

3 1761 11554952 9



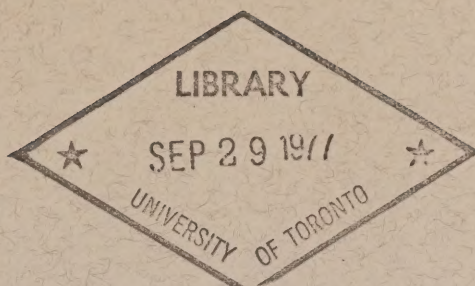


Digitized by the Internet Archive
in 2022 with funding from
University of Toronto

<https://archive.org/details/31761115549529>

CAI
EP 321
77R11

(7)



Numerical Model Studies of Semi-diurnal Tides in the Southern Beaufort Sea

by

R.F. Henry and M.G.G. Foreman

**INSTITUTE OF OCEAN SCIENCES, PATRICIA BAY
Victoria, B.C.**



For additional copies or further information please write to:

Department of Fisheries and the Environment

Institute of Ocean Sciences, Patricia Bay

512 - 1230 Government Street

Victoria, B.C..

V8W 1Y5

Pacific Marine Science Report 77-11

NUMERICAL MODEL STUDIES OF SEMI-DIURNAL
TIDES IN THE SOUTHERN BEAUFORT SEA

by

R.F. Henry and M.G.G. Foreman

Institute of Ocean Sciences, Patricia Bay
Victoria, B.C.

July 1977

This is a manuscript which has received only limited circulation. On citing this report in a bibliography, the title should be followed by the words "UNPUBLISHED MANUSCRIPT" which is in accordance with accepted bibliographic custom.

Abstract

Tide gauge and current meter data available from the southern Beaufort Sea are summarised and the existence of large seasonal variation in tidal constituents is discussed. Existing cotidal charts for the ice-free season are then reviewed. A series of numerical model studies of the semi-diurnal tides, particularly the M_2 tide, is described and extended cotidal charts for the semi-diurnal tides, based on the model results, are presented.

1.1 Analysis of Surface Elevation Records	1
1.1.1 Cotidal charts for surface elevations	1
1.2 Analysis of Current Meter Data	2
1.2.1 Cotidal charts for currents	2
2. Numerical Model Studies of Tidal Constituents	3
2.1 Preliminary Simulation of Semi-diurnal Surface Elevation: Model 1	4
2.2 Refined Simulation: Model 2	5
2.3 Semi-diurnal Currents	7
2.3.1 Progress of Current in Model 2	8
2.4 Mean Energy Flux for M_2 Constituents	9
References	10
Tables	11
Figures	12
Appendix 1: Representation of Tidal Constituents	17
Appendix 2: Energy Flux	21

Table of Contents

	<u>Page No.</u>
Acknowledgements	2
1. Tidal Observations in the Southern Beaufort Sea	3
1.1 Available Records	3
1.2 Analysis of Surface Elevation Records	3
1.2.1 Cotidal charts for surface elevation	5
1.3 Analysis of Current Meter Data	5
1.3.1 Cotidal charts for currents.	5
2. Numerical Model Studies of Tidal Constituents	5
2.1 Preliminary Simulation of Semi-diurnal Surface Elevation: Model 1 .	6
2.2 Refined Simulation: Model 2	7
2.3 Semi-diurnal Current	7
2.3.1 Progress of Current in Model 2	8
2.4 Mean Energy Flux for M_2 constituent	9
References	10
Tables	11
Figures	23
Appendix 1: Representation of Tidal Currents	62
Appendix 2: Energy Flux	70

Acknowledgements

The authors wish to thank Messrs. W. Rapatz, S. Huggett and F. Stephenson of Tides and Currents Section, Institute of Ocean Sciences, Patricia Bay, for their assistance in obtaining tidal data and for many helpful discussions; Mr. I. Taylor of Marine Environmental Data Service, Ottawa for provision of notes mentioned in the text; and Mrs. C. Wallace for preparation of the illustrations.

1. TIDAL OBSERVATIONS IN THE SOUTHERN BEAUFORT SEA

1.1 Available Records

Permanent tide gauges have been maintained at Tuktoyaktuk, Cape Parry and Sachs Harbour (Fig. 1) since 1961, 1966 and 1972 respectively, though occasional gaps in the records have occurred because of difficult operating conditions. Figure 2 indicates the sites of various temporary gauges in Canadian waters, while Figure 3 shows where tidal heights have been recorded on the north Alaskan coast. A few temporary sites have been omitted because either the records were too short or analysis showed serious inconsistencies between records from the same site or neighbouring sites. Herschel Island, off-shore site 13 and Point Barrow are the only locations, besides the three permanent stations, where records have been obtained during the winter months.

The periods for which Canadian records are available in digitized form are given in Tables 1-6. The Alaskan records listed in Table 7 are obtainable from the U.S. Coast and Geodetic Survey in tabular form.

Current meters were installed near the sea bottom at various sites indicated in Figure 2 over the summers of 1974 and 1975 and the periods for which records were obtained are given in Table 8.

Until the 1970s, tidal heights were collected manually or on continuous ('analog') recording devices from which hourly heights were extracted by manual sampling. Recently, recordings of tidal heights and currents have been made directly in digital form at hourly or shorter intervals. Information on the exact locations, sampling intervals, periods recorded and types of instrument used is held by Canadian Hydrographic Service, Victoria.

1.2 Analysis of Surface Elevation Records

Mean sea level at gauge sites on the Beaufort Sea coast is difficult to establish, as there is considerable seasonal variation in level caused mainly by discharge from the Mackenzie River. The effect is most marked in bad ice years when the persistent ice cover appears to partly dam the river water against the coast, augmenting the normal steric increase in level to as much as 0.3 m. However, this uncertainty in the mean level has little effect on the analysis of diurnal and higher frequency tidal constituents to which attention is confined in this report. The shallow coastal waters are very responsive to meteorological influences, in particular to winds during ice-free summer months. Fluctuations in level lasting a few days and reaching 0.5 m above or below mean level are quite frequent and larger variations are not uncommon. Low-frequency constituents of genuinely tidal origin are masked by these meteorologically induced variations and for this reason are not considered further in this report.

The method used to analyze the hourly tidal heights is described by Godin (1972) and Foreman (1977). A least square fit to the observations is effected using a sum of up to 63 constituents, selection of constituents being on the basis of adequate frequency separation from neighbouring constituents. Certain constituents which would normally be excluded on grounds of

insufficient frequency separation (i.e. short record length) are inferred from neighbouring major constituents in whose calculated amplitudes and phases they would otherwise cause cyclic variations (Godin, 1972).

Table 9 shows the results of 1-year analyses at Tuktoyaktuk for the four years in which substantially complete records were collected. Only those constituents clearly above the noise level are shown. The great variability of the calculated low-frequency constituents confirms the pointlessness of considering tides below diurnal frequency. Quite clearly the semi-diurnal constituents account for most of the remaining tide, M_2 being predominant.

The large amplitudes found for H_1 and H_2 , the Horn constituents close to M_2 , are far larger than can be accounted for by the tidal driving forces at the corresponding frequencies and can be attributed to variation in the amplitude or phase of M_2 (Godin, 1972, p. 174). There is a similar spread of S_2 into R_2 and T_2 . The variations in some major constituents in one particular year can be seen clearly from the monthly analyses in Table 10. In the case of M_2 and S_2 , it can be said with reasonable certainty that systematic seasonal changes occur. During the summer months the phases are in advance of winter values and the amplitudes are larger; the seasonal changes occur relatively smoothly, with minor irregularities which are probably attributable to storm surges. For the smaller constituents, storm surge or other effects obscure any systematic trends which may be present.

It seems that these variations in the tide at Tuktoyaktuk are due primarily to the seasonal nature of the ice cover on the Herschel-Bathurst shelf. At Pt. Barrow, where there is normally little open water even in summer, the phase of the M_2 constituent is constant year round to within 1° (Matthews, private communication). Monthly analyses show that at Herschel Island, the M_2 tide arrives about 10° earlier in summer than in winter, whereas at Tuktoyaktuk the difference is at least 60° . Even in ice-free summers, there is not usually a great extent of open water west of Herschel Island, the direction from which the semi-diurnal tides approach. There is consistent evidence therefore that the presence of ice cover delays the tide, the amount of the delay being very roughly proportional to the increase in extent of the ice.

An important implication of such seasonal changes is that care must be taken when comparing tidal behaviour at different sites. In particular, cotidal charts of the area must be based on records covering similar periods. At the present time, enough observations are available from the Herschel-Bathurst shelf to draw up rough cotidal charts for ice-free summer conditions, see for instance, Figures 4 and 5.

If measurements are made at more sites during the winter months, it should be possible also to prepare cotidal charts for fully ice-covered conditions, but it seems very unlikely that enough observations will ever be made to provide cotidal charts valid for all the great variety of partial ice-cover configurations found in the interim season. It was in the hope of coping to some extent with this problem that the numerical modelling study described later in this report was begun.

1.2.1 Cotidal charts for surface elevation

Cotidal charts prepared on the basis of observations made mainly during the 1974 and 1975 spring and summer field seasons are shown in Figures 4 and 5 (Huggett *et al.*, 1976). The phases shown are Greenwich phases relative to time zone +6 (see footnote p. 11). The behaviour of M_2 and K_1 are typical of all the major semi-diurnal and diurnal constituents respectively, in that the former all propagate eastwards from Alaskan waters while the latter apparently propagate southwards. The chart for K_1 is probably less reliable than that for M_2 since the amplitude of K_1 is closer to the noise level. One aim of the numerical modelling study was to extend the coverage of these cotidal charts to all navigable parts of the Canadian sector of the Beaufort Sea.

1.3 Analysis of Current Meter Data

The current meter record from each site was resolved into tidal constituents according to the method outlined in Godin (1972). The computer program used for this analysis reduces each constituent into clockwise and anticlockwise rotating vectors which it specifies in terms of their respective amplitudes a^+ , a^- and phases ϵ^+ , ϵ^- . The definitions of these parameters and their relationships to other representations of tidal current constituents, in particular the 'current ellipse' and the 'Greenwich phase', are discussed in some detail in Appendix 1.

1.3.1 Cotidal charts for currents

Figure 6 shows a tentative cotidal chart for the M_2 tide (Huggett *et al.*, 1976) based on analyses of current meter records from eight sites. Results from a ninth site, No. 3, which became available later, have been added. The apparent increase from east to west of the Greenwich phase can be viewed as a westerly progression of the time of maximum flow, a situation contradictory to the eastward progression of surface elevation discussed in §1.2.1. However, due to arbitrariness in the definition of Greenwich phases of tidal current constituents (Appendix 1), there are possible ambiguities of 180° in the observed phases at isolated sites and indeed as is shown in §2.4, this problem is not always overcome when intermediate values are available. On selecting the possible alternative values (shown in parentheses) at some sites, it can be argued that the time of maximum flow, pertaining to the M_2 constituent, in fact progresses eastward.

In the case of K_1 there is no similar difficulty in the interpretation of observed current phases. Figure 7 indicates a southward progression of time of maximum flow, which is concordant with the progression of surface elevation shown in Figure 5.

2. NUMERICAL MODEL STUDIES OF TIDAL CONSTITUENTS

The availability of a two-dimensional vertically-integrated finite-difference model covering the southern Beaufort Sea (Henry and Heaps, 1976) prompted attempts to simulate the behaviour of major tidal constituents, with the aims of extending cotidal charts, resolving uncertainty about the direction of propagation of the semi-diurnal tide and determining optimum sites for future measurements. The area covered by the model is shown in Figure 8.

Although the governing equations include a quadratic friction term, the total tidal range is small enough that this nonlinearity may be ignored and the constituents of interest simulated separately. While all efforts to simulate the diurnal tides failed, the semi-diurnal constituents were reproduced with reasonable accuracy in the Canadian sector.

2.1 Preliminary Simulation of Semi-diurnal Surface Elevation: Model 1

A fundamental assumption made was that the tides in the area considered are essentially 'co-oscillating', that is, the local contribution of the tidal generating potential is small and the tides originate in the adjacent deeper ocean areas. In simulation of co-oscillating tides it is usually necessary to know beforehand the amplitudes and phases of the constituents along the sea boundaries of the model, in this case the western and northern boundaries (the boundary conditions applied in the narrow eastern channels were found to affect the model behaviour locally only). Point Barrow, close to the southern end of the western boundary is in fact the only point near either sea boundary where observations have been made. In a preliminary simulation (Model 1), it was assumed, on the basis of Figure 4, that the M_2 and other semi-diurnal constituents probably entered the domain of the model over the western boundary. Secondly, it was assumed that the amplitude and phase of each constituent were the same all along this relatively short boundary.

With zero initial conditions throughout the interior of the model and periodic surface elevation imposed at the western boundary, a wave propagates eastward into the model domain. From general knowledge of the Kelvin wave-like behaviour of tidal waves in the northern hemisphere, it was assumed that such waves would leave the model domain travelling northwards, parallel to the Banks Island shore. For this reason, the radiation condition used on the northern boundary in the original model was retained, as it was designed to permit the free escape of the northward component of any long wave reaching this boundary, clearly an appropriate condition in the present case.

The model was run in the above manner with an imposed periodic surface elevation on the western boundary at M_2 frequency and with an amplitude of 6 cm, that is, the observed amplitude of M_2 at Point Barrow. After only five cycles, approximately steady periodic conditions obtained throughout the model. Amplitudes and phases were found by fitting sinusoids to the elevations computed for three subsequent cycles. Part of the resulting cotidal amplitude and phase charts are shown in Figures 9 and 10, which also show, for comparison, values obtained from summer records at various sites. It must be noted that the computed phases shown in Figure 10 do not come directly from the model, which simply provides phases relative to the driving periodic condition on the western boundary. The phases shown were obtained by adding to all the computed phases an arbitrary angle such that the simulated tides at Herschel Island and Cape Parry (two stations where substantial series of observations have been made) agreed well with observed values. Using a least square fit, the error at the two stations was less than 3° for the M_2 tide.

From Figure 9 it can be seen that there is quite good agreement between simulated and observed amplitudes. M_2 phases from the simulation as shown in Figure 10 were satisfactory and there was also fair agreement with the few observations available in Amundsen Gulf, but the observed phases along the Alaskan coast, which did not become available until after Model 1 had been devised and run, were not at all well reproduced.

2.2 Refined Simulation: Model 2

The Alaskan observations indicated roughly simultaneous phase for the M_2 wave all along the coast from Point Barrow to Herschel Island. This fact, together with closer study of the bottom topography north and west of Point Barrow led to a second model, in which a periodic boundary condition was arranged which introduced a travelling wave through the northwest part of the model domain. For computational convenience, this was achieved by imposing a periodic surface elevation at the 3650 m depth contour, the amplitude and phase being kept constant all along the contour. The remaining sea boundaries, including now the western boundary, were governed by the radiation condition permitting outward passage of the normal components of incident long waves.

On starting from rest with periodic elevation of 6 cm at M_2 frequency imposed on the 3650 m contour, Model 2 settled to steady oscillation in a few cycles. The resulting amplitudes and phases, obtained as for Model 1, are shown in Figures 11 a,b and 12 a,b. The simulation was now in satisfactory agreement with practically all the observed values and it was concluded that the M_2 wave in all likelihood does enter the area from the north-west. Better agreement between the simulated and observed amplitudes could very probably have been obtained by rerunning with a driving amplitude somewhat greater than 6 cm, but this was not done on account of computational cost.

Simulation of S_2 , the next largest semi-diurnal constituent, was performed in the same way as for M_2 ; some of the results are shown in Figures 13 and 14. Essentially, the cotidal charts for M_2 and S_2 are very similar and the following comments apply as much to S_2 as to M_2 .

Comparison of Figures 9 and 10 with Figures 11b and 12b respectively shows that the simulated semi-diurnal tide in the Canadian sector is relatively insensitive to the choice of driving conditions applied at the western end of the model domain; this encourages placing of some confidence in the results shown in Figures 11b and 12b at least. The outstanding feature of these is the near-degenerate amphidromic point off Cape Kellett on Banks Island. Its discovery led to the installation in the summer of 1976 of the shore-based tide gauges at Rabbit Island and Masik River (Figure 2), the data from which confirmed the general correctness of the simulation in the Canadian sector.

In view of the rather arbitrary placement of the periodic boundary in Model 2, no reliance should really be placed on simulated amplitudes and phases in Figures 11a and 12a. The simulated tides in Prince of Wales Strait and Dolphin and Union Strait (Figs. 11b, 12b) are also probably unrealistic, as a radiating condition was simply assumed at the boundaries there.

2.3 Semi-diurnal Current

Figure 15 presents for comparison the M_2 constituent of the observed currents together with simulated M_2 currents at the same sites from Model 2. It is clear that while there is partial agreement as to the orientation of current ellipses, the observed currents are far smaller than the simulation leads one to expect. It must be noted that the observed currents were generally close to or below the operating threshold of the meters for an

appreciable fraction of the time and that the current data are inherently somewhat unreliable. The meters were approximately 4 m above sea bottom, which should preclude boundary layer effects as the cause of the discrepancies. Unfortunately, no near-surface meters were recovered, so that the assumption of barotrophy is unconfirmed.

2.3.1 Progress of Current in Model 2

The contoured presentation in Figure 16 of the M_2 current phase from Model 2 shows a generally eastward progression of time of maximum flow, thus favouring the alternative interpretation of Figure 6 discussed in §1.3.1. The time zone, (z+6), used in Figure 16 is the same as that of Figure 6.

There are difficulties in contouring current phase which deserve some discussion. Figure 17 shows current ellipses from a small rectangular area indicated in Figure 16. The arrow shown with each ellipse indicates the position of the current vector at the instant of maximum surface elevation. For convenience individual ellipses in Figure 17 will be designated (i, j) according to their row number, i, and column number, j in the figure. The Greenwich phases shown in large numbers are the conventional values from the current analysis program, which always selects the north-pointing major semi-axis as reference axis. Considering ellipses (4, 5) and (5, 5), it can be seen that despite the obvious continuity in the nature of the current, an artificial jump occurs in this Greenwich phase due to difference in inclination of the ellipses (OA indicates the reference major semi-axis in each case). A similar effect is obvious on comparing ellipses (3, 4) and (4, 4) or (3, 3) and (4, 3). This difficulty can apparently be avoided by relaxing the requirement that the northern major semi-axis should always be used as reference axis. Thus if the southern major semi-axis is chosen instead for ellipses (5, 5) and (6, 5), (4, 4), (5, 4) and (6, 4), and (4, 3), (5, 3) and (6, 3), the resulting modified Greenwich phase, shown, where relevant, in small numbers, varies smoothly over the last three columns of ellipses*. Unfortunately, other difficulties remain.

Consider two paths from (1, 5) to (6, 1), in one case via (1,1) and in the second via (6, 5). On the first path, visual examination of the ellipses indicates that the northern major semi-axis is the appropriate reference axis throughout, the phases shown in large numbers apply, and it appears that the correct Greenwich phase angle for ellipse (6, 1) must be 196° . However, on taking the second path and making the switch from northern to southern major semi-axis between (4, 5) and (5, 5) as mentioned above, continuity along the remainder of the path is maintained by using the phases shown in small numbers, leading to the conflicting conclusion that the Greenwich phase angle for (6, 1) should be 16° .

* A 180° change in reference axis inclination produces a 180° change in Greenwich phase (see Appendix 1).

Another difficulty is evident when ellipses (3, 2), (4, 2) and (5, 2) are examined. At some point intermediate between (4, 2) and (5, 2), the current ellipse degenerates to a circle and there is a consequent interchange in roles of the semi-axes, from major to minor and vice-versa. This results in a 90° change in reference axis and a corresponding jump of 90° in the Greenwich phase.

While the difficulty of 180° discontinuities in Greenwich phase can be removed to some extent by ignoring the direction of the current and considering only its magnitude, the second type of discontinuity (90° in phase) seems to be unavoidable.

It is proper to consider whether the discontinuities just described do not occur in nature but are simply a feature of the model, the result of imperfect simulation. As a check on the physical consistency of the model results, it was decided to examine another quantity, the mean energy flux, since any violation of conservation of energy would indicate some defect.

2.4 Mean Energy Flux

The mean energy flux, a vector quantity defined in Appendix 2, was calculated from the output of Model 2 for the M_2 constituent. The results for the eastern portion of the model domain are² shown in Figure 18. The northern portion shows that in the deeper water there is net transmission of energy in the direction of propagation of the wave, as would be the case with a Kelvin wave for instance. On the shallow Herschel-Bathurst shelf, energy flow is directed particularly towards very shallow regions where it is effectively dissipated.

In Appendix 2 it is shown that the direction of the mean energy flux vector coincides with that of the current at the instant of maximum surface elevation. Since the latter vector is shown at each grid-point in Figure 17, a detailed picture is already available of the directional variation of mean energy flux in a region where characteristic parameters of the current are known to exhibit marked spatial variation.

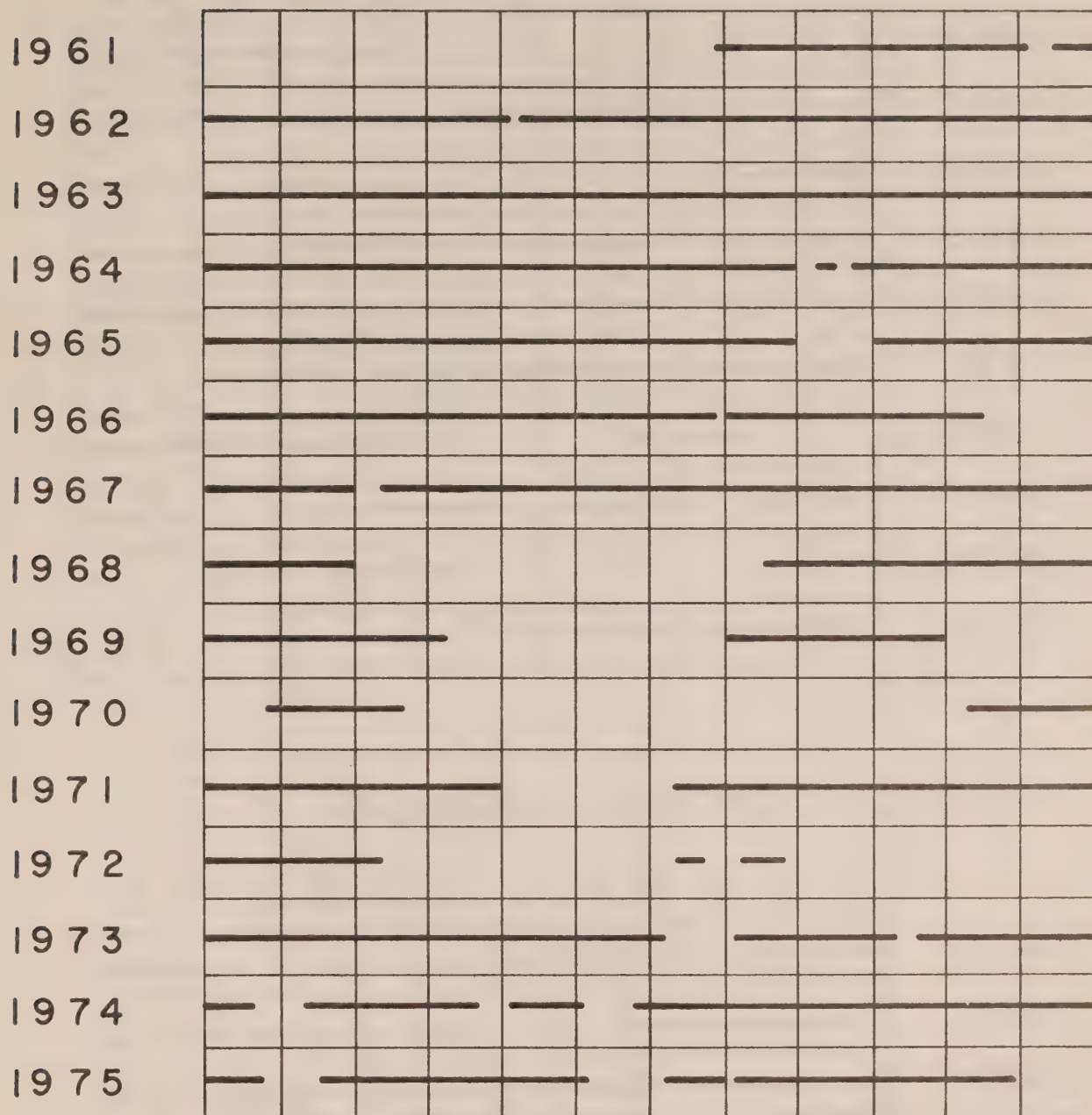
The smooth spatial variation of mean energy flux in Figures 17 and 18 certainly encourages the conclusion that no anomalous effects have been introduced by the modelling procedure. Judging from the results presented here, examination of the mean energy flux may cast a more useful light on tidal behaviour than preparation of cotidal charts of more erratically-varying quantities such as Greenwich phase of the current or time of maximum flow.

REFERENCES

- Foreman, M.G.G., 1977. Manual for Tidal Heights Analysis and Prediction. Pacific Marine Science Report 77-10, Institute of Ocean Sciences, Patricia Bay, Victoria, B.C.
- Godin, G.G., 1972. The Analysis of Tides. University of Toronto Press.
- Godin, G.G., 1976. The Reduction of Current Observations with the Help of the Admittance Function. Technical Note No. 14, Environment Canada, Ottawa. Marine Environmental Data Service.
- Henry, R.F. and Heaps, N.S., 1976. Storm Surges in the Southern Beaufort Sea. J. Fish. Res. Board Can., Vol. 33, 2362-76.
- Huggett, W.S., Woodward, M.J., Stephenson, F., Hermiston, F.V. and Douglas A., 1976. Near Bottom Currents and Offshore Tides. Technical Report No. 16, Beaufort Sea Project, Victoria, B.C.
- Phillips, O.M., 1969. The Dynamics of the Upper Ocean. Cambridge University Press.

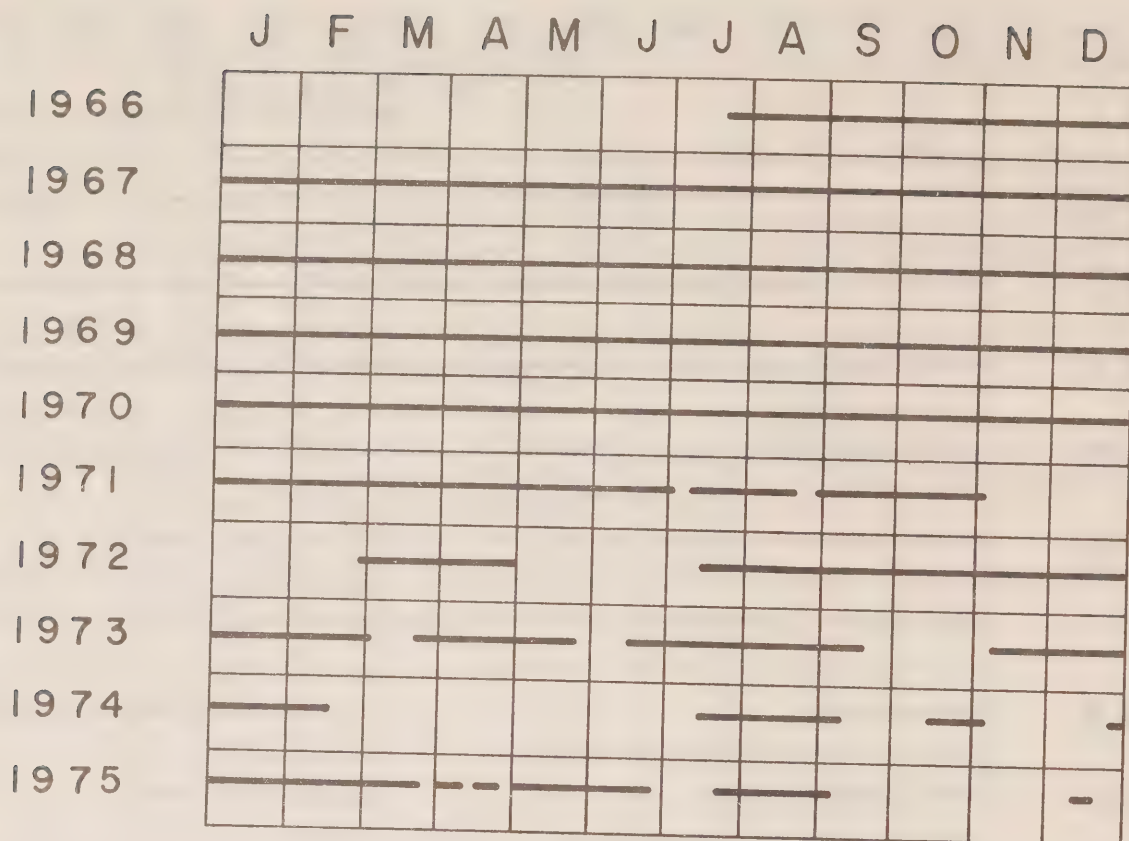
TUKTOYAKTUK

J F M A M J J A S O N D

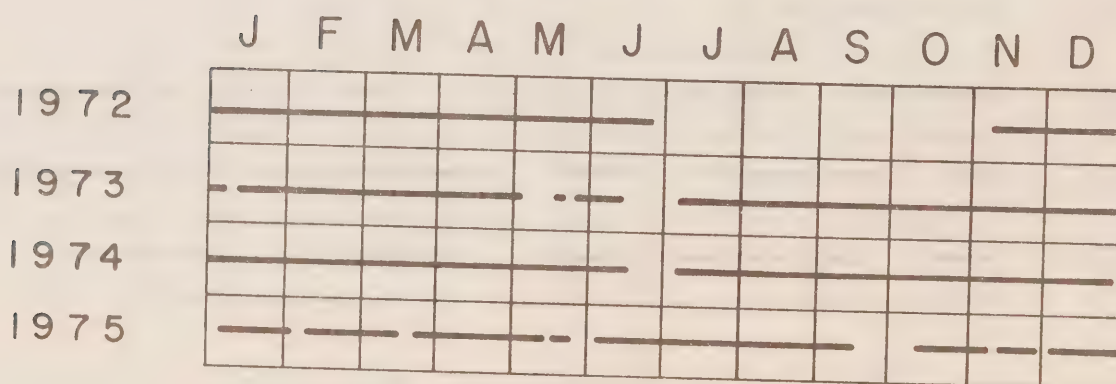


Bar Charts of Available Records
of Surface Elevation
Table I

CAPE PARRY

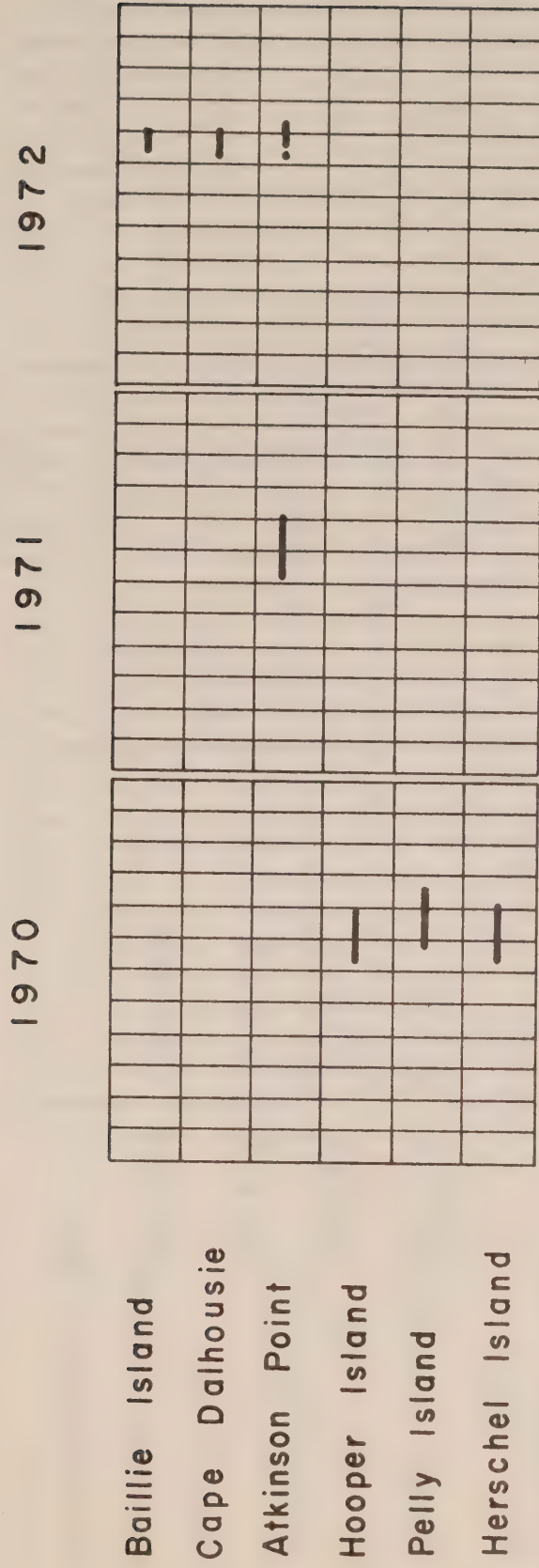


SACHS HARBOUR



Bar Charts of Available Records
of Surface Elevation

Table 2

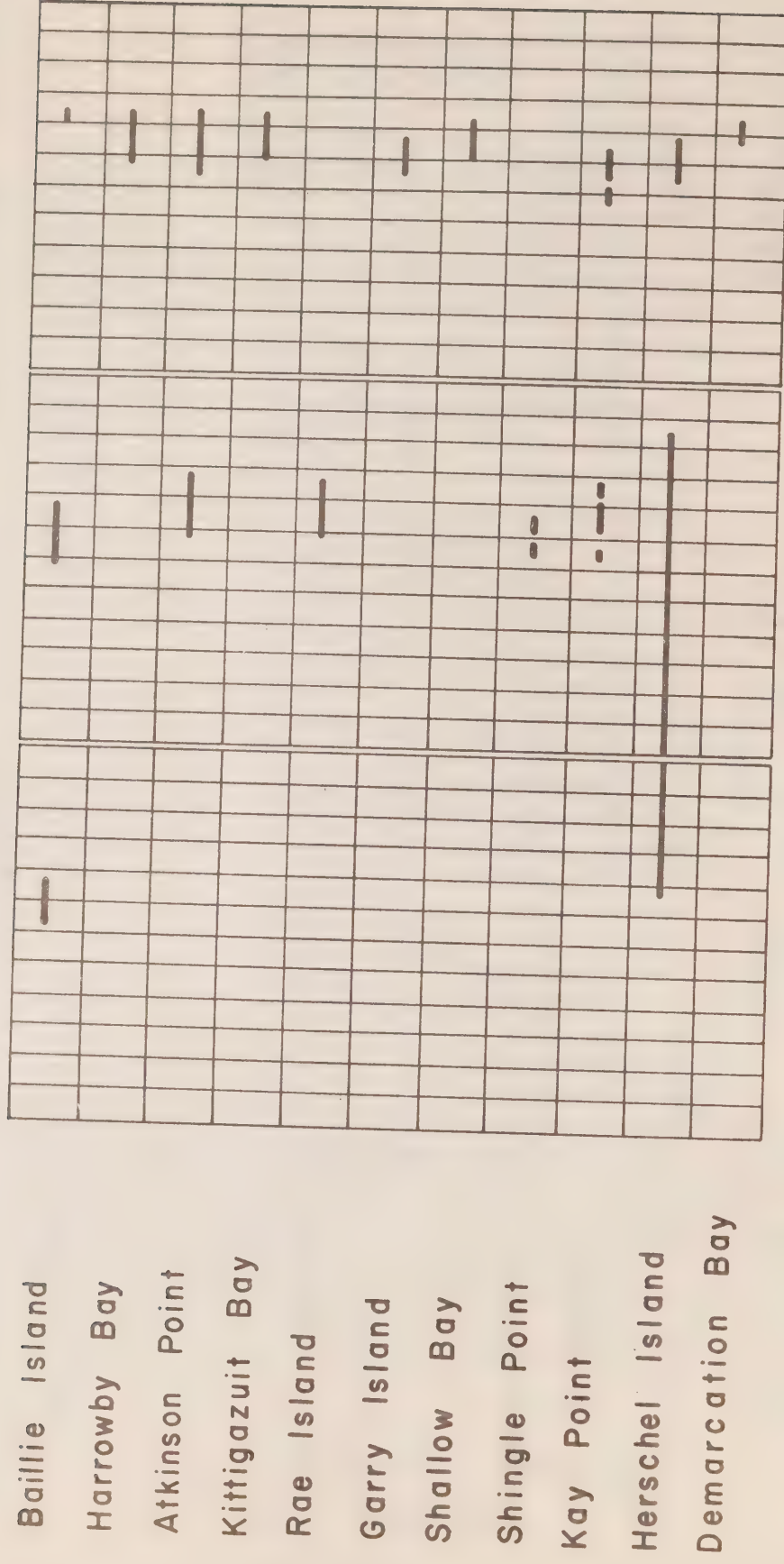


Bar Charts of Available Records from Shore Based Gauges
Table 3

1973

1974

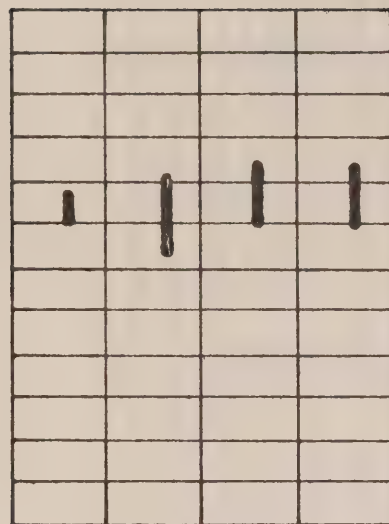
1975



Bar Charts of Available Records from Shore Based Gauges

Table 4

1976



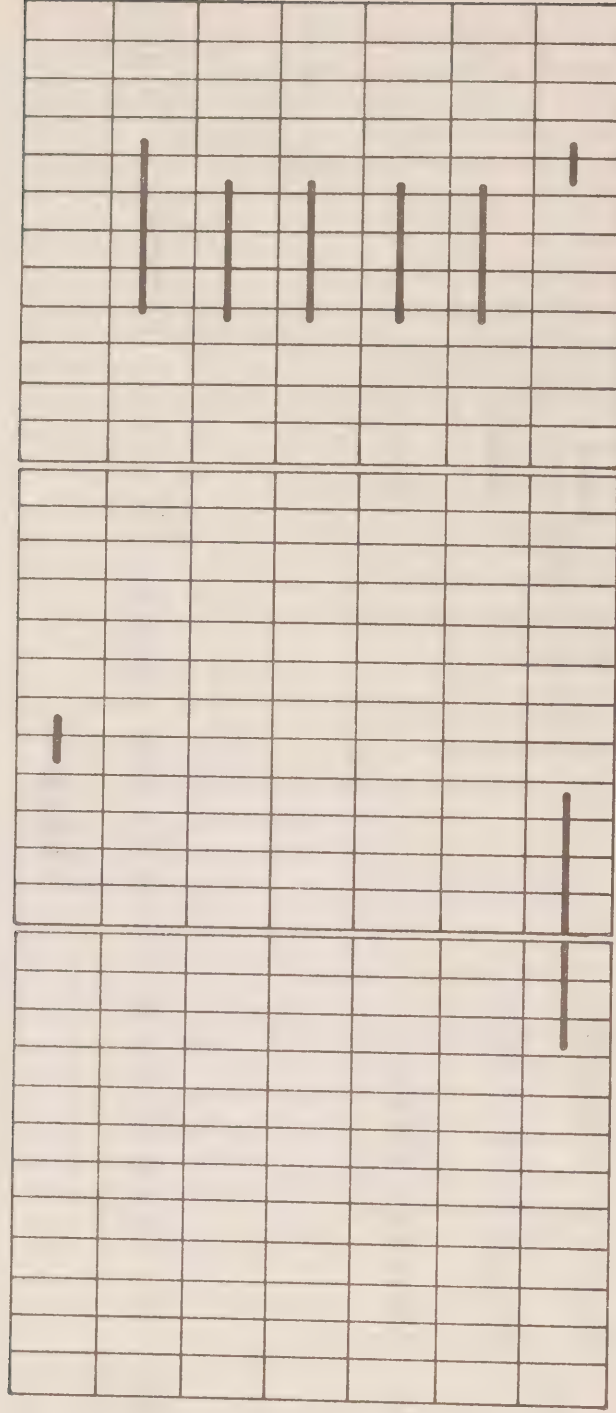
Bar Charts of Available Records from Shore Based Gauges

Table 5

1973

1974

1975

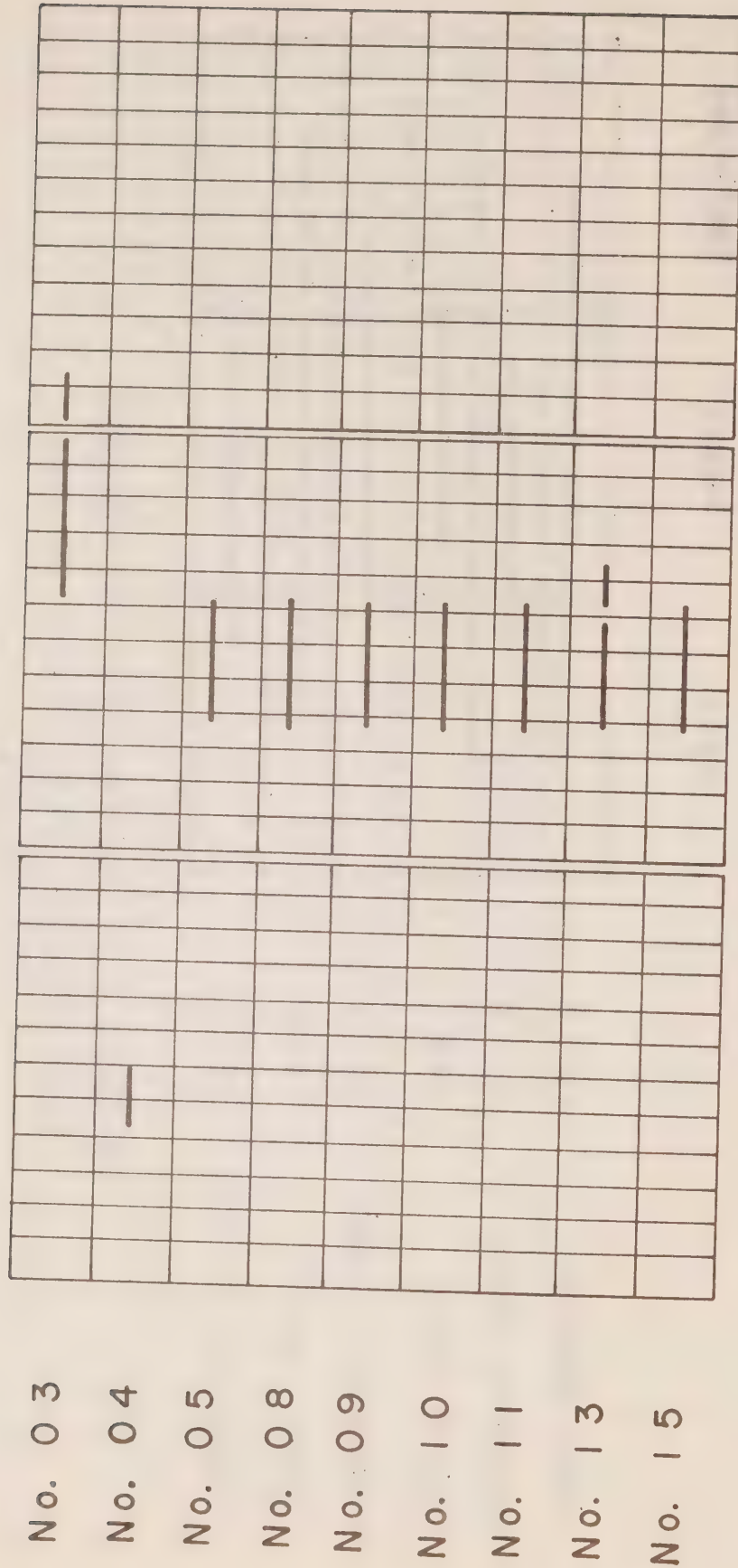


Bar Charts of Available Records from Off Shore Gauges

Table 6

		July	August	September
Point Barrow	1972			
Saktuina Point	1953			
Oliktok Point	1951			
Tigvariak Island	1949			
Barter Island	1948			
Demarcation Bay	1952			

Bar Charts of Surface Elevation Records
from Alaskan Shore Based Gauges
Table 7



Bar Charts of Available Current Meter Records
Table 8

Constituent		1962		1963		1964		1967	
		Amp. (cm)	Phase (°)	Amp. (cm)	Phase (°)	Amp. (cm)	Phase (°)	Amp. (cm)	Phase (°)
Low frequency	Sa	17.0	182.6	10.8	209.8	10.9	162.6	9.0	188.6
	Ssa	12.2	251.6	5.0	158.5	9.9	224.8	8.4	196.6
	MSm	6.5	198.0	1.8	71.4	1.1	23.8	2.1	52.4
	Mm	5.4	181.0	4.4	172.6	4.7	161.9	0.8	301.0
	MSf	0.6	26.7	2.4	345.1	2.8	74.4	1.4	97.3
	Mf	1.9	218.8	2.9	109.5	3.8	260.0	4.5	235.1
Diurnal	Q ₁	0.5	214.7	1.0	214.5	0.7	197.0	0.6	187.6
	O ₁	2.5	186.3	2.9	190.2	2.8	188.5	2.5	187.7
	P ₁	0.9	145.3	1.3	166.3	1.2	167.8	0.7	149.3
	K ₁	3.1	162.3	3.2	158.8	3.1	161.2	3.2	157.9
Semidiurnal	N ₂	1.8	280.3	1.6	295.3	1.9	305.7	1.5	285.3
	OP ₂	1.7	110.3	1.4	143.6	1.1	124.4	1.4	101.9
	H ₁	4.9	177.0	3.8	184.6	2.7	162.3	4.8	172.5
	M ₂	11.5	309.5	11.9	310.4	12.9	312.8	11.2	309.9
	H ₂	4.5	116.0	3.9	108.0	2.8	131.9	3.9	109.8
	MKS ₂	1.4	139.4	1.6	131.8	1.1	174.5	1.8	149.0
	L ₂	0.7	341.8	1.1	244.6	0.7	279.2	0.4	13.4
	T ₂	2.2	57.9	1.9	73.9	1.4	38.8	2.0	44.9
	S ₂	4.9	1.2	5.2	6.2	5.3	5.0	4.8	3.3
	R ₂	1.9	22.1	1.3	18.6	1.3	39.3	1.7	13.0
	K ₂	1.1	333.5	1.1	338.9	1.5	341.9	0.9	340.7

Principal tidal constituents at Tuktoyaktuk
based on 1-year analyses

Table 9

	M ₂		S ₂		N ₂		K ₁		O ₁	
	Amp. (cm)	Phase (°)	Amp. (cm)	Phase (°)	Amp. (cm)	Phase (°)	Amp. (cm)	Phase (°)	Amp. (cm)	Phase (°)
Jan.	11.4	334.3	4.6	28.6	1.2	306.2	2.6	164.5	2.7	205.2
Feb.	11.8	335.4	4.4	43.9	1.2	307.9	3.0	155.9	2.9	194.6
Mar.	11.5	337.6	4.2	37.9	2.1	332.0	4.4	165.8	3.1	206.7
Apr.	11.4	338.1	4.2	33.3	2.4	329.0	2.5	175.1	2.8	205.1
May	11.6	329.9	4.8	23.9	2.2	284.1	2.9	171.9	2.7	189.1
June	12.5	311.5	6.0	5.3	1.6	225.4	2.9	158.8	3.0	189.3
July	19.0	278.1	5.5	332.8	0.5	387.4	5.2	159.6	3.6	191.6
Aug.	15.1	271.6	8.2	335.0	2.1	239.2	3.5	155.8	1.7	67.2
Sep.	16.6	284.0	8.3	357.6	1.8	255.1	4.6	171.5	4.4	199.1
Oct.	13.9	295.5	6.7	349.3	1.8	251.2	5.2	122.0	4.7	170.4
Nov.	11.5	317.1	5.1	5.7	2.0	290.4	2.9	162.7	2.4	181.5
Dec.	11.4	325.6	4.7	13.4	2.3	296.1	3.2	154.1	2.3	182.5

Major Tidal Constituents at Tuktoyaktuk based on 30-day analyses in 1963

Table 10

Fig. 1 THE SOUTHERN BEAUFORT SEA

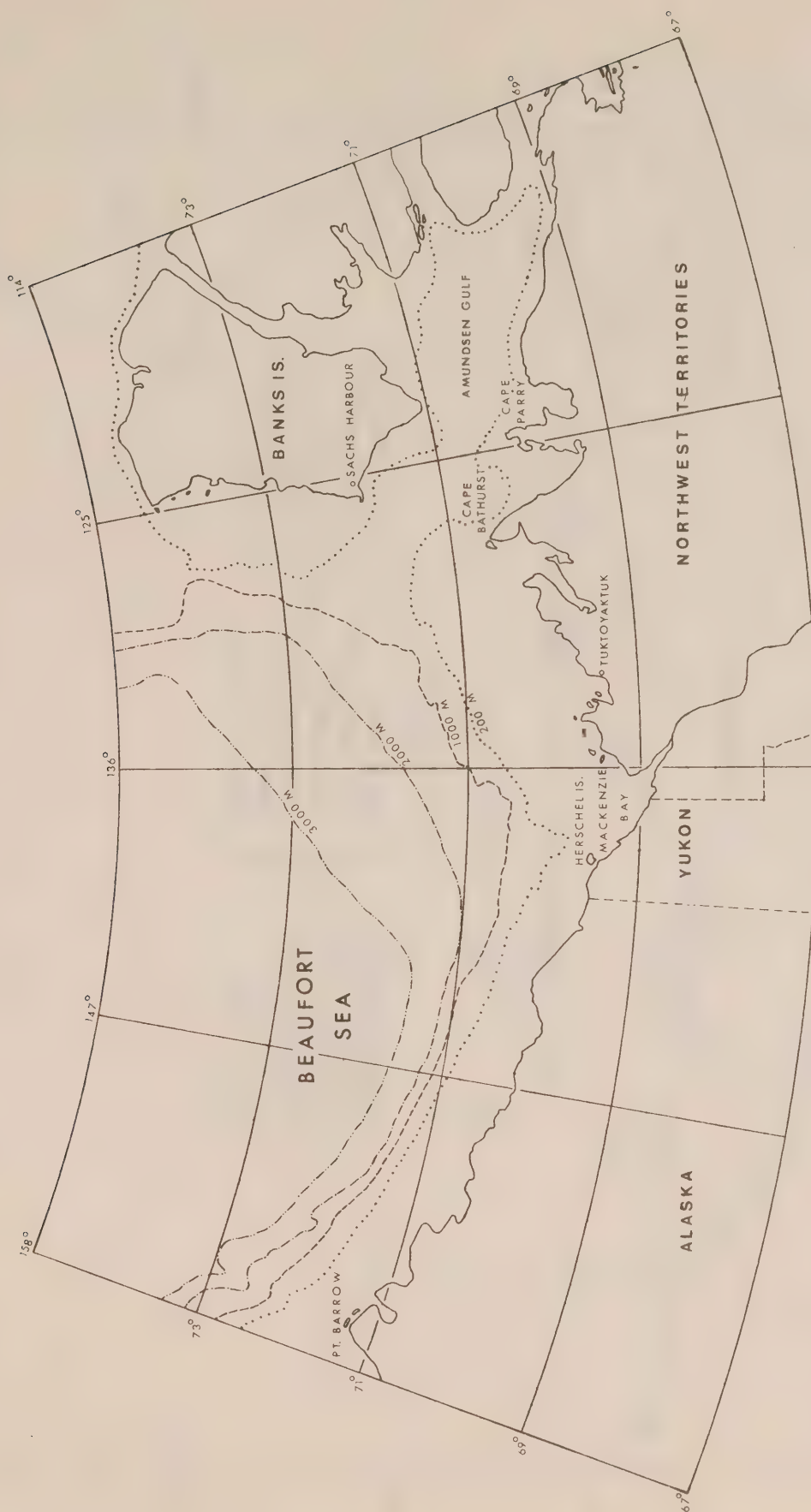


Fig. 2 OBSERVATION SITES IN CANADIAN SECTOR

	○ Tide gauge				
	+	Current meter			
F	Demarcation Bay	L	Rae Island	T	Harrowby Bay
G	Herschel Island	M	Kittigazuit Bay	U	Cape Parry
H	Kay Point	N	Tuktoyaktuk	V	Paulatuk
I	Shingle Point	P	Atkinson Point	W	Rabbit Island
J	Shallow Bay	R	Cape Dalhousie	X	Sachs Harbour
K	Garry Island	S	Baillie Island	Y	Masik River

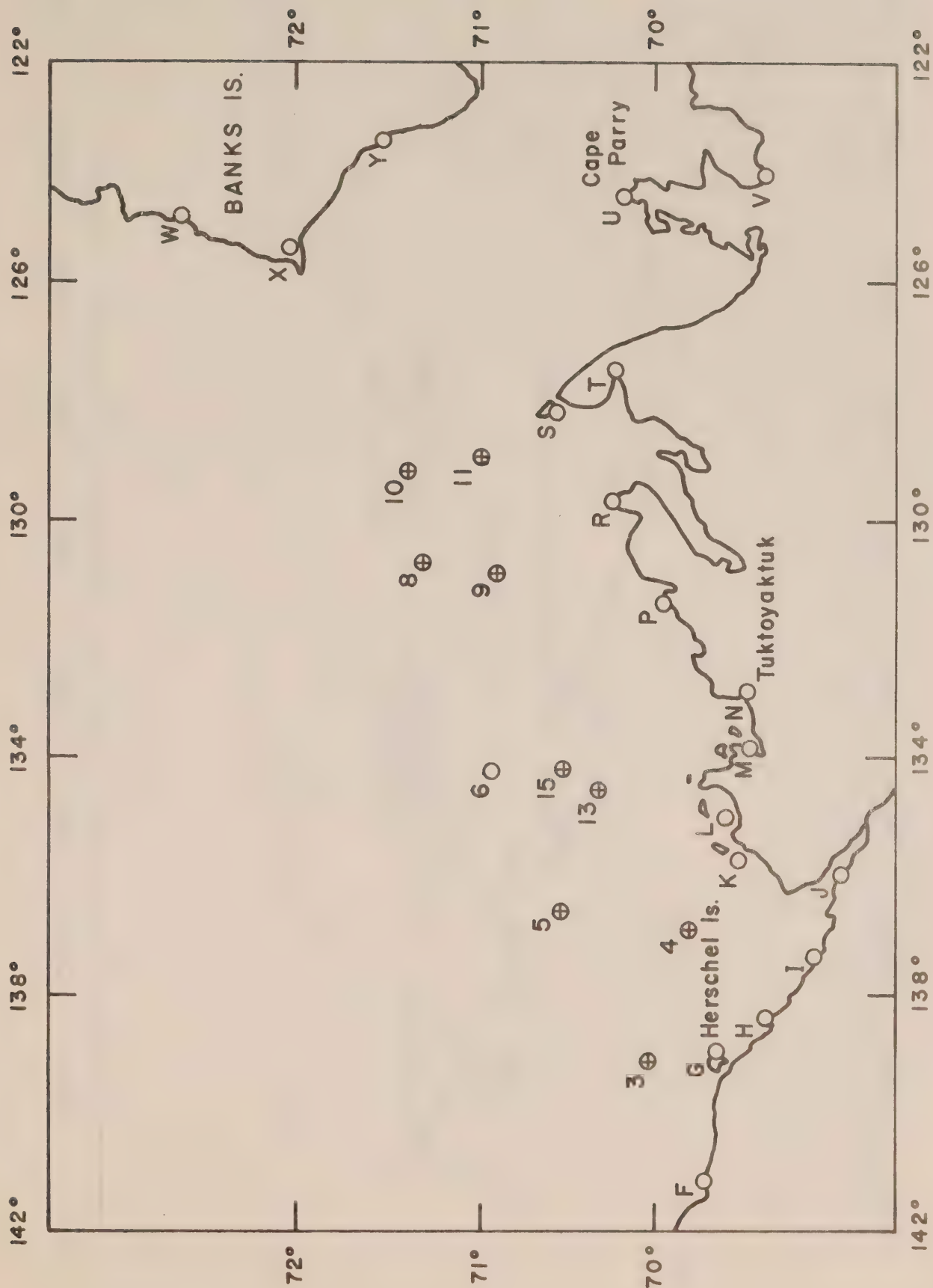


Fig. 3 OBSERVATION SITES IN U.S. SECTOR

O Tide gauge

- | | | | |
|---|----------------|---|------------------|
| A | Point Barrow | D | Tigvariak Island |
| B | Saktuina Point | E | Barter Island |
| C | Oliktok Point | F | Demarcation Bay |

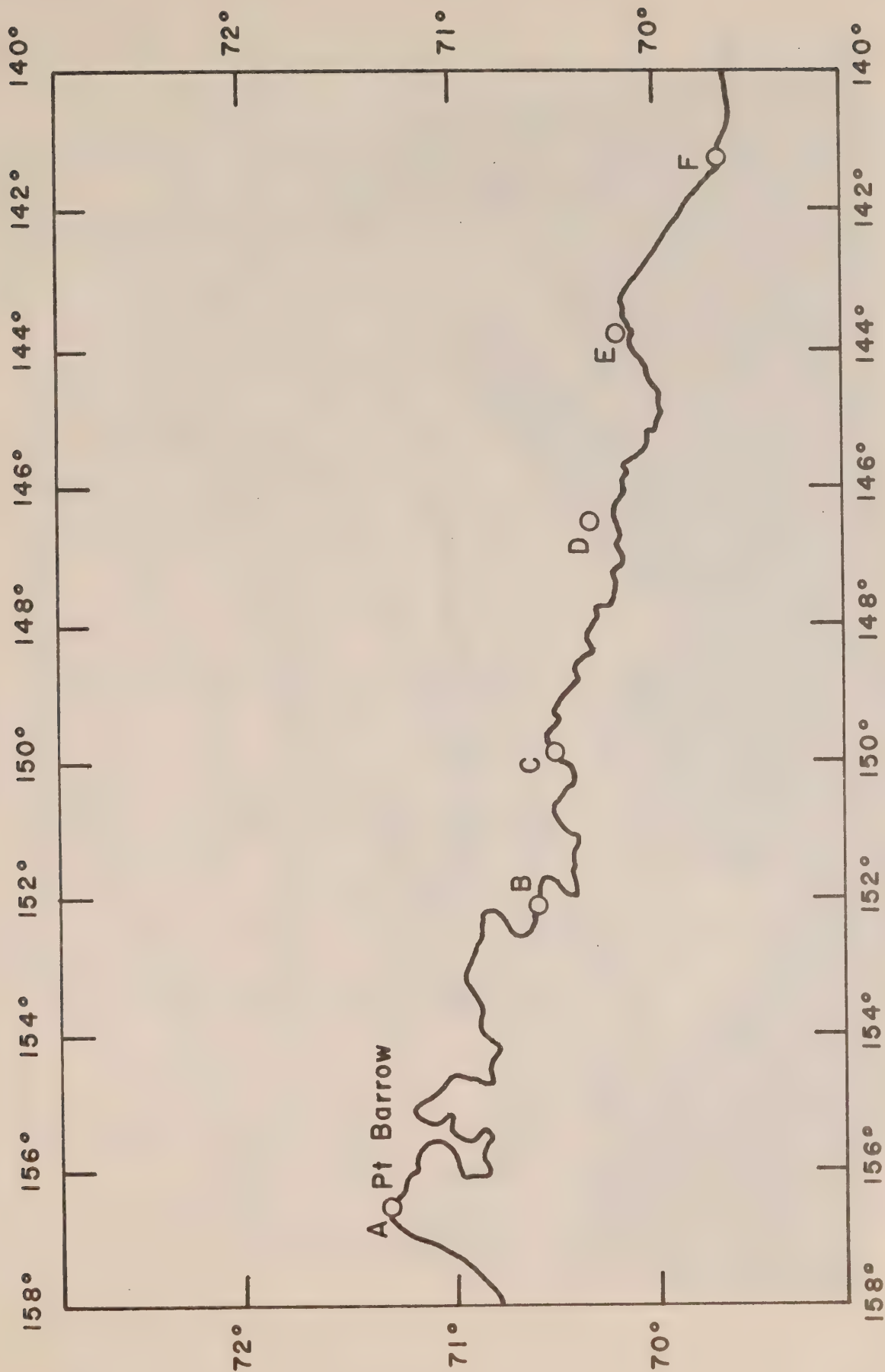
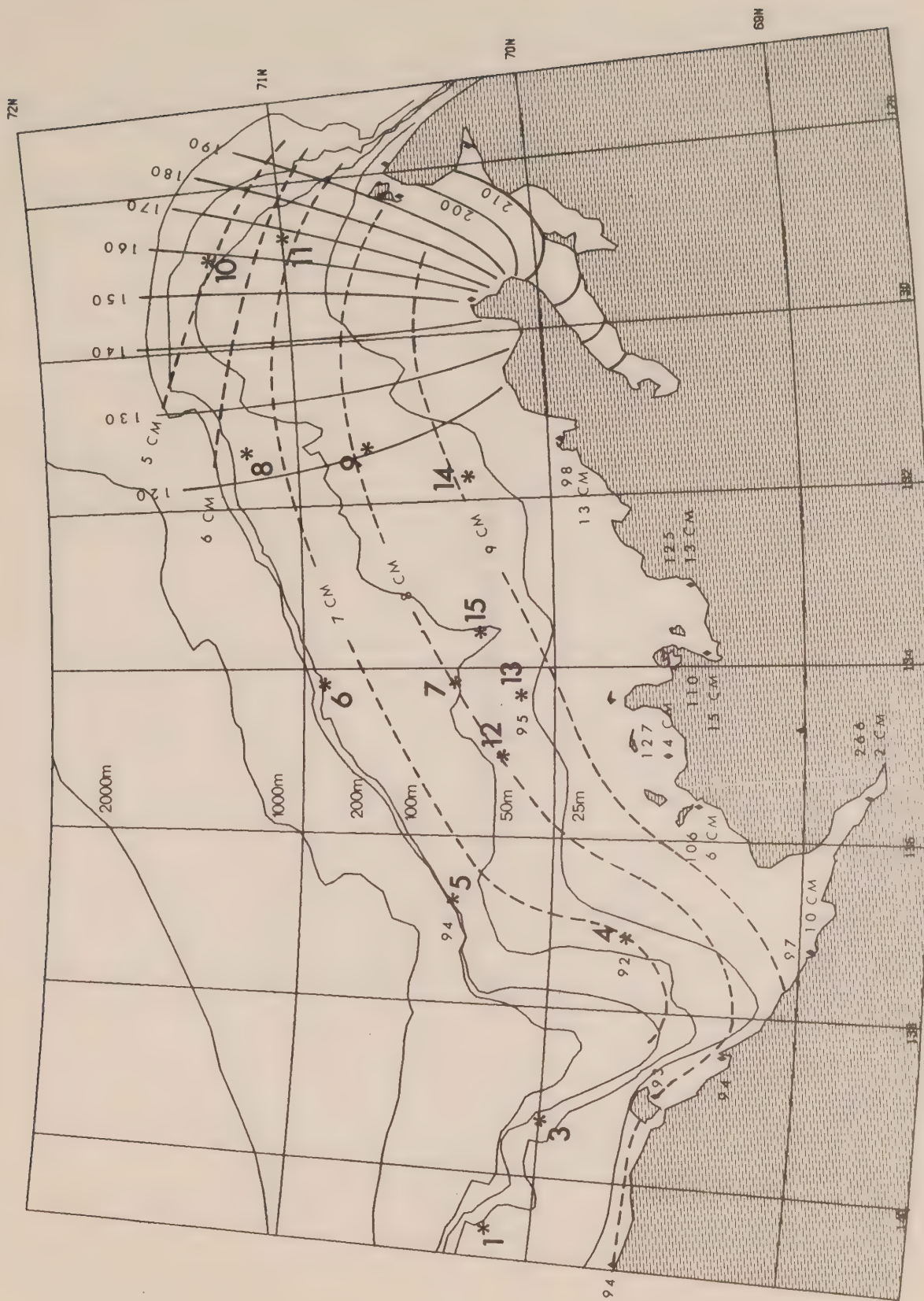
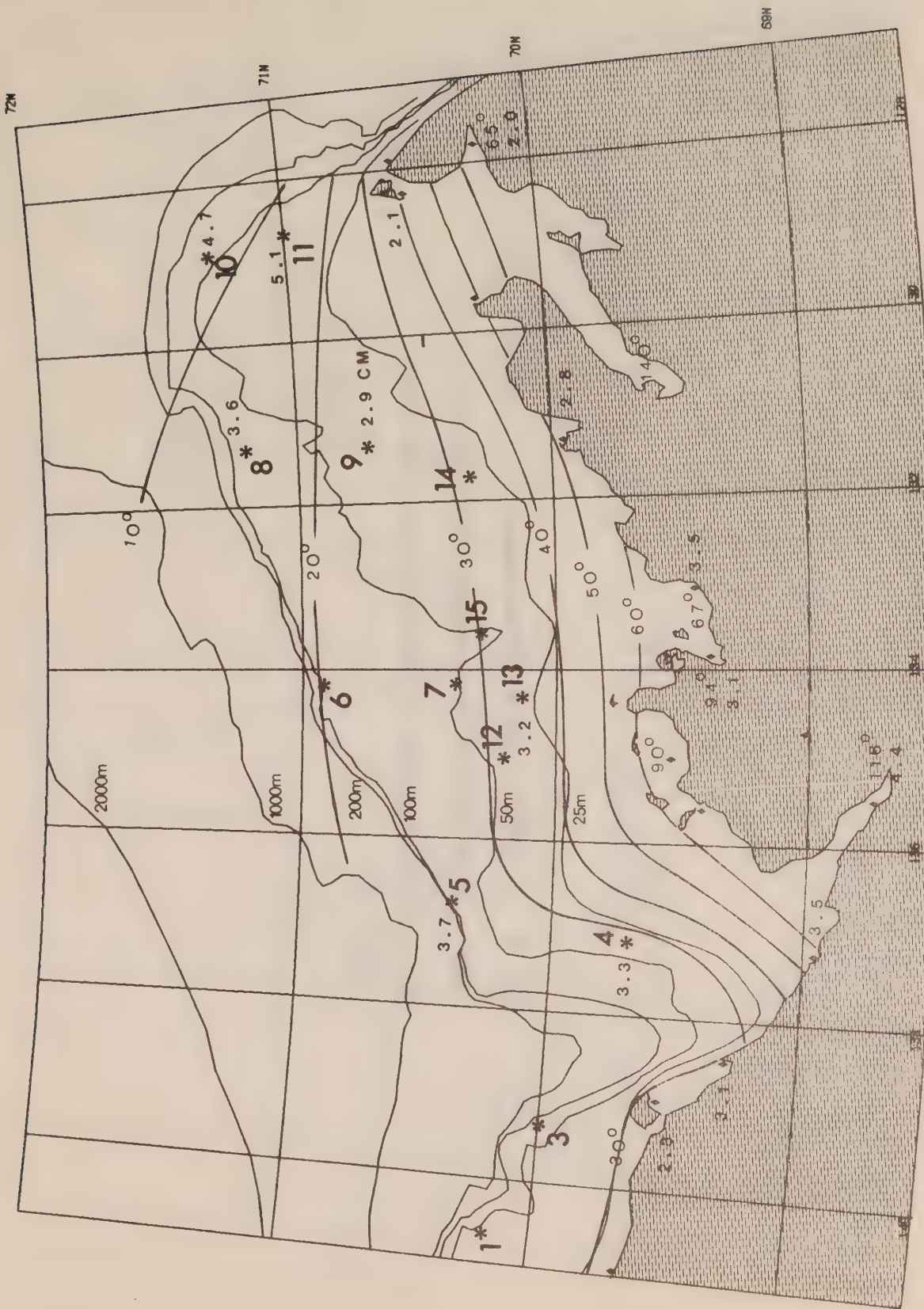


Fig. 4 M_2 SURFACE ELEVATION (from Huggett *et al.*, 1976)



M₂ COTIDAL CHART - WATER LEVELS (Z + 6)

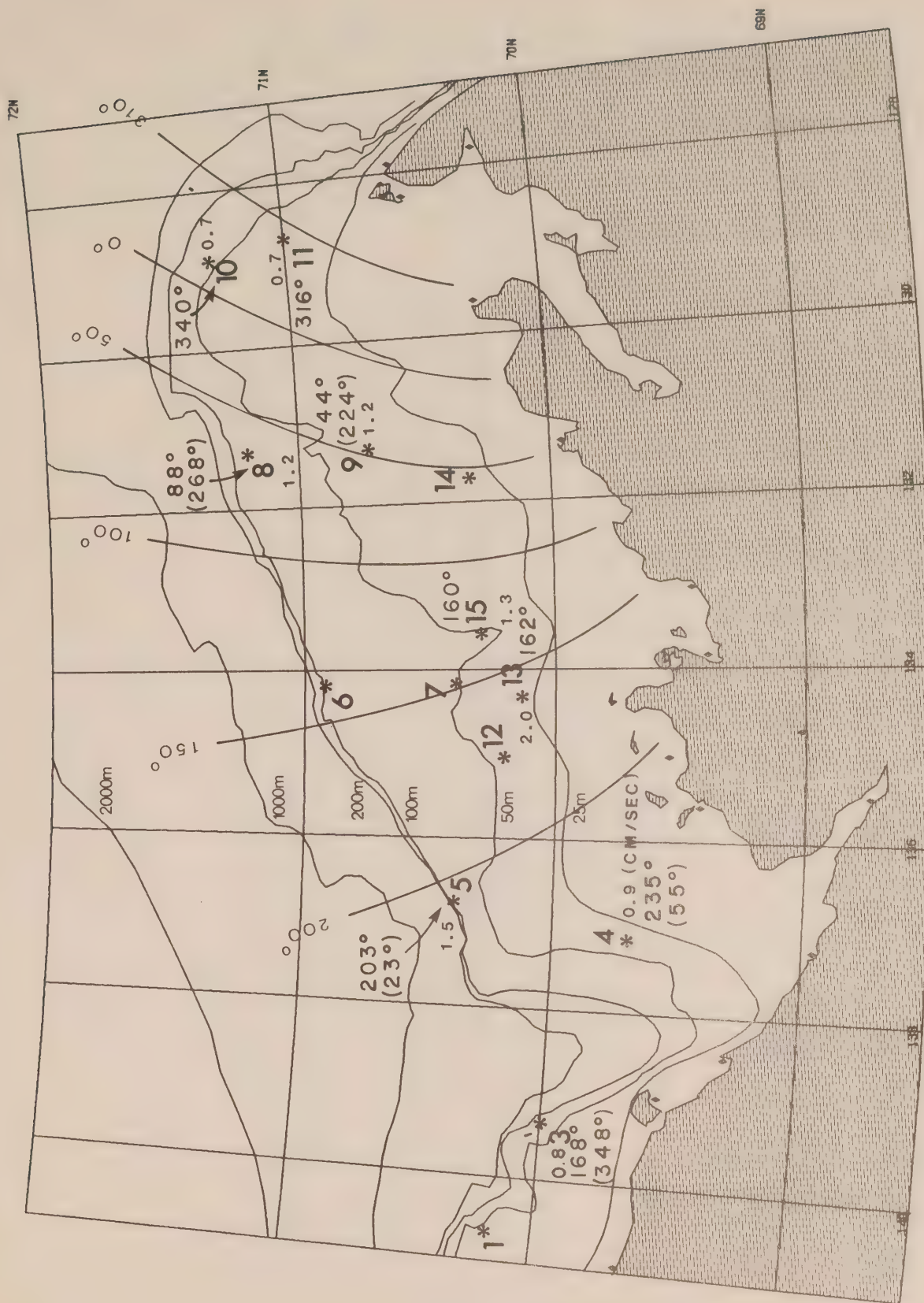
Fig. 5 K_1 SURFACE ELEVATION (from Huggett *et al.*, 1976)



K₁ COTIDAL CHART - WATER LEVELS (Z+6)

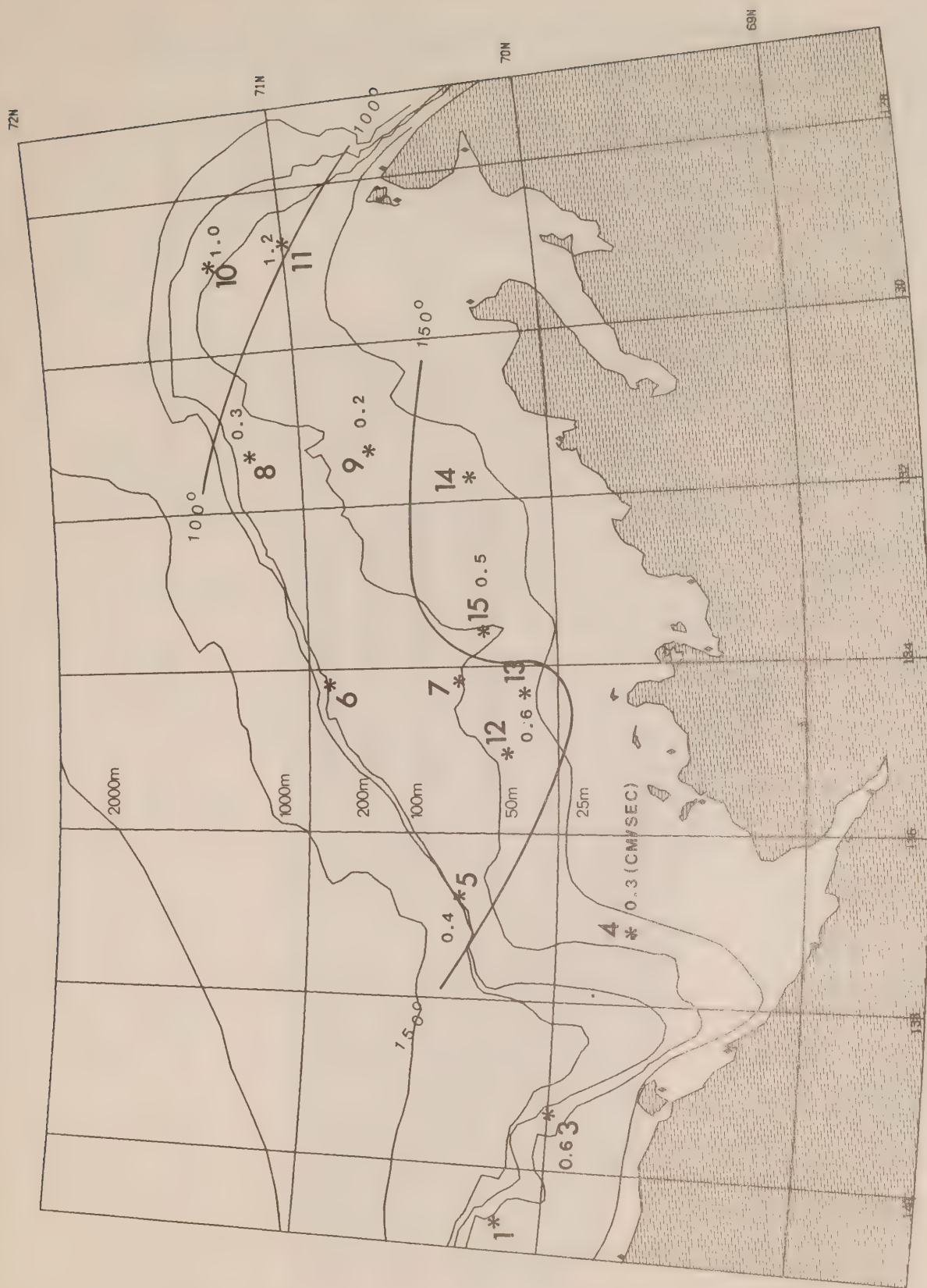
AMPLITUDES IN CM

Fig. 6 M_2 CURRENT (adapted from Huggett *et al.*, 1976)
235° - Phase relative to northern major semi-axis
(55°) - Phase relative to southern major semi-axis



M₂ COTIDAL CHART - TIDAL CURRENTS (Z+6)

Fig. 7 K_1 CURRENT (adapted from Huggett *et al.*, 1976)



K₁ COTIDAL CHART - TIDAL CURRENTS (Z+6)

Fig. 8 GRID FOR NUMERICAL MODEL

-- Radiating sea boundary
— Closed land boundary
.... 200m depth contour

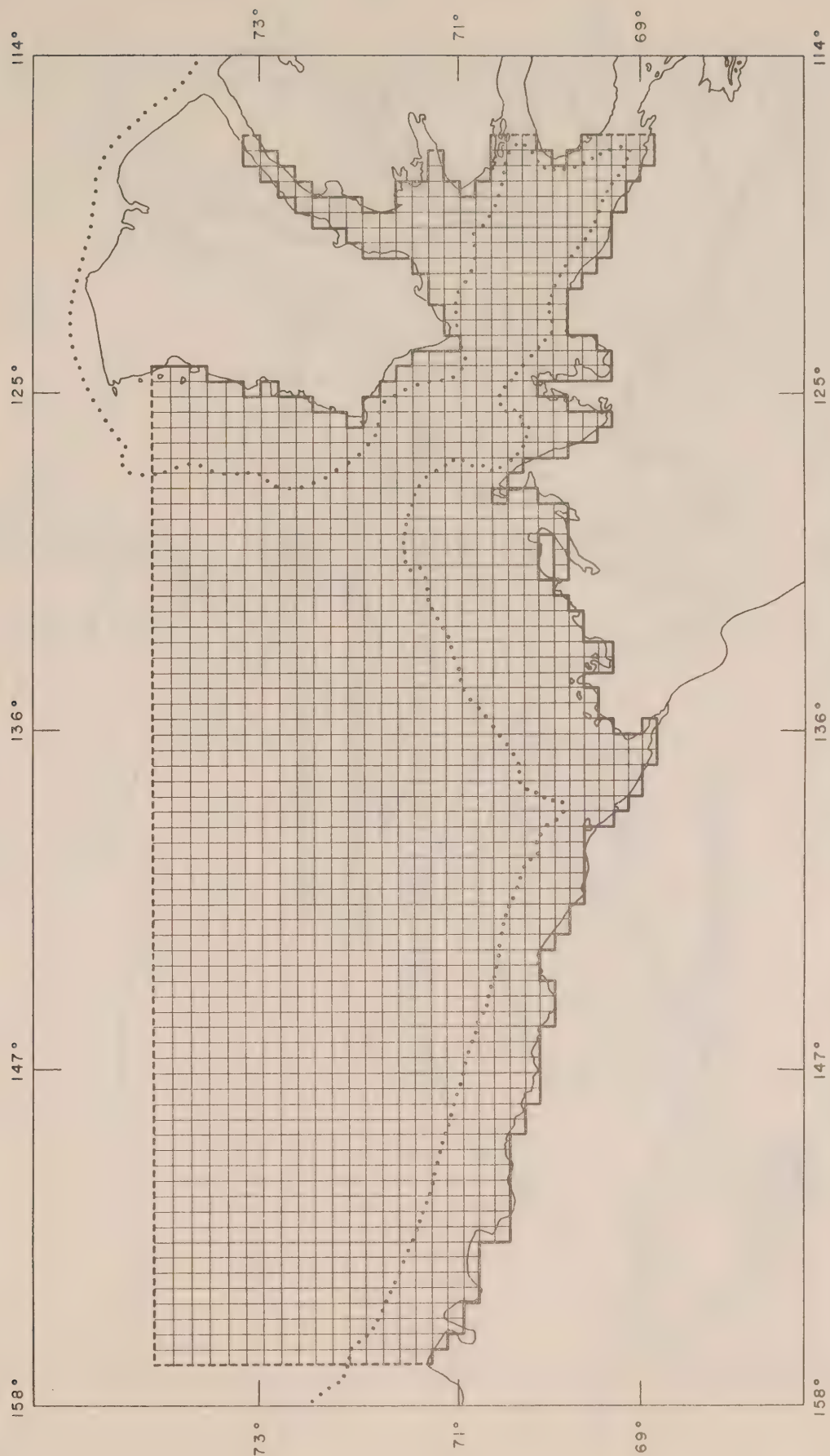


Fig. 9 AMPLITUDE OF M_2 SURFACE ELEVATION FROM MODEL 1

10	Simulated amplitude (cm)
8.6	Observed amplitude (cm)

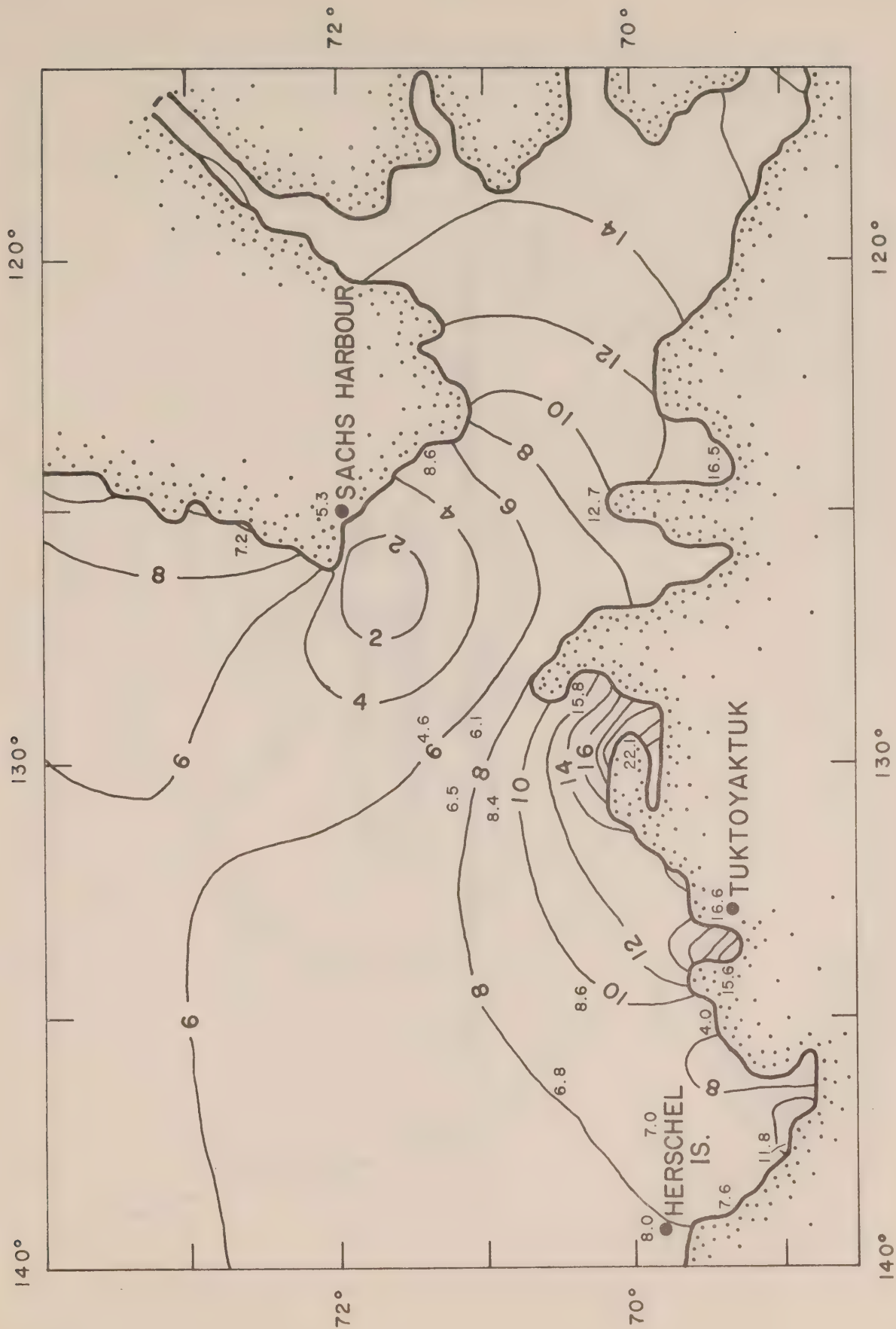


Fig. 10 GREENWICH PHASE (Z+0) OF M_2 SURFACE ELEVATION FROM MODEL 1

270	Simulated phase (deg)
262	Observed phase (deg)

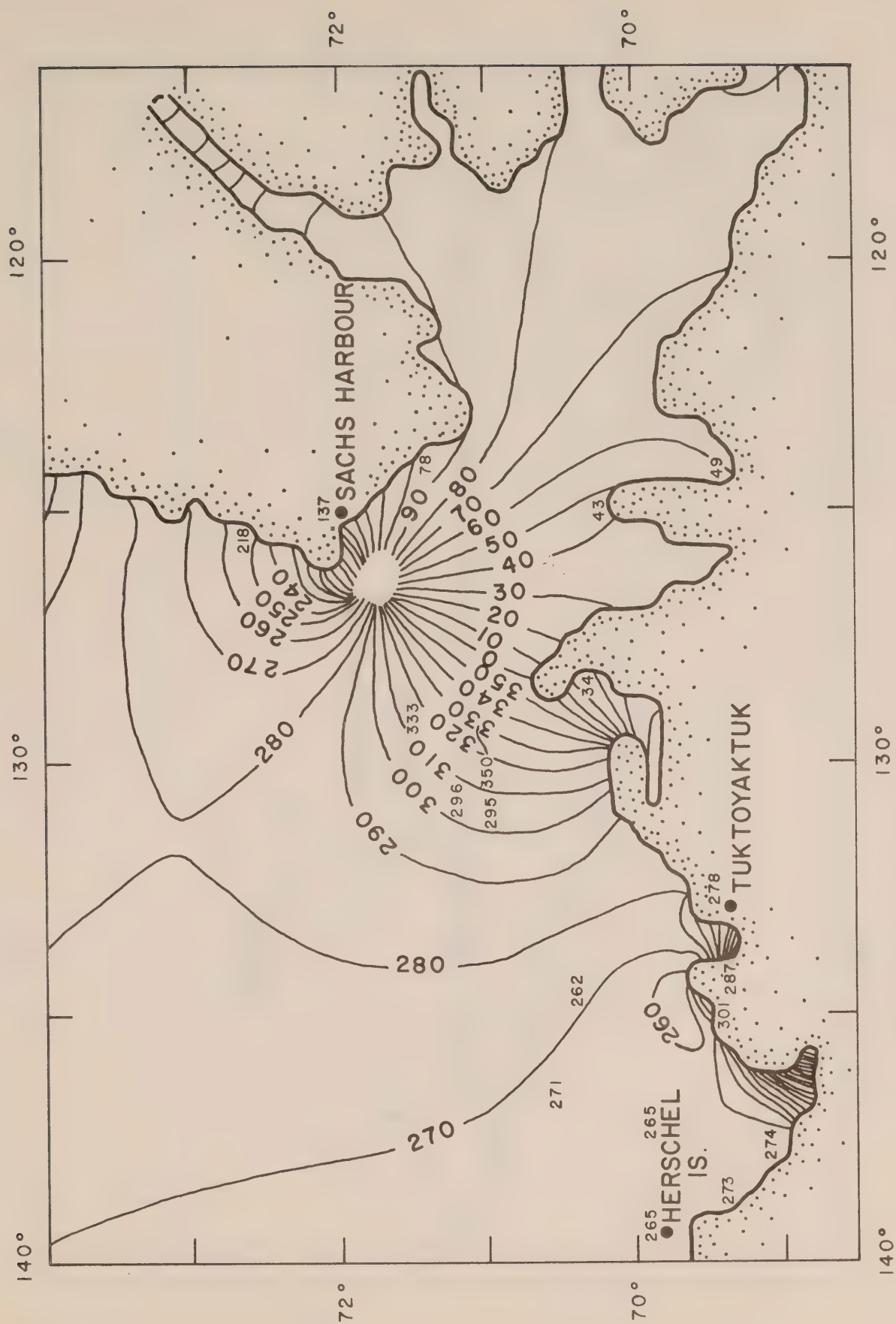


Fig. 11a AMPLITUDE OF M_2 SURFACE ELEVATION FROM MODEL 2 - U.S. SECTOR

6 Simulated amplitude (cm)

6.6 Observed amplitude (cm)

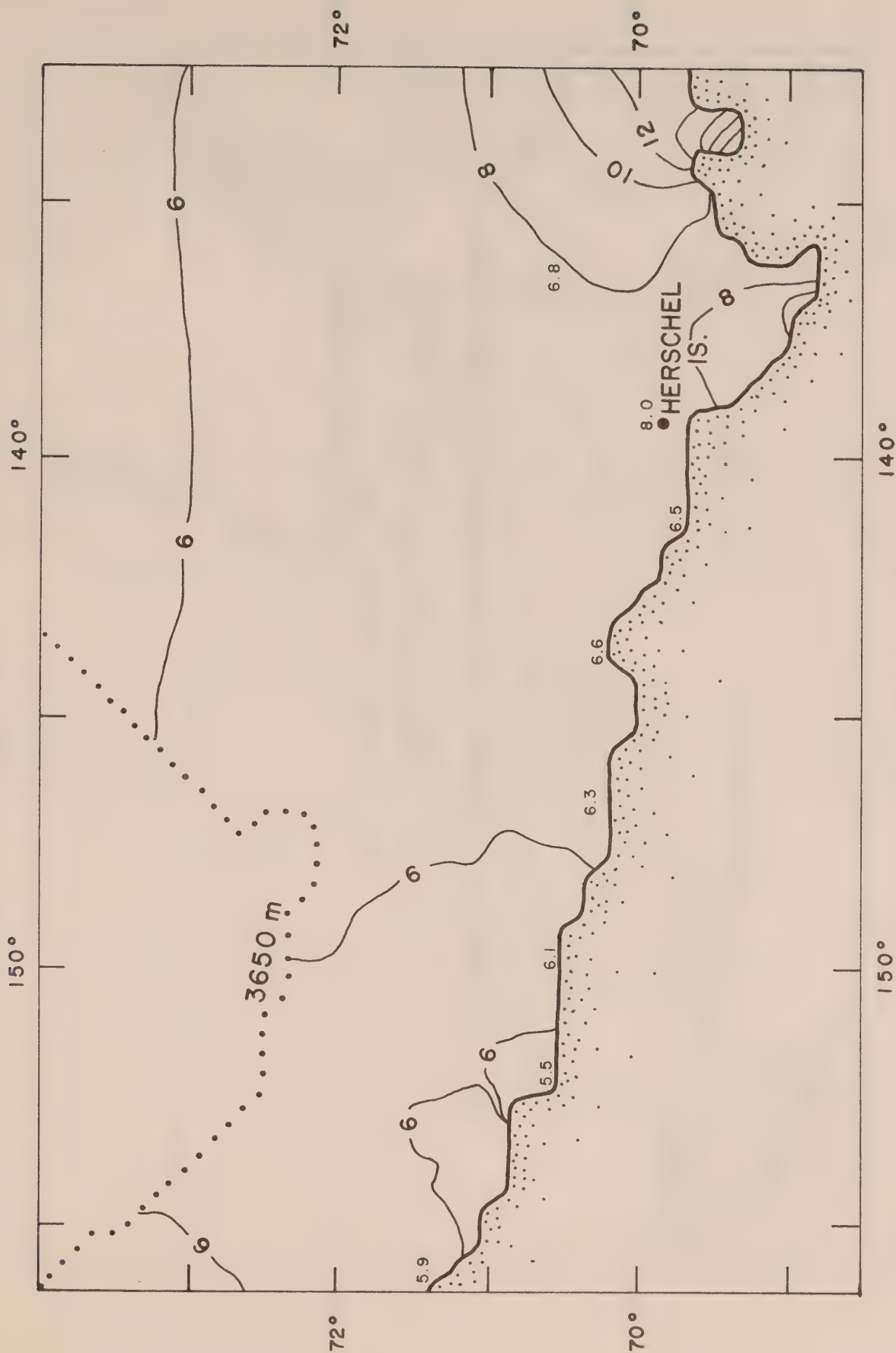


Fig. 11b AMPLITUDE OF M_2 SURFACE ELEVATION FROM MODEL 2 - CANADIAN SECTOR

10	Simulated amplitude (cm)
8.6	Observed amplitude (cm)

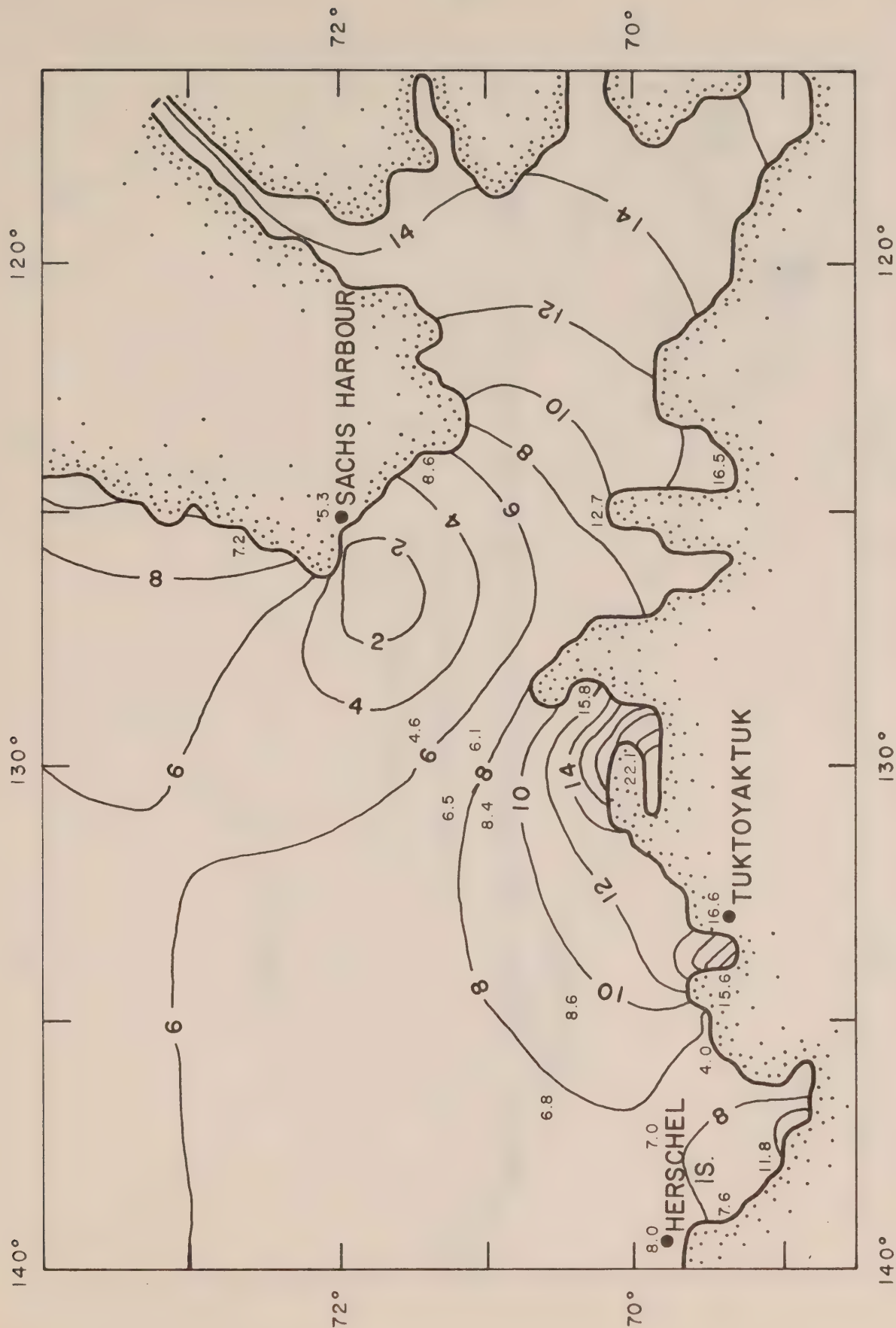


Fig. 12a GREENWICH PHASE (Z+0) OF M_2 SURFACE ELEVATION FROM MODEL 2 - U.S. SECTOR

270	Simulated phase (deg)
271	Observed phase (deg)

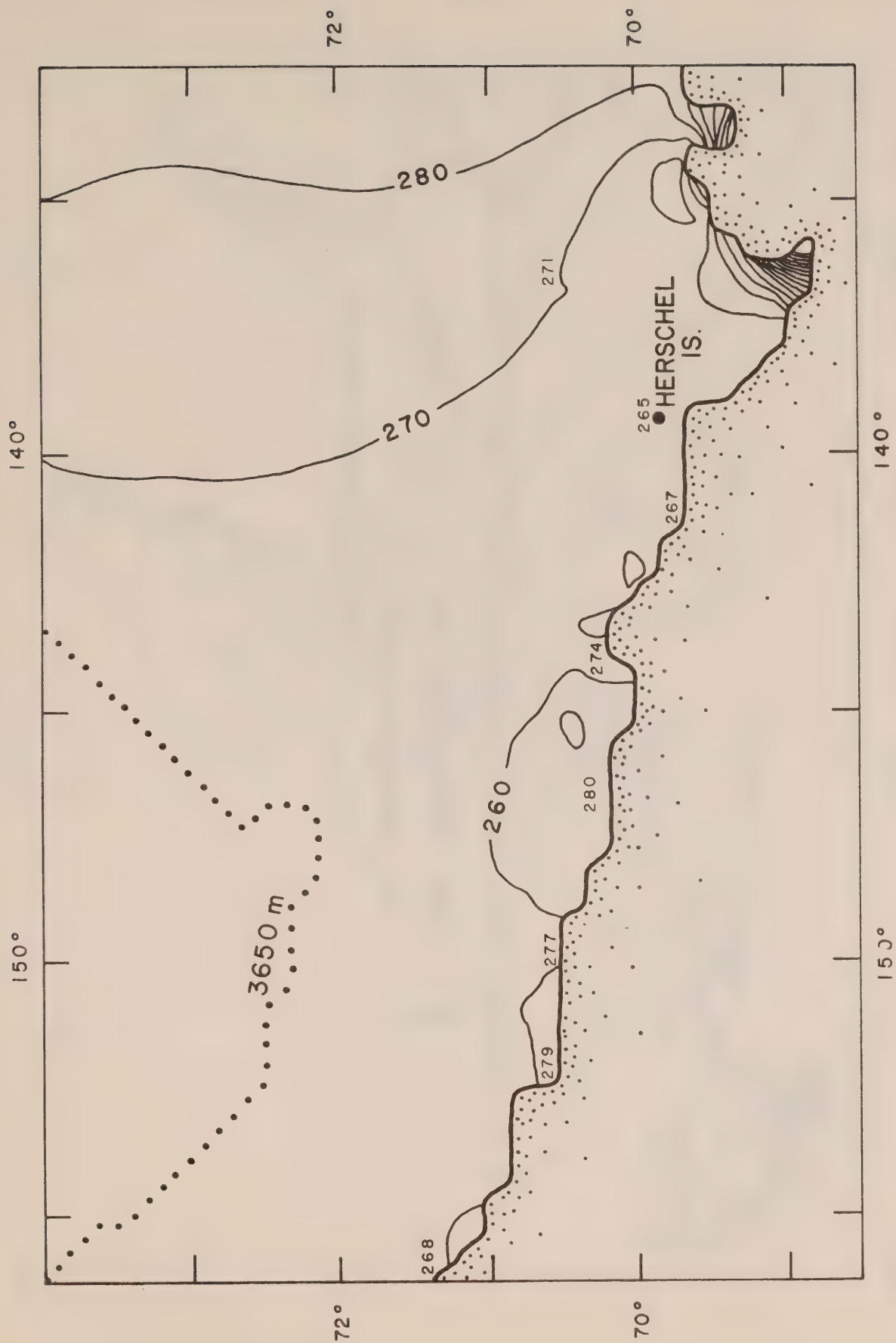


Fig. 12b GREENWICH PHASE (Z+0) OF M_2 SURFACE ELEVATION FROM MODEL 2 - CANADIAN SECTOR

270	Simulated phase (deg)
271	Observed phase (deg)

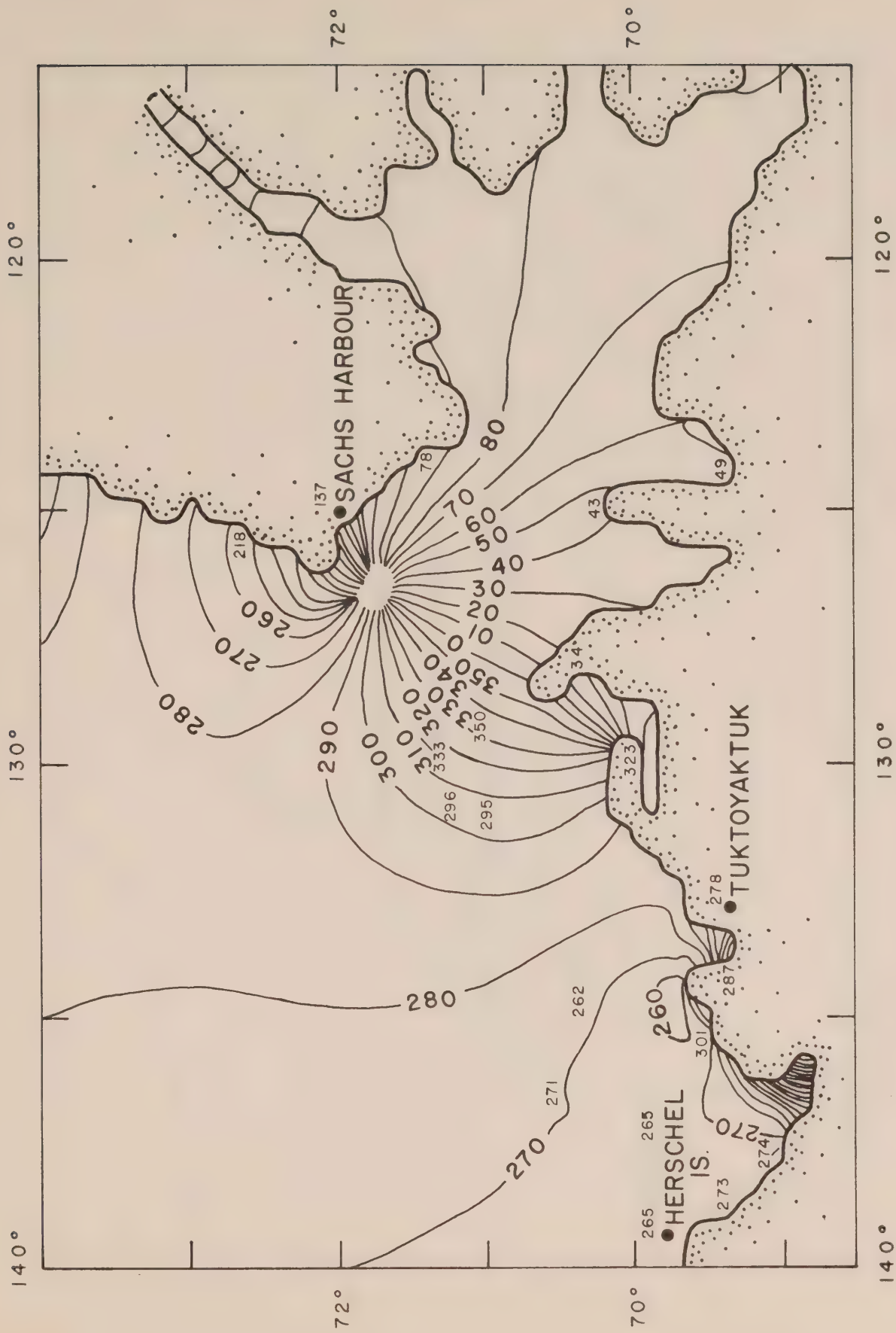


Fig. 13 AMPLITUDE OF S_2 SURFACE ELEVATION FROM MODEL 2

4 Simulated amplitude (cm)

2.7 Observed amplitude (cm)

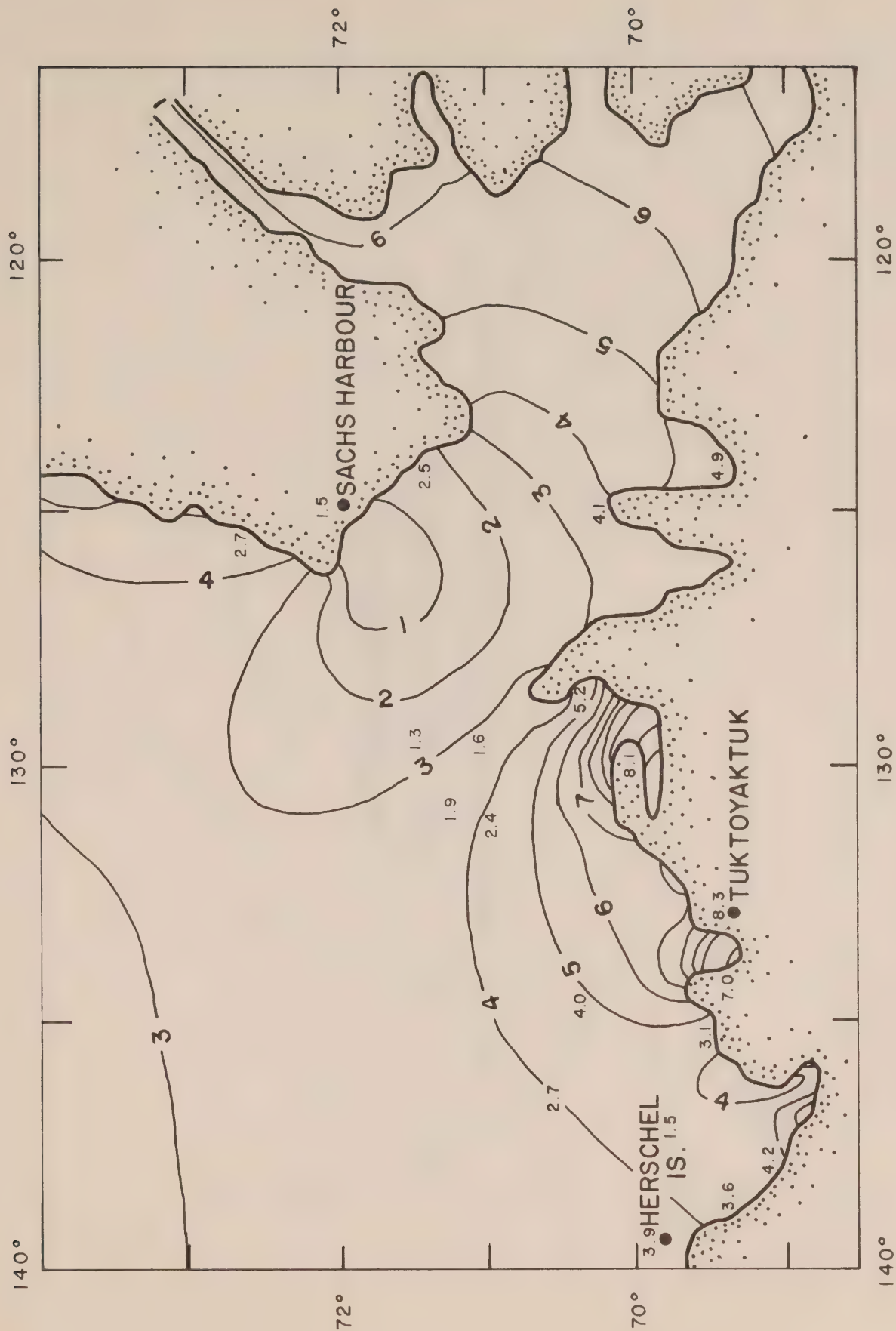


Fig. 14 GREENWICH PHASE (Z+0) OF S_2 SURFACE ELEVATION IN MODEL 2

330	Simulated phase (deg)
316	Observed phase (deg)

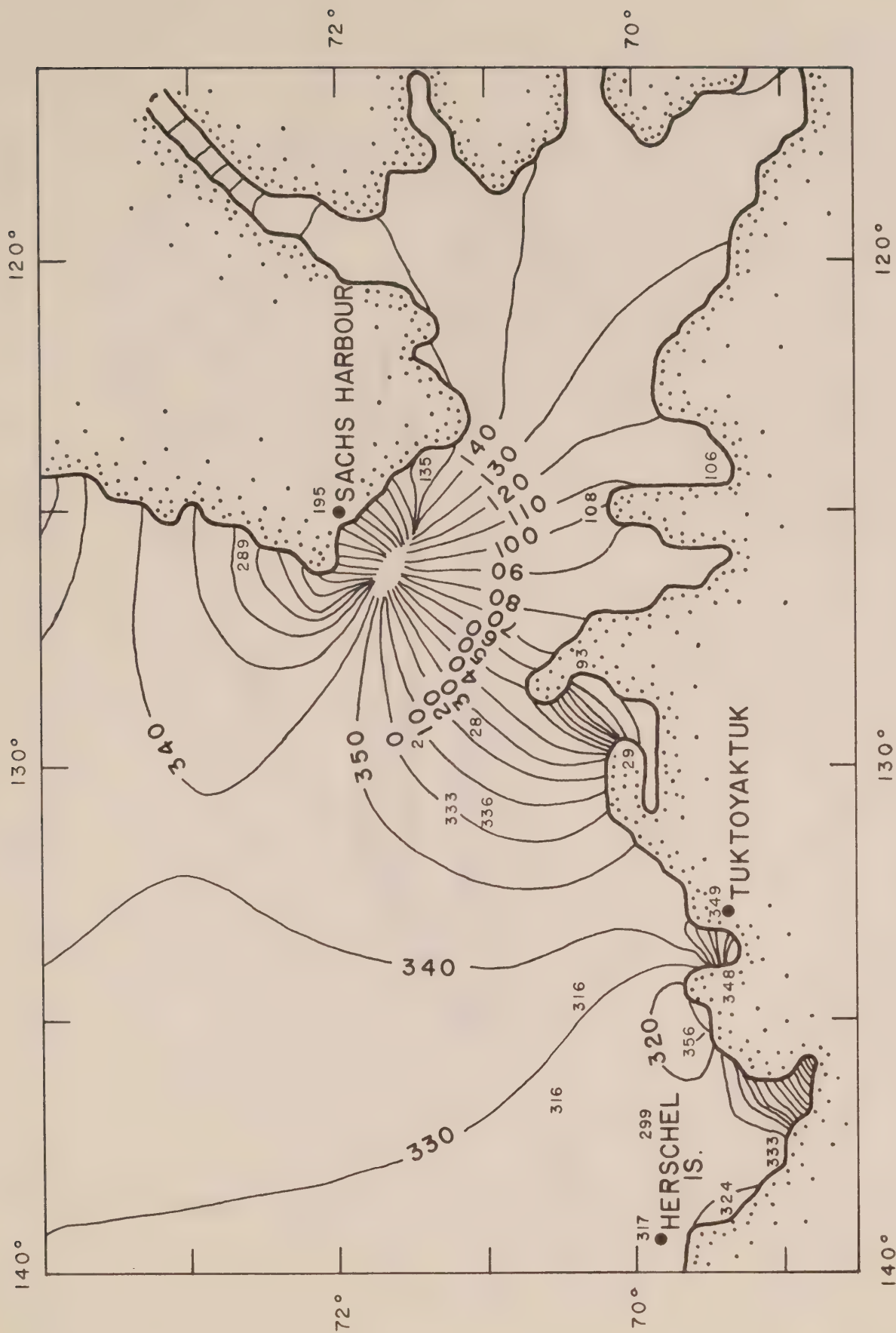


Fig. 15 OBSERVED AND SIMULATED M_2 CURRENTS AT CURRENT METER SITES

Ellipses correspond to simulated currents in Model 2; crossed lines are major and minor axes of corresponding ellipses for observed currents.



Fig. 16 GREENWICH PHASE (Z+6) OF M_2 CURRENT MODEL 2

- - - Outline of area utilized in fig. 17

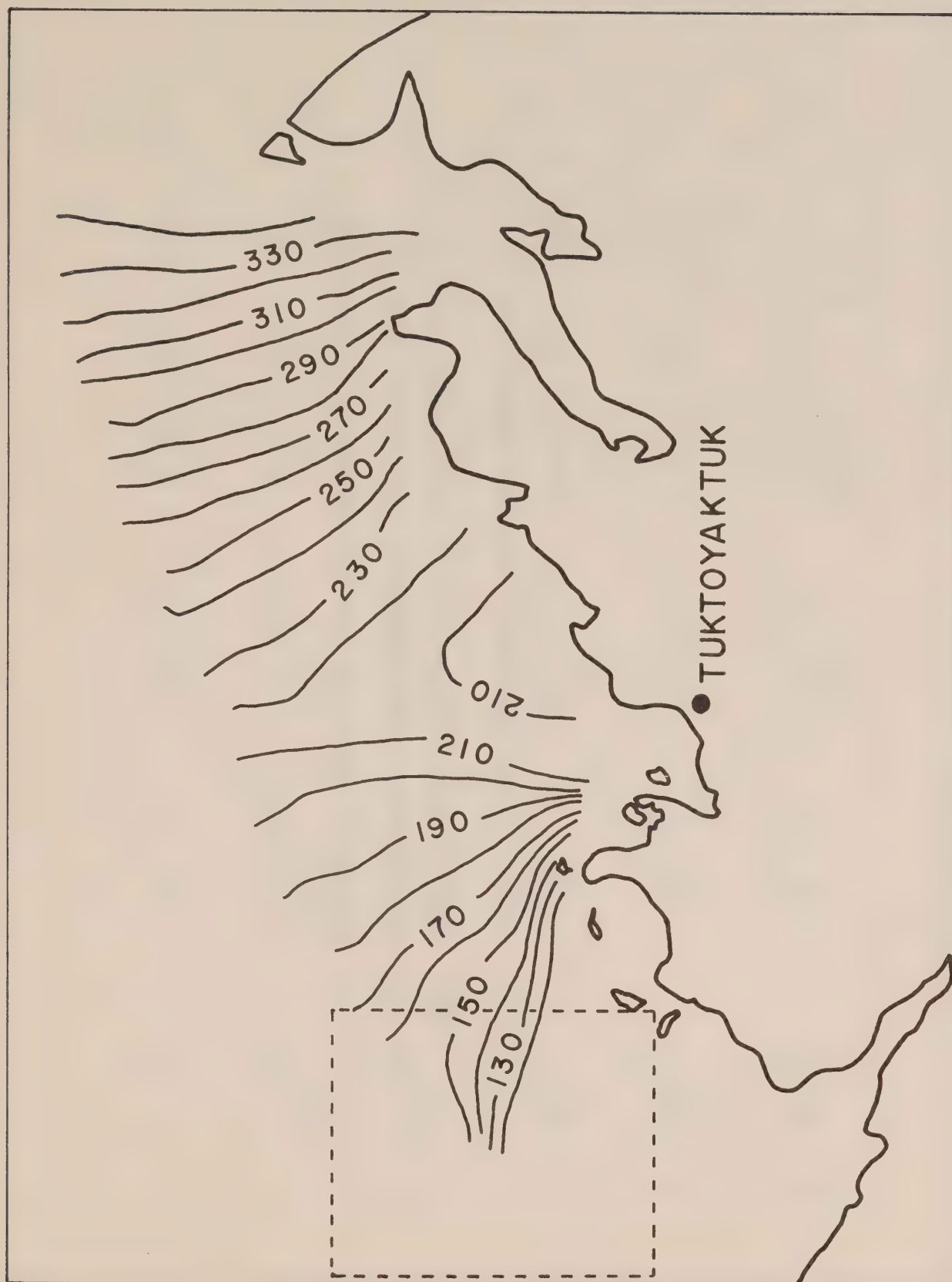


Fig. 17 CURRENT ELLIPSES FROM MODEL 2 FOR AREA OUTLINED IN FIG. 16

196° Greenwich phase (Z+0) referred to northern major semi-axis

16° Greenwich phase (Z+0) referred to southern major semi-axis

↙ Direction of current at instant of maximum surface elevation

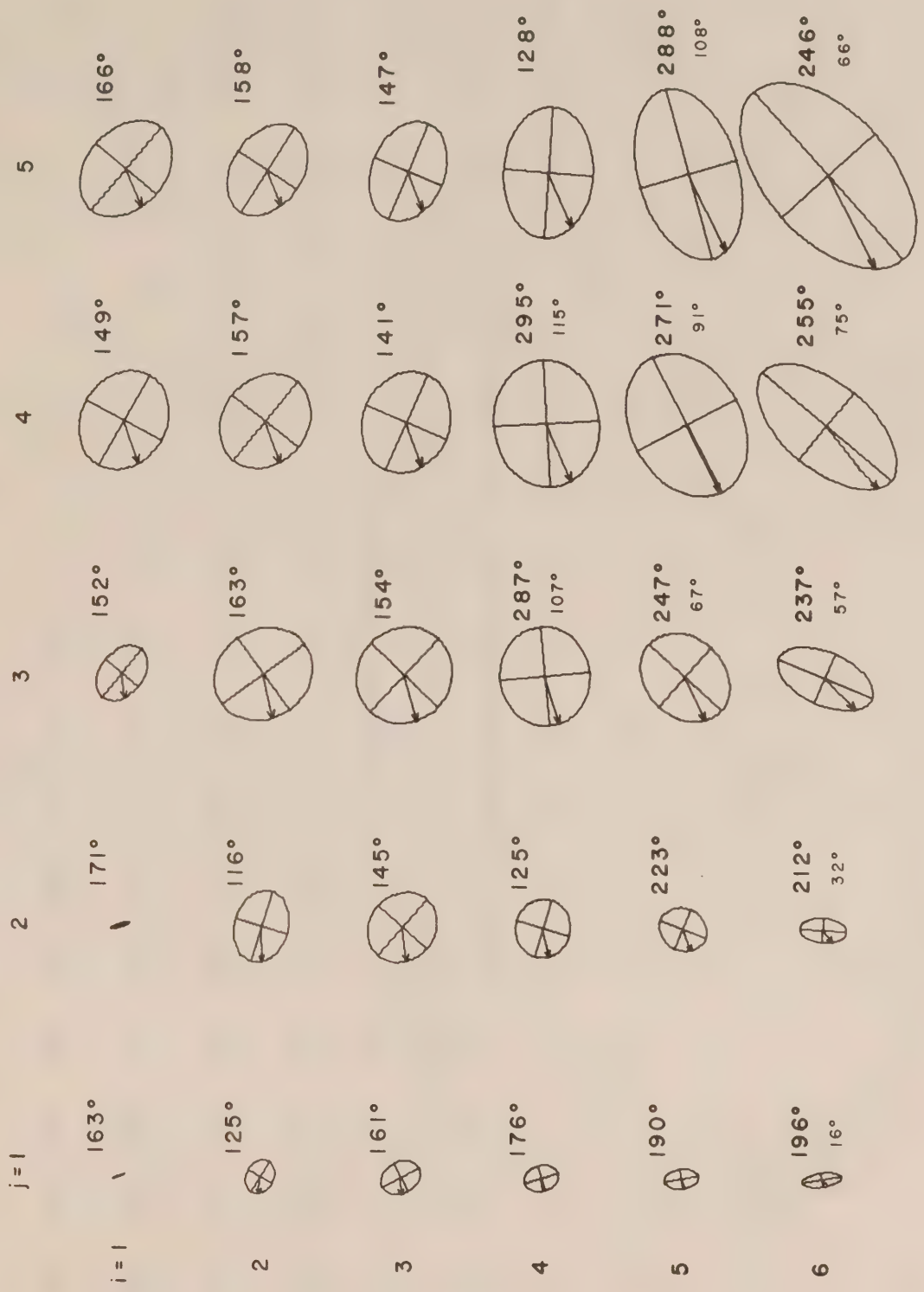
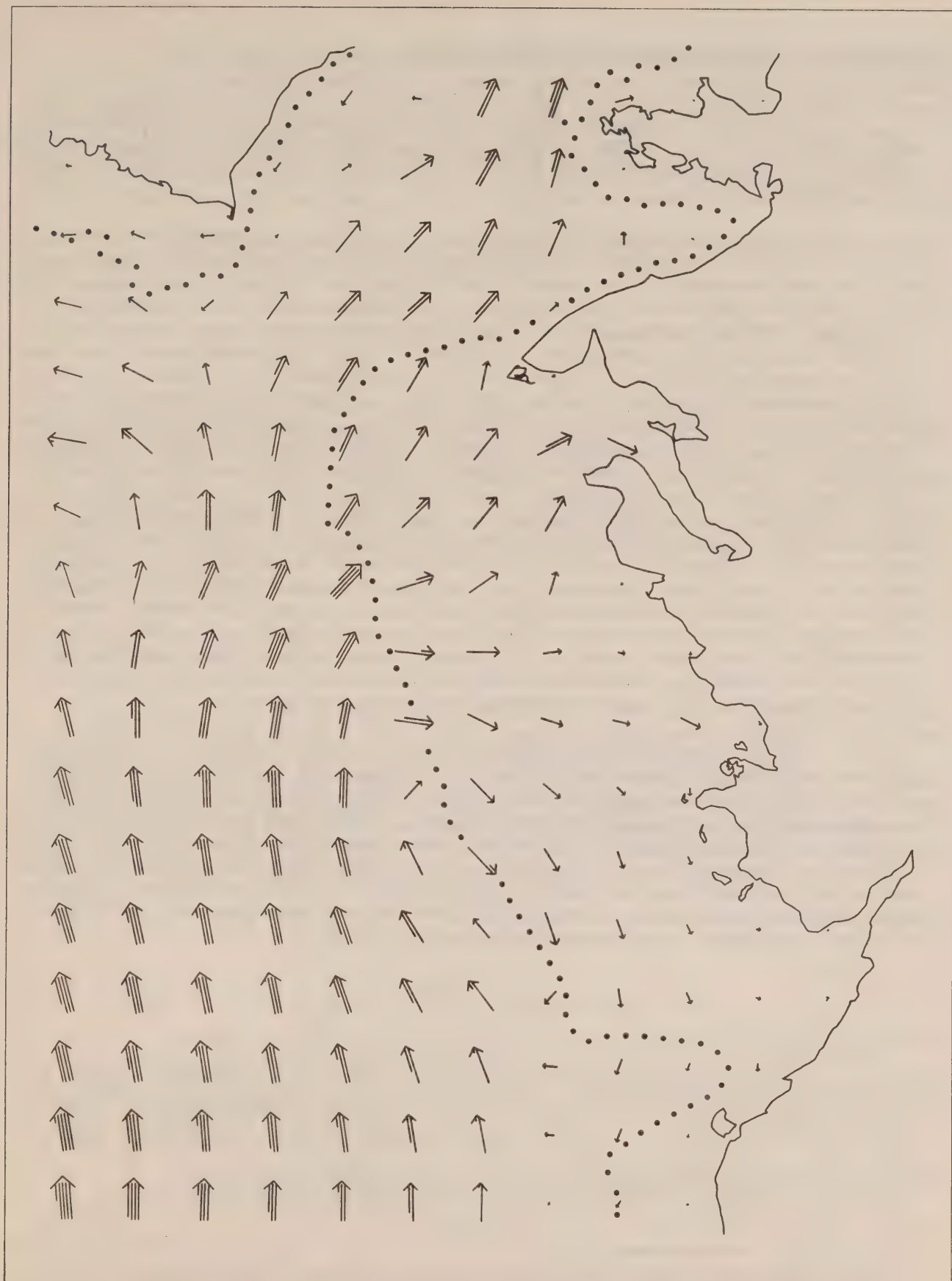


Fig. 18 MEAN ENERGY FLUX FOR M_2 TIDE FROM MODEL 2

Flux vector scale: each full shaft represents 500 kg.m.s^{-3}

. . . 200m depth contour



Appendix 1: Representation of Tidal Currents

A succinct description of the method of current analysis most widely used in Canada is to be found in Godin [1972, 1976]. The following account is based on brief unpublished notes by J. Taylor on Godin's method and the associated computer program.

In analysing tidal heights, it is sometimes convenient to associate with each tidal constituent a 'fictitious star' whose longitude is taken as equal to the argument of the constituent in question. Then a given constituent in the equilibrium tide at any place is at a maximum when the corresponding fictitious star is overhead. The phase angle between the local transit of the star and the actual occurrence of a maximum in the constituent under consideration is known as the local 'epoch' of the constituent. The transit of the fictitious star cannot be observed, of course, and must be calculated. Since the arguments of tidal potential constituent, i.e. the longitudes of the respective fictitious stars, used to be readily available only in tabulated form relative to Greenwich, it became customary to state the phase delay of each constituent as a 'Greenwich phase', a more artificial but, in some respects, more convenient concept than the epoch. The Greenwich phase (delay) of a tidal constituent is obtained by converting the record to G.M.T. and then analyzing it as though it pertains to the longitude of Greenwich.* The phase lag of each constituent, measured in constituent degrees (360° equalling one cycle of the constituent) is calculated relative to some time datum, normally the central point of the record. The longitude relative to Greenwich of the corresponding fictitious star at the central time is then found and the sum of this and the phase lag calculated from the record is the Greenwich phase of the constituent at the location where the record was taken.

In the case of tidal currents, the choice of reference vector from which to measure the phase lag of each constituent is less obvious. The current analysis method described by Godin [1972, 1976] employs concepts based on those familiar from tidal height analysis; phase lags are expressed relative to the time at which certain fictitious stars pass a given point on the current ellipse of the constituent in question. As a first step, the observed current vector is resolved from its initial representation as two rectangular components (normally northerly and easterly) into constituents consisting of pairs of counterclockwise - and clockwise-rotating vectors:

$$V_k(t) = V_k^+(t) + V_k^-(t) = A_k^+ e^{2\pi i \sigma_k t} + A_k^- e^{-2\pi i \sigma_k t} \quad (A1.1)$$

The amplitudes A_k^+ and A_k^- associated with the component vectors of the k^{th} constituent are in general complex; angles are measured counterclockwise from the W-E axis; the datum for time t is taken at the central point of the record. Whereas the angular speed of each constituent vector V_k varies as it traces out its ellipse, the component vectors V_k^+ and V_k^- rotate at constant constituent speed σ_k , making it possible to define steady phase angles.

*Some writers omit the conversion to GMT, yet retain the term 'Greenwich phase'. In that case the relevant time zone must be stated and conversion to the same time zone is necessary before phases from different locations can be compared.

The choice of W-E and S-N axis or any other rectangular coordinate system for the original current measurements is quite arbitrary, and if angles are measured with respect to such axes there is a corresponding arbitrariness in the phases of V_k^+ and V_k^- . One aim of Godin's analysis is to obtain invariant phases for V_k^+ and V_k^- by referring angular measurements to a major semi-axis of the constituent ellipse. Since the orientation of each ellipse is unknown prior to the analysis, the calculation of phase proceeds in two stages.

Dropping the constituent-numbering suffix k , the expression (A1.1) for any given constituent can be rewritten as

$$V(t) = V^+(t) + V^-(t) = a^+ e^{i\epsilon^+} e^{2\pi i \sigma^+ t} + a^- e^{i\epsilon^-} e^{-2\pi i \sigma^- t} \quad (A1.2)$$

where a^+ , a^- , ϵ^+ and ϵ^- are real and a^+ , $a^- \geq 0$. The meaning of these constants is clear from Figures A1.1(i) and A1.1(ii). (Note that if $a^+ > a^-$, the current vector V rotates counterclockwise, otherwise it rotates clockwise.) a^+ , a^- , ϵ^+ and ϵ^- are all computed directly in the first stage of the analysis of the W-E, S-N current components. The counterclockwise - and clockwise-rotating vectors V^+ and V^- coincide on the major axis of the ellipse; consequently, if θ is the inclination of the ellipse to the W-E axis, then $\epsilon^+ - \theta = \theta - \epsilon^-$ and

$$\theta = \frac{\epsilon^+ + \epsilon^-}{2} \quad (A1.3)$$

In order to define phases relative to the tidal potential, fictitious stars, S^+ and S^- (Fig. A1.1(iii)), may be considered rotating at the same speed and in the same direction as the respective vectors V^+ and V^- . The angular location L of each star is calculated at the central time ($t = 0$) and since tidal constituent arguments relative to Greenwich are available, it is convenient to take L relative to Greenwich.* In consequence, the constant phase angles g^+ and g^- by which S^+ and S^- lead (or lag) the respective vectors V^+ and V^- may be termed 'Greenwich phases' and can readily be evaluated as follows:

$$\begin{aligned} g^+ &= L - \epsilon^+ \\ g^- &= L + \epsilon^- \end{aligned} \quad (A1.4)$$

Insofar as any physical picture can be attached to the fictitious stars in this case, they can be visualized as circling the periphery of a 'celestial disk' tangential to the earth at the measurement site, each 'generating' a respective current vector V^+ or V^- which follows it round in the same plane, lagging by g^+ or g^- respectively.

To obtain a representation of the current independent of the initial choice of rectangular coordinates, Godin employs the construction in Figure A1.1(iv), in which the major semi-axis OA of the constituent ellipse is used as the reference axis; in particular, the fictitious stars, Σ^+ and Σ^- , are now visualized as being at angular distance L from OA. An advantage of this

*The angle L is generally designated " $V + u$ " in the tidal literature.

approach is that the phase of both rotating vectors relative to their respective stars can now be expressed by a single (Greenwich) phase angle g . As can be seen from Figure A1.1(iv),

$$2g + \varepsilon^+ - \varepsilon^- = 2L \quad (\text{A1.5})$$

and since L has the same magnitude in Figures A1.1(iii) and A1.1(iv), it follows from (A1.4) and (A1.5) that g is expressible in terms of known quantities g^+ and g^- as

$$g = \frac{g^+ + g^-}{2} \quad (\text{A1.6})$$

g , which is normally measured in constituent degrees (as are g^+ and g^-), is the interval by which the instant of maximum current (when V^+ and V^- coincide along OA) lags the simultaneous transits of the fictitious stars at OA.

Unfortunately, the factor 2 in the denominators of (A1.3) and (A1.6) can introduce an ambiguity of 180° into the values computed for θ and g , since any of the angles ε^+ , ε^- , g^+ or g^- can be altered by 360° without changing the representation of the original current. In the computer program in use at present, ambiguity is avoided by imposing the condition

$$0 \leq g^- - g^+ < 360^\circ \quad (\text{A1.7})$$

prior to computation of g with (A1.6). The fact that this eliminates ambiguities in θ and g and also implies that the *northern* major semi-axis of the constituent is always to be used as reference axis is clear only if the problem of reference semi-axis is considered from the outset.

Figure A1.2 shows the two basically different configurations which can occur. Assuming that, initially, $0 \leq \varepsilon^+, \varepsilon^- < 360^\circ$, it can be seen that the angular position, θ , of the northern major semi-axis is given by

$$\theta = \frac{\varepsilon^+ + \varepsilon^-}{2} \text{ if } \varepsilon^+ + \varepsilon^- < 360^\circ \quad (\text{Fig. A1.2(i)})$$

$$\text{or} \quad \theta = \frac{\varepsilon^+ + \varepsilon^-}{2} - 180^\circ \text{ if } \varepsilon^+ + \varepsilon^- \geq 360^\circ \quad (\text{Fig. A1.2(ii)})$$

Both cases can be condensed into the single formula

$$\theta = \frac{\varepsilon^+ + \varepsilon^-}{2} \bmod(180^\circ) \quad (\text{A1.8}) *$$

* The notation $\phi \bmod(N^\circ)$ indicates that a suitable integer multiple of N is added to or subtracted from ϕ to bring it into the range $0 \leq \phi < N^\circ$.

Figures A1.3 and A1.4 show separately the angular relationships for the two rotating vectors V^+ and V^- in cases (i) and (ii) respectively of Figure A1.2. Allowing for the fact that larger values of L may occur than are shown in these figures, all possible cases can be summarized in the formulas

$$\begin{aligned} g &= g^+ + \theta \pmod{360^\circ} \\ g &= g^- - \theta \pmod{360^\circ} \end{aligned} \quad (\text{A1.9})$$

For the same reason, (A1.4) should in general be written

$$\begin{aligned} g^+ &= L - \varepsilon^+ \pmod{360^\circ} \\ g^- &= L + \varepsilon^+ \pmod{360^\circ} \end{aligned} \quad (\text{A1.4})'$$

Of course, if g^+ and g^- are not required, (A1.4)' and (A1.9) can be combined to give

$$\begin{aligned} g &= L - \varepsilon^+ + \theta \pmod{360^\circ} \\ g &= L + \varepsilon^- - \theta \pmod{360^\circ} \end{aligned} \quad (\text{A1.10})$$

Using θ as defined in (A1.8), the possibility of ambiguity in g does not arise.

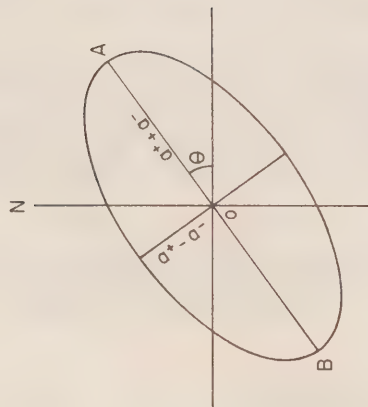
From (A1.9) it follows that $2\theta = g^- - g^+ \pmod{360}$, which, in view of (A1.8), shows that condition (A1.7) used in the computer program implies choice of the northern major semi-axis as reference axis. Condition (A1.7) also ensures that (A1.6), when interpreted in the sense $g = \frac{1}{2}(g^+ + g^-) \pmod{360^\circ}$, gives unambiguous values for g identical to those from (A1.10).

The appearance of θ in (A1.10) indicates that if the southern major semi-axis OB should be chosen as reference axis for some reason, the consequent change of 180° in θ produces a similar change in g . As Godin notes [1976 p. 5], this is only a change in *representation* of the constituent ellipse; the ellipse itself is not affected.

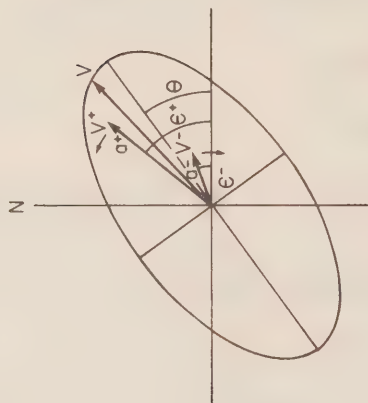
From Figures A1.3 and A1.4, it can readily be deduced that maximum current (in the sense that V^+ and V^- coincide on OA) occurs at times

$$t = \frac{g-L + n.360^\circ}{\sigma}, \quad n = \dots, -1, 0, 1, \dots \quad (\text{A1.11})$$

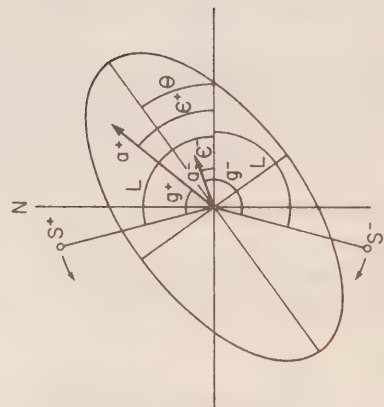
relative to the central time of the record.



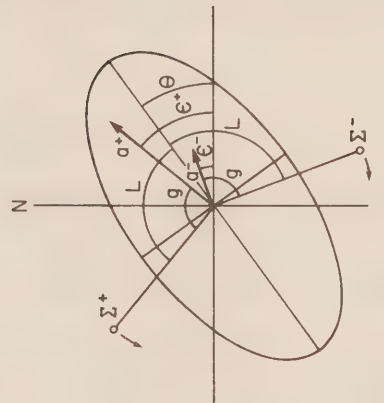
(i) Dimensions of a Constituent Ellipse



(ii) Configuration at $t=0$

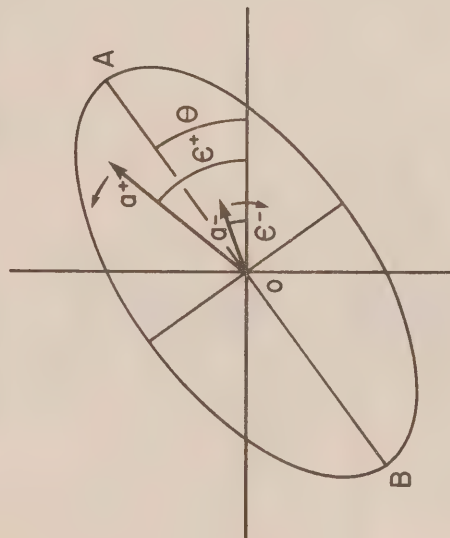


(iii) Fictitious stars related to E-W axis

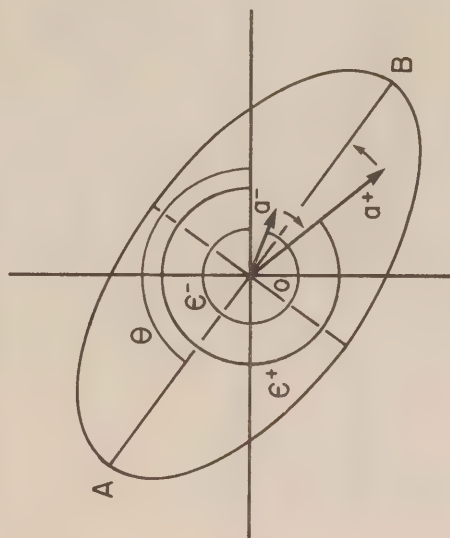


(iv) Fictitious stars related to major semi-axis

FIGURE A11 DELINEATION OF CURRENT ELLIPSE NOTATION

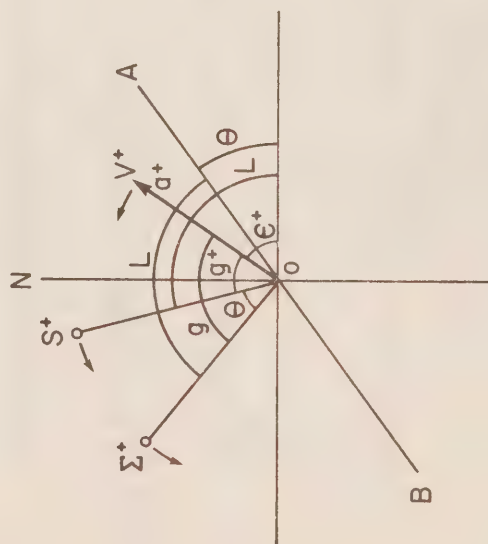


$$(i) \quad \epsilon^+ + \epsilon^- < 360^\circ, \quad \theta = \frac{\epsilon^+ + \epsilon^-}{2}$$

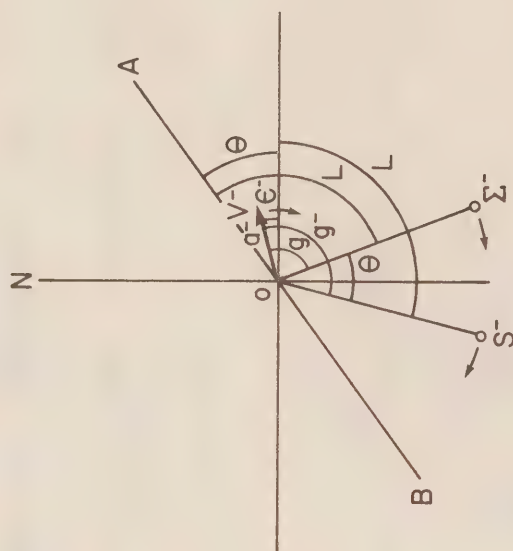


$$(ii) \quad \epsilon^+ + \epsilon^- \geq 360^\circ, \quad \theta = \frac{\epsilon^+ + \epsilon^-}{2} - 180^\circ$$

FIGURE A1.2 DEFINITION OF SEMI-AXIS USED AS REFERENCE AXIS

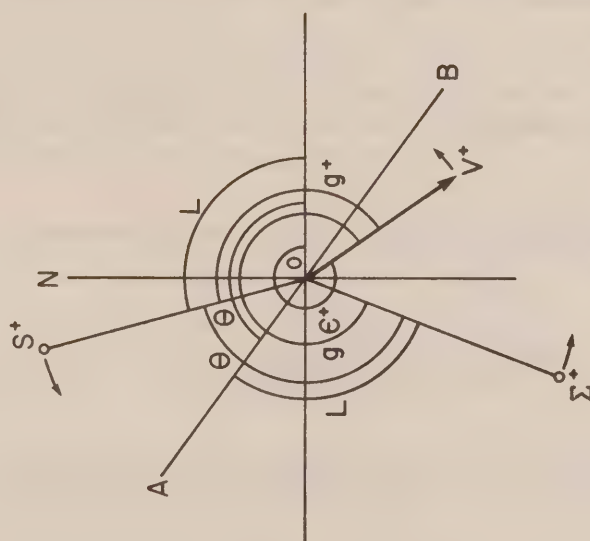


$$g = g^+ + \theta$$

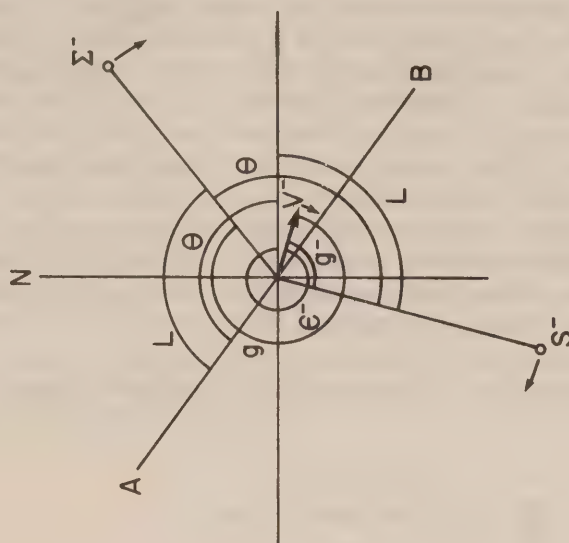


$$g = g^- - \theta$$

FIGURE A I.3 ANGULAR RELATIONSHIPS WHEN $\epsilon^+ \cdot \epsilon^- < 360^\circ$



$$g = g^+ + \theta$$



$$g = g^- + (360^\circ - \theta)$$

FIGURE A I.4 ANGULAR RELATIONSHIPS WHEN $\epsilon^+ + \epsilon^- \approx 360^\circ$

Appendix 2: Energy Flux

In essentially one-dimensional systems such as rivers or narrow inlets, a tidal constituent may occur as a standing wave in which the surface elevation and current phase differ by 90° , as a travelling wave in which height and current have equal or opposite phase, or as a mixture of these two types. A standing wave normally occurs when an incident travelling wave is reflected, e.g. by a coast. The energy-transmitting capabilities of standing and travelling waves are radically different; the mean energy flux (energy flow averaged over the cycle) is zero for a standing wave, whereas a travelling wave transports energy. In this appendix, the applicability of the concepts of standing and travelling waves and mean energy flux are discussed in the context of vertically-integrated models.

Phillips (1966) shows that the instantaneous energy flux per unit volume is

$$\underline{\mathcal{F}} = \underline{u}(P + \frac{1}{2}\rho u^2 + \rho g\zeta)$$

where \underline{u} is velocity, u its magnitude, p is pressure and ζ is height, which in the present case will be measured upwards from mean water level. Implicit in the derivation of the governing equations [Henry and Heaps, 1976] is the assumption of hydrostatic pressure, i.e. $p = \rho g(\eta - \zeta)$, where η is surface elevation. Consequently the sum of the pressure and potential energy density contributions to $\underline{\mathcal{F}}$, i.e. $\rho g(\eta - \zeta) + \rho g\zeta = \rho g\eta$, is uniform throughout the water column. Since it can be assumed that velocity is uniform with depth and that the vertical component of velocity is negligible, the vertically integrated energy flux is

$$\underline{F} = (h+\eta)\underline{\mathcal{F}} = (h+\eta)\left\{\rho\left[\frac{1}{2}(u^2+v^2)+g\eta\right]u, \rho\left[\frac{1}{2}(u^2+v^2)+g\eta\right]v\right\}$$

Except in very shallow water it is usually adequate to use the first-order approximation

$$\underline{F} = F_{x,y} = \left\{\rho gh\eta u, \rho gh\eta v\right\}$$

The mean energy flux is the average of F over one cycle and will be written

$$\overline{F}_{x,y} = \left\{\rho gh\overline{\eta u}, \rho gh\overline{\eta v}\right\} \quad (A2.1)$$

Quite clearly if some other pair of rectangular coordinates x', y' are chosen in the horizontal plane and the current is resolved into components p and q in the x', y' directions respectively, then the mean energy flux has components

$$F_{x', y'} = \left\{ \rho g h \overline{\eta p}, \rho g h \overline{\eta q} \right\} \quad (A2.2)$$

in the new coordinate system.

When evaluating the mean energy flux associated with a single tidal constituent, it is most convenient to consider axes x', y' aligned respectively with the reference major semi-axis OA of the current ellipse and the axis 90° counterclockwise from OA. Then since at any time the angle through which V^+ and V^- have rotated since last passing the reference axis is $L - g \bmod (360^\circ)$ (in the notation of Appendix 1), the surface elevation and current components can be written as

$$\begin{aligned} \eta &= \eta_0 \cos(L - g_\eta) \\ p &= (a^+ + a^-) \cos(L - g) \\ q &= (a^+ - a^-) \sin(L - g) \end{aligned} \quad (A2.3)$$

where η_0 is the amplitude and g_η the Greenwich phase of the surface elevation. Substituting (A2.3) into (A2.4) gives mean energy flux

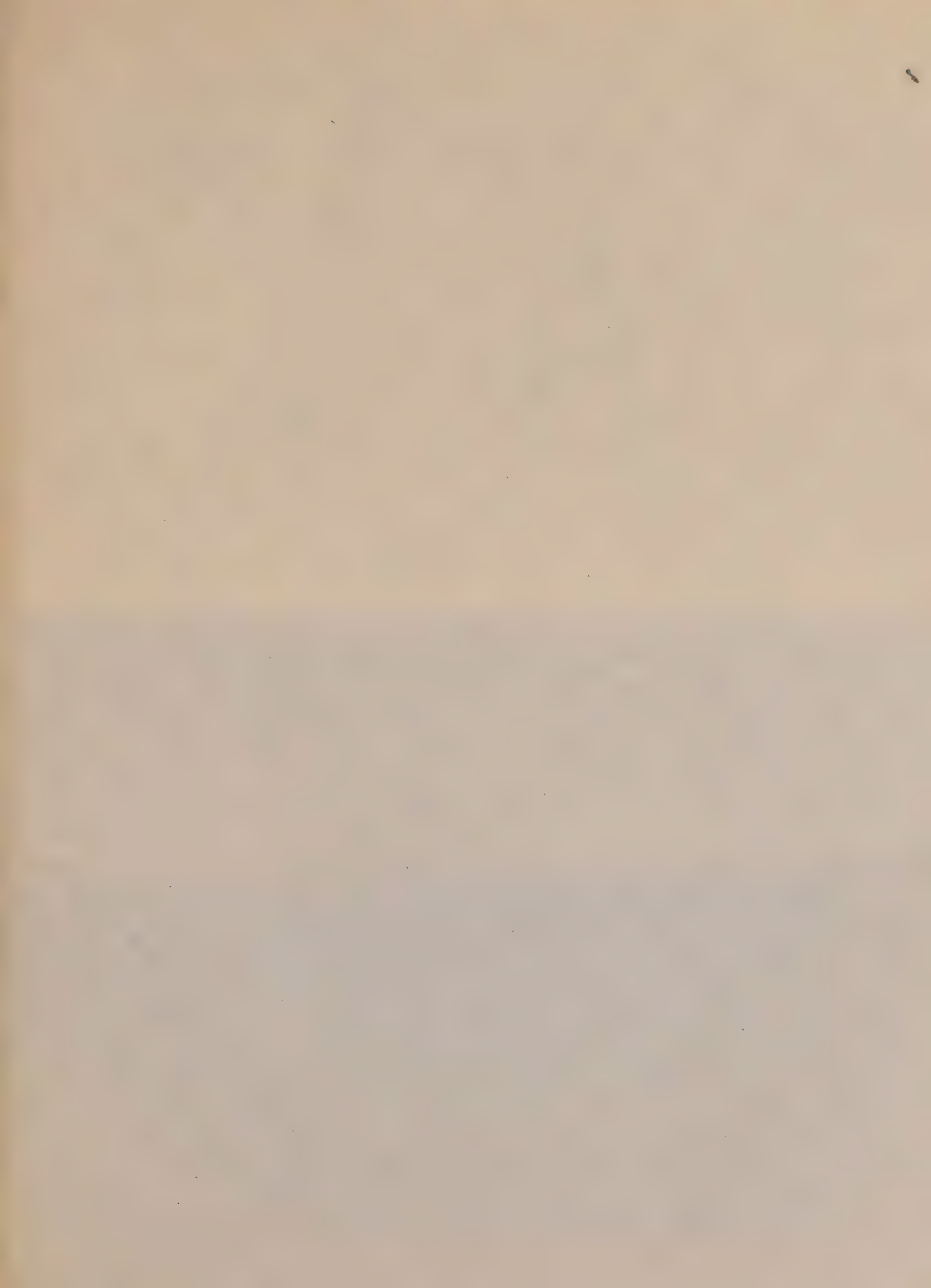
$$\overline{F}_{x', y'} = \left\{ \frac{\rho g h \eta_0}{2} (a^+ + a^-) \cos(g_\eta - g), \frac{\rho g h \eta_0}{2} (a^+ - a^-) \sin(g_\eta - g) \right\} \quad (A2.4)$$

It is worth noting that the direction of the mean energy flux vector is coincident with the direction of the current vector V at the instant of maximum surface elevation. This follows from the fact that η is a maximum when $L = g_\eta$, hence, at maximum elevation,

$$\begin{aligned} p &= (a^+ + a^-) \cos(g_\eta - g) \\ q &= (a^+ - a^-) \sin(g_\eta - g) \end{aligned} \quad (A2.5)$$

from (A2.3). On comparison of (A2.5) with (A2.4), it can be seen that the resultant current V is then aligned with \underline{F} .

From equations (A2.4) it is clear that standing wave behaviour, in the sense of there being zero mean energy flux, is uncommon in 2-dimensional tidal systems and occurs only if the flow is locally one-dimensional (i.e. $a^+ = a^-$ and the current ellipse degenerates to a straight line) and elevation and current are 90° out of phase ($g_\eta = g \pm 90^\circ$).



CA1
EP 321
-77R12



STATIC ANALYSIS OF SINGLE-POINT MOORINGS

by
W.H. Bell

INSTITUTE OF OCEAN SCIENCES, PATRICIA BAY
Victoria, B.C.



For additional copies or further information please write to:

Department of Fisheries and the Environment
Institute of Ocean Sciences, Patricia Bay
512 - 1230 Government Street
Victoria, B.C.
V8W 1Y4

STATIC ANALYSIS OF SINGLE-POINT MOORINGS

by

W.H. Bell

Institute of Ocean Sciences, Patricia Bay
Victoria, B.C.
August 1977

This is a manuscript which has received only limited circulation. On citing this report in a bibliography, the title should be followed by the words "UNPUBLISHED MANUSCRIPT" which is in accordance with accepted bibliographic custom.

ABSTRACT

A static mooring model is developed for use in the design and analysis of moored instrument arrays. The model incorporates the steady two-dimensional hydrodynamic forces exerted by a space-varying velocity field on a surface or subsurface buoy and on a flexible, extensible cable and instruments supported beneath the buoy. Suitable equations for the normal and longitudinal components of cable drag are provided from an examination of existing data. The model behaviour is verified using an analytical solution for a free-streaming cable. An example is given of the model applied to a mooring which consists of a toroidal surface float, an extensible synthetic plastic cable, five instrument packages and a heavy chain anchor.

TABLE OF CONTENTS

	<u>Page</u>
Abstract	i
Table of Contents	ii
List of Figures	iii
List of Tables	iii
Introduction	1
Theoretical Analysis of a Buoy-Cable System	2
A. The Buoy	2
B. The Cable	3
C. Cable Drag	8
D. The Instruments	16
E. Method of Solution	18
Computer Solution of The Buoy-Cable System	18
A. The Buoy	18
B. The Velocity Profile	18
C. The Instruments	19
D. The Cable	19
E. The Iteration Procedure	21
F. Program Output	22
Verification of the Model	22
Limitations of the Present Model	24
References	25
Appendix A - Buoy Calculations	26
Appendix B - Sample Computation	28
Appendix C - Program Source Listing	38

LIST OF FIGURES

	<u>Page</u>
Fig. 1 Buoy Free-body Diagram	4
Fig. 2 Cable Free-body Diagram	6
Fig. 3 Drag of Smooth Cylinders	11
Fig. 4 Normal Drag Coefficient <u>vs</u> Cable Inclination	12
Fig. 5 Longitudinal Drag Coefficient <u>vs</u> Cable Inclination	14
Fig. 6 Drag Force Component Magnitudes	15
Fig. 7 Instrument Package Free-body Diagram	17

LIST OF TABLES

Table I	FORTTRAN Coding Form for Mooring Program Example	31
Table II	Output Listing for Mooring Program Example	32

Introduction

The Coastal Zone Oceanography Group at the Institute of Ocean Sciences, Patricia Bay, makes widespread use of moored instrument arrays for the measurement of seawater properties. The moorings are usually single-point taut-line types, supported by either a surface or a subsurface buoy, with a length of heavy chain or a clump of railway wheels and a Danforth anchor at the lower end. The moorings are normally made in fairly protected waters, so the response to wave action is not often a problem. However, questions have arisen from time to time concerning the actual depths of the instruments. For subsurface buoys, drag forces on the whole system can result in a considerable reduction in the elevation above bottom of any point in the system. For surface buoys, where synthetic lines are normally used, the stretch of the line can cause uncertainties in instrument positions. The elevations could be determined, after the fact, by using depth sensors, but it was desirable to have some means of estimating the instrument positions, for a given set of conditions, before deploying an array. Thus a theoretical investigation of the static behaviour of taut-line moorings was indicated.

A survey of available literature (e.g. McCormick, 1973; Schram, 1968) indicated there were some existing mooring models, most of them not as comprehensive as one might desire, and none of them completely suitable for our needs. Therefore, we decided to develop a mooring system model specifically oriented to the requirements of the group. It would incorporate such details as a varying velocity profile, elastic cable, varying cable types, surface or subsurface buoy, attached instruments and slack or taut line into one computer program. A two-dimensional model was deemed sufficient for our purposes. The information available from such a model includes:

- the length to which an elastic line should be cut for a taut-line surface mooring in a given water depth;
- the attachment points along the unstretched cable for instruments to end up at the required depths;
- the differences in a taut-line surface mooring configuration for low and high tide situations;
- the required buoyancy to attain or maintain a particular depth with a subsurface buoy;
- the tension in the mooring line;
- the required minimum anchor weight;
- the horizontal excursion of the mooring;
- the excursions through depth of instruments suspended below a subsurface buoy for various velocity profiles;
- the line angle at any point along its length.

The mooring model development is outlined in the following sections. The engineering system of units (ft-lb-sec) is used throughout the model, in preference to the metric system, because of the present utility of the engineering force unit in connection with the purchase and use of cables, buoys and anchors.

Theoretical Analysis of a Buoy-Cable System

A. The Buoy

Several types of buoys, having various shapes, are used in moorings. The toroidal buoy has been the most commonly used type for surface floats. It supports a tripod superstructure for increased visibility. The small amount of wind drag on the superstructure, and on the exposed portion of the buoy, will be ignored here, as will the effect of buoy tilt due to waves. Sub-surface moorings are usually effected with spherical buoys, or with cylindrical buoys having a horizontal axis. The latter include tail fins to provide stability. If such a buoy develops a large degree of tilt, then an analysis of the forces involved can become very complicated. For example, the separate lift and drag forces of the main body and the fins, together with their moments about the centre of gravity (CG), must be considered. The lift and drag coefficients, and their points of action, will be functions of the angle of tilt. The buoyancy, weight and tensile forces will be unlikely to act through the same point, creating additional moments to complicate the problem. For such a case, the obvious solution is to redesign the buoy for adequate longitudinal stability at small tilt angles. Principally, this requires tail fins of sufficient size to respond to small disturbances, suitably placed to avoid a loss of efficiency if separation of flow occurs over any portion of the buoy. Surface or subsurface buoys which are symmetrical about a vertical axis present no problems due to tilt, provided that the lift and drag coefficients do not change by any substantial amount over the range of tilt angles. There will be moments involved if the tensile force in the cable doesn't act along the axis (unless the cable is attached at the CG position), and if the centre of buoyancy (CB) doesn't correspond approximately with the CG. The simplest case will be considered here, the basic assumptions being:

1. The line of action of the cable tension is through the CG of the buoy.
2. The point of cable attachment is at the lower surface of the buoy.
3. There is no change in drag coefficient with a change in buoy aspect.
4. There is no fluid dynamic lift force.
5. There is no wind drag.
6. The water drag is proportional to the greatest immersed cross-sectional area in a vertical plane normal to the flow direction.
7. There is no buoy tilt insofar as buoyancy and drag calculations are concerned.

The justification for the simplifications made in these assumptions is that the buoy drag will seldom be as important as cable drag in determining the system configuration, and that small tilt angles will not much affect the

buoyant force. Appendix A contains the immersed area and volume calculations for several buoy types.

A free-body diagram of a simple buoy is shown in Figure 1. A summation of forces in static equilibrium gives:

$$B - W - T_B \sin \phi_B = 0 \quad (1)$$

$$D - T_B \cos \phi_B = 0 \quad (2)$$

Here, B is the buoyancy force, obtained from the immersed volume. W is the weight force, T_B is the cable tension and ϕ_B is the cable angle. The drag force, D , is represented by:

$$D = C_D \frac{\rho}{2} A V |V| \quad (3)$$

where C_D is the drag coefficient for the shape under consideration, ρ is the fluid density, A is the immersed area (Appendix A) and V is the fluid velocity. Solving equations (1) and (2) simultaneously, one obtains:

$$T_B^2 = (B-W)^2 + D^2 \quad (4)$$

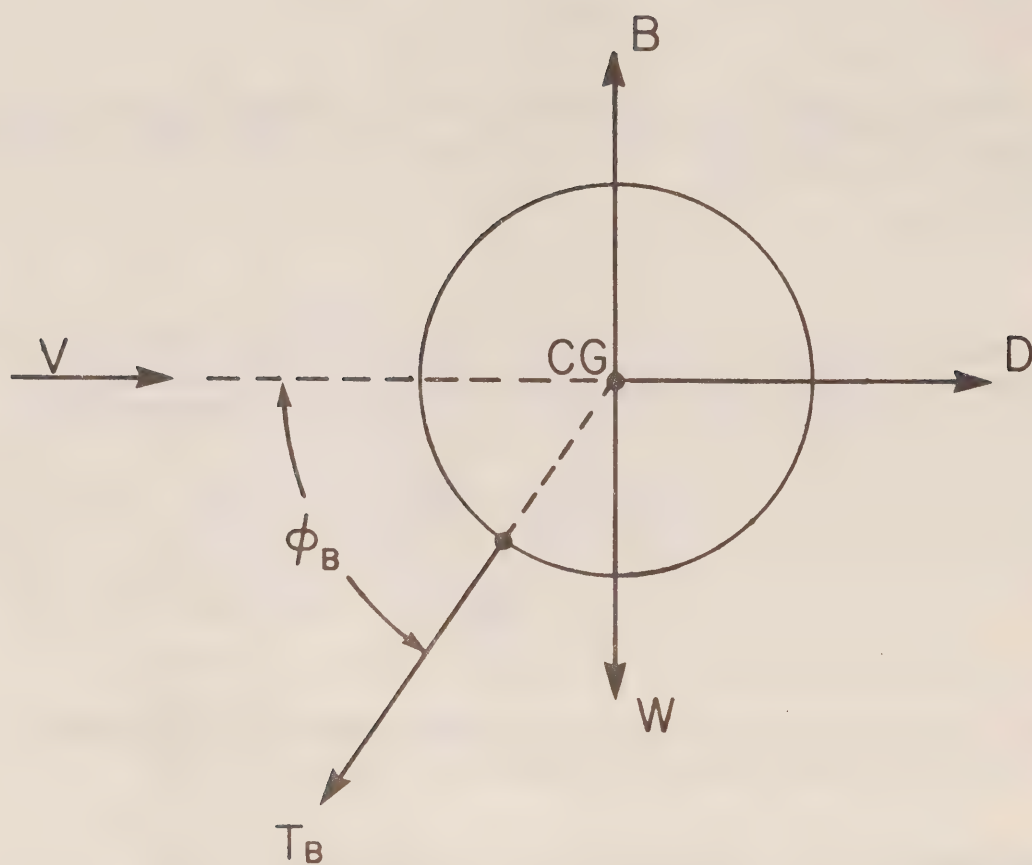
$$\phi_B = \tan^{-1} \left(\frac{B-W}{D} \right) \quad (5)$$

T_B and ϕ_B form the boundary conditions at the upper end of the cable.

B. The Cable

Cables used for mooring are of two principal types - synthetic (plastic) rope and wire rope. Occasionally, a section of chain may be included. Cables are probably the most difficult part of the system to analyze accurately since some of their characteristics are ill-defined. Further paragraphs of this section will examine the problem in more detail. For the present, it is sufficient to assume the following:

1. The cable is flexible and extensible.
2. The cable diameter is not significantly reduced when stretching occurs, i.e., the radial strain is neglected for the purpose of calculating the drag cross-sectional area.
3. The drag on the cable can be separated into normal and



BUOY FREE-BODY DIAGRAM

Figure 1

longitudinal components.

4. There are no side forces on the cable and no vortices are shed in the wake (thus, there is no possibility of "strumming").
5. The cable lies in a vertical plane and the flow is coplanar with the cable.

A free-body diagram of a cable segment is shown in Figure 2. The unstretched case is illustrated for simplicity. The independent variable is taken to be the length S along the cable. The dependent variables are then the cable angle ϕ and tension T , and the x and z coordinates for any point on the cable. An elemental length of the cable is represented by ΔS . The weight force and buoyant force of the cable are, respectively, w and b pounds per unit length. The drag force D_C is also in pounds per unit length and is shown resolved into normal and longitudinal components, F_N and F_L , respectively. The appropriate form for these components, especially F_L , is open to some conjecture and will be considered in detail in the next section.

Resolving all of the forces into components, and summing in the normal and longitudinal directions, respectively, one obtains:

$$2T \sin \frac{\Delta\phi}{2} = \{F_N + (w-b) \cos \phi\} \Delta S \quad (6)$$

$$\Delta T \cos \frac{\Delta\phi}{2} = \{-F_L + (w-b) \sin \phi\} \Delta S \quad (7)$$

Taking these equations to the infinitesimal limit, and neglecting second order quantities, gives:

$$\frac{d\phi}{dS} = \frac{1}{T} \{F_N + (w-b) \cos \phi\} \quad (8)$$

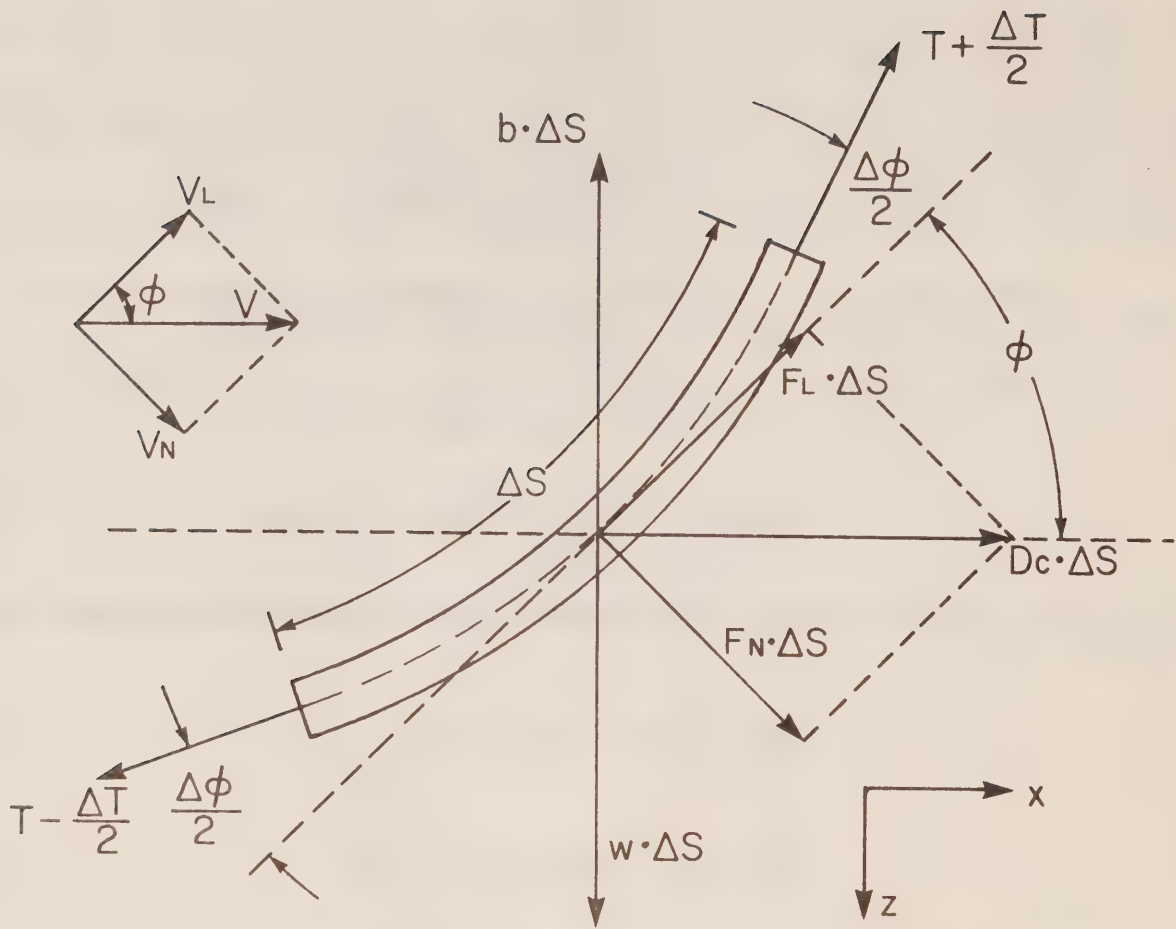
$$\frac{dT}{dS} = -F_L + (w-b) \sin \phi \quad (9)$$

In addition, there are two parametric equations (directional derivatives) describing the cable shape, namely:

$$\frac{dx}{dS} = \cos \phi \quad (10)$$

$$\frac{dz}{dS} = \sin \phi \quad (11)$$

The preceding four equations are all that are necessary to describe an inextensible cable. They can be solved simultaneously, obtaining the boundary conditions from the buoy equations and from a condition on the water



CABLE FREE-BODY DIAGRAM

Figure 2

depth, to provide the configuration of the cable and the tension in the cable. However, if the cable is extensible, with an elongation per unit length represented by ϵ , an additional relationship is required to relate this strain to the tension in the cable. For materials obeying Hooke's law:

$$\epsilon = \frac{\Delta L}{L} = \frac{T}{AE} \quad (12)$$

where E is the static modulus of elasticity, A is the load-bearing cross-sectional area, L is the unstretched length of cable and ΔL is the actual elongation. The strain of non-Hookeian (non-linear) materials is best approximated by fitting a power curve to empirical data, if such is available. The information regarding elongation of a particular material is often provided by the manufacturer in the form of a graph or table giving strain vs. the ratio of cable tension T to ultimate strength T_{\max} , both in percentages. In this case, one can obtain the strain in the form:

$$\epsilon = \frac{a}{100} + b \left(\frac{T}{T_{\max}} \right) + 100 c \left(\frac{T}{T_{\max}} \right)^2 \quad (13)$$

where a , b , c are constants to be determined from the graph. Only the portion of the graph covering the normal working range of the material should be considered. The considerations above assume that pre-stretched cable is used, so that any elongation resulting from mechanical deformation (readjustment of strand positions) is not included.

Synthetic plastic cables are non-linear in their elastic behaviour, but the situation is complicated further by their plastic behaviour. This is especially so when a history factor is involved, that is, the stress-strain relationship depends somewhat on the previous loads experienced by the cable, and may be affected by the number of wet/dry cycles undergone. Also, some materials creep under load, even after pre-stretching has settled the strands along the core. Some materials (e.g., nylon) absorb water and swell. This can result in a contraction of cable length, because the expansion in the plane of the cross-section forces individual strands into a longer helical path about the core. Little of an exact nature is known about these effects and they are not dealt with here since their influence on the static behaviour of the mooring is normally small.

The total strained length of cable is $(1 + \epsilon)$ times the original unstretched length. From Equation 13, we obtain the form used in the present model:

$$1 + \epsilon = a_0 + a_1 T + a_2 T^2 \quad (14)$$

where a_0 , a_1 , a_2 are constants to be determined, as before. For an inextensible cable: $a_0 = 1$, $a_1 = 0$, $a_2 = 0$. For a cable obeying Hooke's Law: $a_0 = 1$, $a_1 = 4/(\pi d^2 E)$, $a_2 = 0$, where E is Young's modulus for the cable itself (not the modulus for the cable material because of the difficulty in

determining the exact cross-section area). For synthetic cables: $a_0 = 1 + (a/100)$, $a_1 = b/T_{\max}$, $a_2 = 100 c/T_{\max}^2$, where T_{\max} is the ultimate stress for the cable. Rewriting equations 8 through 11 in terms of a strained element gives:

$$\frac{d\phi}{dS} = \frac{1}{T} \{ (1+\epsilon)F_N + (w-b) \cos \phi \} \quad (15)$$

$$\frac{dT}{dS} = - (1+\epsilon)F_L + (w-b) \sin \phi \quad (16)$$

$$\frac{dx}{dS} = (1+\epsilon) \cos \phi \quad (17)$$

$$\frac{dz}{dS} = (1+\epsilon) \sin \phi \quad (18)$$

Here, the implication is that the weight of one foot of stretched cable is $w/(1+\epsilon)$ so there is no change in total weight. Further, the buoyancy per foot of stretched cable happens also to be taken as $b/(1+\epsilon)$, so that some compensation for the effect of radial strain on the displaced water volume is included, although not in the correct formal manner. Any error in this term is small compared to the other forces involved, so it was not considered necessary to formalize it. As mentioned previously, the effect of radial strain on the drag force term is neglected, again because of its relative insignificance.

C. Cable Drag

A suitable representation of the cable drag forces is a very important consideration for any mooring model, the more so when high current speeds are involved since the drag is proportional to the square of the velocity. For the most part, the literature is not too helpful in this matter. Usually, as is done here, the forces involved are resolved into components normal to the cable axis and components along the cable. The form of the normal component of drag is almost standardized, although there is a considerable range in the actual drag coefficient values used. Many different forms have been proposed for the longitudinal component (Casarella & Parsons, 1970), but it is often ignored completely since it is usually small compared to the normal component. However, this is not necessarily the case when the cable angle becomes large for some reason, such as high water velocities or inadequate buoyancy on a subsurface mooring. Relative magnitudes will be examined below. A problem that confronts one in attempting to determine the most suitable form for drag force components is that very few measurements of force as a function of cable inclination to the flow have been reported and some of these do not appear to be reliable, especially where longitudinal drag is concerned. This latter quantity is a difficult one to measure accurately because of its relative magnitude and the fact that

it is usually the result of the subtraction of two large quantities, the drag of the supporting structure being included in the measurement. The preferred data set, in my view, is that due to Relf and Powell, made in 1917! Their longitudinal drag curve for a smooth wire is a good fit to a theoretically-derived form, as will be shown, with the lack of scatter in the data points being an indication of reasonable accuracy in the measurements. This gives one some confidence in their subsequent drag determinations for wire ropes. The Relf and Powell data is used below to estimate normal and longitudinal drag coefficients for cables inclined to the flow.

According to the "crossflow" or "independence" principle which states, in effect, that the nature of the boundary layer depends only on the normal velocity component (Hoerner, 1958; Schlichting, 1960), the pressure force and the normal friction force will also depend only on that component. This holds true while laminar (sub-critical) flow prevails but does not necessarily apply to turbulent boundary layers. Thus, in sub-critical Reynolds number flow, the total drag force normal to the cable axis can be expressed as a function of $V \sin \phi$, where V is the free-stream velocity and ϕ is the cable inclination referenced to a horizontal plane (Fig. 2). Typical mooring systems will almost always operate in the sub-critical flow regime. We can define the normal drag force component, per unit length of cable, as:

$$F_N = C_{DN} \frac{\rho}{2} d u^2 \quad (19)$$

where $u = V \sin \phi$ and d is the cable diameter. C_{DN} is based on frontal area and includes the effects of both pressure and skin friction, i.e.

$$C_{DN} = C_p + C_{FN} \quad (20)$$

Over the Reynolds number range of interest, say $10^2 < R < 10^5$, C_p is usually considered approximately constant. It is much larger than C_{FN} except at the low end of the range. The logical definition for Reynolds number here makes use of the normal velocity component as the characteristic velocity, since it is the key to the changing state of the boundary layer, as suggested by the independence principle. Thus,

$$R_u = \frac{dV \sin \phi}{\nu} = R \sin \phi \quad (21)$$

where ν is the kinematic viscosity and R is the Reynolds number at $\phi = 90^\circ$. Since it is R which is generally reported in the literature, its use in various expressions will be retained here, but in conjunction with $\sin \phi$. The value of R_u may become small at large cable angles, even though the free stream velocity is high, with the result that the friction component of the normal drag force may assume some relative importance. Therefore, C_{FN} should probably not be excluded from consideration.

Goldstein (1938) presents some drag data, which he attributes to Relf and Thom, for a smooth cylinder normal to the flow. This is shown in Fig. 3. The total drag curve is by Relf; the rest of the results are due to Thom, who derived a numerical solution for skin friction and found that a good fit to the points provided by this solution was given by:

$$C_{FN} = \frac{4}{R_u^{1/2}} \quad (22)$$

for $\phi = 90^\circ$. With the inclusion of the Reynolds number in the appropriate form, the effect of cable angle is accounted for, i.e.

$$C_{FN} = \frac{4}{(R \sin \phi)^{1/2}} \quad (23)$$

This equation should hold so long as the flow is laminar, at least. Thus, it may not apply to rough cylinders such as wire rope. An examination of the pressure drag curve in Fig. 3 suggests that, rather than taking it as constant, a power law fit might be worthwhile. In any case, the normal force has the form:

$$\begin{aligned} \frac{F_N}{\frac{\rho}{2} d V^2} &= C_{DN} \sin^2 \phi \\ &= \left[C_p + \left(\frac{16}{R \sin \phi} \right)^{1/2} \right] \sin^2 \phi \end{aligned} \quad (24)$$

where C_p is determined at the angle $\phi = 90^\circ$ and $R = \frac{dV}{\nu}$.

The previously mentioned Relf and Powell (R&P) data were obtained using a smooth wire and several different wire ropes. The data were taken near $R = 10^4$, so that the friction drag is only a small fraction of the pressure drag. Even at an extreme angle of $\phi = 10^\circ$, the boundary layer Reynolds number R_u is about 10^3 . Then the friction drag is about 1/10 of the pressure drag, so it is probably hidden within the measurement error of the small forces involved. The normal drag coefficient values, derived from R&P normal force measurements, are plotted in Fig. 4. The measurements on the different cable types were made at slightly different values of R , but the scatter in the data is more likely due to differences in cable construction rather than to any R -dependence. The solid line in the figure is a $\sin^2 \phi$ curve, which is readily fitted to any of the data sets, including both the smooth wire and the wire ropes.

The longitudinal, or along-cable, flow field is, in one sense, influenced by both flow components. This is a result of the fact that the

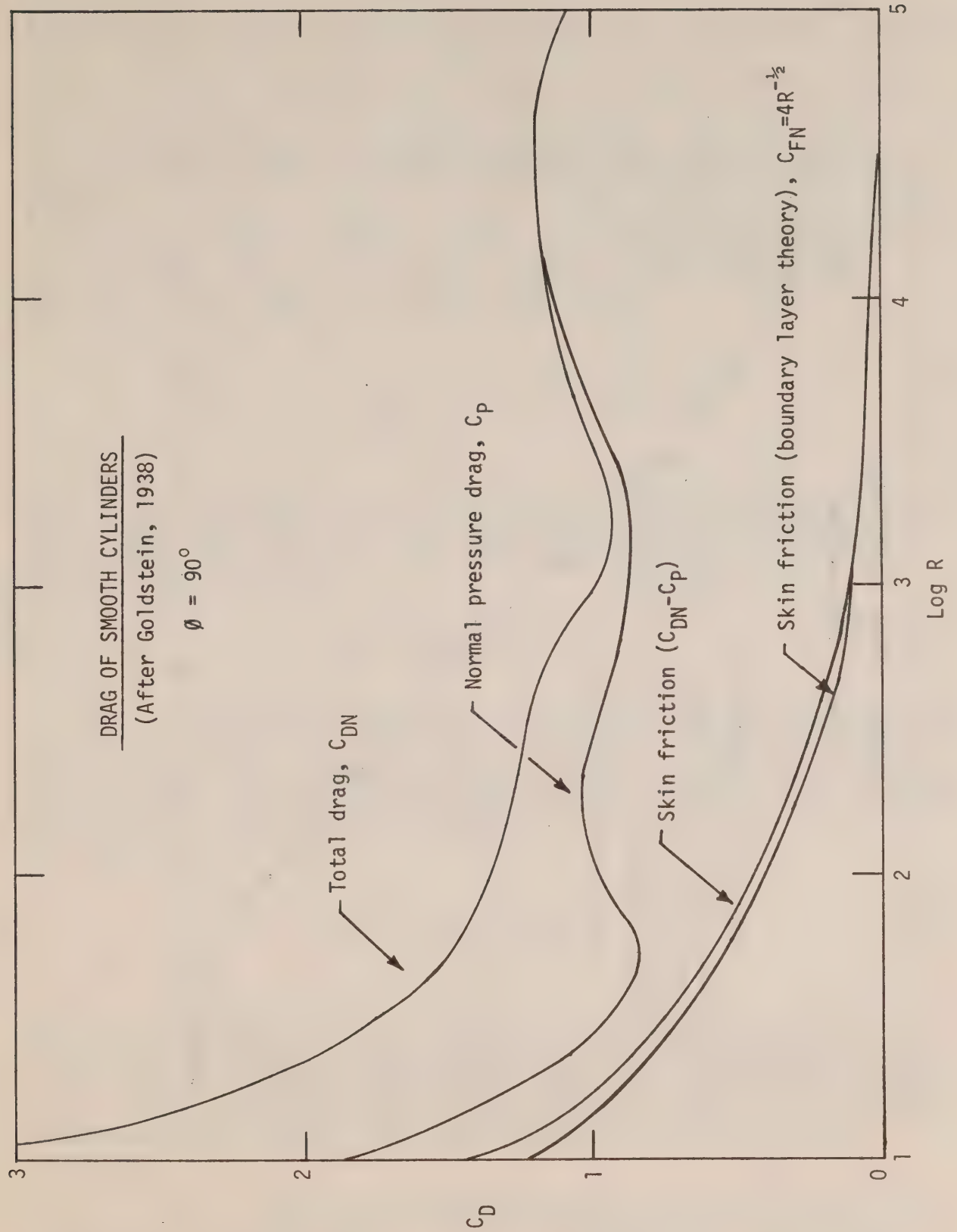


Figure 3

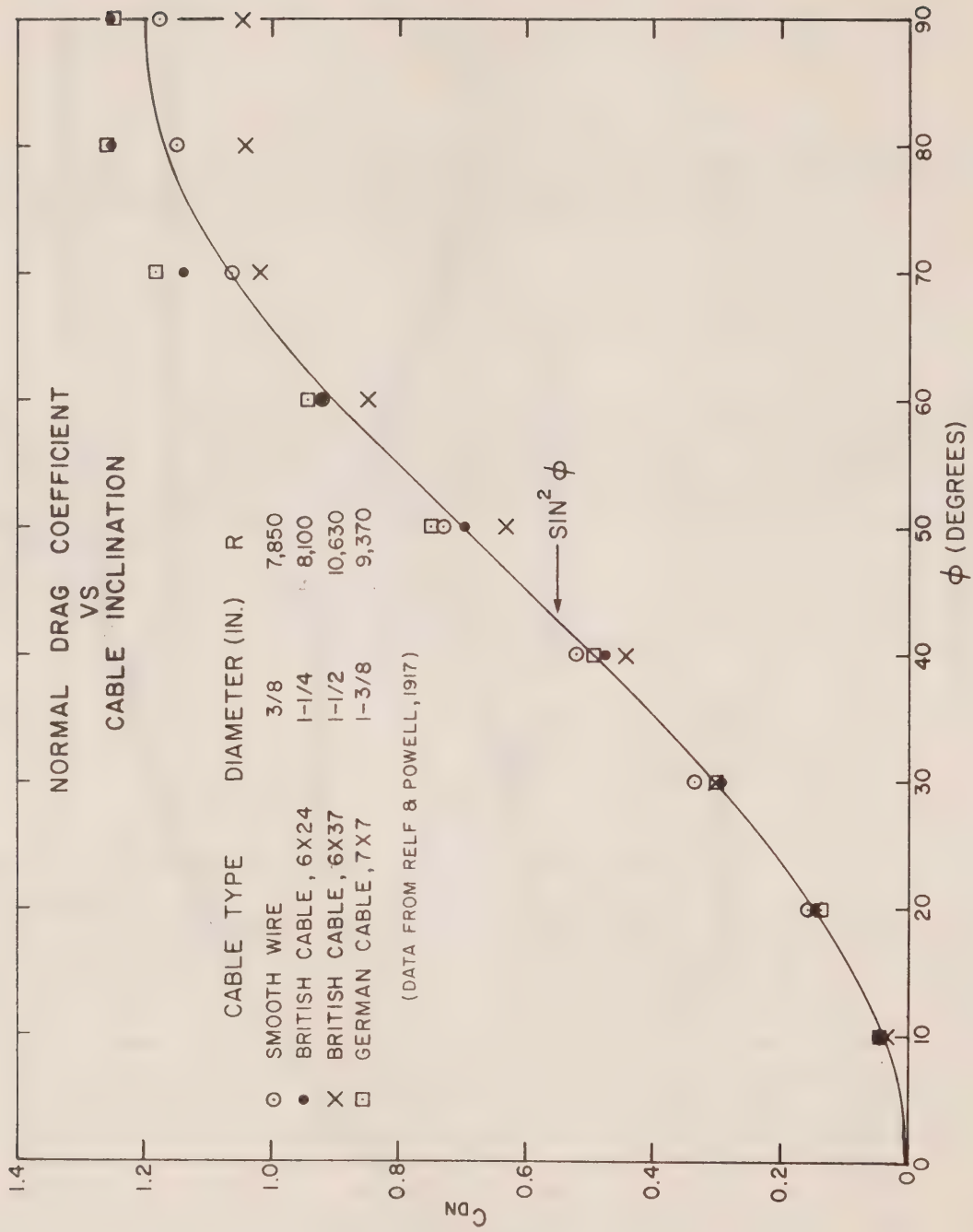


Figure 4

boundary layer thickness is determined by the normal velocity component. A boundary layer build-up in the direction of the cable is prevented because the normal velocity "blows" away any excess retarded fluid layer. (This theory obviously breaks down for the limiting case of pure longitudinal flow at $\phi = 0^\circ$.) However, the longitudinal stress distribution within the boundary layer is determined only by the along-cable velocity. When the stress distribution is known it can be integrated over the cable to obtain the longitudinal drag force. The method for making this calculation has been suggested by Schlichting (1960) and carried out by Schram (1968) and Topham (1976) for the case of a smooth cylinder. A similar solution to the problem is arrived at through an analogy with the heat flow equation (Schlichting, 1960; Taylor, 1952). The theoretical result is a function which depends on both the sine and cosine of the angle ϕ (and not simply on $\cos^2\phi$ in an analogous fashion to the normal drag force), namely:

$$\frac{F_L}{\frac{\rho}{2} \pi d V^2} = C_{FL} = \alpha R^{-\frac{1}{2}} \cos \phi \sin^{\frac{1}{2}} \phi \quad (25)$$

where α is a constant to be determined and C_{FL} is based on surface area. There is no longitudinal pressure drag component because it is assumed that the cable is infinitely long. Note that, for convenience in subsequent manipulation, we may write:

$$C_{FL} = \frac{\alpha}{4} \left(\frac{16}{R \sin \phi} \right)^{\frac{1}{2}} \cos \phi \sin \phi \quad (26)$$

The longitudinal drag coefficients derived from R&P data are shown in Fig. 5. The empirical result for the smooth wire shows good agreement with Equation 25. However, the wire rope data shows considerable variance from this function. This is probably a consequence of flow modification resulting from the spiral construction of the cable. Fitting a straight line to the wire rope data gives a curve of the form:

$$C_{FL} = \left(1 - \frac{\phi}{90} \right) \left(\frac{16}{R \sin \phi} \right)^{\frac{1}{2}} \sin \phi \quad (27)$$

where ϕ is in degrees. All of the data were obtained near $R = 10^4$, as previously mentioned. If this is beyond the flow transition point for the rough cables involved, then the boundary layer theory is inapplicable in any case. The relatively high normal drag coefficients (seen in Fig. 4) would seem to argue, though, that the flow is still sub-critical. Just where the transition region lies for such cable has not been determined, to my knowledge.

Fig. 6 summarizes the foregoing equations and allows one to easily determine the relative magnitudes of the component forces at a given cable inclination and Reynolds number. It can be seen that there may be occasions

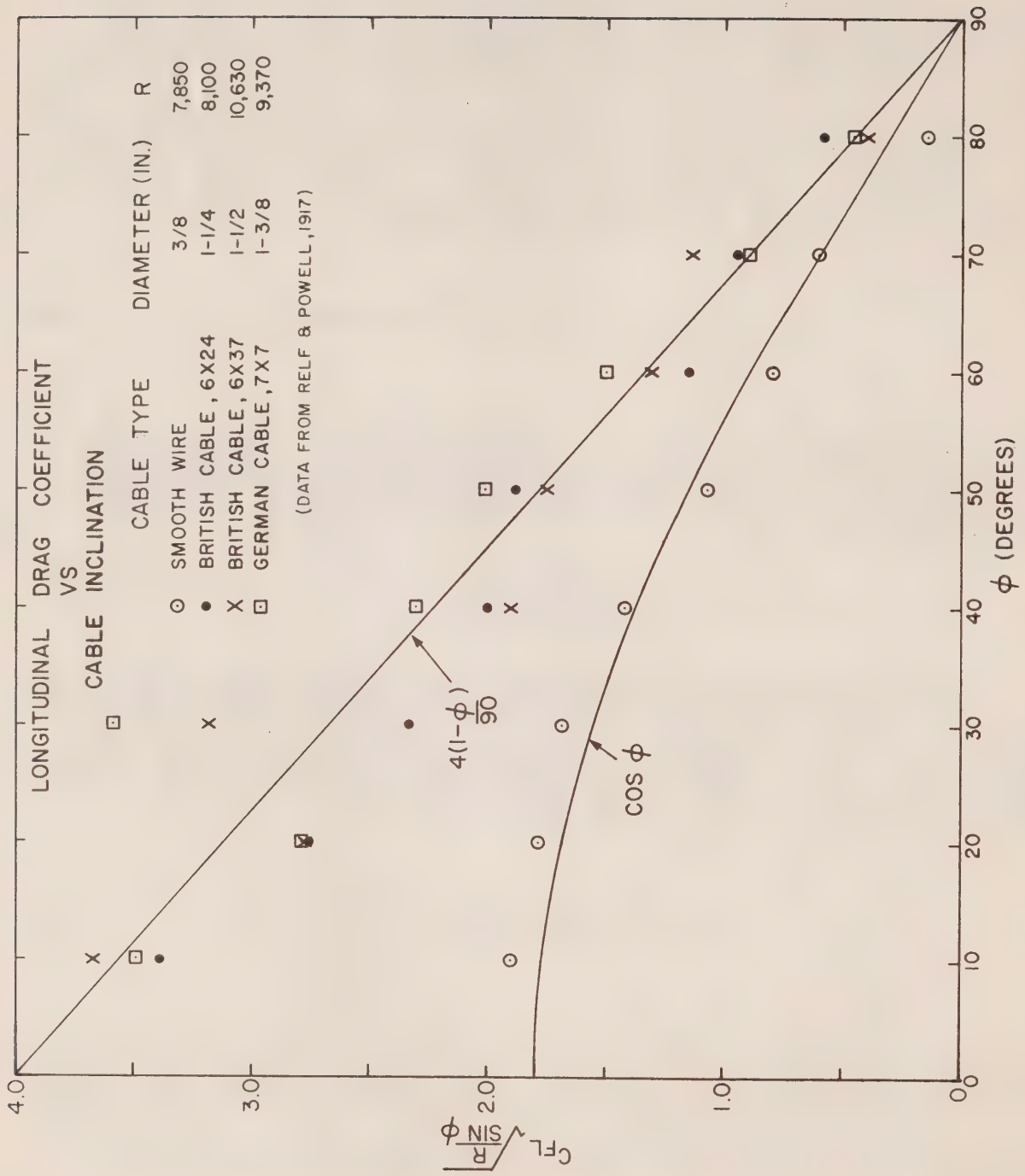


Figure 5

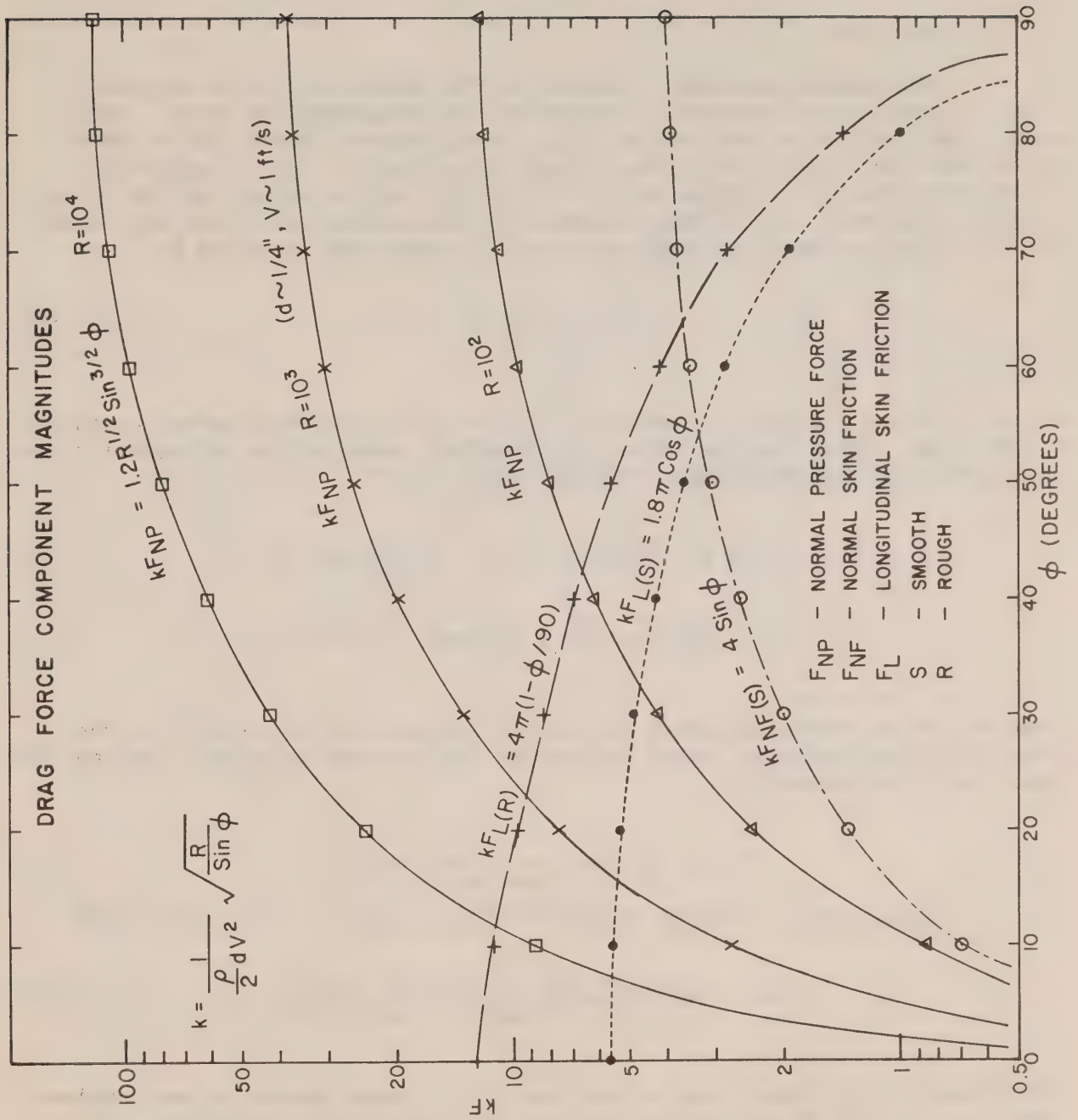


Figure 6

on which the skin frictional forces should not be ignored. However, the equations are derived or verified on the basis of very limited empirical results. A definite need exists for force measurements on various cable types inclined to the flow over a reasonable range of Reynolds numbers. For the present, however, we will be satisfied to use the results outlined in Equations 19 through 27 to simulate drag in our mooring model.

D. The Instruments

Instrument packages, attached to the cable, may be of various shapes and sizes, and the method and points of attachment may vary. Here, as for the buoy, only the simplest case is considered, namely one in which all of the forces act through the CG and any effect of tilt is neglected. A free-body diagram is presented in Fig. 7. W_I is the package weight in air, B_I is its buoyancy, $\Delta\phi$ is the increment in cable angle due to the instrument and ΔT is the increment in cable tension. Package drag is given by:

$$D_I = C_I \frac{\rho}{2} A V |V| \quad (28)$$

where C_I is the drag coefficient and A is the cross-sectional area presented to the flow. Resolving the forces in directions parallel to and normal to the cable and summing, one obtains, respectively:

$$T + D_I \cos \phi - (W_I - B_I) \sin \phi = (T - \Delta T) \cos \Delta\phi \quad (29)$$

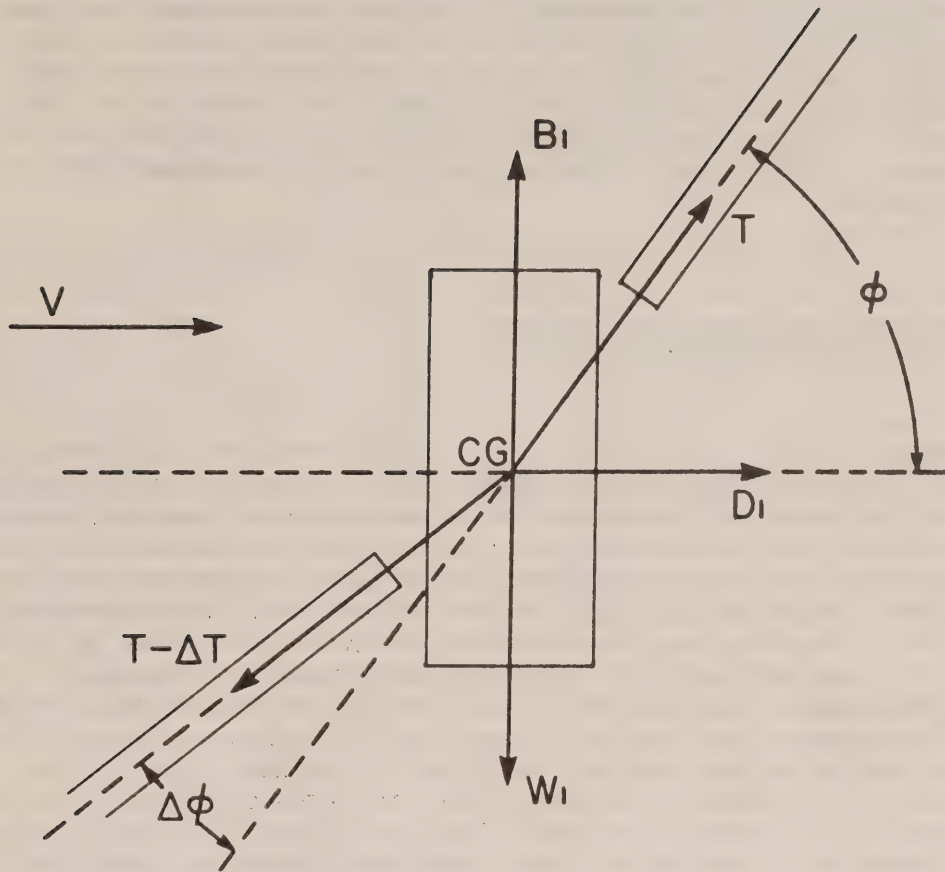
$$D_I \sin \phi + (W_I - B_I) \cos \phi = (T - \Delta T) \sin \Delta\phi \quad (30)$$

Some of the instrument packages may be very buoyant or very heavy, so the simplifying assumption of small changes in angle cannot be made. Solving the equations simultaneously:

$$T - \Delta T = \frac{D_I \sin \phi + (W_I - B_I) \cos \phi}{\sin \Delta\phi} \quad (31)$$

$$\Delta\phi = \tan^{-1} \left[\frac{D_I \sin \phi + (W_I - B_I) \cos \phi}{T + D_I \cos \phi - (W_I - B_I) \sin \phi} \right] \quad (32)$$

The boundary conditions (tension and angle) for these equations are obtained from the solution of the cable system on one side of the instrument. The equations, in turn, provide the boundary conditions for the next cable segment.



INSTRUMENT PACKAGE FREE-BODY DIAGRAM

Figure 7

E. Method of Solution

The equations for the complete buoy-cable system are first-order non-linear and form a boundary-value problem requiring boundary conditions at each end of the cable. The buoy boundary condition is satisfied by assuming an elevation for the buoy which, in turn, fixes the cross-sectional area and volume immersed. The anchor boundary condition is that the elevation of the anchor must coincide with that of the sea bottom, within acceptable limits. The governing equations are solved for the unknown quantities (ϕ , T , x , z) by a step-wise integration along the cable, beginning at the buoy end, to a point of discontinuity resulting from the concentrated loads caused by the presence of an instrument package. The effect of the forces on the package is added to the cable forces and the integration is continued in a similar fashion until the lower end of the cable is reached. If the anchor boundary condition is not satisfied within the specified error limits, then a new buoy position is chosen and the procedure is repeated.

Computer Solution of the Buoy-Cable System

A. The Buoy

The buoy geometry is incorporated into a subroutine (Appendix C), so that the ability to cope with various types of buoys can be added to the program with no difficulty. The subroutine is entered with the buoy elevation and the water velocity at that elevation. The buoyancy and water drag forces are calculated and returned to the main program to provide the upper boundary condition on the cable. The limitations on these calculations have been mentioned in a previous section. The buoy elevation is taken to be at the bottom of the buoy, which is the point of attachment for the cable. Thus, for a surface buoy, the difference between the water surface elevation and the buoy elevation is the depth of immersion of the buoy. Three pertinent dimensions of a buoy can be specified in the data input. The vertical dimension of the buoy is of particular importance, since it is used in conjunction with the buoyancy to modify the position of the buoy during the iteration procedure. Surface or subsurface buoy types are specified by a flag in the main program, to permit some minor processing differences.

B. The Velocity Profile

Since the model is two-dimensional, the water motion is confined to a vertical plane. The flow is also assumed to have no vertical component. Any speed versus depth relationship which can be represented by a second order profile of the form:

$$v = a + bz + cz^2 \quad (33)$$

is permissible. Likewise, various profiles of this form can be pieced together in segments, as desired. The profile segments can be any convenient size and do not have to correspond to multiples of the cable segment length (discussed in a following section). Negative speeds are allowed. The only limitation is that strong discontinuities in the profile may make convergence to the correct solution more difficult. In the program, the velocity profile information is stored in an array, the first element in each row being the lower depth limit of applicability (measured from the sea-bed) of the particular segment whose coefficients (a,b,c) are given by the other elements of that row. Presently, storage is provided for five segments. A conditional branch on the depth is used in subsequent calculations to calculate the correct velocity for a given depth.

C. The Instruments

The program permits all kinds of instrument packages to be inserted in the system. They should be positioned at multiples of the basic cable segment length, as used for integration along the cable (and discussed in the next section). If they are not so positioned, the program will round the position to a segment multiple. The instrument locations, in feet along the cable from the buoy, are read into the computer, converted into an integer number of cable segments and stored in an array capable of holding ten different values. Because of the conversion, the instrument locations are still correct when the cable is stretched. Before each integration is made, the program checks to see if there is an instrument at the upper end of the cable segment. If so, the velocity is determined and the instrument drag calculated. Then the resulting increments in cable tension and angle are combined with the preceding values of these variables. No separate subroutine is provided for the instruments, as was the case for the buoy, so the buoyancy and drag cross-sectional area must be read in as data. Any swivels, shackles or other fittings located near an instrument should have their weights accounted for by including them in the instrument weight.

D. The Cable

The integration along the cable is carried out over a series of cable segments which are of equal length when unstretched, this length being a sub-multiple of the total cable length. The choice of segment size depends on the problem parameters, such as the complexity of the velocity profile, the number and location of instrument packages, etc. The integration routine uses the Runge-Kutta method with error control. The user must code an external subroutine which specifies the functions required for an evaluation of the derivatives given in Equations 24 through 27. The integration routine also requires the specification of an error tolerance on the integral, a step size, and a value of the independent variable at the end-point of the integration. Double precision is used throughout to reduce the possibility of cumulative rounding errors.

For an extensible cable and step-wise integration, the end point

must correspond to the strained length of each cable segment. This requires that the independent variable be stretched as well, i.e. Equations 24 through 27 are divided through by the quantity $(1 + \epsilon)$, giving $(1 + \epsilon)dS$ as the independent variable instead of dS . In the program, the strained unit length $(1 + \epsilon)$ is represented by the function STRCH. The function is presently calculated on the basis of the tension at the upper end of a cable segment. For greater accuracy, this tension could include one-half of the tension increment for the previous segment. Generally speaking, however, the increment is usually no more than a few tenths of one percent of the tension, so this correction is ignored here. If required, the accuracy can be improved by reducing the segment length. Any necessity for this is easily checked by running the model for two different segment lengths.

The boundary conditions for the first cable segment are provided by the buoy calculations, and for subsequent segments by the results of the integration over the preceding cable segment. The velocity used for calculating cable drag is that which occurs at the midpoint of the segment, the midpoint elevation being estimated on the basis of the cable angle for the preceding segment. An iteration on the cable angle would result in a slightly more accurate midpoint location and, therefore, a slightly more accurate velocity (only when the velocity profile is not uniform). This was not deemed worthwhile since, for the calculation of drag, the midpoint velocity is assumed to apply over the whole segment in any case. Likewise, one could incorporate a varying velocity (when such is the case) throughout the integration over a cable segment, but at the expense of a considerable increase in program complexity. Again, if concern is felt about the outcome of the procedure as presently used, especially when the velocity is changing rapidly with depth, the program can be run with small segment lengths. Some trial runs in which the segment lengths were varied by factors of two or more, all other variables remaining unchanged, showed no variation in the results. Thus, the indication is that the simple procedure used to obtain the velocity for the drag determination is adequate. Also, while only an average velocity value is used in the drag calculation, the dependence of the drag on the actual cable angle is included throughout the integration along a cable segment since the angle is one of the dependent variables. At the conclusion of each call to the integration subroutine, the resulting cable angle is tested for a negative value. The program is terminated if such a value occurs, since it indicates either that the buoy has insufficient buoyancy or that the cable is much too long. Thus the model will only cope with a slack line mooring up to the point at which the slack is sufficient to result in a portion of the cable assuming a horizontal position. The length of cable involved, at this critical point, depends on the cable loading.

The mooring line used in the model is not restricted to one size or one kind of material throughout its length. Presently, ten different cable types can be handled. Information on these, including the lower end position of each type in feet from the buoy, is read into an array. Then (as is done for the instruments), the end position is converted into an integer number of cable segments, the conversion permitting an easy check on type changes as well as allowing cable stretch without causing any additional problems. The form of the longitudinal drag equation used with each type is optional, the choice being either that for smooth cable, for wire rope, or no axial drag at all. The selection is made by assigning an

appropriate logical flag in the input data.

The program incorporates a provision for using a length of chain, rather than a dead-weight anchor, at the lower end of the cable in a taut-line surface mooring. The chain acts to reduce changes in cable tension resulting from changes in water surface elevation, i.e. changes in the buoyant force at the upper end of the cable. It does this by means of chain links being picked up or lowered to the bottom to permit small changes in buoy elevation. A flag in the program indicates when chain is present, in which case the integration is carried out beyond the end of the cable to the point where the vertical component of tension in the chain is just less than the weight of one increment of chain. The present chain drag routine arbitrarily incorporates a sine-squared dependence on the angle of inclination for the normal component and a cosine-squared dependence for the longitudinal component. The current speed occurring at the bottom end of the cable is assumed to apply for all of the chain links above the bottom.

E. The Iteration Procedure

The solution of the buoy-cable model is based on making an estimate of the buoy position with respect to the bottom and, proceeding from there, integrating along the cable to the anchor. If the anchor elevation doesn't coincide with the bottom elevation, within specified limits, the estimate of the buoy position is modified and another integration is performed. For the case where a length of chain replaces the anchor, it is the end of the last suspended link which must coincide with the bottom. A simple additive modification of the buoy position is made for the first iteration, using the error in the anchor location. Subsequent iterations use a procedure somewhat akin to the Newton-Raphson method (Appendix C).

A marked change in the velocity profile at the location of a subsurface buoy can result in slow convergence, or even non-convergence, of an iteration procedure unless certain steps are taken. Even more difficult is the case of a surface buoy on a taut-line mooring using an elastic cable. Here, the buoyancy force and the cable strain combine to increase convergence problems. A very small change in buoy elevation can result in a very large change in the calculated anchor position. To avoid these problems and assist in attaining reasonably rapid convergence, a fairly elaborate system of testing and revision is used. This begins in the buoy subroutine, but is contained mostly in the main program. Record is kept of anchor position errors obtained from revised buoy elevation estimates. The only corrections subsequently permitted to the estimate are those which will result in the error at the anchor being smaller than the error obtained on any previous iteration. The correction term involving the ratio of differences in successive buoy position estimates and resultant anchor locations, multiplied by the most recent anchor location, usually provides a rapid initial convergence but becomes less effective as the final answer is approached. To offset this, an additional correction term is included which subtracts a further fraction of the most recently-obtained coordinate for the anchor location from the previous estimate of buoy elevation.

The program halts when more than fifteen iterations are required.

If this happens, then a second run of the program, using a position estimate based on the results of the first run, will normally achieve the desired solution. In fact, subsurface moorings seldom take more than one iteration, and surface moorings may typically require several.

F. Program Output

The first portion of the program output lists information associated with the integration and iteration routines. In particular, the various estimates of buoy elevation and the resulting anchor position are given for each iteration. Following this there is a listing of all of the pertinent input and output data about the buoy-cable system and the velocity profile, including items such as instrument package drag and position coordinates.

Next, a table of cable coordinates, tensions, slope angle and drag is printed. This contains the results of a solution of the system equations for each segment of the cable, the number of segments having been specified in the data input. The cable drag values given in this table are for unit cable length. The drag value listed in the j-th row applies to the segment whose lower-end coordinates are also listed in the j-th row.

Verification of the Model

A model user must have some assurance that the physics of the system being modelled are represented in a reliable fashion so that he may place confidence in the predicted results. If an analytical solution is available for the system, this provides the best possible check on the correctness of the model behaviour, confirming that any mathematical procedures involved in the model are being properly carried out. For the present case, a problem with an analytical solution can be formulated to verify that the system of four simultaneous differential equations describing the cable behaviour is being solved correctly by the computer program. The problem concerns a so-called free-streaming cable, i.e. a mooring line unencumbered by any attachments except at the anchor point and supported only by its own buoyancy. Under these circumstances, the cable will stream into a position where the normal forces are in balance, i.e. the normal drag force will be just equal to the normal component of the weight or buoyant force at every point along the cable. Thus, referring back to Equation 8:

$$F_N + (w-b) \cos \phi = 0 \quad (34)$$

and:

$$T \frac{d\phi}{dS} = 0 \quad (35)$$

Since T is obviously non-zero, then the change in angle, $\frac{d\phi}{dS}$, must be zero and the solution of Equation 35 is:

$$\phi = \text{constant} \quad (36)$$

Therefore, the cable streams in a straight line (if it is everywhere exposed to water having the same velocity and density). Equation 34 can be solved, by iteration if necessary, to obtain the exact value of the angle. It might also be mentioned that the cable angle at the fixed end of any moored system using buoyant line (or any surface-towed system with a 'weighty' line) will be asymptotic to the free-streaming angle, no matter what the configuration of floats or weights. Next, the tension along the line can be calculated from Equation 9, since all of the variables in the equation are now known.

Four simulations of a free-streaming cable were carried out by applying the model to a 100-ft length of $\frac{1}{4}$ -inch diameter buoyant cable subjected to four different flow velocities. A buoy having a nominal buoyancy of 1 lb was added to the system to circumvent some program logic that requires support at the upper end of a mooring cable. A segment length of 2 ft was used. In each simulation, the free-streaming angle was achieved at a distance of several segment lengths from the buoy. For velocities ranging from 5 to 20 ft/sec, the angles ranged from 20 to 5 degrees above the horizontal, approximately. The agreement between the predicted angles and the angles calculated analytically reached to at least six significant figures. The same degree of correspondence was found for predicted and calculated tensions. Therefore, the veracity of the program procedures seems unquestionable and there only remains the problem of supplying adequate input data to the program.

The provision of suitable information to the mooring model is certainly the key to obtaining accurate predictions regarding the system configuration. In particular, a reasonable representation of the velocity profile is required because of the square law dependence of drag on flow speed. Even if a test mooring is deployed with the specific intent of defining the nature of the profile at a given location by measuring velocities at a number of depths, there is still no assurance that the velocity is not considerably different at positions between the measuring points. Also, the profile may vary with tidal range or with the seasons. Lacking any reliable information concerning the profile required for a simulation, the most straightforward approach is to assume a uniform velocity. Suitable estimates of drag coefficients are also important, with the emphasis on accuracy depending somewhat on the mooring configuration. If a long line is used, carrying few instruments, then the cable drag is likely to be the dominant force. For a short line and a large number of instruments, the total drag of the instruments may equal or exceed the cable drag. The flow Reynolds numbers for the components should be considered when selecting the drag coefficients.

Lacking an analytical solution for a particular model, any attempt at verification on the basis of data from an actual mooring would be very difficult because of the aforementioned problems associated with the correctness of the model parameters. If such verification must be attempted, it is preferable to make use of a subsurface mooring, rather than a surface one, because of the much greater sensitivity of its configuration to variations in the forces involved.

Limitations of the Present Model

Some of the limitations of the model have already been mentioned as assumptions connected with the mathematical development. The effect of these assumptions is to restrict the model to static two-dimensional cases in which all moments of forces are neglected. The extension of the model to three dimensions is not difficult in principle, but would add some complexity to the computer program. Moments on the buoy and instruments could also be readily included, but would require a good knowledge of the fluid dynamic behaviour of these bodies, e.g. lift and drag coefficients vs angle of incidence, and centre-of-pressure travel. Wind drag on surface buoys is presently ignored but this restriction is easily modified. Instruments must be attached between cable segments but this is of little consequence because the segment lengths can be made as small as reasonably desired. Moorings using more than a single anchor point require a different program. For a two-point mooring, the model might still be two-dimensional. For a larger number of anchors than two, a three-dimensional model is obviously required. Multiple-point mooring models might encounter structural redundancy problems.

In conclusion, the present model incorporates the steady two-dimensional hydrodynamic drag forces exerted by a space-varying velocity on a surface or subsurface buoy and on a flexible, extensible cable and instruments supported beneath the buoy. The accuracy of results obtained from the model will depend in large measure on the provision of accurate velocity information and, to a lesser degree, on an adequate knowledge of the cable characteristics.

References

- Casarella, M.J. and M. Parsons. 1970. Cable Systems Under Hydrodynamic Loading. *MTS Journal* 4(4):27-44.
- Goldstein, S. 1938. Modern Developments in Fluid Dynamics, p. 425. Oxford: Clarendon Press.
- Hoerner, S.F. 1958. Fluid Dynamic Drag. Published by the author. Brick Town, N.J.
- McCormick, M.E. 1973. Ocean Engineering Wave Mechanics. John Wiley & Sons, N.Y.
- Relf, E.F. and C.H. Powell. 1917. Tests on Smooth and Stranded Wires Inclined to the Wind Direction and a Comparison of Results on Stranded Wires in Air and Water. Advisory Comm. for Aeronautics (Gt. Britain) Reports & Memoranda (New Series) No. 307.
- Schlichting, H. 1960. Boundary Layer Theory. McGraw-Hill, N.Y.
- Schram, J.W. 1968. A Three-Dimensional Analysis of a Towed System. Ph.D. Thesis, Rutgers - The State University, New Brunswick, N.J.
- Taylor, G. 1952. Analysis of the Swimming of Long and Narrow Animals. *Proc. Roy. Soc.*, A214:158-183.
- Topham, D. 1976. Personal communication.

APPENDIX A - BUOY CALCULATIONS

1. Spherical Buoy

(a) Immersed volume:

$$V(z) = \int_{-r}^b C(z) dz$$

where V is immersed volume, C is the area of a horizontal section of the buoy, z is the vertical coordinate (positive upwards), r is the radius of the buoy, and b is the distance from the water surface to the centre of the buoy. The horizontal coordinate is x . Now:

$$C(z) = \pi x^2 = \pi(r^2 - z^2)$$

Therefore:

$$V(z) = \pi \left[r^2 z - \frac{z^3}{3} \right]_{-r}^b$$

$$= \frac{\pi}{3} (3r^2 b - b^3 + 2r^3)$$

where r is given for a particular buoy and the quantity $(r + b)$ is equal to the difference in elevation of the water surface and the bottom of the buoy.

(b) Immersed area:

$$A(z) = \int_{-r}^b 2x dz = \int_{-r}^b 2(r^2 - z^2)^{1/2} dz$$

where A is the immersed area in a vertical plane and the other variables are as given in the previous section. Then:

$$\begin{aligned} A(z) &= \left[z(r^2 - z^2)^{1/2} + r^2 \sin^{-1} \frac{z}{r} \right]_{-r}^b \\ &= b(r^2 - b^2)^{1/2} + r^2 \left(\frac{\pi}{2} + \sin^{-1} \frac{b}{r} \right) \end{aligned}$$

2. Cylindrical Buoy with Horizontal Axis

(a) Immersed area:

The equation for the immersed area in a vertical plane is identical to that given for the spherical buoy, above.

(b) Immersed volume:

$$V(z) = LA(z)$$

where L is the length of the buoy (the average length in the case where cone-shaped end pieces are fastened to the cylinder).

3. Toroidal Buoy

(a) Immersed area:

The immersed area of a toroidal buoy is just twice that of a spherical buoy, where r is now the minor radius of the toroid (i.e., it is the radius of a cylindrical section of the toroid).

(b) Immersed volume:

$$V(z) = 2\pi RA(z)$$

where $A(z)$ is as given for the spherical buoy and R is the major axis of the toroid, i.e., the centreline radius or mean value of the inside and outside radii of the toroid.

APPENDIX B - SAMPLE COMPUTATION

The program is here applied to a system comprised of a toroidal surface float, a synthetic plastic cable, five instruments and a heavy chain anchor to illustrate the procedure. The FORTRAN coding form for this example is given in Table I at the end of this section.

The first data card provides all the information about the buoy type and its specifications. A letter "T" is required in the j-th column to call the j-th buoy subroutine. The remainder of the first five columns, corresponding to other buoy types, should contain the letter "F". In the present case, BUOY3 (toroid) is called. The letter "F" is found in Column 11, indicating that the buoy is at the water surface; a "T" would have been required for a subsurface buoy. Columns 21-30 contain the buoy weight (700.0 lb) in air and Columns 31-40 contain the drag coefficient (1.0). The principal vertical dimension (for displacement - see Appendix A) is listed in Columns 41-50. In this instance, it is the minor radius (1.25 ft) of the toroid. The next two sets of ten columns are available for other pertinent dimensions of the buoy. Here, only one is required, it being the major radius (2.75 ft) of the toroid.

The second data card lists the cable parameters. Columns 1-7 contain the distance from the buoy to the lower end of the cable type, in the unstretched condition. In the present example, only one type of cable is used, with a length of 900.0 ft. The next five sets of seven columns each are used to supply information on, in the order given, the cable buoyancy (0.045 lb/ft), weight (0.050 lb/ft), diameter (0.036 ft), drag coefficient (1.2) for flow in a direction normal to the cable and drag coefficient (0.1) for flow parallel to the cable axis. Beginning in Column 43, there are three sets of ten columns each which contain the coefficients for a second order fit to the fractional stress-strain relationship for the cable. In this instance, the cable is taken to be Samson 2-in-1 nylon. From a graph supplied by the manufacturer, a least squares fit to the working portion of the stress-strain curve was obtained in the form of Equation 13 with $a = 4.48$, $b = 0.675$ and $c = -0.005$. The ultimate stress for a line having a diameter of 0.036 ft (7/16 in.) is 6000 lbs. Thus, in terms of Equation 14, one obtains $a_0 = 1.045$, $a_1 = 1.125 \times 10^{-4}$ and $a_2 = 1.389 \times 10^{-8}$. These are the data which are used on the card in the given sequence. Columns 73-75 contain logical variables used for selecting the form of longitudinal drag equation considered appropriate to the occasion. If a "T" appears in Column 73, Equation 26 is used; if in Column 74, Equation 27 is used; if in Column 75, longitudinal drag is ignored altogether. Up to ten different cable types may be represented in the model, each with its own card for data input. If the number is less than ten, the sequence must be terminated by an end-of-file indication. Hence, the third card here contains @EOF.

The fourth data card indicates, in Column 1, the presence (T) or absence (F) of a length of chain at the lower end of the cable. If, as here, chain is used in the system then seven parameters are given, commencing in Column 11 and occupying ten columns each. These are given in the following order: buoyancy (lb/ft), weight (lb/ft), cross-sectional area (ft²) per ft of length, drag coefficient for normal flow, drag coefficient for axial flow, total length of chain (ft) and the length of chain (ft) over which each

integration is performed. For this example, it is assumed that chain is used in lieu of an anchor. For easier handling, two lengths of 17 lb/ft chain are used together, giving a weight of 34 lb/ft. The buoyancy is about 4 lb/ft and the cross-sectional area is taken as 0.4 ft²/ft. The drag coefficients are not known with any accuracy, but the drag force is small in any case. Here the normal- and longitudinal-flow drag coefficients are assumed to be 1.2 and 0.6, respectively. The increment of chain over which each integration is made is 1 ft. Total length of chain (i.e., of the doubled-up chain) is 40 ft.

The next five data cards provide information about the instrument packages. Up to ten different types of instruments can be used, but five identical current meters are involved here. Columns 1-10 on each card contain the instrument locations in feet from the buoy along the unstretched cable. The instruments must be positioned at multiples of the basic cable segment length, as mentioned in the text. For this example, the segment length will be 20 ft (determined by a subsequent card), and the five instrument locations are 20, 100, 200, 500 and 800 ft. Then Columns 11-20 of each card contain the buoyancy (lbs), Columns 21-30 the weight (lbs), Columns 31-40 the cross-sectional area (ft²) for the drag calculation and Columns 41-50 the drag coefficient. Here, the values for the above parameters are assumed to be 15, 50, 0.7 and 1.0, respectively. Since the number of instrument data cards is less than ten, the next card must be an end-of-file indicator.

Another five cards are used, next, to provide the velocity profile information. Each card lists up to four numbers, each number occupying ten columns. The last three numbers are the coefficients for a second order velocity vs depth equation of the form $v = a + bz + cz^2$. The first number is the lower limit of applicability of the coefficients, given in feet above bottom. If fewer than five segments (cards) are used, they must be followed by an end-of-file card. The easiest way of determining the coefficients is to graph the desired velocity profile, for clarity, then obtain a zero-, first- or second-order fit to each segment separately. In the present example, the current speed is 0.83 ft/sec from the bottom to a height of 600 ft above bottom. It then increases linearly to 1.64 ft/sec at 700 ft. It remains constant at this value for another 100 ft, and from 800 to 900 ft it increases linearly to 5 ft/sec. Above 900 ft, the speed remains constant at 5 ft/sec.

The sixteenth card in this data deck contains the desired number of cable segments in Columns 1-10, the cable length (ft) in Columns 11-20 and the integration error tolerance in Columns 21-30. The number of segments is here taken as 45, with a cable length of 900 ft, resulting in a segment length of 20 ft, as mentioned above. The integration error tolerance is required by the integration subroutine. Too large a value reduces the computational accuracy and too small a value increases the computation time. A value of 0.1 appears reasonable in this application. Column 31 contains the value of a logical variable which, if given as "T", will result in the printing of various data as a diagnostic aid, when required.

The seventeenth data card contains, in Columns 1-10, an initial estimate or guess of the buoy position in feet above bottom. The value of

this guess can be almost any number because the iteration procedure usually ensures a rapid approach to the correct position. However, for a subsurface buoy a reasonable value to use is that of the cable length, and for a surface buoy one could assume that it is immersed to about one-half of its height. Columns 11-20 list the permissible iteration error (ft) for the anchor position. An accuracy equivalent to one-tenth of one percent of the total cable length appears to be a reasonable requirement. Columns 21-30 give the elevation of the water surface in feet above bottom. For this example, the water depth is 960 ft, the permissible iteration error is 1 ft and the buoy elevation is estimated to be 958.8 ft.

After the program is run, the listings mentioned in the section on Program Output are produced. These are shown in Table II for the given example. The initial guess for the buoy elevation was too low, as indicated by the resulting large negative value for the anchor position, seen under the column headed Y(3). The iteration procedure then provided a rather ludicrous second estimate (in the column headed ZED) for the buoy elevation, since the suggested value put the buoy above the water surface. However, the buoy subroutine recognized this and substituted a more reasonable value before commencing on the first iteration. Note from the results how a small change in elevation, for a surface buoy, can result in a large change in anchor position.

TABLE II - Output Listing for Mooring Program Example

NO. OF CABLE SEGMENTS = 45.
 INTEGRATION ERROR TOLERANCE = .10000
 PERMISSIBLE ITERATION ERROR = 1.00 FT
 INITIAL GUESS FOR BUOY POSITION = 958.80 FT ABOVE BOTTOM

ZED	Y(3)	ZMAX	ZLOW	YMAX	YMIN
958.80	-154.87				
1113.67	-154.87	1268.55	958.80	154.87	-154.87
959.37	255.93				
959.10	255.93	1268.55	958.80	154.87	-154.87
959.10	-54.33				
959.19	-54.33	1268.55	959.10	154.87	-54.33
959.19	-11.35				
959.21	-11.35	1268.55	959.19	154.87	-11.35
959.21	3.75				
959.20	3.75	959.21	959.19	3.75	-11.35
959.20	-2.23				
959.21	-2.23	959.21	959.20	3.75	-2.23
959.21	1.21				
959.21	1.21	959.21	959.20	1.21	-2.23
959.21	-.63				

NO. OF ITERATIONS REQUIRED WAS 7 .

TABLE II (Continued)

BUOY PARAMETERS :

BUOYANCY = 1483.389 LBS
 WEIGHT IN AIR = 700.000 LBS
 KB = 1.250 FT
 KC = 2.750 FT
 KD = .000 FT
 DRAG COEFFICIENT = 1.000
 BUOY TYPE IS TOROIDAL.
 BUOY COORDINATES (336.43 , 959.21).
 VERTICAL EXCURSION = -59.21 FT
 BUOY DRAG IS 67.07 LBS.
 BUOY IS IMMersed TO A DEPTH OF .795 FT.

CABLE PARAMETERS - TYPE 1 :

BUOYANCY = .0450 LBS PER FT
 WEIGHT IN AIR = .0500 LBS PER FT
 DIAMETER = .0360 FT
 NORMAL DRAG COEFFICIENT = 1.2000
 AXIAL DRAG COEFFICIENT = .1000
 ELASTIC COEFFICIENTS: A0 = .1045+001 ; A1 = .1125-003 ; A2 = -.1389-007
 LENGTH = 900.000 FT.

TOTAL LENGTH OF CABLE = 900.000 FT.

INSTRUMENT PARAMETERS - NO. 1 :

DISTANCE ALONG UNSTRETCHED CABLE FROM BUOY = 20. FT
 BUOYANCY = 15.000 LBS
 WEIGHT IN AIR = 50.000 LBS
 CROSS-SECTIONAL AREA = .700 SQ FT
 DRAG COEFFICIENT = 1.000
 INSTRUMENT DRAG IS 17.50 LBS
 INSTRUMENT COORDINATES (336.16 , 936.82).

TABLE II (Continued)

VERTICAL EXCURSION =	-50.82	FT
INSTRUMENT PARAMETERS - NO. 2 :		
DISTANCE ALONG UNSTRETCHED CABLE FROM BUOY =	100.	FT
BUOYANCY =	15.000	LBS
WEIGHT IN AIR =	50.000	LBS
CROSS-SECTIONAL AREA =	.700	SQ FT
DRAG COEFFICIENT =	1.000	
INSTRUMENT DRAG IS	7.48	LBS
INSTRUMENT COORDINATES (317.91 ,	848.93)
VERTICAL EXCURSION =	-48.93	FT
INSTRUMENT PARAMETERS - NO. 3 :		
DISTANCE ALONG UNSTRETCHED CABLE FROM BUOY =	200.	FT
BUOYANCY =	15.000	LBS
WEIGHT IN AIR =	50.000	LBS
CROSS-SECTIONAL AREA =	.700	SQ FT
DRAG COEFFICIENT =	1.000	
INSTRUMENT DRAG IS	1.88	LBS
INSTRUMENT COORDINATES (285.92 ,	741.64)
VERTICAL EXCURSION =	-41.64	FT
INSTRUMENT PARAMETERS - NO. 4 :		
DISTANCE ALONG UNSTRETCHED CABLE FROM BUOY =	500.	FT
BUOYANCY =	15.000	LBS
WEIGHT IN AIR =	50.000	LBS
CROSS-SECTIONAL AREA =	.700	SQ FT
DRAG COEFFICIENT =	1.000	
INSTRUMENT DRAG IS	.48	LBS
INSTRUMENT COORDINATES (175.98 ,	425.36)
VERTICAL EXCURSION =	-25.36	FT

TABLE II (Continued)

INSTRUMENT PARAMETERS - NO. 5 :

DISTANCE ALONG UNSTRETCHED CABLE FROM BUOY = 800. FT
 BUOYANCY = 15.000 LBS
 WEIGHT IN AIR = 50.000 LBS
 CROSS-SECTIONAL AREA = .700 SQ FT
 DRAG COEFFICIENT = 1.000
 INSTRUMENT DRAG IS .48 LBS
 INSTRUMENT COORDINATES (X, Y) = 55.29 , 114.03)
 VERTICAL EXCURSION = -14.03 FT

VELOCITY PROFILE :

LOWER LIMIT (FT ABOVE BOTTOM)	COEF(0)	COEF(1)	COEF(2)	VELOCITY (FT/SEC)
900.	.5000+001	.0000	.0000	5.00
800.	-.2500+002	.3330-001	.0000	1.64
700.	.1640+001	.0000	.0000	1.64
600.	-.4150+001	.8330-002	.0000	.85
0.	.8300+000	.0000	.0000	.83

CHAIN PARAMETERS :

BUOYANCY = 4.000 LBS PER FT
 WEIGHT IN AIR = 34.000 LBS PER FT
 DRAG CROSS-SECTION AREA = .400 SQ FT PER FT LENGTH
 NORMAL DRAG COEFFICIENT = 1.200
 AXIAL DRAG COEFFICIENT = .600
 TOTAL LENGTH = 40.000 FT
 INCREMENT LENGTH FOR INTEGRATION = 1.000 FT
 LENGTH OF CHAIN ON BOTTOM = 22.000 FT

Table II (Continued)

TABLE OF CABLE COORDINATES, LENGTH, DEFLECTIONS, ANGLES & DRAG :						
X (FT)	Z (FT)	S (FT)	T (LB)	PHI (DEG)	NORMAL DRAG (LB/FT)	AXIAL DRAG (LB/FT)
333.43	959.21	1022.06	786.26	85.11		
336.16	936.82	999.56	786.29	83.30	1.098	.0077
332.54	914.62	977.06	754.01	79.81	1.078	.0116
328.22	892.60	954.62	754.18	77.98	1.065	.0136
323.29	870.71	932.18	754.33	76.61	.802	.0123
317.91	848.93	909.74	754.44	75.66	.554	.0100
311.75	827.35	887.30	722.63	73.77	.351	.0081
305.43	805.88	864.92	722.64	73.41	.200	.0054
299.00	784.44	842.54	722.61	73.21	.112	.0035
292.50	763.03	820.16	722.59	73.00	.112	.0036
285.92	741.64	797.78	722.56	72.80	.112	.0036
278.89	720.39	775.40	689.77	71.59	.110	.0039
271.80	699.23	753.08	689.75	71.38	.110	.0039
264.03	678.09	730.76	689.73	71.19	.103	.0038
257.41	656.97	708.44	689.69	71.03	.081	.0032
250.13	635.87	686.12	689.65	70.91	.063	.0026
242.82	614.70	663.80	689.59	70.82	.046	.0021
235.47	593.71	641.48	689.52	70.76	.032	.0016
228.11	572.64	619.16	689.44	70.70	.029	.0015
220.72	551.57	596.84	689.37	70.65	.029	.0015
213.32	530.52	574.52	689.30	70.59	.029	.0015
205.89	509.47	552.21	689.23	70.54	.028	.0015
198.44	488.43	529.89	689.15	70.48	.028	.0015
190.98	467.40	507.57	689.08	70.42	.028	.0015
183.49	446.36	485.25	689.01	70.37	.028	.0015
175.96	425.36	462.93	688.94	70.31	.028	.0015
168.00	404.49	440.61	656.19	69.19	.028	.0016
160.14	383.69	418.36	656.12	69.13	.028	.0016
152.20	362.90	396.10	656.05	69.07	.028	.0016
144.24	342.12	373.84	655.98	69.01	.028	.0016
136.20	321.34	351.59	655.91	68.95	.028	.0016
128.25	300.57	329.33	655.84	68.90	.028	.0016
120.23	279.81	307.07	655.78	68.84	.028	.0016

Table II (Continued)

112.18	259.06	284.82	655.71	68.78	.028	.0016
104.12	238.32	262.56	655.64	68.72	.028	.0016
96.03	217.58	240.31	655.57	68.67	.028	.0016
87.93	196.86	218.05	655.50	68.61	.028	.0016
79.80	176.14	195.80	655.44	68.55	.028	.0016
71.65	155.43	173.54	655.37	68.49	.028	.0016
63.48	134.73	151.28	655.30	68.44	.028	.0016
55.29	114.03	129.03	655.23	68.38	.028	.0016
46.64	93.53	106.77	622.95	67.09	.027	.0017
37.99	73.09	84.58	622.89	67.03	.027	.0017
29.32	52.66	62.39	622.82	66.97	.027	.0017
20.82	32.24	40.19	622.76	66.91	.027	.0017
11.91	11.83	18.00	622.69	66.85	.027	.0017
11.51	10.91	17.00	595.26	65.69	.275	.0280
11.09	10.01	16.00	568.08	64.42	.269	.0308
10.64	9.11	15.00	541.21	63.02	.263	.0340
10.18	8.23	14.00	514.70	61.47	.255	.0377
9.69	7.35	13.00	488.59	59.76	.247	.0419
9.17	6.50	12.00	462.97	57.86	.237	.0468
8.62	5.66	11.00	437.91	55.75	.226	.0524
8.04	4.85	10.00	413.52	53.37	.213	.0588
7.43	4.06	9.00	389.92	50.71	.198	.0663
6.78	3.30	8.00	367.27	47.72	.181	.0748
6.08	2.56	7.00	345.75	44.34	.162	.0846
5.34	1.91	6.00	325.58	40.54	.140	.0955
4.56	1.26	5.00	307.04	36.25	.116	.1075
3.73	.73	4.00	290.43	31.46	.090	.1203
2.86	.24	3.00	276.09	26.12	.064	.1333
1.94	-.15	2.00	264.40	20.26	.040	.1455
.98	-.44	1.00	255.72	13.93	.019	.1558
.00	-.63	.00	250.36	7.25	.005	.1627

FINAL VERTICAL TENSION COMPONENT = 31.59 LB
 FINAL HORIZONTAL TENSION COMPONENT = 248.36 LB

APPENDIX C - PROGRAM SOURCE LISTING

A complete source listing for the main program and all subroutines is given in the following pages.

C--SURFACE & SUBSURFACE SINGLE-POINT MOORED BUOY PROGRAM

W. H. BELL - 1977

C--THIS ROUTINE CALCULATES CABLE SHAPE, TENSION, DRAG AND ANGLE.

C--ORIGIN OF THE SYSTEM IS AT THE BUOY FOR THE INITIAL CALCULATIONS,
C AND AT THE ANCHOR FOR THE LIST.

C CABLE ANGLE IS REFERRED TO THE HORIZONTAL.

C IF MORE THAN 300 DEPTH SEGMENTS ARE REQUIRED, ALL OF THE
C ARRAY DIMENSIONS MUST BE INCREASED ACCORDINGLY.

C--DENSITY OF WATER IS TAKEN AS 2 SLUGS PER CU.FT., I.E. $\text{RHO}/2 = 1$.
C KINEMATIC VISCOSITY IS 0.000015 SQ FT/SEC.

C--NOMENCLATURE :

BB - BUOY BUOYANCY (LBS)

WB - BUOY WEIGHT IN AIR (LBS)

AB - BUOY CROSS-SECTIONAL AREA (SQ FT)

CD - BUOY DRAG COEFFICIENT

DB - DRAG FORCE ON BUOY (LBS)

B() - BUOY TYPE

RB - VERTICAL DIMENSION OF BUOY

ZED - VERTICAL DISTANCE OF BUOY ABOVE BOTTOM.

BC - CABLE BUOYANCY (LBS PER FT)

WC - CABLE WEIGHT (LBS PER FT)

CP - CABLE DRAG COEFFICIENT FOR NORMAL FLOW

CL - CABLE DRAG COEFFICIENT FOR AXIAL FLOW

D() - DRAG TYPE

DIAC - CABLE DIAMETER (FT)

STRCH - STRETCHED LENGTH OF UNIT CABLE

ZCBL - TOTAL CABLE LENGTH (FT)

CHLZ - DISTANCE FROM BUOY TO END OF CABLE TYPE

A() - ELASTIC COEFFICIENTS FOR CABLE

```

CABLE - ARRAY OF CABLE PARAMETERS
NSEG - NO. OF CABLE SEGMENTS USED IN CALCULATIONS
DELZ - LENGTH OF CABLE SEGMENT
X - INDEPENDENT VARIABLE - CABLE LENGTH
Y(1) - CABLE ANGLE (RADIAN)
Y(2) - CABLE TENSION (LBS)
Y(3) - CABLE Z-COORDINATE (FT)
Y(4) - CABLE X-COORDINATE (FT)

BCH - CHAIN BUOYANCY (LBS PER FT)
WCH - CHAIN WEIGHT (LBS PER FT)
CNCH - CHAIN DRAG COEFFICIENT FOR NORMAL FLOW
CTCH - CHAIN DRAG COEFFICIENT FOR AXIAL FLOW
DCH - CHAIN CROSS-SECTION AREA PER FT LENGTH
ZCHN - TOTAL CHAIN LENGTH (FT)
LINK - CHAIN INCREMENT (FT) FOR INTEGRATION

BI - INSTRUMENT BUOYANCY (LBS)
WI - INSTRUMENT WEIGHT (LBS)
AI - INSTRUMENT CROSS-SECTIONAL AREA (SQ FT)
CI - INSTRUMENT DRAG COEFFICIENT
DI - DRAG FORCE ON INSTRUMENT (LBS)
DELPH - INCREMENT IN CABLE ANGLE DUE TO INSTR.
INSTR - ARRAY OF INSTRUMENT PARAMETERS

VEL - WATER VELOCITY (FT PER SEC)
RN - REYNOLDS NO.
N - NO. OF SIMULTANEOUS EQUATIONS
E - INTEGRATION ERROR TOLERANCE
SURF - WATER SURFACE ELEVATION
LOOP - NO. OF ITERATIONS REQUIRED.
IT - PERMISSIBLE ITERATION ERROR

IMPLICIT REAL*8 ( A-H,O-Z )
DIMENSION IDEPTH(300)/300*0/, Y(4), F(4), G(4), S(4),
+T(4), SAVE(16), XXI(10), ZZI(10), XX(301), ZZ(301),
+CUIS(301), TENS(301), PHI(301), VP(4,5)/20*0.000/,
+JDEPTH(300)/300*0/,DRGIN(301),DRGL(301)

```

```

REAL*8 IDRG(10), NSEG, MIDZ, MERS, LINK, LCHN, IT,
+CABLE(9,10)/90*0.0D0/, INSTR(5,10)/50*0.0D0/
LOGICAL SUB,B1,B2,B3,B4,B5,D1,D2,D3,FLAG/.FALSE./,TRBL/.FALSE./,
+DRAG(3,10)
COMMON /ALL/ VEL,PI
COMMON /RKFN/ DN,DL,CP,CL,DIAC,GAMMA,D1,D2,D3
COMMON /RKCH/ CNCH,DCH,WCH,BCH,CTCH
COMMON /BUOY/ RB,RC,RD,SURF,YY,ZCBL,CD,ZED
EXTERNAL FUNC,FCHN

C
C--READ BUOY PARAMETERS.
C A LETTER T IN COLUMN J CALLS BUOY(J) SUBROUTINE. (B1-SPHERICAL,
C B2-CYLINDRICAL, B3-TOROIDAL, B4 & B5 NOT PRESENTLY USED.) OTHER 4
C OF 5 COLUMNS REQUIRE F.
C SUB IS T FOR SUBSURFACE OR F FOR SURFACE BUOY.
C RB IS A VERTICAL DIMENSION. RC & RD ARE 2 OTHER DIMENSIONS
C DESCRIBING BUOY GEOMETRY, IF REQUIRED.
C
C READ(5,40) B1,B2,B3,B4,B5,SUB,WB,CD,RB,RC,RD
C 40 FORMAT(5L1,5X,L1,9X,5F10.2)
C
C--READ CABLE PARAMETERS.
C ONE CARD FOR EACH CABLE TYPE, IN CORRECT SEQUENCE STARTING AT THE
C BUOY. ORDER OF PARAMETERS IS CBLZ,BC,WC,DIAC,CP,CL,A0,A1,A2,D1,D2,D3.
C CBLZ IS THE DISTANCE FROM THE BUOY TO THE LOWER END OF THE CABLE
C TYPE. THE LENGTH OF EACH TYPE MUST BE A MULTIPLE OF DELZ.
C A0,A1,A2, ARE COEFFICIENTS FOR A SECOND ORDER FIT TO A FRACTIONAL
C STRAIN VS. STRESS RELATIONSHIP.
C D1,D2,D3 ARE LOGICAL FLAGS FOR AXIAL DRAG ROUTINES. (D1-SMOOTH,
C D2-ROUGH,D3-NONE.)
C LAST CARD MUST BE @EOF UNLESS ARRAY IS FILLED.
C
C 50 54 J=1,10
C READ(5,50,END=34) (CABLE(I,J),I=1,9),(DRAG(K,J),K=1,3)
C 50 FORMAT(6F7.2,3E10.4,3L1)
C 54 CONTINUE
C
C--READ FLAG & CHAIN PARAMETERS.

```

```

C IF FLAG IS TRUE, THERE IS A LENGTH OF CHAIN AT THE LOWER END OF THE
C CABLE. SEE NOMENCLATURE FOR EXPLANATION OF VARIABLES.
C
  34 READ(5,303) FLAG,BCH,WCH,DCH,CNCH,CTCH,ZCHN,LINK
  303 FORMAT(L1,9X,7F10.2)
C
C--READ INSTRUMENT PARAMETERS.
C ONE CARD FOR EACH INSTRUMENT, IN CORRECT SEQUENCE FROM BUOY.
C ORDER OF PARAMETERS IS INSTZ,BI,WI,AI,CI. INSTZ IS THE LOCATION
C OF THE INSTRUMENT IN FEET ALONG THE CABLE FROM THE BUOY.
C INSTRUMENTS MUST BE POSITIONED AT MULTIPLES OF DELZ.
C LAST CARD MUST BE @EOF UNLESS ARRAY IS FILLED.
C
  READ(5,145,END=15) INSTR
  145 FORMAT(5F10.2)
C
C--READ VELOCITY PROFILE INFORMATION.
C THE LAST THREE NUMBERS ARE THE COEFFICIENTS FOR A SECOND ORDER
C VELOCITY VS. DEPTH EQUATION. THE FIRST NUMBER IS THE LOWER LIMIT OF
C APPLICABILITY, ZMIN (POSITIVE FT ABOVE BOTTOM), OF THE EQUATION.
C LAST CARD MUST BE @EOF UNLESS ARRAY IS FILLED.
C
  15 READ (5,121,END=123) VP
  121 FORMAT(F10.0,3E10.4)
C
C--READ NO. OF CABLE SEGMENTS, CABLE LENGTH, ERROR TOLERANCE & LOGICAL
C FLAG. IF TRBL IS SET, DRKC VALUES WILL BE LISTED FOR DIAGNOSTIC USE.
C
  123 READ(5,60) NSEG,ZCBL,E,TRBL
  60 FORMAT(2F10.2,F10.5,L1)
C
C--READ A FIRST ESTIMATE OF THE BUOY POSITION IN FEET ABOVE
C BOTTOM, THE PERMISSIBLE ITERATION ERROR & THE WATER SURFACE
C ELEVATION IN FEET ABOVE BOTTOM.
C
  READ(5,122) ZED,IT,SURF
  122 FORMAT(3F10.2)
C

```

```

      WRITE(6,102) NSEG,E
102  FORMAT('1',//,' NO. OF CABLE SEGMENTS =',
      +F10.0,//,' INTEGRATION ERROR TOLERANCE =',F10.5,/)
C
      WRITE(6,31) IT,ZED
31  FORMAT(' ','PERMISSIBLE ITERATION ERROR =',F10.2,3X,'FT',//,1X,
      + 'INITIAL GUESS FOR BUOY POSITION =',F10.2,3X,'FT ABOVE BOTTOM',//)
C
      WRITE(6,206)
206  FORMAT(' ','5X,ZED',9X,'Y(3)',9X,'ZMAX',9X,'ZLOW',9X,
      + 'YMAX',9X,'YMIN',/)
C
C--INITIALIZE SOME ITEMS.
C
      Z=ZCBL
      X=0.0D0
      PI=3.141593D0
      RAD=PI/180.D0
      ZINC=0.0D0
      LOOP=0
      YY=Y(3)
      DELZ=-(Z-X)/NSEG
C
C--LOAD AN ARRAY INDICATING THE INSTRUMENT LOCATIONS FOR
C  SUBSEQUENT PROCESSING ROUTINES
C
      DO 75 J=1,10
      II=-DELZ
      JJ=INSTR(1,J)
      K=JJ/II
      IF(K) 75,75,85
85  IDEPTH(K+1)=J
75  CONTINUE
C
C--LOAD AN ARRAY INDICATING THE LOCATION OF
C  CHANGES IN CABLE MATERIAL.
C
      DO 46 J=1,10

```

```

II=-DELZ
JJ=CABLE(1,J)
K=JJ/II
IF(K) 46,46,47
47 JDEPTH(K)=J+1
46 CONTINUE
C-----ITERATIVE LOOP BEGINS HERE-----
C
C--CALCULATE THE VELOCITY AT THE BUOY.
C
245 DO 200 I=1,5
    ZMIN=VP(1,I)
    IF(ZMIN-ZED) 210,200,200
210 VEL=VP(2,I)+VP(3,I)*ZED+VP(4,I)*ZED*ZED
    GO TO 220
200 CONTINUE
C
C--EMPTY THE STORAGE ARRAYS.
C XXI & ZZI ARE INSTRUMENT COORDS. IDRG IS INSTRUMENT DRAG. XX & ZZ ARE
C CABLE COORDS. TENS IS CABLE TENSION. PHI IS CABLE ANGLE. CDIST IS
C DISTANCE ALONG THE CABLE FROM THE BUOY (STRETCHED DISTANCE, IF
C APPLICABLE). CDRG IS THE AVERAGE DRAG FORCE ON A CABLE SEGMENT,
C RESOLVED HORIZONTALLY.
C
220 DO 32 I=1,301
    CDIST(I)=0.0D0
    TENS(I)=0.0D0
    PHI(I)=0.0D0
    DRGN(I)=0.0D0
    DRGL(I)=0.0D0
    XX(I)=0.0D0
    ZZ(I)=0.0D0
    DO 35 I=1,10
        IDRG(I)=0.0D0
        XXI(I)=0.0D0
        ZZI(I)=0.0D0
32
35

```

```

C--CALCULATE BUOY DRAG & BUOYANCY. ADD MORE SUBROUTINES AS REQUIRED.
C
    IF(B1) CALL BUOY1(HB,DB)
    IF(B2) CALL BUOY2(HB,DB)
    IF(B3) CALL BUOY3(HB,DB)
C
C--DETERMINE INITIAL VALUES FOR CABLE ANGLE,TENSION & COORDINATES
C AT THE BUOY END OF THE CABLE
C
    A=BB-WB
    IF(DB.EQ.0.0D0) GO TO 3
    IF(A) 1,92,92
    1 IF(SUB) GO TO 93
    2 IF(SURF.GE.(ZED+2.0D0*RB)) GO TO 91
    ZINC=ZINC+RB/2.0D0
    ZED=ZED-ZINC
    GO TO 245
    92 Y(1)=DATAN2(A,DB)
    GO TO 90
    3 IF(ZCBL.GE.SURF) GO TO 86
    IF(A) 1,1,83
    83 Y(1)=PI/2.0D0
    90 Y(2)=(A*DB*DB)**0.5D0
    Y(3)=ZED
    Y(4)=0.0D0
    X=0.0D0
    XX(1)=Y(4)
    ZZ(1)=Y(3)
    YDEG=Y(1)/RAD
    CDIST(1)=X
    TENS(1)=Y(2)
    PHI(1)=YDEG
    PRIORX=0.0D0
C
C--INITIALIZE CABLE PARAMETERS.
C
    JJ=1
    BC=CABLE(2,JJ)

```

```

WC=CABLE(3,JJ)
UIAC=CABLE(4,JJ)
CP=CABLE(5,JJ)
CL=CABLE(6,JJ)
A0=CABLE(7,JJ)
A1=CABLE(8,JJ)
A2=CABLE(9,JJ)
D1=DRAG(1,JJ)
D2=DRAG(2,JJ)
D3=DRAG(3,JJ)
GAMMA=WC-BC

C
C--PARAMETERS REQUIRED BY DRKC ROUTINE FOR SIMULTANEOUS D.E.'S
C
      N=4
      STRCH=A0+A1*Y(2)+A2*Y(2)*Y(2)
      Z=DELZ*STRCH
      H=(Z-X)/64.000
      HMIN=.0001D0*H

C
C-----INTEGRATION LOOP BEGINS HERE-----
C
      K=IDFIX(NSEG)
      DO 10 J=1,K

C
C--IF THERE IS AN INSTRUMENT AT THE UPPER END OF A CABLE SEGMENT,
C  CALCULATE THE VELOCITY THERE.
C
      IF(IDEPH(J)) 106,106,107
107  DO 250 I=1,5
      ZMIN=VP(1,I)
      IF(ZMIN-Y(3)) 255,250,250
255  VEL=VP(2,I)+VP(3,I)*Y(3)+VP(4,I)*Y(3)*Y(3)
      GO TO 105
250  CONTINUE

C
C--SET INSTRUMENT PARAMETERS & CALCULATE THE DRAG
C

```

```

105 JJ=IDEPH(J)
    BI=INSTR(2,JJ)
    WI=INSTR(3,JJ)
    AI=INSTR(4,JJ)
    CI=INSTR(5,JJ)
    DI=CI*AI*VEL*DABS(VEL)
C
C-- CALCULATE CHANGE IN ANGLE & TENSION DUE TO INSTRUMENT
C
    DELP=(WI-BI)*DSIN(Y(1))-DI*DCOS(Y(1))
    DELN=(WI-BI)*DCOS(Y(1))+DI*DSIN(Y(1))
    DEL1=Y(2)-DELP
    DELPH=DATAN2(DELN,DEL1)
    Y(2)=DELN/DSIN(DELP)
    Y(1)=Y(1)-DELP
    YDEG=Y(1)/RAD
    6 IF (YDEG) 97,96,96
C
C--LOAD INSTRUMENT COORDINATE ARRAY
C
    96 IDRG(JJ)=DI
    XXI(JJ)=Y(4)
    ZZI(JJ)=Y(3)
C
C--CALCULATE THE VELOCITY AT THE CABLE MIDPOINT (APPROXIMATELY).
C
    106 STRCH=A0+A1*Y(2)+A2*Y(2)*Y(2)
    MIDZ=Y(3)+(DELZ*STRCH*DSIN(Y(1)))/2.D0
    DO 108 I=1,5
    ZMIN=VP(1,I)
    IF(ZMIN-MIDZ) 109,108,108
    109 VEL=VP(2,I)+VP(3,I)*MIDZ+VP(4,I)*MIDZ*MIDZ
    GO TO 265
    108 CONTINUE
C
    265 IF(.NOT.TRBL) GO TO 260
    WRITE(6,11) X,Z,Y,VEL
    11 FORMAT(' ', ' IN:',3X,'X=',F10.4,2X,'Z=',F10.4,2X,'Y1=',F10.4,

```

```

C      +2X,'Y2=',F10.4,2X,'Y3=',F10.4,2X,'Y4=',F10.4,2X,'VEL=',F10.4)
C
C--CALCULATE THE DEPENDENT VARIABLES.
C  DRKC CALLS SUBROUTINE FUNC & RETURNS VALUES FOR Y(I).
C
C      260  CALL DRKC(N,X,Z,Y,F,H,HMIN,E,FUNC,G,S,T)
C
C      IF(.NOT.TRBL) GO TO 12
C      WRITE(6,13) X,Z,Y,F
C      13  FORMAT(' ',OUT:',2(4X,F10.4),4(5X,F10.4),/,6X,
C      +F1=',F10.4,2X,'F2=',F10.4,2X,'F3=',F10.4,2X,'F4=',F10.4)
C
C--CHECK FOR TOO SMALL A CABLE ANGLE.
C
C      12  YDEG=Y(1)/RAD
C      IF(YDEG) 4,95,95
C      4  IF(SUB) GO TO 22
C      5  GO TO 84
C
C--LOAD CABLE COORDINATE ARRAY. (SEE AFTER LABEL 200 FOR LIST.)
C
C      95  STRCH=A0+A1*Y(2)+A2*Y(2)*Y(2)
C      Z=Z+DELZ*STRCH
C      L=J+1
C      XX(L)=Y(4)
C      ZZ(L)=Y(3)
C      CDIST(L)=X
C      TENS(L)=Y(2)
C      PHI(L)=YDEG
C      DRGN(L)=DN
C      DRGL(L)=DL
C      PRIORX=X
C
C--CHECK FOR CHANGE IN CABLE TYPE.
C
C      IF(JDEPTH(J)) 10,10,49
C      49  JJ=JDEPTH(J)
C      BC=CABLE(2,JJ)

```

```

WC=CABLE(3,JJ)
DIAC=CABLE(4,JJ)
CP=CABLE(5,JJ)
CL=CABLE(6,JJ)
A0=CABLE(7,JJ)
A1=CABLE(8,JJ)
A2=CABLE(9,JJ)
D1=DRAG(1,JJ)
D2=DRAG(2,JJ)
D3=DRAG(3,JJ)
GAMMA=WC-BC
10 CONTINUE
C
YZ=Y(2)*DSIN(Y(1))
YX=Y(2)*DCOS(Y(1))
SVCBL=X
LC=L
C
C--IF FLAG IS SET,DO CHAIN ROUTINE
C
IF(.NOT.FLAG) GO TO 308
Z=X
Z=Z-LINK
LC=LC+1
IF(LC.GT.301) GO TO 308
CALL DRKC(N,X,Z,Y,F,H,HMIN,E,FCHN,G,S,T)
UN=CNCH*DCH*VEL*DABS(VEL)*DSIN(Y(1))*DSIN(Y(1))
DL=CTCH*DCH*VEL*DABS(VEL)*DCOS(Y(1))*DCOS(Y(1))
YDEG=Y(1)/RAD
IF(YDEG.LT.0.000) STOP 100
XX(LC)=Y(4)
ZZ(LC)=Y(3)
CUIST(LC)=X
TENS(LC)=Y(2)
PHI(LC)=YDEG
DRGN(LC)=DN
DRGL(LC)=DL
PRIORX=X
309

```

```

YZ=Y(2)*DSIN(Y(1))
YX=Y(2)*DCOS(Y(1))
IF(YZ-WCH*LINK) 308,308,309
308 CONTINUE
    SVCHN=X
C
    WRITE(6,189) ZED,Y(3)
189 FORMAT(F10.2,3X,F10.2)
C
C-- DETERMINE IF AN ITERATION IS NECESSARY.
C
    L=LOOP+1
    SAVE(L)=ZED
    IF(Y(3)) 270,275,280
270 ERR=Y(3)+IT
    IF(ERR) 285,275,275
280 ERR=Y(3)-IT
    IF(ERR) 275,275,285
C
C--ITERATION PROCEDURE
C
285 IF(LOOP-1) 286,287,287
286 IF(Y(3).LT.0.0D0) GO TO 146
    IF(Y(3).GT.0.0D0) GO TO 147
146 YMAX=-Y(3)
    YMIN=Y(3)
    ZMAX=ZED-2.0D0*Y(3)
    ZLOW=ZED
    GO TO 146
147 YMAX=Y(3)
    YMIN=-Y(3)
    ZMAX=ZED
    ZLOW=ZED-2*Y(3)
    ZED=ZED-Y(3)
148 GO TO 201
287 SAVE2=SAVE(L-1)
    IF(Y(3).GT.0.0D0.AND.Y(3).LT.YMAX) GO TO 141
    IF(Y(3).GT.0.0D0.AND.Y(3).GT.YMAX) GO TO 142

```

```

141 IF(Y(3).LT.0.0D0.AND.Y(3).GT.YMIN) GO TO 143
    IF(Y(3).LT.0.0D0.AND.Y(3).LT.YMIN) GO TO 144
    ZMAX=ZED
    YMAX=Y(3)
    GO TO 111
142 ZED=ZLOW+Y(3)*RB/BB
    GO TO 204
143 ZLOW=ZED
    YMIN=Y(3)
    GO TO 111
144 ZED=ZMAX+Y(3)*RB/BB
    GO TO 204
111 IF(SUB) GO TO 29
    ZED=ZED-Y(3)*DABS(ZED-SAVEZ)/(DABS(Y(3))+DABS(SAVEY))-Y(3)*RB/BB
    GO TO 204
29 ZED=ZED-Y(3)*(ZED-SAVEZ)/(Y(3)-SAVEY)-Y(3)*RB/BB
204 IF(ZED.LE.ZLOW) ZED=ZMAX-Y(3)*RB/BB
    IF(ZED.GE.ZMAX) ZED=ZLOW-Y(3)*RB/BB
    IF(LOOP-15) 201,201,202
202 WRITE(6,203)
203 FORMAT('0',' PROGRAM TERMINATED BECAUSE THE NO. OF ITERATIONS EXCE
    +EDS 15.,/, MAKE A BETTER GUESS & TRY AGAIN.',/)
    GO TO 300
201 LOOP=LOOP+1
    WRITE(6,65) ZED,Y(3),ZMAX,ZLOW,YMAX,YMIN
65 FORMAT(6(F10.2,3X),/)
    SAVEY=Y(3)
    GO TO 245
275 CONTINUE
    LCHN=ZCHN-SVCBL+SVCHN
    XRV=XX(LC)
    CBLMX=-CDIST(LC)
C
C--PRINT THE NO. OF ITERATIONS REQUIRED.
C
C
    WRITE(6,33) LOOP
33 FORMAT('0',' NO. OF ITERATIONS REQUIRED WAS',I5,1X,'.',.,//)
C

```

```

C--LIST ALL PARAMETERS
C
C--PRINT BUOY DATA.
C
300 WRITE(6,100) BB,WB,RB,RC,RD,CD
100 FORMAT('1BUOY PARAMETERS :',/,/, BUOYANCY =,F10.3,3X,'LBS',/,
+ ' WEIGHT IN AIR =,F10.3,3X,'LBS',/,/, RB =,F10.3,3X,'FT',/,
+ ' RC =,F10.3,3X,'FT',/,/, RD =,F10.3,3X,'FT',/,
+ ' DRAG COEFFICIENT =,F10.3)
C
51 IF(B1) WRITE(6,51)
   FORMAT(' BUOY TYPE IS SPHERICAL.')
52 IF(B2) WRITE(6,52)
   FORMAT(' BUOY TYPE IS CYLINDRICAL WITH HORIZONTAL AXIS.')
53 IF(B3) WRITE(6,53)
   FORMAT(' BUOY TYPE IS TOROIDAL.')
C
   XXB=XX(1)-XRV
   EXC=ZCBL-ZZ(1)
   WRITE(6,76) XXB,ZZ(1),EXC,DB
76  FORMAT(' BUOY COORDINATES (,F10.2,1X',/,/,F10.2,1X',/,/,
+ ' VERTICAL EXCURSION =,F10.2,2X,'FT',/,
+ ' BUOY DRAG IS, F10.2,2X,'LBS.')
C
   IF(SUB) GO TO 77
   IF(SURF-2.*RB-ZED) 61,78,78
78  WRITE(6,79)
79  FORMAT(' ***** BUOY IS COMPLETELY IMMERSED. *****')
   GO TO 77
61  MERS=SURF-ZZ(1)
   WRITE(6,62)MERS
62  FORMAT(' BUOY IS IMMERSED TO A DEPTH OF',F10.3,3X,'FT.')
C
   IF(FLAG.AND.(YZ.GT.(WCH*LINK))) GO TO 902
   GO TO 77
902 WRITE(6,903)
903 FORMAT('0*****INVALID RESULT - SOLUTION COINCIDED WITH BOTTOM',
+ ' WITHOUT PROPER',/, 'REDUCTION IN VERTICAL COMPONENT OF TENSION.')

```

```

+,, TRY AGAIN.*****')
STOP 99

C
C--PRINT CABLE DATA.
C
77 DO 14 K=1,10
  IF(CABLE(1,K).EQ.0.0D0) GO TO 14
  KTYPE=K
  IF(K.EQ.1) CLEN=CABLE(1,1)
  IF(K.NE.1) CLEN=CABLE(1,K)-CABLE(1,K-1)
  WRITE(6,101) KTYPE,(CABLE(J,K),J=2,9),CLEN
101 FORMAT(' ',//,' CABLE PARAMETERS - TYPE ',I1,' :',//,' BUOYANCY',
+ ' =',F10.4,3X,'LBS PER FT',//,
+ ' WEIGHT IN AIR =',F10.4,3X,'LBS PER FT',//, DIAMETER =',F10.4,3X,
+ 'FT',//, NORMAL DRAG COEFFICIENT =',F10.4,//, AXIAL DRAG ',
+ 'COEFFICIENT =',F10.4,//,
+ ' ELASTIC COEFFICIENTS: A0=',E10.4,2X,'; A1=',E10.4,2X,'; A2=',
+ 'E10.4,//, LENGTH =',F10.3,3X,'FT.')
14 CONTINUE
C
  WRITE(6,17) ZCBL
17 FORMAT(' ',//,' TOTAL LENGTH OF CABLE =',F10.3,3X,'FT.',//)
C
C--PRINT INSTRUMENT DATA.
C
DO 16 K=1,10
  IF(INSTR(1,K).EQ.0.0D0) GO TO 16
  ITYPE=K
  EXC=ZCBL-INSTR(1,K)-ZZI(K)
  XXI(K)=XXI(K)-XRV
  WRITE(6,135) ITYPE,(INSTR(J,K),J=1,5),IDRG(K),XXI(K),ZZI(K),EXC
135 FORMAT(' ',//,' INSTRUMENT PARAMETERS - NO. ',I1,' :',//,
+ ' DISTANCE ALONG UNSTRETCHED CABLE FROM BUOY =',F8.0,3X,'FT',//,
+ ' BUOYANCY =',F10.3,3X,'LBS',//, WEIGHT IN AIR =',F10.3,3X,
+ 'LBS',//, CROSS-SECTIONAL AREA =',F10.3,3X,'SQ FT',//,
+ ' DRAG COEFFICIENT =',F10.3,//, INSTRUMENT DRAG IS',F10.2,2X,'LBS',
+ //, INSTRUMENT COORDINATES ('F10.2,1X,'',F10.2,1X,'').',//,
+ ' VERTICAL EXCURSION =',F10.2,2X,'FT',//)

```

```

16 CONTINUE
C
C--PRINT VELOCITY DATA.
C
      WRITE(6,230)
230  FORMAT('0',/, ' VELOCITY PROFILE :',/,3X,'LOWER LIMIT',8X,
+ 'COEF(0)',5X,'COEF(1)',5X,'COEF(2)',5X,'VELOCITY',/,
+ ' (FT ABOVE BOTTOM)',41X,'(FT/SEC)')
      DO 235 I=1,5
      IF(I.EQ.1) GO TO 236
      IF((VP(1,I).EQ.0.0D0).AND.(VP(1,I-1).EQ.0.0D0)) GO TO 235
236  VEL=VP(2,I)+VP(3,I)*VP(1,I)+VP(4,I)*VP(1,I)*VP(1,I)
      WRITE(6,240) (VP(J,I),J=1,4),VEL
240  FORMAT(' ',3X,F10.0,4X,3(2X,E10.4),3X,F10.2)
235  CONTINUE
C
C--PRINT CHAIN DATA.
C
      IF(FLAG) GO TO 305
      GO TO 307
305  WRITE(6,306) BCH,WCH,DCH,CNCH,CTCH,ZCHN,LINK,LCHN
306  FORMAT(' ',/, ' CHAIN PARAMETERS :',/, ' BUOYANCY =',F10.3,3X,
+ 'LBS PER FT',/, ' WEIGHT IN AIR =',F10.3,3X,'LBS PER FT',/,
+ ' DRAG CROSS-SECTION AREA =',F10.3,3X,'SQ FT PER FT LENGTH',/,
+ ' NORMAL DRAG COEFFICIENT =',F10.3,/,
+ ' AXIAL DRAG COEFFICIENT =',F10.3,/, ' TOTAL LENGTH =',
+ F10.3,3X,'FT',/, ' INCREMENT LENGTH FOR INTEGRATION =',F10.3,3X,
+ 'FT',/, ' LENGTH OF CHAIN ON BOTTOM =',F10.3,3X,'FT')
307  CONTINUE
C
C--PRINT A TABLE OF CABLE COORDINATES, TENSIONS, ANGLES & DRAG
C
      WRITE(6,30)
30  FORMAT('1TABLE OF CABLE COORDINATES,LENGTH,TENSIONS',,
+ ' ANGLES & DRAG :',/,4X,'X (FT)',4X,'Z (FT)',4X,'S (FT)',4X,
+ 'T (LB)',2X,'PHI (DEG)',2X,'NORMAL DRAG',2X,'AXIAL DRAG',
+/,55X,'(LB/FT)',6X,'(LB/FT)',/,)
      CDIST(1)=CBLMX+CDIST(1)

```

```

XX(1)=XX(1)-XRV
WRITE(6,24) XX(1),ZZ(1),CDIST(1),TENS(1),PHI(1)
24  FORMAT(5F10.2)
   K=LC
   DO 70 I=2,K
   XX(I)=XX(I)-XRV
   CDIST(I)=CBLMX+CDIST(I)
   WRITE(6,20) XX(I),ZZ(I),CDIST(I),TENS(I),PHI(I),DRGN(I),DRGL(I)
20  FORMAT(5F10.2,F10.3,3X,F10.4)
70  CONTINUE
C
WRITE(6,310) YZ,YX
310  FORMAT(/,' FINAL VERTICAL TENSION COMPONENT =',F10.2,3X,'LB',/,/,
+ ' FINAL HORIZONTAL TENSION COMPONENT =',F10.2,3X,'LB',/,/)
GO TO 205
C
C
97  WRITE(6,98)
98  FORMAT('0',' PROGRAM TERMINATED AT LABEL 6.',/,1X,
+ 'CABLE ANGLE IS TOO SMALL. ADD BUOYANCY.',/)
GO TO 300
C
C
84  WRITE(6,63)
63  FORMAT('0',' PROGRAM TERMINATED AT LABEL 5.',/,1X,
+ 'CABLE ANGLE IS TOO SMALL. INCREASE VELOCITY.',/)
GO TO 300
C
C
22  WRITE(6,64)
64  FORMAT('0',' PROGRAM TERMINATED AT LABEL 4.',/,1X,
+ 'CABLE ANGLE IS TOO SMALL. ADD BUOYANCY.',/)
GO TO 300
C
C
86  WRITE(6,87)
87  FORMAT('0',' PROGRAM TERMINATED AT LABEL 3.',/,1X,
+ 'THE CABLE IS TOO LONG FOR THE WATER DEPTH.',/)
GO TO 300
C
C
91  WRITE(6,99)

```

```

99  FORMAT('0','PROGRAM TERMINATED AT LABEL 2.'/,1X,
+ 'BUOY PULLED UNDER DUE TO INSUFFICIENT BUOYANCY.',/)
GO TO 300
C
93  WRITE(6,94)
94  FORMAT('0','PROGRAM TERMINATED AT LABEL 1.'/,1X,
+ 'THE BUOY SANK DUE TO INSUFFICIENT BUOYANCY.',/)
GO TO 300
205 STOP
END
C
C--SUBROUTINE TO PROVIDE THE FUNCTIONAL RELATIONSHIPS FOR DRKC.
C THE FUNCTIONS ARE THE STATIC CABLE EQUATIONS.
C
SUBROUTINE FUNC(X,Y,F)
IMPLICIT REAL*8 ( A-H,O-Z )
LOGICAL D1,D2,D3
COMMON /ALL/ VEL,PI
COMMON /RKFN/ DN,DL,CP,CL,DIAC,GAMMA,D1,D2,D3
DIMENSION Y(1),F(1)
STRCH=A0+A1*Y(2)+A2*Y(2)*Y(2)
GCOMP=GAMMA/STRCH
C
C--CALCULATE DRAG FORCES PER UNIT LENGTH.
C
RN=DIAC*DABS(VEL)/1.5D-05
DP=DIAC*VEL*DABS(VEL)
RP=(16.D0/(RN*DSIN(Y(1))))**0.5D0
CDN=CP+RP
IF(D1) CFL=(CL/4.D0)*RP*DCOS(Y(1))*DSIN(Y(1))
IF(D2) CFL=RP*(1.D0-(Y(1)*2.D0)/PI)*DSIN(Y(1))
IF(D3) CFL=0.D0
DN=CDN*DP*DSIN(Y(1))*DSIN(Y(1))
DL=PI*DP*CFL
C
F(1)=(DN+GCOMP*DCOS(Y(1)))/Y(2)
F(2)=GCOMP*DSIN(Y(1))-DL
F(3)=DSIN(Y(1))

```

```

F(4)=DCOS(Y(1))
RETURN
END

C
C--SUBROUTINE TO PROVIDE THE FUNCTIONAL RELATIONSHIPS FOR DRKC.
C THE FUNCTIONS ARE THE CHAIN EQUATIONS.
C
SUBROUTINE FCHN(X,Y,F)
IMPLICIT REAL*8 ( A-H,O-Z )
COMMON /ALL/ VEL,PI
COMMON /RKCH/ CNCH,DCH,WCH,BCH,CTCH
DIMENSION Y(1),F(1)
F(1)=(CNCH*DCH*VEL*DABS(VEL)*DSIN(Y(1))*DSIN(Y(1))+(WCH-BCH)*DCOS(
+Y(1)))/Y(2)
F(2)=(WCH-BCH)*DSIN(Y(1))-CTCH*DCH*VEL*DABS(VEL)*DCOS(Y(1))*DCOS(Y
+(1))
F(3)=DSIN(Y(1))
F(4)=DCOS(Y(1))
RETURN
END

C
C-- SUBROUTINE TO DETERMINE BUOYANCY & DRAG FOR A SPHERICAL BUOY.
C
SUBROUTINE BUOY1(BB,DB)
IMPLICIT REAL*8 ( A-H,O-Z )
COMMON /ALL/ VEL,PI
COMMON /BUOY/ RB,RC,RD,SURF,YY,ZCBL,CD,ZED
ZS=ZED+RB-SURF
IF(ZS-RB) 11,12,12

C
C BUOY IS PARTLY OR COMPLETELY SUBMERGED.
C
11 IF(ZS+RB) 16,16,17
C
C BUOY IS ABOVE THE WATER SURFACE.
C
12 ZED=SURF-RB*YY/ZCBL
ZS=ZED+RB-SURF

```

```

      GO TO 17
C
C   BUOY IS COMPLETELY SUBMERGED.
C
16  AB=PI*RB*RB
    VOL=(4.00*PI*RB*RB*RB)/3.00
    GO TO 13
C
C   BUOY IS PARTLY SUBMERGED.
C
17  BYIM=RB-ZS
    BYEX=RB+ZS
    AB=-ZS*DSQRT(BYIM*BYEX)+RB*RB*(PI/2.00-DARSIN(ZS/RB))
    VOL=PI*(-3.00*RB*RB*ZS+ZS*ZS+2.00*RB*RB*RB)/3.00
13  DB=CD*AB*VEL*DABS(VEL)
    BB=VOL*64.00
    RETURN
    END
C
C--- SUBROUTINE TO DETERMINE BUOYANCY & DRAG FOR A CYLINDRICAL BUOY.
C   THE AXIS IS HORIZONTAL.
C
      SUBROUTINE BUOY2(RB,DB)
      IMPLICIT REAL*8 ( A-H,O-Z )
      COMMON /ALL/ VEL,PI
      COMMON /BUOY/ RB,RC,RD,SURF,YY,ZCBL,CD,ZED
      ZS=ZED+RB-SURF
      IF(ZS-RB) 11,12,12
C
C   BUOY IS PARTLY OR COMPLETELY SUBMERGED.
C
11  IF(ZS+RB) 16,16,17
C
C   BUOY IS ABOVE THE WATER SURFACE.
C
12  ZED=SURF-RB*YY/ZCBL
    ZS=ZED+RB-SURF
    GO TO 17

```

```

C
C BUOY IS COMPLETELY SUBMERGED.
C
16 AB=PI*RB*RB
VOL=AB*RC
GO TO 13

C
C BUOY IS PARTLY SUBMERGED.
C
17 BYIM=RB-ZS
BYEX=RB+ZS
AB=-ZS*DSQRT(BYIM*BYEX)+RB*RB*(PI/2.D0-DARSIN(ZS/RB))
VOL=AB*RC
13 DB=CD*AB*VEL*DABS(VEL)
BB=VOL*64.D0
RETURN
END

C
C-- SUBROUTINE TO DETERMINE BUOYANCY & DRAG FOR A TOROIDAL BUOY.
C
SUBROUTINE BUOY3(BB,DB)
IMPLICIT REAL*8 ( A-H,O-Z )
COMMON /ALL/ VEL,PI
COMMON /BUOY/ RB,RC,RD,SURF,YY,ZCBL,CD,ZED
ZS=ZED+RB-SURF
IF(ZS-RB) 11,12,12

C
C BUOY IS PARTLY OR COMPLETELY SUBMERGED.
C
11 IF(ZS+RB) 16,16,17
C
C BUOY IS ABOVE THE WATER SURFACE.
C
12 ZED=SURF-RB*YY/ZCBL
ZS=ZED+RB-SURF
GO TO 17

C
C BUOY IS COMPLETELY SUBMERGED.

```

```

C
16 AB=2.00*PI*RB*RB
VOL=AB*PI*RC
GO TO 13
C
C BUOY IS PARTLY SUBMERGED.
C
17 BYIM=RB-ZS
BYEX=RB+ZS
AB=2.00*(-ZS*DSQRT(BYIM*BYEX)+RB*RB*(PI/2.00-DARSIN(ZS/RB)))
VOL=AB*PI*RC
13 DB=CD*AB*VEL*DABS(VEL)
BB=VOL*64.00
RETURN
END
C
C--SUBROUTINE FOR SOLVING SIMULTANEOUS ORDINARY DIFFERENTIAL EQUATIONS
C USING THE RUNGE-KUTTA METHOD (ADAPTED FROM UBC DRKC.)
C
C N - NO. OF D.E.'S TO BE SOLVED.
C X - INDEPENDENT VARIABLE. INITIAL VALUE ON ENTRY TO DRKC
C & FINAL VALUE ON EXIT.
C Z - FINAL VALUE OF X AT END OF INTEGRATION.
C Y - VECTOR OF DEPENDENT VARIABLES. INITIAL VALUES ON ENTRY
C TO DRKC & FINAL VALUES ON EXIT.
C F - OUTPUT VECTOR OF DERIVATIVES, DY/DX AT X=Z.
C H - INPUT STEP-SIZE.
C HMIN - INPUT LOWER BOUND ON STEP-SIZE.
C E - INPUT ERROR TOLERANCE.
C FUNC - EXTERNAL SUBROUTINE FOR EVALUATING DERIVATIVES.
C G,S,T - SCRATCH VECTORS.
C
C SYSTEM OF EGNS IS: F(I)=DY(I)/DX=FN(X,Y,Y(1),...,Y(N)) ,I=1,...,N
C
SUBROUTINE DRKC(N,X,Z,Y,F,H,HMIN,E,FUNC,G,S,T)
IMPLICIT REAL*8(A-H,O-Z)
DIMENSION Y(N),F(N),T(N),S(N),G(N)
INTEGER SW

```

```

LOGICAL BC,BE,BH,BR,BX
IF (HMIN .LT. 0.00) HMIN=.01D0*DABS(H)
BH=.TRUE.
BR=.TRUE.
BX=.TRUE.
BC=.FALSE.
IF (E .LT. 1.00) BC=.TRUE.
E=DABS(E)
E5=5.00*E
IF (Z .GT. X .AND. H .LT. 0.00) H=-H
IF (Z .LT. X .AND. H .GT. 0.00) H=-H
XS = X
10 DO 15 J=1,N
15 G(J) = Y(J)
20 HS=H
Q=X+H-Z
BE=.TRUE.
IF (H .GT. 0.00 .AND. Q .GE. 0.00) GO TO 30
IF (H .LT. 0.00 .AND. Q .LE. 0.00) GO TO 30
GO TO 40
30 H=Z-X
BR=.FALSE.
H3=H/3.00
40 DO 240 SW=1,5
CALL FUNC(X,Y,F)
DO 200 I=1,N
Q=H3*F(I)
GO TO (50,60,70,80,90),SW
50 T(I)=Q
R=Q
GO TO 100
60 R=.5D0*(Q+T(I))
GO TO 100
70 R=3.00*Q
S(I)=R
R=.375D0*(R+T(I))
GO TO 100
80 R=T(I)+4.00*Q

```

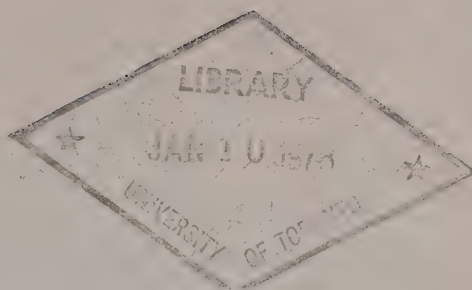
```

T(I)=R
R=1.5D0*(R-S(I))
GO TO 100
90  R=.5D0*(Q+T(I))
    Q=DABS(R+R-1.5D0*(Q+S(I)))
    Y(I)=G(I)+R
    IF (SW.NE. 5) GO TO 200
    IF (.NOT. BC) GO TO 200
    R=DABS(Y(I))
    IF (R.LT. .001D0) GO TO 110
    R=E5*R
    GO TO 120
110  R=E5
120  IF (Q.LT. R) GO TO 190
    IF (.NOT. BX) GO TO 190
    BR=.TRUE.
    BH=.FALSE.
    H=.5D0*H
    IF ( DABS(H) .GE. HMIN) GO TO 180
    SIGH=1.D0
    IF ( H.LT. 0.D0) SIGH=-1.D0
    H=SIGH*HMIN
    BX=.FALSE.
    DO 185J=1,N
180  Y(J)=G(J)
185  X=XS
    GO TO 20
    CONTINUE
190  IF (Q.GE. .03125D0*R) BE=.FALSE.
    CONTINUE
200  GO TO (210,240,220,230,240),SW
210  X=X+H3
    GO TO 240
220  X=X+.5D0*H3
    GO TO 240
230  X=X+.5D0*H
240  CONTINUE
    IF (.NOT. BC) GO TO 300

```

```
250 IF (BE .AND. BH .AND. BR) GO TO 250  
    GO TO 260  
    H= H+H  
    BX=.TRUE.  
260 BH=.TRUE.  
300 IF (BR) GO TO 10  
    H=HS  
    RETURN  
    END
```


CAI
EP 321
- 77R13



**OCEANOGRAPHIC OBSERVATIONS
AT OCEAN STATION P
(50°N, 145°W)**

VOLUME 79

7 January - 17 February 1977

by

Seakem Oceanography Ltd.

**Institute of Ocean Sciences, Patricia Bay
Sidney, B.C.**



For addition copies or further information please write to:

Department of Fisheries and the Environment

Institute of Ocean Sciences, Patricia Bay

P.O. Box 5000

Sidney, B.C.

V8L 4B2

OCEANOGRAPHIC OBSERVATIONS AT OCEAN STATION P (50°N, 145°W)

Volume 79

7 January - 17 February 1977

by

Seakem Oceanography Ltd.

Institute of Ocean Sciences, Patricia Bay

Sidney, B.C.

September 1977

This is a manuscript which has received only limited circulation. On citing this report in a bibliography, the title should be followed by the words "UNPUBLISHED MANUSCRIPT" which is in accordance with accepted bibliographic custom.

ABSTRACT

Physical, chemical and biological oceanographic observations are made from the weathership at Ocean Weather Station Papa, and between Esquimalt and Station Papa, on a routine continuing basis. Physical oceanography data only are shown, including surface observations and profiles obtained with bottle casts and conductivity-temperature-pressure instruments.

TABLE OF CONTENTS

ABSTRACT.....	i
TABLE OF CONTENTS.....	iii
INTRODUCTION.....	1
PROGRAM OF OBSERVATIONS.....	2
OBSERVATIONAL PROCEDURES.....	4
COMPUTATIONS.....	4
REFERENCES.....	5
LOG OF HYDROGRAPHIC AND STD OBSERVATIONS.....	6
RESULTS OF HYDROGRAPHIC OBSERVATIONS.....	11
RESULTS OF STD OBSERVATIONS.....	39
SURFACE SALINITY AND TEMPERATURE OBSERVATIONS.....	147
LIST OF OMISSIONS FROM DATA.....	150

LIST OF FIGURES

Figure 1. Chart showing Line P station positions.....	8
Figure 2. Composite plot of temperature vs \log_{10} depth for Line P stations.....	12
Figure 3. Composite plot of salinity vs \log_{10} depth for Line P stations.....	13
Figure 4. Composite plot of temperature vs \log_{10} depth for Station P.....	14
Figure 5. Composite plot of salinity vs \log_{10} depth for Station P.....	15
Figure 6. Composite plot of oxygen vs \log_{10} depth for Station P.....	16
Figure 7. Salinity difference between hydro data and STD.....	40
Figure 8. Temperature difference between hydro data and STD.....	41

INTRODUCTION

Canadian operation of Ocean Weather Station P (Latitude $50^{\circ}00'N$, Longitude $145^{\circ}00'W$) was inaugurated in December, 1950. The station is occupied primarily to make meteorological observations of the surface and upper air and to provide an air-sea rescue service. The station is manned by two vessels operated by the Marine Services Branch of the Ministry of Transport. They are the CCGS Vancouver and the CCGS Quadra. Each ship remains on station for a period of six weeks, and is then relieved by the alternate ship, thus maintaining a continuous watch.

Bathythermograph observations have been made at Station P since July 1952. A program of more extensive oceanographic observations commenced in August 1956. This was extended in April 1959, by the addition of a series of oceanographic stations along the route to and from Station P and Swiftsure Bank. These stations are known as Line P stations. The number of stations on Line P has been increased twice and now consists of twelve stations (Fig. 1). Bathythermograph observations and surface salinity sample collections, in addition to being made on Line P oceanographic stations, are also made at odd meridians at $40'$, i.e. $139^{\circ}40'W$, $141^{\circ}40'W$, etc. These stations are known as Line P BT stations. Data observed prior to 1968 have been indexed by Collins et al (1969).

The present record includes hydrographic, continuously sampled STP and surface salinity and temperature data collected from the CCGS Vancouver during the period 7 January to 17 February 1977.

All physical oceanographic data have been stored by the Canadian Oceanographic Data Centre (CODC), 615 Booth Street, Ottawa, Ontario, Canada. Requests for these data should be directed to CODC.

Biological and productivity data are published in the Manuscript Report series of the Fisheries Research Board of Canada (FRB), Pacific Biological Station, Nanaimo, British Columbia, Canada. Requests for these data should be directed to FRB.

Marine geochemical data are for the Ocean Chemistry Group, Ocean and Aquatic Sciences, Environment Canada, Institute of Ocean Sciences, P.O. Box 5000, Sidney, B.C. V8L 4B2.

PROGRAM OF OBSERVATION FROM CCGS VANCOUVER, 7 JANUARY - 17 FEBRUARY 1977 (P-77-1)
(CODC Ref. No. 15-77-001)

Oceanographic observations were made by Mr. B. Canning of Seakem Oceanography Ltd., Victoria, B.C.

En Route to Station P

Line P Stations 1 to 12 were occupied and an STP profile made to near bottom or 1500 metres. Two hydrocasts to 1500 m were done at Stations 6 and 10.

Samples for salinity, nitrate, nutrient, alkalinity and total CO_2 were taken from the seawater loop at all whole stations, with salinity also taken at all half stations. Surface bucket salinities were taken at all whole stations 1 to 5. Surface bucket temperatures were taken at all whole and half stations.

Surface tarball tows were made at Stations 2, 4, 6, 8, 10 and 12.

The thermosalinograph, surface temperature recorder and PCO_2 system were run continuously.

Mechanical BT's or XBT's were taken at all whole and half stations.

On Station P

The oceanographic program was carried out as follows:

Physical Oceanography:

- 1) Profiles of salinity, temperature and oxygen were obtained from 6 hydrographic casts to near bottom (4200 metres) (one cast was to 400 m only since the bottles at 500 and 600 m did not trip).
- 2) 32 STP profiles to 1500 metres and 1 to 600 metres were obtained.
- 3) BT's or XBT's were taken every three hours to coincide with meteorological observations, encoded and transmitted according to the IGOSS format.
- 4) Salinity samples were collected daily at 0000 hrs GMT from the seawater loop.

Marine Geochemistry:

- 1) Nutrient and salinity samples were collected daily at 0000 hrs GMT from the seawater loop. One 24 hour series of nutrient samples was taken each hour from the seawater loop. Two profiles for nutrients to 500 m and one profile for tritium to 500 m were taken. One loop sample and one rain-water sample were also collected for tritium.
- 2) Alkalinity and total CO_2 samples were taken every 3 days from the seawater loop or bucket and in addition, 2 profiles each to 500 m were taken.
- 3) Air CO_2 samples were taken in quadruplicate at weekly intervals.

- 4) 3 surface tarball tows were completed.
- 5) 1 seawater C-14 sample was extracted from 45 gallons of seawater taken from the seawater loop along with 1 seawater C-13 and 2 air C-13 samples.
- 6) PCO_2 carboys were filled every 3 days when the loop system was operational.

Biological Oceanography:

Samples were obtained as follows:

- 1) 26 - 150 metre vertical plankton hauls.
2 - 1200 metre vertical plankton hauls.
3 groups of subsurface plankton hauls were taken on 3 consecutive nights at sunset.
- 2) 2 profiles to 200 metres for each of plant pigment, nitrate and C_{14} productivity were obtained, as well as 3 surface samples each.

An emergency run was made towards the Queen Charlotte Islands during which time surface salinity samples and temperatures were taken every 3 hours. Stations 12½ to 8½ were missed as a result of this run.

En Route from Station P

An STP profile was made at Stations 8 to 6 and 4 to 1. Two hydrocasts were done at Stations 8 and 4. Nutrient, nitrate, alkalinity and total CO_2 samples were taken from the seawater loop at Stations 8 to 1. Salinity samples were taken at all whole and half stations 8 to 1. Surface bucket temperatures were taken at all whole stations 8 to 1. Tarball tows were taken at Stations 8, 7, 6, 4, 3, and 2. Mechanical BT's or XBT's were taken at all whole and half Stations 8 to 1.

Observations for Other Agencies

- 1) Marine mammal observations were made by the ship's officers for Mr. I. McAskie, Fisheries Research Board of Canada, Pacific Biological Station, Nanaimo, B.C., Canada.
- 2) Bird observations were made by the ship's officers for Dr. M. Myres, University of Alberta, Calgary, Alberta, Canada and Mr. J. Guiguet, Curator of Birds and Mammals, Provincial Museum, Department of Provincial Secretary and Travel Industry, Victoria, British Columbia, Canada.
- 3) Air CO_2 samples were taken weekly in duplicate for Scripps Institution of Oceanography, La Jolla, California, U.S.A.

Data were processed for publication by Ms. M. Sainsbury of Seakem Oceanography Ltd., Victoria, B.C.

OBSERVATIONAL PROCEDURES

Observations for salinity, oxygen and temperature from all hydrographic casts, including the surface, were obtained with Niskin water sample bottles equipped with either Richter and Wiese and/or Yoshino Keiki Co. reversing thermometers. Two protected thermometers were used on all bottles and one unprotected thermometer was used on each bottle at depths of 300 m or greater. The accuracy of protected reversing thermometers is believed to be $\pm 0.02^{\circ}\text{C}$.

The daily surface water temperatures were measured from a bucket sample using a deck thermometer of $\pm 0.1^{\circ}\text{C}$ accuracy. The daily surface salinity samples were obtained from the seawater loop. When the seawater loop was not operational these samples were obtained with a bucket, and are indicated with a 'b' in this data record.

Salinity determinations were made aboard ship with either an Autolab Model 601 Mark III inductive salinometer or a Hytech Model 6220 lab salinometer. Accuracy using duplicate determinations is estimated to be $\pm 0.003^{\circ}/\text{oo}$.

Depth determinations were made using the "depth difference" method described in the U. S. N. Hydrographic Office Publication No. 607 (1955). Depth estimates have an approximate accuracy of ± 5 m for depths less than 1000 m, and $\pm 0.5\%$ of depth for depths greater than 1000 m.

The dissolved oxygen analyses were done in shipboard laboratory by a modified Winkler method (Carpenter, 1955).

Line P engine intake continuous temperature on both ships were recorded by a Honeywell Elektronik 15 Recorder. The temperature probe is at a depth of approximately 3 metres below the sea surface and the instrument accuracy is believed to be $\pm 0.1^{\circ}\text{C}$.

Each ship is equipped with a Plessey Model 6600-T thermosalinograph which is used, on Line P, for continuous recording of surface temperatures and salinities from the ship's seawater loop. The temperature probe is mounted at the seawater loop intake (approximately 3 metres below the surface) and the salinity probe and recorder are situated in the dry lab. The accuracy of this instrument is believed to be $\pm 0.1^{\circ}\text{C}$ for temperature and $\pm 0.1^{\circ}/\text{oo}$ for salinity.

STP profiles were taken with a Guildline Model 8700 STP system.

COMPUTATIONS

All hydrographic data were processed with the aid of an IBM 370 computer and a UNIVAC 1100 computer. Reversing thermometer temperature corrections, thermometric depth calculations and accepted depth from the "depth difference" method were computed. Extraneous thermometric depths caused by thermometer malfunctions were automatically edited and replaced. A Calcomp 565 Offline Plotter was used to plot temperature-salinity, and temperature-oxygen diagrams, as well as plots of temperature, salinity, and dissolved oxygen vs \log_{10} depth. These plots were used to check the data for errors.

Missing hydrographic data were obtained using a weighted parabolas interpolation method (Reiniger and Ross, 1968). These data are indicated with an asterisk in this data record.

Data values which we suspect but which we have included in this data record are indicated with a plus. These data have been removed from punch card and magnetic tape records.

Analog records from the salinity-temperature-pressure instrument have been machine digitized, then replotted using the Calcomp plotter.

Digitization was continued until original and computer plotted traces were coincident. Temperature and salinity values were listed at standard pressures; integrals (depths, geopotential anomaly, and potential energy anomaly) were computed from the entire array of digitized data.

The headings for the data listings are explained as follows:

PRESS	is pressure (decibars)
TEMP	is temperature (degrees Celsius)
SAL	is salinity (parts per thousand)
DEPTH	is reported in metres
SIGMA-T	is specific gravity anomaly
SVA	is specific volume anomaly
THETA	is potential temperature (degrees Celsius)
SVA (THETA)	is potential specific volume anomaly
DELTA D	is geopotential anomaly (J/kg)
POT EN	is potential energy in units of 10^8 ergs/cm ²
OXY	is the concentration of dissolved oxygen expressed in millilitres per litre
SOUND	is the velocity of sound in m/sec.

REFERENCES

- Carpenter, J.H., 1965. The Chesapeake Bay Institute technique for the Winkler dissolved oxygen method. *Limnol. and Oceanogr.* 10: 141-143.
- Collins, C.A., R.L. Tripe, D.A. Healey and J. Joergensen, 1969. The time distribution of serial oceanographic data from the Ocean Station P programme. *Fish. Res. Bd. Can. Tech. Rept. No. 106.*
- MacNeill, M., 1977. A study of anomalous salinity and oxygen values in the deep water at Ocean Station P from 1960-1976 (unpublished manuscript). *Pacific Marine Science Report* 77-9.
- Reiniger, R.F. and C.K. Ross, 1968. A method of interpolation with application to oceanographic data. *Deep Sea Res.*, 15: 185-193.
- U. S. N. Hydrographic Office, 1955. *Instruction Manual for oceanographic observations*, Publ. No. 607.

LOG OF HYDROGRAPHIC AND STD OBSERVATIONS

Consec #	Positions	Date (Z)	Time (Z)	STD (m)	Hydrocasts (m)	Comments
1	125-33 ⁰ W	7/1/77	2335	90		
2	126-00 ⁰ W	8/1/77	0110	90		
3	126-40 ⁰ W	8/1/77	0320	1,200		
4	127-40 ⁰ W	8/1/77	0635	1,425		
5	128-40 ⁰ W	8/1/77	1015	1,425		
6	130-40 ⁰ W	8/1/77	1630	1,425		
7	130-40 ⁰ W	8/1/77	1755		1,500	T,S
8	132-40 ⁰ W	9/1/77	0015	1,425		
9	134-40 ⁰ W	9/1/77	0610	1,425		
10	136-40 ⁰ W	9/1/77	1230	1,425		
11	138-40 ⁰ W	9/1/77	1825	1,425		
12	138-40 ⁰ W	9/1/77	2000		1,500	T,S
13	140-40 ⁰ W	10/1/77	0225	1,425		
14	142-40 ⁰ W	10/1/77	0905	1,425		
15	P	10/1/77	1735		4,200	T,S,O,Alk.
16	P	10/1/77	2110	1,425		
17	P	11/1/77	1725	1,425		
18	P	12/1/77	1715	1,425		
19	P	13/1/77	1720	1,425		
20	P	14/1/77	0515	1,425		
21	P	15/1/77	1720	600		
22	P	16/1/77	1820	1,425		
23	P	17/1/77	1747		4,200	T,S,O,Alk.
24	P	17/1/77	2110	1,425		
25	P	18/1/77	1735	1,425		
26	P	19/1/77	2110	1,425		
27	P	20/1/77	1750	1,425		
28	P	22/1/77	0235	1,425		
29	P	22/1/77	1720	1,425		
30	P	23/1/77	1805	1,425		
31	P	24/1/77	2145	1,425		
32	P	25/1/77	1735		400	T,S, O
33	P	25/1/77	1825	1,425		
34	P	26/1/77	1745	1,425		
35	P	27/1/77	1730		4,200	T,S,O,Alk.
36	P	27/1/77	2055	1,425		
37	P	28/1/77	1725	1,425		
38	P	29/1/77	1740	1,425		
39	P	30/1/77	1735	1,425		
40	P	31/1/77	1735	1,425		
41	P	2/2/77	0015	1,425		
42	P	2/2/77	1730		4,200	T,S,O,Alk.
43	P	2/2/77	2045	1,425		
44	P	3/2/77	1740	1,425		
45	P	4/2/77	1815	1,425		
46	P	5/2/77	1730	1,425		
47	P	6/2/77	1750	1,425		

LOG OF HYDROGRAPHIC AND STD OBSERVATIONS (Continued)

Consec #	Positions	Date (Z)	Time (Z)	STD (m)	Hydrocasts (m)	Comments
48	P	7/2/77	1730	1,425		
49	P	8/2/77	1725	1,425		
50	P	9/2/77	1730		4,200	T,S,O,Alk.
51	P	9/2/77	2025	1,425		
52	P	10/2/77	1730	1,425		
53	P	11/2/77	1745	1,425		
54	134-40°W	14/2/77	1500	1,425		
55	134-40°W	14/2/77	1630		1,500	T,S.
56	132-40°W	15/2/77	0050	1,425		
57	130-40°W	15/2/77	0950	1,425		
58	128-40°W	15/2/77	1815	1,425		
59	127-40°W	15/2/77	2330		1,500	T,S
60	127-40°W	16/2/77	0020	1,425		
61	126-40°W	16/2/77	0510	1,200		
62	126-00°W	16/2/77	0845	85		
63	125-33°W	16/2/77	1055	85		

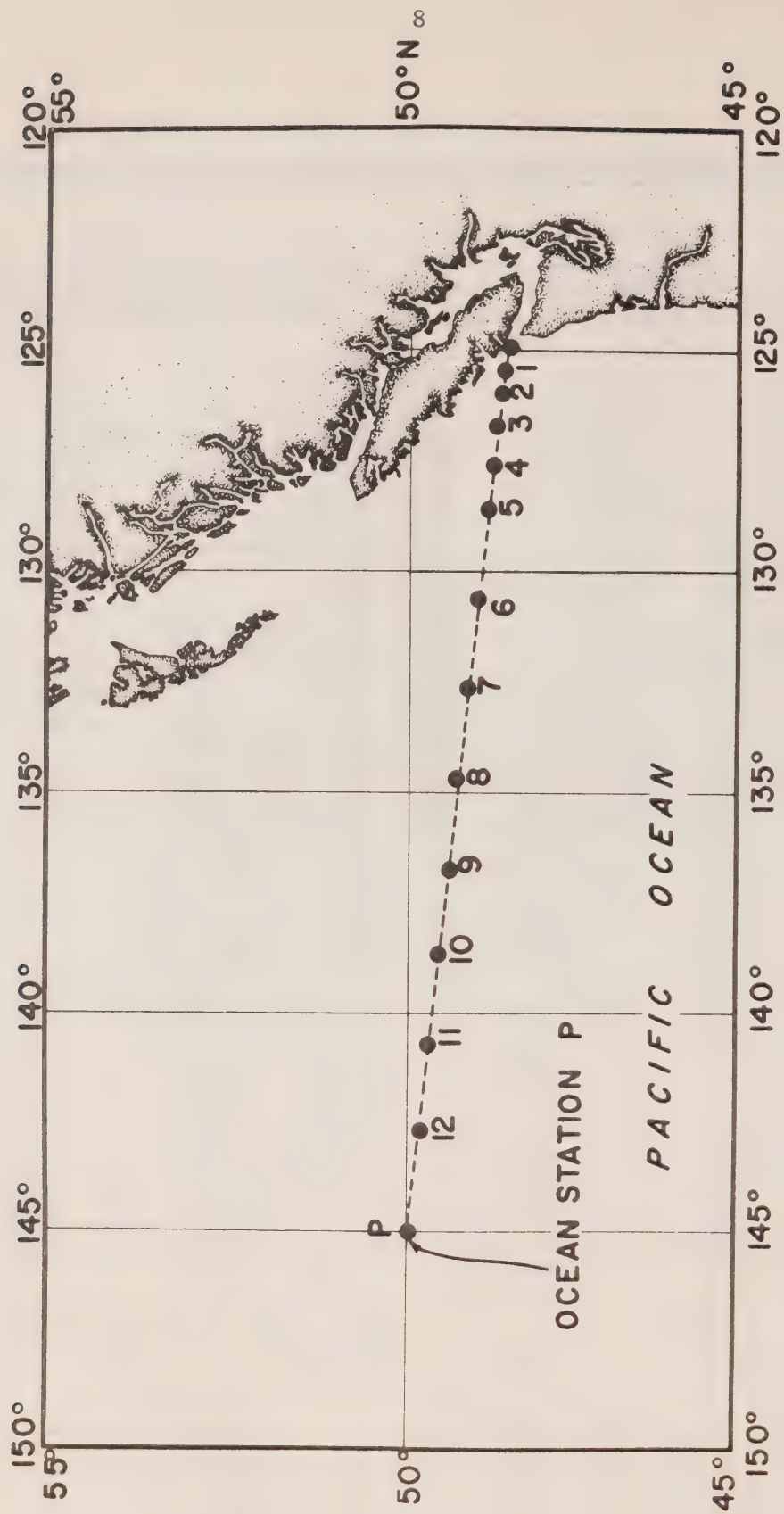


Fig. 1 Chart showing Line P station positions.

Oceanographic Data Obtained on Cruise P-77-1

(CODC Reference No. 15-77-001)

Results of Hydrographic Observations

(P-77-1)

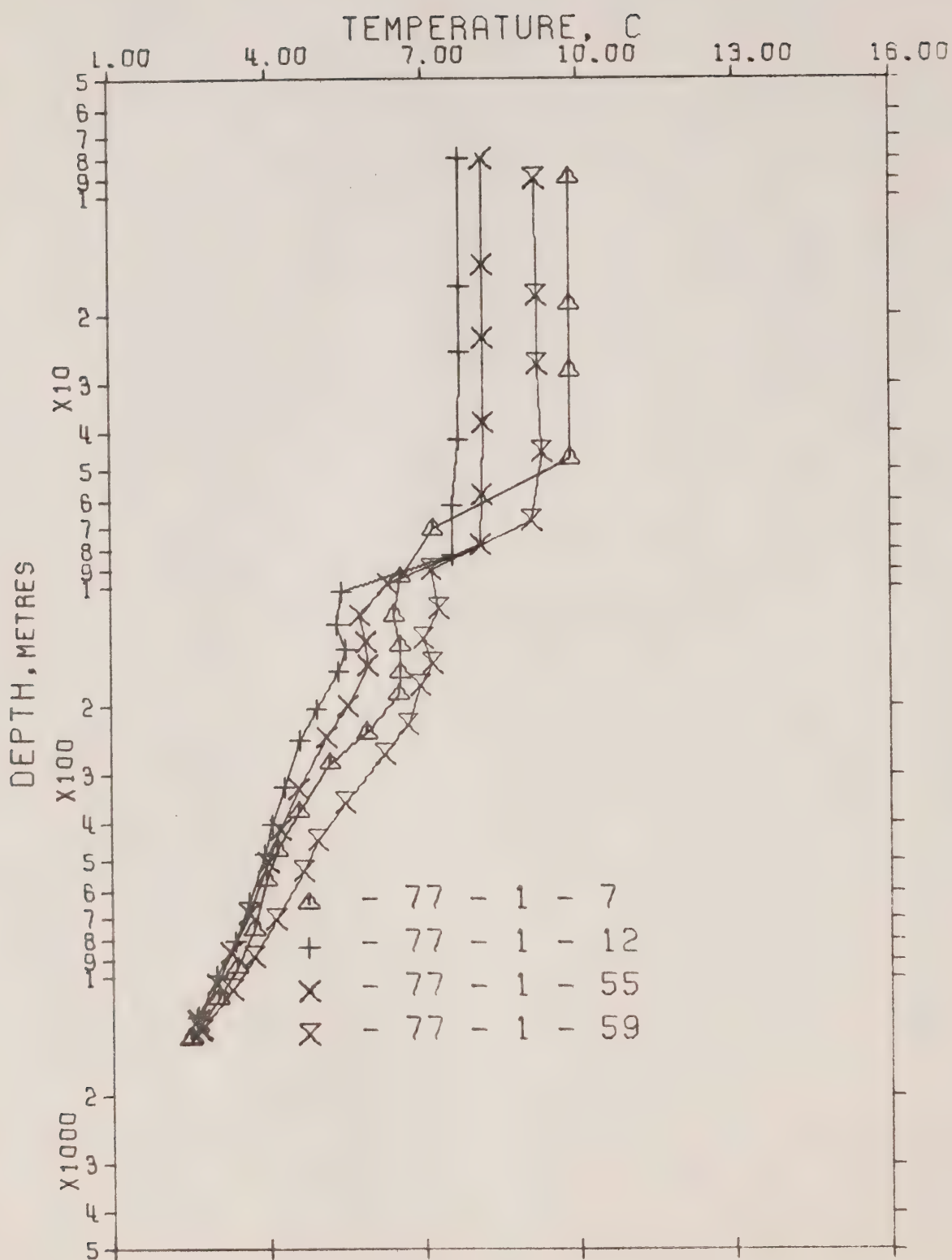


Figure 2. Composite plot of temperature vs \log_{10} depth for Line P stations. P-77-1.

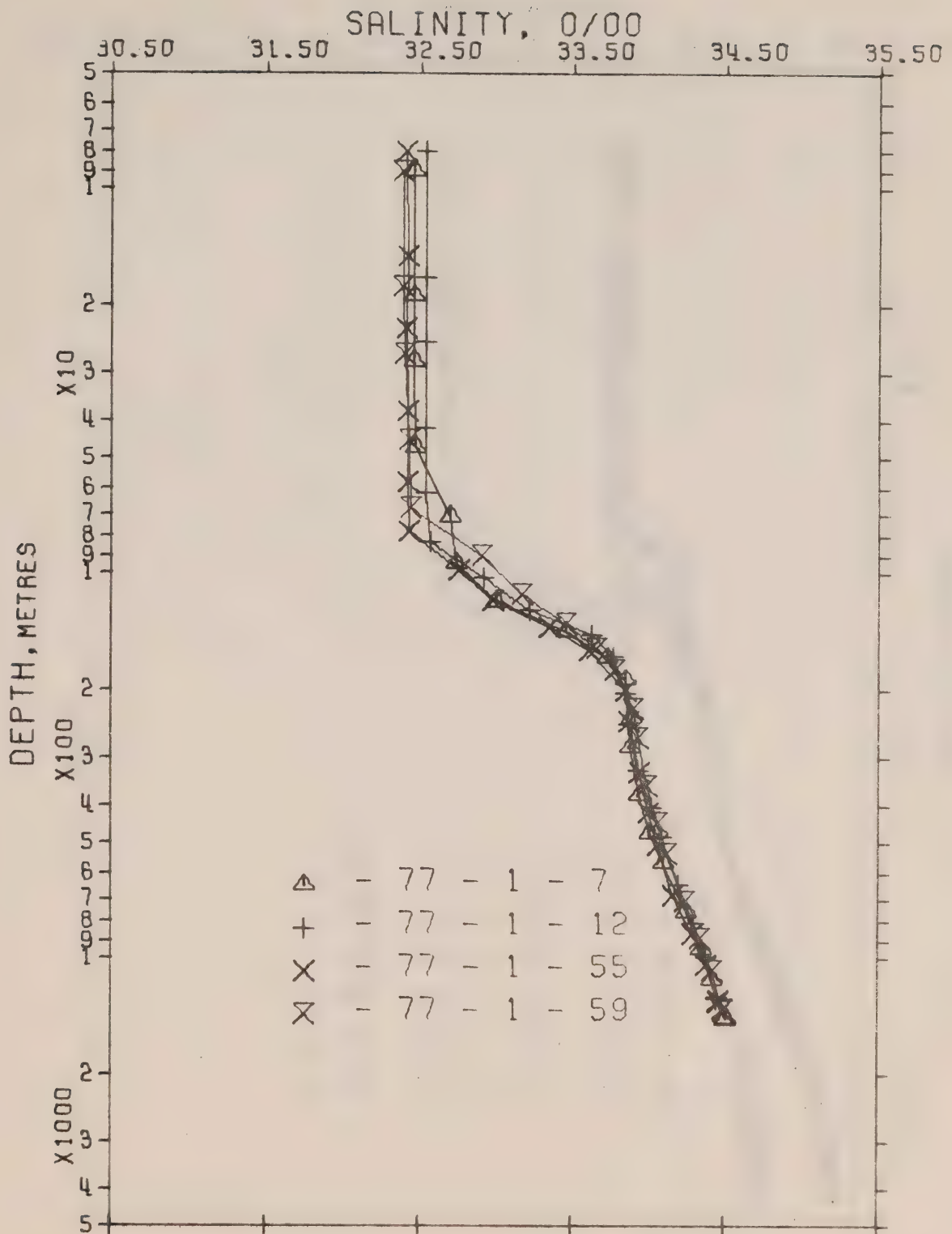


Figure 3. Composite plot of salinity vs \log_{10} depth for Line P stations. P-77-1.

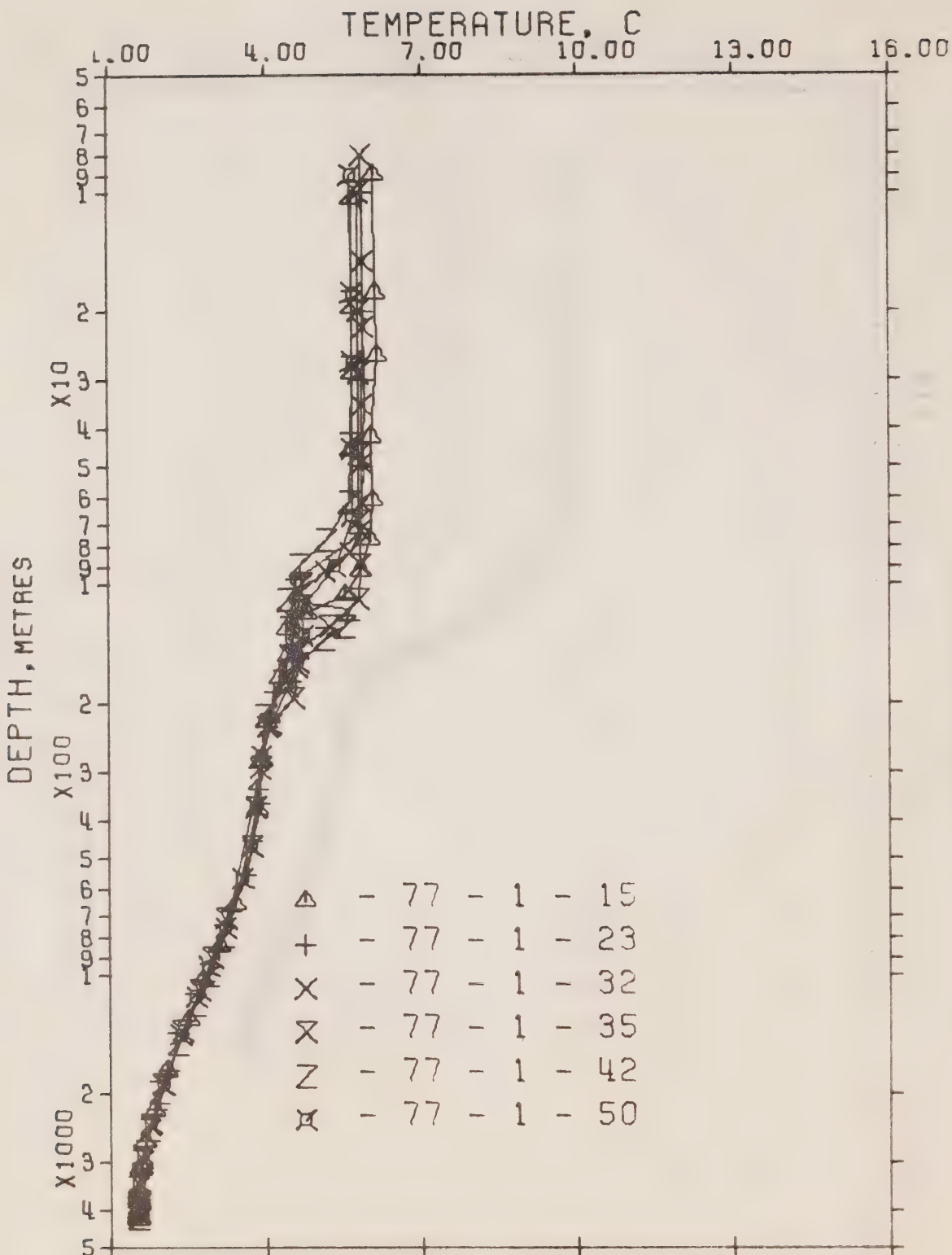


Figure 4. Composite plot of temperature vs \log_{10} depth for Station P. P-77-1.

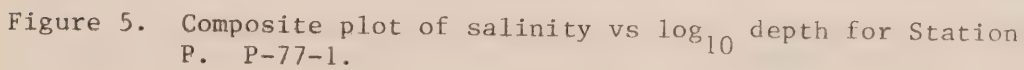


Figure 5. Composite plot of salinity vs \log_{10} depth for Station P. P-77-1.

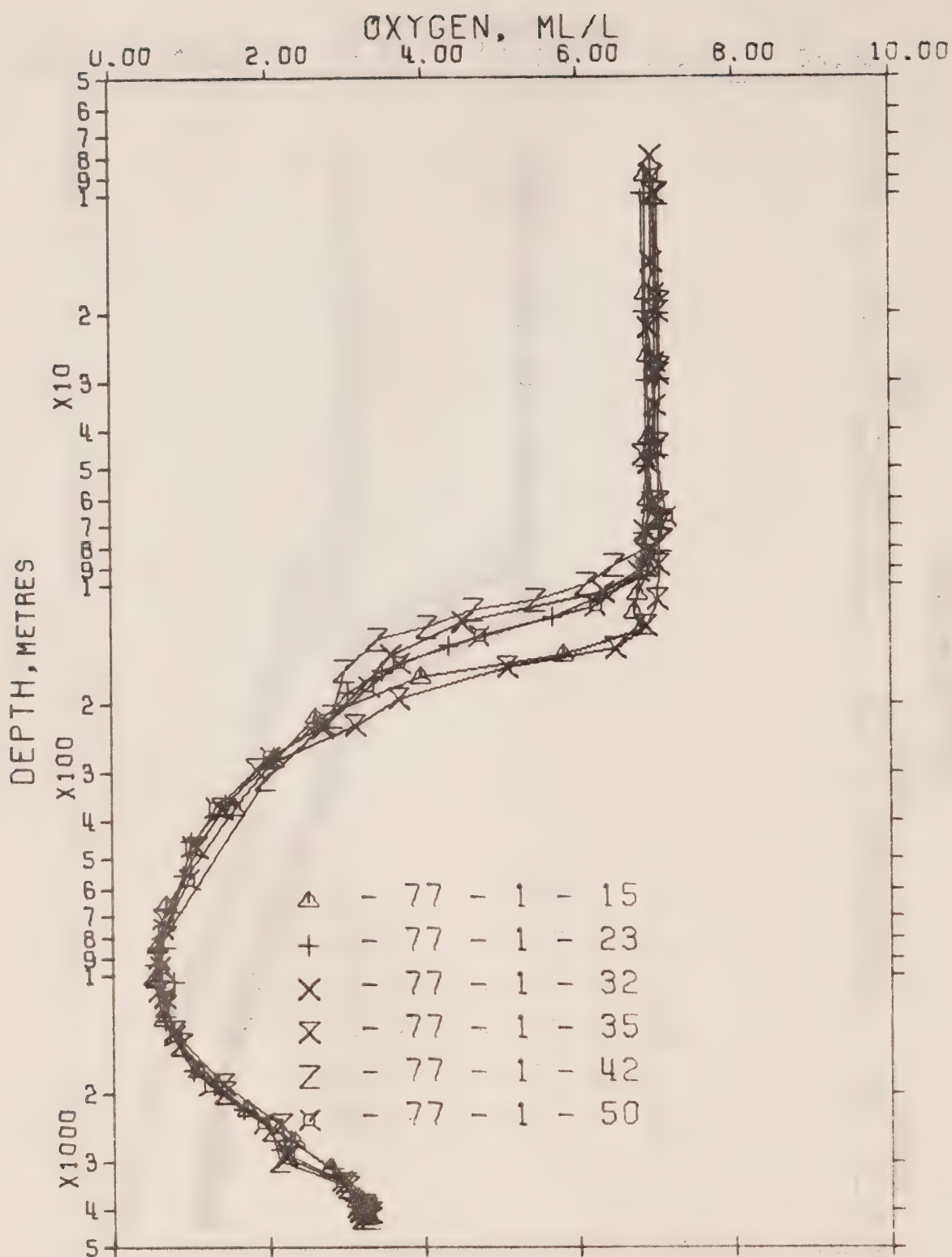
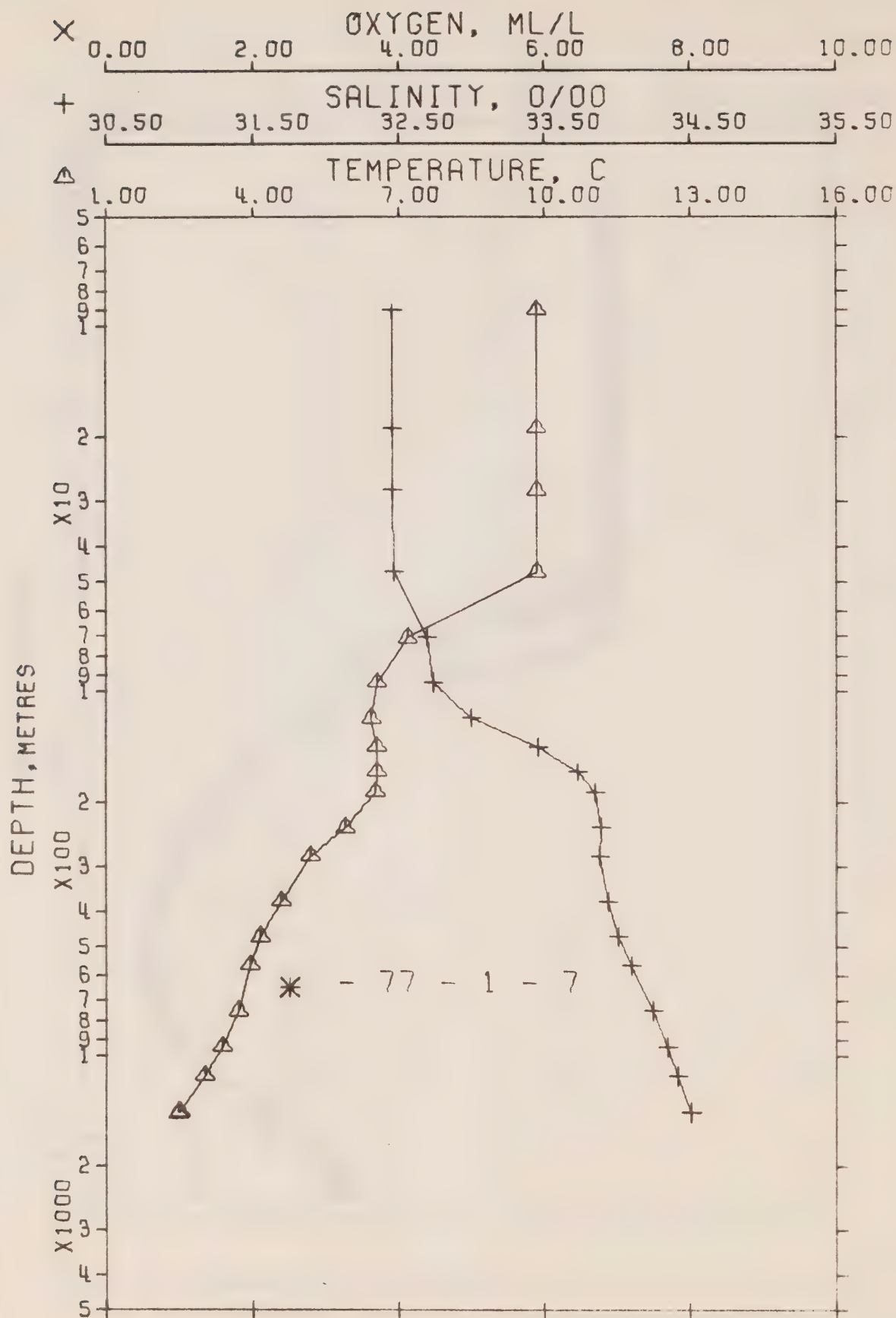


Figure 6. Composite plot of oxygen vs \log_{10} depth for Station P. P-77-1.



OFFSHORE OCEANOGRAPHY GROUP

REFERENCE NO. 77- 1- 7 DATE 8/ 1/77 GMT 17.8

POSITION 49- 2.0 N, 130-40.0 W

STATION 6

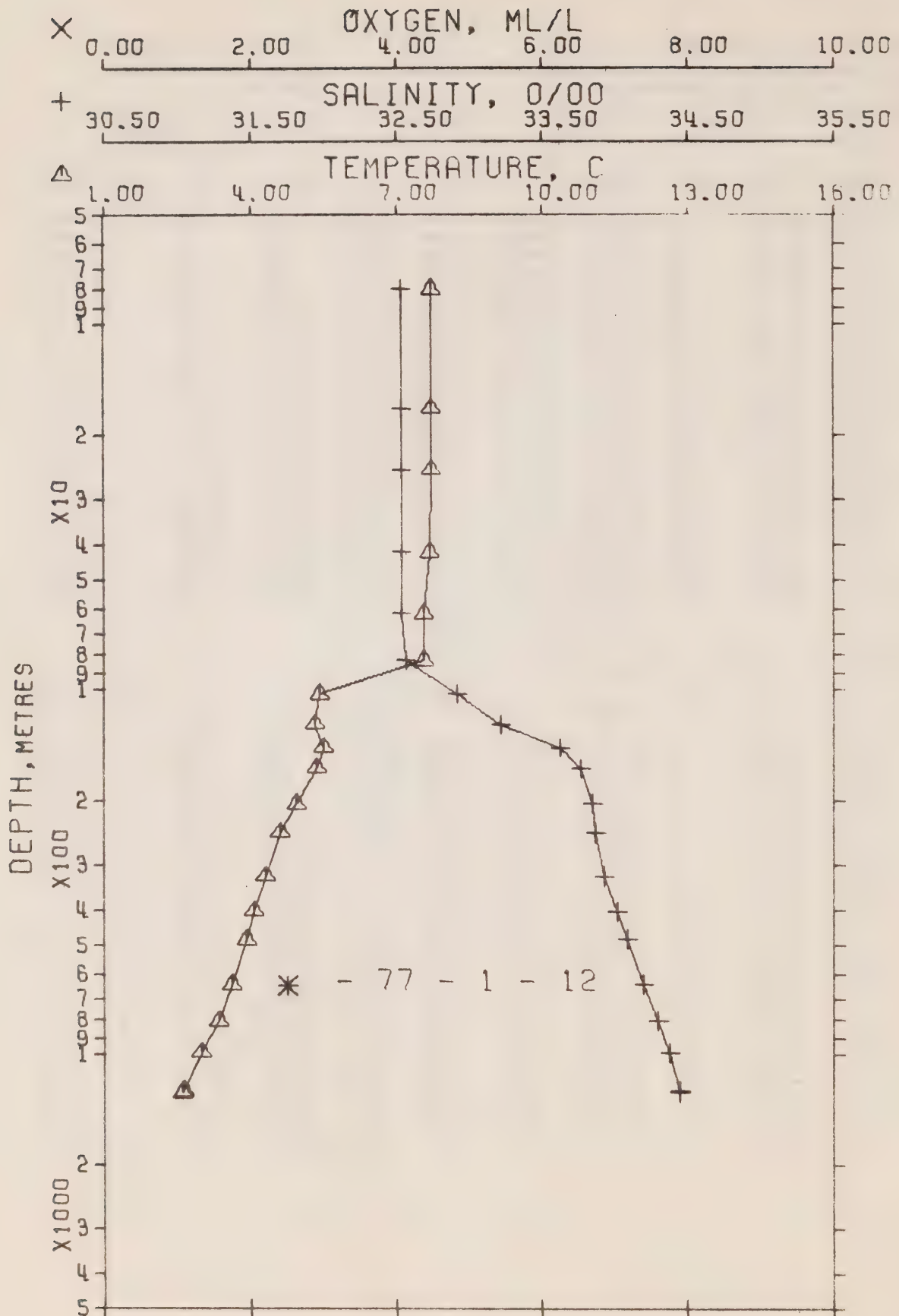
HYDROGRAPHIC CAST DATA

OBSERVED DATA

PRESS	TEMP	SAL	DEPTH	SIGMA T	SVA	THETA	SVA (THETA)	DELTA D	POT. EN	OXY	SOUND
0	9.87	32.462	0	25.017	295.0	9.87	295.0	.00	.00		1487.
9	9.85	32.462	9	25.021	294.9	9.85	294.7	.27	.01		1487.
19	9.86	32.460	19	25.017	295.4	9.86	295.0	.56	.05		1487.
28	9.86	32.459	28	25.017	295.6	9.86	295.0	.83	.12		1487.
47	9.85	32.471	47	25.028	294.9	9.84	293.9	1.40	.34		1487.
71	7.19	32.704	71	25.610	239.6	7.18	238.5	2.05	.73		1478.
95	6.56	32.740	94	25.722	229.2	6.55	227.9	2.59	1.19		1476.
119	6.44	32.996	118	25.939	208.9	6.43	207.2	3.12	1.76		1476.
142	6.54	33.465	141	26.295	175.5	6.53	173.4	3.57	2.35		1478.
166	6.56	33.735	165	26.504	156.0	6.54	153.5	3.97	2.98		1478.
189	6.51	33.849	188	26.601	147.2	6.49	144.3	4.32	3.61		1479.
237	5.86	33.892	235	26.715	136.6	5.86	133.4	4.99	5.07		1477.
284	5.16	33.879 +	282	26.792	129.5	5.14	126.2	5.62	6.74		1475.
378	4.58	33.939	375	26.904	119.4	4.55	115.4	6.78	10.67		1474.
473	4.15	34.014	469	27.010	109.9	4.12	105.4	7.87	15.38		1474.
567	3.94	34.101	562	27.100	101.9	3.90	96.8	8.86	20.63		1475.
757	3.71	34.251	750	27.243	89.8	3.65	83.2	10.68	32.85		1477.
949	3.37	34.355	940	27.358	79.7	3.30	72.1	12.30	46.94		1479.
1144	3.00	34.423	1133	27.447	71.8	2.92	63.6	13.78	62.70		1481.
1438	2.50	34.506	1423	27.557	61.7	2.40	53.1	15.75	88.63		1483.
1448	2.48	34.511	1433	27.563	61.1	2.38	52.5	15.81	89.55		1484.

INTERPOLATED TO STANDARD PRESSURE

PRESS	TEMP	SAL	DEPTH	SIGMA T	SVA	THETA	SVA (THETA)	DELTA D	POT. EN	OXY	SOUND
0	9.87	32.462	0	25.017	295.0	9.87	295.0	.00	.00		1487.
10	9.85	32.462	10	25.020	294.9	9.85	294.7	.29	.02		1487.
20	9.86	32.460	20	25.017	295.4	9.86	295.0	.59	.06		1487.
30	9.86	32.460	30	25.018	295.5	9.86	294.9	.89	.14		1487.
50	9.49	32.503	50	25.111	287.0	9.48	286.0	1.48	.38		1486.
75	7.08	32.710	75	25.630	237.7	7.07	236.6	2.13	.79		1478.
100	6.53	32.803	99	25.775	224.2	6.52	222.8	2.71	1.31		1476.
125	6.47	33.132	124	26.042	199.2	6.46	197.5	3.25	1.92		1477.
150	6.55	33.560	149	26.369	168.6	6.53	166.4	3.71	2.56		1478.
175	6.54	33.781	174	26.543	152.4	6.52	149.8	4.10	3.22		1478.
200	6.35	33.860	199	26.629	144.5	6.34	141.6	4.47	3.92		1478.
225	6.02	33.882	224	26.690	139.0	6.00	135.9	4.83	4.69		1477.
250	5.66	33.868	248	26.739	134.5	5.64	131.2	5.17	5.52		1476.
300	5.05	33.891	298	26.813	127.6	5.02	124.1	5.82	7.35		1475.
400	4.47	33.958	397	26.931	117.0	4.44	112.9	7.04	11.71		1474.
500	4.08	34.041	496	27.038	107.4	4.05	102.7	8.17	16.84		1474.
600	3.89	34.131	595	27.129	99.5	3.85	94.1	9.20	22.63		1475.
700	3.77	34.211	694	27.204	93.0	3.72	86.8	10.16	29.01		1476.
800	3.63	34.277	793	27.271	87.3	3.57	80.4	11.06	35.89		1477.
900	3.45	34.331	891	27.332	82.0	3.38	74.7	11.91	43.22		1478.
1000	3.27	34.374	991	27.383	77.5	3.19	69.7	12.70	50.93		1479.
1200	2.90	34.440	1188	27.470	69.7	2.81	61.4	14.18	67.41		1481.



OFFSHORE OCEANOGRAPHY GROUP

REFERENCE NO. 77- 1- 12 DATE 9/ 1/77 GMT 20.0

POSITION 49-34.0 N, 138-40.0 W

STATION 10

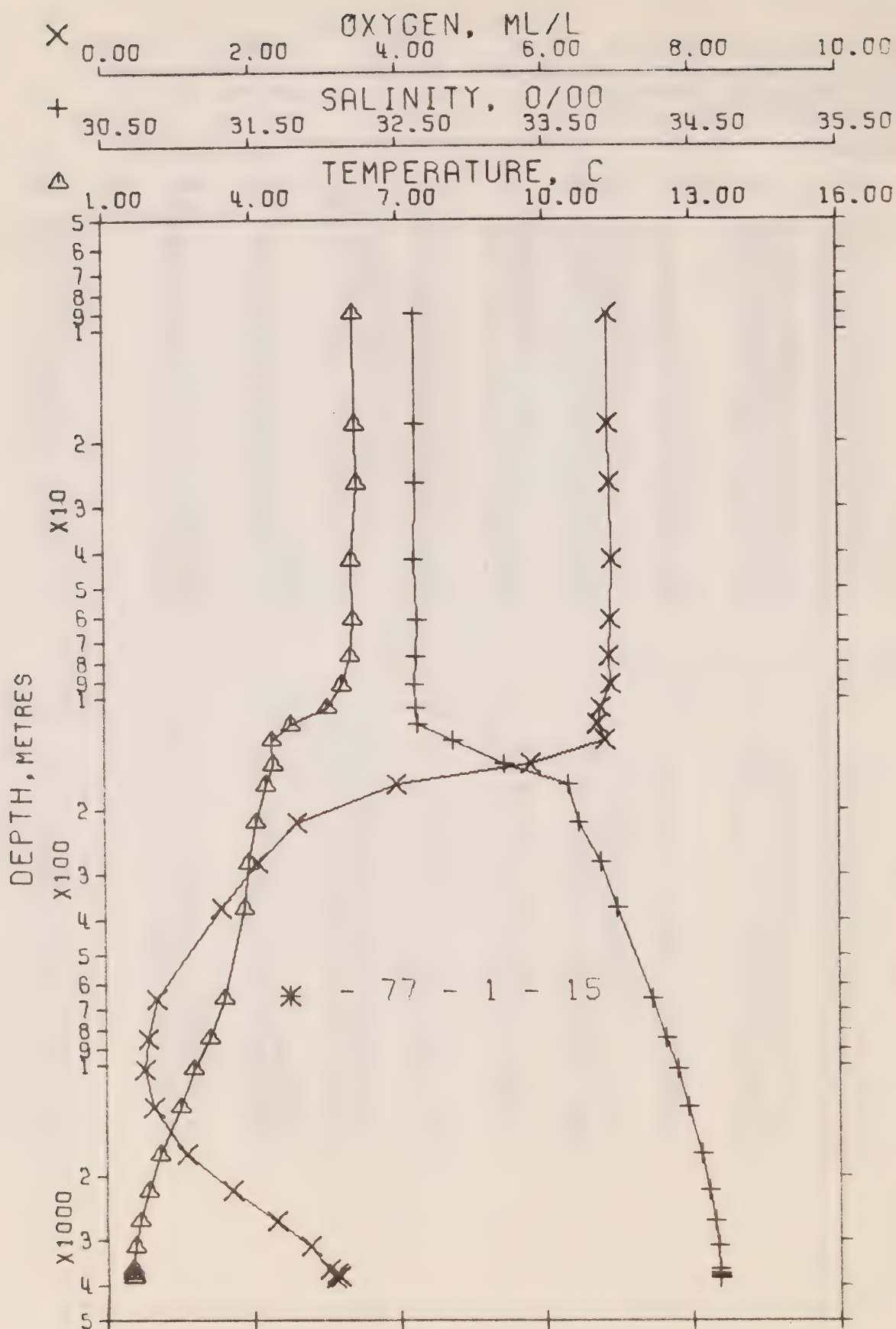
HYDROGRAPHIC CAST DATA

OBSERVED DATA

PRESS	TEMP	SAL	DEPTH	SIGMA T	SVA	THETA	SVA (THETA)	DELTA D	POT. EN	OXY	SOUND
0	7.76	32.546	0	25.407	257.9	7.76	257.9	.00	.00		1479.
8	7.71	32.545	8	25.413	257.5	7.71	257.3	.21	.01		1479.
17	7.71	32.544	17	25.413	257.7	7.71	257.4	.44	.04		1479.
25	7.73	32.543	25	25.409	258.1	7.73	257.7	.65	.08		1479.
42	7.69	32.541	42	25.413	258.0	7.69	257.3	1.09	.23		1479.
62	7.58	32.537	62	25.425	257.1	7.57	256.1	1.61	.51		1479.
84	7.56	32.575	83	25.458	254.3	7.55	253.0	2.15	.91		1479.
104	5.42	32.924	103	26.007	201.9	5.41	200.8	2.61	1.35		1472.
125	5.31	33.224	124	26.257	178.5	5.30	177.1	3.01	1.81		1472.
145	5.49	33.628	144	26.555	150.6	5.48	148.8	3.34	2.27		1474.
165	5.36	33.772	164	26.684	138.5	5.35	136.5	3.63	2.73		1474.
206	4.92	33.849	205	26.795	128.2	4.90	125.9	4.18	3.77		1473.
247	4.61	33.870	245	26.846	123.6	4.59	121.0	4.69	4.94		1472.
326	4.30	33.933	324	26.930	116.3	4.28	113.1	5.64	7.73		1472.
407	4.06	34.023	404	27.026	107.7	4.03	103.9	6.55	11.10		1472.
487	3.90	34.091	483	27.097	101.6	3.86	97.2	7.38	14.90		1473.
650	3.61	34.205	644	27.216	91.3	3.56	85.8	8.94	23.94		1475.
817	3.34	34.302	810	27.319	82.4	3.28	75.9	10.40	34.79		1477.
995	2.99	34.383	985	27.416	73.7	2.92	66.6	11.77	47.52		1478.
1274	2.63	34.452	1261	27.503	66.3	2.54	58.3	13.73	70.05		1481.
1284	2.60	34.451	1271	27.505	66.1	2.51	58.1	13.79	70.92		1481.

INTERPOLATED TO STANDARD PRESSURE

PRESS	TEMP	SAL	DEPTH	SIGMA T	SVA	THETA	SVA (THETA)	DELTA D	POT. EN	OXY	SOUND
0	7.76	32.546	0	25.407	257.9	7.76	257.9	.00	.00		1479.
10	7.71	32.545	10	25.413	257.5	7.71	257.3	.26	.01		1479.
20	7.72	32.544	20	25.411	257.8	7.72	257.5	.52	.05		1479.
30	7.72	32.542	30	25.410	258.1	7.71	257.6	.77	.12		1479.
50	7.64	32.539	50	25.418	257.6	7.64	256.8	1.29	.33		1479.
75	7.57	32.561	75	25.446	255.3	7.56	254.1	1.93	.74		1479.
100	5.77	32.866	99	25.920	210.3	5.77	209.1	2.53	1.27		1473.
125	5.31	33.224	124	26.257	178.5	5.30	177.1	3.01	1.81		1472.
150	5.46	33.666	149	26.589	147.4	5.44	145.6	3.41	2.38		1474.
175	5.25	33.792	174	26.713	135.8	5.23	133.7	3.76	2.96		1473.
200	4.98	33.838	199	26.780	129.7	4.97	127.4	4.10	3.60		1473.
225	4.77	33.859	224	26.820	126.0	4.75	123.5	4.41	4.29		1472.
250	4.60	33.873	248	26.850	123.3	4.58	120.7	4.73	5.04		1472.
300	4.39	33.914	298	26.905	118.5	4.37	115.5	5.33	6.73		1472.
400	4.08	34.016	397	27.018	108.4	4.05	104.6	6.47	10.79		1472.
500	3.87	34.101	496	27.108	100.6	3.84	96.1	7.51	15.57		1473.
600	3.69	34.174	594	27.183	94.1	3.65	88.9	8.48	21.01		1474.
700	3.52	34.237	694	27.250	88.3	3.47	82.6	9.39	27.05		1475.
800	3.37	34.293	793	27.310	83.2	3.31	76.8	10.25	33.60		1476.
900	3.17	34.342	891	27.367	78.1	3.11	71.3	11.06	40.59		1477.
1000	2.96	34.385	990	27.418	73.5	2.91	66.5	11.82	47.93		1478.
1200	2.72	34.435	1188	27.482	68.1	2.63	60.3	13.23	63.77		1480.



OFFSHORE OCEANOGRAPHY GROUP

REFERENCE NO. 77- 1- 15

DATE 10/ 1/77 GMT 17.6

POSITION 50- .0 N, 145-

.0 W

STATION P

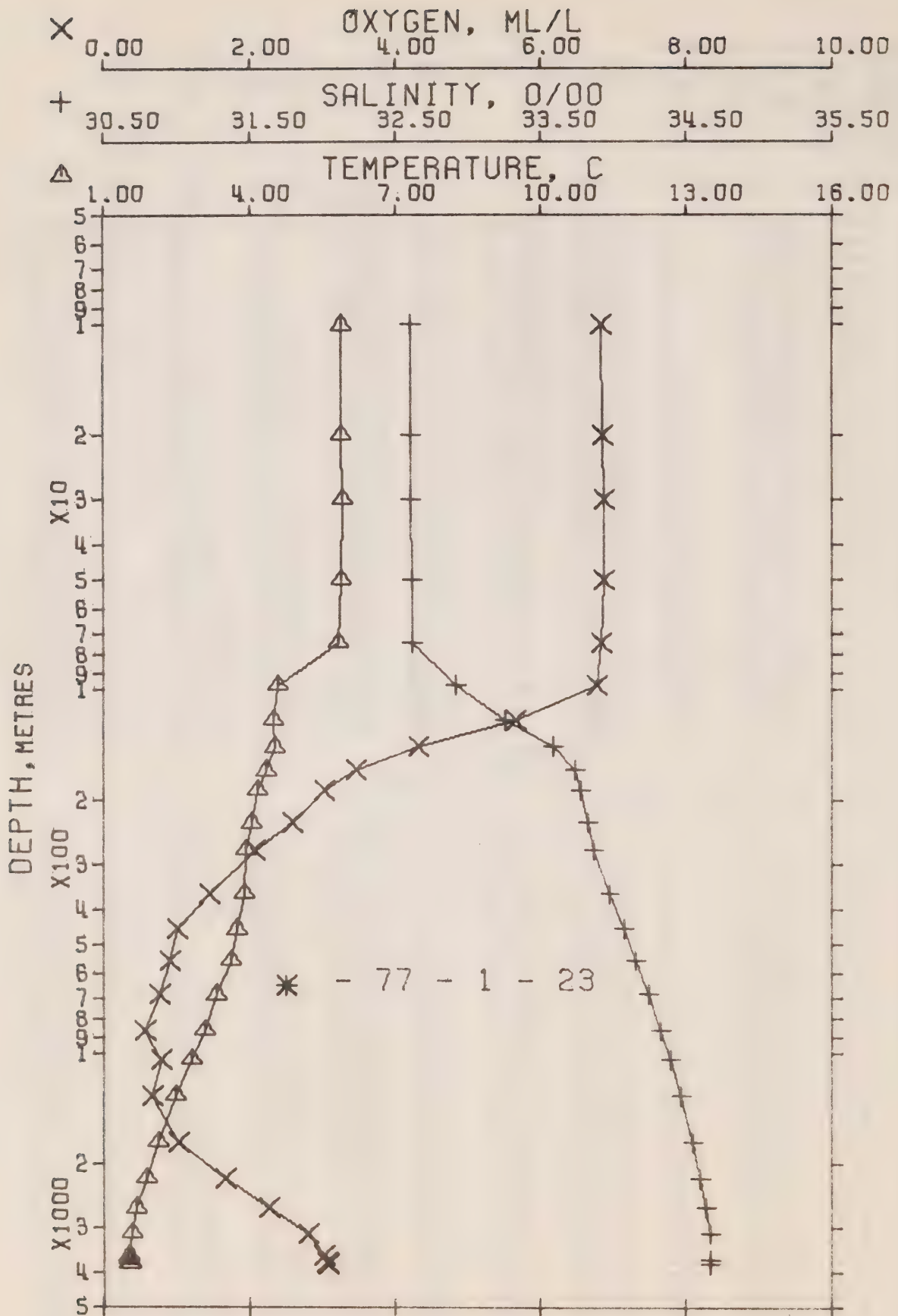
HYDROGRAPHIC CAST DATA

OBSERVED DATA

PRESS	TEMP	SAL	DEPTH	SIGMA T	SVA	THETA	SVA (THETA)	DELTA D	POT. EN	OXY	SOUND
0	6.15	32.618	0	25.678	232.2	6.15	232.2	.00	.00	6.83	1473.
9	6.10	32.617	9	25.684	231.7	6.10	231.6	.21	.01	6.87	1472.
18	6.12	32.617	18	25.681	232.1	6.12	231.9	.42	.04	6.88	1473.
26	6.15	32.617	26	25.677	232.5	6.15	232.2	.61	.08	6.90	1473.
42	6.04	32.613	42	25.688	231.7	6.04	231.2	.98	.21	6.91	1473.
61	6.06	32.626	61	25.696	231.2	6.05	230.4	1.42	.45	6.91	1473.
77	6.01	32.622	77	25.699	231.1	6.00	230.1	1.80	.71	6.88	1473.
93	5.84	32.615	92	25.714	229.8	5.83	228.7	2.14	1.01	6.91	1473.
107	5.53	32.617	106	25.752	226.2	5.52	225.0	2.47	1.34	6.75	1472.
119	4.78	32.631	118	25.848	217.0	4.77	215.9	2.73	1.65	6.73	1469.
131	4.39	32.874	130	26.081	194.9	4.38	193.7	2.98	1.96	6.82	1468.
152	4.42	33.225	151	26.356	169.0	4.41	167.6	3.37	2.51	5.81	1469.
173	4.27	33.663	172	26.719	134.8	4.26	133.2	3.69	3.05	3.97	1469.
220	4.05	33.732	218	26.796	127.8	4.03	125.8	4.30	4.26	2.59	1469.
283	3.92	33.877	281	26.925	116.1	3.90	113.6	5.07	6.24	2.07	1470.
377	3.83	33.993	374	27.026	107.3	3.80	104.0	6.12	9.75	1.56	1471.
664	3.40	34.233	658	27.259	87.0	3.35	81.7	8.87	24.25	.69	1474.
850	3.09	34.323	842	27.359	78.3	3.03	72.1	10.41	36.07	.56	1476.
1035	2.78	34.405	1025	27.453	70.0	2.71	63.2	11.78	49.23	.52	1478.
1312	2.49	34.471	1298	27.530	63.5	2.40	55.7	13.62	71.20	.65	1481.
1773	2.09	34.556	1752	27.631	54.8	1.97	46.0	16.34	113.80	1.07	1487.
2234	1.84	34.613	2206	27.696	49.4	1.68	39.6	18.74	162.73	1.70	1494.
2703	1.66	34.647	2666	27.737	46.2	1.47	35.5	20.97	218.99	2.31	1501.
3182	1.56	34.666	3135	27.760	44.9	1.32	33.1	23.15	284.29	2.75	1509.
3675	1.51	34.678	3616	27.773	44.6	1.22	31.5	25.35	361.15	3.03	1517.
3775	1.50	34.676	3714	27.772	44.8	1.20	31.5	25.80	378.18	3.11	1519.
3867	1.53	34.677	3803	27.771	45.5	1.22	31.6	26.22	394.42	3.16	1520.
3877	1.51	34.680	3813	27.774	45.0	1.20	31.2	26.26	396.25	3.11	1521.

INTERPOLATED TO STANDARD PRESSURE

PRESS	TEMP	SAL	DEPTH	SIGMA T	SVA	THETA	SVA (THETA)	DELTA D	POT. EN	OXY	SOUND
0	6.15	32.618	0	25.678	232.2	6.15	232.2	.00	.00	6.83	1473.
10	6.10	32.617	10	25.683	231.8	6.10	231.7	.23	.01	6.87	1473.
20	6.13	32.617	20	25.680	232.2	6.13	231.9	.46	.05	6.89	1473.
30	6.12	32.616	30	25.680	232.3	6.12	231.9	.70	.11	6.91	1473.
50	6.05	32.619	50	25.691	231.5	6.04	230.9	1.16	.30	6.91	1473.
75	6.02	32.623	75	25.698	231.1	6.01	230.2	1.74	.66	6.88	1473.
100	5.67	32.616	99	25.735	227.8	5.66	226.7	2.31	1.18	6.82	1472.
125	4.57	32.759	124	25.971	205.3	4.57	204.2	2.87	1.81	6.77	1468.
150	4.42	33.194	149	26.332	171.3	4.41	170.0	3.33	2.46	5.90	1469.
175	4.26	33.666	174	26.722	134.5	4.25	132.9	3.71	3.09	3.91	1469.
200	4.14	33.705	198	26.766	130.6	4.12	128.7	4.04	3.72	3.13	1469.
225	4.04	33.746	223	26.809	126.7	4.02	124.7	4.37	4.42	2.54	1469.
250	3.98	33.806	248	26.862	121.8	3.97	119.6	4.68	5.17	2.33	1469.
300	3.90	33.900	298	26.945	114.3	3.88	111.7	5.26	6.82	1.97	1470.
400	3.78	34.018	397	27.050	105.1	3.76	101.6	6.36	10.72	1.47	1471.
500	3.62	34.113	496	27.142	97.1	3.58	92.9	7.37	15.35	1.13	1472.
600	3.46	34.190	595	27.217	90.6	3.44	85.7	8.31	20.60	.84	1473.
700	3.33	34.252	694	27.280	85.1	3.28	79.7	9.18	26.42	.66	1474.
800	3.17	34.301	792	27.335	80.4	3.11	74.5	10.01	32.74	.59	1475.
900	3.00	34.347	891	27.386	75.9	2.94	69.5	10.79	39.52	.55	1476.
1000	2.83	34.391	990	27.436	71.5	2.77	64.8	11.53	46.65	.53	1477.
1200	2.60	34.446	1188	27.501	65.9	2.52	58.5	12.90	61.94	.60	1480.
1500	2.31	34.509	1483	27.575	59.6	2.21	51.4	14.78	87.79	.84	1484.
2000	1.96	34.586	1975	27.665	52.0	1.82	42.6	17.55	137.11	1.40	1491.
2500	1.73	34.633	2466	27.720	47.5	1.56	37.2	20.02	193.74	2.06	1498.
3000	1.60	34.659	2957	27.751	45.3	1.37	34.0	22.33	258.38	2.59	1506.
3500	1.53	34.674	3446	27.768	44.7	1.26	32.1	24.57	332.65	2.93	1514.



OFFSHORE OCEANOGRAPHY GROUP
REFERENCE NO. 77- 1- 23
POSITION 50- .0 N, 145-
HYDROGRAPHIC CAST DATA

DATE 17/ 1/77 GMT 17.8

.0 W

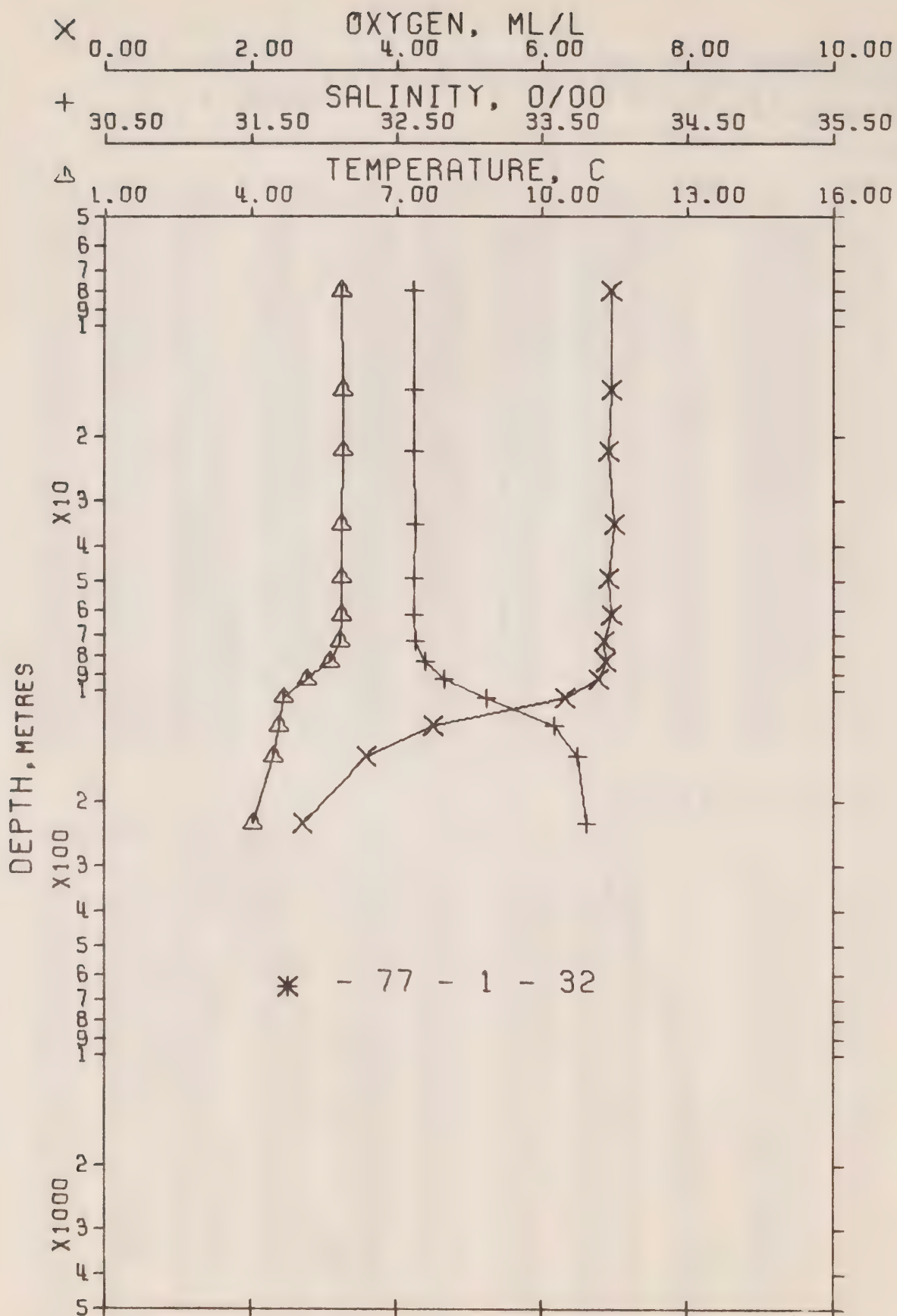
STATION P

OBSERVED DATA

PRESS	TEMP	SAL	DEPTH	SIGMA T	SVA	THETA	SVA (THETA)	DELTA D	POT. EN	OXY	SOUND
0	6.08	32.611	0	25.681	231.9	6.08	231.9	.00	.00	6.75	1472.
10	5.89	32.610	10	25.704	229.8	5.89	229.7	.23	.01	6.85	1472.
20	5.89	32.612	20	25.705	229.8	5.89	229.5	.46	.05	6.86	1472.
30	5.91	32.614	30	25.705	230.0	5.91	229.6	.69	.11	6.87	1472.
50	5.88	32.616	50	25.710	229.7	5.88	229.1	1.16	.30	6.89	1472.
74	5.84	32.616	74	25.715	229.5	5.83	228.6	1.73	.66	6.85	1472.
98	4.56	32.924	97	26.103	192.6	4.55	191.7	2.21	1.09	6.77	1468.
122	4.49	33.261	121	26.377	166.8	4.48	165.7	2.65	1.57	5.67	1469.
144	4.52	33.590	143	26.635	142.7	4.51	141.2	2.99	2.03	4.33	1469.
167	4.34	33.741	166	26.773	129.7	4.33	128.0	3.30	2.53	3.47	1469.
189	4.16	33.784	188	26.826	124.8	4.15	123.0	3.59	3.04	3.01	1469.
233	4.03	33.831	231	26.877	120.3	4.01	118.2	4.12	4.19	2.57	1469.
276	3.92	33.866	274	26.916	116.9	3.90	114.5	4.63	5.52	2.06	1469.
365	3.87	33.984	362	27.015	108.3	3.84	105.0	5.63	8.78	1.44	1471.
457	3.74	34.082	453	27.105	100.3	3.71	96.4	6.59	12.78	1.00	1472.
557	3.60	34.160	552	27.181	93.8	3.56	89.1	7.56	17.78	.90	1473.
693	3.32	34.248	687	27.278	85.3	3.27	79.9	8.77	25.53	.75	1474.
868	3.06	34.333	860	27.370	77.4	3.00	71.1	10.19	36.81	.56	1476.
1044	2.80	34.398	1034	27.445	70.8	2.73	63.9	11.50	49.50	.78	1478.
1312	2.48	34.475	1298	27.534	63.1	2.39	55.3	13.28	70.92	.66+	1481.
1766	2.10	34.552	1745	27.627	55.2	1.98	46.4	15.96	112.76	1.01	1487.
2228	1.87	34.603	2200	27.686	50.5	1.71	40.6	18.40	162.36	1.65	1494.
2696	1.66	34.643	2659	27.734	46.5	1.47	35.8	20.66	219.14	2.25	1501.
3170	1.56	34.668	3123	27.761	44.7	1.32	32.9	22.82	283.56	2.80	1509.
3647	1.51	34.670 *	3589	27.766	45.1	1.22	32.2	24.95	357.83	3.02	1517.
3744	1.51	34.670	3683	27.766	45.3	1.21	32.1	25.39	374.23	3.04 *	1518.
3830	1.53	34.674 *	3767	27.768	45.6	1.22	31.9	25.78	389.46	3.05	1520.
3839	1.51	34.674	3776	27.770	45.3	1.20	31.7	25.83	391.09	3.07	1520.

INTERPOLATED TO STANDARD PRESSURE

PRESS	TEMP	SAL	DEPTH	SIGMA T	SVA	THETA	SVA (THETA)	DELTA D	POT. EN	OXY	SOUND
0	6.08	32.611	0	25.681	231.9	6.08	231.9	.00	.00	6.75	1472.
10	5.89	32.610	10	25.704	229.8	5.89	229.7	.23	.01	6.85	1472.
20	5.89	32.612	20	25.705	229.8	5.89	229.5	.46	.05	6.86	1472.
30	5.91	32.614	30	25.705	230.0	5.91	229.6	.69	.11	6.87	1472.
50	5.88	32.616	50	25.710	229.7	5.88	229.1	1.16	.30	6.89	1472.
75	5.81	32.624	75	25.725	228.5	5.80	227.6	1.74	.67	6.84	1472.
100	4.55	32.960	99	26.133	189.8	4.55	188.9	2.26	1.13	6.65	1468.
125	4.49	33.312	124	26.417	163.1	4.49	161.9	2.70	1.64	5.46	1469.
150	4.47	33.631	149	26.673	139.1	4.46	137.6	3.08	2.16	4.09	1469.
175	4.27	33.757	174	26.793	127.9	4.26	126.2	3.41	2.71	3.30	1469.
200	4.13	33.796	199	26.840	123.6	4.11	121.7	3.72	3.31	2.90	1469.
225	4.05	33.823	223	26.869	121.0	4.04	119.0	4.02	3.97	2.65	1469.
250	3.98	33.846	248	26.893	118.9	3.97	116.6	4.32	4.69	2.36	1469.
300	3.91	33.901	298	26.945	114.3	3.88	111.7	4.91	6.33	1.87	1470.
400	3.82	34.024	397	27.052	105.0	3.79	101.5	6.00	10.24	1.26	1471.
500	3.68	34.118	496	27.140	97.3	3.64	93.1	7.01	14.86	.96	1472.
600	3.50	34.190	595	27.214	90.9	3.46	86.0	7.96	20.14	.85	1473.
700	3.31	34.252	694	27.282	84.9	3.26	79.5	8.83	25.95	.74	1474.
800	3.15	34.302	792	27.337	80.2	3.10	74.3	9.66	32.25	.63	1475.
900	3.01	34.346	891	27.385	76.1	2.95	69.7	10.44	39.02	.60	1477.
1000	2.86	34.363	990	27.428	72.4	2.79	65.6	11.18	46.20	.73	1478.
1200	2.60	34.445	1188	27.500	66.1	2.52	58.7	12.56	61.68	.71	1480.
1500	2.31	34.510	1483	27.576	59.5	2.21	51.3	14.43	87.41	.82	1484.
2000	1.98	34.579	1975	27.659	52.7	1.84	43.3	17.22	136.98	1.36	1491.
2500	1.74	34.627	2466	27.715	48.1	1.57	37.7	19.74	194.60	2.02	1498.
3000	1.59	34.659	2957	27.752	45.3	1.37	33.9	22.05	259.50	2.61	1506.
3500	1.52	34.669	3446	27.765	45.0	1.25	32.4	24.29	333.69	2.96	1514.



OFFSHORE OCEANOGRAPHY GROUP
 REFERENCE NO. 77- 1- 32
 POSITION 50- .0 N, 145-
 HYDROGRAPHIC CAST DATA

DATE 25/ 1/77 GMT 17.6
 .0 W

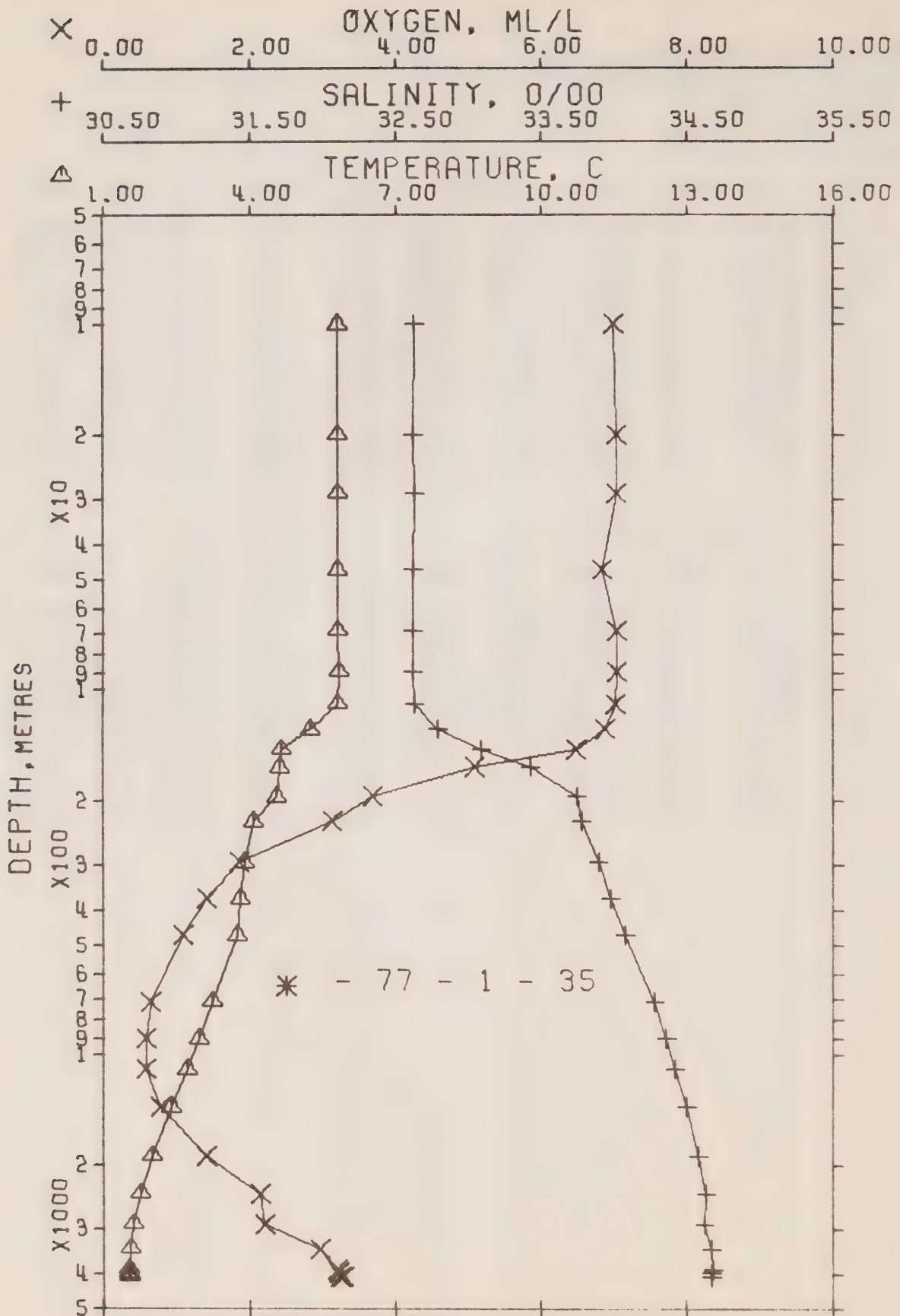
STATION P

OBSERVED DATA

PRSS	TEMP	SAL	DEPTH	SIGMA T	SVA	THETA	SVA (THETA)	DELTA D	POT. EN	OXY	SOUND
0	5.98	32.624	0	25.704	229.7	5.98	229.7	.00	.00	6.94	1472.
8	5.87	32.621	8	25.715	228.7	5.87	228.7	.18	.01	6.96	1472.
15	5.88	32.623	15	25.715	228.8	5.88	228.6	.35	.03	6.95	1472.
22	5.88	32.625	22	25.717	228.7	5.88	228.5	.51	.06	6.92	1472.
35	5.86	32.626	35	25.720	228.6	5.86	228.1	.81	.14	7.00	1472.
49	5.86	32.624	49	25.719	228.9	5.86	228.3	1.13	.28	6.91	1472.
62	5.87	32.624	62	25.717	229.1	5.86	228.4	1.43	.45	6.96	1472.
73	5.84	32.630	73	25.726	228.4	5.83	227.6	1.68	.63	6.87	1472.
84	5.61	32.699	83	25.808	220.7	5.60	219.8	1.91	.81	6.88	1472.
94	5.15	32.829	93	25.963	206.0	5.14	205.0	2.13	1.01	6.78	1470.
105	4.67	33.124	104	26.250	178.8	4.66	177.8	2.34	1.22	6.32	1469.
126	4.56	33.586	125	26.627	143.2	4.55	141.9	2.68	1.62	4.49	1469.
152	4.44	33.748	151	26.768	130.1	4.43	128.5	3.03	2.12	3.58	1469.
233	4.02	33.813	231	26.864	121.5	4.00	119.4	4.04	4.09	2.70	1469.

INTERPOLATED TO STANDARD PRESSURE

PRESS	TEMP	SAL	DEPTH	SIGMA T	SVA	THETA	SVA (THETA)	DELTA D	POT. EN	OXY	SOUND
0	5.98	32.624	0	25.704	229.7	5.98	229.7	.00	.00	6.94	1472.
10	5.87	32.622	10	25.715	228.8	5.87	228.6	.23	.01	6.96	1472.
20	5.88	32.624	20	25.716	228.7	5.88	228.5	.46	.05	6.93	1472.
30	5.87	32.626	30	25.719	228.6	5.86	228.2	.69	.10	6.97	1472.
50	5.86	32.624	50	25.718	228.9	5.86	228.3	1.14	.29	6.91	1472.
75	5.80	32.641	75	25.739	227.2	5.80	226.3	1.72	.66	6.87	1472.
100	4.87	33.003	99	26.133	189.9	4.86	188.9	2.25	1.13	6.51	1469.
125	4.56	33.569	124	26.613	144.5	4.55	143.3	2.67	1.60	4.56	1469.
150	4.45	33.736	149	26.758	131.0	4.44	129.5	3.00	2.08	3.65	1469.
175	4.30	33.769	174	26.800	127.2	4.29	125.5	3.32	2.61	3.29	1469.
200	4.17	33.790	198	26.830	124.5	4.16	122.7	3.64	3.21	3.02	1469.
225	4.05	33.808	223	26.856	122.2	4.04	120.2	3.94	3.88	2.77	1469.



OFFSHORE OCEANOGRAPHY GROUP
 REFERENCE NO. 77- 1- 35
 POSITION 50- .0 N, 145-
 HYDROGRAPHIC CAST DATA

DATE 27/ 1/77 GMT 17.5
 .0 W

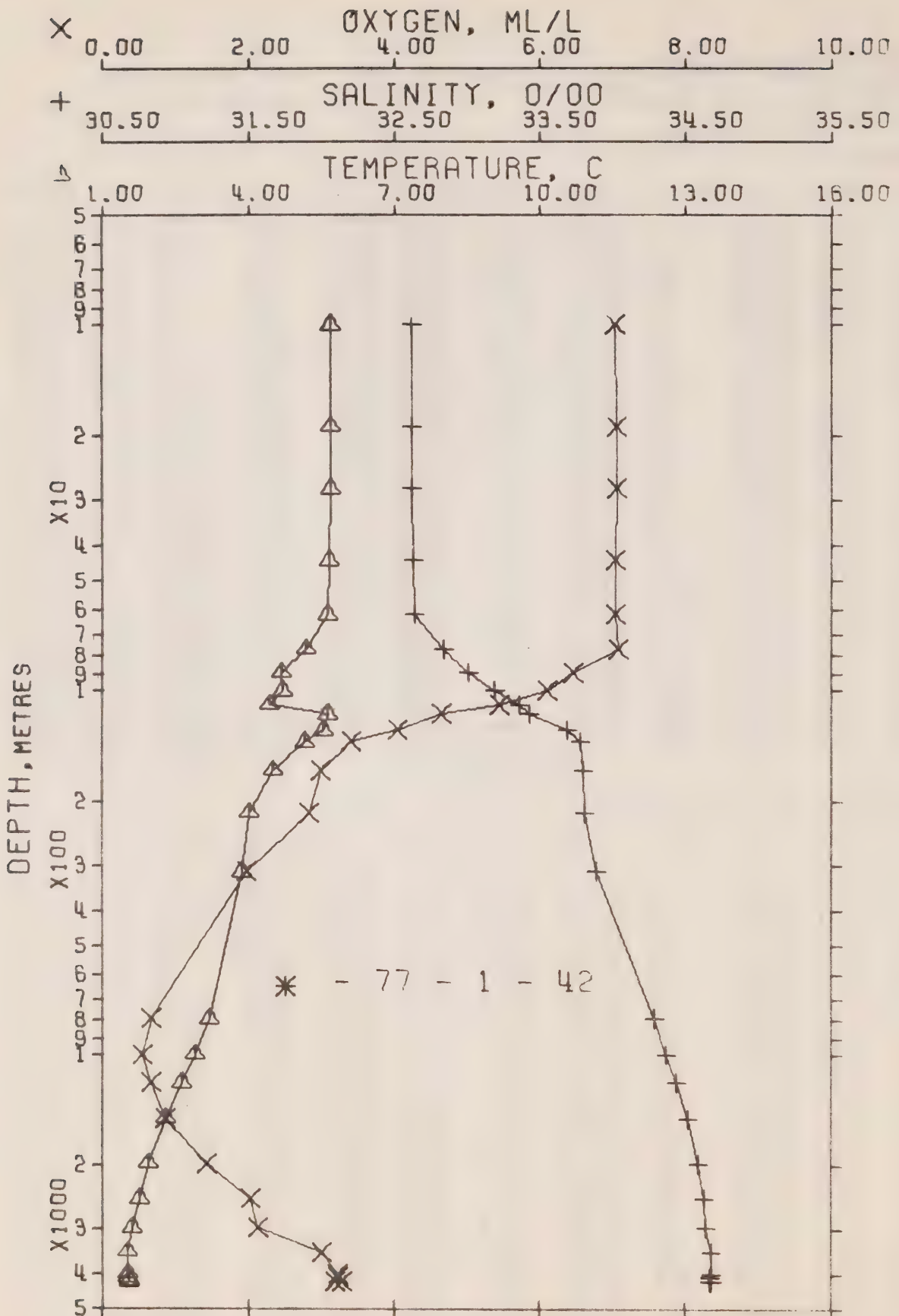
STATION P

OBSERVED DATA

PRESS	TEMP	SAL	DEPTH	SIGMA	SVA	THETA	SVA	DELTA	POT.	OXY	SOUND
				T			(THETA)	U	EN		
0	5.89	32.625	0	25.716	228.6	5.89	228.6	.00	.00	7.01	1471.
10	5.81	32.628	10	25.728	227.6	5.81	227.4	.23	.01	7.00	1471.
20	5.81	32.623	20	25.724	228.0	5.81	227.8	.46	.05	7.04	1471.
29	5.81	32.627	29	25.727	227.8	5.81	227.5	.67	.10	7.03	1472.
47	5.80	32.625	47	25.727	228.1	5.80	227.5	1.08	.26	6.84	1472.
69	5.80	32.621	69	25.723	228.6	5.79	227.8	1.58	.56	7.05	1472.
90	5.82	32.624	89	25.723	228.8	5.81	227.8	2.04	.93	7.05	1473.
110	5.79	32.634	109	25.735	227.9	5.78	226.7	2.50	1.40	7.03	1473.
129	5.22	32.795	128	25.929	209.6	5.21	208.3	2.92	1.91	6.89	1471.
146	4.62	33.089	145	26.227	181.3	4.61	179.9	3.26	2.38	6.47	1469.
164	4.60	33.430	163	26.499	155.7	4.59	154.0	3.56	2.86	5.07	1470.
197	4.53	33.751	196	26.761	131.2	4.52	129.2	4.04	3.73	3.67	1471.
231	4.05	33.780	229	26.834	124.3	4.03	122.2	4.46	4.66	3.13	1469.
298	3.87	33.899	296	26.947	114.1	3.85	111.5	5.26	6.82	1.84	1470.
376	3.79	33.979	373	27.019	107.9	3.76	104.7	6.13	9.78	1.40	1471.
473	3.73	34.080	469	27.105	100.5	3.70	96.4	7.13	14.14	1.09	1472.
719	3.23	34.284	713	27.315	81.8	3.18	76.4	9.37	27.61	.64	1474.
912	2.95	34.360	903	27.401	74.5	2.89	68.1	10.86	40.04	.57	1476.
1108	2.71	34.422	1097	27.472	68.4	2.64	61.3	12.26	54.45	.59	1479.
1409	2.37	34.497	1394	27.561	60.7	2.28	52.8	14.20	79.26	.77	1482.
1922	1.98	34.579	1899	27.658	52.4	1.85	43.3	17.10	128.30	1.41	1489.
2443	1.75	34.630	2411	27.717	47.8	1.58	37.6	19.69	185.72	2.14	1497.
2963	1.61	34.619+	2920	27.718	48.3	1.39	37.1	22.20	255.09	2.21	1505.
3471	1.53	34.671	3417	27.766	44.8	1.26	32.3	24.55	331.96	2.97	1514.
3960	1.51	34.682+	3894	27.776	45.0	1.19	31.0	26.72	414.20	3.20	1522.
4054	1.51	34.672	3986	27.768	46.0	1.18	31.7	27.15	431.75	3.22	1524.
4138	1.53	34.671*	4068	27.766	46.6	1.19	31.8	27.54	448.02	3.27	1525.
4148	1.52	34.671	4077	27.767	46.4	1.18	31.8	27.58	449.83	3.25	1525.

INTERPOLATED TO STANDARD PRESSURE

PRESS	TEMP	SAL	DEPTH	SIGMA	SVA	THETA	SVA	DELTA	POT.	OXY	SOUND
				T			(THETA)	U	EN		
0	5.89	32.625	0	25.716	228.6	5.89	228.6	.00	.00	7.01	1471.
10	5.81	32.628	10	25.728	227.6	5.81	227.4	.23	.01	7.00	1471.
20	5.81	32.623	20	25.724	228.0	5.81	227.8	.46	.05	7.04	1471.
30	5.81	32.627	30	25.727	227.8	5.81	227.5	.68	.10	7.02	1472.
50	5.80	32.624	50	25.726	228.1	5.80	227.6	1.14	.29	6.87	1472.
75	5.81	32.622	75	25.723	228.7	5.80	227.8	1.71	.65	7.05	1472.
100	5.80	32.629	100	25.730	228.3	5.80	227.2	2.28	1.16	7.04	1473.
125	5.33	32.765	124	25.892	213.0	5.32	211.7	2.84	1.81	6.92	1471.
150	4.62	33.168	149	26.291	175.3	4.60	173.9	3.33	2.49	6.15	1469.
175	4.58	33.542	174	26.590	147.1	4.56	145.4	3.73	3.14	4.58	1470.
200	4.49	33.753	199	26.767	130.6	4.47	128.6	4.07	3.80	3.62	1470.
225	4.13	33.775	224	26.823	125.4	4.11	123.3	4.39	4.49	3.22	1469.
250	3.99	33.817	249	26.870	121.1	3.98	118.8	4.70	5.24	2.73	1469.
300	3.87	33.901	298	26.949	113.9	3.85	111.3	5.28	6.88	1.83	1470.
400	3.77	34.006	397	27.042	105.9	3.75	102.4	6.38	10.79	1.31	1471.
500	3.66	34.107	496	27.133	98.0	3.63	93.7	7.40	15.48	1.03	1472.
600	3.45	34.196	595	27.225	89.8	3.40	85.0	8.34	20.73	.83	1473.
700	3.26	34.271	694	27.302	83.0	3.21	77.7	9.21	26.45	.67	1474.
800	3.10	34.318	792	27.354	78.5	3.05	72.6	10.01	32.60	.61	1475.
900	2.97	34.356	891	27.397	74.9	2.90	68.5	10.78	39.24	.58	1476.
1000	2.84	34.389	990	27.435	71.6	2.77	64.9	11.51	46.32	.58	1477.
1200	2.60	34.447	1188	27.502	65.9	2.52	58.5	12.88	61.71	.65	1480.
1500	2.29	34.514	1483	27.581	59.1	2.19	50.9	14.75	87.33	.90	1484.
2000	1.94	34.587	1975	27.668	51.7	1.80	42.4	17.51	136.41	1.53	1490.
2500	1.73	34.629	2466	27.717	47.8	1.56	37.5	19.96	192.55	2.15	1498.
3000	1.60	34.623	2957	27.722	48.0	1.38	36.7	22.38	260.55	2.27	1506.
3500	1.53	34.672	3447	27.766	44.9	1.26	32.2	24.68	336.58	2.98	1514.
4000	1.51	34.678	3933	27.773	45.4	1.19	31.3	26.90	421.57	3.21	1523.
4100	1.52	34.672	4031	27.767	46.3	1.19	31.8	27.36	440.52	3.25	1524.



OFFSHORE OCEANOGRAPHY GROUP
REFERENCE NO. 77- 1- 42
POSITION 50- .0 N, 145-
HYDROGRAPHIC CAST DATA

DATE 2/ 2/77 GMT 17.5
.0 W

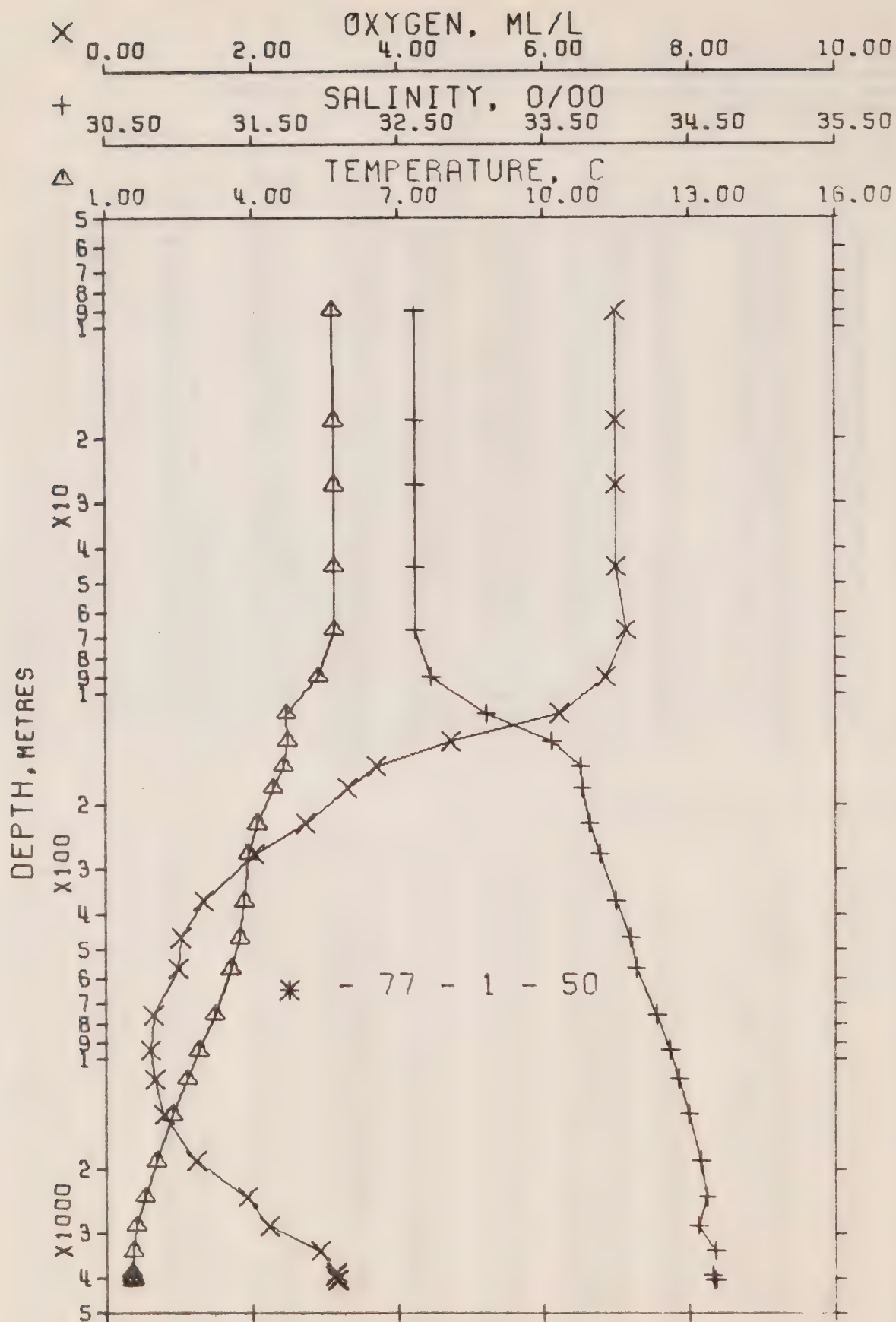
STATION P

OBSERVED DATA

PRESS	TEMP	SAL	DEPTH	SIGMA T	SVA	THETA	SVA (THETA)	DELTA D	POT. EN	OXY	SOUND
0	5.70	32.624	0	25.738	226.5	5.70	226.5	.00	.00	7.11	1471.
10	5.67	32.623	10	25.741	226.3	5.67	226.2	.23	.01	7.04	1471.
19	5.68	32.624	19	25.740	226.5	5.68	226.3	.43	.04	7.07	1471.
28	5.69	32.624	28	25.739	226.7	5.69	226.4	.64	.09	7.07	1471.
44	5.64	32.627	44	25.747	226.1	5.64	225.6	1.00	.23	7.05	1471.
62	5.63	32.637	62	25.756	225.4	5.62	224.7	1.41	.45	7.04	1471.
78	5.16	32.838	77	25.969	205.2	5.15	204.4	1.74	.68	7.08	1470.
90	4.66	33.014	89	26.164	186.8	4.65	186.0	1.97	.88	6.45	1468.
101	4.68	33.188	100	26.299	174.1	4.67	173.1	2.17	1.08	6.10	1469.
110	4.43	33.363	109	26.464	158.4	4.42	157.4	2.33	1.24	5.44	1468.
117	5.63	33.435	116	26.386	166.3	5.62	164.9	2.44	1.37	4.65	1473.
129	5.52	33.691	128	26.601	146.0	5.51	144.4	2.63	1.61	4.05	1473.
139	5.13	33.776	138	26.714	135.3	5.12	133.7	2.77	1.80	3.39	1472.
166	4.49	33.801	165	26.805	126.7	4.48	125.1	3.13	2.35	2.99	1470.
218	4.01	33.808	216	26.861	121.7	3.99	119.7	3.76	3.60	2.83	1469.
316	3.84	33.893	314	26.945	114.4	3.82	111.6	4.93	6.76	1.97	1470.
802	3.19	34.289	795	27.323	81.6	3.13	75.6	9.56	32.54	.67	1476.
1004	2.88	34.374	994	27.419	73.2	2.81	66.4	11.11	46.84	.54	1478.
1204	2.61	34.441	1192	27.496	66.5	2.53	59.0	12.51	62.57	.66	1480.
1507	2.29	34.518	1490	27.584	58.7	2.19	50.5	14.39	88.60	.86	1484.
2013	1.94	34.590	1988	27.670	51.5	1.80	42.2	17.19	138.63	1.42	1491.
2521	1.75	34.632	2487	27.718	47.9	1.57	37.4	19.70	196.59	2.03	1498.
3032	1.59	34.636	2988	27.733	47.0	1.37	35.7	22.11	264.89	2.12	1506.
3547	1.52	34.677	3491	27.771	44.5	1.25	31.8	24.47	343.99	3.01	1515.
4065	1.51	34.683	3996	27.777	45.2	1.18	30.9	26.78	433.56	3.21	1524.
4169	1.51	34.674 +	4098	27.770	46.1	1.17	31.5	27.26	453.62	3.21	1526.
4263	1.55	34.670 +	4189	27.764	47.3	1.20	32.0	27.70	472.58	3.19	1527.
4273	1.53	34.681	4199	27.774	46.2	1.18	31.0	27.74	474.67	3.27	1528.

INTERPOLATED TO STANDARD PRESSURE

PRESS	TEMP	SAL	DEPTH	SIGMA T	SVA	THETA	SVA (THETA)	DELTA D	POT. EN	OXY	SOUND
0	5.70	32.624	0	25.738	226.5	5.70	226.5	.00	.00	7.11	1471.
10	5.67	32.623	10	25.741	226.3	5.67	226.2	.23	.01	7.04	1471.
20	5.68	32.624	20	25.740	226.5	5.68	226.3	.45	.05	7.07	1471.
30	5.68	32.624	30	25.740	226.6	5.68	226.2	.68	.10	7.07	1471.
50	5.64	32.631	50	25.750	225.8	5.63	225.2	1.13	.29	7.05	1471.
75	5.23	32.808	75	25.937	208.3	5.23	207.5	1.69	.64	7.07	1470.
100	4.68	33.178	99	26.291	174.8	4.67	173.8	2.16	1.06	6.12	1469.
125	5.55	33.612	124	26.534	152.3	5.54	150.8	2.57	1.53	4.24	1473.
150	4.86	33.787	149	26.753	131.6	4.84	130.0	2.92	2.01	3.22	1471.
175	4.40	33.802	174	26.816	125.7	4.39	124.0	3.24	2.54	2.96	1470.
200	4.16	33.806	198	26.844	123.2	4.15	121.4	3.55	3.14	2.88	1469.
225	3.99	33.816	223	26.868	121.0	3.98	119.0	3.85	3.80	2.75	1469.
250	3.95	33.839	248	26.892	118.9	3.93	116.7	4.15	4.53	2.51	1469.
300	3.86	33.881	298	26.933	115.4	3.84	112.8	4.74	6.17	2.09	1470.
400	3.68	33.993	397	27.041	105.9	3.65	102.5	5.85	10.12	1.64	1471.
500	3.52	34.088	496	27.131	97.9	3.49	93.9	6.86	14.78	1.33	1472.
600	3.39	34.165	595	27.205	91.6	3.35	86.8	7.81	20.09	1.07	1473.
700	3.29	34.231	694	27.268	86.2	3.24	80.9	8.70	25.97	.86	1474.
800	3.19	34.288	793	27.322	81.7	3.14	75.7	9.54	32.38	.67	1476.
900	3.03	34.333	891	27.372	77.3	2.97	70.9	10.33	39.27	.60	1477.
1000	2.89	34.373	990	27.417	73.4	2.82	66.5	11.09	46.56	.54	1478.
1200	2.62	34.440	1188	27.495	66.6	2.53	59.1	12.48	62.22	.66	1480.
1500	2.30	34.516	1483	27.583	58.9	2.19	50.7	14.36	88.01	.85	1484.
2000	1.95	34.588	1975	27.668	51.7	1.81	42.4	17.12	137.30	1.41	1491.
2500	1.76	34.630	2466	27.716	48.0	1.58	37.5	19.60	194.03	2.01	1498.
3000	1.60	34.636	2956	27.733	47.0	1.38	35.8	21.96	260.23	2.11	1506.
3500	1.53	34.674	3444	27.768	44.7	1.26	32.1	24.26	336.49	2.93	1514.
4000	1.51	34.682	3931	27.776	45.1	1.19	31.0	26.49	421.59	3.19	1523.
4100	1.51	34.680	4030	27.774	45.5	1.18	31.1	26.94	440.25	3.21	1524.
4200	1.52	34.673	4128	27.768	46.5	1.18	31.6	27.40	459.69	3.20	1526.



OFFSHORE OCEANOGRAPHY GROUP
 REFERENCE NO. 77- 1- 50
 POSITION 50- .0 N, 145- .0 W
 HYDROGRAPHIC CAST DATA

DATE 9/ 2/77 GMT 17.5

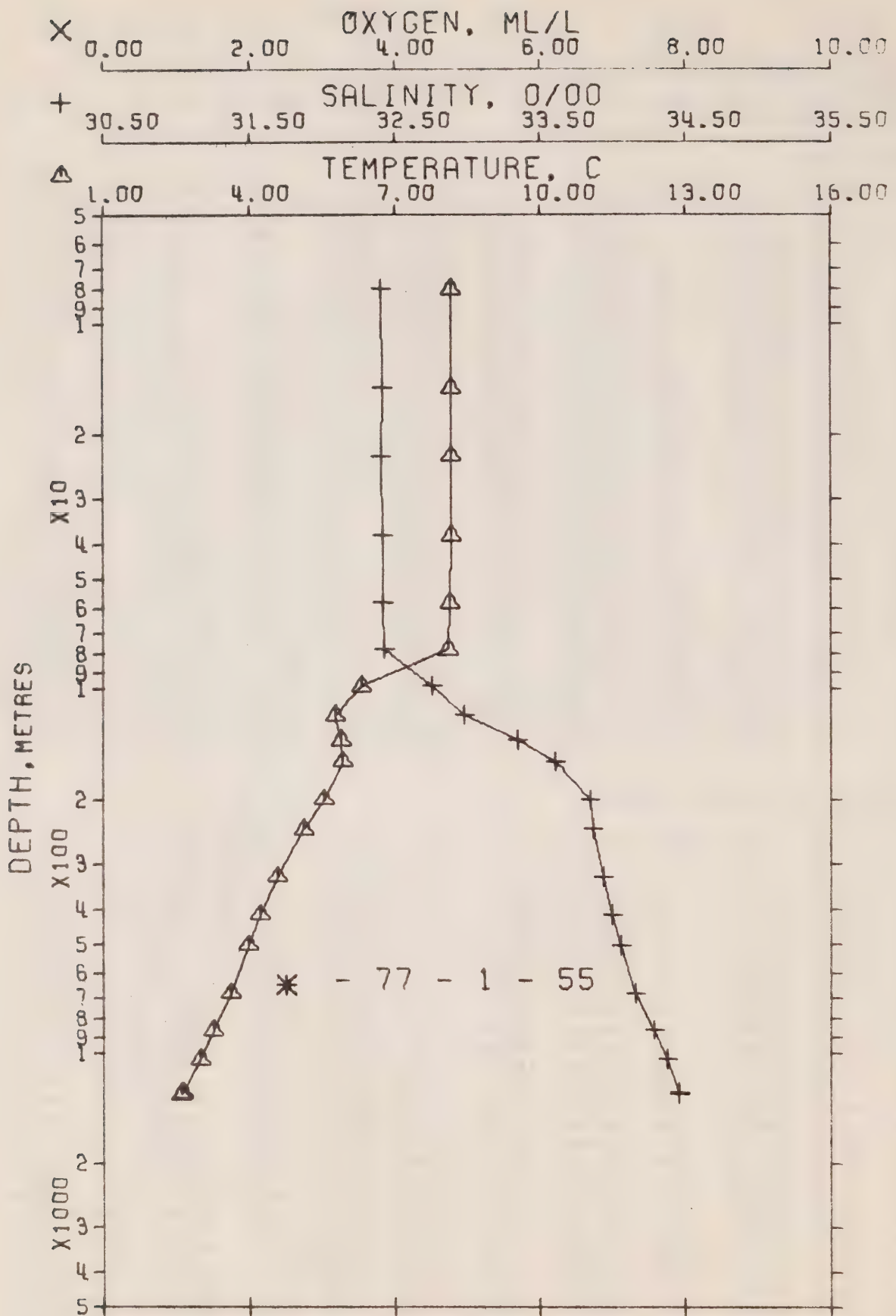
STATION P

OBSERVED DATA

PRESS	TEMP	SAL	DEPTH	SIGMA T	SVA	THETA	SVA (THETA)	DELTA D	POT. EN	OXY	SOUND
0	5.73	32.622	0	25.733	227.0	5.73	227.0	.00	.00	6.94	1471.
9	5.66	32.622	9	25.741	226.3	5.66	226.2	.21	.01	7.00	1471.
18	5.69	32.620	18	25.736	226.9	5.69	226.7	.41	.04	7.01	1471.
27	5.69	32.619	27	25.735	227.0	5.69	226.7	.62	.09	7.01	1471.
45	5.68	32.621	45	25.738	227.0	5.68	226.5	1.03	.24	7.00	1471.
67	5.67	32.620	67	25.738	227.2	5.66	226.4	1.53	.53	7.15	1472.
91	5.34	32.729	90	25.863	215.5	5.33	214.5	2.04	.94	6.86	1471.
114	4.69	33.115	113	26.240	179.8	4.68	178.7	2.50	1.41	6.22	1469.
136	4.73	33.563	135	26.590	146.8	4.72	145.4	2.86	1.87	4.72	1470.
159	4.63	33.762	158	26.759	131.1	4.62	129.4	3.18	2.35	3.70	1470.
182	4.42	33.766	181	26.785	128.8	4.41	127.0	3.48	2.88	3.29	1470.
229	4.08	33.825	227	26.867	121.2	4.06	119.1	4.06	4.09	2.72	1469.
276	3.92	33.888	274	26.933	115.2	3.90	112.8	4.62	5.53	2.01	1470.
372	3.81	34.000	369	27.033	106.5	3.78	103.3	5.68	9.03	1.32	1471.
470	3.72	34.096	466	27.119	99.2	3.69	95.1	6.69	13.33	1.02	1472.
571	3.54	34.145	566	27.175	94.4	3.50	89.7	7.67	18.52	.98	1473.
762	3.22	34.279	755	27.312	82.4	3.17	76.6	9.35	29.92	.65	1475.
953	2.88	34.374	944	27.419	72.9	2.82	66.4	10.83	42.84	.61	1477.
1146	2.65	34.433	1134	27.486	67.2	2.57	60.0	12.18	57.22	.65	1479.
1436	2.36	34.499	1420	27.564	60.6	2.26	52.5	14.02	81.49	.78	1483.
1925	2.01	34.579	1902	27.656	52.8	1.88	43.6	16.80	128.86	1.23	1490.
2420	1.78	34.622	2388	27.708	48.6	1.61	38.4	19.27	183.57	1.91	1497.
2918	1.61	34.561+	2876	27.672	52.3	1.40	41.6	21.83	253.39	2.22	1504.
3418	1.53	34.676	3365	27.770	44.4	1.27	32.0	24.21	329.92	2.91	1513.
3917	1.51	34.665*	3852	27.762	46.1	1.20	32.3	26.46	414.29	3.15	1521.
4016	1.51	34.663+	3949	27.761	46.5	1.18	32.4	26.93	432.91	3.12	1523.
4106	1.53	34.680	4036	27.773	45.8	1.19	31.2	27.34	450.01	3.14	1525.
4116	1.52	34.668+	4046	27.764	46.5	1.18	32.0	27.39	452.00	3.16	1525.

INTERPOLATED TO STANDARD PRESSURE

PRESS	TEMP	SAL	DEPTH	SIGMA T	SVA	THETA	SVA (THETA)	DELTA D	POT. EN	OXY	SOUND
0	5.73	32.622	0	25.733	227.0	5.73	227.0	.00	.00	6.94	1471.
10	5.66	32.622	10	25.740	226.4	5.66	226.3	.23	.01	7.00	1471.
20	5.69	32.620	20	25.736	226.9	5.69	226.7	.45	.05	7.01	1471.
30	5.69	32.619	30	25.736	227.0	5.69	226.7	.68	.10	7.01	1471.
50	5.68	32.621	50	25.738	227.0	5.67	226.4	1.13	.29	7.04	1471.
75	5.55	32.659	75	25.783	223.0	5.55	222.1	1.70	.65	7.04	1471.
100	5.06	32.896	99	26.027	200.0	5.05	198.9	2.24	1.13	6.58	1470.
125	4.71	33.352	124	26.426	162.3	4.70	161.1	2.69	1.65	5.43	1470.
150	4.67	33.688	149	26.696	137.0	4.66	135.4	3.06	2.16	4.08	1470.
175	4.48	33.765	174	26.777	129.5	4.47	127.7	3.39	2.71	3.41	1470.
200	4.28	33.790	199	26.819	125.7	4.27	123.7	3.71	3.32	3.06	1470.
225	4.10	33.821	223	26.861	121.7	4.09	119.7	4.02	3.99	2.76	1469.
250	4.00	33.855	248	26.899	118.4	3.99	116.1	4.32	4.71	2.38	1469.
300	3.89	33.919	298	26.961	112.8	3.87	110.1	4.90	6.33	1.82	1470.
400	3.78	34.030	397	27.060	104.2	3.75	100.7	5.98	10.19	1.23	1471.
500	3.66	34.112	496	27.137	97.6	3.63	93.4	6.98	14.80	1.00	1472.
600	3.48	34.168	595	27.199	92.3	3.44	87.4	7.94	20.14	.92	1473.
700	3.31	34.240	694	27.272	85.9	3.27	80.5	8.83	26.04	.74	1474.
800	3.15	34.300	793	27.336	80.3	3.09	74.4	9.66	32.39	.64	1475.
900	2.97	34.350	891	27.392	75.3	2.91	69.0	10.44	39.12	.62	1476.
1000	2.82	34.389	990	27.437	71.4	2.75	64.7	11.17	46.21	.62	1477.
1200	2.59	34.447	1188	27.502	65.8	2.51	58.4	12.54	61.55	.68	1480.
1500	2.31	34.511	1483	27.577	59.4	2.21	51.2	14.41	87.28	.85	1484.
2000	1.97	34.586	1975	27.665	52.1	1.83	42.7	17.19	136.72	1.34	1491.
2500	1.75	34.611	2466	27.702	49.3	1.57	38.9	19.66	193.40	1.97	1498.
3000	1.60	34.581	2956	27.689	50.9	1.37	39.9	22.26	266.19	2.34	1506.
3500	1.53	34.674	3445	27.769	44.7	1.26	32.0	24.57	342.81	2.95	1514.
4000	1.51	34.663	3933	27.761	46.4	1.19	32.4	26.85	429.82	3.12	1523.
4100	1.53	34.679	4030	27.772	45.9	1.19	31.3	27.31	448.94	3.14	1525.



OFFSHORE OCEANOGRAPHY GROUP

REFERENCE NO. 77- 1- 55 DATE 14/ 2/77 GMT 16.5

POSITION 49-17.0 N, 134-40.0 W

STATION 8

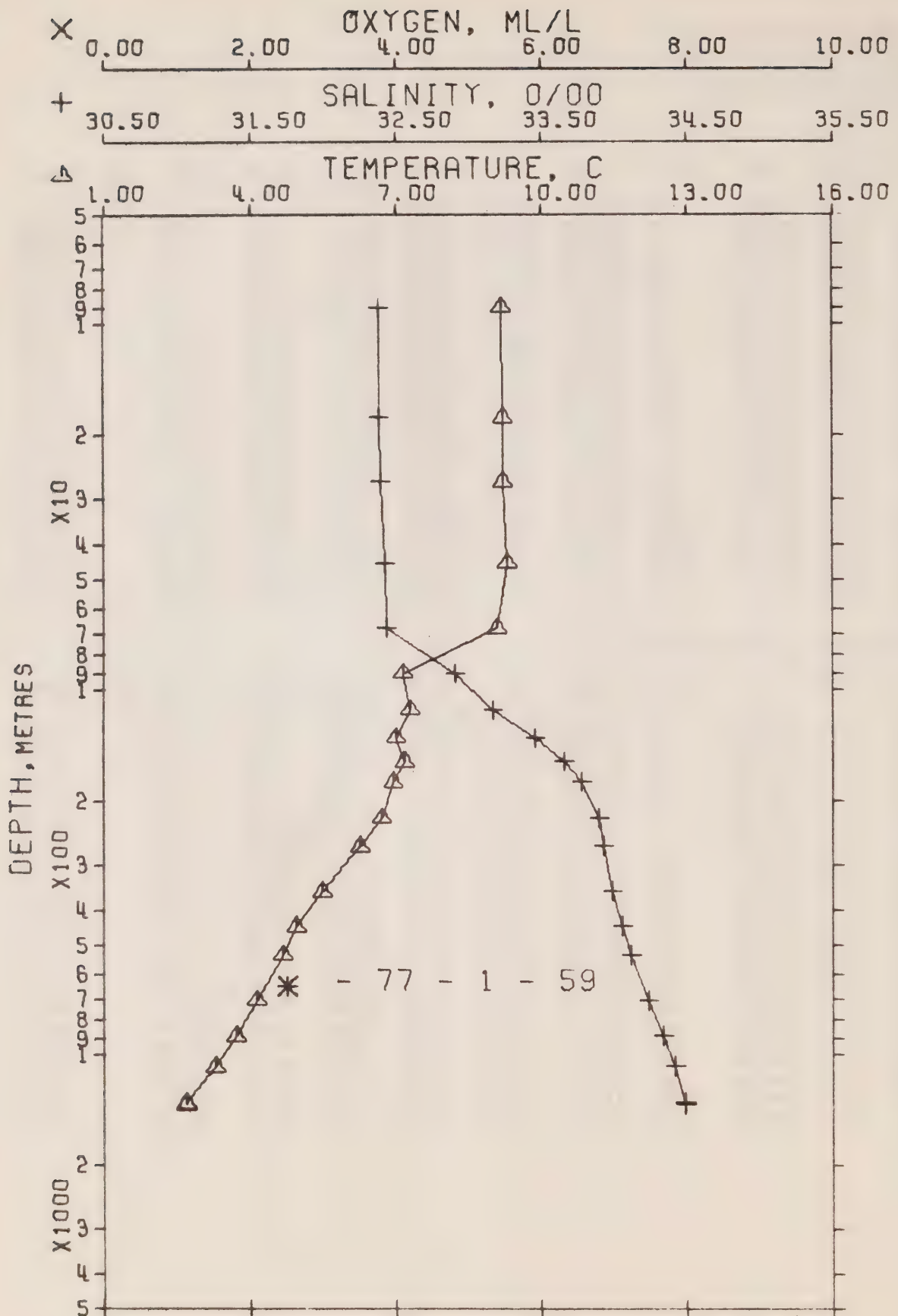
HYDROGRAPHIC CAST DATA

OBSERVED DATA

PRESS	TEMP	SAL	DEPTH	SIGMA T	SVA	THETA	SVA (THETA)	DELTA D	POT. EN	OXY	SOUND
0	8.22	32.408	0	25.233	274.5	8.22	274.5	.00	.00		1480.
8	8.17	32.408	8	25.240	274.0	8.17	273.8	.22	.01		1480.
15	8.17	32.420	15	25.249	273.2	8.17	272.9	.41	.03		1480.
23	8.18	32.412	23	25.242	274.0	8.18	273.6	.63	.07		1481.
38	8.16	32.418	38	25.249	273.5	8.16	272.9	1.05	.20		1481.
58	8.14	32.420	58	25.254	273.4	8.13	272.4	1.60	.47		1481.
78	8.10	32.429	78	25.267	272.5	8.09	271.2	2.15	.86		1481.
99	6.32	32.758	98	25.767	224.9	6.31	223.6	2.65	1.31		1475.
119	5.76	32.977	118	26.009	202.1	5.75	200.6	3.08	1.78		1473.
139	5.88	33.353	138	26.290	175.6	5.87	173.9	3.46	2.28		1475.
159	5.91	33.607	158	26.487	157.3	5.90	155.2	3.79	2.79		1475.
201	5.54	33.851	200	26.725	135.2	5.52	132.6	4.41	3.92		1475.
244	5.11	33.875	242	26.794	128.8	5.09	126.0	4.96	5.18		1474.
329	4.56	33.940	327	26.907	118.7	4.53	115.2	6.02	8.27		1473.
417	4.21	34.002	414	26.994	111.0	4.18	106.9	7.03	12.09		1473.
507	3.98	34.063	503	27.066	104.7	3.94	100.0	8.00	16.65		1474.
688	3.60	34.165	682	27.185	94.4	3.55	88.7	9.79	27.58		1475.
870	3.26	34.292	862	27.319	82.6	3.20	75.9	11.40	40.31		1477.
1049	2.99	34.382	1039	27.415	74.1	2.92	66.7	12.80	54.00		1479.
1298	2.62	34.460	1285	27.510	65.7	2.53	57.6	14.54	74.75		1482.
1307	2.60	34.461	1293	27.513	65.4	2.51	57.3	14.59	75.46		1482.

INTERPOLATED TO STANDARD PRESSURE

PRESS	TEMP	SAL	DEPTH	SIGMA T	SVA	THETA	SVA (THETA)	DELTA D	POT. EN	OXY	SOUND
0	8.22	32.408	0	25.233	274.5	8.22	274.5	.00	.00		1480.
10	8.17	32.412	10	25.243	273.7	8.17	273.5	.27	.01		1480.
20	8.18	32.415	20	25.244	273.7	8.17	273.4	.55	.06		1481.
30	8.17	32.415	30	25.245	273.8	8.17	273.3	.82	.13		1481.
50	8.15	32.419	50	25.252	273.4	8.14	272.6	1.37	.35		1481.
75	8.11	32.428	75	25.265	272.6	8.10	271.4	2.05	.78		1481.
100	6.28	32.775	99	25.786	223.1	6.27	221.8	2.68	1.34		1475.
125	5.80	33.100	124	26.101	193.4	5.79	191.8	3.20	1.94		1474.
150	5.90	33.497	149	26.402	165.2	5.88	163.2	3.65	2.56		1475.
175	5.76	33.706	174	26.583	148.3	5.75	146.0	4.03	3.20		1475.
200	5.55	33.844	199	26.718	135.8	5.53	133.3	4.39	3.88		1475.
225	5.29	33.865	223	26.765	131.5	5.27	128.7	4.72	4.60		1474.
250	5.06	33.880	248	26.804	128.0	5.04	125.1	5.04	5.38		1474.
300	4.73	33.920	298	26.873	121.8	4.71	118.5	5.67	7.13		1473.
400	4.27	33.991	397	26.979	112.3	4.24	108.4	6.84	11.29		1473.
500	4.00	34.059	496	27.061	105.2	3.96	100.5	7.92	16.27		1474.
600	3.77	34.119	594	27.132	99.0	3.73	93.8	8.94	21.99		1475.
700	3.57	34.174	693	27.195	93.5	3.53	87.7	9.91	28.39		1475.
800	3.38	34.247	792	27.271	86.8	3.33	80.5	10.81	35.27		1476.
900	3.21	34.308	891	27.336	81.0	3.15	74.2	11.65	42.53		1477.
1000	3.06	34.359	990	27.391	76.3	2.99	69.0	12.43	50.14		1478.
1200	2.76	34.431	1187	27.475	68.8	2.67	60.9	13.88	66.33		1480.



OFFSHORE OCEANOGRAPHY GROUP

REFERENCE NO. 77- 1- 59 DATE 15/ 2/77 GMT 23.5

POSITION 48-46.0 N, 127-40.0 W

STATION 4

HYDROGRAPHIC CAST DATA

OBSERVED DATA

PRESS	TEMP	SAL	DEPTH	SIGMA T	SVA	THETA	SVA (THETA)	DELTA D	POT. EN	OXY	SOUND
0	9.25	32.396	0	25.066	290.4	9.25	290.4	.00	.00		1484.
9	9.19	32.392	9	25.072	289.9	9.19	289.8	.26	.01		1484.
18	9.21	32.392	18	25.069	290.4	9.21	290.0	.53	.05		1484.
27	9.23	32.397	27	25.070	290.5	9.23	290.0	.79	.11		1485.
45	9.30	32.428	45	25.083	289.5	9.30	288.7	1.31	.30		1485.
68	9.11	32.436	68	25.119	286.5	9.10	285.2	1.99	.70		1485.
91	7.16	32.906	90	25.773	224.4	7.15	223.1	2.55	1.15		1478.
114	7.31	33.166	113	25.956	207.4	7.30	205.6	3.05	1.67		1480.
136	7.00	33.459	135	26.229	181.8	6.99	179.7	3.48	2.22		1479.
158	7.17	33.656	157	26.360	169.7	7.15	167.2	3.87	2.80		1481.
180	6.93	33.784	179	26.493	157.4	6.91	154.5	4.23	3.42		1480.
226	6.71	33.904	224	26.617	146.2	6.69	142.7	4.92	4.84		1480.
270	6.24	33.932	268	26.701	138.6	6.22	134.7	5.55	6.43		1479.
359	5.46	33.993	356	26.846	125.5	5.43	120.9	6.72	10.17		1477.
447	4.94	34.056	444	26.957	115.5	4.90	110.4	7.79	14.55		1477.
536	4.65	34.116	532	27.037	108.6	4.61	102.7	8.78	19.54		1477.
715	4.12	34.242	709	27.194	94.7	4.07	87.8	10.59	31.06		1478.
897	3.71	34.342	889	27.315	84.1	3.64	76.2	12.22	44.39		1479.
1085	3.29	34.416	1075	27.415	75.2	3.21	66.7	13.72	59.50		1481.
1372	2.68	34.486	1358	27.526	64.9	2.58	56.1	15.72	84.58		1483.
1383	2.67	34.492	1369	27.532	64.4	2.57	55.5	15.79	85.60		1483.

INTERPOLATED TO STANDARD PRESSURE

PRESS	TEMP	SAL	DEPTH	SIGMA T	SVA	THETA	SVA (THETA)	DELTA D	POT. EN	OXY	SOUND
0	9.25	32.396	0	25.066	290.4	9.25	290.4	.00	.00		1484.
10	9.19	32.392	10	25.072	290.0	9.19	289.8	.29	.01		1484.
20	9.21	32.393	20	25.069	290.4	9.21	290.0	.58	.06		1484.
30	9.24	32.403	30	25.073	290.3	9.24	289.7	.87	.13		1485.
50	9.25	32.430	50	25.092	288.8	9.25	287.8	1.45	.37		1485.
75	8.47	32.591	75	25.338	265.7	8.46	264.4	2.17	.83		1483.
100	7.23	33.020	99	25.853	217.0	7.22	215.4	2.76	1.35		1479.
125	7.14	33.322	124	26.101	193.7	7.13	191.8	3.28	1.95		1479.
150	7.11	33.588	149	26.315	173.9	7.10	171.5	3.73	2.58		1480.
175	6.98	33.756	174	26.464	160.1	6.97	157.3	4.15	3.27		1480.
200	6.83	33.840	199	26.551	152.1	6.81	149.0	4.54	4.01		1480.
225	6.71	33.903	224	26.616	146.3	6.69	142.8	4.91	4.82		1480.
250	6.44	33.920	248	26.666	141.8	6.42	138.1	5.27	5.69		1479.
300	5.95	33.955	298	26.756	133.6	5.92	129.5	5.96	7.62		1478.
400	5.20	34.024	397	26.901	120.5	5.17	115.7	7.23	12.14		1477.
500	4.76	34.093	496	27.006	111.3	4.72	105.7	8.38	17.43		1477.
600	4.44	34.165	595	27.098	103.1	4.40	96.9	9.46	23.44		1477.
700	4.16	34.233	694	27.182	95.8	4.11	88.9	10.45	30.02		1478.
800	3.92	34.291	793	27.254	89.5	3.86	82.0	11.38	37.10		1479.
900	3.70	34.343	892	27.317	84.0	3.64	76.0	12.24	44.60		1479.
1000	3.47	34.384	991	27.372	79.0	3.40	70.8	13.06	52.49		1480.
1200	3.03	34.446	1187	27.463	70.8	2.94	62.1	14.55	69.23		1482.

Results of STP Observations

(P-77-1)

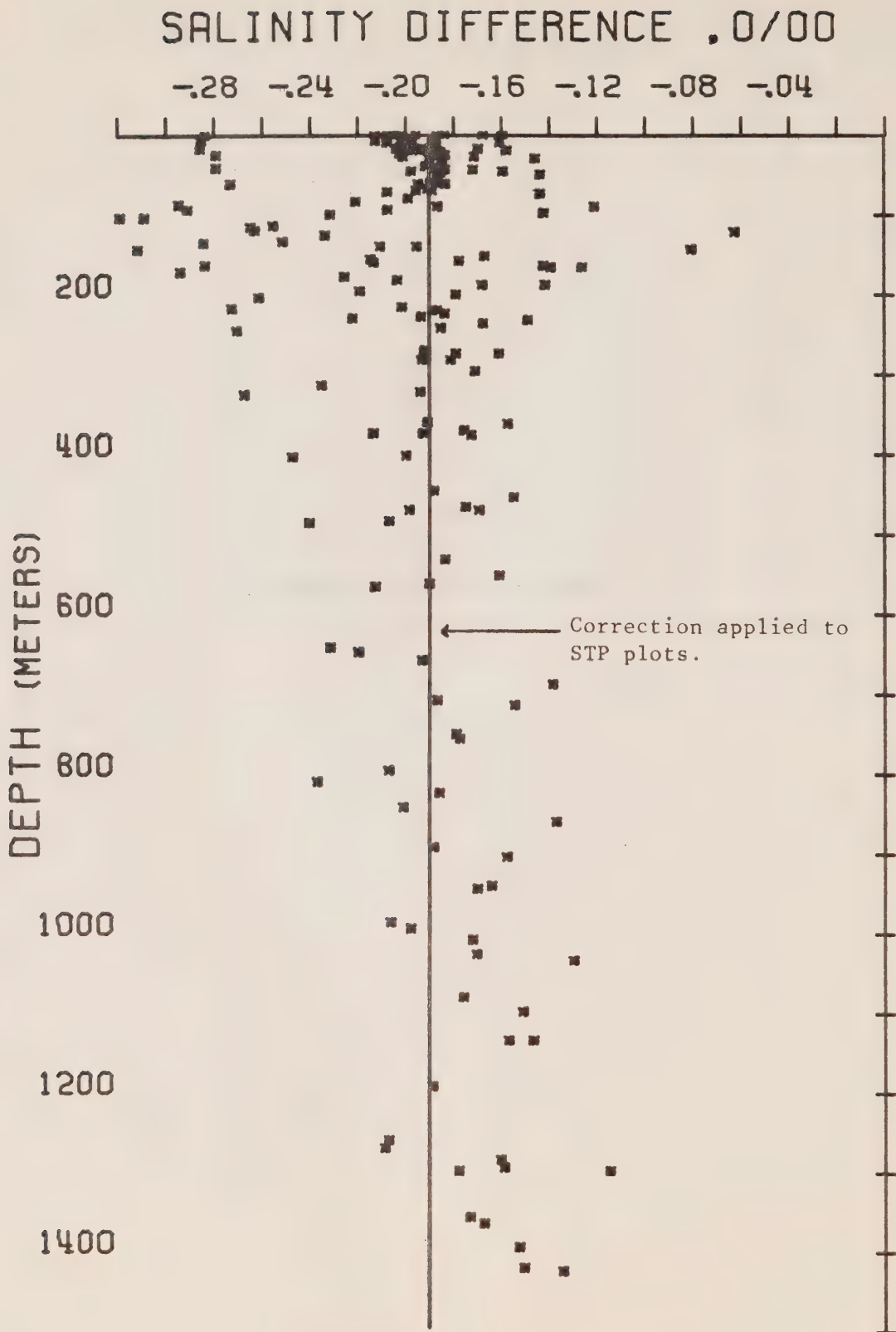


Figure 7. Salinity difference between hydro data and STP.
P-77-1.

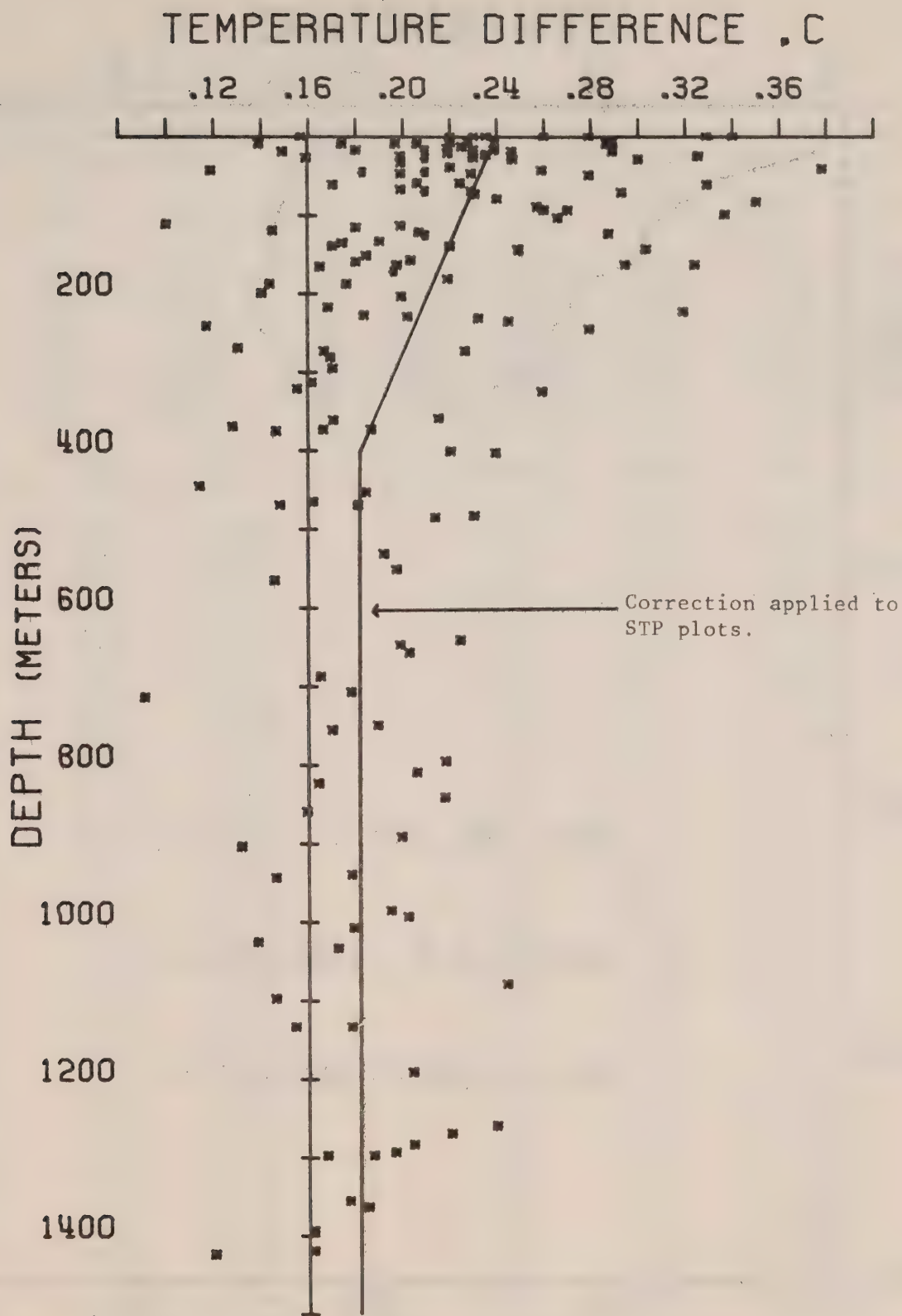
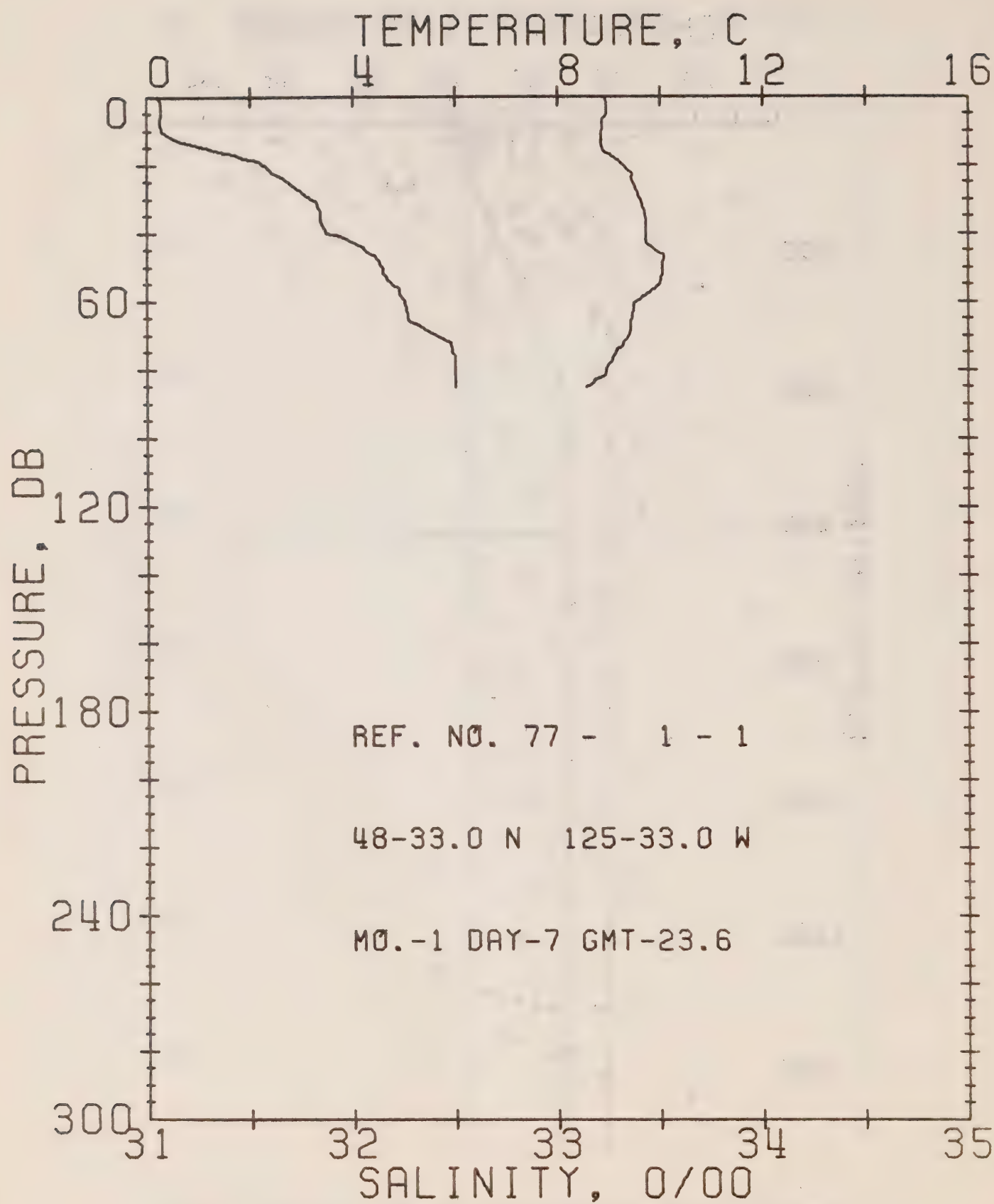


Figure 8. Temperature difference between hydro data and STP.
P-77-1.



OFFSHORE OCEANOGRAPHY GROUP

REFERENCE NO. 77- 1- 1

DATE 7/ 1/77

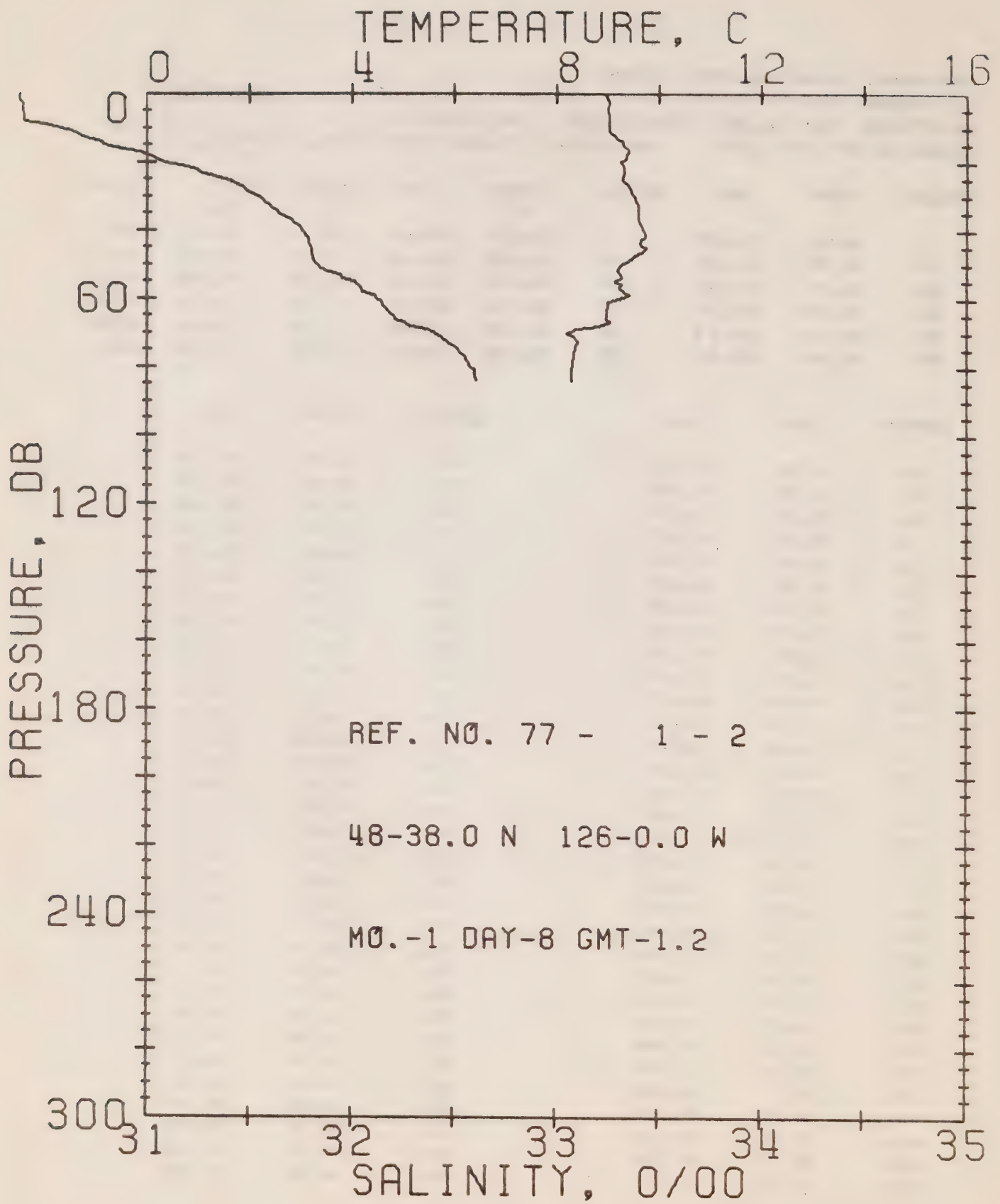
STATION 1

POSITION 48-33.0N, 125-33.0W GMT 23.0

RESULTS OF STP CAST 64 POINTS TAKEN FROM ANALOG TRACE

PRESS	TEMP	SAL	DEPTH	SIGMA T	SVA	DELTA D	POT. EN	SOUND
0	8.94	31.05	0	24.06	385.8	0.0	0.0	1481.
10	8.88	31.07	10	24.09	383.8	0.38	0.02	1481.
20	9.27	31.56	20	24.41	353.3	0.75	0.08	1484.
30	9.60	31.79	30	24.54	341.0	1.10	0.16	1485.
50	10.06	32.14	50	24.74	323.0	1.77	0.44	1488.
75	9.14	32.49	75	25.16	283.2	2.53	0.92	1485.

DEPTH	TEMP	SAL	DEPTH	TEMP	SAL
0.	8.94	31.05	44.	9.85	32.05
1.	8.94	31.06	45.	9.91	32.06
2.	8.95	31.07	46.	10.04	32.09
3.	8.95	31.07	47.	10.07	32.11
5.	8.95	31.07	50.	10.06	32.14
6.	8.94	31.07	51.	10.06	32.15
7.	8.89	31.06	52.	10.06	32.15
8.	8.88	31.06	55.	9.99	32.19
10.	8.88	31.07	56.	9.93	32.22
11.	8.86	31.09	57.	9.85	32.23
13.	8.86	31.15	58.	9.73	32.23
14.	8.85	31.22	60.	9.55	32.25
15.	8.85	31.28	61.	9.50	32.25
16.	8.91	31.35	62.	9.49	32.26
17.	9.02	31.42	65.	9.47	32.27
18.	9.11	31.47	66.	9.45	32.28
19.	9.21	31.54	67.	9.44	32.32
21.	9.33	31.58	68.	9.43	32.35
22.	9.42	31.60	70.	9.40	32.41
23.	9.47	31.63	72.	9.31	32.48
24.	9.45	31.66	73.	9.27	32.48
27.	9.52	31.72	74.	9.18	32.49
29.	9.58	31.77	75.	9.14	32.49
31.	9.62	31.82	76.	9.13	32.50
32.	9.66	31.83	78.	9.04	32.50
34.	9.71	31.84	79.	8.99	32.50
37.	9.74	31.84	80.	8.97	32.50
39.	9.73	31.86	81.	8.97	32.50
40.	9.73	31.87	82.	8.90	32.50
41.	9.72	31.94	83.	8.76	32.50
42.	9.72	31.98	84.	8.69	32.50
43.	9.72	32.01	85.	8.56	32.50



OFFSHORE OCEANOGRAPHY GROUP

REFERENCE NO. 77- 1- 2

DATE 8/ 1/77

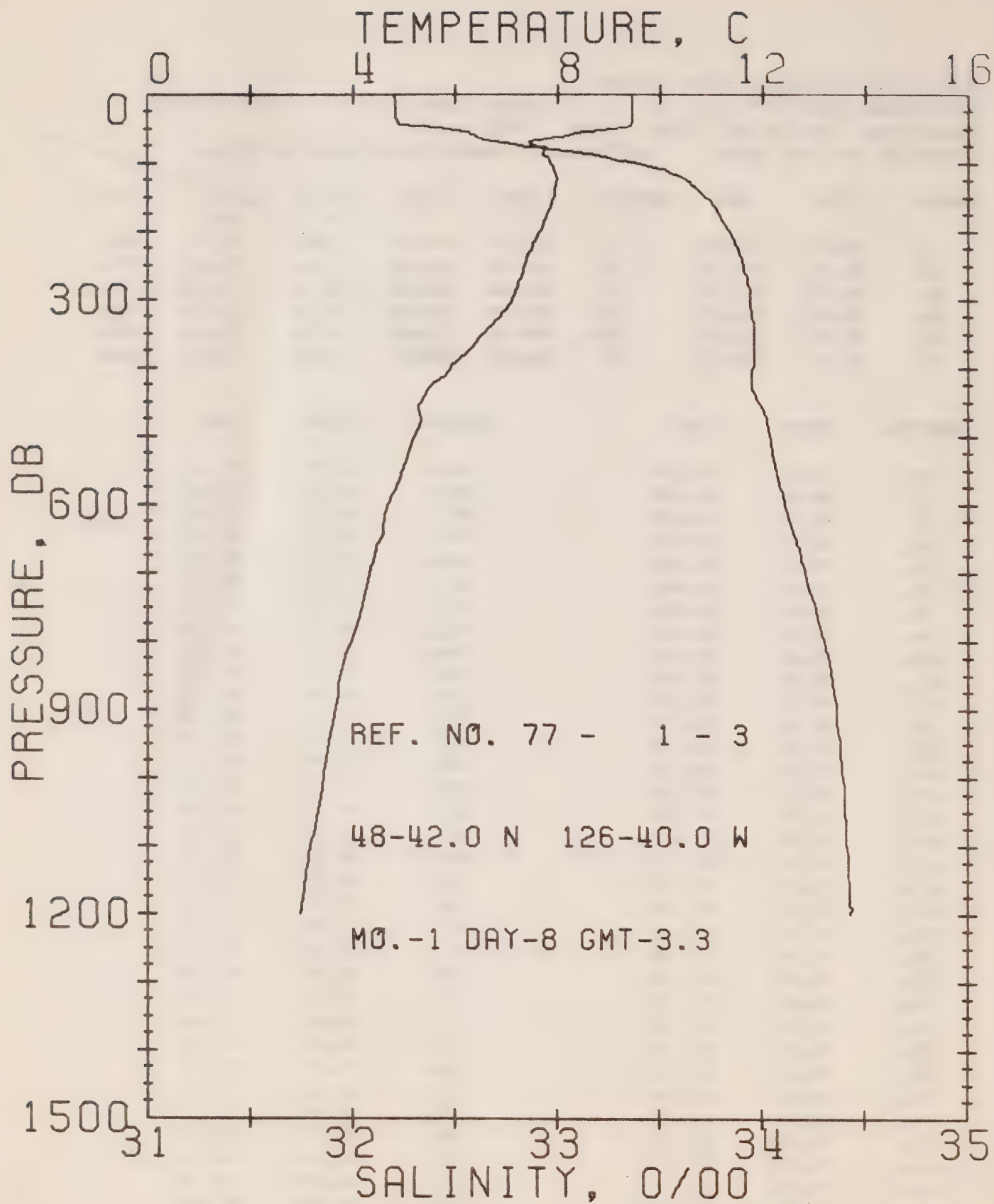
STATION 2

POSITION 48-38.0N, 126- 0.0W GMT 1.2

RESULTS OF STP CAST 68 POINTS TAKEN FROM ANALOG TRACE

PRESS	TEMP	SAL	DEPTH	SIGMA T	SVA	DELTA D	POT. EN	SOUND
0	9.00	30.39	0	23.54	435.8	0.0	0.0	1481.
10	9.04	30.59	10	23.69	421.9	0.43	0.02	1481.
20	9.25	31.08	20	24.04	388.6	0.84	0.08	1433.
30	9.52	31.55	30	24.36	358.0	1.21	0.18	1485.
50	9.29	31.83	50	24.62	334.1	1.90	0.46	1485.
75	8.35	32.52	75	25.30	269.7	2.66	0.94	1482.

DEPTH	TEMP	SAL	DEPTH	TEMP	SAL
0.	9.00	30.39	45.	9.75	31.80
1.	8.98	30.39	46.	9.70	31.80
2.	9.02	30.39	47.	9.59	31.80
3.	9.03	30.40	49.	9.41	31.81
5.	9.01	30.40	50.	9.29	31.83
7.	9.03	30.41	51.	9.23	31.84
8.	9.03	30.41	52.	9.20	31.88
9.	9.04	30.50	53.	9.26	31.94
10.	9.04	30.59	54.	9.27	31.95
11.	9.04	30.64	55.	9.14	32.01
13.	9.18	30.71	56.	9.28	32.03
14.	9.30	30.78	57.	9.23	32.04
15.	9.31	30.79	58.	9.33	32.05
16.	9.39	30.88	59.	9.44	32.11
17.	9.41	30.96	60.	9.22	32.12
19.	9.36	31.05	61.	9.00	32.14
20.	9.25	31.08	62.	9.00	32.15
21.	9.30	31.17	64.	8.99	32.18
22.	9.33	31.24	65.	8.99	32.20
23.	9.33	31.25	66.	8.99	32.21
25.	9.30	31.40	67.	9.06	32.25
27.	9.42	31.46	68.	8.82	32.28
28.	9.43	31.48	69.	8.40	32.37
30.	9.52	31.55	70.	8.22	32.40
31.	9.54	31.56	71.	8.33	32.43
33.	9.59	31.60	73.	8.42	32.47
34.	9.60	31.63	74.	8.36	32.50
35.	9.61	31.64	77.	8.34	32.55
37.	9.61	31.70	79.	8.32	32.57
39.	9.65	31.74	80.	8.31	32.58
41.	9.72	31.77	81.	8.30	32.60
42.	9.73	31.78	82.	8.29	32.60
43.	9.66	31.79	83.	8.29	32.60
44.	9.65	31.79	84.	8.28	32.61



OFFSHORE OCEANOGRAPHY GROUP

REFERENCE NO. 77- 1- 3

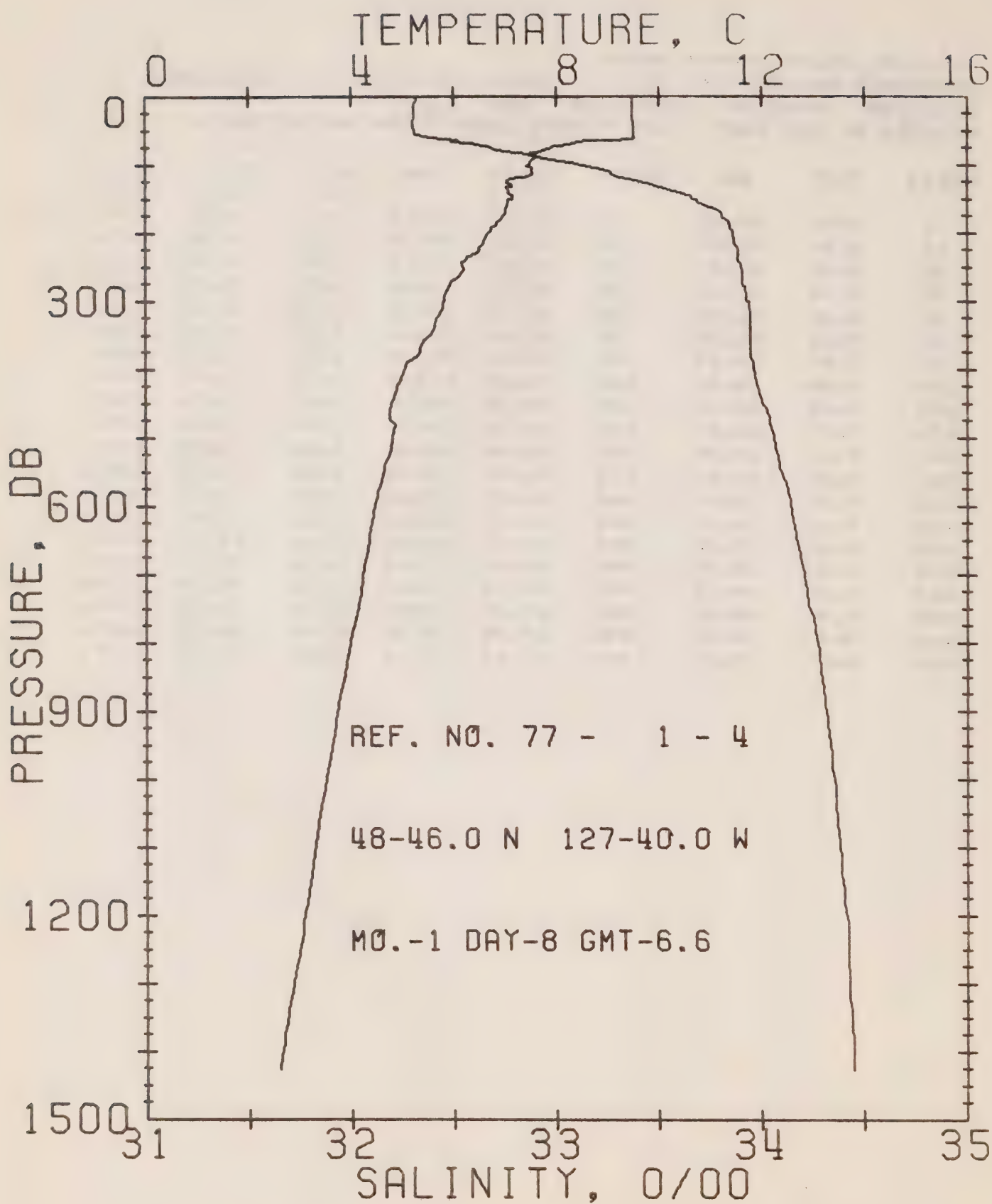
DATE 8/ 1/77

STATION 3

POSITION 48-42.0N. 126-40.0W GMT 3.3

RESULTS OF STP CAST 177 POINTS TAKEN FROM ANALOG TRACE

PRESS	TEMP	SAL	DEPTH	SIGMA T	SVA	DELTA D	POT. EN	SOUND
0	9.46	32.20	0	24.88	308.0	0.0	0.0	1485.
10	9.46	32.21	10	24.89	307.7	0.31	0.02	1485.
20	9.46	32.21	20	24.89	307.9	0.62	0.06	1485.
30	9.46	32.21	30	24.89	308.1	0.92	0.14	1485.
50	9.09	32.46	50	25.14	284.2	1.53	0.39	1485.
75	7.64	32.85	75	25.66	235.0	2.17	0.80	1480.
100	7.89	33.39	99	26.05	198.9	2.71	1.27	1482.
125	7.99	33.63	124	26.22	182.7	3.19	1.81	1483.
150	7.92	33.72	149	26.31	175.4	3.63	2.44	1483.
175	7.79	33.79	174	26.38	168.9	4.06	3.15	1483.
200	7.65	33.84	199	26.44	163.4	4.48	3.95	1483.
225	7.49	33.88	223	26.49	158.6	4.88	4.82	1483.
250	7.36	33.91	248	26.53	155.3	5.27	5.77	1483.
300	7.11	33.94	298	26.59	150.1	6.03	7.90	1483.
400	5.89	33.96	397	26.77	134.0	7.45	12.96	1480.
500	5.21	34.04	496	26.91	120.9	8.72	18.77	1479.
600	4.68	34.11	595	27.03	110.2	9.88	25.26	1478.
800	3.96	34.30	793	27.26	89.4	11.88	39.45	1479.
1000	3.41	34.39	991	27.39	77.8	13.53	54.55	1480.
1200	2.97	34.43	1188	27.46	71.4	15.02	71.18	1481.



OFFSHORE OCEANOGRAPHY GROUP

REFERENCE NO. 77- 1- 4

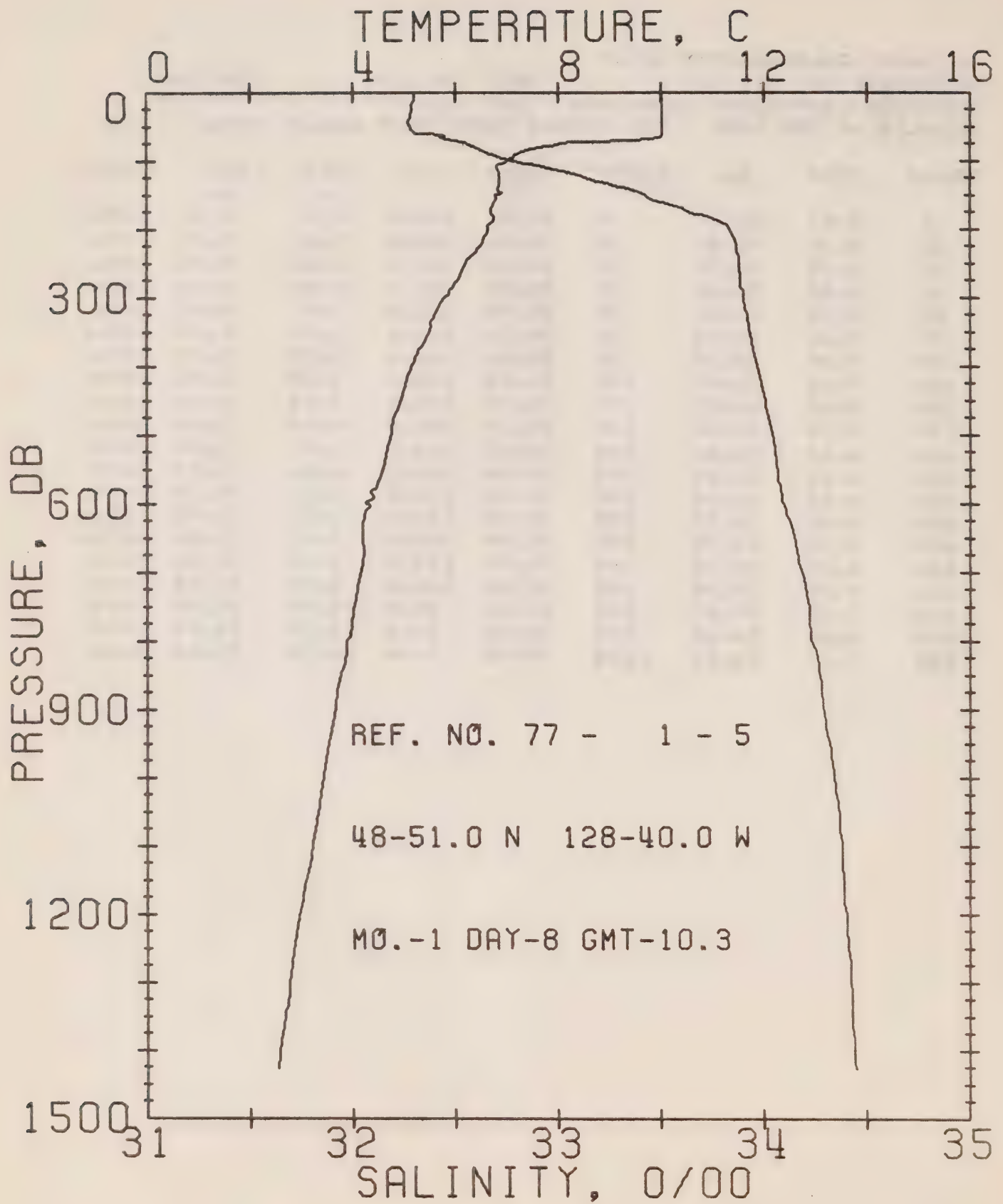
DATE 8/ 1/77

STATION 4

POSITION 48-46.0N, 127-40.0W GMT 6.6

RESULTS OF STP CAST 226 POINTS TAKEN FROM ANALOG TRACE

PRESS	TEMP	SAL	DEPTH	SIGMA T	SVA	DELTA D	POT. EN	SOUND
0	9.49	32.31	0	24.96	300.4	0.0	0.0	1485.
10	9.50	32.31	10	24.96	300.5	0.30	0.02	1485.
20	9.50	32.31	20	24.96	301.1	0.60	0.06	1485.
30	9.50	32.31	30	24.96	301.4	0.90	0.14	1486.
50	9.52	32.31	50	24.95	302.2	1.51	0.38	1486.
75	7.85	32.69	75	25.51	249.8	2.21	0.83	1481.
100	7.46	33.13	99	25.91	212.1	2.79	1.34	1480.
125	7.03	33.43	124	26.20	184.3	3.29	1.92	1479.
150	7.15	33.67	149	26.38	168.4	3.73	2.53	1480.
175	6.96	33.81	174	26.51	155.8	4.13	3.20	1480.
200	6.67	33.86	199	26.59	148.7	4.51	3.92	1480.
225	6.48	33.89	223	26.64	144.5	4.88	4.72	1479.
250	6.19	33.90	248	26.68	140.2	5.24	5.58	1478.
300	5.80	33.93	298	26.76	133.7	5.92	7.49	1478.
400	5.02	33.96	397	26.88	123.0	7.21	12.08	1476.
500	4.80	34.06	496	26.98	114.2	8.39	17.48	1477.
600	4.45	34.14	595	27.08	105.0	9.48	23.63	1477.
800	3.97	34.27	793	27.24	91.6	11.45	37.65	1479.
1000	3.49	34.35	991	27.35	81.8	13.19	53.50	1480.
1200	3.07	34.41	1188	27.43	73.8	14.74	70.93	1482.



OFFSHORE OCEANOGRAPHY GROUP

REFERENCE NO. 77- 1- 5

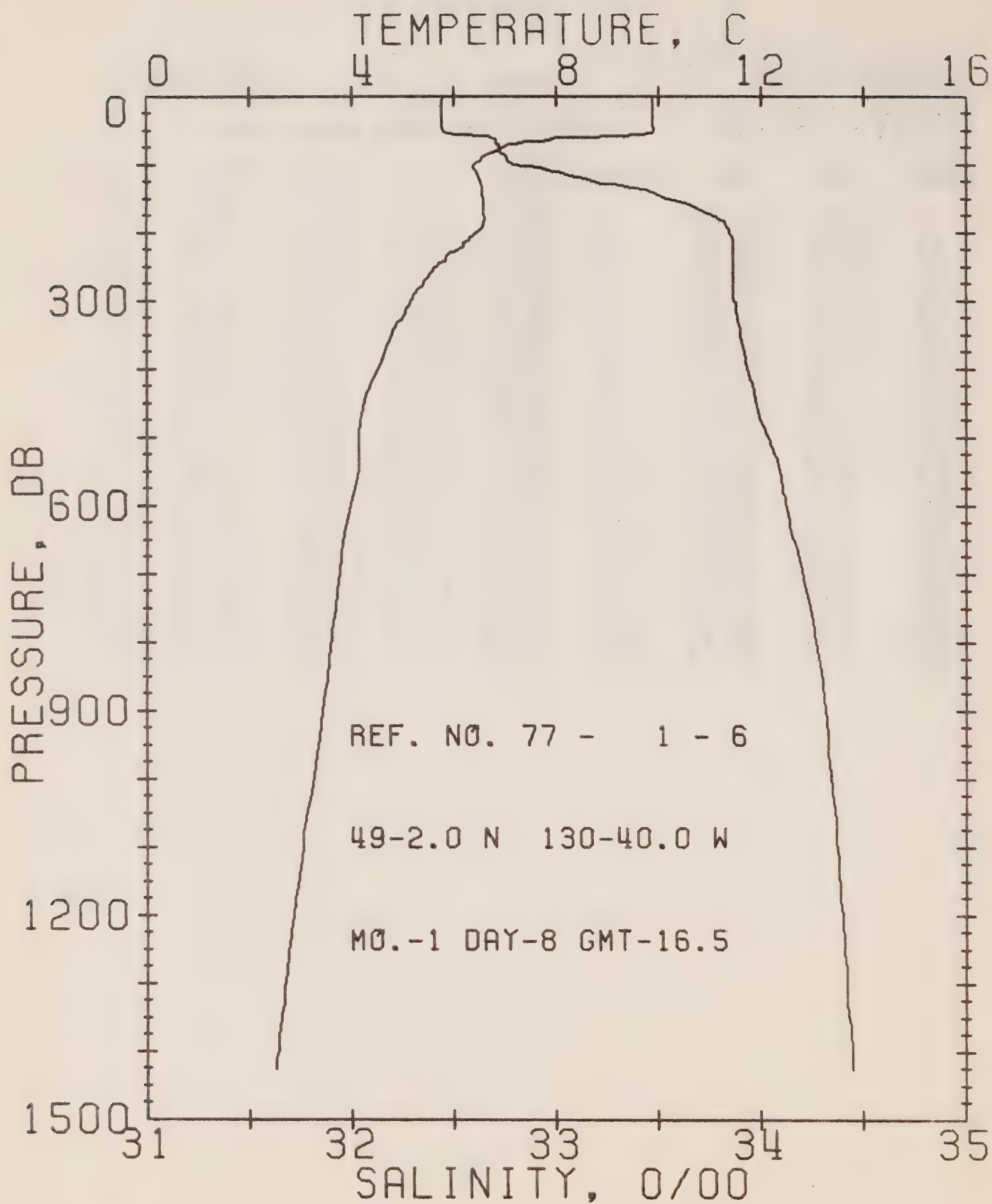
DATE 8/ 1/77

STATION 5

POSITION 48-51.0N, 128-40.0W GMT 10.3

RESULTS OF STP CAST 210 POINTS TAKEN FROM ANALOG TRACE

PRESS	TEMP	SAL	DEPTH	SIGMA T	SVA	DELTA D	POT. EN	SOUND
0	10.02	32.30	0	24.87	309.3	0.0	0.0	1487.
10	10.02	32.30	10	24.87	309.8	0.31	0.02	1487.
20	10.03	32.29	20	24.86	310.7	0.62	0.06	1487.
30	10.03	32.29	30	24.85	311.4	0.93	0.14	1488.
50	10.03	32.27	50	24.85	312.6	1.56	0.40	1488.
75	8.05	32.56	75	25.37	262.4	2.30	0.87	1481.
100	7.00	32.78	99	25.69	232.2	2.92	1.42	1478.
125	6.86	33.14	124	26.00	203.7	3.46	2.03	1478.
150	6.81	33.42	149	26.23	182.3	3.94	2.71	1479.
175	6.70	33.64	174	26.41	165.1	4.37	3.43	1479.
200	6.63	33.83	199	26.57	150.2	4.76	4.17	1479.
225	6.46	33.87	224	26.63	145.6	5.13	4.97	1479.
250	6.18	33.88	248	26.67	141.6	5.49	5.84	1478.
300	5.77	33.90	298	26.74	135.6	6.19	7.79	1478.
400	5.12	33.97	397	26.87	123.8	7.48	12.41	1477.
500	4.72	34.04	496	26.97	114.5	8.67	17.86	1477.
600	4.26	34.09	595	27.06	106.6	9.79	24.09	1477.
800	3.87	34.23	793	27.21	93.6	11.77	38.22	1478.
1000	3.41	34.34	991	27.35	81.6	13.51	54.15	1480.
1200	2.94	34.40	1188	27.44	73.4	15.06	71.45	1481.



OFFSHORE OCEANOGRAPHY GROUP

REFERENCE NO. 77- 1- 6

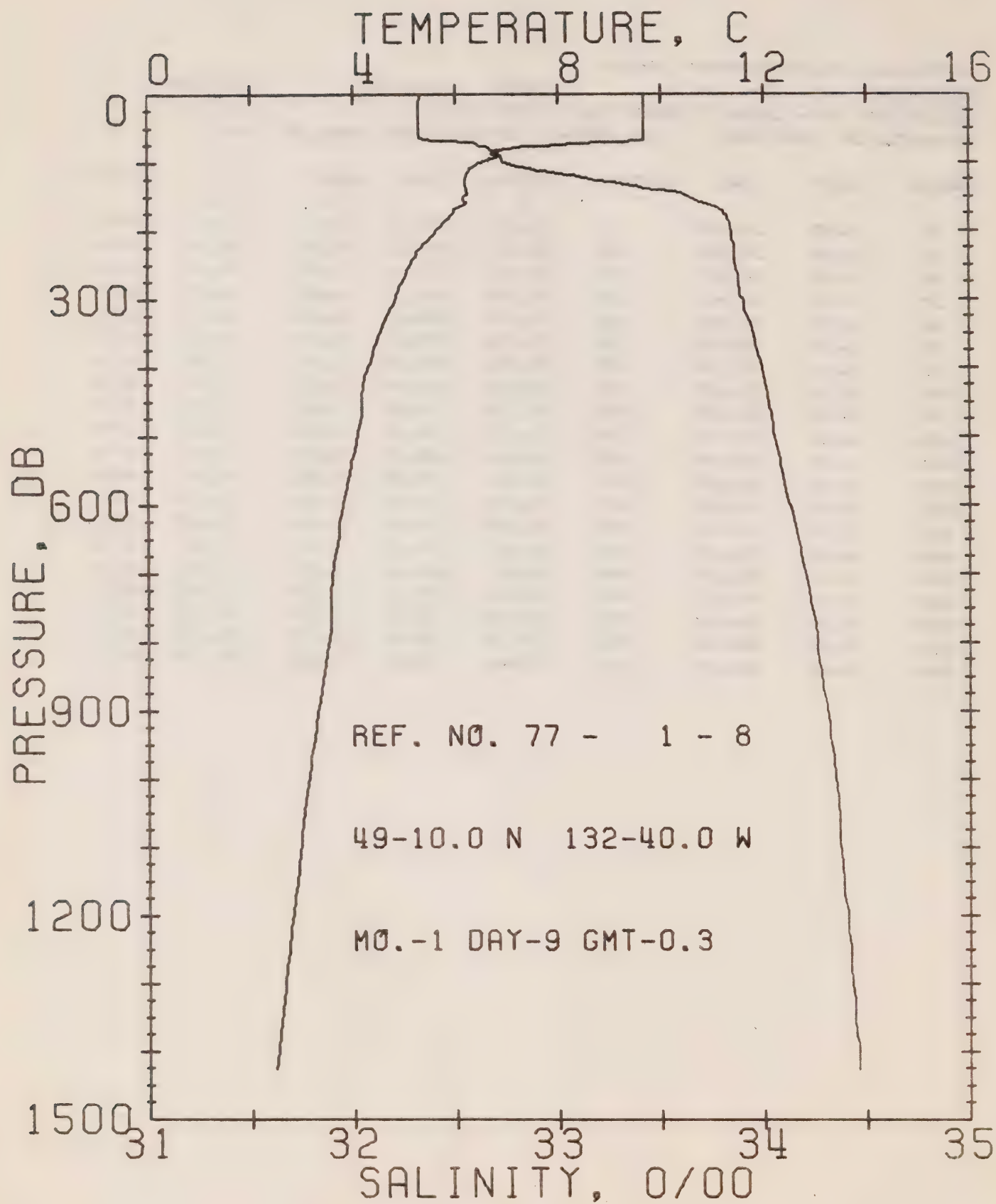
DATE 8/ 1/77

STATION 6

POSITION 49- 2.0N, 130-40.0W GMT 16.5

RESULTS OF STP CAST 188 POINTS TAKEN FROM ANALOG TRACE

PRESS	TEMP	SAL	DEPTH	SIGMA T	SVA	DELTA D	POT. EN	SOUND
0	9.89	32.45	0	25.01	296.2	0.0	0.0	1487.
10	9.89	32.44	10	25.00	297.2	0.30	0.02	1487.
20	9.89	32.44	20	25.00	297.6	0.59	0.06	1487.
30	9.89	32.44	30	25.00	297.7	0.89	0.14	1487.
50	9.91	32.44	50	25.00	298.2	1.49	0.38	1488.
75	6.97	32.72	75	25.65	235.8	2.14	0.79	1477.
100	6.41	32.79	99	25.78	223.8	2.72	1.30	1475.
125	6.53	33.19	124	26.08	195.8	3.23	1.90	1477.
150	6.59	33.54	149	26.35	170.8	3.68	2.53	1478.
175	6.61	33.77	174	26.53	154.1	4.09	3.19	1479.
200	6.46	33.85	199	26.61	146.7	4.46	3.91	1479.
225	6.09	33.87	223	26.67	140.8	4.82	4.68	1478.
250	5.65	33.87	248	26.73	135.7	5.16	5.52	1476.
300	5.14	33.87	298	26.79	130.3	5.83	7.38	1475.
400	4.50	33.94	397	26.91	119.0	7.07	11.81	1474.
500	4.13	34.04	496	27.03	108.4	8.21	17.01	1474.
600	3.97	34.12	595	27.12	101.0	9.25	22.86	1475.
800	3.59	34.27	793	27.27	87.7	11.13	36.19	1477.
1000	3.23	34.34	991	27.36	79.4	12.79	51.43	1479.
1200	2.85	34.40	1188	27.44	72.3	14.30	68.37	1481.



OFFSHORE OCEANOGRAPHY GROUP

REFERENCE NO. 77- 1- B

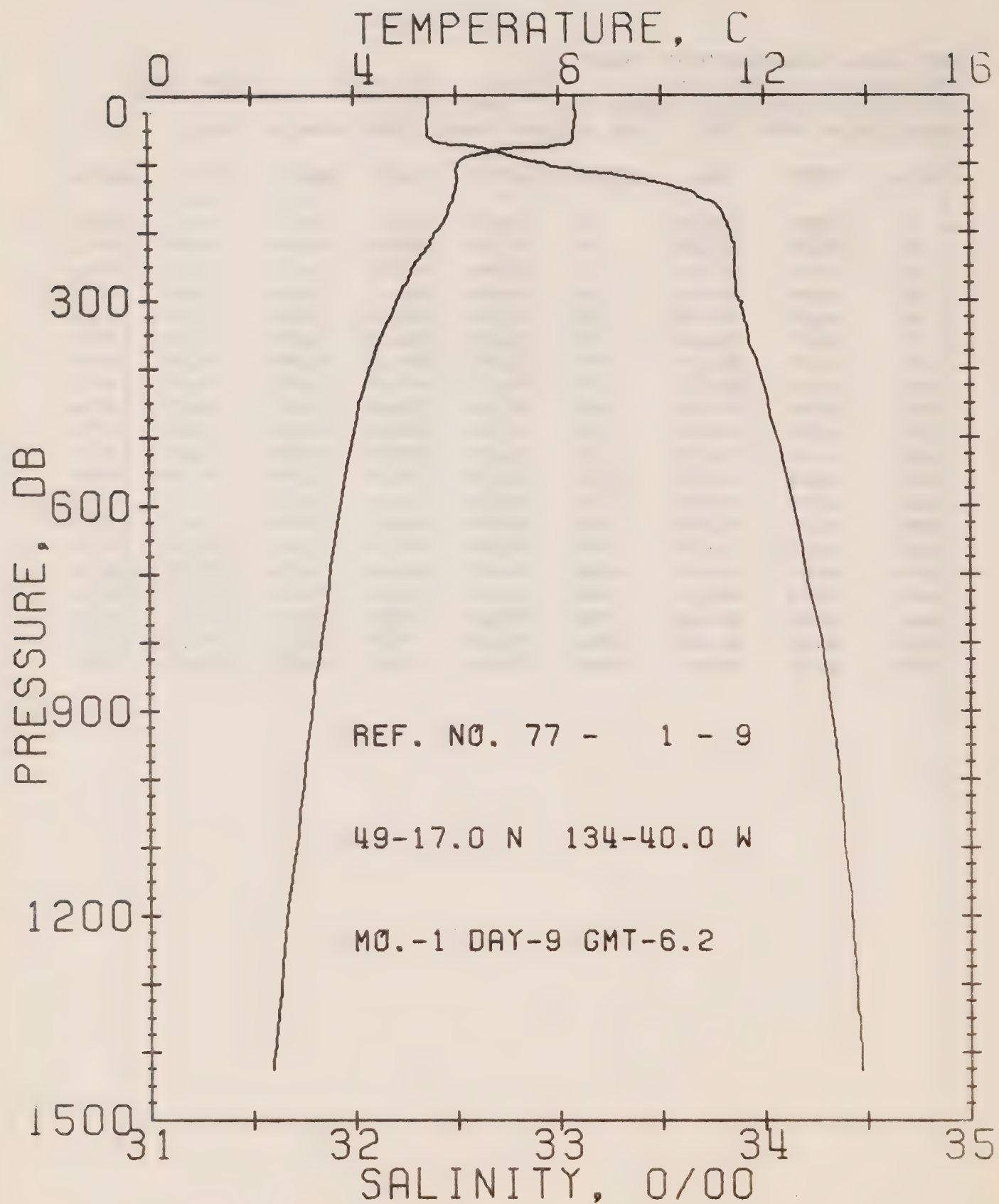
DATE 9/ 1/77

STATION 7

POSITION 49-10.0N, 132-40.0W GMT 0.3

RESULTS OF STP CAST 194 POINTS TAKEN FROM ANALOG TRACE

PRESS	TEMP	SAL	DEPTH	SIGMA T	SVA	DELTA D	POT. EN	SOUND
0	9.68	32.33	0	24.95	301.8	0.0	0.0	1486.
10	9.68	32.33	10	24.94	302.5	0.30	0.02	1486.
20	9.68	32.32	20	24.94	303.2	0.61	0.06	1486.
30	9.68	32.32	30	24.94	303.4	0.91	0.14	1486.
50	9.68	32.32	50	24.94	303.7	1.52	0.39	1487.
75	7.74	32.62	75	25.47	253.5	2.25	0.85	1480.
100	6.47	32.74	99	25.73	228.3	2.84	1.38	1476.
125	6.19	33.19	124	26.12	191.6	3.37	1.98	1475.
150	6.19	33.63	149	26.48	158.6	3.81	2.59	1476.
175	5.94	33.81	174	26.65	142.5	4.18	3.21	1476.
200	5.61	33.85	199	26.71	136.4	4.53	3.88	1475.
225	5.28	33.86	223	26.76	131.8	4.87	4.60	1474.
250	5.09	33.86	248	26.79	129.7	5.19	5.40	1474.
300	4.80	33.90	298	26.85	124.1	5.83	7.17	1474.
400	4.28	33.99	397	26.98	112.3	7.01	11.37	1473.
500	4.07	34.05	496	27.05	106.4	8.10	16.37	1474.
600	3.78	34.12	595	27.14	98.9	9.13	22.13	1475.
800	3.51	34.26	793	27.27	87.3	10.97	35.23	1477.
1000	3.10	34.35	990	27.38	77.5	12.61	50.29	1479.
1200	2.78	34.41	1188	27.46	70.7	14.10	66.95	1481.



OFFSHORE OCEANOGRAPHY GROUP

REFERENCE NO. 77- 1- 9

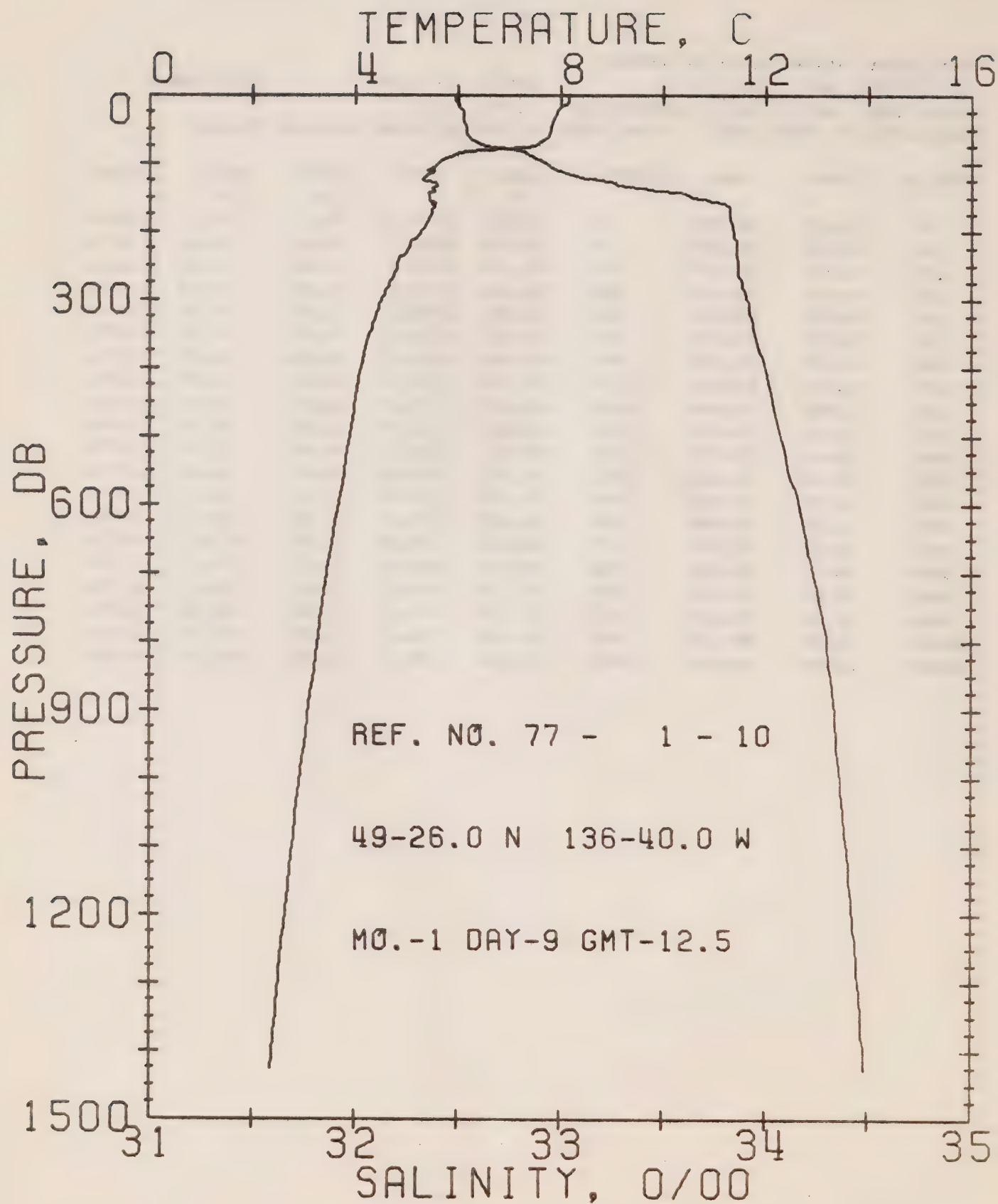
DATE 9/ 1/77

STATION 8

POSITION 49-17.0N, 134-40.0W GMT 6.2

RESULTS OF STP CAST 164 POINTS TAKEN FROM ANALOG TRACE

PRESS	TEMP	SAL	DEPTH	SIGMA T	SVA	DELTA D	POT. EN	SOUND
0	8.32	32.38	0	25.20	278.0	0.0	0.0	1481.
10	8.32	32.37	10	25.19	279.1	0.28	0.01	1481.
20	8.33	32.37	20	25.19	279.4	0.56	0.06	1481.
30	8.34	32.37	30	25.19	279.8	0.84	0.13	1481.
50	8.30	32.36	50	25.18	280.3	1.40	0.36	1481.
75	7.77	32.62	75	25.46	253.8	2.09	0.80	1480.
100	6.03	32.93	99	25.94	208.4	2.66	1.30	1474.
125	6.02	33.44	124	26.34	170.8	3.13	1.84	1475.
150	5.95	33.69	149	26.55	151.7	3.53	2.40	1476.
175	5.82	33.80	174	26.65	141.9	3.90	3.00	1476.
200	5.60	33.84	199	26.71	136.8	4.24	3.67	1475.
225	5.42	33.86	223	26.75	133.4	4.58	4.40	1475.
250	5.15	33.86	248	26.78	130.6	4.91	5.20	1474.
300	4.84	33.88	298	26.83	126.0	5.56	7.00	1474.
400	4.31	33.97	397	26.96	114.0	6.75	11.27	1473.
500	3.97	34.06	496	27.07	104.8	7.85	16.27	1474.
600	3.71	34.14	595	27.16	96.7	8.85	21.89	1474.
800	3.33	34.28	793	27.30	83.9	10.66	34.75	1476.
1000	3.00	34.37	990	27.40	75.1	12.24	49.26	1478.
1200	2.65	34.42	1188	27.48	68.3	13.68	65.32	1480.



OFFSHORE OCEANOGRAPHY GROUP

REFERENCE NO. 77- 1- 10

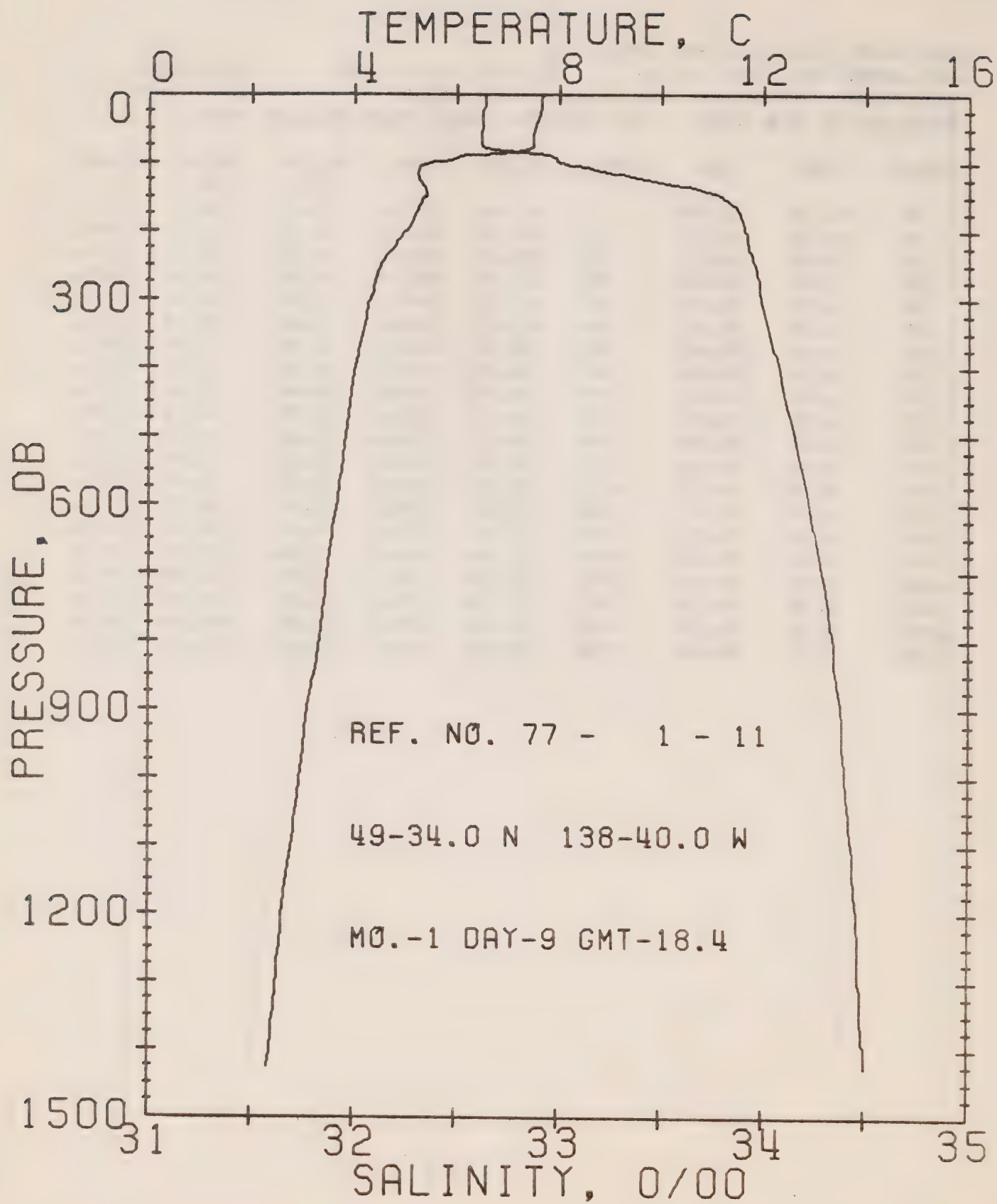
DATE 9/ 1/77

STATION 9

POSITION 49-26.0N, 136-40.0W GMT 12.5

RESULTS OF STP CAST 191 POINTS TAKEN FROM ANALOG TRACE

PRESS	TEMP	SAL	DEPTH	SIGMA T	SVA	DELTA D	POT. EN	SOUND
0	8.16	32.49	0	25.31	267.6	0.0	0.0	1480.
10	8.15	32.50	10	25.31	267.4	0.27	0.01	1480.
20	7.99	32.51	20	25.35	264.0	0.53	0.05	1480.
30	7.90	32.53	30	25.38	261.6	0.80	0.12	1480.
50	7.82	32.54	50	25.39	260.1	1.32	0.33	1480.
75	7.33	32.67	75	25.57	244.2	1.96	0.74	1479.
100	5.62	32.92	99	25.98	204.3	2.50	1.22	1472.
125	5.38	33.23	124	26.25	178.9	2.99	1.78	1472.
150	5.44	33.65	149	26.58	148.5	3.40	2.36	1473.
175	5.46	33.83	174	26.72	135.6	3.75	2.93	1474.
200	5.27	33.85	199	26.75	132.4	4.08	3.57	1474.
225	5.00	33.86	223	26.80	128.6	4.41	4.28	1473.
250	4.79	33.87	248	26.83	125.8	4.73	5.05	1473.
300	4.50	33.91	298	26.89	120.0	5.34	6.78	1472.
400	4.08	34.00	397	27.01	109.9	6.49	10.87	1472.
500	3.88	34.07	496	27.09	102.9	7.56	15.75	1473.
600	3.67	34.16	595	27.18	94.7	8.55	21.30	1474.
800	3.26	34.30	793	27.33	81.5	10.31	33.80	1476.
1000	2.91	34.37	990	27.41	74.2	11.87	48.06	1478.
1200	2.63	34.42	1188	27.48	68.1	13.29	63.98	1480.



OFFSHORE OCEANOGRAPHY GROUP

REFERENCE NO. 77- 1- 11

DATE 9/ 1/77

STATION 10

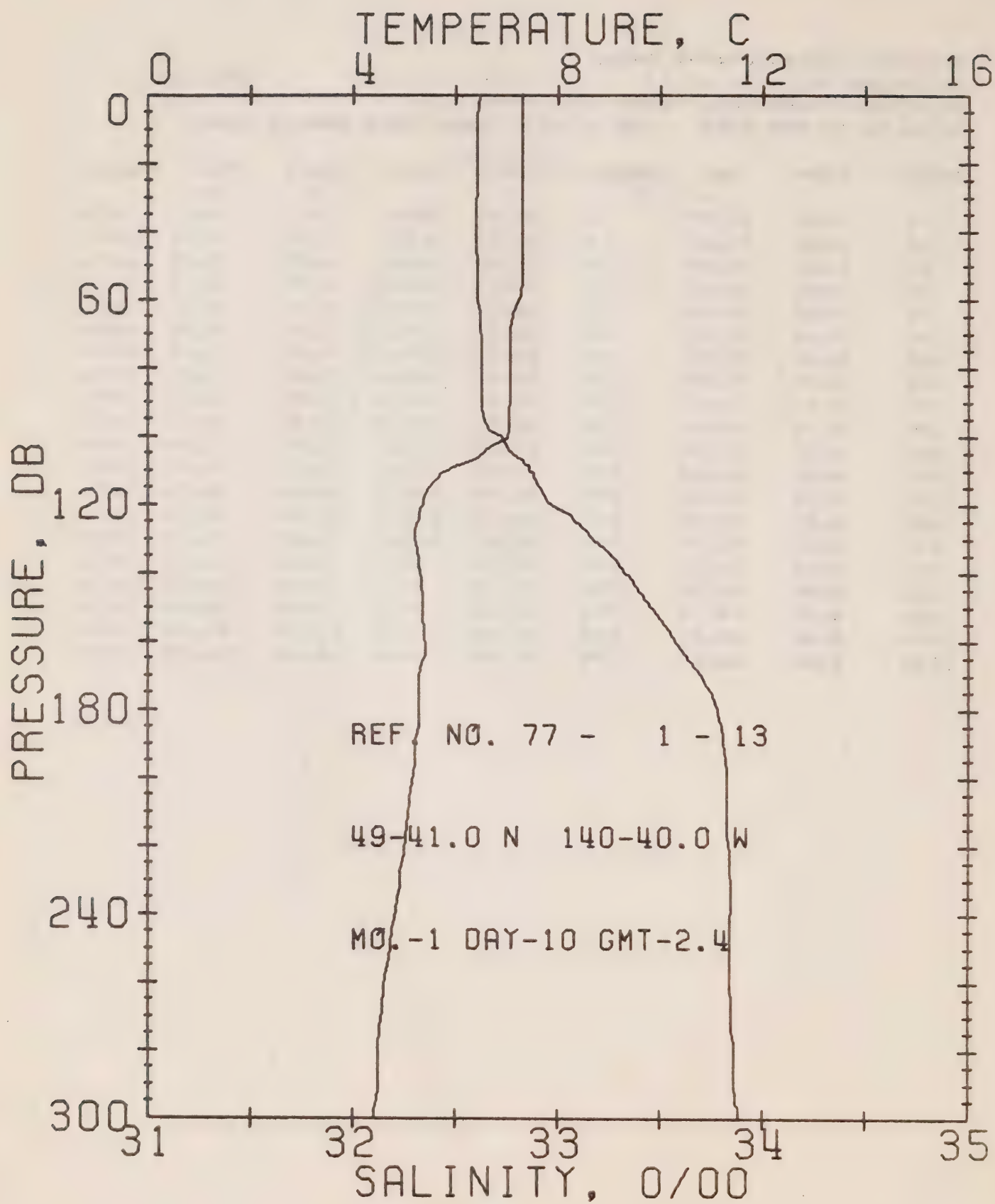
POSITION 49-34.0N. 138-40.0W

GMT 18.4

RESULTS OF STP CAST

152 POINTS TAKEN FROM ANALOG TRACE

PRESS	TEMP	SAL	DEPTH	SIGMA T	SVA	DELTA D	POT. EN	SOUND
0	7.67	32.64	0	25.49	249.7	0.0	0.0	1479.
10	7.66	32.64	10	25.50	249.9	0.25	0.01	1479.
20	7.66	32.64	20	25.49	250.2	0.50	0.05	1479.
30	7.62	32.63	30	25.49	250.4	0.75	0.11	1479.
50	7.53	32.63	50	25.51	249.5	1.25	0.32	1479.
75	7.48	32.62	75	25.51	249.9	1.87	0.72	1479.
100	5.45	33.01	99	26.07	196.0	2.43	1.21	1472.
125	5.28	33.44	124	26.43	161.9	2.88	1.72	1472.
150	5.41	33.80	149	26.70	137.0	3.25	2.23	1474.
175	5.19	33.89	174	26.80	128.3	3.57	2.78	1473.
200	5.01	33.91	199	26.84	124.7	3.89	3.38	1473.
225	4.75	33.93	223	26.88	120.6	4.20	4.05	1472.
250	4.51	33.96	248	26.93	116.0	4.49	4.76	1472.
300	4.31	33.99	298	26.98	112.0	5.06	6.35	1472.
400	4.01	34.08	397	27.08	103.3	6.14	10.19	1472.
500	3.84	34.15	496	27.15	96.6	7.14	14.78	1473.
600	3.66	34.22	595	27.23	90.1	8.07	20.00	1474.
800	3.32	34.34	793	27.36	79.0	9.76	32.00	1476.
1000	2.94	34.40	990	27.44	72.0	11.26	45.75	1478.
1200	2.60	34.46	1188	27.51	65.2	12.63	61.08	1480.



OFFSHORE OCEANOGRAPHY GROUP

REFERENCE NO. 77- 1- 13

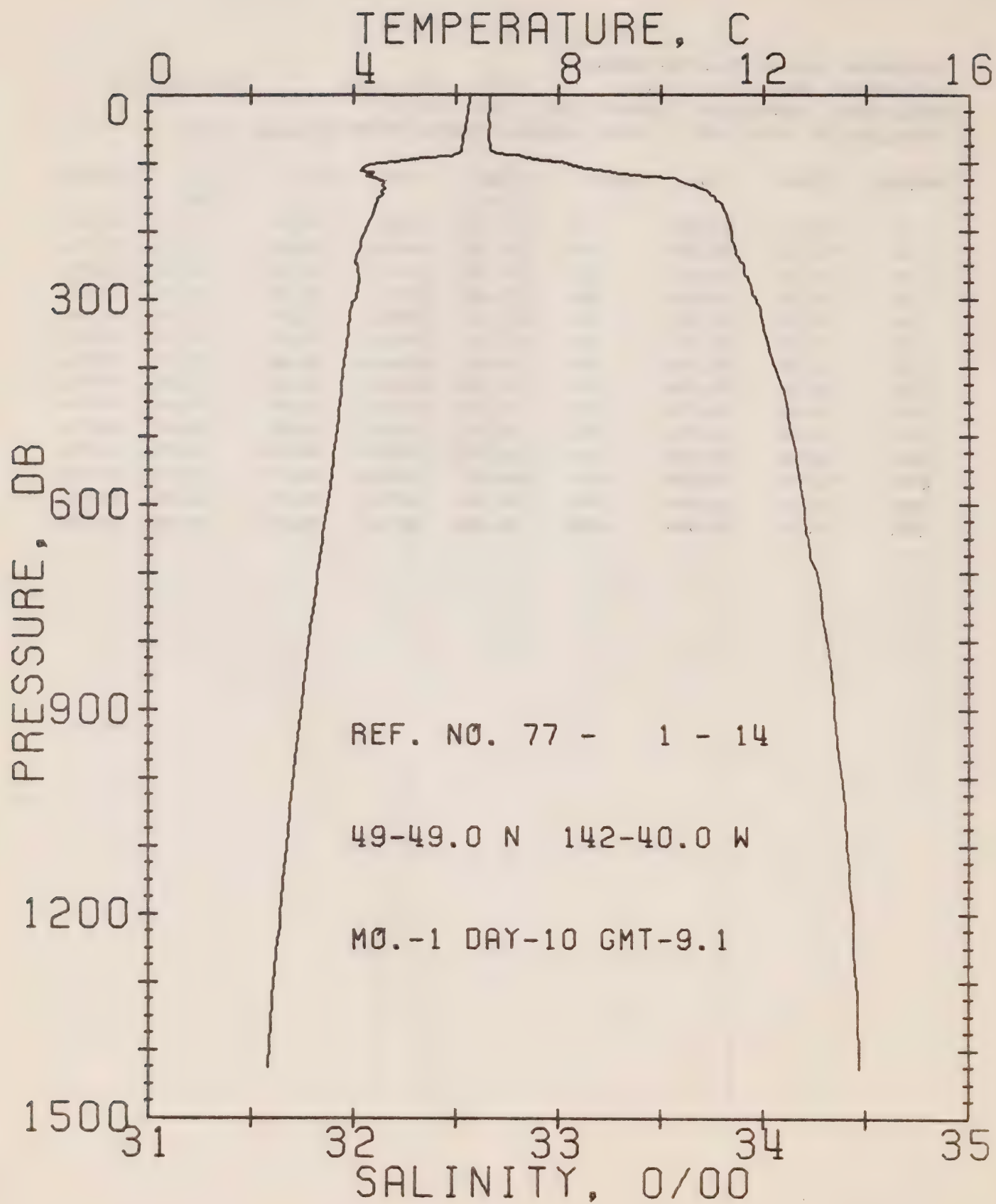
DATE 10/ 1/77

STATION 11

POSITION 49-41.0N, 140-40.0W GMT 2.4

RESULTS OF STP CAST 110 POINTS TAKEN FROM ANALOG TRACE

PRESS	TEMP	SAL	DEPTH	SIGMA T	SVA	DELTA D	POT. EN	SOUND
0	7.31	32.62	0	25.53	246.4	0.0	0.0	1477.
10	7.31	32.61	10	25.52	247.5	0.25	0.01	1477.
20	7.32	32.61	20	25.52	247.7	0.49	0.05	1477.
30	7.31	32.61	30	25.52	248.1	0.74	0.11	1478.
50	7.31	32.61	50	25.52	248.1	1.24	0.32	1478.
75	7.08	32.63	75	25.57	243.9	1.85	0.71	1477.
100	7.00	32.72	99	25.65	236.5	2.46	1.25	1478.
125	5.24	33.09	124	26.16	187.9	2.99	1.85	1472.
150	5.36	33.46	149	26.44	162.0	3.42	2.46	1473.
175	5.29	33.75	174	26.68	139.5	3.80	3.08	1473.
200	5.16	33.83	199	26.75	132.5	4.14	3.73	1473.
225	4.95	33.84	223	26.79	129.6	4.47	4.44	1473.
250	4.71	33.84	248	26.81	127.1	4.79	5.21	1472.
300	4.39	33.88	298	26.88	121.1	5.41	6.95	1472.



OFFSHORE OCEANOGRAPHY GROUP

REFERENCE NO. 77- 1- 14

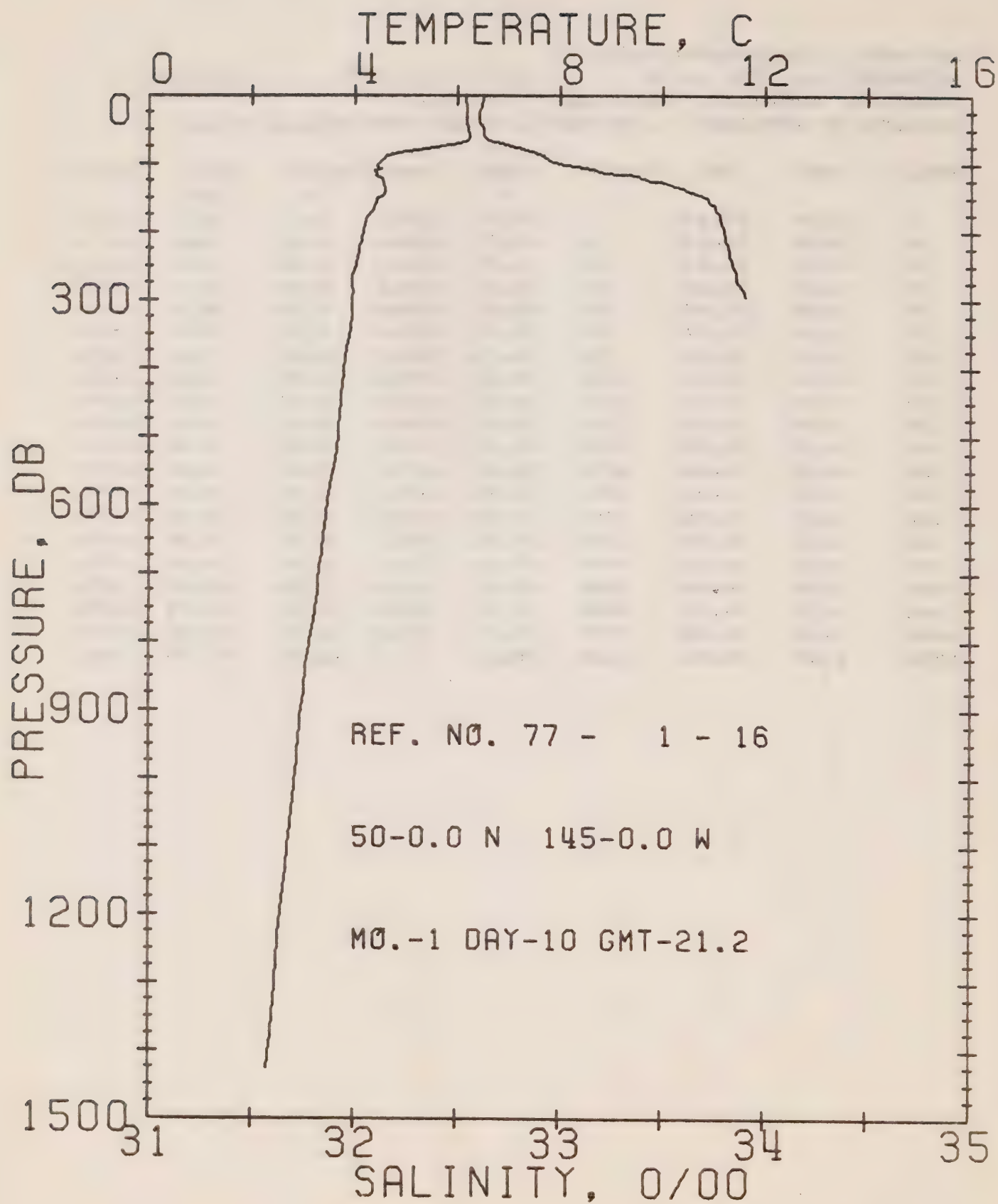
DATE 10/ 1/77

STATION 12

POSITION 49-49.0N, 142-40.0W GMT 9.1

RESULTS OF STP CAST 178 POINTS TAKEN FROM ANALOG TRACE

PRESS	TEMP	SAL	DEPTH	SIGMA T	SVA	DELTA D	POT. EN	SOUND
0	6.26	32.68	0	25.71	228.8	0.0	0.0	1473.
10	6.26	32.67	10	25.71	229.9	0.23	0.01	1473.
20	6.24	32.67	20	25.71	229.8	0.46	0.05	1473.
30	6.22	32.66	30	25.71	230.1	0.69	0.11	1473.
50	6.20	32.67	50	25.71	229.6	1.15	0.29	1474.
75	6.11	32.67	75	25.72	228.8	1.72	0.66	1474.
100	4.52	33.03	99	26.19	184.4	2.26	1.14	1468.
125	4.52	33.58	124	26.63	143.4	2.68	1.61	1469.
150	4.51	33.75	149	26.77	130.4	3.02	2.09	1470.
175	4.36	33.82	174	26.83	124.4	3.33	2.61	1470.
200	4.22	33.85	199	26.87	121.0	3.64	3.20	1470.
225	4.11	33.86	223	26.89	119.0	3.94	3.85	1469.
250	4.04	33.90	248	26.94	115.1	4.23	4.56	1470.
300	4.03	33.96	298	26.98	111.3	4.80	6.15	1470.
400	3.81	34.05	397	27.08	102.7	5.87	9.94	1471.
500	3.66	34.14	496	27.16	95.6	6.85	14.46	1472.
600	3.49	34.20	595	27.22	90.4	7.78	19.67	1473.
800	3.13	34.31	793	27.35	79.4	9.48	31.73	1475.
1000	2.82	34.38	990	27.43	72.0	10.99	45.55	1477.
1200	2.57	34.44	1188	27.50	66.2	12.37	61.03	1480.



OFFSHORE OCEANOGRAPHY GROUP

REFERENCE NO. 77- 1- 16

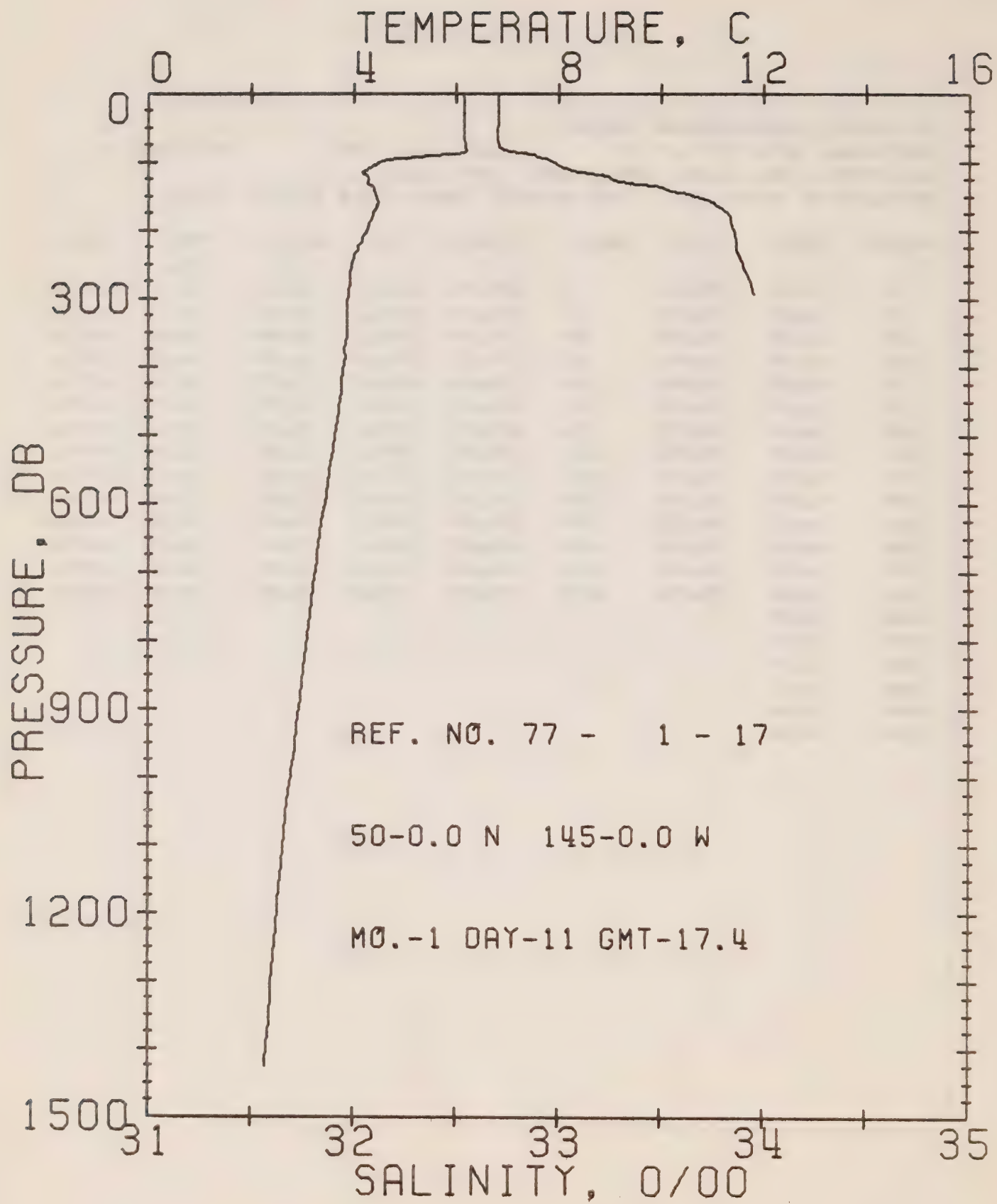
DATE 10/ 1/77

STATION P

POSITION 50- 0.0N. 145- 0.0W GMT 21.2

RESULTS OF STP CAST 169 POINTS TAKEN FROM ANALOG TRACE

PRESS	TEMP	SAL	DEPTH	SIGMA T	SVA	DELTA D	POT. EN	SOUND
0	6.16	32.64	0	25.70	230.6	0.0	0.0	1473.
10	6.17	32.63	10	25.68	232.1	0.23	0.01	1473.
20	6.18	32.62	20	25.67	233.0	0.46	0.05	1473.
30	6.19	32.61	30	25.67	233.8	0.70	0.11	1473.
50	6.22	32.63	50	25.68	232.8	1.17	0.30	1474.
75	5.63	32.77	75	25.87	215.4	1.74	0.66	1472.
100	4.46	32.98	99	26.16	187.2	2.23	1.10	1468.
125	4.55	33.44	124	26.51	154.1	2.66	1.59	1469.
150	4.49	33.71	149	26.73	133.5	3.01	2.09	1470.
175	4.27	33.78	174	26.81	126.4	3.34	2.62	1469.
200	4.15	33.80	199	26.84	123.7	3.65	3.22	1469.
225	4.09	33.82	223	26.87	121.6	3.96	3.88	1469.
250	4.01	33.84	248	26.89	119.6	4.26	4.61	1469.
300	3.95	33.91	298	26.95	114.2	4.84	6.25	1470.
400	3.79							
500	3.67							
600	3.47							
800	3.11							
1000	2.84							
1200	2.56							



OFFSHORE OCEANOGRAPHY GROUP

REFERENCE NO. 77- 1- 17

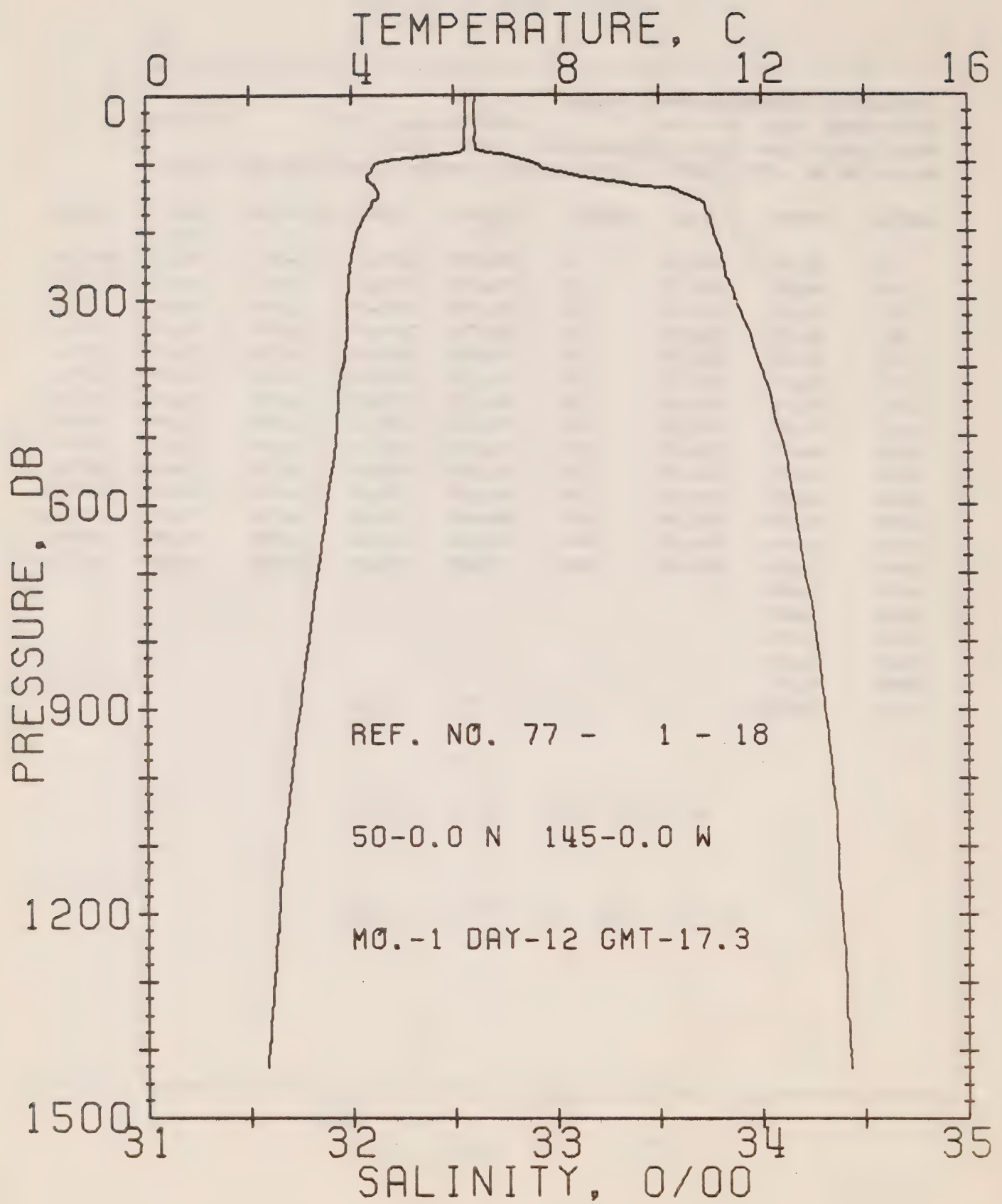
DATE 11/ 1/77

STATION P

POSITION 50- 0.0N, 145- 0.0W GMT 17.4

RESULTS OF STP CAST 167 POINTS TAKEN FROM ANALOG TRACE

FRESS	TEMP	SAL	DEPTH	SIGMA T	SVA	DELTA D	POT. EN	SOUND
0	6.14	32.71	0	25.75	225.1	0.0	0.0	1473.
10	6.16	32.71	10	25.75	225.7	0.23	0.01	1473.
20	6.15	32.71	20	25.75	225.7	0.45	0.05	1473.
30	6.15	32.71	30	25.75	225.8	0.68	0.10	1473.
50	6.16	32.71	50	25.75	226.5	1.13	0.29	1474.
75	6.19	32.71	75	25.74	227.0	1.70	0.65	1474.
100	4.51	32.97	99	26.15	188.5	2.23	1.12	1468.
125	4.29	33.27	124	26.41	164.2	2.67	1.62	1468.
150	4.45	33.67	149	26.71	136.1	3.04	2.14	1469.
175	4.37	33.83	174	26.84	123.5	3.36	2.68	1470.
200	4.25	33.86	199	26.88	120.5	3.67	3.26	1470.
225	4.08	33.87	223	26.90	118.0	3.96	3.90	1469.
250	3.96	33.90	248	26.94	114.6	4.26	4.61	1469.
300	3.88	33.96	298	27.00	109.8	4.82	6.18	1470.
400	3.80							
500	3.63							
600	3.44							
800	3.09							
1000	2.77							
1200	2.50							



OFFSHORE OCEANOGRAPHY GROUP

REFERENCE NO. 77- 1- 18

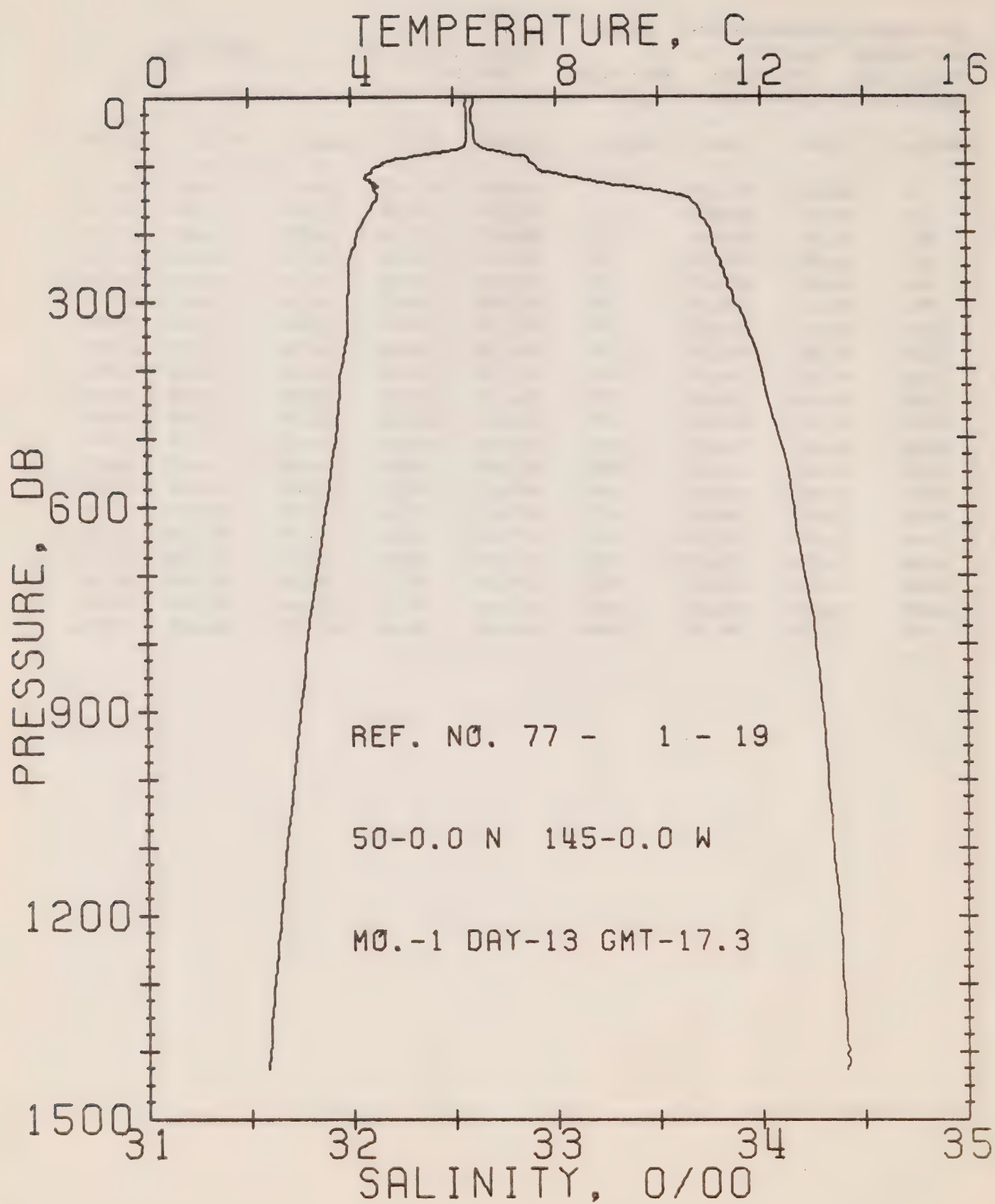
DATE 12/ 1/77

STATION P

POSITION 50- 0.0N, 145- 0.0W GMT 17.3

RESULTS OF STP CAST 153 POINTS TAKEN FROM ANALOG TRACE

PRESS	TEMP	SAL	DEPTH	SIGMA T	SVA	DELTA D	POT. EN	SOUND
0	6.23	32.61	0	25.66	233.7	0.0	0.0	1473.
10	6.23	32.61	10	25.66	234.2	0.23	0.01	1473.
20	6.24	32.60	20	25.65	234.9	0.47	0.05	1473.
30	6.23	32.60	30	25.65	234.9	0.70	0.11	1473.
50	6.22	32.61	50	25.66	234.5	1.17	0.30	1474.
75	6.22	32.61	75	25.66	234.7	1.76	0.67	1474.
100	4.50	32.90	99	26.09	194.0	2.31	1.16	1468.
125	4.32	33.23	124	26.38	167.1	2.76	1.68	1468.
150	4.53	33.67	149	26.70	136.9	3.14	2.20	1470.
175	4.28	33.74	174	26.78	129.5	3.47	2.75	1469.
200	4.11	33.77	199	26.82	125.5	3.79	3.36	1469.
225	4.03	33.79	223	26.85	123.0	4.10	4.03	1469.
250	3.98	33.82	248	26.88	120.8	4.40	4.77	1469.
300	3.90	33.87	298	26.92	116.7	5.00	6.44	1470.
400	3.82	34.00	397	27.03	107.1	6.12	10.42	1471.
500	3.68	34.09	496	27.12	99.6	7.15	15.14	1472.
600	3.50	34.16	595	27.19	93.3	8.11	20.52	1473.
800	3.14	34.26	793	27.31	83.1	9.87	33.05	1475.
1000	2.79	34.34	990	27.40	74.8	11.44	47.47	1477.
1200	2.55	34.39	1188	27.46	69.9	12.89	63.62	1480.



OFFSHORE OCEANOGRAPHY GROUP

REFERENCE NO. 77- 1- 19

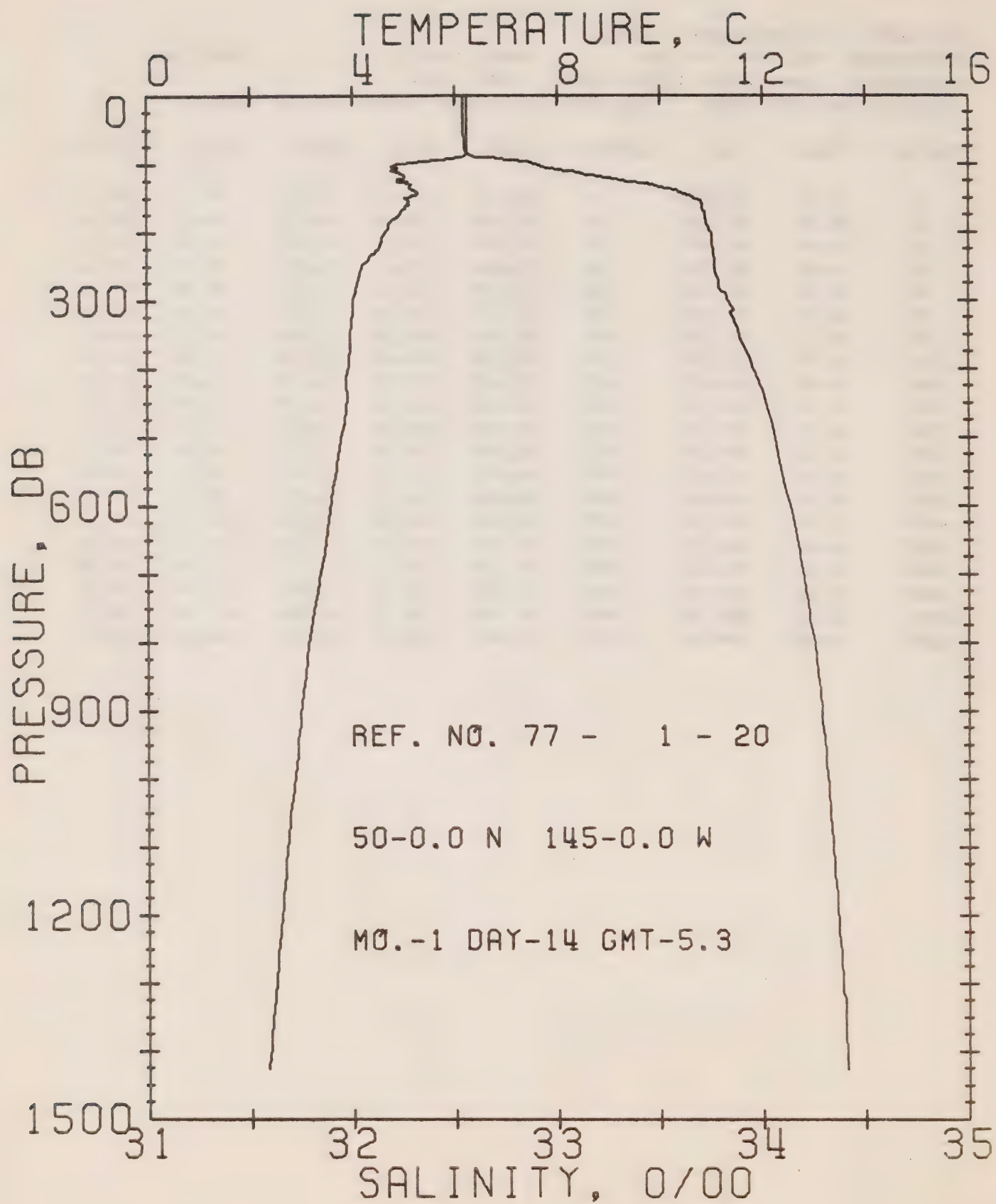
DATE 13/ 1/77

STATION P

POSITION 50- 0.0N, 145- 0.0W GMT 17.3

RESULTS OF STP CAST 182 POINTS TAKEN FROM ANALOG TRACE

PRESS	TEMP	SAL	DEPTH	SIGMA T	SVA	DELTA D	POT. EN	SOUND
0	6.25	32.60	0	25.65	234.7	0.0	0.0	1473.
10	6.25	32.60	10	25.65	235.0	0.23	0.01	1473.
20	6.26	32.59	20	25.64	236.0	0.47	0.05	1473.
30	6.26	32.59	30	25.64	236.1	0.71	0.11	1473.
50	6.26	32.60	50	25.65	235.5	1.18	0.30	1474.
75	6.18	32.64	75	25.70	231.6	1.77	0.67	1474.
100	4.57	32.89	99	26.08	195.2	2.29	1.14	1468.
125	4.37	33.21	124	26.35	169.6	2.75	1.67	1468.
150	4.51	33.65	149	26.69	137.9	3.13	2.20	1470.
175	4.29	33.71	174	26.76	131.6	3.47	2.76	1469.
200	4.11	33.75	199	26.81	126.8	3.79	3.37	1469.
225	4.01	33.78	223	26.84	124.0	4.10	4.05	1469.
250	3.94	33.81	248	26.87	121.2	4.41	4.79	1469.
300	3.91	33.87	298	26.92	116.8	5.01	6.46	1470.
400	3.80	34.00	397	27.04	106.5	6.12	10.42	1471.
500	3.67	34.09	496	27.12	99.6	7.15	15.16	1472.
600	3.48	34.16	595	27.19	93.1	8.11	20.54	1473.
800	3.11	34.26	793	27.31	83.0	9.87	33.05	1475.
1000	2.82	34.32	990	27.38	76.7	11.46	47.61	1477.
1200	2.58	34.38	1188	27.45	70.7	12.94	64.11	1480.



OFFSHORE OCEANOGRAPHY GROUP

REFERENCE NO. 77- 1- 20

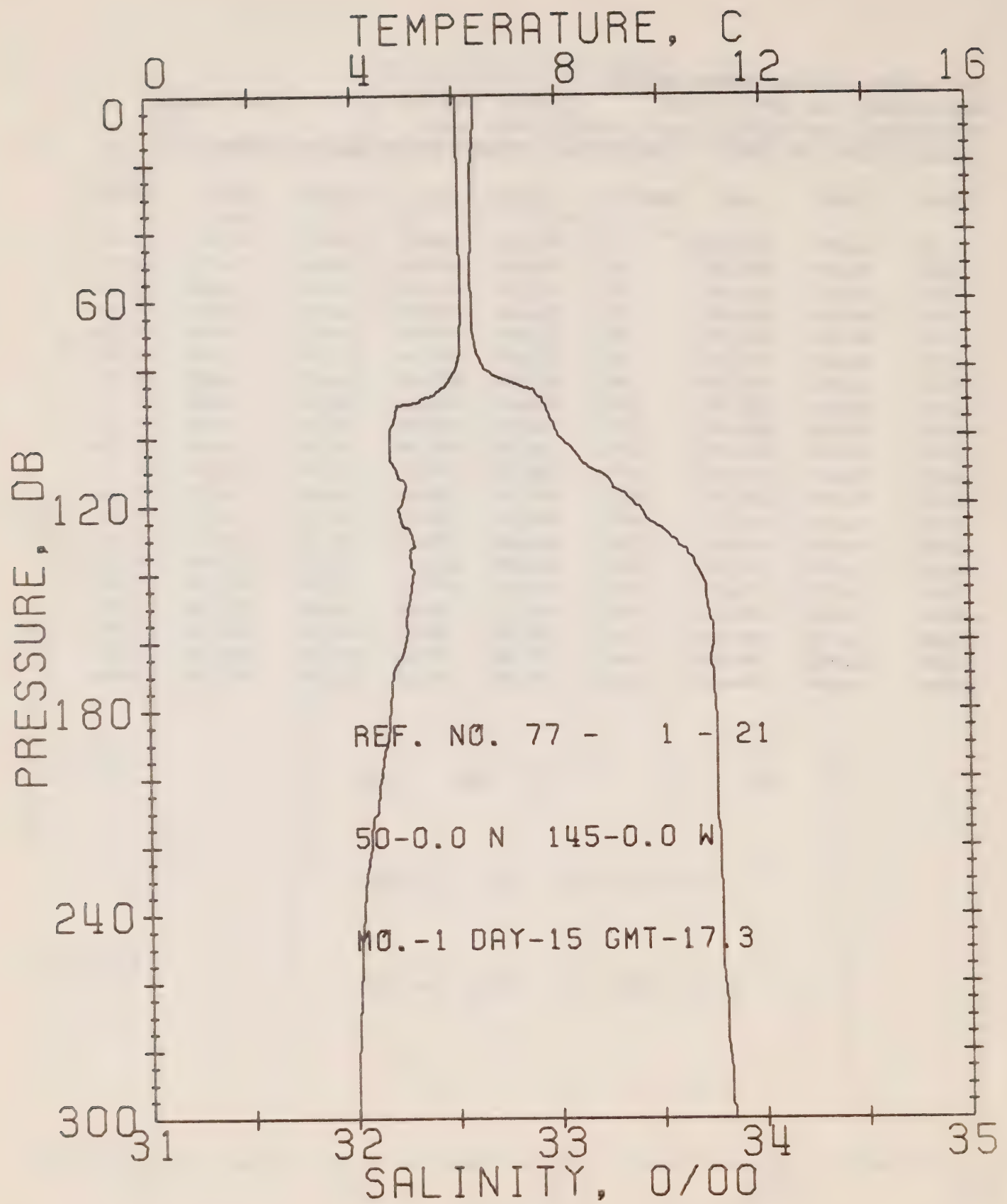
DATE 14/ 1/77

STATION P

POSITION 50- 0.0N, 145- 0.0W GMT 5.3

RESULTS OF STP CAST 195 POINTS TAKEN FROM ANALOG TRACE

PRESS	TEMP	SAL	DEPTH	SIGMA T	SVA	DELTA D	POT. EN	SOUND
0	6.24	32.55	0	25.61	238.3	0.0	0.0	1473.
10	6.24	32.54	10	25.61	239.3	0.24	0.01	1473.
20	6.24	32.54	20	25.61	239.4	0.48	0.05	1473.
30	6.24	32.54	30	25.61	239.6	0.72	0.11	1473.
50	6.24	32.54	50	25.61	239.8	1.20	0.31	1474.
75	6.24	32.55	75	25.61	239.4	1.80	0.69	1474.
100	5.00	32.89	99	26.03	200.0	2.37	1.20	1470.
125	4.88	33.35	124	26.41	164.4	2.83	1.72	1470.
150	5.10	33.66	149	26.63	143.9	3.21	2.26	1472.
175	4.89	33.72	174	26.70	137.4	3.56	2.84	1472.
200	4.63	33.74	199	26.75	133.0	3.90	3.48	1471.
225	4.48	33.76	223	26.78	130.4	4.23	4.20	1471.
250	4.18	33.77	248	26.81	126.6	4.55	4.97	1470.
300	4.00	33.83	298	26.88	120.7	5.17	6.71	1470.
400	3.90	33.95	357	26.99	111.1	6.33	10.85	1472.
500	3.77	34.06	496	27.09	102.8	7.40	15.74	1473.
600	3.56	34.13	595	27.17	95.8	8.40	21.31	1474.
800	3.14	34.25	793	27.30	84.1	10.19	34.08	1475.
1000	2.85	34.32	990	27.38	77.3	11.80	48.78	1477.
1200	2.59	34.36	1188	27.44	72.0	13.29	65.46	1480.



OFFSHORE OCEANOGRAPHY GROUP

REFERENCE NO. 77- 1- 21

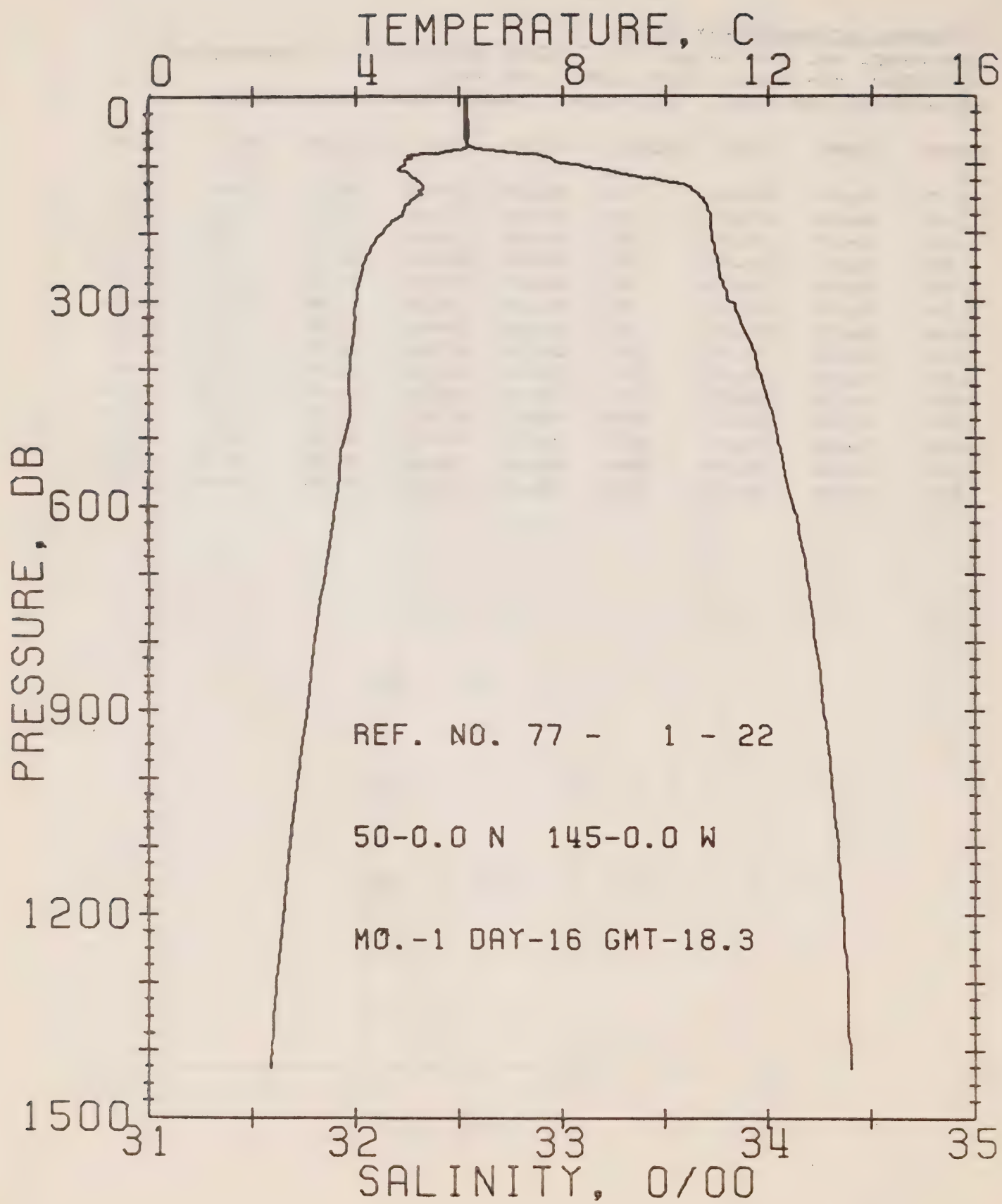
DATE 15/ 1/77

STATION P

POSITION 50- 0.0N. 145- 0.0W GMT 17.3

RESULTS OF STP CAST 108 POINTS TAKEN FROM ANALOG TRACE

PRESS	TEMP	SAL	DEPTH	SIGMA T	SVA	DELTA D	POT. EN	SOUND
0	6.09	32.61	0	25.68	232.0	0.0	0.0	1472.
10	6.09	32.61	10	25.68	232.6	0.23	0.01	1472.
20	6.10	32.59	20	25.67	233.8	0.47	0.05	1473.
30	6.11	32.59	30	25.66	234.3	0.70	0.11	1473.
50	6.12	32.58	50	25.65	235.3	1.17	0.30	1473.
75	6.10	32.61	75	25.68	233.2	1.76	0.67	1474.
100	4.72	33.01	99	26.16	188.0	2.28	1.13	1469.
125	4.95	33.45	124	26.48	157.3	2.71	1.63	1471.
150	5.03	33.73	149	26.69	137.8	3.07	2.14	1472.
175	4.70	33.75	174	26.75	132.8	3.41	2.70	1471.
200	4.48	33.77	199	26.78	129.4	3.74	3.32	1470.
225	4.23	33.78	223	26.82	126.2	4.06	4.01	1470.
250	4.08	33.79	248	26.84	124.2	4.37	4.77	1470.
300	3.98	33.84	298	26.89	119.7	4.98	6.48	1470.



OFFSHORE OCEANOGRAPHY GROUP

REFERENCE NO. 77- 1- 22

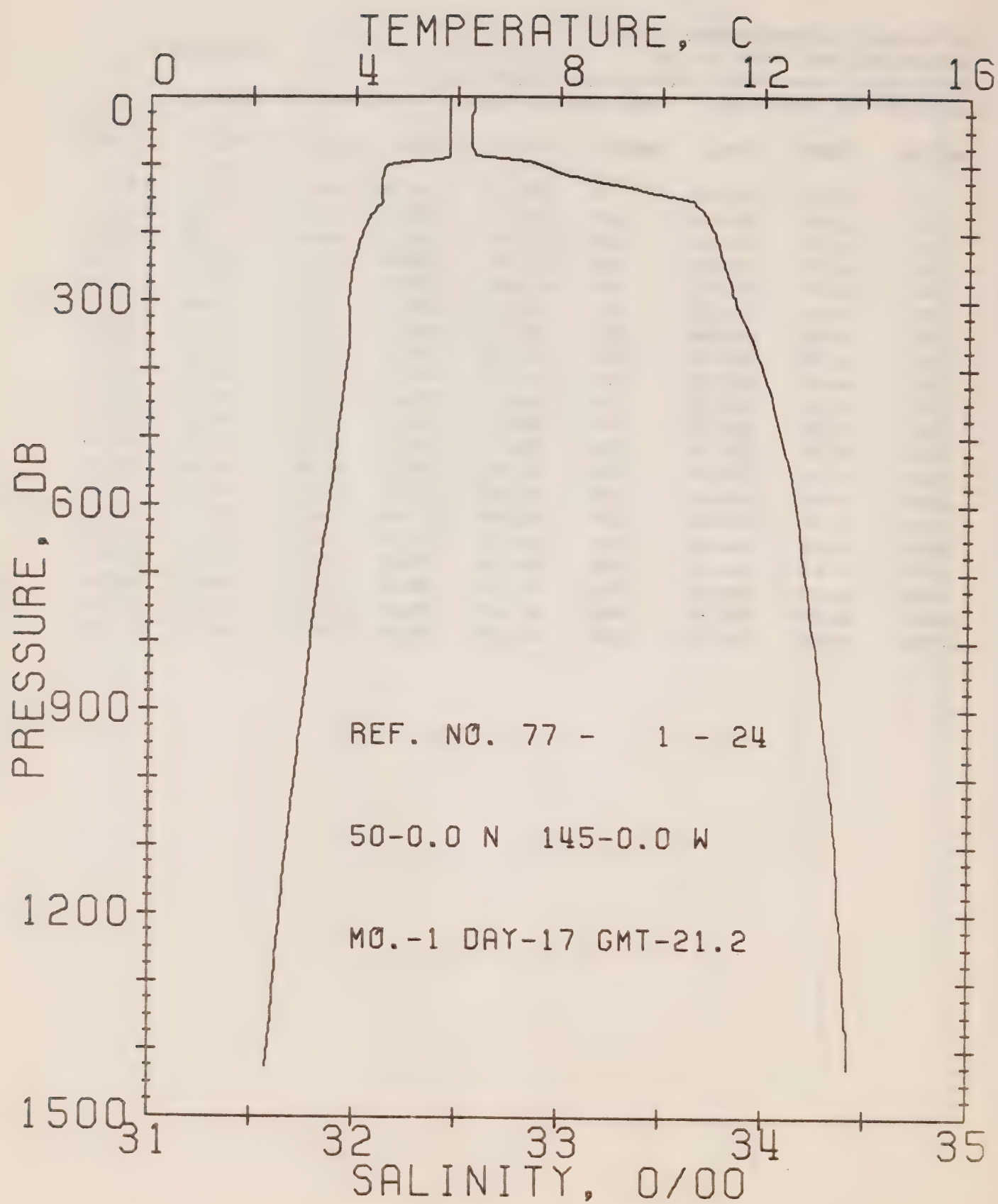
DATE 16/ 1/77

STATION P

POSITION 50- 0.0N, 145- 0.0W GMT 18.3

RESULTS OF STP CAST 186 POINTS TAKEN FROM ANALOG TRACE

PRESS	TEMP	SAL	DEPTH	SIGMA T	SVA	DELTA D	POT. EN	SOUND
0	6.17	32.53	0	25.61	238.9	0.0	0.0	1472.
10	6.17	32.53	10	25.61	239.2	0.24	0.01	1473.
20	6.17	32.53	20	25.61	239.4	0.48	0.05	1473.
30	6.17	32.53	30	25.61	239.6	0.72	0.11	1473.
50	6.18	32.53	50	25.61	239.9	1.20	0.31	1473.
75	6.13	32.58	75	25.65	235.8	1.80	0.69	1474.
100	4.95	33.06	99	26.17	186.7	2.31	1.15	1470.
125	5.25	33.52	124	26.50	155.8	2.74	1.63	1472.
150	5.13	33.68	149	26.64	142.4	3.11	2.15	1472.
175	4.87	33.72	174	26.70	137.1	3.46	2.73	1472.
200	4.50	33.73	199	26.75	132.6	3.80	3.37	1471.
225	4.27	33.74	223	26.78	129.5	4.12	4.08	1470.
250	4.14	33.76	248	26.81	127.0	4.44	4.86	1470.
300	4.01	33.81	298	26.86	122.3	5.07	6.61	1470.
400	3.89	33.95	397	26.99	111.4	6.23	10.73	1472.
500	3.78	34.05	496	27.07	103.8	7.30	15.66	1473.
600	3.60	34.12	595	27.15	97.2	8.31	21.30	1474.
800	3.19	34.22	793	27.27	86.6	10.13	34.26	1475.
1000	2.87	34.31	990	27.37	78.2	11.77	49.30	1478.
1200	2.60	34.36	1188	27.44	72.1	13.27	66.07	1480.



OFFSHORE OCEANOGRAPHY GROUP

REFERENCE NO. 77- 1- 24

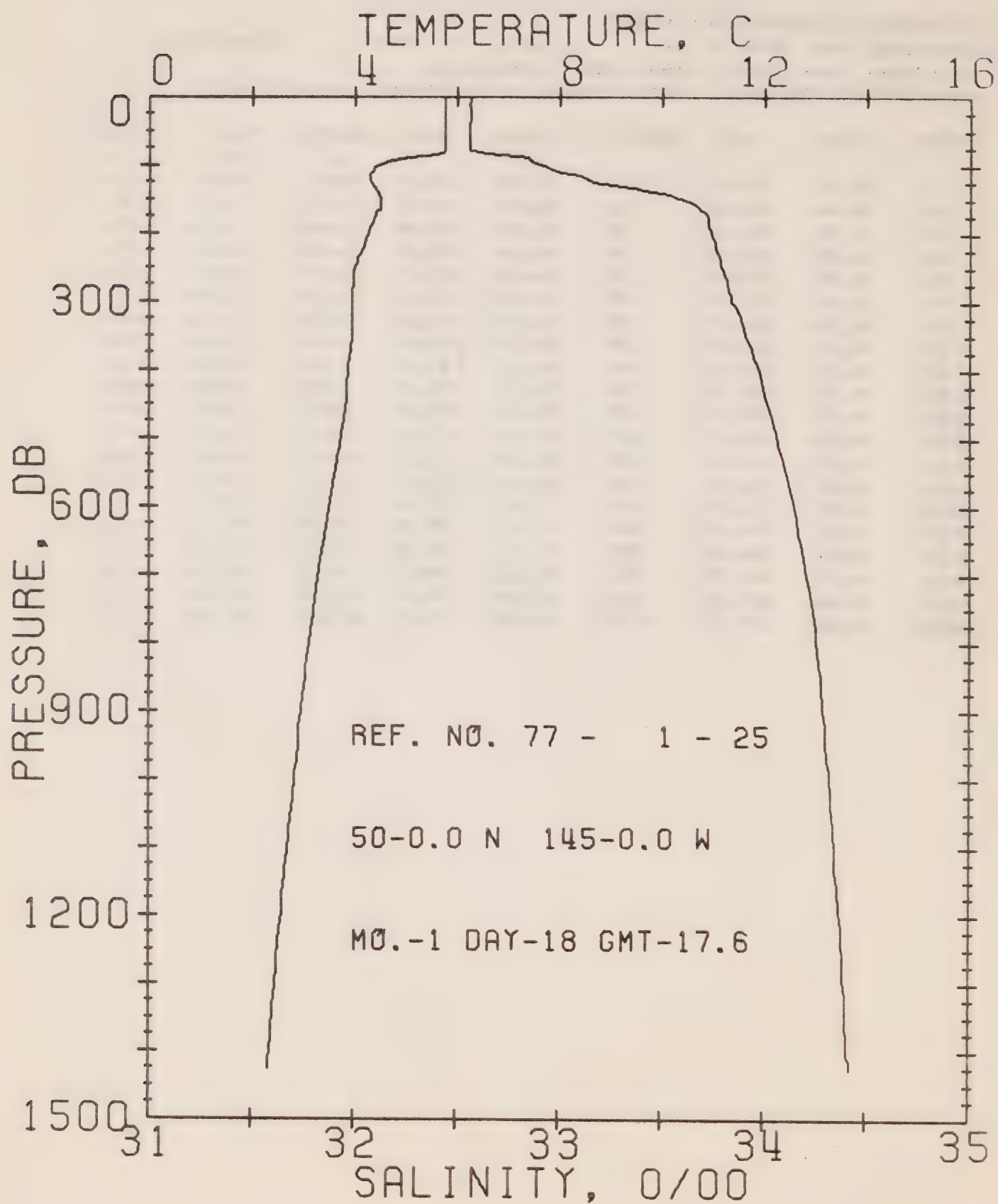
DATE 17/ 1/77

STATION P

POSITION 50- 0.0N, 145- 0.0W GMT 21.2

RESULTS OF STP CAST 171 POINTS TAKEN FROM ANALOG TRACE

PRESS	TEMP	SAL	DEPTH	SIGMA T	SVA	DELTA D	POT. EN	SOUND
0	5.85	32.58	0	25.69	231.5	0.0	0.0	1471.
10	5.84	32.58	10	25.69	231.7	0.23	0.01	1471.
20	5.84	32.58	20	25.69	231.8	0.46	0.05	1472.
30	5.85	32.57	30	25.68	232.7	0.70	0.11	1472.
50	5.84	32.57	50	25.68	232.9	1.16	0.30	1472.
75	5.85	32.57	75	25.68	233.2	1.74	0.67	1472.
100	4.70	32.90	99	26.07	196.0	2.30	1.16	1469.
125	4.50	33.20	124	26.33	171.9	2.76	1.69	1469.
150	4.51	33.61	149	26.65	141.2	3.15	2.24	1470.
175	4.30	33.72	174	26.76	131.3	3.49	2.80	1469.
200	4.14	33.75	199	26.81	127.0	3.81	3.41	1469.
225	4.04	33.78	223	26.84	123.9	4.13	4.09	1469.
250	3.95	33.81	248	26.87	121.3	4.43	4.83	1469.
300	3.87	33.86	298	26.92	117.1	5.03	6.50	1470.
400	3.84	33.99	397	27.03	107.6	6.15	10.51	1471.
500	3.67	34.09	496	27.12	99.6	7.19	15.24	1472.
600	3.50	34.16	595	27.19	93.2	8.15	20.63	1473.
800	3.15	34.25	793	27.30	84.3	9.92	33.24	1475.
1000	2.84	34.32	990	27.39	76.5	11.53	47.93	1477.
1200	2.57	34.37	1188	27.45	71.1	12.99	64.35	1480.



OFFSHORE OCEANOGRAPHY GROUP

REFERENCE NO. 77- 1- 25

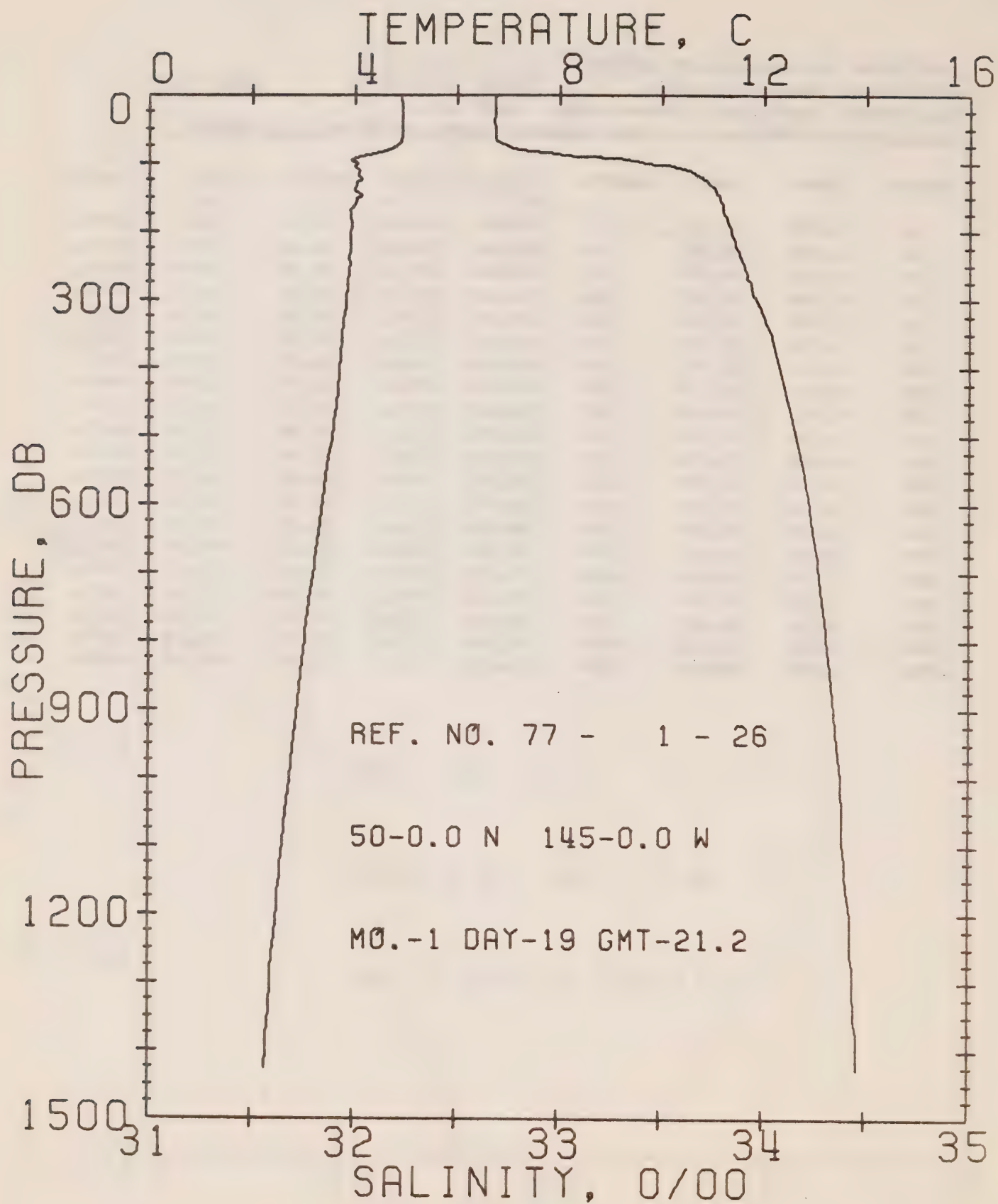
DATE 18/ 1/77

STATION P

POSITION 50- 0.0N, 145- 0.0W GMT 17.6

RESULTS OF STP CAST 173 POINTS TAKEN FROM ANALOG TRACE

PRESS	TEMP	SAL	DEPTH	SIGMA T	SVA	DELTA D	POT. EN	SOUND
0	5.76	32.57	0	25.69	231.2	0.0	0.0	1471.
10	5.76	32.56	10	25.68	232.0	0.23	0.01	1471.
20	5.76	32.57	20	25.69	231.7	0.46	0.05	1471.
30	5.76	32.57	30	25.69	231.7	0.70	0.11	1471.
50	5.76	32.56	50	25.68	232.7	1.16	0.30	1472.
75	5.76	32.56	75	25.68	232.9	1.74	0.67	1472.
100	4.51	32.91	99	26.10	192.9	2.27	1.14	1468.
125	4.31	33.19	124	26.34	170.5	2.73	1.66	1468.
150	4.51	33.60	149	26.65	142.0	3.11	2.19	1470.
175	4.39	33.72	174	26.76	131.7	3.45	2.76	1470.
200	4.25	33.74	199	26.78	129.2	3.78	3.38	1469.
225	4.13	33.77	223	26.82	126.0	4.10	4.07	1469.
250	4.00	33.79	248	26.85	123.1	4.41	4.82	1469.
300	3.94	33.84	298	26.90	119.3	5.01	6.51	1470.
400	3.87	33.97	397	27.01	109.3	6.15	10.57	1471.
500	3.72	34.06	496	27.09	101.9	7.21	15.42	1473.
600	3.50	34.15	595	27.18	94.1	8.19	20.91	1473.
800	3.12	34.25	793	27.30	83.8	9.96	33.48	1475.
1000	2.83	34.32	990	27.38	76.6	11.55	48.09	1477.
1200	2.57	34.37	1188	27.45	71.1	13.03	64.65	1480.



OFFSHORE OCEANOGRAPHY GROUP

REFERENCE NO. 77- 1- 26

DATE 19/ 1/77

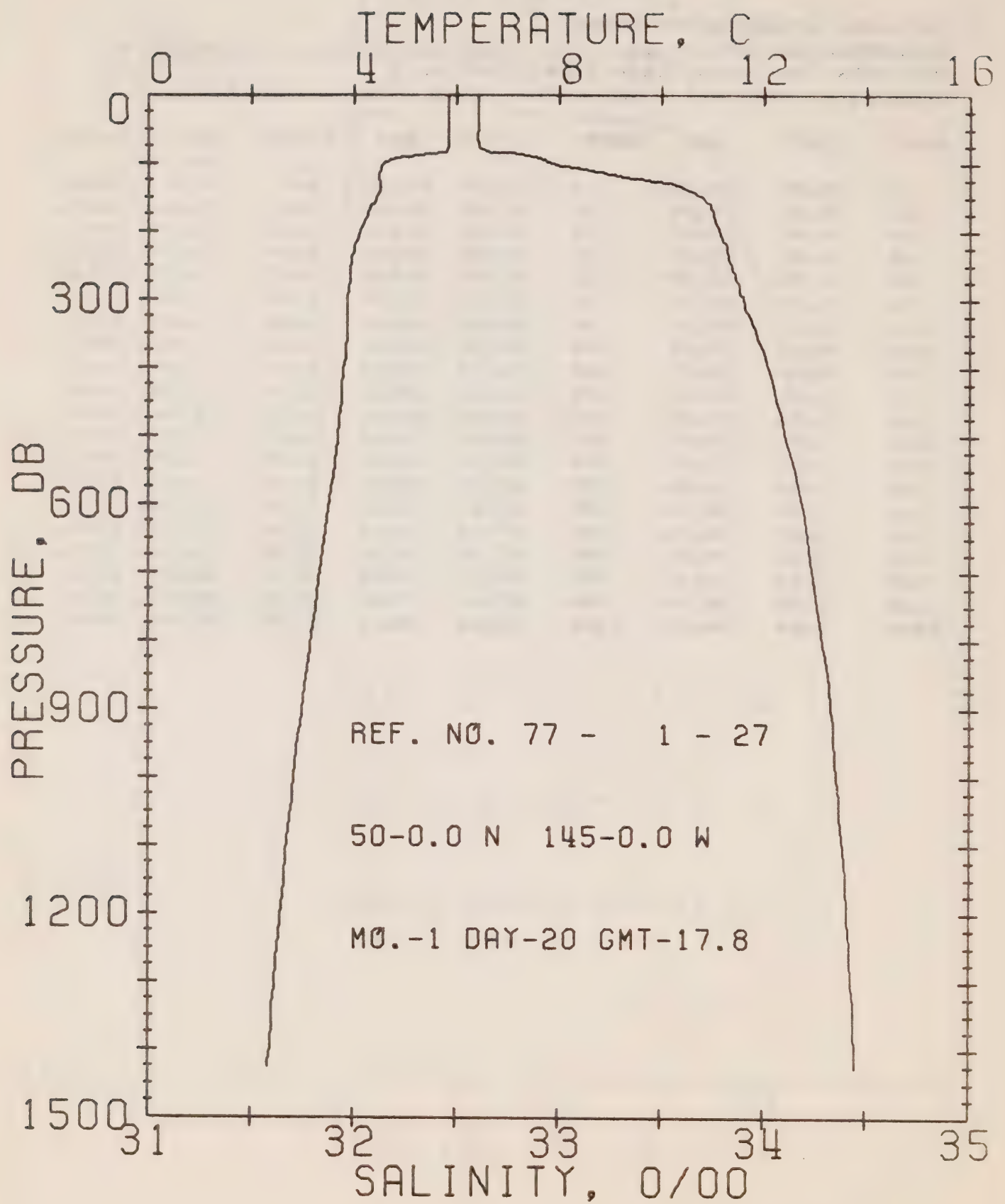
STATION P

POSITION 50- 0.0N. 145- 0.0W

GMT 21.2

RESULTS OF STP CAST 155 POINTS TAKEN FROM ANALOG TRACE

PRESS	TEMP	SAL	DEPTH	SIGMA T	SVA	DELTA D	POT. EN	SOUND
0	4.92	32.70	0	25.89	212.3	0.0	0.0	1468.
10	4.93	32.69	10	25.88	213.4	0.21	0.01	1468.
20	4.94	32.69	20	25.88	213.7	0.43	0.04	1468.
30	4.94	32.69	30	25.88	213.7	0.64	0.10	1468.
50	4.94	32.69	50	25.88	214.0	1.07	0.27	1468.
75	4.83	32.74	75	25.93	208.8	1.60	0.61	1469.
100	4.02	33.43	99	26.56	149.3	2.05	1.01	1466.
125	4.11	33.71	124	26.78	129.1	2.39	1.40	1468.
150	4.10	33.78	149	26.83	123.9	2.70	1.84	1468.
175	3.92	33.80	174	26.87	120.7	3.01	2.34	1468.
200	3.93	33.84	199	26.90	118.4	3.31	2.91	1468.
225	3.92	33.87	223	26.92	116.3	3.60	3.55	1469.
250	3.91	33.90	248	26.95	113.8	3.89	4.24	1469.
300	3.83	33.96	298	27.00	109.2	4.45	5.81	1470.
400	3.71	34.08	397	27.11	100.1	5.49	9.51	1471.
500	3.57	34.16	496	27.18	93.4	6.46	13.95	1472.
600	3.38	34.22	595	27.26	87.1	7.36	18.99	1473.
800	3.03	34.31	793	27.36	78.3	9.01	30.73	1475.
1000	2.75	34.38	990	27.44	71.4	10.50	44.43	1477.
1200	2.49	34.43	1188	27.50	66.3	11.89	59.94	1479.



OFFSHORE OCEANOGRAPHY GROUP

REFERENCE NO. 77- 1- 27

DATE 20/ 1/77

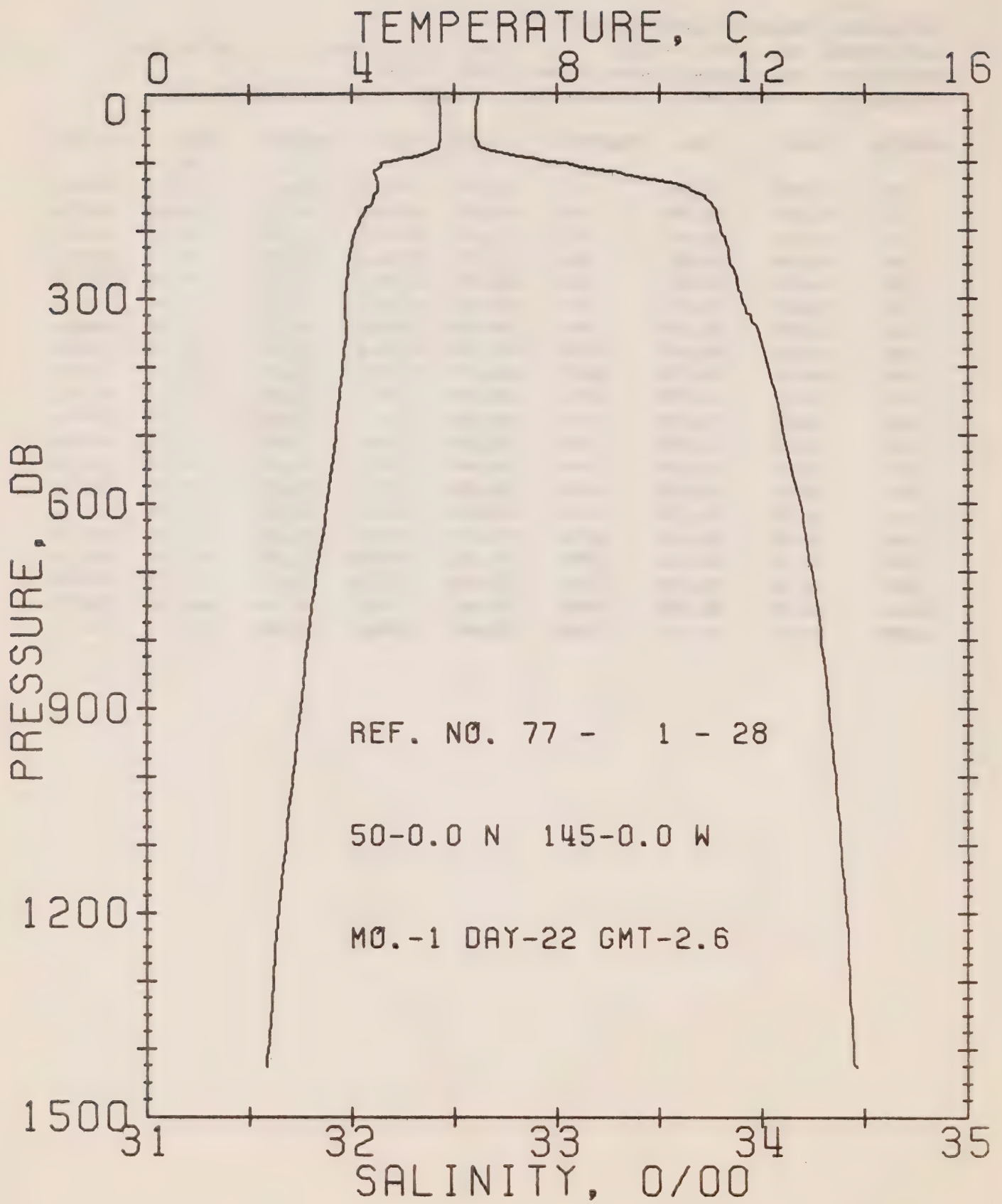
STATION P

POSITION 50- 0.0N, 145- 0.0W

GMT 17.8

RESULTS OF STP CAST 166 POINTS TAKEN FROM ANALOG TRACE

PRESS	TEMP	SAL	DEPTH	SIGMA T	SVA	DELTA D	POT. EN	SOUND
0	5.83	32.61	0	25.71	229.0	0.0	0.0	1471.
10	5.83	32.61	10	25.71	229.4	0.23	0.01	1471.
20	5.83	32.61	20	25.71	229.5	0.46	0.05	1472.
30	5.84	32.61	30	25.71	229.7	0.69	0.11	1472.
50	5.84	32.61	50	25.71	229.9	1.15	0.29	1472.
75	5.83	32.61	75	25.71	230.1	1.72	0.66	1472.
100	4.58	32.96	99	26.13	190.0	2.25	1.13	1468.
125	4.50	33.47	124	26.54	151.4	2.68	1.62	1469.
150	4.44	33.70	149	26.73	133.7	3.03	2.11	1469.
175	4.27	33.75	174	26.79	128.4	3.36	2.65	1469.
200	4.10	33.78	199	26.83	124.5	3.68	3.26	1469.
225	4.00	33.82	223	26.87	120.8	3.98	3.92	1469.
250	3.93	33.84	248	26.90	118.8	4.28	4.64	1469.
300	3.87	33.90	298	26.95	114.1	4.86	6.28	1470.
400	3.80	34.02	397	27.05	105.3	5.96	10.18	1471.
500	3.69	34.11	496	27.13	98.4	6.98	14.84	1472.
600	3.52	34.19	595	27.21	91.4	7.93	20.14	1474.
800	3.16	34.29	793	27.33	81.6	9.65	32.44	1475.
1000	2.83	34.35	990	27.41	74.2	11.20	46.60	1477.
1200	2.57	34.41	1188	27.48	68.4	12.62	62.52	1480.



OFFSHORE OCEANOGRAPHY GROUP

REFERENCE NO. 77- 1- 28 .

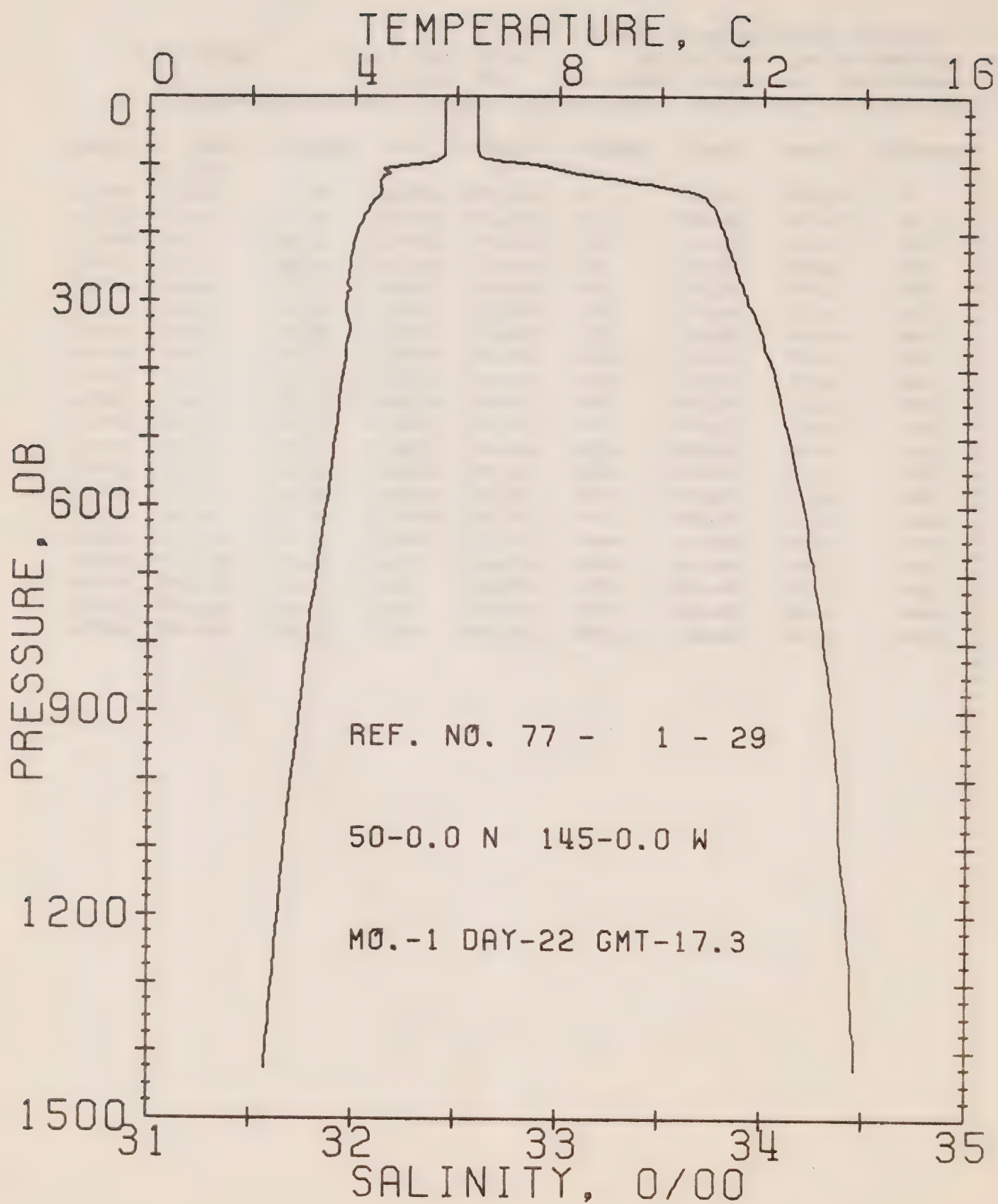
DATE 22/ 1/77

STATION P

POSITION 50- 0.0N, 145- 0.0W GMT 2.6

RESULTS OF STP CAST 163 POINTS TAKEN FROM ANALOG TRACE

PRESS	TEMP	SAL	DEPTH	SIGMA T	SVA	DELTA D	POT. EN	SOUND
0	5.72	32.62	0	25.73	226.9	0.0	0.0	1471.
10	5.72	32.62	10	25.73	227.4	0.23	0.01	1471.
20	5.73	32.61	20	25.73	228.1	0.45	0.05	1471.
30	5.73	32.61	30	25.72	228.4	0.68	0.10	1471.
50	5.73	32.61	50	25.72	228.6	1.14	0.29	1472.
75	5.72	32.62	75	25.73	228.0	1.71	0.65	1472.
100	4.69	32.97	99	26.13	190.7	2.25	1.13	1469.
125	4.48	33.44	124	26.52	153.5	2.68	1.62	1469.
150	4.43	33.71	149	26.74	132.6	3.03	2.11	1469.
175	4.21	33.78	174	26.82	125.6	3.35	2.65	1469.
200	4.07	33.80	199	26.85	122.8	3.66	3.24	1469.
225	3.98	33.83	223	26.89	119.7	3.96	3.89	1469.
250	3.93	33.85	248	26.90	118.0	4.26	4.61	1469.
300	3.86	33.90	298	26.95	114.1	4.84	6.24	1470.
400	3.81	34.03	397	27.06	104.6	5.93	10.12	1471.
500	3.68	34.10	496	27.13	98.4	6.94	14.75	1472.
600	3.52	34.18	595	27.21	91.4	7.89	20.07	1474.
800	3.13	34.29	793	27.33	81.0	9.61	32.29	1475.
1000	2.83	34.36	990	27.41	73.9	11.16	46.47	1477.
1200	2.56	34.41	1188	27.48	68.1	12.58	62.38	1480.



OFFSHORE OCEANOGRAPHY GROUP

REFERENCE NO. 77- 1- 29

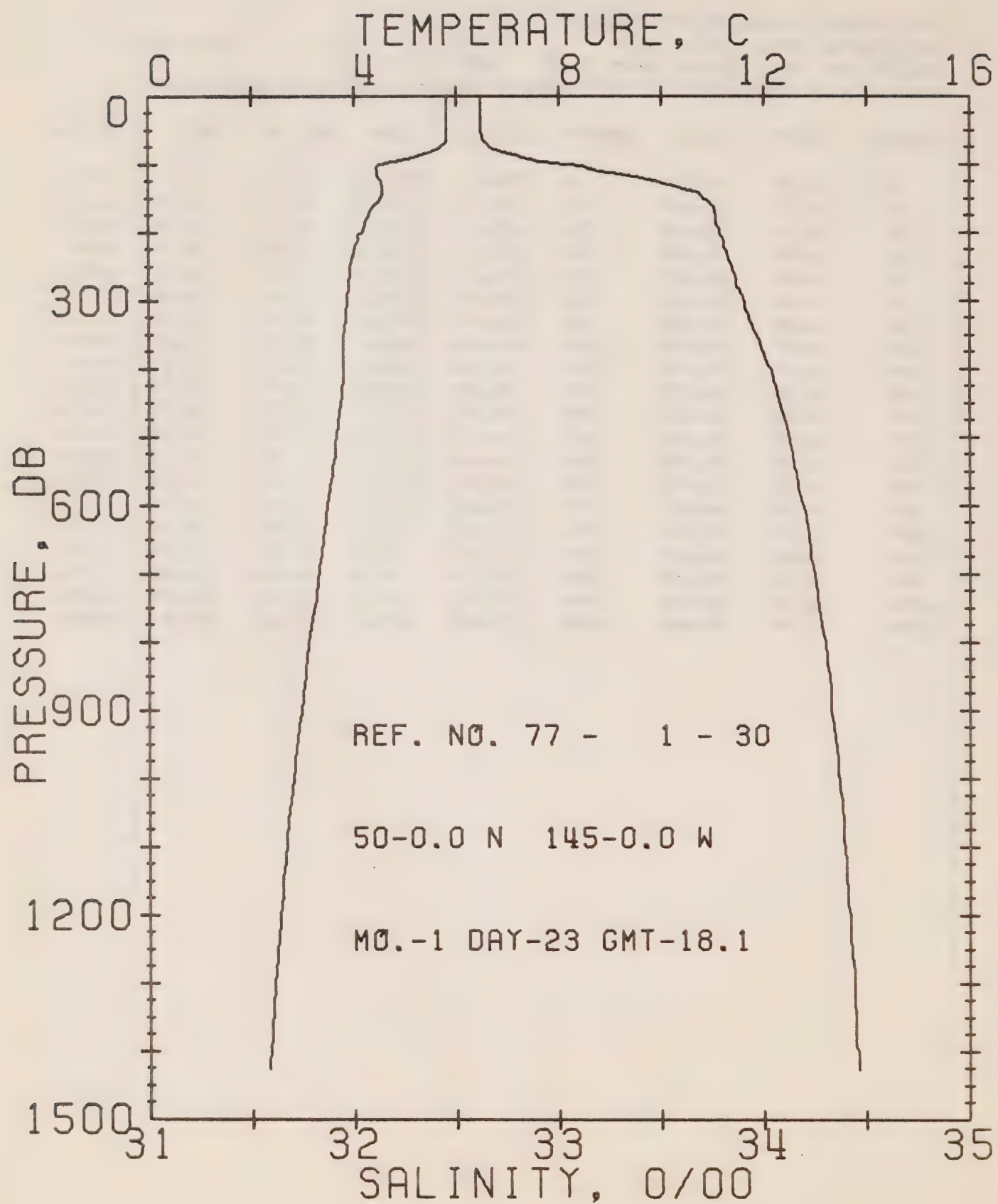
DATE 22/ 1/77

STATION P

POSITION 50- 0.0N, 145- 0.0W GMT 17.3

RESULTS OF STP CAST 176 POINTS TAKEN FROM ANALOG TRACE

PRESS	TEMP	SAL	DEPTH	SIGMA T	SVA	DELTA D	POT. EN	SOUND
0	5.78	32.60	0	25.71	229.2	0.0	0.0	1471.
10	5.77	32.60	10	25.71	229.4	0.23	0.01	1471.
20	5.77	32.60	20	25.71	229.5	0.46	0.05	1471.
30	5.76	32.60	30	25.71	229.5	0.69	0.11	1471.
50	5.76	32.60	50	25.71	229.8	1.15	0.29	1472.
75	5.75	32.60	75	25.71	229.9	1.72	0.66	1472.
100	5.28	32.85	99	25.97	205.8	2.29	1.16	1471.
125	4.51	33.34	124	26.44	161.2	2.74	1.68	1469.
150	4.45	33.72	149	26.75	132.5	3.10	2.18	1469.
175	4.18	33.77	174	26.82	125.6	3.42	2.71	1469.
200	4.04	33.81	199	26.86	121.7	3.73	3.30	1469.
225	3.96	33.83	223	26.89	119.4	4.03	3.96	1469.
250	3.91	33.86	248	26.91	117.1	4.33	4.67	1469.
300	3.85	33.92	298	26.97	112.4	4.90	6.28	1470.
400	3.80	34.05	397	27.08	102.9	5.98	10.11	1471.
500	3.64	34.13	496	27.15	96.2	6.97	14.66	1472.
600	3.47	34.20	595	27.23	89.8	7.90	19.86	1473.
800	3.10	34.30	793	27.34	79.8	9.59	31.87	1475.
1000	2.79	34.38	990	27.43	72.2	11.10	45.73	1477.
1200	2.54	34.42	1188	27.49	67.2	12.50	61.44	1480.



OFFSHORE OCEANOGRAPHY GROUP

REFERENCE NO. 77- 1- 30

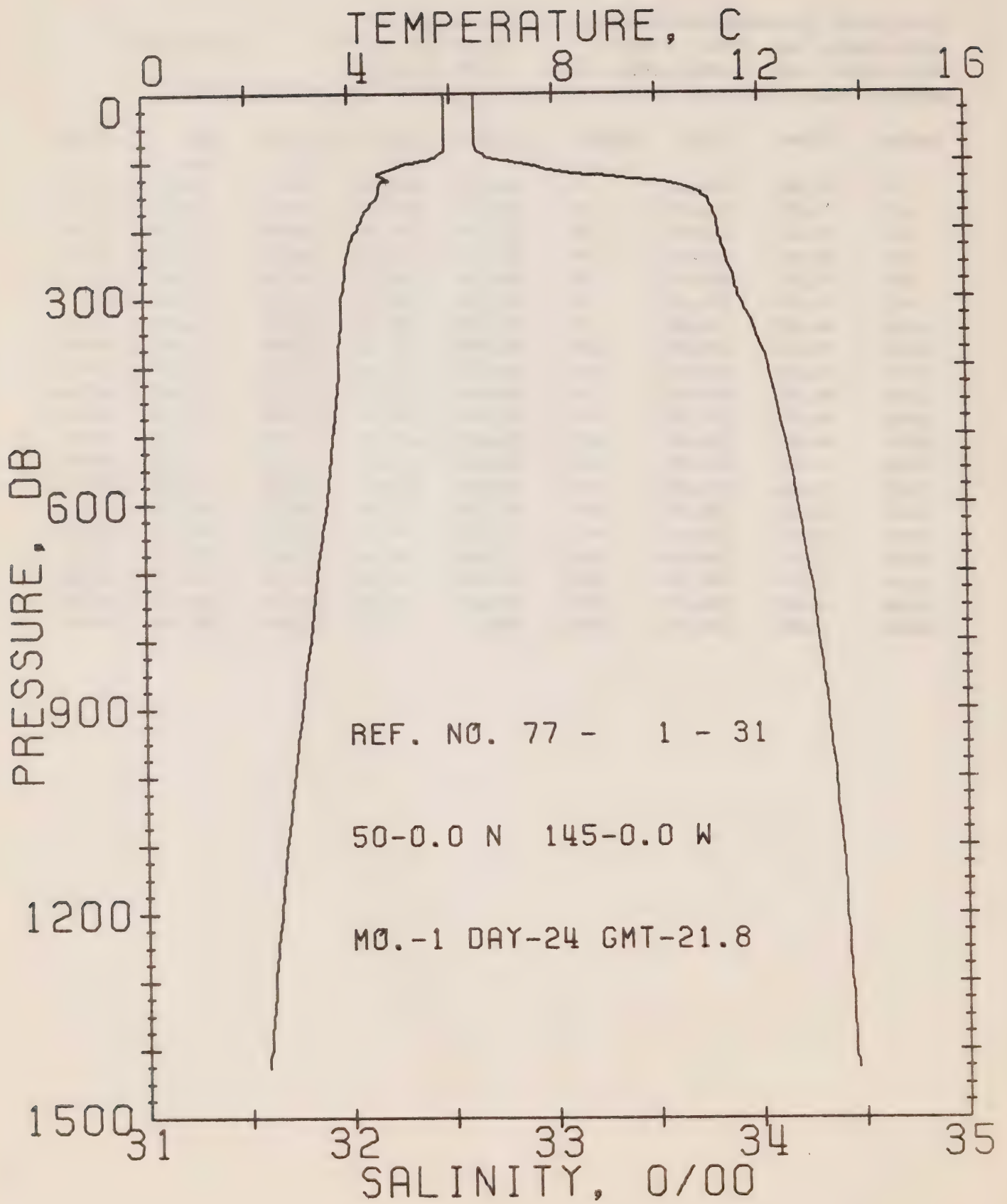
DATE 23/ 1/77

STATION P

POSITION 50- 0.0N, 145- 0.0W GMT 18.1

RESULTS OF STP CAST 188 POINTS TAKEN FROM ANALOG TRACE

PRESS	TEMP	SAL	DEPTH	SIGMA T	SVA	DELTA D	POT. EN	SOUND
0	5.82	32.62	0	25.72	228.1	0.0	0.0	1471.
10	5.82	32.62	10	25.72	228.5	0.23	0.01	1471.
20	5.82	32.62	20	25.72	228.6	0.46	0.05	1472.
30	5.82	32.62	30	25.72	228.7	0.69	0.10	1472.
50	5.82	32.62	50	25.72	228.9	1.14	0.29	1472.
75	5.69	32.67	75	25.78	223.9	1.71	0.65	1472.
100	4.51	33.03	99	26.19	184.3	2.23	1.12	1468.
125	4.53	33.48	124	26.55	151.0	2.65	1.59	1469.
150	4.52	33.71	149	26.73	133.8	3.00	2.09	1470.
175	4.28	33.77	174	26.80	127.2	3.33	2.62	1469.
200	4.15	33.79	199	26.83	124.4	3.64	3.23	1469.
225	4.00	33.81	223	26.87	121.5	3.95	3.89	1469.
250	3.93	33.84	248	26.90	118.7	4.25	4.62	1469.
300	3.86	33.90	298	26.95	114.1	4.83	6.24	1470.
400	3.80	34.03	397	27.06	104.6	5.92	10.14	1471.
500	3.65	34.12	496	27.15	96.8	6.93	14.74	1472.
600	3.48	34.19	595	27.22	90.5	7.87	19.99	1473.
800	3.10	34.30	793	27.34	80.0	9.58	32.15	1475.
1000	2.80	34.37	990	27.42	73.1	11.10	46.14	1477.
1200	2.54	34.42	1188	27.49	67.3	12.50	61.83	1480.



OFFSHORE OCEANOGRAPHY GROUP

REFERENCE NO. 77- 1- 31

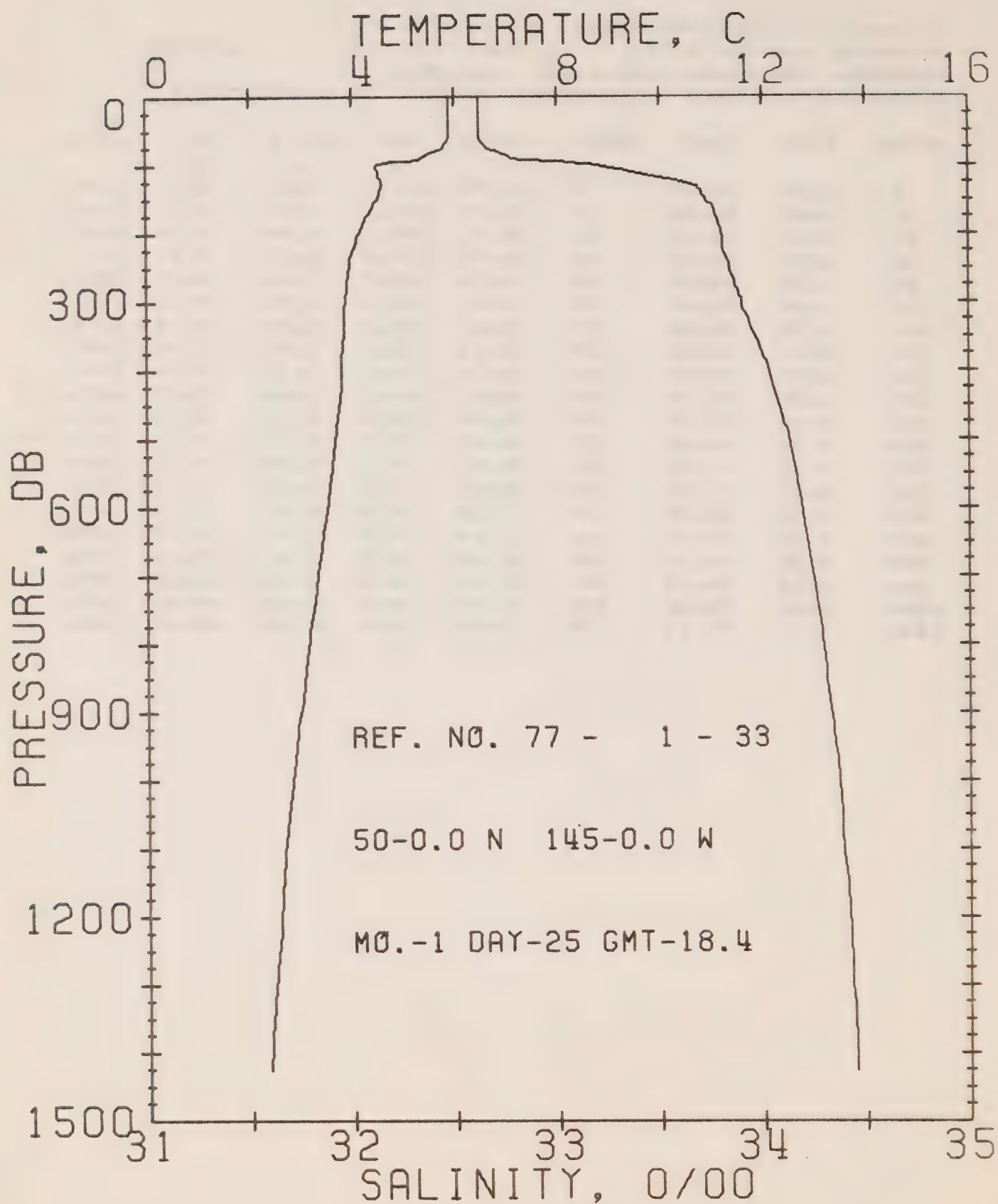
DATE 24/ 1/77

STATION P

POSITION 50- 0.0N, 145- 0.0W GMT 21.8

RESULTS OF STP CAST 161 POINTS TAKEN FROM ANALOG TRACE

PRESS	TEMP	SAL	DEPTH	SIGMA T	SVA	DELTA D	POT. EN	SOUND
0	5.88	32.63	0	25.72	228.0	0.0	0.0	1471.
10	5.89	32.62	10	25.71	229.3	0.23	0.01	1472.
20	5.89	32.62	20	25.71	229.4	0.46	0.05	1472.
30	5.90	32.62	30	25.71	229.6	0.69	0.11	1472.
50	5.89	32.62	50	25.71	229.7	1.15	0.29	1472.
75	5.89	32.62	75	25.71	229.9	1.72	0.66	1473.
100	5.36	32.80	99	25.92	210.7	2.29	1.16	1471.
125	4.73	33.36	124	26.43	162.1	2.76	1.70	1470.
150	4.57	33.73	149	26.74	132.9	3.11	2.19	1470.
175	4.30	33.78	174	26.81	126.5	3.43	2.73	1469.
200	4.16	33.81	199	26.85	123.3	3.75	3.33	1469.
225	4.00	33.82	223	26.87	120.7	4.05	3.98	1469.
250	3.93	33.85	248	26.90	118.1	4.35	4.71	1469.
300	3.84	33.90	298	26.95	113.8	4.93	6.32	1470.
400	3.79	34.04	397	27.07	103.3	6.01	10.17	1471.
500	3.66	34.12	496	27.14	97.2	7.01	14.77	1472.
600	3.53	34.18	595	27.21	91.7	7.95	20.05	1474.
800	3.19	34.28	793	27.32	82.2	9.68	32.36	1476.
1000	2.86	34.36	990	27.41	74.0	11.24	46.62	1478.
1200	2.58	34.41	1188	27.48	68.5	12.66	62.47	1480.



OFFSHORE OCEANOGRAPHY GROUP

REFERENCE NO. 77- 1- 33

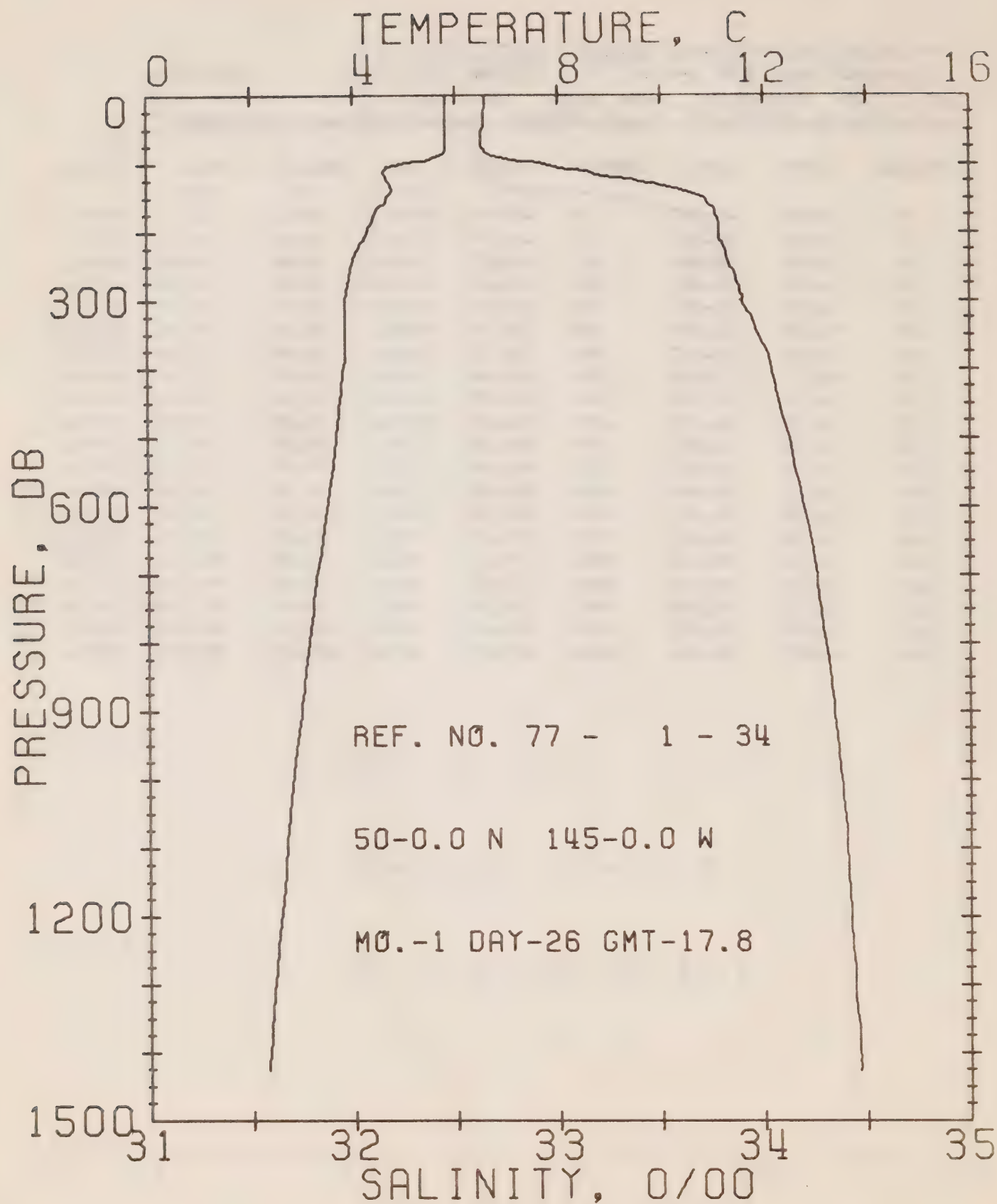
DATE 25/ 1/77

STATION P

POSITION 50- 0.0N, 145- 0.0W GMT 18.4

RESULTS OF STP CAST 143 POINTS TAKEN FROM ANALOG TRACE

PRESS	TEMP	SAL	DEPTH	SIGMA T	SVA	DELTA D	POT. EN	SOUND
0	5.89	32.62	0	25.71	228.9	0.0	0.0	1471.
10	5.89	32.62	10	25.71	229.3	0.23	0.01	1472.
20	5.90	32.62	20	25.71	229.5	0.46	0.05	1472.
30	5.90	32.62	30	25.71	229.6	0.69	0.11	1472.
50	5.90	32.62	50	25.71	229.8	1.15	0.29	1472.
75	5.75	32.66	75	25.76	225.3	1.72	0.66	1472.
100	4.46	33.17	99	26.31	172.9	2.24	1.12	1468.
125	4.57	33.61	124	26.65	141.4	2.63	1.56	1469.
150	4.50	33.72	149	26.74	132.7	2.97	2.04	1470.
175	4.27	33.77	174	26.81	126.6	3.29	2.57	1469.
200	4.12	33.80	199	26.85	123.3	3.60	3.17	1469.
225	4.01	33.81	223	26.86	121.7	3.91	3.83	1469.
250	3.93	33.84	248	26.90	118.8	4.21	4.56	1469.
300	3.86	33.90	298	26.95	114.1	4.79	6.19	1470.
400	3.79	34.03	397	27.06	104.4	5.88	10.08	1471.
500	3.66	34.13	496	27.15	96.4	6.89	14.69	1472.
600	3.49	34.19	595	27.22	90.7	7.82	19.92	1473.
800	3.13	34.29	793	27.33	80.7	9.54	32.11	1475.
1000	2.80	34.37	990	27.42	72.7	11.07	46.17	1477.
1200	2.57	34.42	1188	27.48	67.9	12.48	61.89	1480.



OFFSHORE OCEANOGRAPHY GROUP

REFERENCE NO. 77- 1- 34

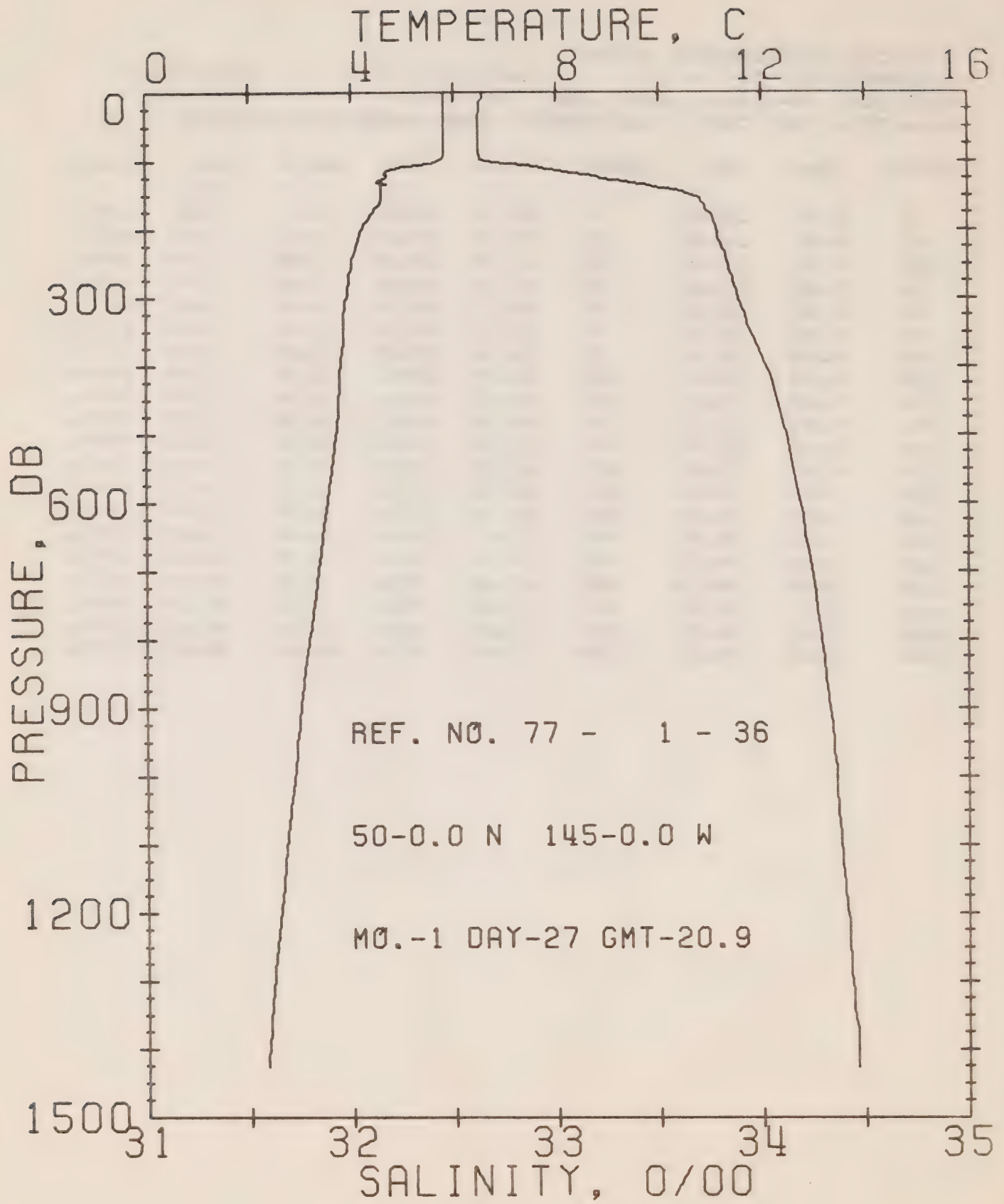
DATE 26/ 1/77

STATION P

POSITION 50- 0.0N, 145- 0.0W GMT 17.8

RESULTS OF STP CAST 164 POINTS TAKEN FROM ANALOG TRACE

PRESS	TEMP	SAL	DEPTH	SIGMA T	SVA	DELTA D	POT. EN	SOUND
0	5.82	32.65	0	25.74	225.9	0.0	0.0	1471.
10	5.81	32.65	10	25.75	226.1	0.23	0.01	1471.
20	5.81	32.65	20	25.74	226.6	0.45	0.05	1472.
30	5.82	32.64	30	25.74	227.2	0.68	0.10	1472.
50	5.82	32.63	50	25.73	227.8	1.13	0.29	1472.
75	5.82	32.63	75	25.73	228.4	1.70	0.65	1472.
100	4.95	32.93	99	26.06	196.7	2.25	1.14	1470.
125	4.69	33.41	124	26.48	157.9	2.70	1.65	1470.
150	4.66	33.71	149	26.72	135.1	3.06	2.16	1470.
175	4.39	33.77	174	26.79	128.3	3.39	2.70	1470.
200	4.26	33.79	199	26.82	125.5	3.71	3.31	1470.
225	4.09	33.81	223	26.86	122.2	4.02	3.98	1469.
250	3.96	33.84	248	26.89	119.0	4.32	4.71	1469.
300	3.84	33.90	298	26.95	113.8	4.90	6.33	1470.
400	3.80	34.04	397	27.07	103.8	5.98	10.20	1471.
500	3.65	34.13	496	27.15	96.6	6.99	14.80	1472.
600	3.49	34.19	595	27.22	90.5	7.93	20.04	1473.
800	3.11	34.30	793	27.34	79.8	9.62	32.09	1475.
1000	2.80	34.37	990	27.43	72.3	11.14	46.00	1477.
1200	2.54	34.42	1188	27.49	67.4	12.53	61.59	1480.



OFFSHORE OCEANOGRAPHY GROUP

REFERENCE NO. 77- 1- 36

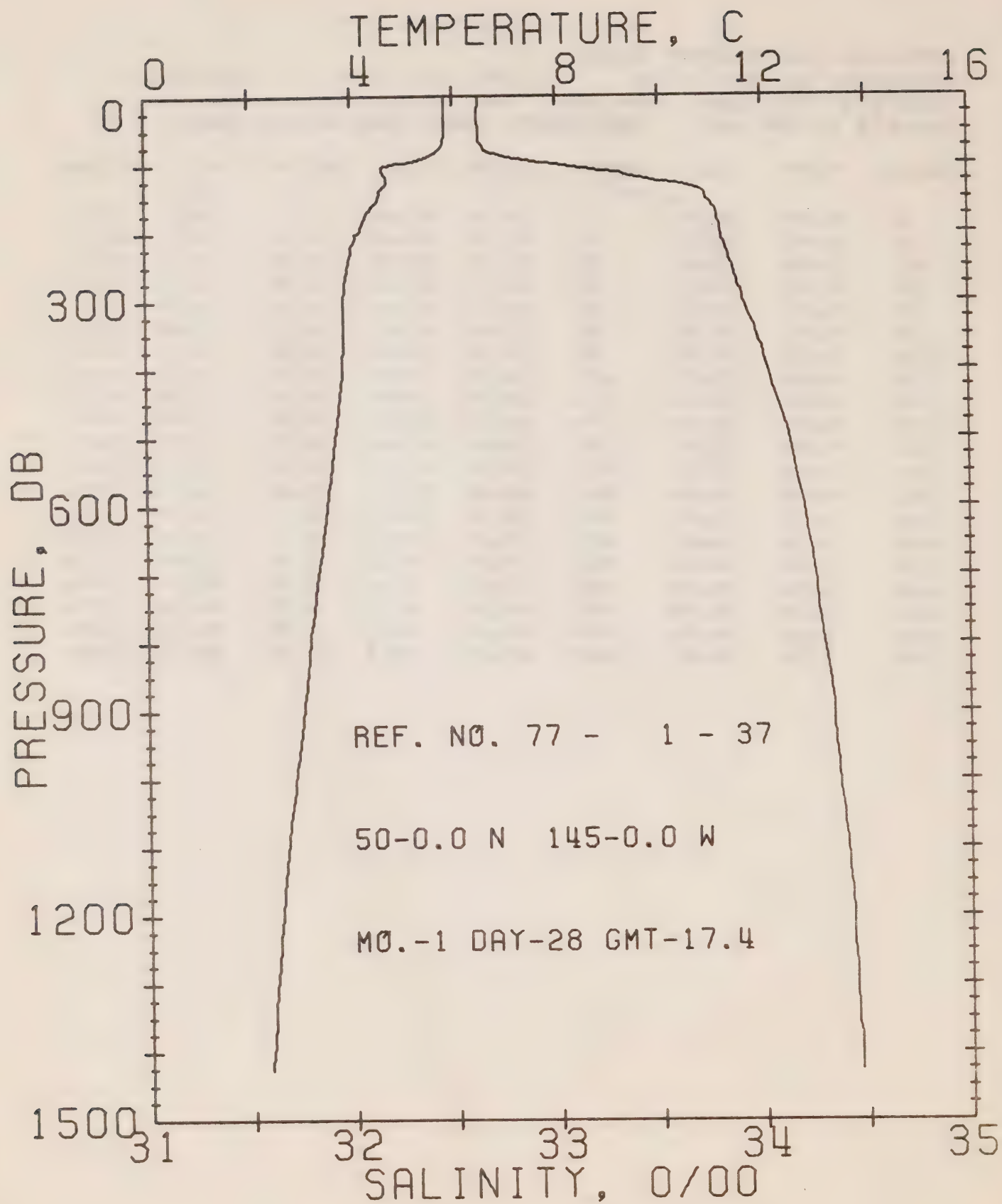
DATE 27/ 1/77

STATION P

POSITION 50- 0.0N, 145- 0.0W GMT 20.9

RESULTS OF STP CAST 153 POINTS TAKEN FROM ANALOG TRACE

PRESS	TEMP	SAL	DEPTH	SIGMA T	SVA	DELTA D	POT. EN	SOUND
0	5.80	32.64	0	25.74	226.4	0.0	0.0	1471.
10	5.81	32.64	10	25.74	226.8	0.23	0.01	1471.
20	5.80	32.63	20	25.73	227.6	0.45	0.05	1471.
30	5.80	32.63	30	25.73	228.0	0.68	0.10	1472.
50	5.81	32.62	50	25.72	228.8	1.14	0.29	1472.
75	5.81	32.62	75	25.72	229.1	1.71	0.66	1472.
100	5.73	32.66	99	25.76	225.6	2.28	1.17	1473.
125	4.64	33.22	124	26.33	171.6	2.77	1.72	1469.
150	4.60	33.65	149	26.68	138.8	3.15	2.26	1470.
175	4.41	33.74	174	26.77	130.5	3.49	2.81	1470.
200	4.19	33.76	199	26.82	125.6	3.81	3.42	1469.
225	4.08	33.81	223	26.85	122.7	4.12	4.09	1469.
250	4.00	33.84	248	26.89	119.9	4.42	4.82	1469.
300	3.90	33.89	298	26.94	115.2	5.01	6.47	1470.
400	3.79	34.02	397	27.05	105.1	6.11	10.40	1471.
500	3.69	34.12	496	27.14	97.5	7.12	15.03	1473.
600	3.50	34.18	595	27.21	91.4	8.07	20.33	1473.
800	3.16	34.29	793	27.33	81.3	9.79	32.58	1475.
1000	2.86	34.36	990	27.41	74.1	11.34	46.75	1478.
1200	2.57	34.41	1188	27.48	68.2	12.77	62.72	1480.



OFFSHORE OCEANOGRAPHY GROUP

REFERENCE NO. 77- 1- 37

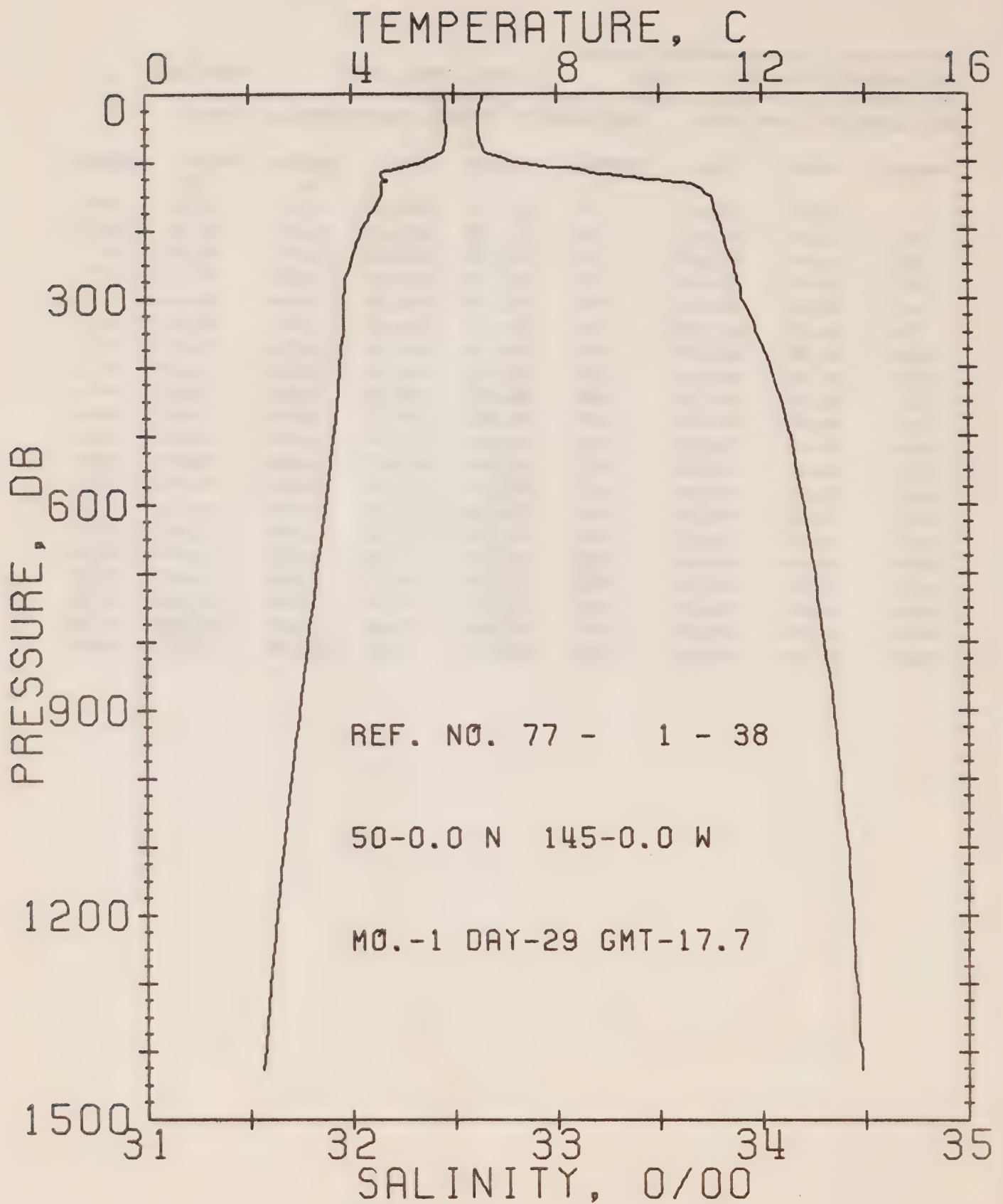
DATE 28/ 1/77

STATION P

POSITION 50- 0.0N, 145- 0.0W GMT 17.4

RESULTS OF STP CAST 149 POINTS TAKEN FROM ANALOG TRACE

PRESS	TEMP	SAL	DEPTH	SIGMA T	SVA	DELTA D	POT. EN	SOUND
0	5.83	32.63	0	25.73	227.5	0.0	0.0	1471.
10	5.84	32.63	10	25.73	227.9	0.23	0.01	1471.
20	5.85	32.62	20	25.72	228.6	0.46	0.05	1472.
30	5.85	32.62	30	25.72	228.9	0.68	0.10	1472.
50	5.83	32.63	50	25.73	228.3	1.14	0.29	1472.
75	5.78	32.65	75	25.75	226.6	1.71	0.65	1472.
100	4.86	32.97	99	26.11	192.1	2.25	1.13	1469.
125	4.71	33.48	124	26.53	152.5	2.67	1.62	1470.
150	4.53	33.73	149	26.75	132.1	3.02	2.10	1470.
175	4.28	33.78	174	26.82	126.0	3.34	2.63	1469.
200	4.12	33.80	199	26.84	123.4	3.65	3.23	1469.
225	4.00	33.83	223	26.88	120.1	3.96	3.89	1469.
250	3.93	33.86	248	26.91	117.5	4.25	4.60	1469.
300	3.83	33.91	298	26.96	113.0	4.83	6.22	1470.
400	3.81	34.03	397	27.06	104.8	5.92	10.09	1471.
500	3.66	34.13	496	27.15	96.5	6.92	14.70	1472.
600	3.49	34.20	595	27.22	90.3	7.86	19.94	1473.
800	3.15	34.30	793	27.33	80.7	9.57	32.08	1475.
1000	2.84	34.37	990	27.42	73.4	11.10	46.13	1477.
1200	2.55	34.43	1188	27.49	66.8	12.50	61.75	1480.



OFFSHORE OCEANOGRAPHY GROUP

REFERENCE NO. 77-1-38

DATE 29/ 1/77

STATION P

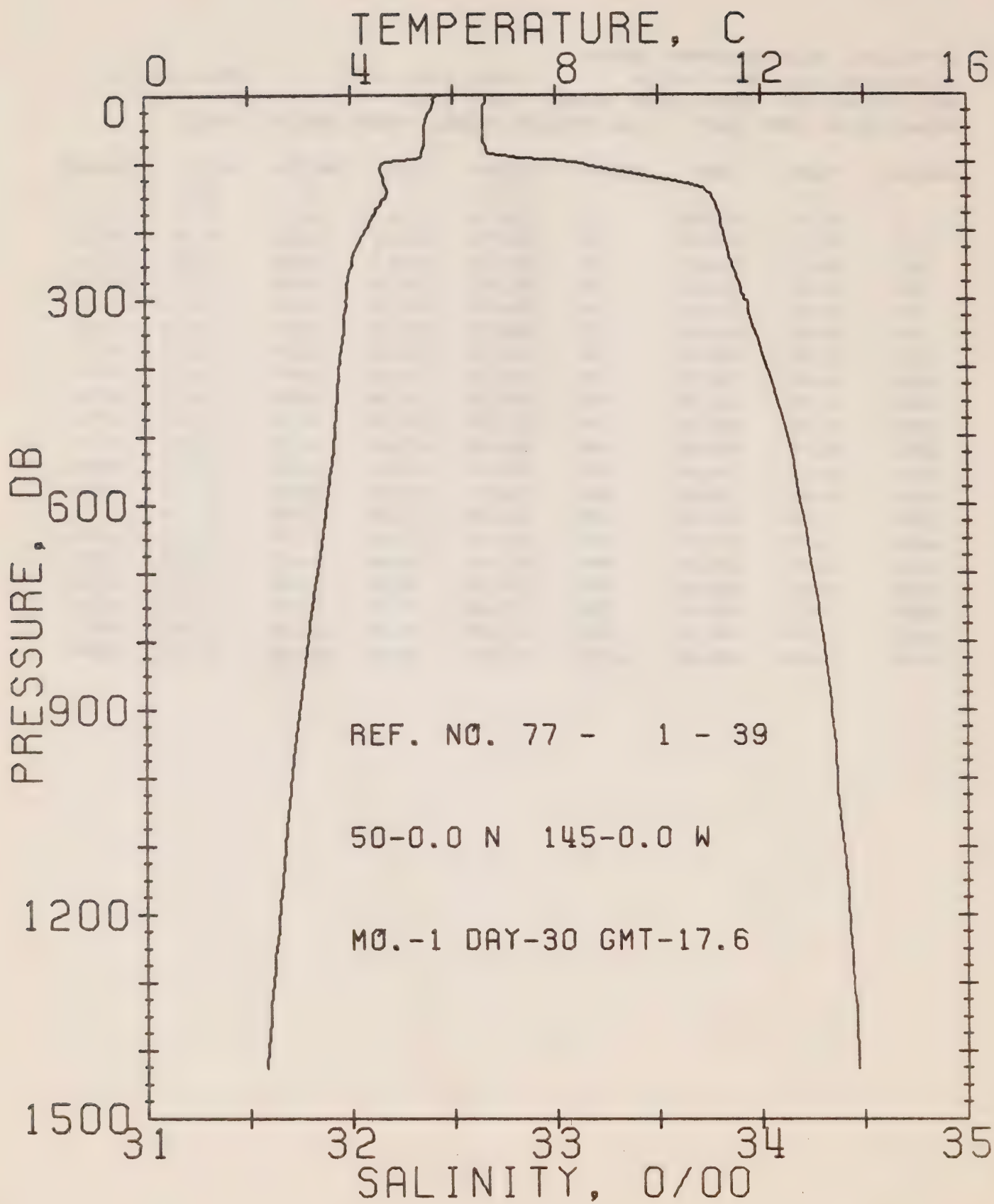
POSITION 50- 0.0N, 145- 0.0W

GMT 17.7

RESULTS OF STP CAST

158 POINTS TAKEN FROM ANALOG TRACE

PRESS	TEMP	SAL	DEPTH	SIGMA T	SVA	DELTA D	POT. EN	SOUND
0	5.82	32.65	0	25.74	225.9	0.0	0.0	1471.
10	5.83	32.64	10	25.74	227.1	0.23	0.01	1471.
20	5.83	32.63	20	25.73	228.0	0.45	0.05	1472.
30	5.84	32.62	30	25.72	228.8	0.68	0.10	1472.
50	5.86	32.62	50	25.72	229.3	1.14	0.29	1472.
75	5.82	32.63	75	25.73	228.1	1.71	0.66	1472.
100	5.38	32.79	99	25.91	211.5	2.27	1.15	1471.
125	4.64	33.44	124	26.50	155.1	2.73	1.67	1469.
150	4.57	33.74	149	26.75	131.8	3.07	2.15	1470.
175	4.37	33.78	174	26.80	127.4	3.39	2.69	1470.
200	4.18	33.81	199	26.85	123.2	3.71	3.29	1469.
225	4.07	33.82	223	26.87	121.2	4.01	3.95	1469.
250	3.97	33.86	248	26.91	117.5	4.31	4.67	1469.
300	3.85	33.90	298	26.95	113.9	4.89	6.29	1470.
400	3.77	34.04	397	27.07	103.4	5.97	10.15	1471.
500	3.65	34.14	496	27.16	95.6	6.97	14.70	1472.
600	3.47	34.20	595	27.23	89.6	7.89	19.89	1473.
800	3.13	34.30	793	27.34	80.3	9.59	31.97	1475.
1000	2.79	34.38	990	27.43	71.9	11.11	45.83	1477.
1200	2.51	34.44	1188	27.51	65.6	12.48	61.18	1479.



OFFSHORE OCEANOGRAPHY GROUP

REFERENCE NO. 77- 1- 39

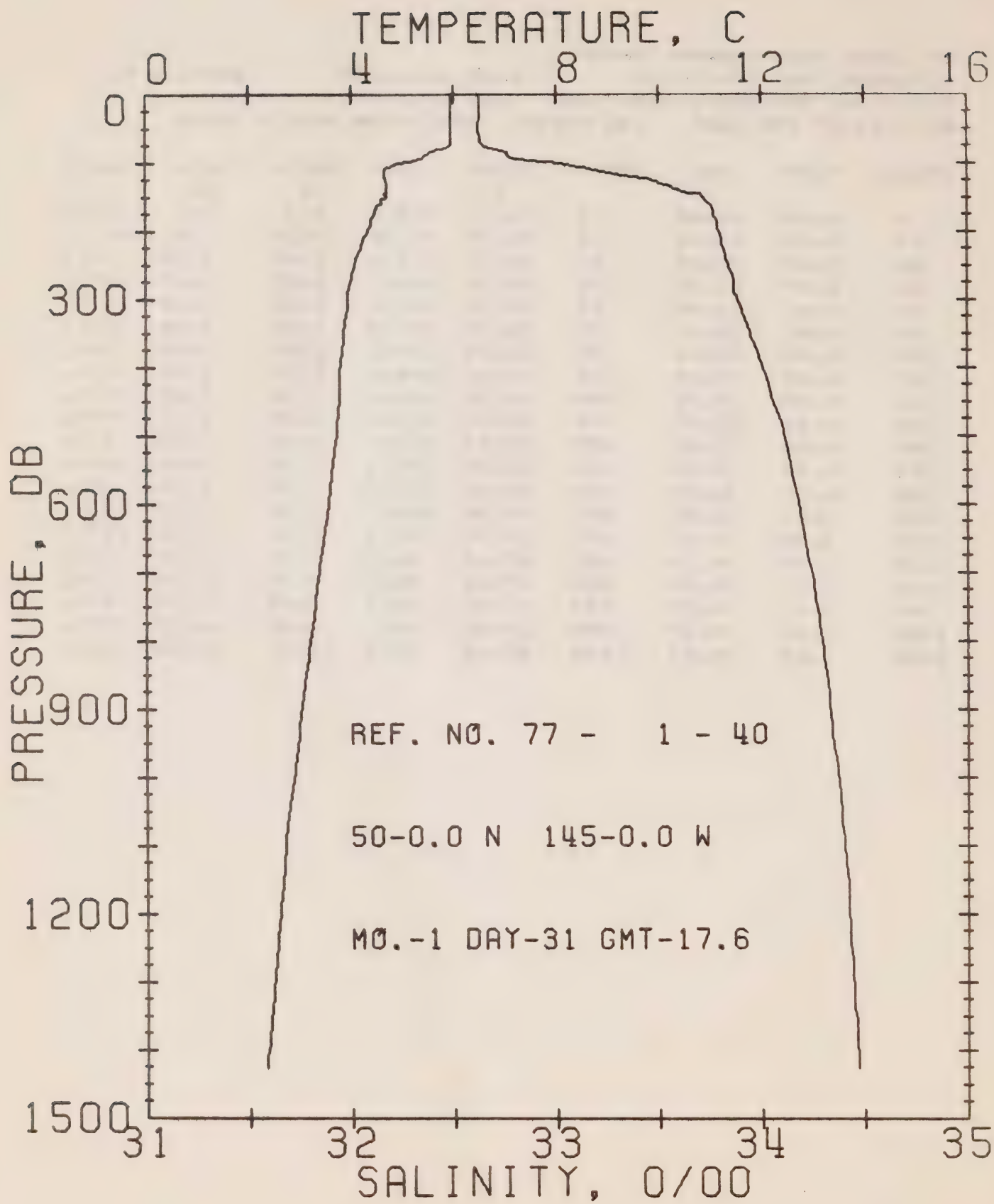
DATE 30/ 1/77

STATION P

POSITION 50- 0.0N, 145- 0.0W GMT 17.6

RESULTS OF STP CAST 132 POINTS TAKEN FROM ANALOG TRACE

PRESS	TEMP	SAL	DEPTH	SIGMA T	SVA	DELTA D	POT. EN	SOUND
0	5.56	32.66	0	25.78	222.2	0.0	0.0	1470.
10	5.62	32.66	10	25.78	223.2	0.22	0.01	1471.
20	5.58	32.65	20	25.77	223.6	0.45	0.05	1471.
30	5.49	32.65	30	25.78	222.7	0.67	0.10	1470.
50	5.44	32.65	50	25.79	222.4	1.11	0.28	1471.
75	5.42	32.66	75	25.80	221.9	1.67	0.64	1471.
100	4.64	33.11	99	26.25	179.3	2.20	1.10	1469.
125	4.65	33.58	124	26.61	144.8	2.61	1.57	1470.
150	4.68	33.76	149	26.75	131.7	2.95	2.05	1470.
175	4.45	33.80	174	26.81	126.6	3.27	2.58	1470.
200	4.28	33.82	199	26.84	123.6	3.58	3.18	1470.
225	4.09	33.84	223	26.88	120.3	3.89	3.84	1469.
250	4.01	33.86	248	26.90	118.2	4.18	4.56	1469.
300	3.90	33.92	298	26.96	112.9	4.76	6.17	1470.
400	3.76	34.03	397	27.06	104.1	5.84	10.04	1471.
500	3.68	34.13	496	27.15	96.7	6.85	14.62	1472.
600	3.51	34.19	595	27.22	90.9	7.78	19.87	1474.
800	3.14	34.30	793	27.34	80.1	9.49	32.00	1475.
1000	2.82	34.37	990	27.42	73.1	11.01	45.97	1477.
1200	2.57	34.43	1188	27.49	67.3	12.41	61.65	1480.



OFFSHORE OCEANOGRAPHY GROUP

REFERENCE NO. 77- 1- 40

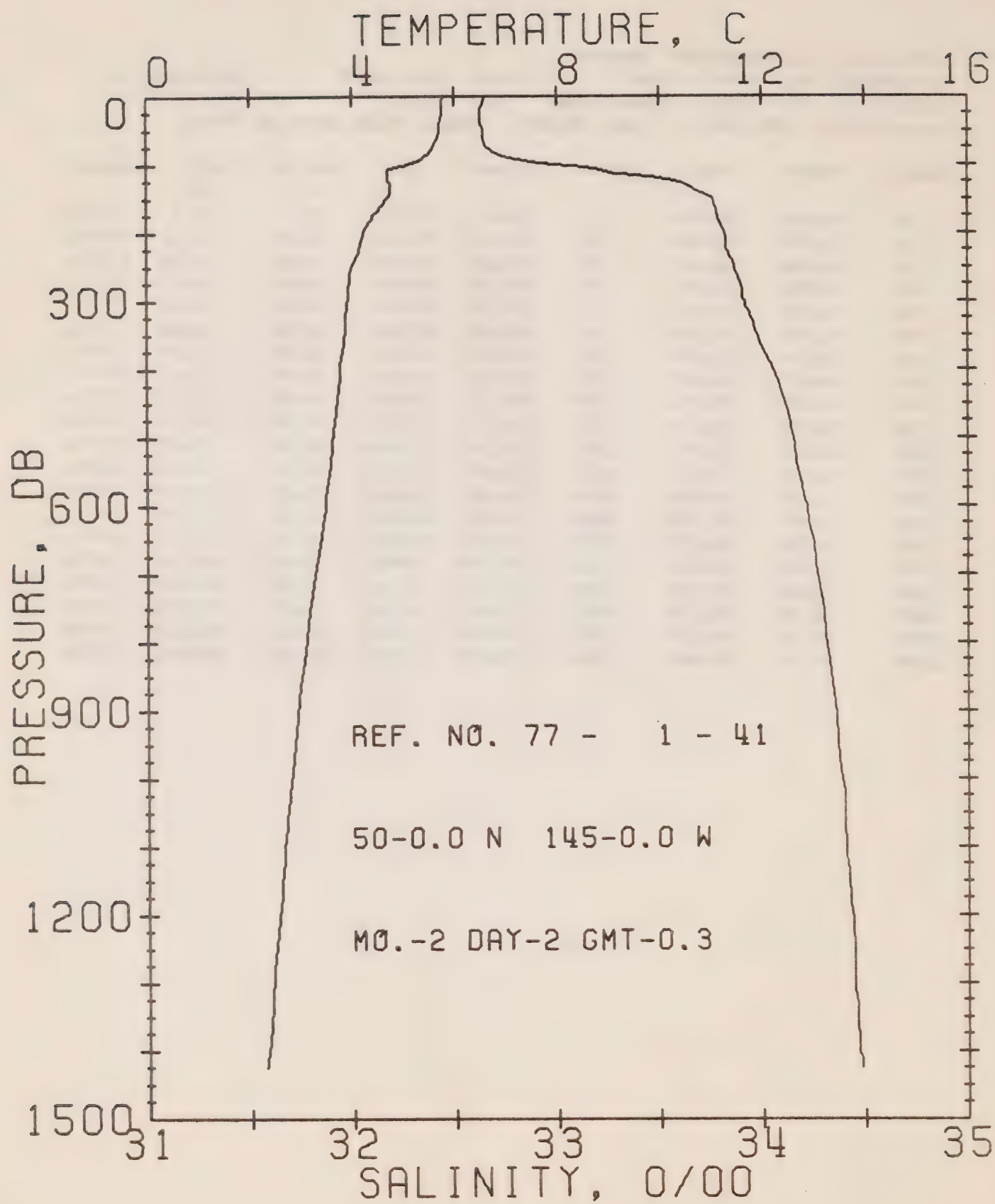
DATE 31/ 1/77

STATION P

POSITION 50- 0.0N, 145- 0.0W GMT 17.6

RESULTS OF STP CAST 167 POINTS TAKEN FROM ANALOG TRACE

PRESS	TEMP	SAL	DEPTH	SIGMA T	SVA	DELTA D	POT. EN	SOUND
0	5.96	32.63	0	25.71	229.0	0.0	0.0	1472.
10	5.96	32.63	10	25.71	229.4	0.23	0.01	1472.
20	5.96	32.63	20	25.71	229.5	0.46	0.05	1472.
30	5.96	32.63	30	25.71	229.6	0.69	0.11	1472.
50	5.96	32.62	50	25.70	230.5	1.15	0.29	1473.
75	5.92	32.64	75	25.73	228.4	1.72	0.66	1473.
100	5.01	32.98	99	26.10	193.0	2.26	1.14	1470.
125	4.67	33.48	124	26.53	152.4	2.69	1.63	1470.
150	4.67	33.72	149	26.72	134.9	3.05	2.13	1470.
175	4.43	33.77	174	26.79	128.6	3.38	2.67	1470.
200	4.32	33.79	199	26.82	125.9	3.70	3.28	1470.
225	4.16	33.81	223	26.85	123.0	4.01	3.95	1470.
250	4.04	33.84	248	26.88	120.0	4.31	4.69	1470.
300	3.91	33.88	298	26.93	116.0	4.90	6.34	1470.
400	3.78	34.01	397	27.04	106.2	6.01	10.28	1471.
500	3.69	34.11	496	27.14	98.0	7.03	14.96	1473.
600	3.54	34.18	595	27.21	91.9	7.98	20.27	1474.
800	3.18	34.29	793	27.33	81.4	9.71	32.59	1476.
1000	2.86	34.37	990	27.42	73.1	11.25	46.73	1478.
1200	2.58	34.42	1188	27.49	67.6	12.65	62.40	1480.



OFFSHORE OCEANOGRAPHY GROUP

REFERENCE NO. 77- 1- 41

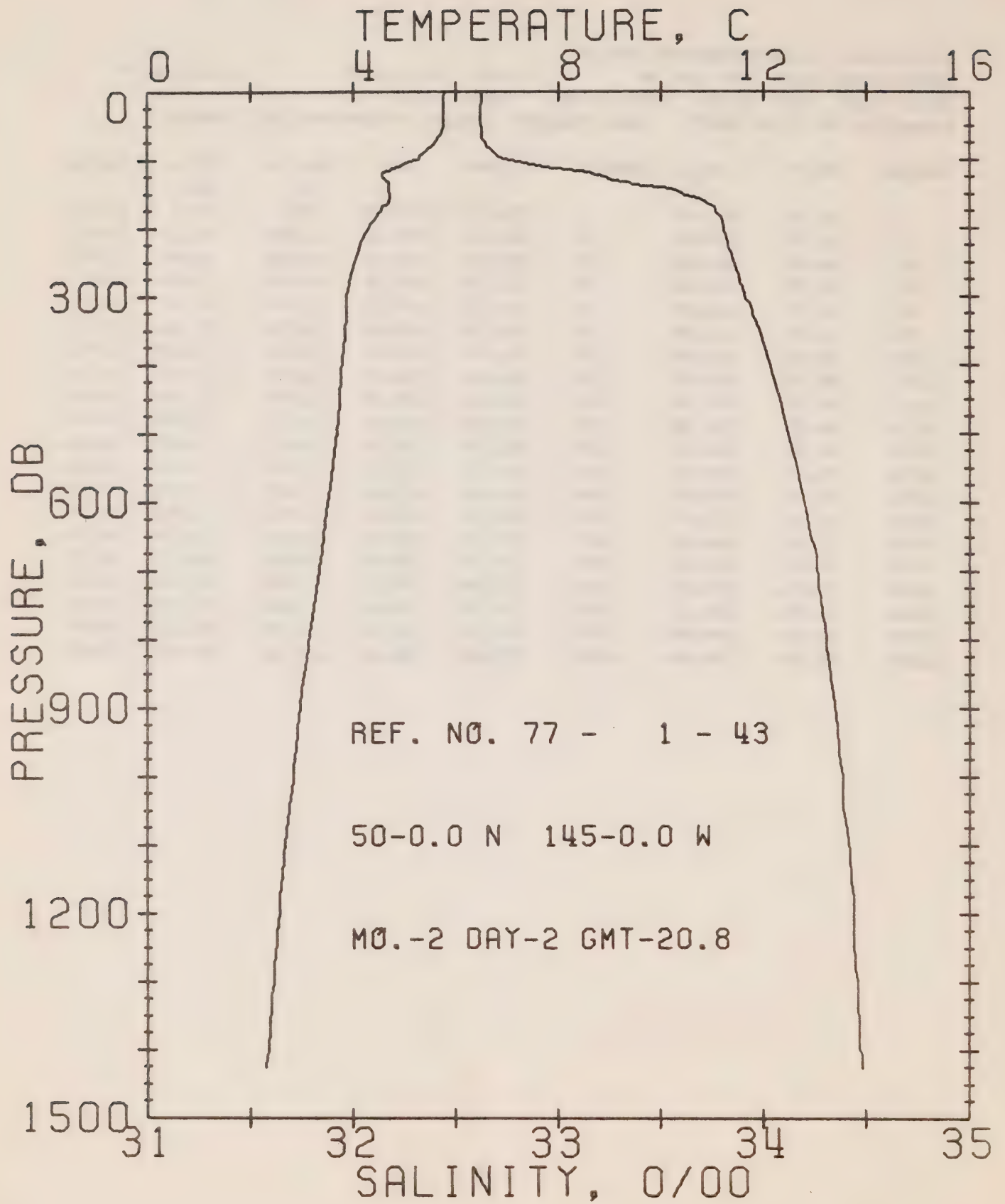
DATE 2/ 2/77

STATION P

POSITION 50- 0.0N. 145- 0.0W GMT 0.3

RESULTS OF STP CAST 141 POINTS TAKEN FROM ANALOG TRACE

PRESS	TEMP	SAL	DEPTH	SIGMA T	SVA	DELTA D	POT. EN	SJUND
0	5.78	32.65	0	25.75	225.4	0.0	0.0	1471.
10	5.75	32.64	10	25.75	226.1	0.23	0.01	1471.
20	5.75	32.63	20	25.74	227.0	0.45	0.05	1471.
30	5.74	32.63	30	25.74	226.9	0.68	0.10	1471.
50	5.70	32.64	50	25.75	226.0	1.13	0.29	1472.
75	5.57	32.66	75	25.78	223.4	1.70	0.65	1471.
100	5.07	32.99	99	26.10	193.2	2.23	1.12	1470.
125	4.72	33.59	124	26.61	144.7	2.65	1.60	1470.
150	4.67	33.76	149	26.75	131.6	2.99	2.08	1470.
175	4.39	33.78	174	26.80	127.3	3.32	2.62	1470.
200	4.22	33.82	199	26.85	122.9	3.63	3.22	1469.
225	4.12	33.83	223	26.87	121.3	3.93	3.88	1469.
250	3.99	33.87	248	26.91	117.3	4.23	4.60	1469.
300	3.90	33.92	298	26.96	112.9	4.81	6.21	1470.
400	3.76	34.06	397	27.08	102.2	5.89	10.06	1471.
500	3.62	34.15	496	27.17	94.4	6.87	14.55	1472.
600	3.46	34.22	595	27.24	88.6	7.79	19.69	1473.
800	3.08	34.31	793	27.35	78.8	9.45	31.53	1475.
1000	2.79	34.39	990	27.44	71.4	10.95	45.21	1477.
1200	2.54	34.44	1188	27.50	66.0	12.32	60.60	1480.



OFFSHORE OCEANOGRAPHY GROUP

REFERENCE NO. 77- 1- 43

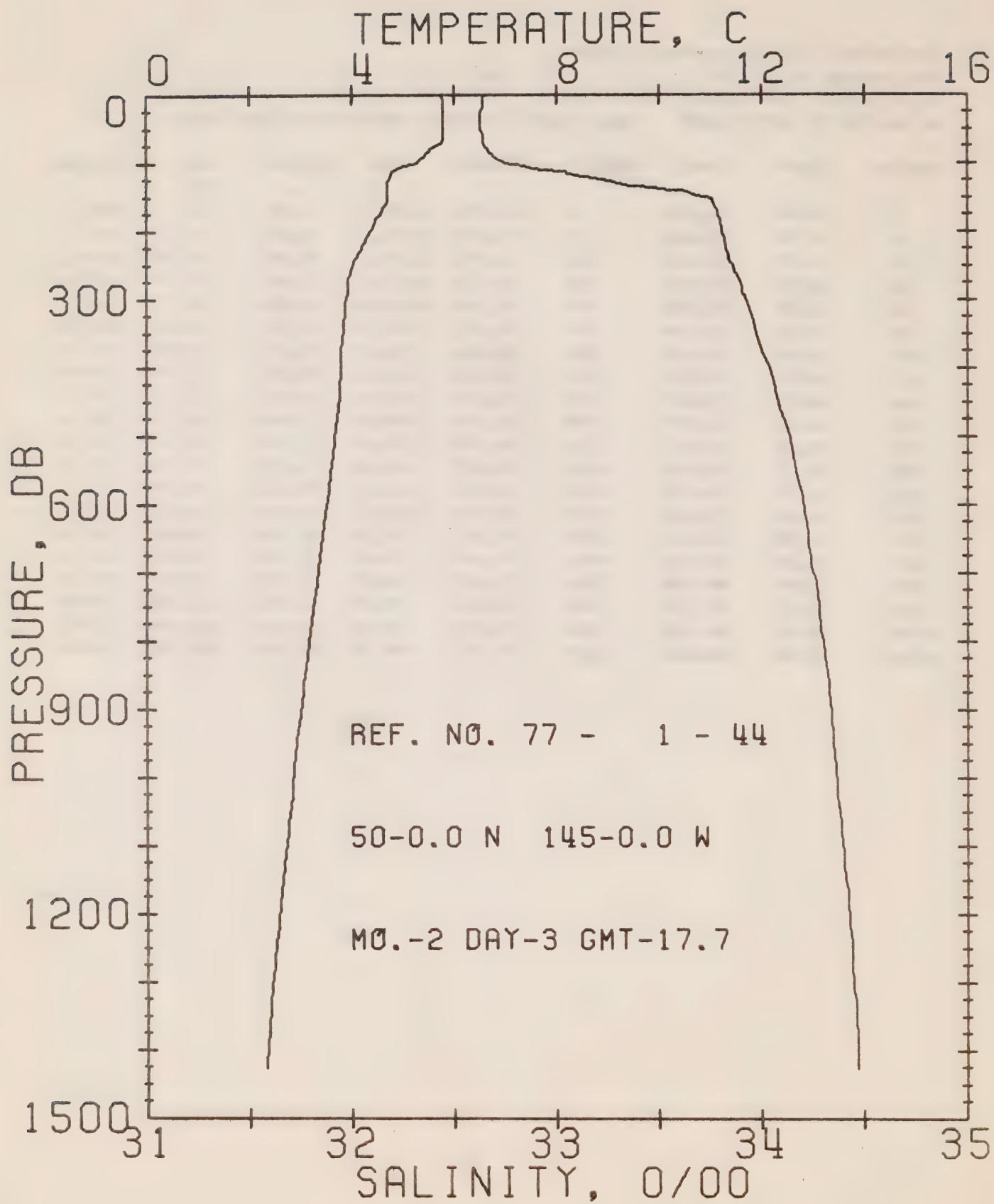
DATE 2/ 2/77

STATION p

POSITION 50- 0.0N, 145- 0.0W GMT 20.8

RESULTS OF STP CAST 156 POINTS TAKEN FROM ANALOG TRACE

PRESS	TEMP	SAL	DEPTH	SIGMA T	SVA	DELTA D	POT. EN	SOUND
0	5.78	32.63	0	25.73	226.9	0.0	0.0	1471.
10	5.77	32.63	10	25.73	227.2	0.23	0.01	1471.
20	5.77	32.62	20	25.73	227.6	0.45	0.05	1471.
30	5.77	32.62	30	25.73	228.1	0.68	0.10	1471.
50	5.75	32.62	50	25.73	227.9	1.14	0.29	1472.
75	5.58	32.64	75	25.77	224.7	1.71	0.65	1471.
100	5.25	32.77	99	25.91	211.7	2.26	1.14	1471.
125	4.58	33.22	124	26.34	171.0	2.73	1.68	1469.
150	4.72	33.61	149	26.63	143.5	3.12	2.23	1470.
175	4.52	33.77	174	26.78	129.6	3.46	2.79	1470.
200	4.28	33.81	199	26.84	124.3	3.78	3.39	1470.
225	4.11	33.83	223	26.87	121.3	4.08	4.06	1469.
250	4.02	33.86	248	26.90	118.5	4.38	4.78	1469.
300	3.86	33.91	298	26.96	113.2	4.96	6.41	1470.
400	3.78	34.03	397	27.06	104.3	6.04	10.26	1471.
500	3.68	34.12	496	27.14	97.4	7.05	14.88	1472.
600	3.50	34.20	595	27.22	90.2	7.99	20.13	1473.
800	3.13	34.31	793	27.35	79.7	9.68	32.16	1475.
1000	2.83	34.39	990	27.44	71.8	11.19	45.99	1477.
1200	2.55	34.44	1188	27.50	65.9	12.57	61.38	1480.



OFFSHORE OCEANOGRAPHY GROUP

REFERENCE NO. 77- 1- 44

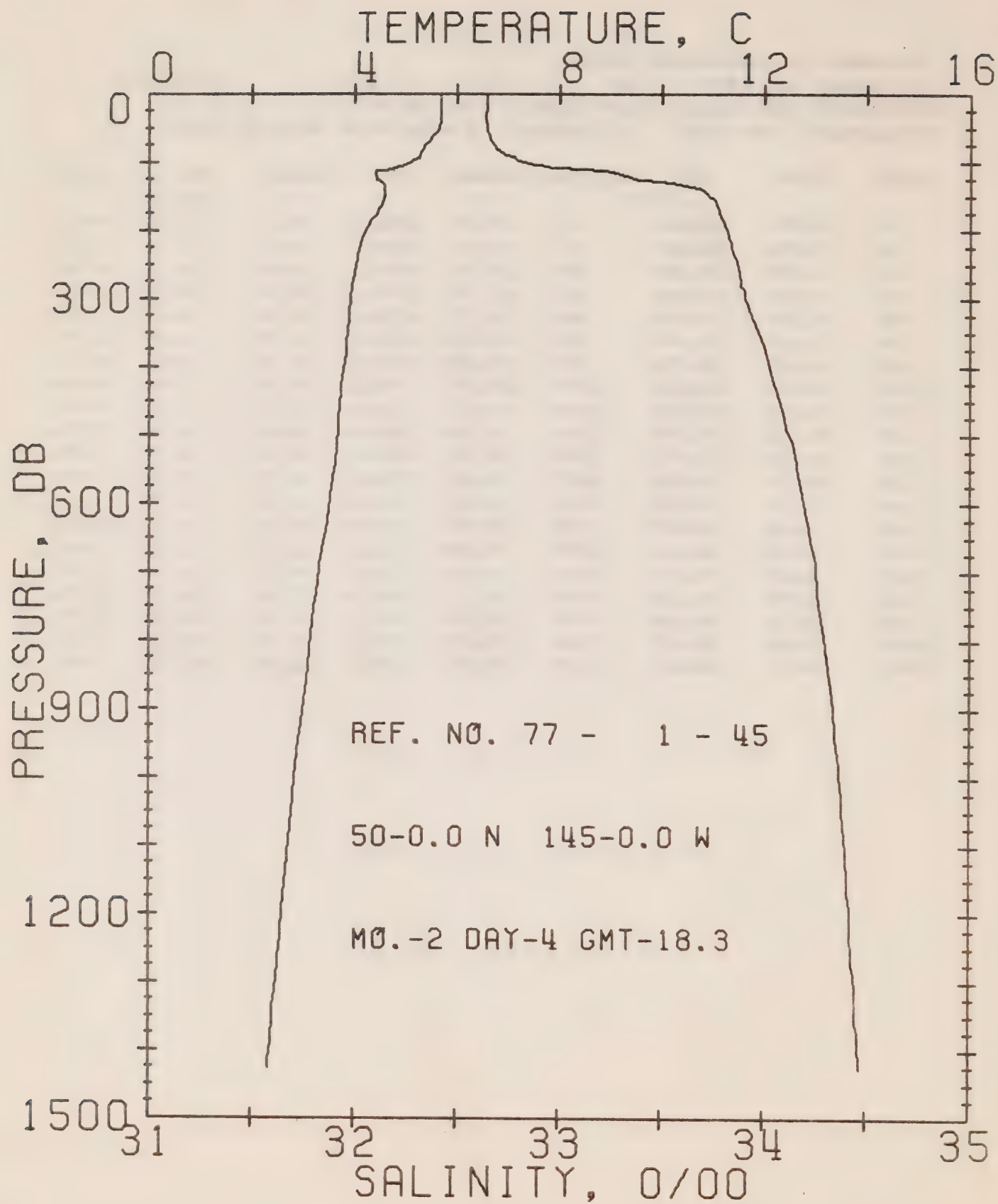
DATE 3/ 2/77

STATION P

POSITION 50- 0.0N, 145- 0.0W GMT 17.7

RESULTS OF STP CAST 172 POINTS TAKEN FROM ANALOG TRACE

PRESS	TEMP	SAL	DEPTH	SIGMA T	SVA	DELTA D	POT. EN	SOUND
0	5.77	32.65	0	25.75	225.3	0.0	0.0	1471.
10	5.78	32.64	10	25.74	226.6	0.23	0.01	1471.
20	5.79	32.64	20	25.74	226.7	0.45	0.05	1471.
30	5.79	32.63	30	25.73	227.6	0.68	0.10	1472.
50	5.79	32.63	50	25.73	227.8	1.14	0.29	1472.
75	5.67	32.64	75	25.76	225.6	1.70	0.65	1472.
100	5.25	32.74	99	25.88	214.0	2.25	1.14	1471.
125	4.70	33.23	124	26.33	171.5	2.73	1.69	1469.
150	4.70	33.72	149	26.72	135.0	3.11	2.22	1471.
175	4.55	33.79	174	26.79	128.4	3.44	2.76	1470.
200	4.35	33.81	199	26.83	125.0	3.76	3.37	1470.
225	4.19	33.83	223	26.86	122.0	4.07	4.04	1470.
250	4.01	33.86	248	26.90	118.2	4.37	4.76	1469.
300	3.89	33.92	298	26.96	112.8	4.94	6.37	1470.
400	3.79	34.04	397	27.07	103.8	6.02	10.23	1471.
500	3.67	34.13	496	27.16	96.1	7.03	14.82	1472.
600	3.49	34.20	595	27.23	89.8	7.96	20.03	1473.
800	3.15	34.30	793	27.34	80.5	9.66	32.13	1475.
1000	2.84	34.37	990	27.42	73.5	11.19	46.17	1477.
1200	2.57	34.43	1188	27.49	67.2	12.60	61.93	1480.



OFFSHORE OCEANOGRAPHY GROUP

REFERENCE NO. 77- 1- 45

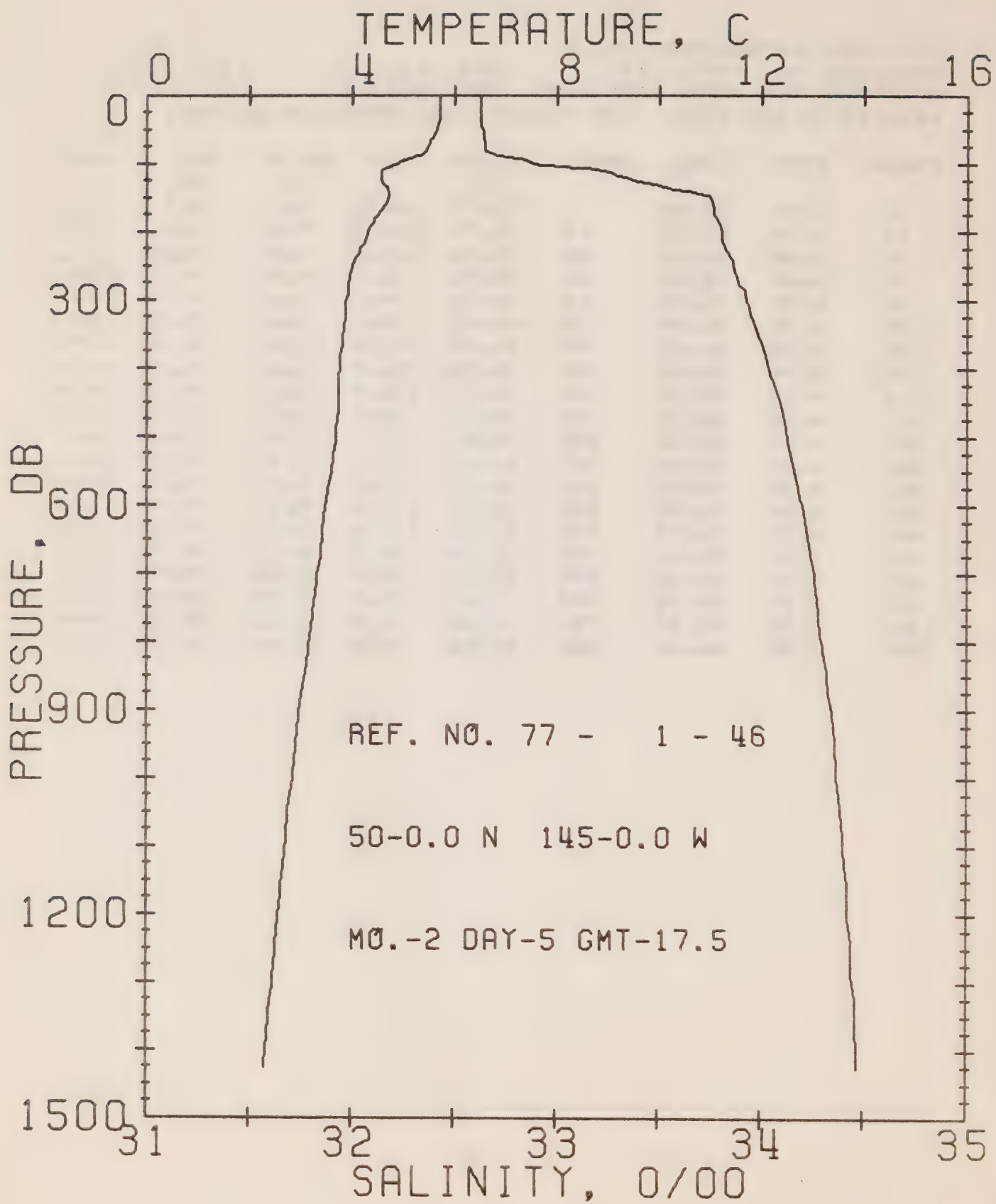
DATE 4/ 2/77

STATION P

POSITION 50- 0.0N, 145- 0.0W GMT 18.3

RESULTS OF STP CAST 135 POINTS TAKEN FROM ANALOG TRACE

PRESS	TEMP	SAL	DEPTH	SIGMA T	SVA	DELTA D	POT. EN	SOUND
0	5.68	32.66	0	25.77	223.5	0.0	0.0	1471.
10	5.68	32.65	10	25.76	224.6	0.22	0.01	1471.
20	5.69	32.65	20	25.76	224.8	0.45	0.05	1471.
30	5.68	32.64	30	25.76	225.3	0.67	0.10	1471.
50	5.65	32.65	50	25.76	224.7	1.12	0.29	1471.
75	5.38	32.68	75	25.82	219.9	1.68	0.64	1471.
100	5.10	32.82	99	25.96	206.4	2.22	1.12	1470.
125	4.44	33.39	124	26.49	156.8	2.66	1.63	1469.
150	4.57	33.74	149	26.75	132.4	3.01	2.11	1470.
175	4.43	33.78	174	26.80	127.8	3.34	2.65	1470.
200	4.21	33.82	199	26.85	123.1	3.65	3.25	1469.
225	4.09	33.84	223	26.88	120.3	3.95	3.91	1469.
250	4.02	33.87	248	26.91	117.5	4.25	4.63	1469.
300	3.91	33.91	298	26.95	113.7	4.83	6.25	1470.
400	3.79	34.03	397	27.06	104.6	5.92	10.13	1471.
500	3.66	34.12	496	27.15	96.9	6.93	14.74	1472.
600	3.50	34.20	595	27.22	90.4	7.86	19.98	1473.
800	3.14	34.29	793	27.33	80.7	9.57	32.10	1475.
1000	2.83	34.37	990	27.42	73.0	11.10	46.12	1477.
1200	2.59	34.42	1188	27.48	67.9	12.50	61.88	1480.



OFFSHORE OCEANOGRAPHY GROUP

REFERENCE NO. 77- 1- 46

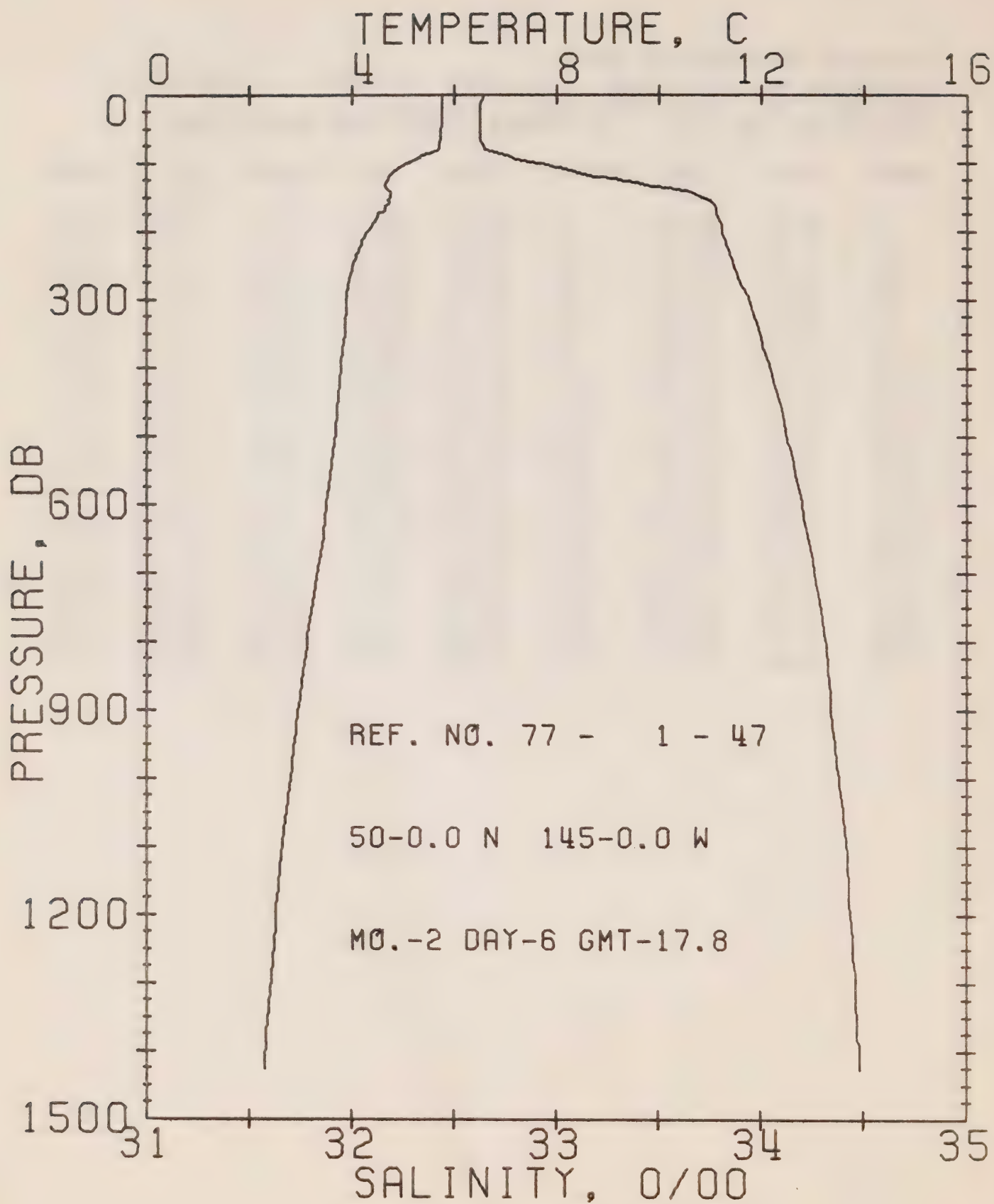
DATE 5/ 2/77

STATION P

POSITION 50- 0.0N, 145- 0.0W GMT 17.5

RESULTS OF STP CAST 162 POINTS TAKEN FROM ANALOG TRACE

PRESS	TEMP	SAL	DEPTH	SIGMA T	SVA	DELTA D	POT. EN	SOUND
0	5.72	32.63	0	25.74	226.2	0.0	0.0	1471.
10	5.72	32.63	10	25.74	226.5	0.23	0.01	1471.
20	5.71	32.63	20	25.74	226.6	0.45	0.05	1471.
30	5.70	32.63	30	25.74	226.6	0.68	0.10	1471.
50	5.65	32.63	50	25.75	225.9	1.13	0.29	1471.
75	5.47	32.65	75	25.79	222.9	1.69	0.65	1471.
100	4.87	32.89	99	26.04	198.6	2.23	1.12	1469.
125	4.57	33.38	124	26.47	158.5	2.66	1.62	1469.
150	4.71	33.74	149	26.74	133.2	3.02	2.12	1471.
175	4.48	33.77	174	26.78	129.1	3.35	2.66	1470.
200	4.30	33.81	199	26.83	124.7	3.67	3.27	1470.
225	4.15	33.82	223	26.86	122.0	3.98	3.94	1470.
250	4.00	33.86	248	26.90	118.1	4.28	4.66	1469.
300	3.88	33.93	298	26.97	112.0	4.85	6.27	1470.
400	3.75	34.04	397	27.07	103.6	5.93	10.12	1471.
500	3.68	34.13	496	27.15	96.8	6.93	14.69	1472.
600	3.48	34.20	595	27.23	90.0	7.87	19.94	1473.
800	3.17	34.29	793	27.33	81.0	9.57	32.06	1475.
1000	2.85	34.37	990	27.42	73.3	11.10	46.05	1478.
1200	2.56	34.42	1188	27.49	67.6	12.50	61.69	1480.



OFFSHORE OCEANOGRAPHY GROUP

REFERENCE NO. 77- 1- 47

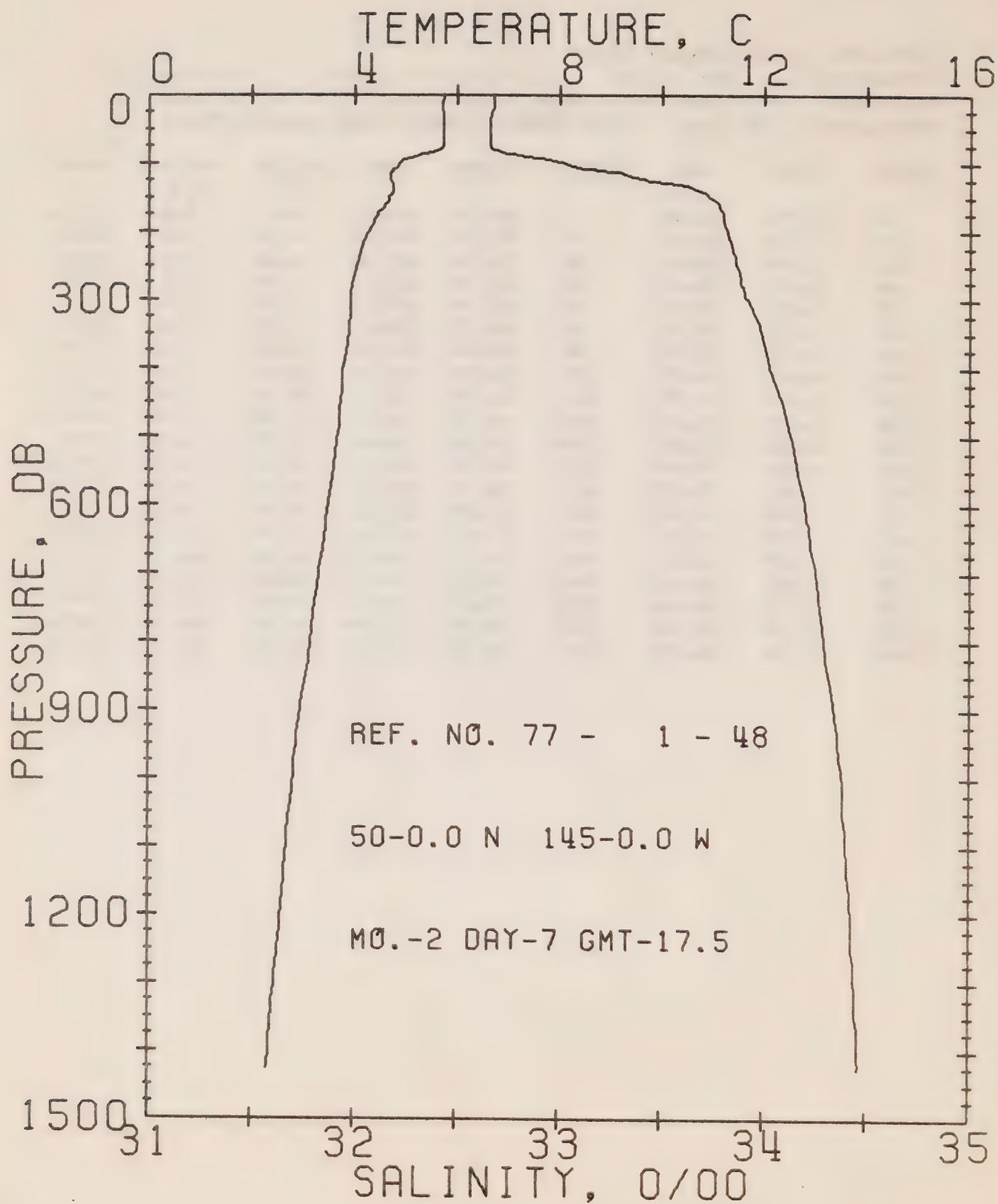
DATE 6/ 2/77

STATION P.

POSITION 50- 0.0N. 145- 0.0W GMT 17.8

RESULTS OF STP CAST 163 POINTS TAKEN FROM ANALOG TRACE

PRESS	TEMP	SAL	DEPTH	SIGMA T	SVA	DELTA D	POT. EN	SOUND
0	5.75	32.64	0	25.75	225.9	0.0	0.0	1471.
10	5.75	32.63	10	25.74	226.6	0.23	0.01	1471.
20	5.75	32.63	20	25.74	227.0	0.45	0.05	1471.
30	5.75	32.63	30	25.74	227.1	0.68	0.10	1471.
50	5.74	32.63	50	25.74	227.2	1.13	0.29	1472.
75	5.71	32.64	75	25.75	226.5	1.70	0.65	1472.
100	5.11	32.89	99	26.02	201.2	2.24	1.13	1470.
125	4.69	33.32	124	26.40	164.8	2.70	1.65	1470.
150	4.75	33.71	149	26.71	136.3	3.07	2.17	1471.
175	4.50	33.78	174	26.79	128.5	3.40	2.72	1470.
200	4.31	33.81	199	26.83	124.6	3.72	3.32	1470.
225	4.14	33.84	223	26.87	120.7	4.02	3.98	1470.
250	4.01	33.87	248	26.91	117.7	4.32	4.71	1469.
300	3.88	33.94	298	26.98	111.2	4.89	6.31	1470.
400	3.79	34.04	397	27.07	103.6	5.97	10.13	1471.
500	3.67	34.12	496	27.15	96.9	6.97	14.71	1472.
600	3.50	34.20	595	27.23	90.1	7.90	19.94	1473.
800	3.12	34.32	793	27.35	78.8	9.59	31.95	1475.
1000	2.79	34.38	990	27.43	71.9	11.10	45.78	1477.
1200	2.51	34.43	1188	27.50	65.8	12.47	61.11	1479.



OFFSHORE OCEANOGRAPHY GROUP

REFERENCE NO. 77- 1- 48

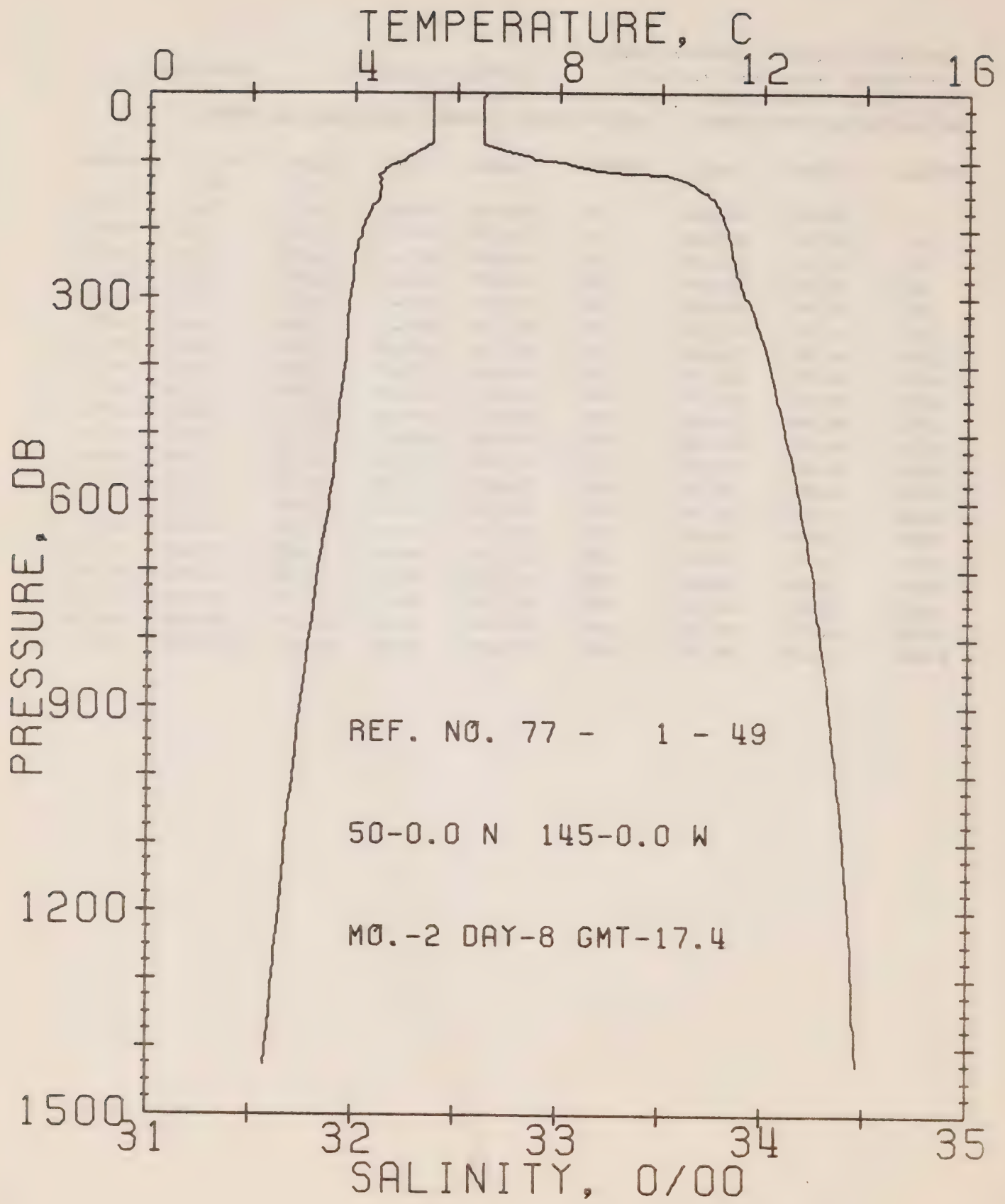
DATE 7/ 2/77

STATION P

POSITION 50- 0.0N, 145- 0.0W GMT 17.5

RESULTS OF STP CAST 165 POINTS TAKEN FROM ANALOG TRACE

PRESS	TEMP	SAL	DEPTH	SIGMA T	SVA	DELTA D	POT. EN	SOUND
0	5.73	32.68	0	25.78	222.6	0.0	0.0	1471.
10	5.72	32.68	10	25.78	222.8	0.22	0.01	1471.
20	5.72	32.68	20	25.78	223.1	0.45	0.05	1471.
30	5.73	32.67	30	25.77	223.9	0.67	0.10	1471.
50	5.74	32.66	50	25.76	225.0	1.12	0.29	1472.
75	5.72	32.66	75	25.76	225.1	1.68	0.64	1472.
100	4.86	33.02	99	26.15	188.8	2.20	1.11	1469.
125	4.71	33.44	124	26.50	155.9	2.63	1.60	1470.
150	4.67	33.74	149	26.74	133.4	2.99	2.09	1470.
175	4.44	33.80	174	26.81	126.5	3.31	2.63	1470.
200	4.26	33.82	199	26.85	123.3	3.62	3.22	1470.
225	4.12	33.85	223	26.88	120.1	3.93	3.88	1469.
250	4.03	33.87	248	26.91	117.9	4.22	4.60	1470.
300	3.92	33.92	298	26.96	113.1	4.80	6.22	1470.
400	3.78	34.03	397	27.06	104.4	5.88	10.08	1471.
500	3.67	34.13	496	27.15	96.4	6.88	14.66	1472.
600	3.49	34.20	595	27.23	90.1	7.82	19.88	1473.
800	3.15	34.29	793	27.33	80.9	9.52	31.99	1475.
1000	2.81	34.38	990	27.44	71.7	11.04	45.92	1477.
1200	2.58	34.43	1188	27.49	67.3	12.43	61.51	1480.



OFFSHORE OCEANOGRAPHY GROUP

REFERENCE NO. 77- 1- 49

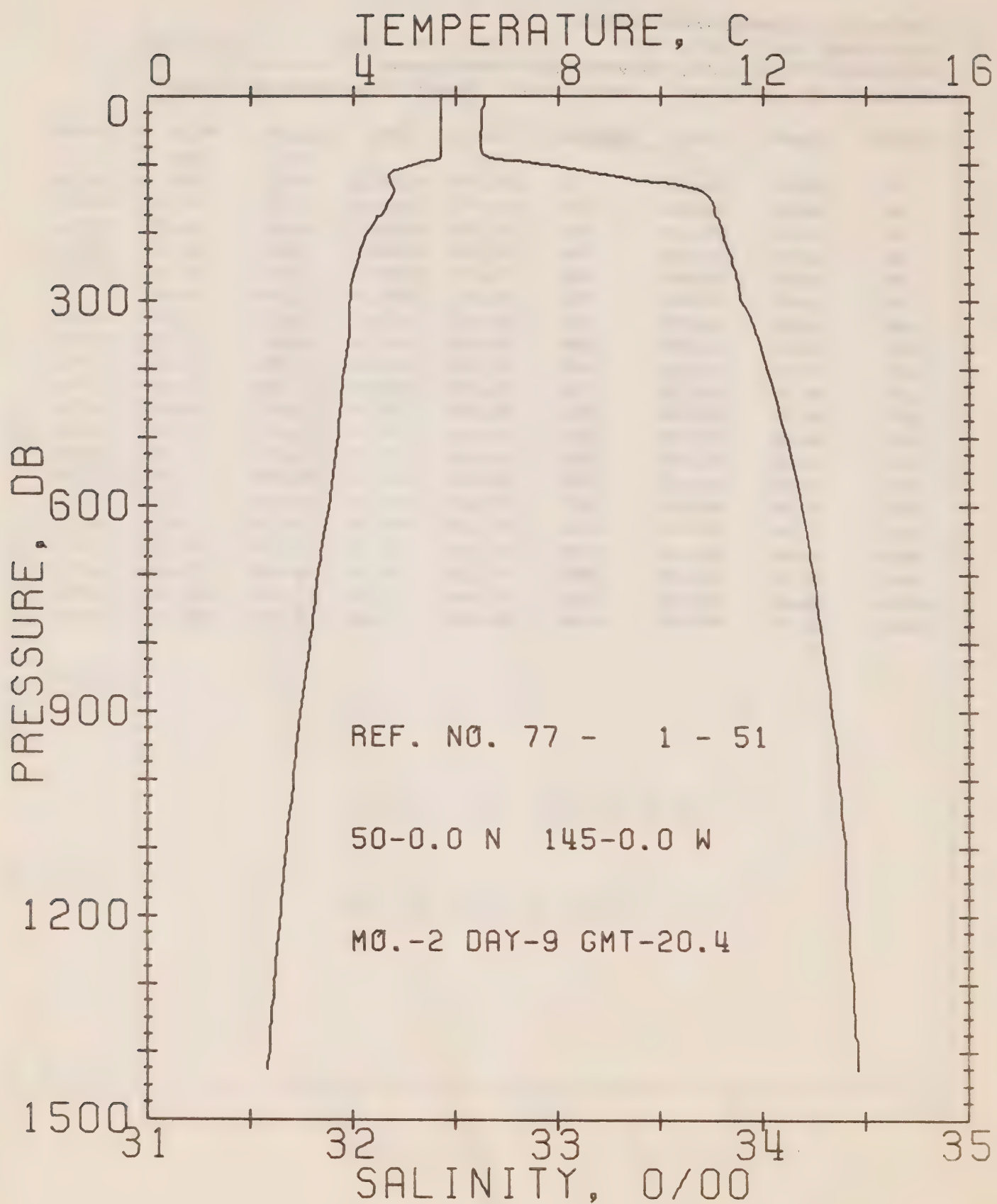
DATE 8/ 2/77

STATION P

POSITION 50- 0.0N, 145- 0.0W GMT 17.4

RESULTS OF STP CAST 160 POINTS TAKEN FROM ANALOG TRACE

PRESS	TEMP	SAL	DEPTH	SIGMA T	SVA	DELTA D	POT. EN	SOUND
0	5.52	32.64	0	25.77	223.2	0.0	0.0	1470.
10	5.52	32.63	10	25.76	224.4	0.22	0.01	1470.
20	5.53	32.63	20	25.76	224.6	0.45	0.05	1470.
30	5.53	32.63	30	25.76	224.6	0.67	0.10	1471.
50	5.52	32.63	50	25.76	224.7	1.12	0.29	1471.
75	5.47	32.63	75	25.77	224.4	1.68	0.64	1471.
100	4.96	32.95	99	26.08	195.0	2.21	1.11	1470.
125	4.50	33.59	124	26.64	142.4	2.64	1.60	1469.
150	4.47	33.73	149	26.75	132.0	2.98	2.08	1470.
175	4.28	33.79	174	26.82	125.6	3.30	2.61	1469.
200	4.14	33.82	199	26.86	121.9	3.61	3.20	1469.
225	4.05	33.84	223	26.88	119.9	3.91	3.86	1469.
250	3.98	33.86	248	26.91	117.9	4.21	4.57	1469.
300	3.91	33.91	298	26.95	113.7	4.79	6.20	1470.
400	3.81	34.03	397	27.06	104.6	5.88	10.07	1471.
500	3.66	34.11	496	27.14	97.8	6.89	14.70	1472.
600	3.52	34.18	595	27.21	91.5	7.84	20.00	1474.
800	3.15	34.29	793	27.33	81.4	9.56	32.28	1475.
1000	2.83	34.36	990	27.42	73.5	11.11	46.42	1477.
1200	2.57	34.42	1188	27.49	67.3	12.51	62.13	1480.



OFFSHORE OCEANOGRAPHY GROUP

REFERENCE NO. 77- 1- 51

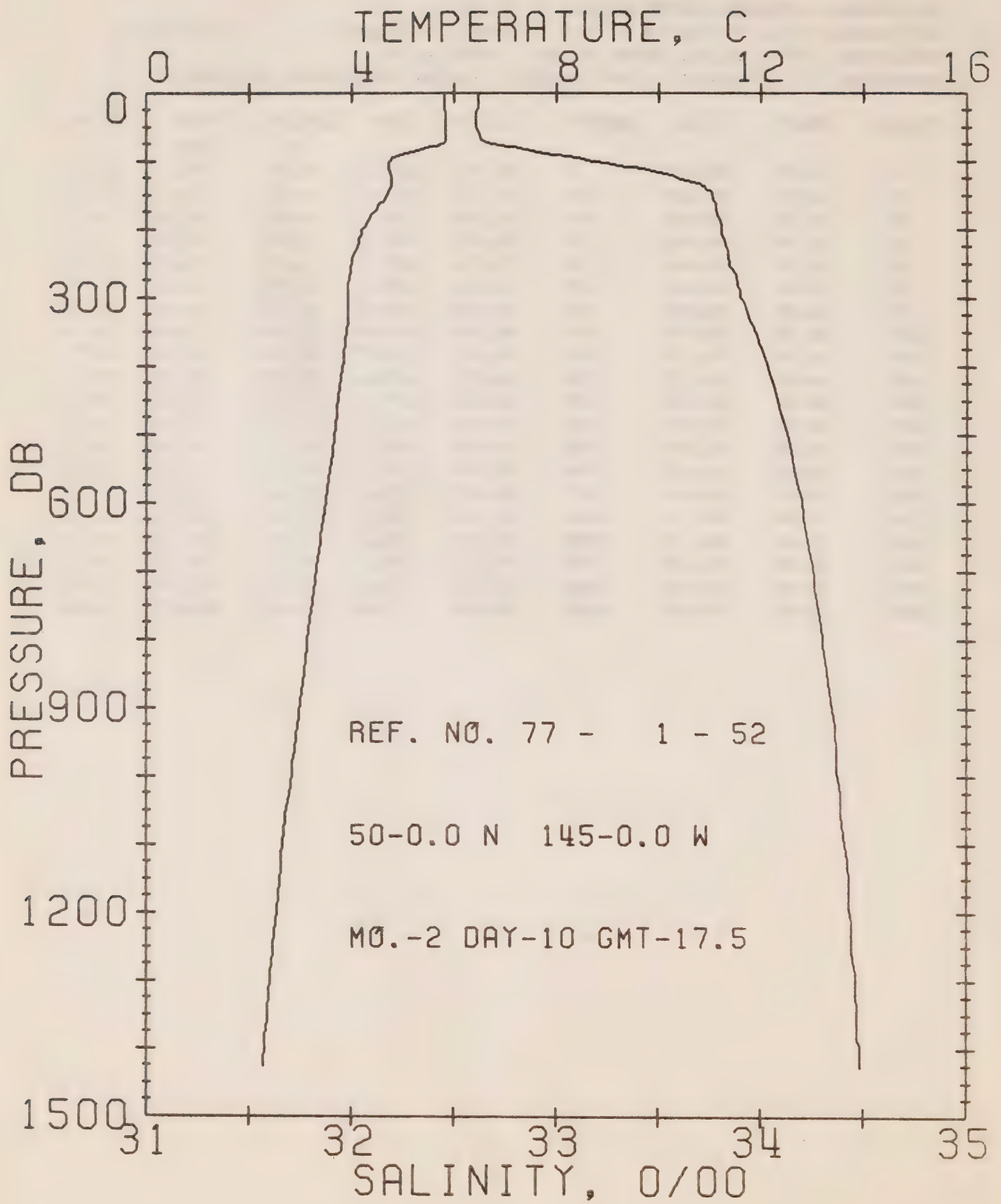
DATE 9/ 2/77

STATION P

POSITION 50- 0.0N, 145- 0.0W GMT 20.4

RESULTS OF STP CAST 147 POINTS TAKEN FROM ANALOG TRACE

PRESS	TEMP	SAL	DEPTH	SIGMA T	SVA	DELTA D	POT. EN	SOUND
0	5.71	32.65	0	25.76	224.6	0.0	0.0	1471.
10	5.70	32.64	10	25.75	225.5	0.23	0.01	1471.
20	5.70	32.63	20	25.74	226.3	0.45	0.05	1471.
30	5.70	32.63	30	25.74	226.6	0.68	0.10	1471.
50	5.71	32.63	50	25.74	227.1	1.13	0.29	1472.
75	5.71	32.62	75	25.73	227.9	1.70	0.65	1472.
100	5.20	32.93	99	26.04	199.2	2.25	1.14	1471.
125	4.72	33.43	124	26.48	157.0	2.69	1.65	1470.
150	4.72	33.74	149	26.73	133.7	3.05	2.14	1471.
175	4.52	33.77	174	26.78	129.6	3.37	2.68	1470.
200	4.26	33.80	199	26.83	124.8	3.69	3.29	1470.
225	4.12	33.82	223	26.86	121.8	4.00	3.96	1469.
250	4.04	33.85	248	26.89	119.1	4.30	4.68	1470.
300	3.92	33.89	298	26.94	115.4	4.88	6.32	1470.
400	3.82	34.02	397	27.05	105.8	5.98	10.24	1471.
500	3.69	34.11	496	27.14	98.0	7.00	14.89	1473.
600	3.51	34.19	595	27.21	91.1	7.95	20.18	1474.
800	3.15	34.29	793	27.33	81.1	9.66	32.39	1475.
1000	2.83	34.37	990	27.42	73.1	11.19	46.42	1477.
1200	2.57	34.41	1188	27.48	67.9	12.60	62.17	1480.



OFFSHORE OCEANOGRAPHY GROUP

REFERENCE NO. 77- 1- 52

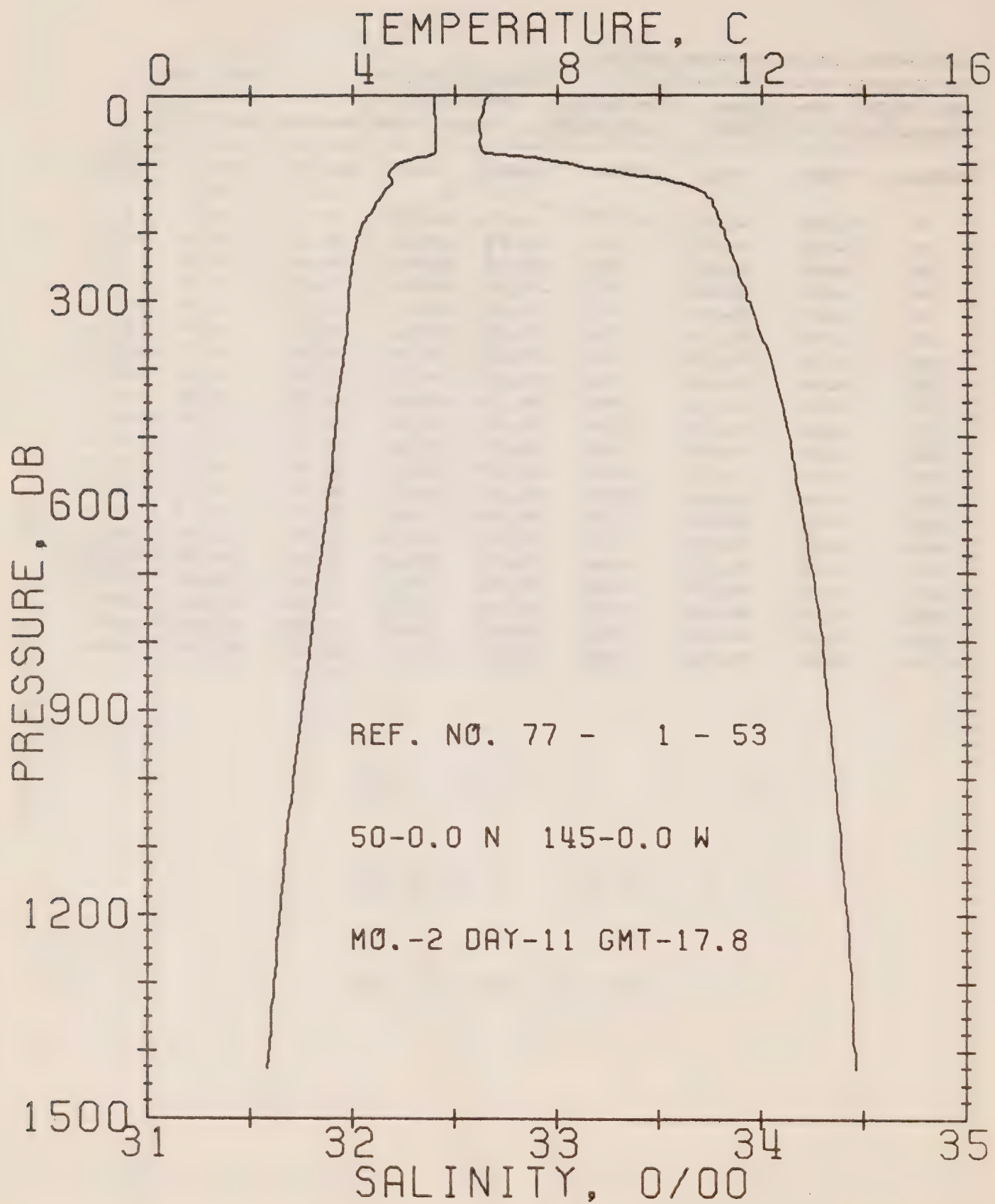
DATE 10/ 2/77

STATION P

POSITION 50- 0.0N, 145- 0.0W GMT 17.5

RESULTS OF STP CAST 157 POINTS TAKEN FROM ANALOG TRACE

PRESS	TEMP	SAL	DEPTH	SIGMA T	SVA	DELTA D	POT. EN	SOUND.
0	5.82	32.63	0	25.73	227.4	0.0	0.0	1471.
10	5.82	32.62	10	25.72	228.5	0.23	0.01	1471.
20	5.82	32.62	20	25.72	228.6	0.46	0.05	1472.
30	5.83	32.61	30	25.71	229.5	0.69	0.10	1472.
50	5.84	32.61	50	25.71	229.9	1.15	0.29	1472.
75	5.75	32.70	75	25.80	222.1	1.72	0.66	1472.
100	4.73	33.18	99	26.29	175.4	2.21	1.09	1469.
125	4.78	33.61	124	26.62	143.9	2.60	1.54	1470.
150	4.67	33.76	149	26.75	131.6	2.94	2.02	1470.
175	4.41	33.78	174	26.80	127.4	3.27	2.56	1470.
200	4.21	33.81	199	26.84	123.5	3.58	3.15	1469.
225	4.10	33.83	223	26.87	121.0	3.89	3.82	1469.
250	3.99	33.85	248	26.90	118.7	4.19	4.54	1469.
300	3.91	33.90	298	26.95	114.5	4.77	6.17	1470.
400	3.81	34.03	397	27.06	104.5	5.86	10.06	1471.
500	3.66	34.13	496	27.15	96.2	6.86	14.66	1472.
600	3.48	34.20	595	27.23	89.9	7.80	19.89	1473.
800	3.13	34.30	793	27.34	80.2	9.50	31.98	1475.
1000	2.81	34.37	990	27.43	72.6	11.02	45.90	1477.
1200	2.52	34.43	1188	27.50	66.1	12.40	61.33	1479.



OFFSHORE OCEANOGRAPHY GROUP

REFERENCE NO. 77- 1- 53

DATE 11/ 2/77

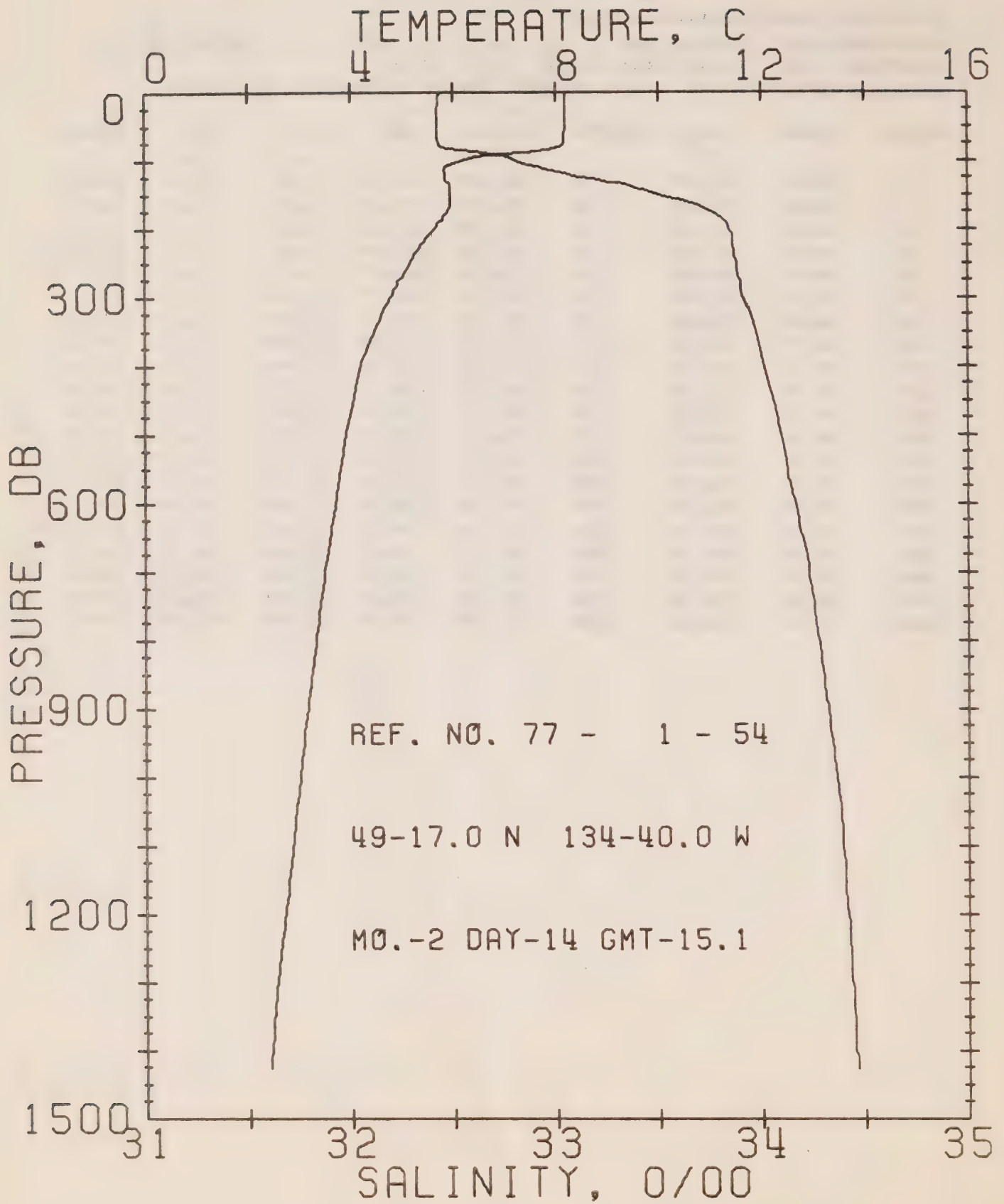
STATION P

POSITION 50- 0.0N, 145- 0.0W

GMT 17.8

RESULTS OF STP CAST 174 POINTS TAKEN FROM ANALOG TRACE

PRESS	TEMP	SAL	DEPTH	SIGMA T	SVA	DELTA D	POT. EN	SOUND
0	5.60	32.67	0	25.79	221.9	0.0	0.0	1470.
10	5.61	32.65	10	25.77	223.8	0.22	0.01	1471.
20	5.61	32.64	20	25.76	224.6	0.45	0.05	1471.
30	5.62	32.63	30	25.76	225.3	0.67	0.10	1471.
50	5.63	32.62	50	25.74	226.7	1.12	0.29	1471.
75	5.63	32.62	75	25.75	226.7	1.69	0.65	1472.
100	4.89	33.06	99	26.17	186.2	2.22	1.12	1470.
125	4.77	33.56	124	26.59	147.5	2.64	1.59	1470.
150	4.52	33.74	149	26.75	131.6	2.98	2.08	1470.
175	4.30	33.78	174	26.81	126.3	3.30	2.61	1469.
200	4.14	33.82	199	26.86	122.0	3.61	3.20	1469.
225	4.04	33.85	223	26.89	119.0	3.92	3.86	1469.
250	3.98	33.88	248	26.92	116.4	4.21	4.57	1469.
300	3.91	33.93	298	26.97	112.3	4.78	6.17	1470.
400	3.79	34.06	397	27.08	102.3	5.85	9.99	1471.
500	3.64	34.13	496	27.16	95.9	6.84	14.52	1472.
600	3.49	34.19	595	27.22	90.8	7.78	19.75	1473.
800	3.17	34.30	793	27.34	80.6	9.49	31.92	1475.
1000	2.84	34.36	990	27.41	74.0	11.04	46.12	1477.
1200	2.57	34.42	1188	27.48	67.9	12.46	61.98	1480.



OFFSHORE OCEANOGRAPHY GROUP

REFERENCE NO. 77- 1- 54

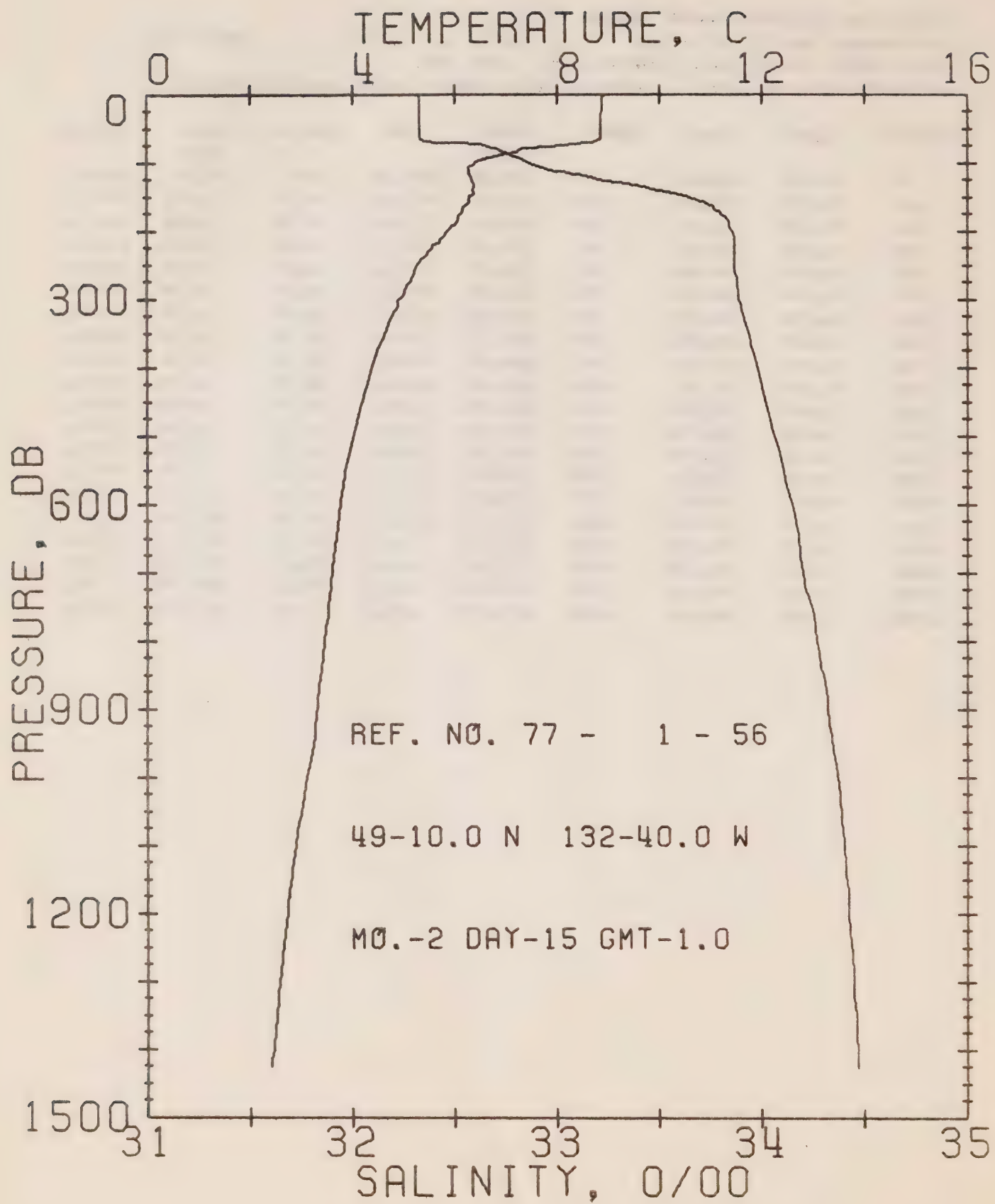
DATE 14/ 2/77

STATION 8

POSITION 49-17.0N, 134-40.0W GMT 15.1

RESULTS OF STP CAST 183 POINTS TAKEN FROM ANALOG TRACE

PRESS	TEMP	SAL	DEPTH	SIGMA T	SVA	DELTA D	POT. EN	SOUND
0	8.18	32.44	0	25.26	271.6	0.0	0.0	1480.
10	8.18	32.43	10	25.26	272.8	0.27	0.01	1480.
20	8.19	32.43	20	25.25	273.2	0.55	0.06	1481.
30	8.18	32.42	30	25.25	273.8	0.82	0.13	1481.
50	8.18	32.42	50	25.25	274.1	1.37	0.35	1481.
75	8.14	32.43	75	25.26	273.5	2.05	0.79	1481.
100	6.16	32.81	99	25.83	219.3	2.67	1.34	1474.
125	5.84	33.14	124	26.13	190.6	3.19	1.92	1474.
150	5.95	33.49	149	26.39	166.2	3.63	2.54	1475.
175	5.87	33.77	174	26.62	144.9	4.02	3.18	1476.
200	5.62	33.84	199	26.71	137.0	4.37	3.85	1475.
225	5.35	33.86	223	26.76	132.6	4.70	4.58	1475.
250	5.14	33.88	248	26.80	129.0	5.03	5.37	1474.
300	4.76	33.91	298	26.86	122.9	5.66	7.14	1473.
400	4.18	34.01	397	27.01	110.0	6.81	11.24	1473.
500	3.89	34.09	496	27.10	101.5	7.87	16.07	1473.
600	3.67	34.17	595	27.18	94.4	8.85	21.57	1474.
800	3.31	34.28	793	27.30	83.8	10.63	34.23	1476.
1000	2.98	34.36	990	27.40	75.4	12.22	48.79	1478.
1200	2.68	34.41	1188	27.47	69.3	13.66	64.95	1480.



OFFSHORE OCEANOGRAPHY GROUP

REFERENCE NO. 77- 1- 56

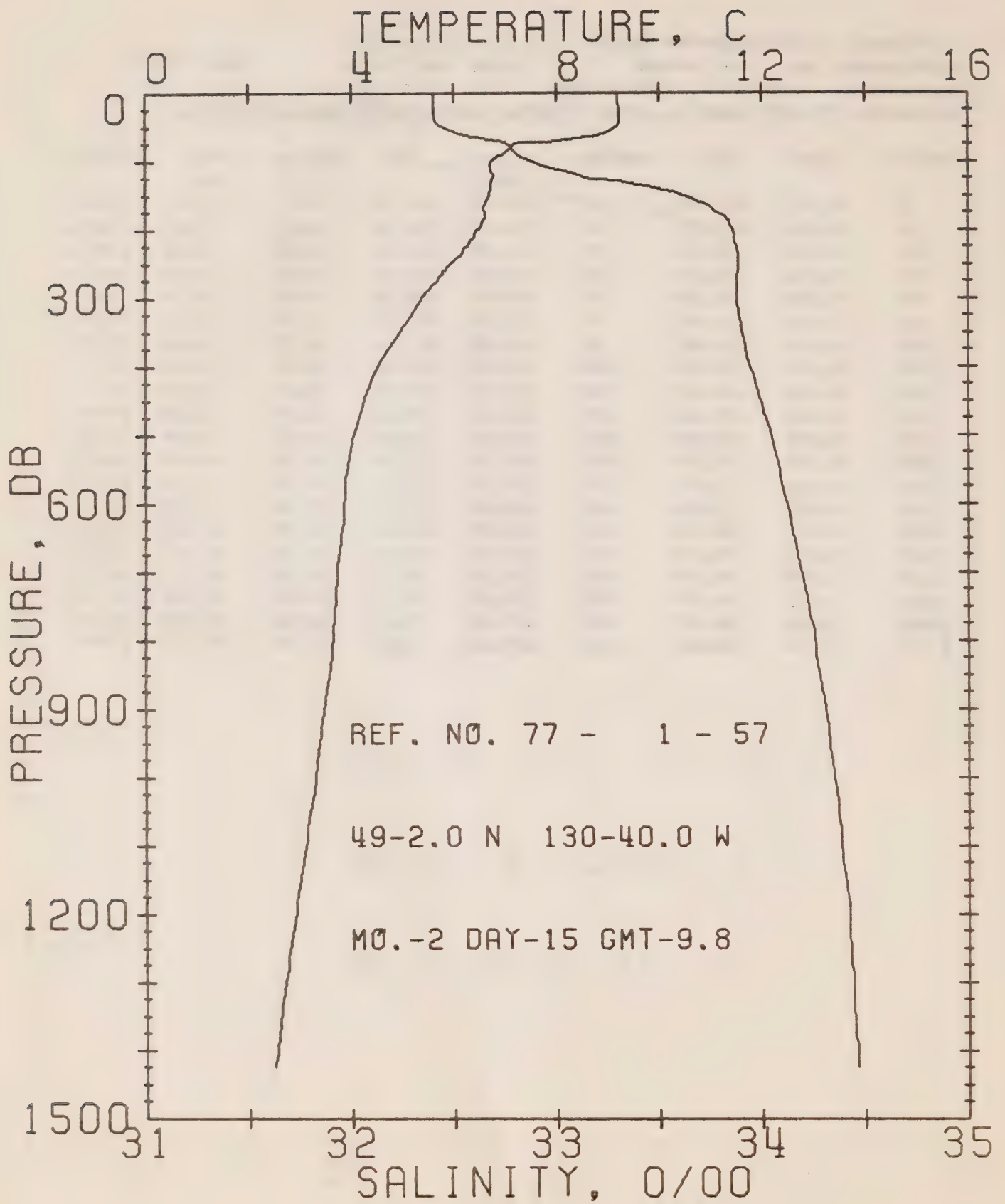
DATE 15/ 2/77

STATION 7

POSITION 49-10.0N, 132-40.0W GMT 1.0

RESULTS OF STP CAST 175 POINTS TAKEN FROM ANALOG TRACE

PRESS	TEMP	SAL	DEPTH	SIGMA T	SVA	DELTA D	POT. EN	SOUND
0	9.00	32.33	0	25.05	291.5	0.0	0.0	1483.
10	8.88	32.33	10	25.07	290.2	0.29	0.01	1483.
20	8.87	32.33	20	25.07	290.2	0.58	0.06	1483.
30	8.86	32.33	30	25.08	290.2	0.87	0.13	1483.
50	8.86	32.33	50	25.08	290.6	1.45	0.37	1484.
75	7.79	32.66	75	25.49	251.1	2.16	0.82	1480.
100	6.38	32.87	99	25.85	217.4	2.75	1.34	1475.
125	6.33	33.22	124	26.13	191.2	3.26	1.93	1476.
150	6.28	33.64	149	26.47	159.4	3.69	2.54	1477.
175	6.09	33.80	174	26.62	145.4	4.07	3.16	1477.
200	5.85	33.85	199	26.69	138.8	4.43	3.84	1476.
225	5.53	33.87	223	26.74	133.9	4.77	4.58	1475.
250	5.25	33.87	248	26.78	131.0	5.10	5.38	1475.
300	4.92	33.89	298	26.83	126.3	5.74	7.18	1474.
400	4.37	33.98	397	26.96	114.5	6.94	11.45	1474.
500	4.00	34.06	496	27.06	105.2	8.04	16.48	1474.
600	3.76	34.15	595	27.16	97.0	9.05	22.13	1475.
800	3.45	34.27	793	27.28	85.9	10.88	35.14	1477.
1000	3.10	34.37	990	27.40	75.9	12.50	49.98	1479.
1200	2.72	34.42	1188	27.47	69.3	13.94	66.11	1480.



OFFSHORE OCEANOGRAPHY GROUP

REFERENCE NO. 77- 1- 57

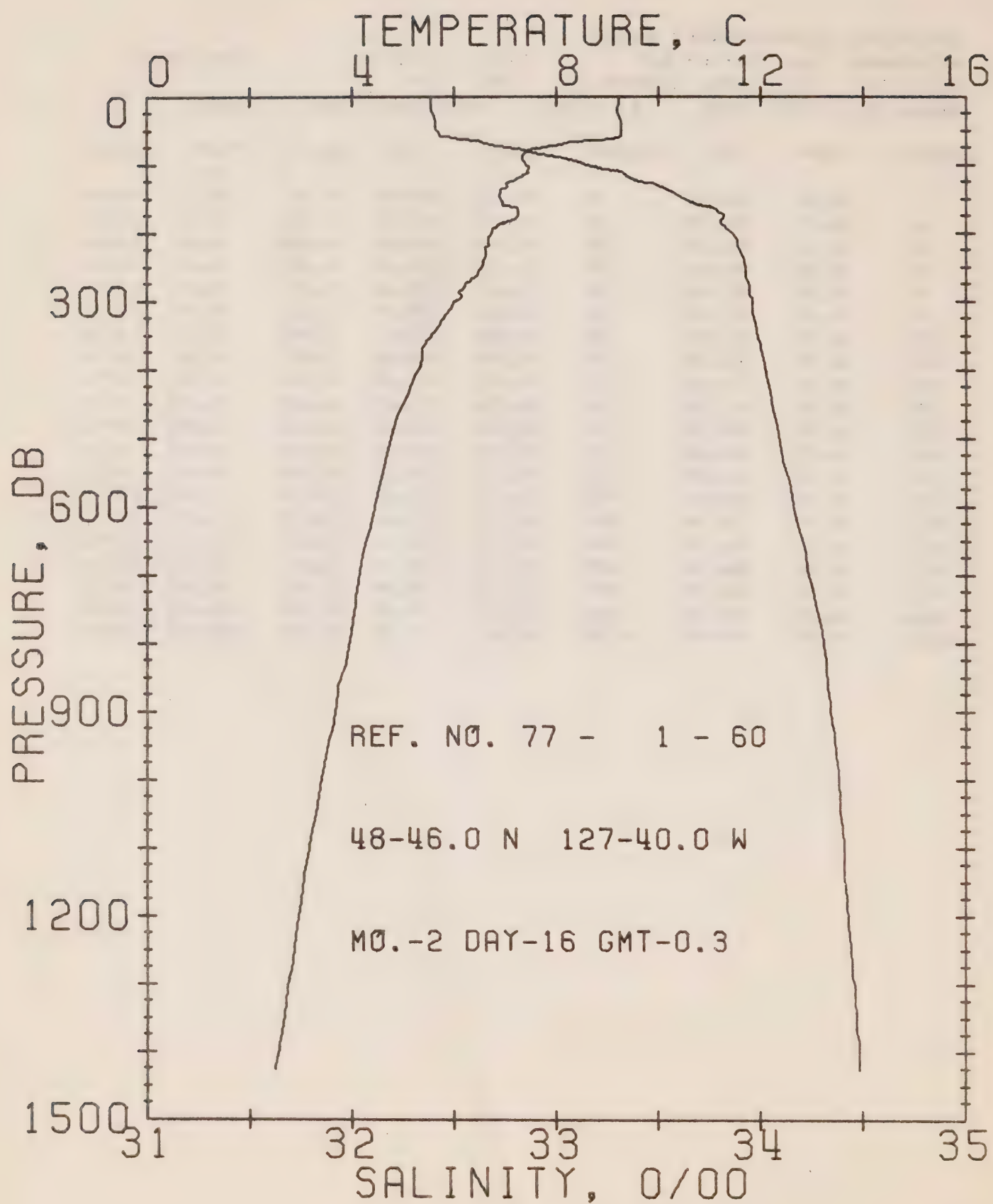
DATE 15/ 2/77

STATION 6

POSITION 49- 2.0N, 130-40.0W GMT 9.8

RESULTS OF STP CAST 183 POINTS TAKEN FROM ANALOG TRACE

PRESS	TEMP	SAL	DEPTH	SIGMA T	SVA	DELTA D	POT. EN	SOUND
0	9.21	32.40	0	25.08	289.4	0.0	0.0	1484.
10	9.21	32.40	10	25.08	289.8	0.29	0.01	1484.
20	9.22	32.40	20	25.07	290.2	0.58	0.06	1484.
30	9.22	32.40	30	25.07	290.4	0.87	0.13	1485.
50	9.18	32.45	50	25.12	286.6	1.45	0.37	1485.
75	7.17	32.76	75	25.66	235.6	2.12	0.79	1478.
100	6.73	32.88	99	25.81	221.1	2.69	1.30	1477.
125	6.76	33.18	124	26.04	199.4	3.22	1.91	1478.
150	6.68	33.62	149	26.40	166.0	3.67	2.54	1478.
175	6.62	33.79	174	26.54	153.2	4.07	3.19	1479.
200	6.47	33.86	199	26.62	146.0	4.44	3.90	1479.
225	6.23	33.88	223	26.66	141.9	4.80	4.69	1478.
250	5.93	33.89	248	26.71	137.7	5.15	5.53	1477.
300	5.38	33.88	298	26.77	132.3	5.82	7.42	1476.
400	4.50	33.94	397	26.92	118.6	7.08	11.90	1474.
500	4.02	34.04	496	27.05	106.8	8.20	17.04	1474.
600	3.85	34.12	595	27.13	100.0	9.24	22.81	1475.
800	3.62	34.25	793	27.26	88.9	11.12	36.20	1477.
1000	3.28	34.35	991	27.37	79.5	12.80	51.61	1479.
1200	2.89	34.42	1188	27.46	71.2	14.30	68.45	1481.



OFFSHORE OCEANOGRAPHY GROUP

REFERENCE NO. 77- 1- 60

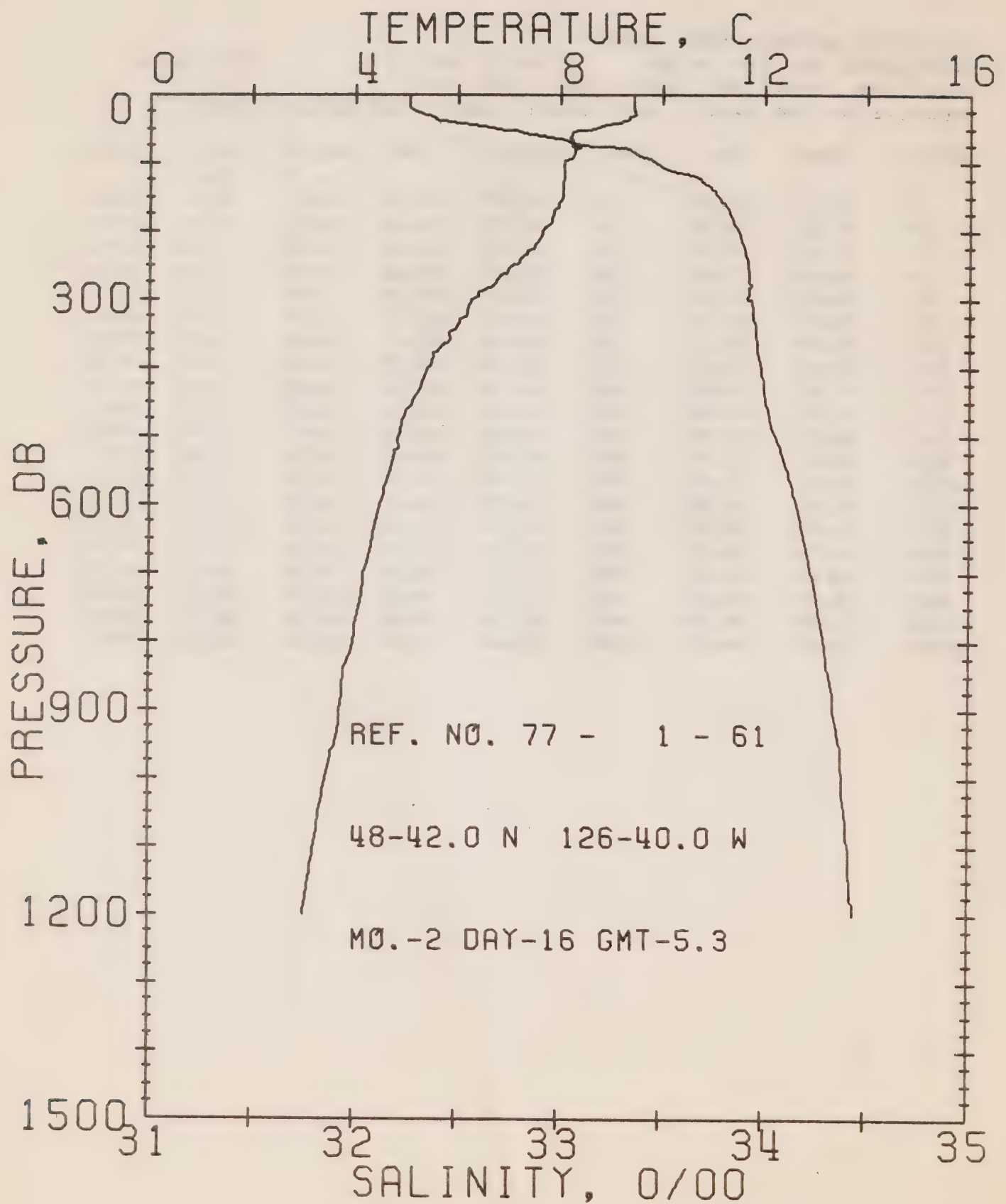
DATE 16/ 2/77

STATION 4

POSITION 48-46.0N, 127-40.0W GMT 0.3

RESULTS OF STP CAST 190 POINTS TAKEN FROM ANALOG TRACE

PRESS	TEMP	SAL	DEPTH	SIGMA T	SVA	DELTA D	POT. EN	SOUND
0	9.23	32.39	0	25.07	290.5	0.0	0.0	1484.
10	9.22	32.39	10	25.07	290.8	0.29	0.01	1484.
20	9.21	32.39	20	25.07	290.8	0.58	0.06	1484.
30	9.24	32.40	30	25.07	290.6	0.87	0.13	1485.
50	9.28	32.41	50	25.08	290.6	1.45	0.37	1485.
75	7.70	32.78	75	25.60	241.0	2.13	0.80	1480.
100	7.42	33.15	99	25.93	210.1	2.69	1.29	1480.
125	7.10	33.42	124	26.19	185.7	3.18	1.86	1479.
150	6.90	33.63	149	26.38	168.1	3.62	2.47	1479.
175	7.22	33.82	174	26.48	158.6	4.03	3.15	1481.
200	6.72	33.86	199	26.58	149.6	4.41	3.88	1480.
225	6.61	33.90	223	26.63	145.2	4.78	4.68	1480.
250	6.53	33.93	248	26.66	142.5	5.14	5.55	1480.
300	6.01	33.96	298	26.75	134.0	5.83	7.49	1479.
400	5.28	34.02	397	26.89	121.5	7.11	12.02	1477.
500	4.75	34.09	496	27.01	111.3	8.27	17.34	1477.
600	4.44	34.16	595	27.10	103.6	9.34	23.35	1477.
800	3.94	34.31	793	27.27	88.6	11.25	36.92	1479.
1000	3.39	34.38	991	27.38	78.4	12.92	52.17	1480.
1200	2.95	34.43	1188	27.46	71.4	14.41	68.90	1481.



OFFSHORE OCEANOGRAPHY GROUP

REFERENCE NO. 77- 1- 61

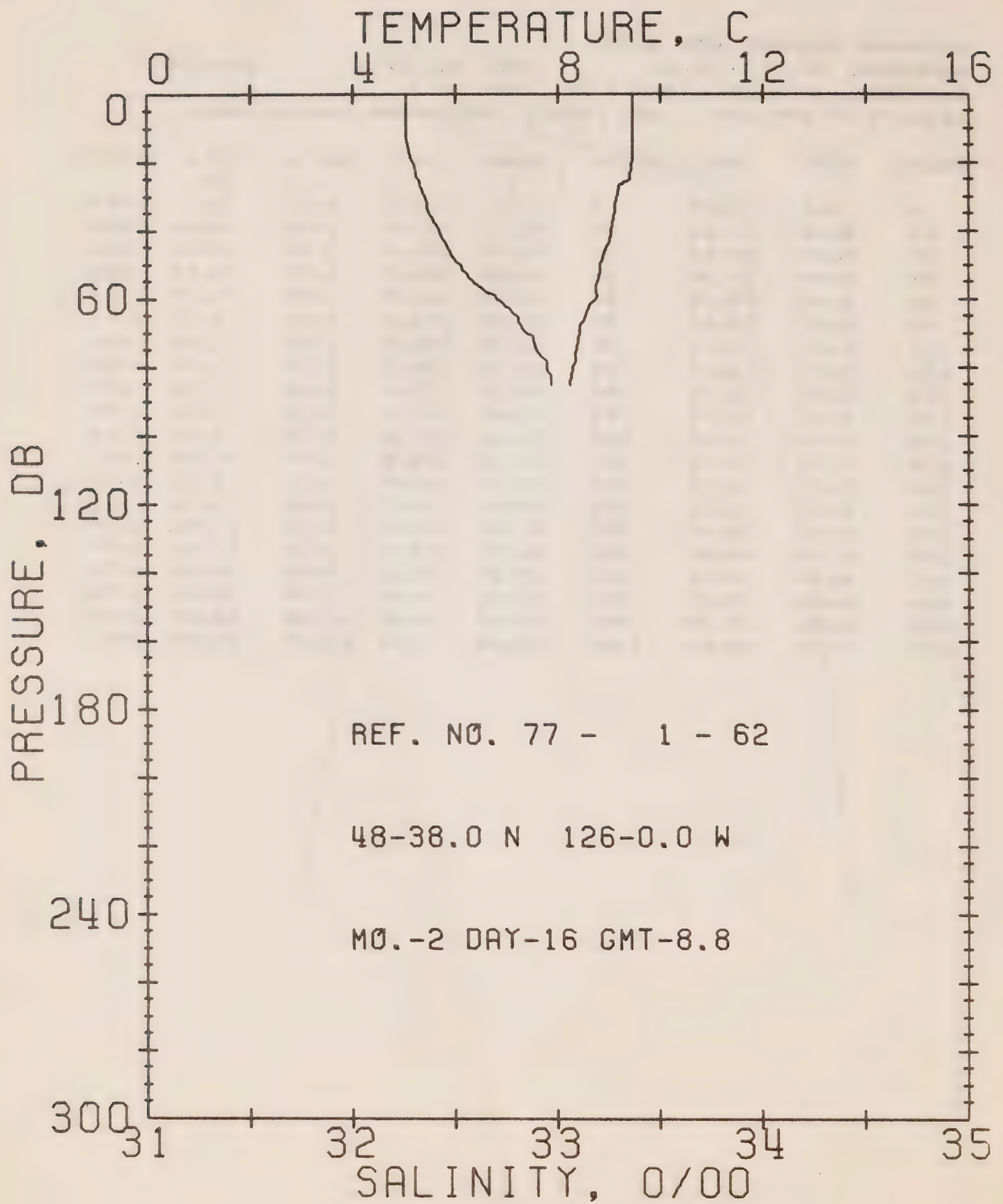
DATE 16/ 2/77

STATION 3

POSITION 48-42.0N, 126-40.0W GMT 5.3

RESULTS OF STP CAST 200 POINTS TAKEN FROM ANALOG TRACE

PRESS	TEMP	SAL	DEPTH	SIGMA T	SVA	DELTA D	POT. EN	SOUND
0	9.44	32.27	0	24.94	302.6	0.0	0.0	1485.
10	9.44	32.26	10	24.93	303.7	0.30	0.02	1485.
20	9.45	32.26	20	24.93	304.1	0.61	0.06	1485.
30	9.48	32.34	30	24.99	298.7	0.91	0.14	1486.
50	8.68	32.68	50	25.38	261.7	1.48	0.37	1483.
75	8.22	33.16	75	25.82	220.0	2.07	0.75	1483.
100	8.07	33.47	99	26.09	195.3	2.58	1.20	1483.
125	8.06	33.69	124	26.26	179.2	3.05	1.74	1483.
150	8.03	33.77	149	26.33	173.1	3.49	2.36	1484.
175	7.87	33.83	174	26.40	166.7	3.92	3.06	1484.
200	7.66	33.87	199	26.46	161.2	4.33	3.84	1483.
225	7.47	33.90	223	26.51	156.8	4.73	4.70	1483.
250	7.05	33.92	248	26.59	149.9	5.11	5.63	1482.
300	6.30	33.92	298	26.69	140.7	5.83	7.66	1480.
400	5.43	33.99	397	26.85	126.3	7.16	12.39	1478.
500	4.84	34.05	496	26.97	115.2	8.37	17.93	1477.
600	4.49	34.16	595	27.09	104.1	9.47	24.06	1478.
800	3.96	34.30	793	27.26	89.8	11.40	37.79	1479.
1000	3.45	34.39	991	27.38	78.5	13.08	53.16	1480.
1200	3.01	34.44	1188	27.46	71.0	14.57	69.90	1482.



OFFSHORE OCEANOGRAPHY GROUP

REFERENCE NO. 77- 1- 62

DATE 16/ 2/77

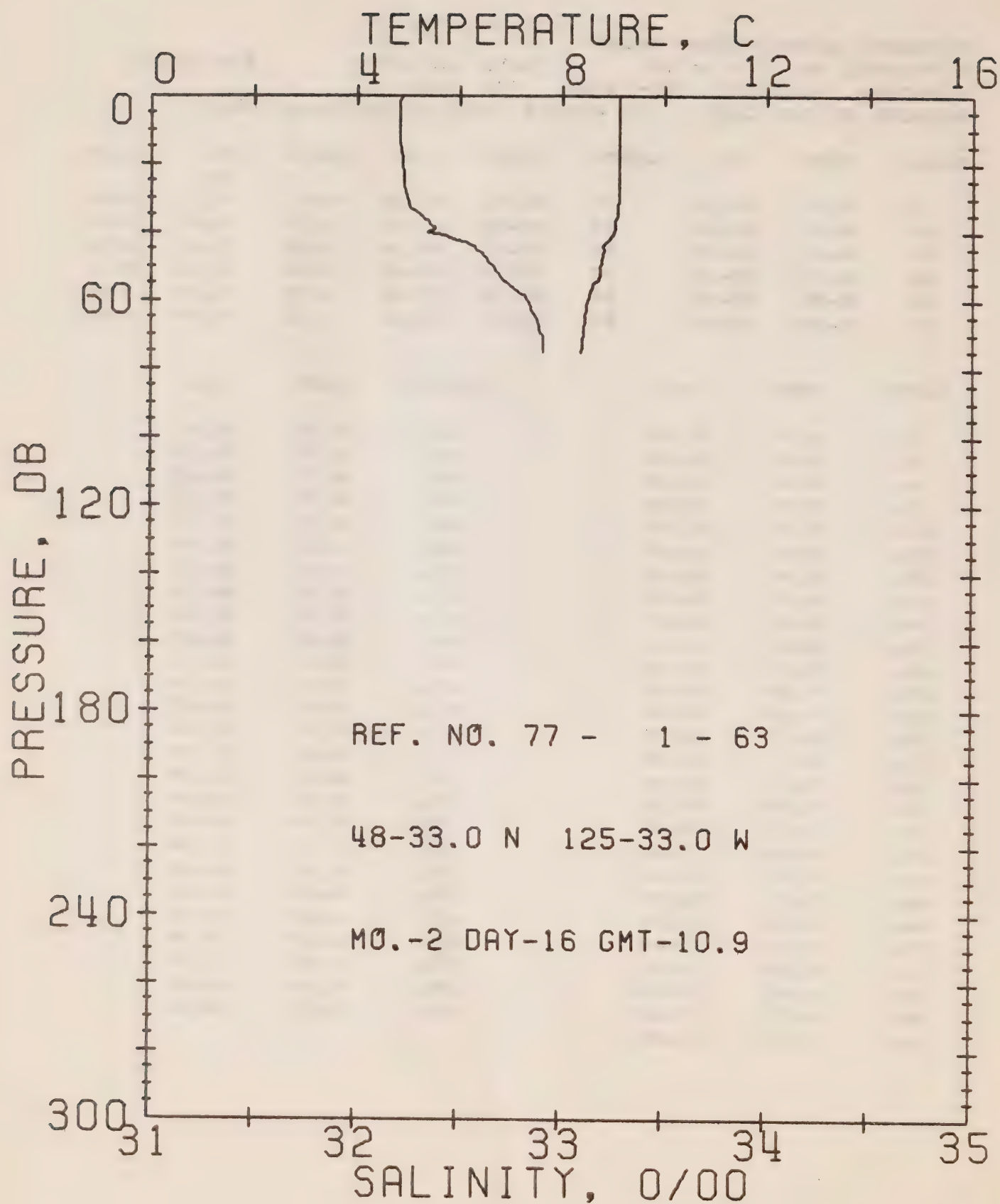
STATION 2

POSITION 48-38.0N, 126- 0.0W GMT 8.8

RESULTS OF STP CAST 53 POINTS TAKEN FROM ANALOG TRACE

PRESS	TEMP	SAL	DEPTH	SIGMA T	SVA	DELTA D	POT. EN	SOUND
0	9.47	32.26	0	24.93	303.8	0.0	0.0	1485.
10	9.47	32.26	10	24.93	304.2	0.30	0.02	1485.
20	9.45	32.29	20	24.95	301.9	0.61	0.06	1485.
30	9.15	32.35	30	25.04	293.3	0.91	0.14	1484.
50	8.84	32.52	50	25.23	276.2	1.48	0.37	1484.
75	8.36	32.90	75	25.60	241.3	2.12	0.78	1483.

DEPTH	TEMP	SAL	DEPTH	TEMP	SAL
0.	9.47	32.26	57.	8.76	32.63
4.	9.47	32.26	58.	8.76	32.65
8.	9.47	32.26	59.	8.77	32.69
9.	9.47	32.26	60.	8.75	32.70
14.	9.47	32.26	61.	8.68	32.72
15.	9.47	32.27	62.	8.62	32.74
19.	9.46	32.28	63.	8.59	32.76
21.	9.45	32.30	64.	8.56	32.78
24.	9.42	32.31	65.	8.54	32.80
25.	9.40	32.32	66.	8.52	32.81
26.	9.30	32.33	67.	8.47	32.81
27.	9.20	32.33	68.	8.43	32.82
29.	9.16	32.34	69.	8.43	32.83
32.	9.13	32.36	70.	8.43	32.85
33.	9.12	32.36	71.	8.41	32.88
34.	9.11	32.36	72.	8.40	32.88
36.	9.09	32.38	74.	8.37	32.89
40.	9.04	32.42	76.	8.35	32.91
41.	9.03	32.42	78.	8.35	32.94
43.	9.01	32.44	79.	8.31	32.95
45.	8.92	32.46	80.	8.29	32.95
46.	8.90	32.47	81.	8.28	32.95
48.	8.87	32.49	82.	8.27	32.96
50.	8.84	32.52	83.	8.26	32.97
52.	8.82	32.54	84.	8.25	32.97
55.	8.77	32.58	85.	8.25	32.97
56.	8.75	32.61			



OFFSHORE OCEANOGRAPHY GROUP

REFERENCE NO. 77- 1- 63

DATE 16/ 2/77

STATION 1

POSITION 48-33.0N, 125-33.0W GMT 10.9

RESULTS OF STP CAST 42 POINTS TAKEN FROM ANALOG TRACE

PRESS	TEMP	SAL	DEPTH	SIGMA T	SVA	DELTA D	POT. EN	SOUND
0	9.11	32.22	0	24.95	301.3	0.0	0.0	1484.
10	9.11	32.21	10	24.94	302.5	0.30	0.02	1484.
20	9.12	32.22	20	24.95	301.9	0.60	0.06	1484.
30	9.11	32.24	30	24.97	300.6	0.91	0.14	1484.
50	8.76	32.66	50	25.35	264.5	1.47	0.37	1484.
75	8.37	32.91	75	25.60	240.7	2.10	0.76	1483.

DEPTH	TEMP	SAL	DEPTH	TEMP	SAL
0.	9.11	32.22	45.	8.84	32.58
2.	9.11	32.21	46.	8.79	32.61
4.	9.11	32.21	49.	8.77	32.64
7.	9.11	32.21	50.	8.76	32.66
9.	9.11	32.21	51.	8.76	32.67
14.	9.12	32.21	52.	8.76	32.68
19.	9.12	32.22	54.	8.71	32.71
25.	9.12	32.23	55.	8.63	32.73
27.	9.12	32.23	57.	8.56	32.77
30.	9.11	32.24	59.	8.53	32.82
33.	9.10	32.25	60.	8.51	32.83
34.	9.09	32.29	61.	8.49	32.84
35.	9.08	32.30	63.	8.47	32.85
37.	9.04	32.35	64.	8.46	32.86
38.	9.03	32.36	66.	8.45	32.88
39.	9.03	32.38	68.	8.43	32.89
40.	9.02	32.34	69.	8.43	32.89
41.	8.98	32.43	70.	8.42	32.90
42.	8.92	32.47	71.	8.41	32.91
43.	8.88	32.52	73.	8.39	32.91
44.	8.81	32.57	75.	8.37	32.91

Surface Salinity and Temperature Observations

(P-77-1)

SURFACE SALINITY AND TEMPERATURE OBSERVATIONS
CRUISE REFERENCE NUMBER 77- 1

DATE/TIME				SALINITY	TEMP	LONGITUDE
YR	MO	DAY	GMT	0/00	C	WEST
77	1	7	2315	31.060	8.2	125-33
77	1	8	105	29.793	9.0	126- 0
77	1	8	315	31.914	9.4	126-40
77	1	8	630	32.233	9.4	127-40
77	1	8	1010	32.502	9.9	128-40
77	1	8	1325	32.437	10.1	129-40
77	1	8	1625	32.461	9.8	130-40
77	1	8	2140	32.409	9.8	131-40
77	1	9	10	32.328	9.7	132-40
77	1	9	325	32.344	8.8	133-40
77	1	9	600	32.372	8.3	134-40
77	1	9	940	32.428	8.2	135-40
77	1	9	1225	32.449	8.0	136-40
77	1	9	1540	32.554	7.7	137-40
77	1	9	1820	32.542	7.7	138-40
77	1	9	2350	32.524	7.4	139-40
77	1	10	220	32.596	7.3	140-40
77	1	10	600	32.606	7.2	141-40
77	1	10	900	32.633	6.2	142-40
77	1	10	1300	32.620	6.1	143-40
77	1	11	0	32.612	6.2	ON STATION
77	1	12	0	32.620	6.0	ON STATION
77	1	13	0	32.624	6.0	ON STATION
77	1	14	0	32.595b	6.0	ON STATION
77	1	15	0	32.581b	6.1	ON STATION
77	1	16	0	32.598b	6.2	ON STATION
77	1	17	0	32.623b	6.0	ON STATION
77	1	18	0	32.621b	5.8	ON STATION
77	1	19	0	32.608b	5.8	ON STATION
77	1	20	0	32.659b	5.3	ON STATION
77	1	21	0	32.621b	5.9	ON STATION
77	1	22	0	32.627b	5.9	ON STATION
77	1	23	0	32.614b	5.8	ON STATION
77	1	24	0	32.618b	5.9	ON STATION
77	1	25	0	32.628b	6.0	ON STATION
77	1	26	0	32.582b	6.0	ON STATION
77	1	27	0	32.628b	5.9	ON STATION
77	1	28	0	32.635b	6.0	ON STATION
77	1	29	0	32.631b	5.9	ON STATION
77	1	30	0	32.621b	6.3	ON STATION
77	1	31	0	32.649b	5.8	ON STATION
77	2	1	0	32.635b	5.7	ON STATION
77	2	2	0	32.611b	5.9	ON STATION
77	2	3	0	32.623	5.9	ON STATION

SURFACE SALINITY AND TEMPERATURE OBSERVATIONS
CRUISE REFERENCE NUMBER 77- I

DATE/TIME				SALINITY	TEMP	LONGITUDE
YR	MO	DY	GMT	0/00	C	WEST
77	2	4	0	32.640b	5.8	ON STATION
77	2	5	0	32.634	6.0	ON STATION
77	2	6	0	32.627b	5.9	ON STATION
77	2	7	0	32.610	5.9	ON STATION
77	2	8	0	32.625	5.8	ON STATION
77	2	9	0	32.635b	5.8	ON STATION
77	2	10	0	32.626	5.9	ON STATION
77	2	11	0	32.614	5.8	ON STATION
77	2	12	0	32.636	6.0	ON STATION
77	2	13	0	32.643b	5.8	ON STATION
77	2	14	1500	32.412	8.2	134-40
77	2	14	2115	32.367b	8.2	133-40
77	2	15	50	32.316	8.9	132-40
77	2	15	520	32.376	9.0	131-40
77	2	15	950	32.407	9.2	130-40
77	2	15	1420	32.510	9.6	129-40
77	2	15	1815	32.336	9.0	128-40
77	2	15	2255	32.397	9.3	127-40
77	2	16	510	32.237	9.5	126-40
77	2	16	845	32.298	9.5	126- 0
77	2	16	1055	32.195	9.3	125-33

b DENOTES SALINITY SAMPLE TAKEN FROM A
BUCKET. ALL OTHER SAMPLES TAKEN FROM
THE SEAWATER LOOP

LIST OF OMISSIONS FROM DATA

Hydrographic data:

Consec. #	Depth (m)	Temp.	Sal.	O ₂	Notes			Comments
					1.	2.	3.	
7	282		*		*			
23	1298			*	*			
	3589		*				*	
	3683			*		*		
	3767		*				*	
35	2920		*		*			
	3894		*		*			
	4068		*				*	
42	4098		*		*			
	4189		*		*			
50	2876		*		*			
	3852		*				*	
	3949		*		*			
	4046		*		*			

Notes (MacNeill, 1977):

1. The data is suspect because of a reversal of gradient by $>.01$ ‰ (salinity) or $>.08$ ml/l (oxygen).
2. The data is deleted because of very irregular data values (usually a mis-tripping or leaking bottle if both oxygen and salinity are irregular).
3. The data is deleted because duplicate samples at a depth were not within $.01$ ‰ (salinity) or $.08$ ml/l (oxygen).

STD Data:

Consecutive #	Comments
16	Deep salinity omitted; too high
17	Deep salinity omitted; too high
58	Not included; traces too erratic

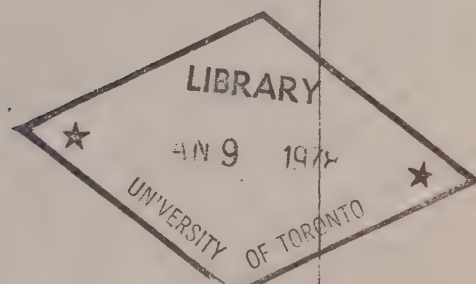
CAI
EP 321
-77R14

**OCEANOGRAPHIC OBSERVATIONS
AT OCEAN STATION P
(50°N, 145°W)**

**VOLUME 80
11 February - 31 March 1977**

by

Seakem Oceanography Ltd.



**Institute of Ocean Sciences, Patricia Bay
Sidney , B.C.**



For addition copies or further information please write to:

Department of Fisheries and the Environment

Institute of Ocean Sciences, Patricia Bay

P.O. Box 5000

Sidney, B.C.

V8L 4B2

OCEANOGRAPHIC OBSERVATIONS AT OCEAN STATION P (50°N, 145°W)

Volume 80

11 February - 31 March 1977

by

Seakem Oceanography Ltd.

Institute of Ocean Sciences, Patricia Bay

Sidney, B.C.

September 1977

This is a manuscript which has received only limited circulation. On citing this report in a bibliography, the title should be followed by the words "UNPUBLISHED MANUSCRIPT" which is in accordance with accepted bibliographic custom.

ABSTRACT

Physical, chemical and biological oceanographic observations are made from the weathership at Ocean Weather Station Papa, and between Esquimalt and Station Papa, on a routine continuing basis. Physical oceanography data only are shown, including surface observations and profiles obtained with bottle casts and conductivity-temperature-pressure instruments.

TABLE OF CONTENTS

ABSTRACT.....	i
TABLE OF CONTENTS.....	iii
INTRODUCTION.....	1
PROGRAM OF OBSERVATIONS.....	2
OBSERVATIONAL PROCEDURES.....	4
COMPUTATIONS.....	4
REFERENCES.....	5
LOG OF HYDROGRAPHIC AND STD OBSERVATIONS.....	6
RESULTS OF HYDROGRAPHIC OBSERVATIONS.....	11
RESULTS OF STD OBSERVATIONS.....	23
SURFACE SALINITY AND TEMPERATURE OBSERVATIONS.....	67
LIST OF OMISSIONS FROM DATA.....	71

LIST OF FIGURES

Figure 1. Chart showing Line P station positions.....	7
Figure 2. Composite plot of temperature vs \log_{10} depth for Line P stations.....	12
Figure 3. Composite plot of salinity vs \log_{10} depth for Line P stations.....	13
Figure 4. Composite plot of temperature vs \log_{10} depth for Station P.....	14
Figure 5. Composite plot of salinity vs \log_{10} depth for Station P.....	15
Figure 6. Composite plot of oxygen vs \log_{10} depth for Station P.....	16
Figure 7. Salinity difference between hydro data and STD.....	24
Figure 8. Temperature difference between hydro data and STD.....	25

INTRODUCTION

Canadian operation of Ocean Weather Station P (Latitude $50^{\circ}00'N$, Longitude $145^{\circ}00'W$) was inaugurated in December, 1950. The station is occupied primarily to make meteorological observations of the surface and upper air and to provide an air-sea rescue service. The station is manned by two vessels operated by the Marine Services Branch of the Ministry of Transport. They are the CCGS Vancouver and the CCGS Quadra. Each ship remains on station for a period of six weeks, and is then relieved by the alternate ship, thus maintaining a continuous watch.

Bathythermograph observations have been made at Station P since July 1952. A program of more extensive oceanographic observations commenced in August 1956. This was extended in April 1959, by the addition of a series of oceanographic stations along the route to and from Station P and Swiftsure Bank. These stations are known as Line P stations. The number of stations on Line P has been increased twice and now consists of twelve stations (Fig. 1). Bathythermograph observations and surface salinity sample collections, in addition to being made on Line P oceanographic stations, are also made at odd meridians at $40'$, i.e. $139^{\circ}40'W$, $141^{\circ}40'W$, etc. These stations are known as Line P BT stations. Data observed prior to 1968 have been indexed by Collins et al (1969).

The present record includes hydrographic, continuously sampled STD and surface salinity and temperature data collected from the CCGS Quadra during the period 11 February to 31 March 1977.

All physical oceanographic data have been stored by the Canadian Oceanographic Data Centre (CODC), 615 Booth Street, Ottawa, Ontario, Canada. Requests for these data should be directed to CODC.

Biological and productivity data are published in the Manuscript Report series of the Fisheries Research Board of Canada (FRB), Pacific Biological Station, Nanaimo, British Columbia, Canada. Requests for these data should be directed to FRB.

Marine geochemical data are for the Ocean Chemistry Group, Ocean and Aquatic Sciences, Environment Canada, Institute of Ocean Sciences, P.O. Box 5000, Sidney, B.C. V8L 4B2.

PROGRAM OF OBSERVATION FROM CCGS QUADRA, 11 FEBRUARY - 31 MARCH 1977 (P-77-2)
(CODC Ref. No. 15-77-002)

Oceanographic observations were made by Mr. B. Whitehouse of Seakem Oceanography Ltd., Victoria, B.C.

En Route to Station P

Rough weather cancelled all hydrographic and STD work. No tarball tows were completed.

Samples for salinity, nitrate, nutrient, alkalinity and total CO_2 were taken from the seawater loop at all whole stations, with salinity also taken at all half stations except Station $9\frac{1}{2}$. Surface bucket temperatures were taken at all whole and half stations.

The thermosalinograph, surface temperature recorder and PCO_2 system were run continuously.

Mechanical BT's or XBT's were taken at all whole and half stations except Stations 1, $5\frac{1}{2}$, and $8\frac{1}{2}$.

On Station P

The oceanographic program was carried out as follows:

Physical Oceanography

- 1) 1 profile of salinity, temperature and oxygen was obtained from a hydrographic cast to near bottom (4200 metres).
- 2) 10 STD profiles to 300 metres and 5 to 1500 metres were obtained.
- 3) BT's or XBT's were taken every three hours to coincide with meteorological observations, encoded and transmitted according to the IGOSS format.
- 4) Salinity samples were collected daily at 0000 hrs GMT from the seawater loop.

Marine Geochemistry

- 1) Nutrient and salinity samples were collected daily at 0000 hrs GMT from the seawater loop. One 24 hour series of nutrient samples was taken each hour from the seawater loop. One profile for nutrients to 500 m and one profile for tritium to 500 m were taken. One bucket sample and one rainwater sample were also collected for tritium.
- 2) Alkalinity and total CO_2 samples were taken every 1 to 4 days from the seawater loop or bucket and in addition 2 profiles each to 500 m were taken.
- 3) Air CO_2 samples were taken in quadruplicate at weekly intervals.

- 4) 4 surface tarball tows were completed.
- 5) 3 seawater C-14 samples were extracted from 45 gallons of seawater taken from the seawater loop along with 3 seawater C-13 and 3 air C-13 samples.
- 6) PCO_2 carboys were filled approximately every 3 days when the loop system was operational.

Biological Oceanography

Samples were obtained as follows:

- 1) 7 - 150 metre vertical plankton hauls.
2 - 1200 metre vertical plankton hauls.
3 groups of subsurface plankton hauls were taken on 3 consecutive nights at sunset.
- 2) 2 chlorophyll "a" loop samples and 1 profile to 75 m were obtained.
- 3) 1 profile to 200 metres for each of plant pigment and nitrates was obtained, as well as 2 surface samples each.
- 4) 3 Secchi disc readings were obtained.

An emergency run was made to Victoria on February 26 for engine repairs. The surface temperature recorder was operated continuously with salinity samples taken every 3 hours. En route back to Station P, the thermosalinograph and surface temperature recorder were run continuously. XBT's were taken when possible. Salinity samples were taken at all whole stations, until Station 10, when the ship left Line P due to high winds. Then, samples were taken every 3 hours until arrival at Station P (March 7).

En Route from Station P

An STD profile was made at Stations 12, 10, 9, 2 and 1. One hydrocast was done at Station 10. Nutrient, nitrate, alkalinity and total CO_2 samples were taken from the seawater loop at Stations 12 to 1. Salinity samples were taken at all whole and half stations $12\frac{1}{2}$ to 1 (except Station $10\frac{1}{2}$). Surface bucket salinities were taken at Stations 12, 10, 9, and 2. Surface bucket temperatures were taken at all whole stations 12 to 1. Tarball tows were taken at Stations 12, 10 and 2. Mechanical BT's or XBT's were taken at all whole and half stations $12\frac{1}{2}$ to 1, except Stations $11\frac{1}{2}$ and $7\frac{1}{2}$.

Observations for Other Agencies

- 1) Marine mammal observations were made by the ship's officers for Mr. I. McAskie, Fisheries Research Board of Canada, Pacific Biological Station, Nanaimo, B.C., Canada.
- 2) Bird observations were made by the ship's officers for Dr. M. Myres, University of Alberta, Calgary, Alberta, Canada and Mr. J. Guiguet, Curator of Birds and Mammals, Provincial Museum, Department of Provincial Secretary and Travel Industry, Victoria, British Columbia, Canada.

PROGRAM OF OBSERVATION FROM CCGS QUADRA, 11 FEBRUARY - 31 MARCH 1977 (P-77-2)
(CODC Ref. No. 15-77-002)

Oceanographic observations were made by Mr. B. Whitehouse of Seakem Oceanography Ltd., Victoria, B.C.

En Route to Station P

Rough weather cancelled all hydrographic and STD work. No tarball tows were completed.

Samples for salinity, nitrate, nutrient, alkalinity and total CO_2 were taken from the seawater loop at all whole stations, with salinity also taken at all half stations except Station $9\frac{1}{2}$. Surface bucket temperatures were taken at all whole and half stations.

The thermosalinograph, surface temperature recorder and PCO_2 system were run continuously.

Mechanical BT's or XBT's were taken at all whole and half stations except Stations 1, $5\frac{1}{2}$, and $8\frac{1}{2}$.

On Station P

The oceanographic program was carried out as follows:

Physical Oceanography

- 1) 1 profile of salinity, temperature and oxygen was obtained from a hydrographic cast to near bottom (4200 metres).
- 2) 10 STD profiles to 300 metres and 5 to 1500 metres were obtained.
- 3) BT's or XBT's were taken every three hours to coincide with meteorological observations, encoded and transmitted according to the IGOSS format.
- 4) Salinity samples were collected daily at 0000 hrs GMT from the seawater loop.

Marine Geochemistry

- 1) Nutrient and salinity samples were collected daily at 0000 hrs GMT from the seawater loop. One 24 hour series of nutrient samples was taken each hour from the seawater loop. One profile for nutrients to 500 m and one profile for tritium to 500 m were taken. One bucket sample and one rainwater sample were also collected for tritium.
- 2) Alkalinity and total CO_2 samples were taken every 1 to 4 days from the seawater loop or bucket and in addition 2 profiles each to 500 m were taken.
- 3) Air CO_2 samples were taken in quadruplicate at weekly intervals.

- 4) 4 surface tarball tows were completed.
- 5) 3 seawater C-14 samples were extracted from 45 gallons of seawater taken from the seawater loop along with 3 seawater C-13 and 3 air C-13 samples.
- 6) PCO_2 carboys were filled approximately every 3 days when the loop system was operational.

Biological Oceanography

Samples were obtained as follows:

- 1) 7 - 150 metre vertical plankton hauls.
2 - 1200 metre vertical plankton hauls.
3 groups of subsurface plankton hauls were taken on 3 consecutive nights at sunset.
- 2) 2 chlorophyll "a" loop samples and 1 profile to 75 m were obtained.
- 3) 1 profile to 200 metres for each of plant pigment and nitrates was obtained, as well as 2 surface samples each.
- 4) 3 Secchi disc readings were obtained.

An emergency run was made to Victoria on February 26 for engine repairs. The surface temperature recorder was operated continuously with salinity samples taken every 3 hours. En route back to Station P, the thermosalinograph and surface temperature recorder were run continuously. XBT's were taken when possible. Salinity samples were taken at all whole stations, until Station 10, when the ship left Line P due to high winds. Then, samples were taken every 3 hours until arrival at Station P (March 7).

En Route from Station P

An STD profile was made at Stations 12, 10, 9, 2 and 1. One hydrocast was done at Station 10. Nutrient, nitrate, alkalinity and total CO_2 samples were taken from the seawater loop at Stations 12 to 1. Salinity samples were taken at all whole and half stations $12\frac{1}{2}$ to 1 (except Station $10\frac{1}{2}$). Surface bucket salinities were taken at Stations 12, 10, 9, and 2. Surface bucket temperatures were taken at all whole stations 12 to 1. Tarball tows were taken at Stations 12, 10 and 2. Mechanical BT's or XBT's were taken at all whole and half stations $12\frac{1}{2}$ to 1, except Stations $11\frac{1}{2}$ and $7\frac{1}{2}$.

Observations for Other Agencies

- 1) Marine mammal observations were made by the ship's officers for Mr. I. McAskie, Fisheries Research Board of Canada, Pacific Biological Station, Nanaimo, B.C., Canada.
- 2) Bird observations were made by the ship's officers for Dr. M. Myres, University of Alberta, Calgary, Alberta, Canada and Mr. J. Guiguet, Curator of Birds and Mammals, Provincial Museum, Department of Provincial Secretary and Travel Industry, Victoria, British Columbia, Canada.

- 3) Air CO₂ samples were taken weekly in duplicate for Scripps Institution of Oceanography, La Jolla, California, U.S.A.

Data were processed for publication by Ms. M. Sainsbury of Seakem Oceanography Ltd., Victoria, B.C.

OBSERVATIONAL PROCEDURES

Observations for salinity, oxygen and temperature from all hydrographic casts, including the surface, were obtained with Niskin water sample bottles equipped with either Richter and Wiese and/or Yoshino Keiki Co. reversing thermometers. Two protected thermometers were used on all bottles and one unprotected thermometer was used on each bottle at depths of 300 m or greater. The accuracy of protected reversing thermometers is believed to be $\pm 0.02^{\circ}\text{C}$.

The daily surface water temperatures were measured from a bucket sample using a deck thermometer of $\pm 0.1^{\circ}\text{C}$ accuracy. The daily surface salinity samples were obtained from the seawater loop. When the seawater loop was not operational these samples were obtained with a bucket, and are indicated with a 'b' in this data record.

Salinity determinations were made aboard ship with either an Autolab Model 601 Mark III inductive salinometer or a Hytech Model 6220 lab salinometer. Accuracy using duplicated determinations is estimated to be $\pm 0.003^{\circ}/\text{oo}$.

Depth determinations were made using the "depth difference" method described in the U. S. N. Hydrographic Office Publication No. 607 (1955). Depth estimates have an approximate accuracy of ± 5 m for depths less than 1000 m, and $\pm 0.5\%$ of depth for depths greater than 1000 m.

The dissolved oxygen analyses were done in the shipboard laboratory by a modified Winkler method (Carpenter, 1955).

Line P engine intake continuous temperature on both ships were recorded by a Honeywell Electronik 15 Recorder. The temperature probe is at a depth of approximately 3 metres below the sea surface and the instrument accuracy is believed to be $\pm 0.1^{\circ}\text{C}$.

Each ship is equipped with a Plessey Model 6600-T thermosalinograph which is used, on Line P, for continuous recording of surface temperatures and salinities from the ship's seawater loop. The temperature probe is mounted at the seawater loop intake (approximately 3 metres below the surface) and the salinity probe and recorder are situated in the dry lab. The accuracy of this instrument is believed to be $\pm 0.1^{\circ}\text{C}$ for temperature and $\pm 0.1^{\circ}/\text{oo}$ for salinity.

STD profiles were taken with a Plessey Model 9006 STD system.

COMPUTATIONS

All hydrographic data were processed with the aid of an IBM 370 computer and a UNIVAC 1100 computer. Reversing thermometer temperature corrections,

thermometric depth calculations and accepted depth from the "depth difference" method were computed. Extraneous thermometric depths caused by thermometer malfunctions were automatically edited and replaced. A Calcomp 565 Offline Plotter was used to plot temperature-salinity, and temperature-oxygen diagrams, as well as plots of temperature, salinity, and dissolved oxygen vs \log_{10} depth. These plots were used to check the data for errors.

Missing hydrographic data were obtained using a weighted parabolas interpolation method (Reiniger and Ross, 1968). These data are indicated with an asterisk in this data record.

Data values which we suspect but which we have included in this data record are indicated with a plus. These data have been removed from punch card and magnetic tape records.

Analog records from the salinity-temperature-pressure instrument have been machine digitized, then replotted using the Calcomp plotter.

Digitization was continued until original and computer plotted traces were coincident. Temperature and salinity values were listed at standard pressures; computed from the entire array of digitized data.

The headings for the data listings are explained as follows:

PRESS	is pressure (decibars)
TEMP	is temperature (degrees Celsius)
SAL	is salinity (parts per thousand)
DEPTH	is reported in metres
SIGMA-T	is specific gravity anomaly
SVA	is specific volume anomaly
THETA	is potential temperature (degrees Celsius)
SVA (THETA)	is potential specific volume anomaly
DELTA D	is geopotential anomaly (J/kg)
POT EN	is potential energy in units of 10^8 ergs/cm ²
OXY	is the concentration of dissolved oxygen expressed in millilitres per litre
SOUND	is the velocity of sound in m/sec

REFERENCES

- Carpenter, J.H., 1965. The Chesapeake Bay Institute technique for the Winkler dissolved oxygen method. *Limnol. and Oceanogr.* 10: 141-143.
- Collins, C.A., R.L. Tripe, D.A. Healey and J. Joergensen, 1969. The time distribution of serial oceanographic data from the Ocean Station P programme. *Fish. Res. Bd. Can. Tech. Rept. No. 106.*
- MacNeill, M., 1977. A study of anomalous salinity and oxygen values in the deep water at Ocean Station P from 1960-1976 (unpublished manuscript) *Pacific Marine Science Report* 77-9.
- Reiniger, R.F. and C.K. Ross, 1968. A method of interpolation with application to oceanographic data. *Deep Sea Res.* 15: 185-193.
- U. S. N. Hydrographic Office, 1955. *Instruction Manual of Oceanographic Observations*, Publ. No. 607.

Log of Hydrographic and STD Observations

Consec #	Positions	Date (Z)	Time (Z)	STD (m)	Hydrocasts (m)	Comments
1	P	15/2/77	1730	300		
2	P	19/2/77	1725	1,500		
3	P	19/2/77	1930		500	Alk., Tot. CO ₂
4	P	20/2/77	1730	300		
5	P	23/2/77	1720	300		
6	P	25/2/77	1730	1,500		
7	P	25/2/77	1825		500	Nutrient & Tritium
8	P	9/3/77	1835	1,500		
9	P	13/3/77	1725	300		
10	P	14/3/77	1730	1,400		
11	P	14/3/77	1850	300		
12	P	15/3/77	1725	1,500		
13	P	15/3/77	1820		4,200	T, O, S
14	P	16/3/77	1715	300		
15	P	17/3/77	1720	300		
16	P	18/3/77	1715	300		
17	P	18/3/77	1740		500	Alk., Tot. CO ₂
18	P	19/3/77	1715	300		
19	P	20/3/77	1715	1,500		
20	P	21/3/77	1715	300		
21	P	21/3/77	1745		200	Biological Cast
22	142-40°W	28/3/77	0600	1,500		
23	138-40°W	28/3/77	1855	1,500		
24	138-40°W	28/3/77	1950		1,500	T, S
25	136-40°W	29/3/77	0300	1,500		
26	126-00°W	30/3/77	1125	80		
27	125-33°W	30/3/77	1315	80		

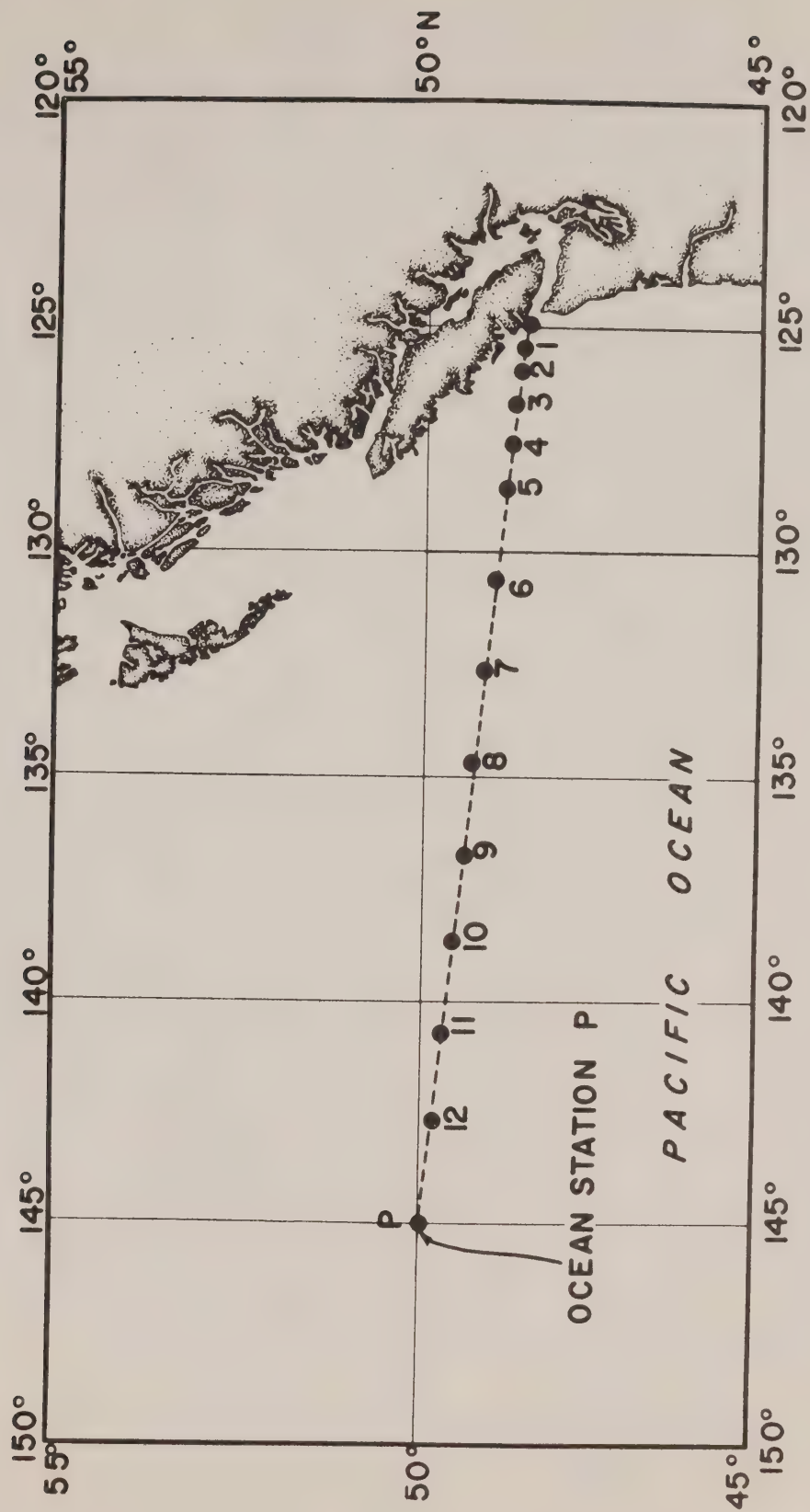


Fig. 1 Chart showing Line P station positions.

Oceanographic Data Obtained on Cruise P-77-2
(CODC Reference No. 15-77-002)

Results of Hydrographic Observations

(P-77-2)

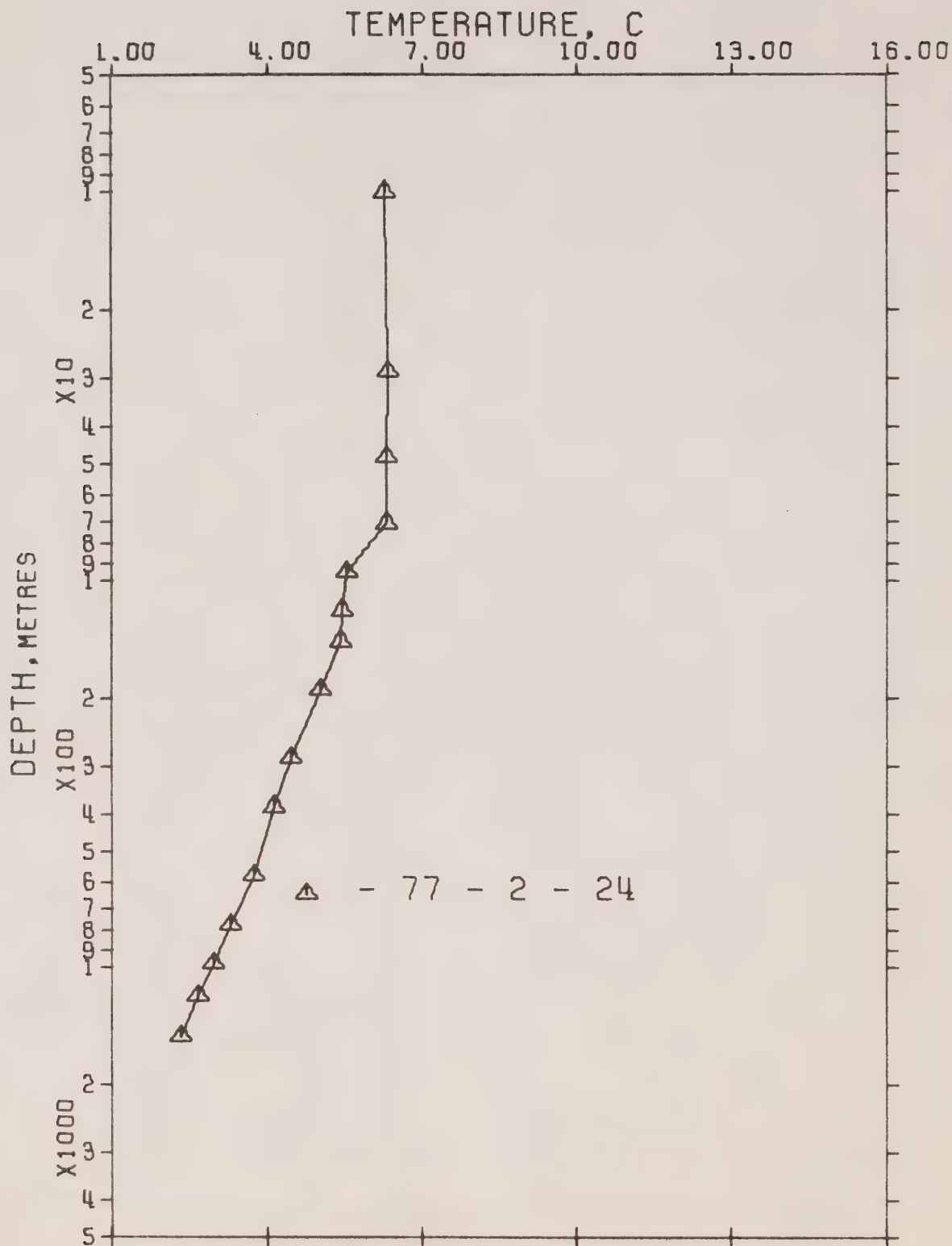


Figure 2. Composite plot of temperature vs \log_{10} depth for Line P stations. P-77-2.

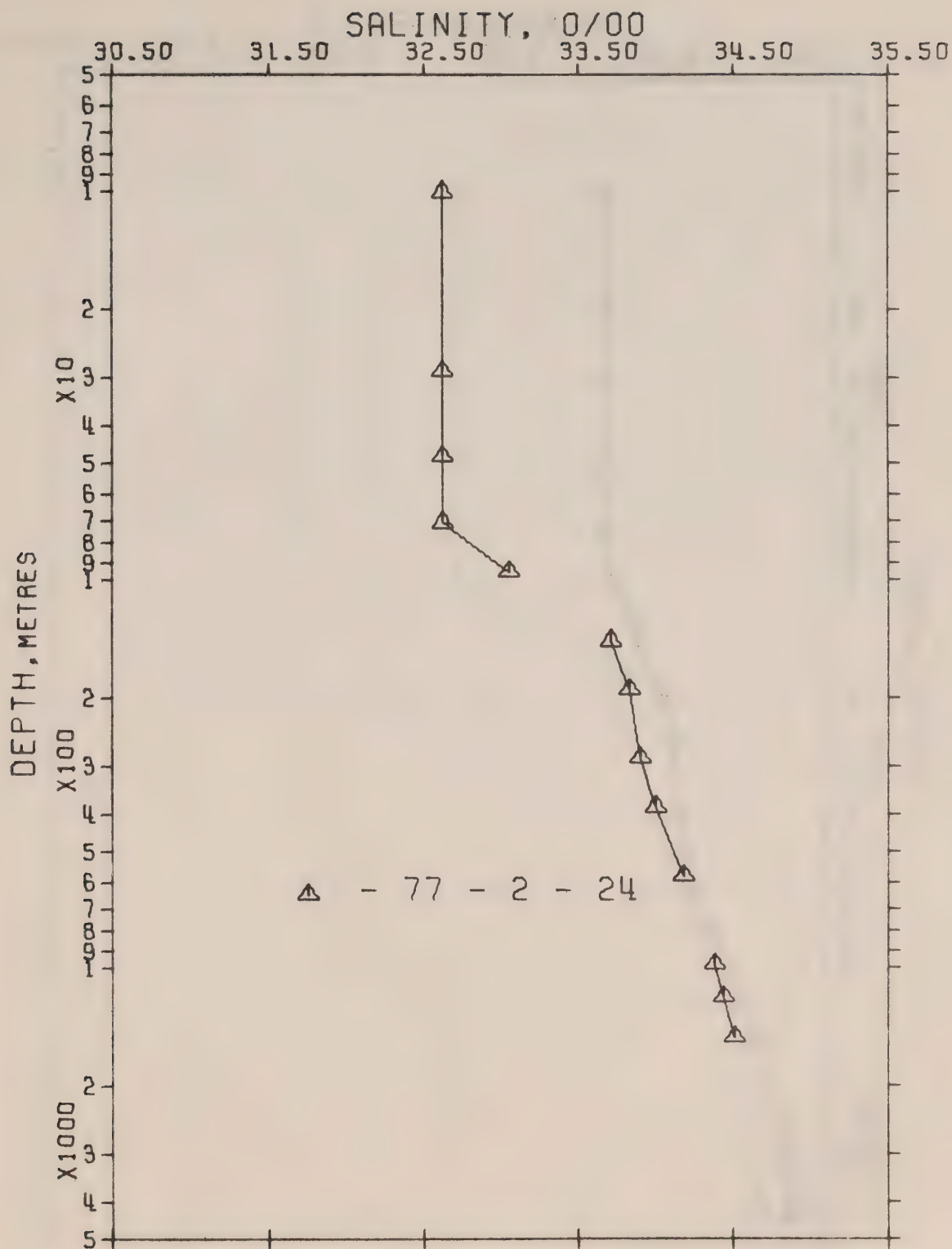


Figure 3. Composite plot of salinity vs \log_{10} depth for Line P stations. P-77-2.

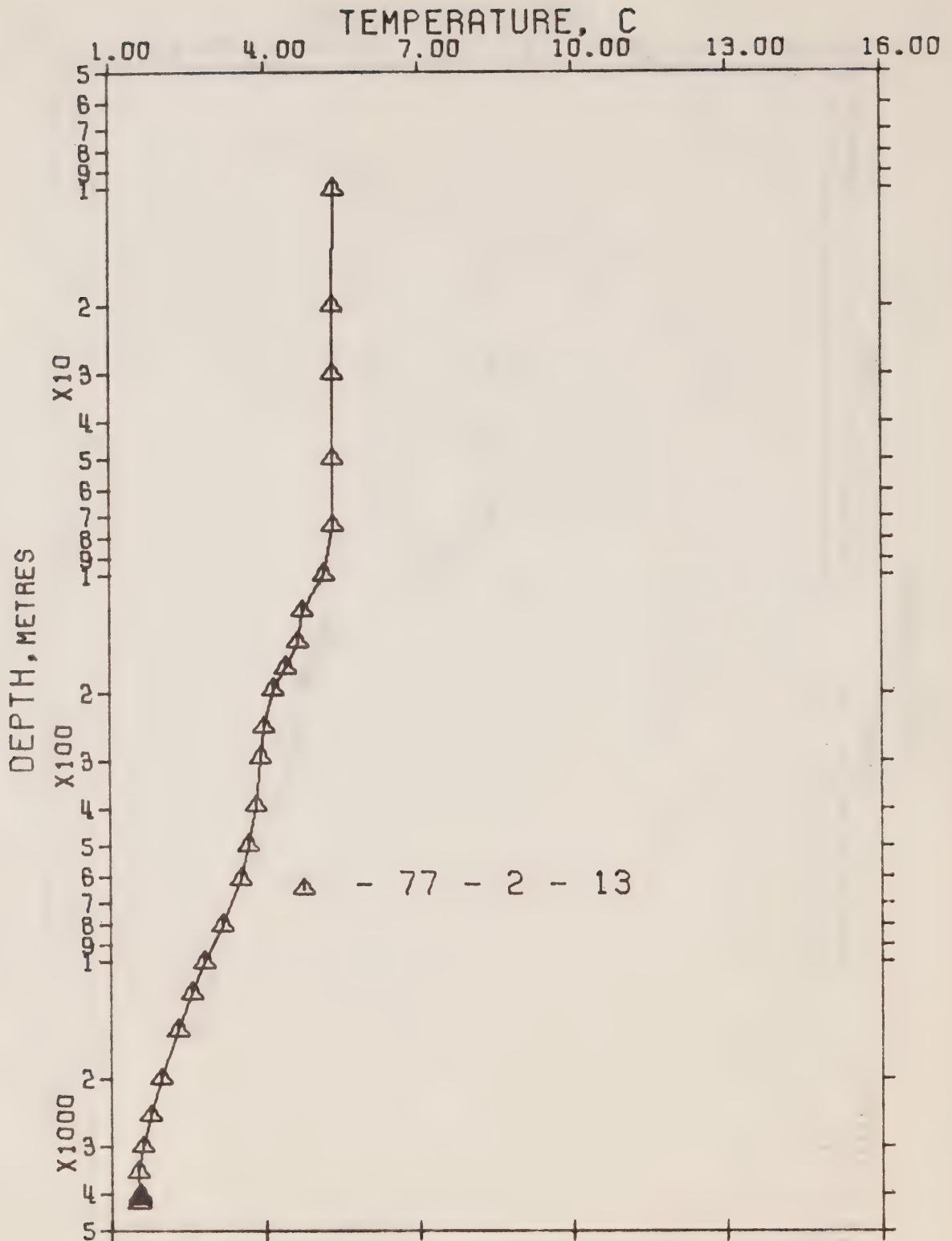


Figure 4. Composite plot of temperature vs \log_{10} depth for Station P. P-77-2.

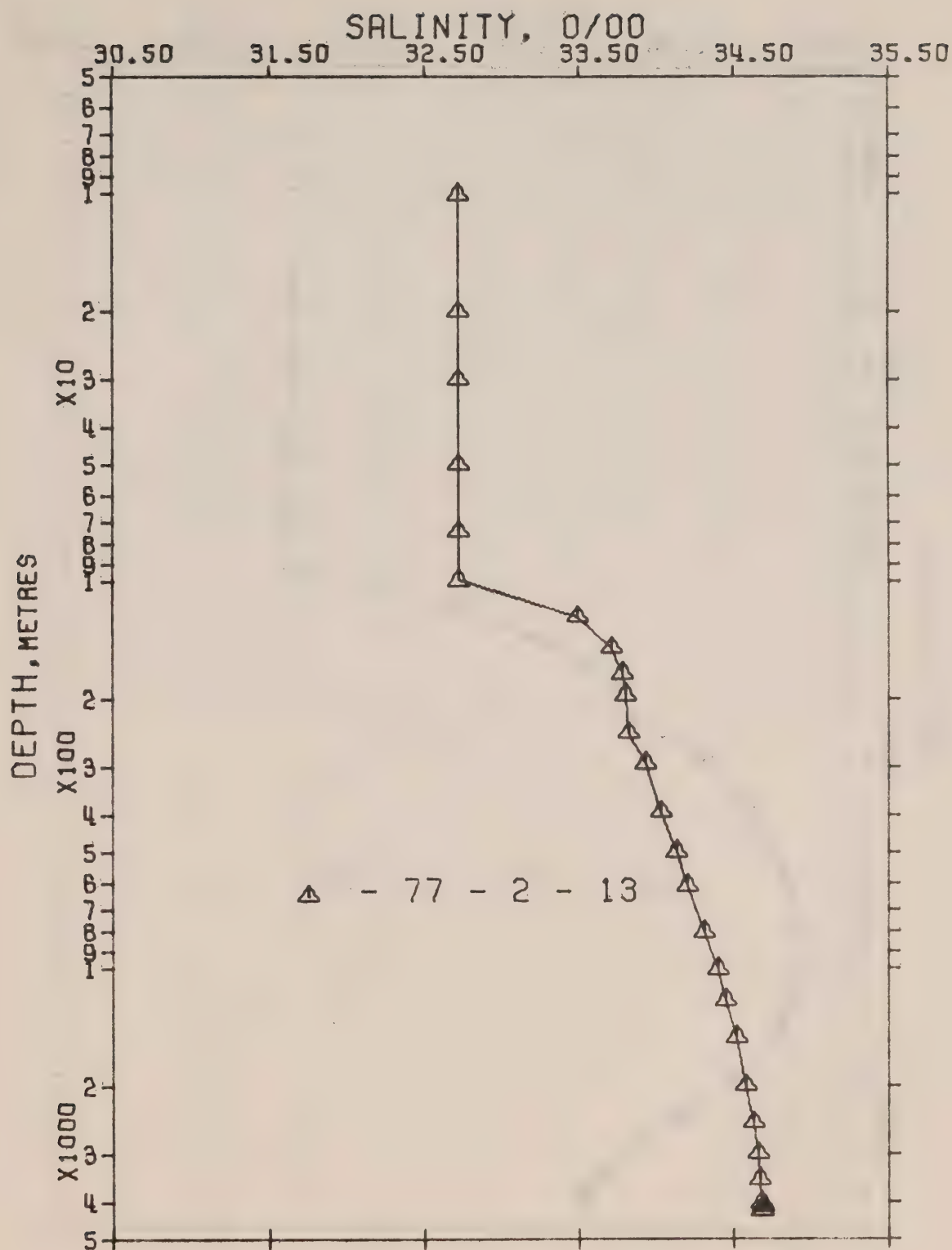
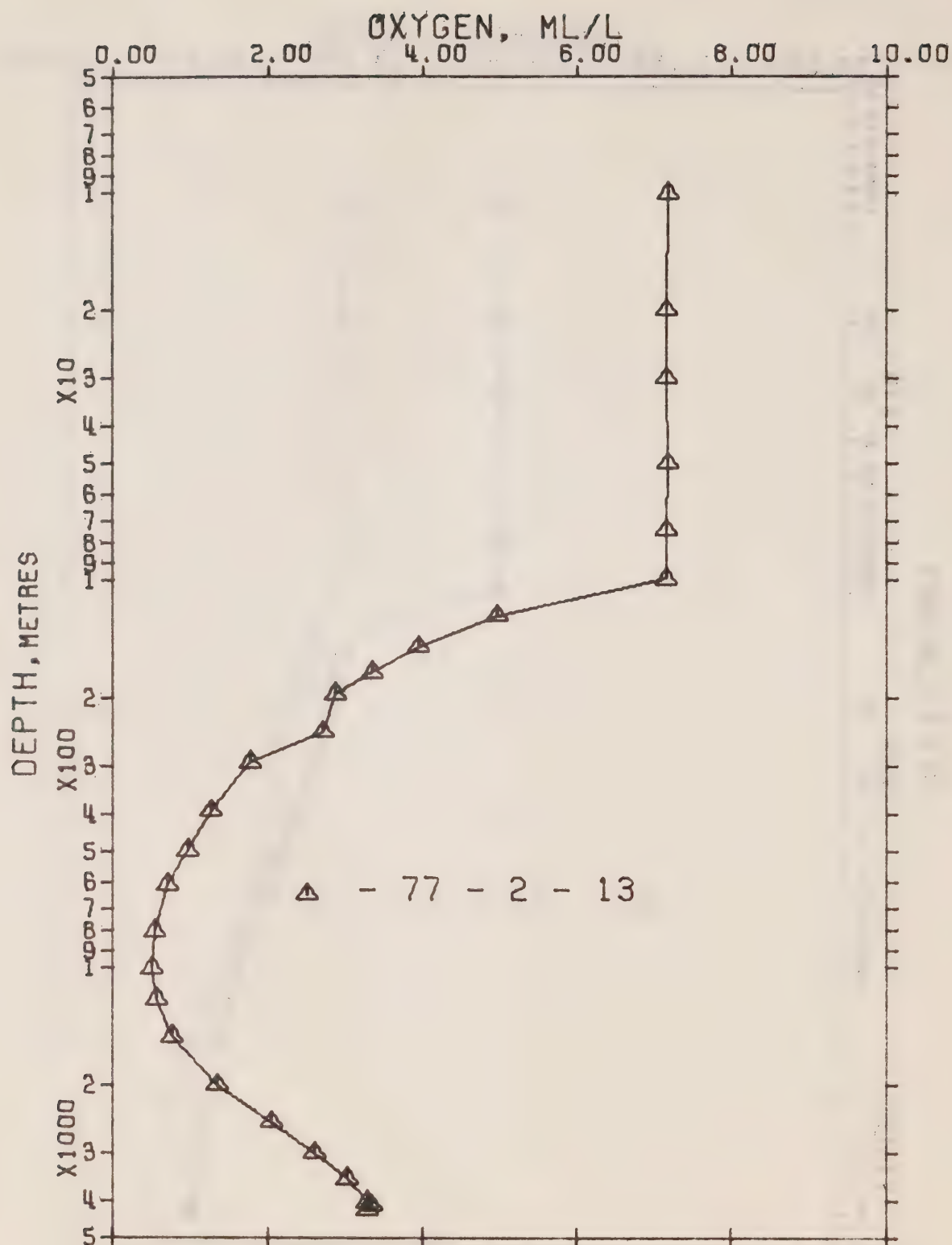
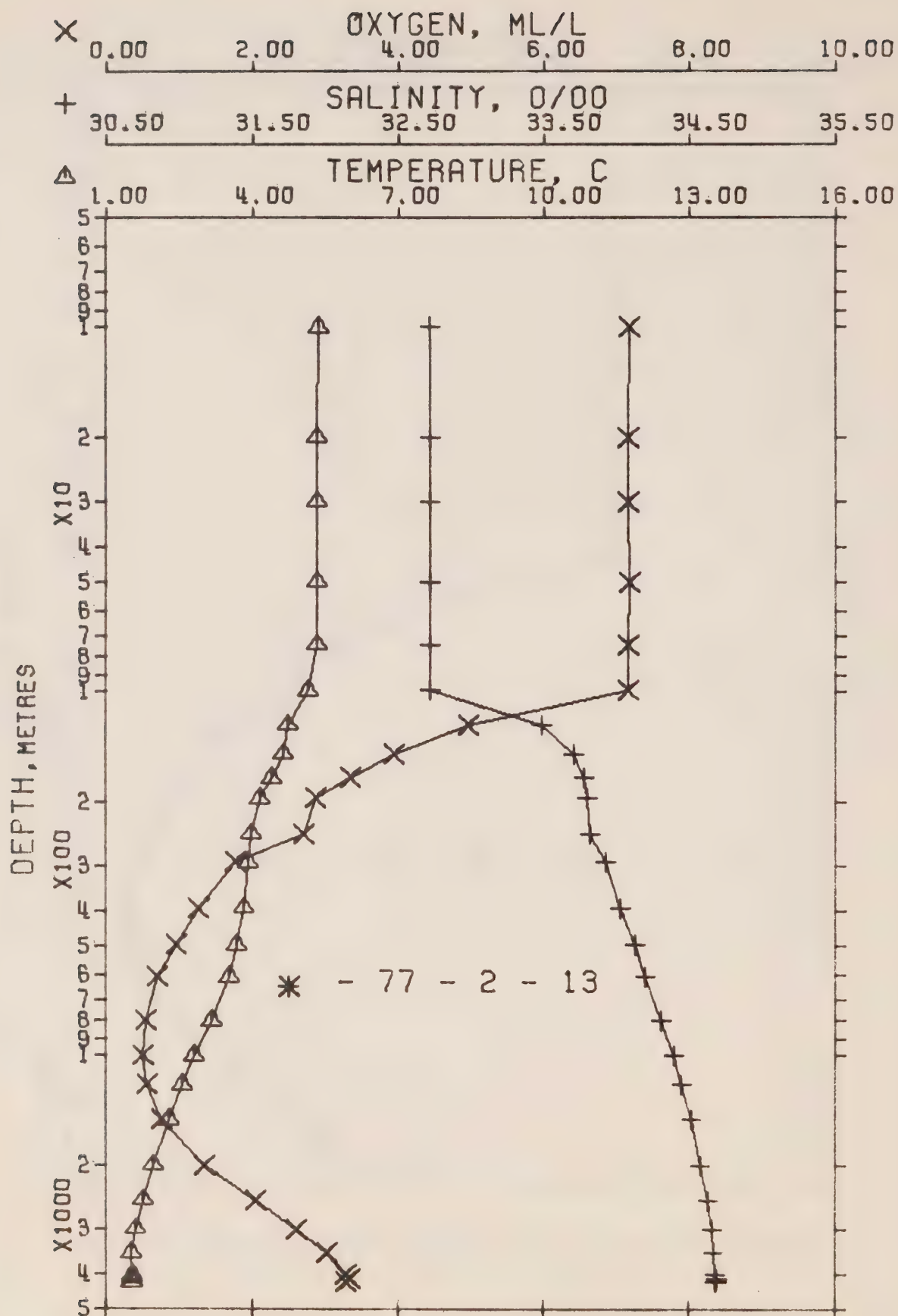


Figure 5. Composite plot of salinity vs \log_{10} depth for Station P. P-77-2.





OFFSHORE OCEANOGRAPHY GROUP

REFERENCE NO. 77- 2- 13

DATE 15/ 3/77

GMT 18.8

POSITION 50- .0 N, 145-

.0 W

STATION P

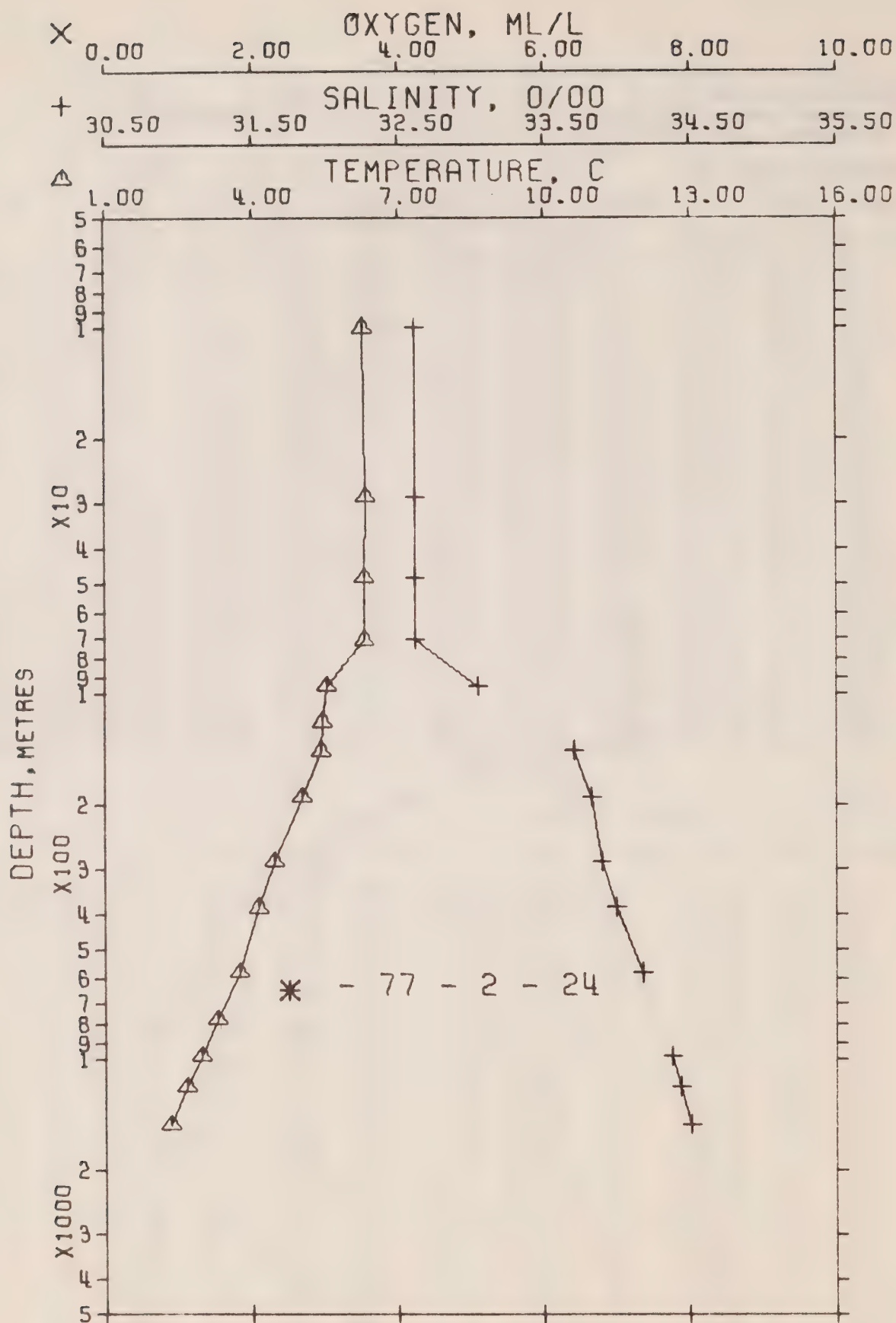
HYDROGRAPHIC CAST DATA

OBSERVED DATA

PRESS	TEMP	SAL	DEPTH	SIGMA T	SVA	THETA	SVA (THETA)	DELTA D	POT. EN	OXY	SOUND
0	5.36	32.718	0	25.852	215.7	5.36	215.7	.00	.00	7.21	1469.
10	5.34	32.719	10	25.855	215.5	5.34	215.4	.22	.01	7.18	1470.
20	5.33	32.719	20	25.856	215.5	5.33	215.2	.43	.04	7.16	1470.
30	5.32	32.718	30	25.856	215.5	5.32	215.2	.65	.10	7.17	1470.
50	5.31	32.721	50	25.860	215.4	5.31	214.9	1.08	.28	7.18	1470.
74	5.32	32.719	74	25.857	215.9	5.31	215.1	1.61	.61	7.16	1471.
100	5.15	32.719	99	25.876	214.2	5.14	213.2	2.16	1.11	7.15	1470.
124	4.71	33.495	123	26.539	151.6	4.70	150.3	2.61	1.61	4.96	1470.
149	4.62	33.713	148	26.721	134.6	4.61	133.0	2.96	2.11	3.94	1470.
173	4.38	33.781	172	26.801	127.1	4.37	125.4	3.28	2.63	3.35	1470.
197	4.14	33.801	196	26.842	123.4	4.13	121.5	3.58	3.20	2.87	1469.
247	3.97	33.817	245	26.872	120.8	3.95	118.6	4.19	4.56	2.70	1469.
296	3.91	33.931	294	26.969	112.1	3.89	109.5	4.76	6.15	1.75	1470.
396	3.81	34.031	393	27.058	104.4	3.78	100.9	5.84	9.96	1.26	1471.
501	3.68	34.129	497	27.149	96.5	3.64	92.2	6.89	14.77	.95	1473.
612	3.53	34.197	607	27.217	90.7	3.49	85.7	7.93	20.67	.70	1474.
807	3.16	34.313	800	27.345	79.5	3.10	73.5	9.59	32.63	.54	1476.
1011	2.81	34.399	1001	27.445	70.7	2.74	63.9	11.11	46.72	.50	1478.
1213	2.56	34.453	1201	27.510	65.1	2.48	57.7	12.48	62.25	.57	1480.
1518	2.29	34.517	1501	27.584	58.9	2.19	50.6	14.36	88.39	.75	1484.
2025	1.96	34.583	2000	27.663	52.3	1.82	42.8	17.19	139.28	1.34	1491.
2535	1.74	34.634	2501	27.721	47.6	1.56	37.1	19.73	198.33	2.05	1499.
3048	1.60	34.665	3003	27.756	45.1	1.37	33.5	22.09	265.68	2.61	1507.
3563	1.51	34.674	3507	27.770	44.6	1.23	31.9	24.40	343.33	3.02	1515.
4082	1.53	34.685	4013	27.777	45.4	1.20	30.8	26.73	434.12	3.27	1524.
4187	1.53	34.687	4115	27.779	45.6	1.19	30.6	27.20	454.21	3.33	1526.
4280	1.52	34.688	4206	27.780	45.6	1.16	30.4	27.62	472.34	3.28	1528.
4290	1.53	34.679 +	4216	27.772	46.4	1.17	31.1	27.67	474.40		1528.

INTERPOLATED TO STANDARD PRESSURE

PRESS	TEMP	SAL	DEPTH	SIGMA T	SVA	THETA	SVA (THETA)	DELTA D	POT. EN	OXY	SOUND
0	5.36	32.718	0	25.852	215.7	5.36	215.7	.00	.00	7.21	1469.
10	5.34	32.719	10	25.855	215.5	5.34	215.4	.22	.01	7.18	1470.
20	5.33	32.719	20	25.856	215.5	5.33	215.2	.43	.04	7.16	1470.
30	5.32	32.718	30	25.856	215.5	5.32	215.2	.65	.10	7.17	1470.
50	5.31	32.721	50	25.860	215.4	5.31	214.9	1.08	.28	7.18	1470.
75	5.32	32.719	75	25.858	215.8	5.31	215.0	1.62	.62	7.16	1470.
100	5.15	32.719	99	25.876	214.2	5.14	213.2	2.16	1.11	7.15	1470.
125	4.71	33.506	124	26.548	150.7	4.70	149.5	2.62	1.63	4.91	1470.
150	4.61	33.716	149	26.725	134.2	4.60	132.7	2.98	2.13	3.92	1470.
175	4.36	33.783	174	26.804	126.8	4.35	125.1	3.30	2.67	3.31	1470.
200	4.13	33.802	199	26.844	123.2	4.12	121.4	3.62	3.26	2.86	1469.
225	4.04	33.810	223	26.860	121.9	4.02	119.8	3.92	3.93	2.77	1469.
250	3.97	33.825	248	26.879	120.2	3.95	118.0	4.23	4.66	2.63	1469.
300	3.91	33.935	298	26.972	111.8	3.88	109.1	4.80	6.28	1.73	1470.
400	3.80	34.035	397	27.062	104.1	3.78	100.6	5.88	10.12	1.25	1471.
500	3.68	34.128	496	27.148	96.6	3.65	92.3	6.88	14.71	.96	1473.
600	3.55	34.190	595	27.210	91.3	3.50	86.3	7.82	19.98	.73	1474.
700	3.35	34.253	694	27.279	85.3	3.30	79.8	8.71	25.83	.63	1475.
800	3.17	34.309	793	27.341	79.9	3.12	73.9	9.53	32.14	.55	1476.
900	2.99	34.355	891	27.393	75.2	2.93	68.9	10.31	38.85	.52	1476.
1000	2.83	34.395	990	27.440	71.1	2.76	64.4	11.04	45.93	.50	1477.
1200	2.58	34.450	1188	27.506	65.4	2.49	58.1	12.40	61.16	.56	1480.
1500	2.30	34.514	1483	27.580	59.2	2.20	50.9	14.26	86.78	.74	1484.
2000	1.97	34.580	1975	27.660	52.6	1.84	43.2	17.06	136.60	1.32	1491.
2500	1.75	34.631	2466	27.717	47.9	1.58	37.5	19.56	194.02	2.00	1498.
3000	1.61	34.662	2955	27.753	45.3	1.39	33.8	21.88	259.05	2.56	1506.
3500	1.52	34.673	3444	27.768	44.6	1.25	32.1	24.12	333.18	2.97	1514.
4000	1.53	34.683	3931	27.776	45.3	1.20	31.0	26.35	418.79	3.23	1523.
4100	1.53	34.685	4031	27.777	45.5	1.19	30.8	26.81	437.53	3.28	1525.
4200	1.53	34.687	4128	27.779	45.6	1.18	30.6	27.26	456.79	3.33	1526.



OFFSHORE OCEANOGRAPHY GROUP

REFERENCE NO. 77- 2- 24

DATE 28/ 3/77

GMT 20.4

POSITION 49-34.0 N, 138-40.0 W

STATION 10

HYDROGRAPHIC CAST DATA

OBSERVED DATA

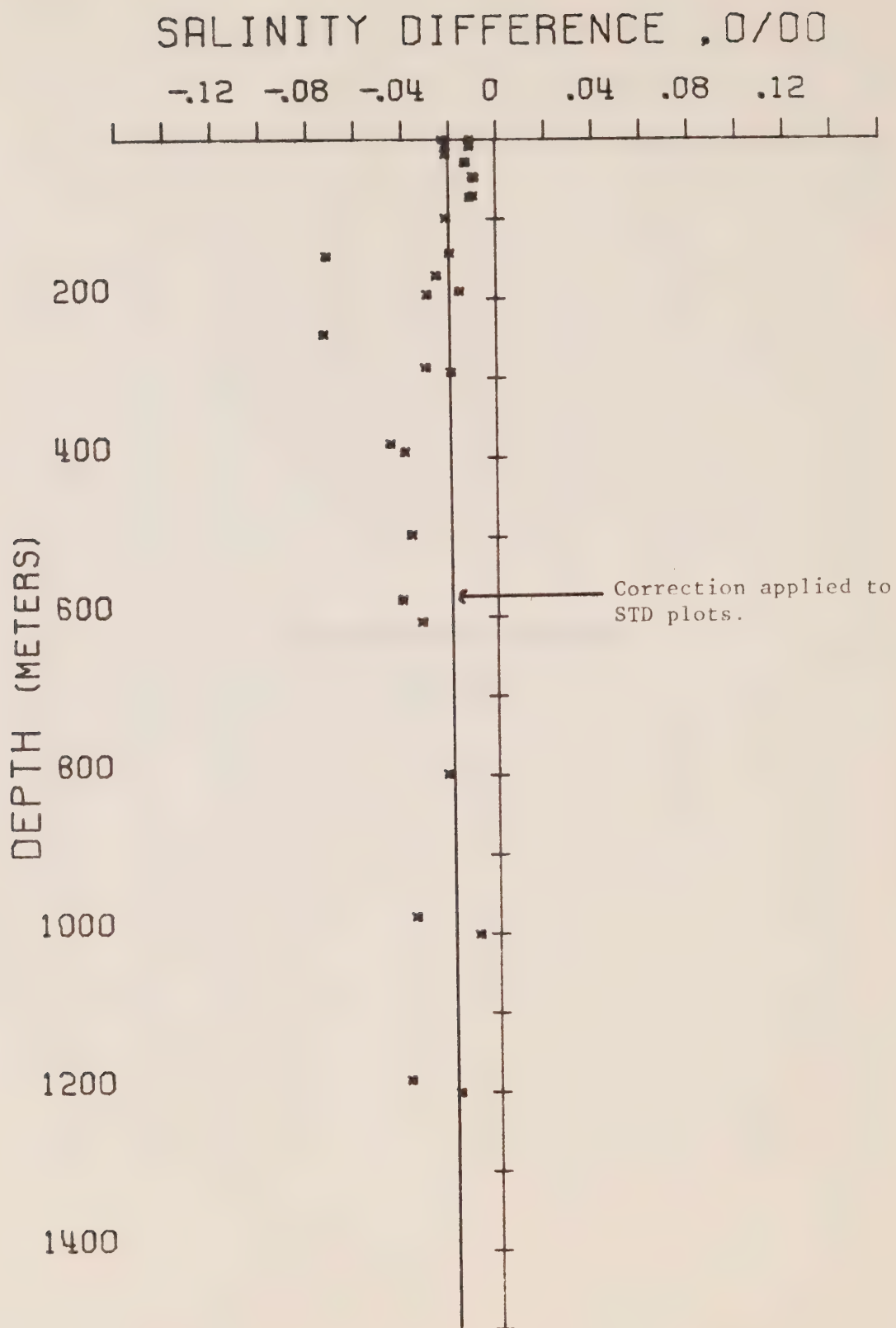
PRESS	TEMP	SAL	DEPTH	SIGMA T	SVA	THETA	SVA (THETA)	DELTA D	POT. EN	OXY	SOUND
0	6.36	32.619	0	25.653	234.6	6.36	234.6	.00	.00		1473.
10	6.29	32.619	10	25.662	233.9	6.29	233.7	.24	.01		1473.
29	6.33	32.617	29	25.655	234.7	6.33	234.3	.68	.10		1474.
48	6.32	32.620	48	25.659	234.6	6.32	234.0	1.13	.28		1474.
71	6.32	32.620	71	25.659	234.9	6.31	234.0	1.69	.62		1474.
96	5.54	33.055	95	26.097	193.4	5.53	192.3	2.20	1.06		1472.
120	5.44	33.415*	119	26.393	165.6	5.43	164.2	2.63	1.53		1473.
144	5.41	33.710	143	26.629	143.5	5.40	141.8	3.01	2.03		1473.
192	5.02	33.834	191	26.772	130.3	5.00	128.1	3.67	3.16		1473.
289	4.46	33.897	287	26.884	120.4	4.44	117.4	4.88	6.12		1472.
387	4.12	33.997	384	26.999	110.1	4.09	106.5	6.00	10.00		1472.
584	3.73	34.177	579	27.182	94.1	3.69	89.0	8.00	19.35		1474.
784	3.27	34.288 *	777	27.315	82.4	3.22	76.3	9.76	32.09		1476.
988	2.96	34.376	979	27.413	73.9	2.89	66.9	11.36	46.46		1478.
1198	2.66	34.440	1186	27.491	67.1	2.58	59.5	12.83	62.86		1480.
1522	2.33	34.511	1505	27.576	59.8	2.23	51.3	14.87	91.20		1484.

INTERPOLATED TO STANDARD PRESSURE

PRESS	TEMP	SAL	DEPTH	SIGMA T	SVA	THETA	SVA (THETA)	DELTA D	POT. EN	OXY	SOUND
0	6.36	32.619	0	25.653	234.6	6.36	234.6	.00	.00		1473.
10	6.29	32.619	10	25.662	233.9	6.29	233.7	.24	.01		1473.
20	6.32	32.618	22	25.657	234.4	6.31	234.1	.47	.05		1474.
30	6.33	32.617	30	25.655	234.7	6.33	234.3	.70	.11		1474.
50	6.32	32.620	50	25.659	234.6	6.32	234.0	1.17	.30		1474.
75	6.19	32.692	75	25.732	227.9	6.18	227.0	1.77	.68		1474.
100	5.52	33.127	99	26.155	187.9	5.51	186.7	2.29	1.14		1472.
125	5.43	33.464	124	26.447	160.5	5.42	159.0	2.72	1.64		1473.
150	5.35	33.728	149	26.649	141.6	5.34	139.8	3.09	2.16		1473.
175	5.15	33.794	174	26.725	134.6	5.13	132.6	3.44	2.73		1473.
200	4.97	33.840	199	26.783	129.4	4.95	127.1	3.77	3.36		1473.
225	4.80	33.858	224	26.816	126.4	4.79	124.0	4.09	4.05		1472.
250	4.66	33.874	248	26.845	123.9	4.64	121.2	4.40	4.81		1472.
300	4.42	33.910	298	26.899	119.1	4.39	116.0	5.01	6.51		1472.
400	4.09	34.011	397	27.014	108.8	4.06	105.1	6.15	10.57		1472.
500	3.88	34.109	496	27.113	100.1	3.84	95.6	7.19	15.35		1473.
600	3.69	34.187	595	27.194	93.0	3.64	87.9	8.15	20.76		1474.
700	3.45	34.246	694	27.264	86.9	3.40	81.2	9.05	26.71		1475.
800	3.24	34.296	793	27.324	81.6	3.19	75.5	9.89	33.14		1476.
900	3.09	34.341	892	27.374	77.3	3.02	70.7	10.69	40.02		1477.
1000	2.94	34.380	991	27.418	73.5	2.87	66.5	11.44	47.32		1478.
1200	2.66	34.440	1188	27.491	67.0	2.58	59.4	12.84	63.00		1480.
1500	2.35	34.507	1483	27.571	60.2	2.25	51.8	14.74	89.20		1484.

Results of STD Observations

(P-77-2)



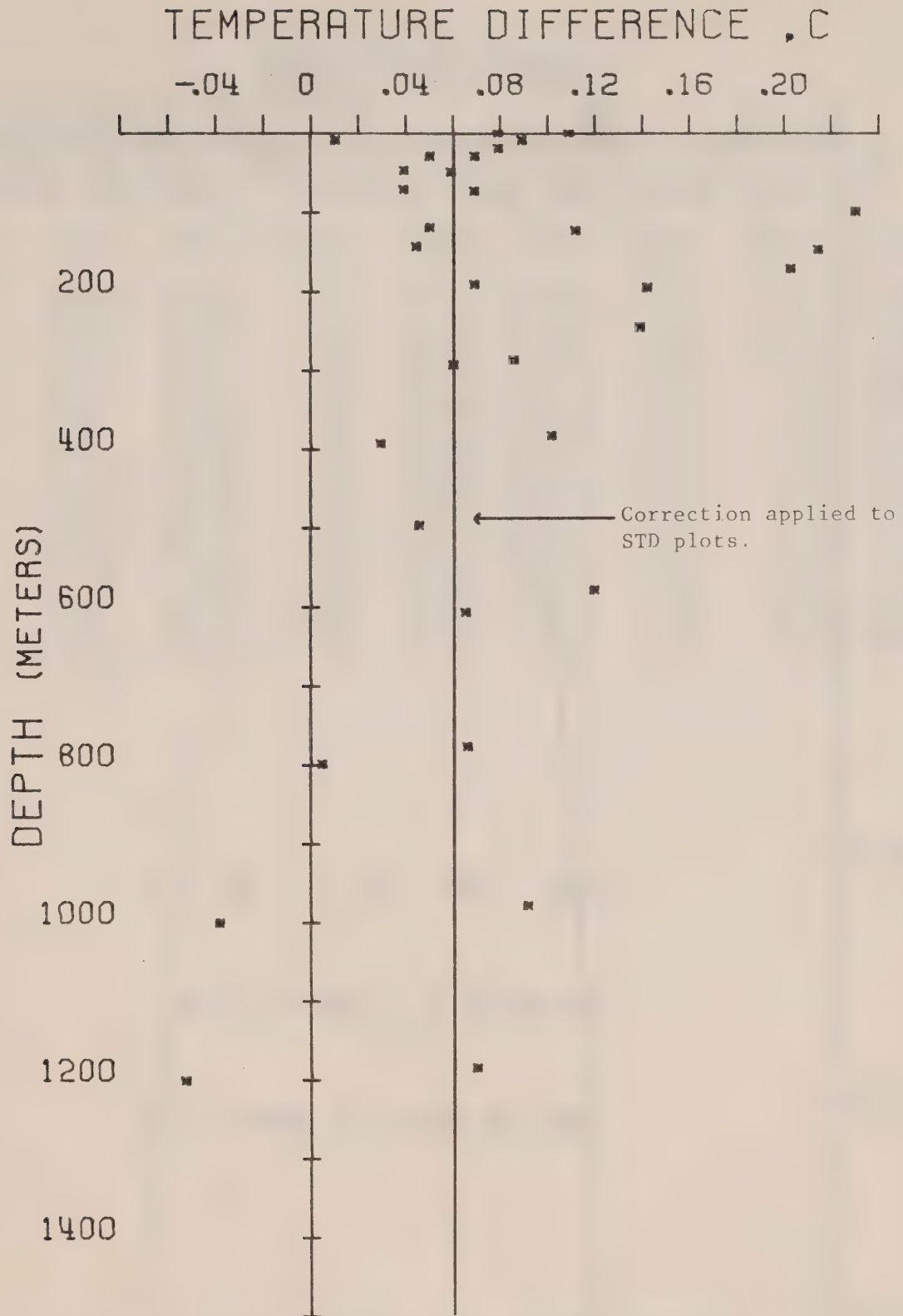
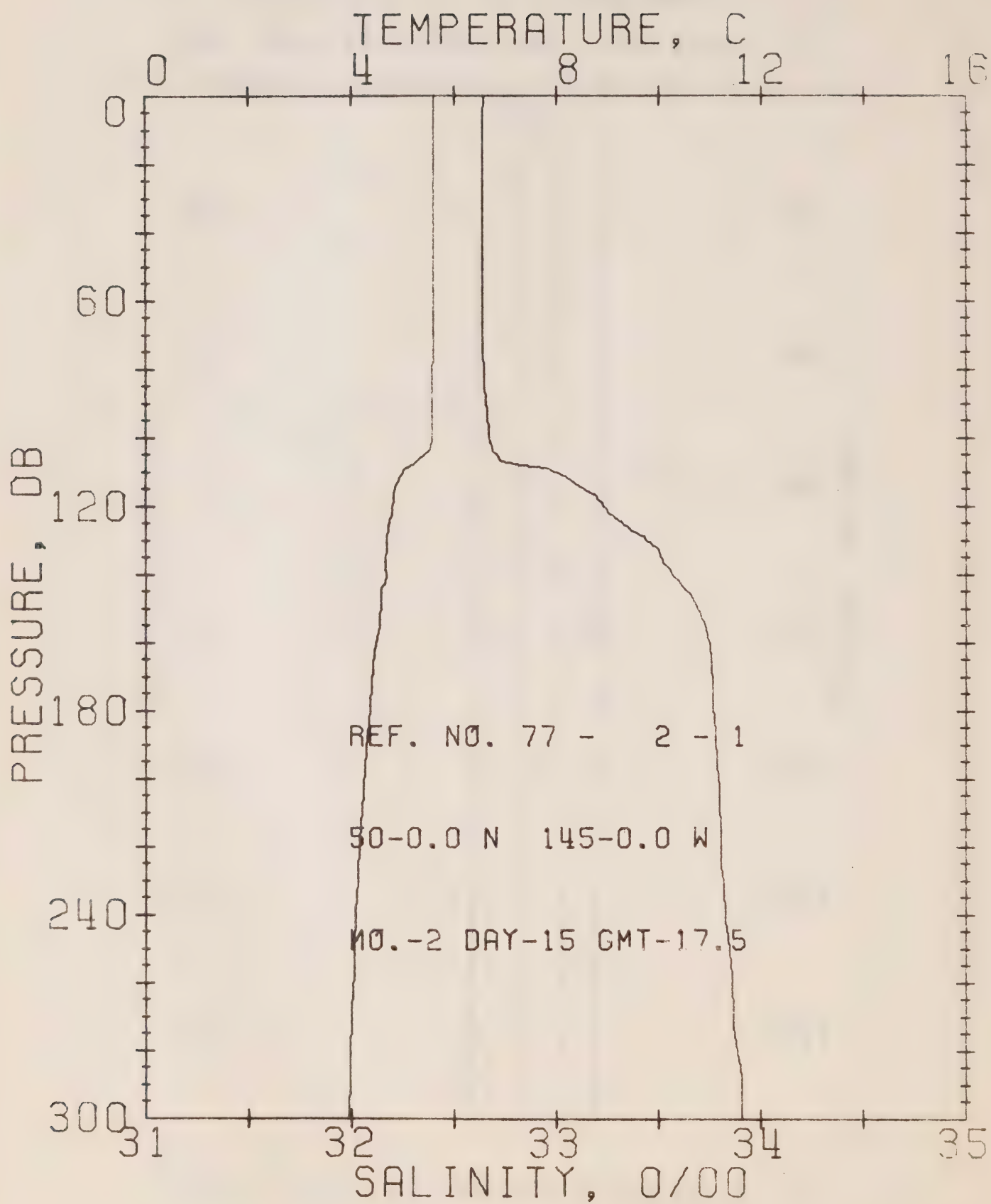


Figure 8. Temperature difference between hydro data and STD.
P-77-2.



OFFSHORE OCEANOGRAPHY GROUP

REFERENCE NO. 77- 2- 1

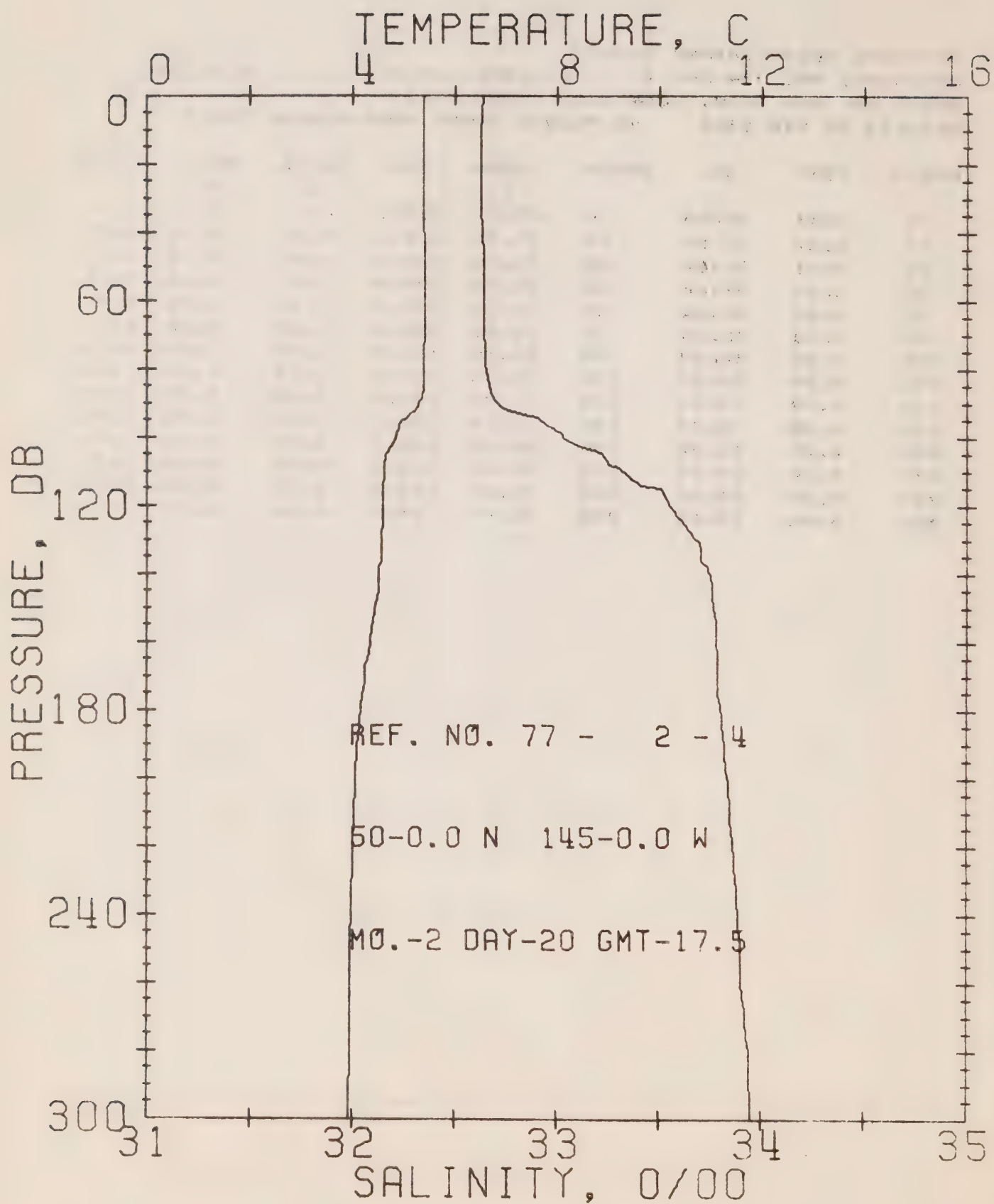
DATE 15/ 2/77

STATION P

POSITION 50- 0.0N, 145- 0.0W GMT 17.5

RESULTS OF STP CAST 82 POINTS TAKEN FROM ANALOG TRACE

PRESS	TEMP	SAL	DEPTH	SIGMA T	SVA	DELTA D	POT. EN	SOUND
0	5.61	32.65	0	25.77	223.5	0.0	0.0	1470.
10	5.61	32.64	10	25.76	224.5	0.22	0.01	1471.
20	5.61	32.64	20	25.76	224.6	0.45	0.05	1471.
30	5.61	32.64	30	25.76	224.8	0.67	0.10	1471.
50	5.61	32.64	50	25.76	225.0	1.12	0.29	1471.
75	5.59	32.64	75	25.77	224.9	1.69	0.64	1472.
100	5.56	32.67	99	25.79	222.7	2.25	1.14	1472.
125	4.74	33.32	124	26.40	164.8	2.73	1.69	1470.
150	4.58	33.69	149	26.71	135.9	3.10	2.21	1470.
175	4.39	33.77	174	26.79	128.3	3.42	2.75	1470.
200	4.25	33.80	199	26.83	125.1	3.74	3.35	1470.
225	4.14	33.81	223	26.85	123.1	4.05	4.03	1470.
250	4.05	33.85	248	26.89	119.5	4.35	4.76	1470.
300	3.96	33.91	298	26.95	114.3	4.94	6.39	1470.



OFFSHORE OCEANOGRAPHY GROUP

REFERENCE NO. 77- 2- 4

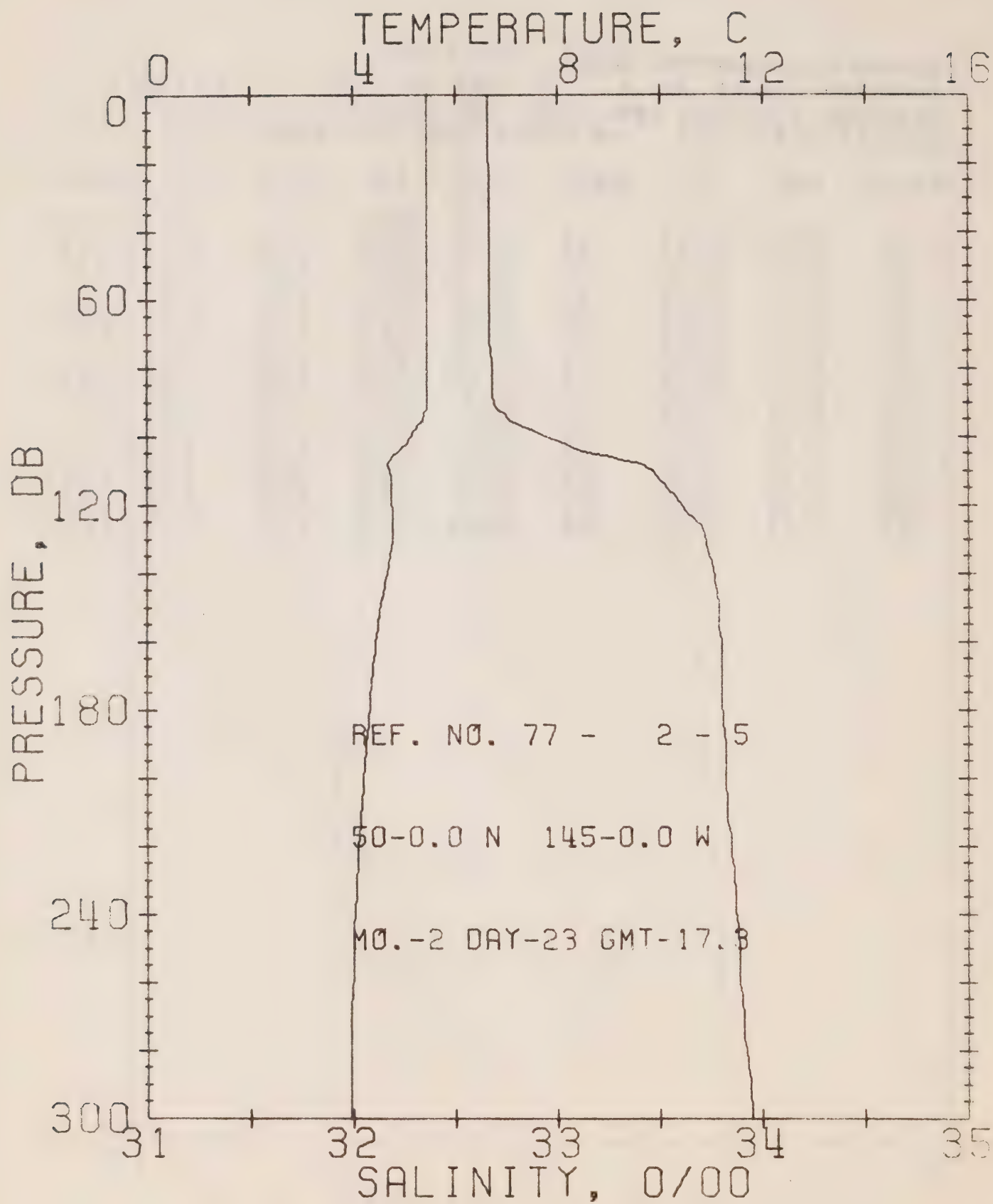
DATE 20/ 2/77

STATION P

POSITION 50- 0.0N, 145- 0.0W GMT 17.5

RESULTS OF STP CAST 94 POINTS TAKEN FROM ANALOG TRACE

PRESS	TEMP	SAL	DEPTH	SIGMA T	SVA	DELTA D	POT. EN	SOUND
0	5.40	32.64	0	25.79	222.0	0.0	0.0	1470.
10	5.40	32.63	10	25.78	222.9	0.22	0.01	1470.
20	5.40	32.63	20	25.78	223.1	0.45	0.05	1470.
30	5.40	32.63	30	25.78	223.2	0.67	0.10	1470.
50	5.41	32.64	50	25.79	222.8	1.11	0.28	1470.
75	5.40	32.65	75	25.79	222.2	1.67	0.64	1471.
100	4.84	33.03	99	26.16	187.8	2.20	1.11	1469.
125	4.59	33.62	124	26.65	140.9	2.60	1.57	1469.
150	4.43	33.77	149	26.79	128.4	2.94	2.03	1469.
175	4.19	33.79	174	26.83	124.6	3.25	2.55	1469.
200	4.05	33.84	199	26.88	119.9	3.56	3.14	1469.
225	4.00	33.87	223	26.91	117.1	3.85	3.78	1469.
250	3.95	33.90	248	26.94	114.5	4.14	4.48	1469.
300	3.93	33.95	298	26.98	111.0	4.71	6.06	1470.



OFFSHORE OCEANOGRAPHY GROUP

REFERENCE NO. 77- 2- 5

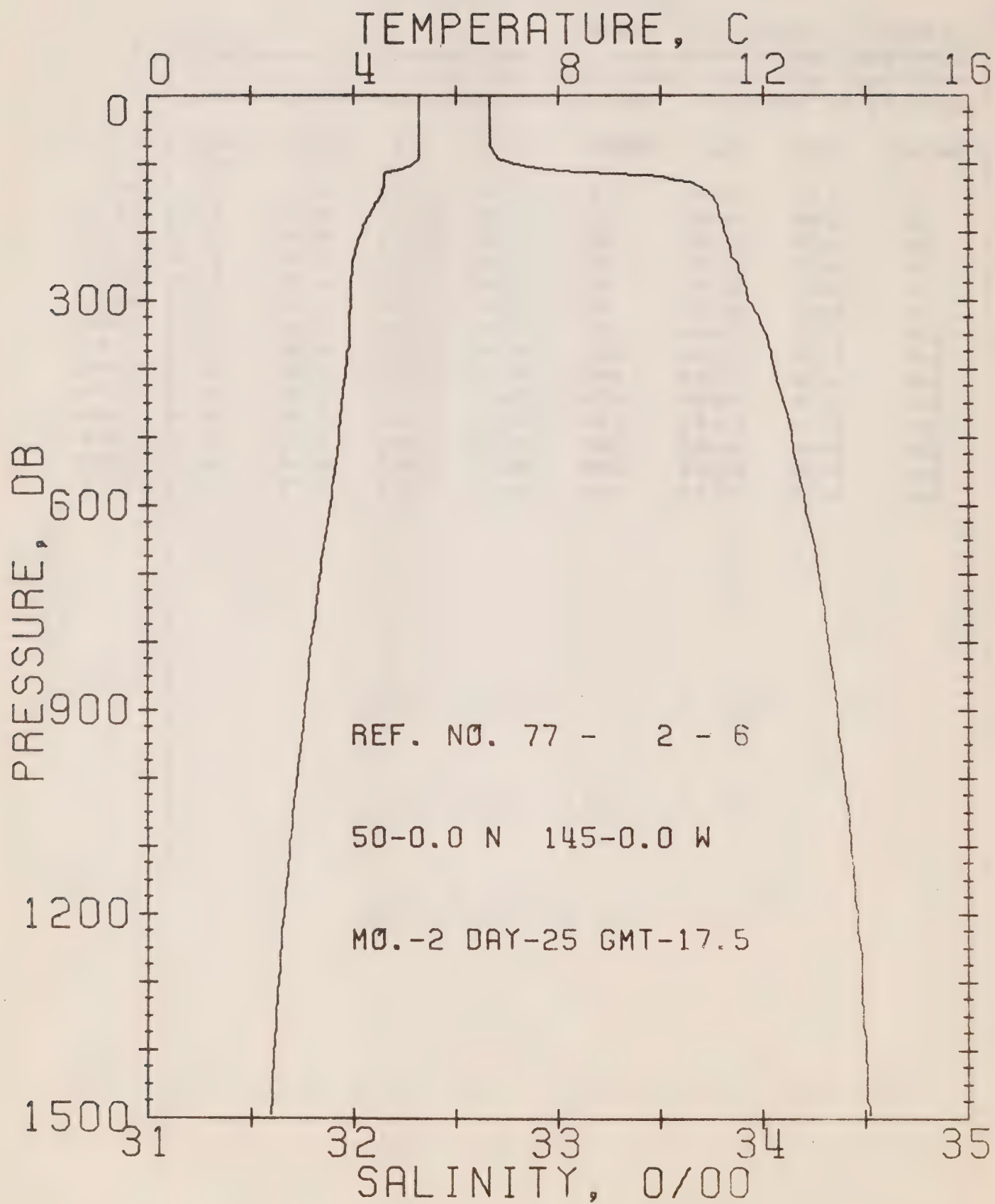
DATE 23/ 2/77

STATION P

POSITION 50- 0.0N, 145- 0.0W GMT 17.3

RESULTS OF STP CAST 106 POINTS TAKEN FROM ANALOG TRACE

PRESS	TEMP	SAL	DEPTH	SIGMA T	SVA	DELTA D	POT. EN	SOUND
0	5.45	32.66	0	25.80	221.0	0.0	0.0	1470.
10	5.45	32.66	10	25.80	221.3	0.22	0.01	1470.
20	5.45	32.66	20	25.80	221.1	0.44	0.05	1470.
30	5.45	32.67	30	25.80	220.8	0.66	0.10	1470.
50	5.45	32.67	50	25.80	221.0	1.10	0.28	1471.
75	5.44	32.67	75	25.81	220.8	1.66	0.63	1471.
100	5.11	32.94	99	26.06	197.4	2.20	1.12	1470.
125	4.77	33.68	124	26.68	138.2	2.60	1.57	1470.
150	4.52	33.79	149	26.79	127.8	2.93	2.03	1470.
175	4.34	33.80	174	26.82	125.3	3.24	2.55	1470.
200	4.19	33.82	199	26.85	122.6	3.55	3.14	1469.
225	4.07	33.85	223	26.89	119.0	3.85	3.80	1469.
250	3.99	33.89	248	26.93	115.7	4.15	4.51	1469.
300	3.95	33.95	298	26.98	111.2	4.72	6.10	1470.



OFFSHORE OCEANOGRAPHY GROUP

REFERENCE NO. 77- 2- 6

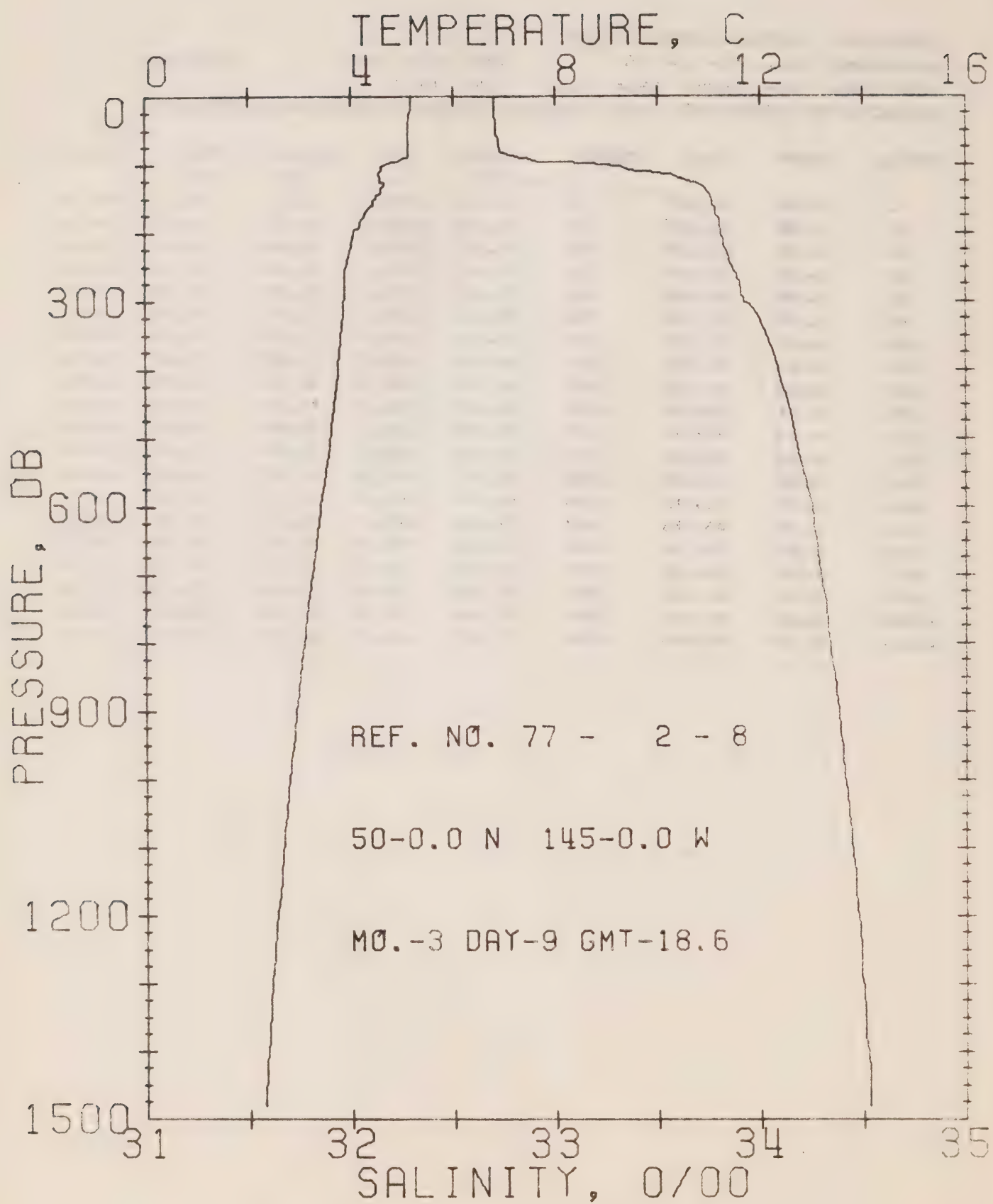
DATE 25/ 2/77

STATION P

POSITION 50- 0.0N, 145- 0.0W GMT 17.5

RESULTS OF STP CAST 172 POINTS TAKEN FROM ANALOG TRACE

PRESS	TEMP	SAL	DEPTH	SIGMA T	SVA	DELTA D	POT. EN	SOUND
0	5.28	32.67	0	25.82	218.3	0.0	0.0	1469.
10	5.28	32.67	10	25.82	218.7	0.22	0.01	1469.
20	5.28	32.67	20	25.82	218.7	0.44	0.04	1469.
30	5.29	32.67	30	25.82	218.9	0.66	0.10	1470.
50	5.29	32.67	50	25.82	219.1	1.09	0.28	1470.
75	5.29	32.67	75	25.82	219.4	1.64	0.63	1470.
100	5.18	32.79	99	25.93	209.5	2.18	1.11	1470.
125	4.60	33.60	124	26.64	142.7	2.63	1.61	1470.
150	4.50	33.75	149	26.77	130.4	2.96	2.08	1470.
175	4.31	33.79	174	26.82	125.9	3.28	2.61	1469.
200	4.14	33.81	199	26.85	122.8	3.59	3.20	1469.
225	4.03	33.84	223	26.89	119.6	3.89	3.86	1469.
250	3.98	33.88	248	26.92	116.3	4.19	4.57	1469.
300	3.94	33.93	298	26.97	112.6	4.76	6.17	1470.
400	3.84	34.05	397	27.08	103.1	5.83	9.98	1471.
500	3.70	34.14	496	27.16	95.9	6.82	14.52	1473.
600	3.54	34.21	595	27.23	90.1	7.75	19.74	1474.
800	3.17	34.32	793	27.35	79.5	9.44	31.72	1476.
1000	2.89	34.40	990	27.44	71.8	10.94	45.53	1478.
1200	2.63	34.46	1188	27.51	65.3	12.31	60.85	1480.



OFFSHORE OCEANOGRAPHY GROUP

REFERENCE NO. 77- 2- B

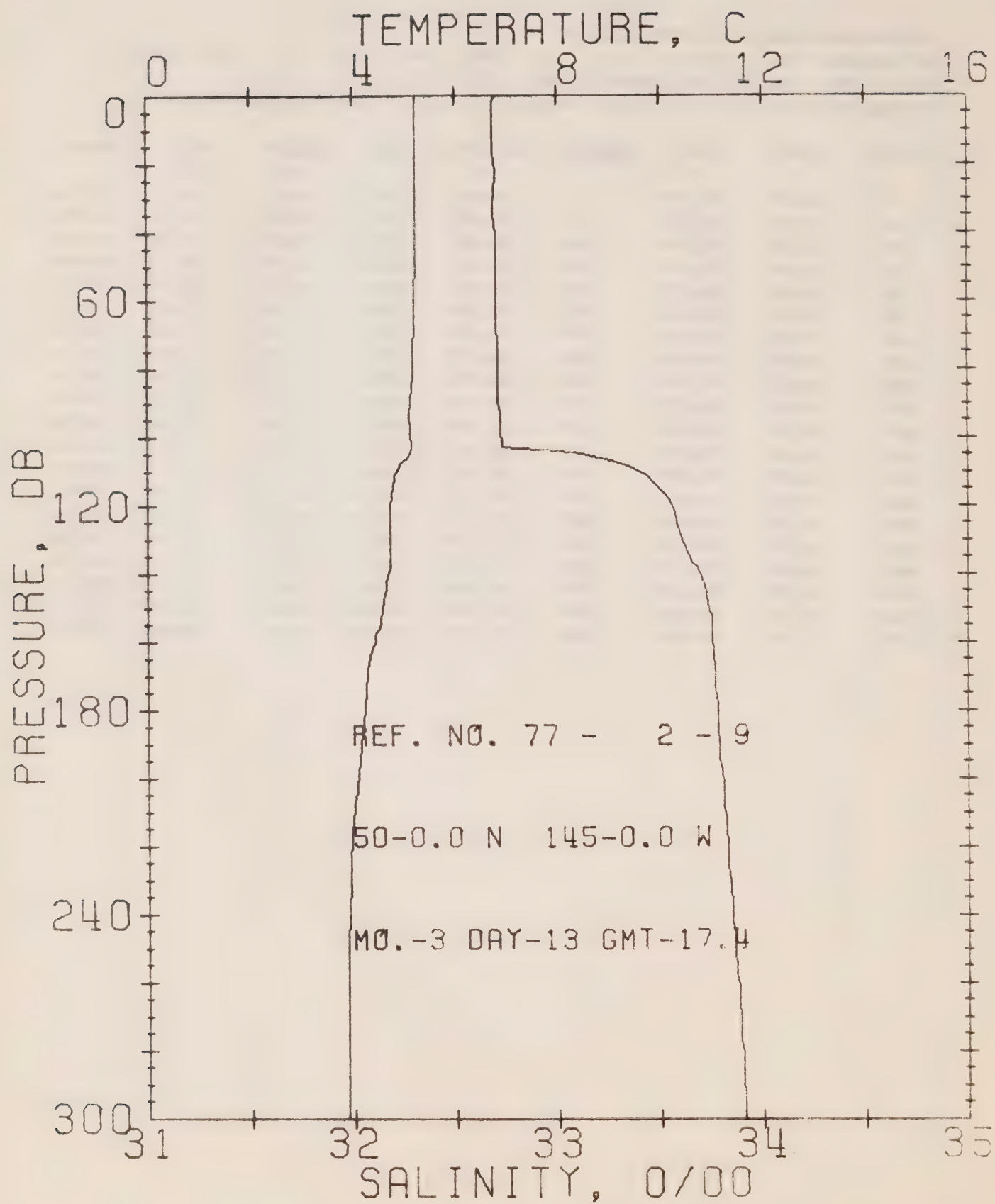
DATE 9/ 3/77

STATION P

POSITION 50- 0.0N, 145- 0.0W GMT 18.6

RESULTS OF STP CAST 203 POINTS TAKEN FROM ANALOG TRACE

PRESS	TEMP	SAL	DEPTH	SIGMA T	SVA	DELTA D	POT. EN	SOUND
0	5.17	32.70	0	25.86	214.9	0.0	0.0	1469.
10	5.17	32.70	10	25.86	215.2	0.22	0.01	1469.
20	5.16	32.70	20	25.86	215.3	0.43	0.04	1469.
30	5.15	32.70	30	25.86	215.2	0.65	0.10	1469.
50	5.12	32.71	50	25.87	214.3	1.07	0.27	1469.
75	5.11	32.72	75	25.89	213.4	1.61	0.61	1470.
100	4.65	33.25	99	26.35	169.3	2.12	1.07	1469.
125	4.55	33.67	124	26.70	136.9	2.50	1.50	1469.
150	4.49	33.76	149	26.77	129.8	2.83	1.96	1470.
175	4.23	33.79	174	26.83	125.0	3.15	2.49	1469.
200	4.04	33.81	199	26.86	121.7	3.46	3.08	1469.
225	3.98	33.83	223	26.88	119.7	3.76	3.74	1469.
250	3.89	33.86	248	26.92	116.7	4.05	4.45	1469.
300	3.85	33.92	298	26.97	112.4	4.63	6.05	1470.
400	3.73	34.09	397	27.11	99.3	5.67	9.77	1471.
500	3.59	34.17	496	27.19	92.4	6.63	14.15	1472.
600	3.40	34.25	595	27.27	85.3	7.52	19.12	1473.
800	3.07	34.34	793	27.38	76.7	9.13	30.64	1475.
1000	2.78	34.41	990	27.46	69.4	10.59	43.97	1477.
1200	2.53	34.47	1188	27.53	63.3	11.91	58.80	1480.



OFFSHORE OCEANOGRAPHY GROUP

REFERENCE NO. 77- 2- 9

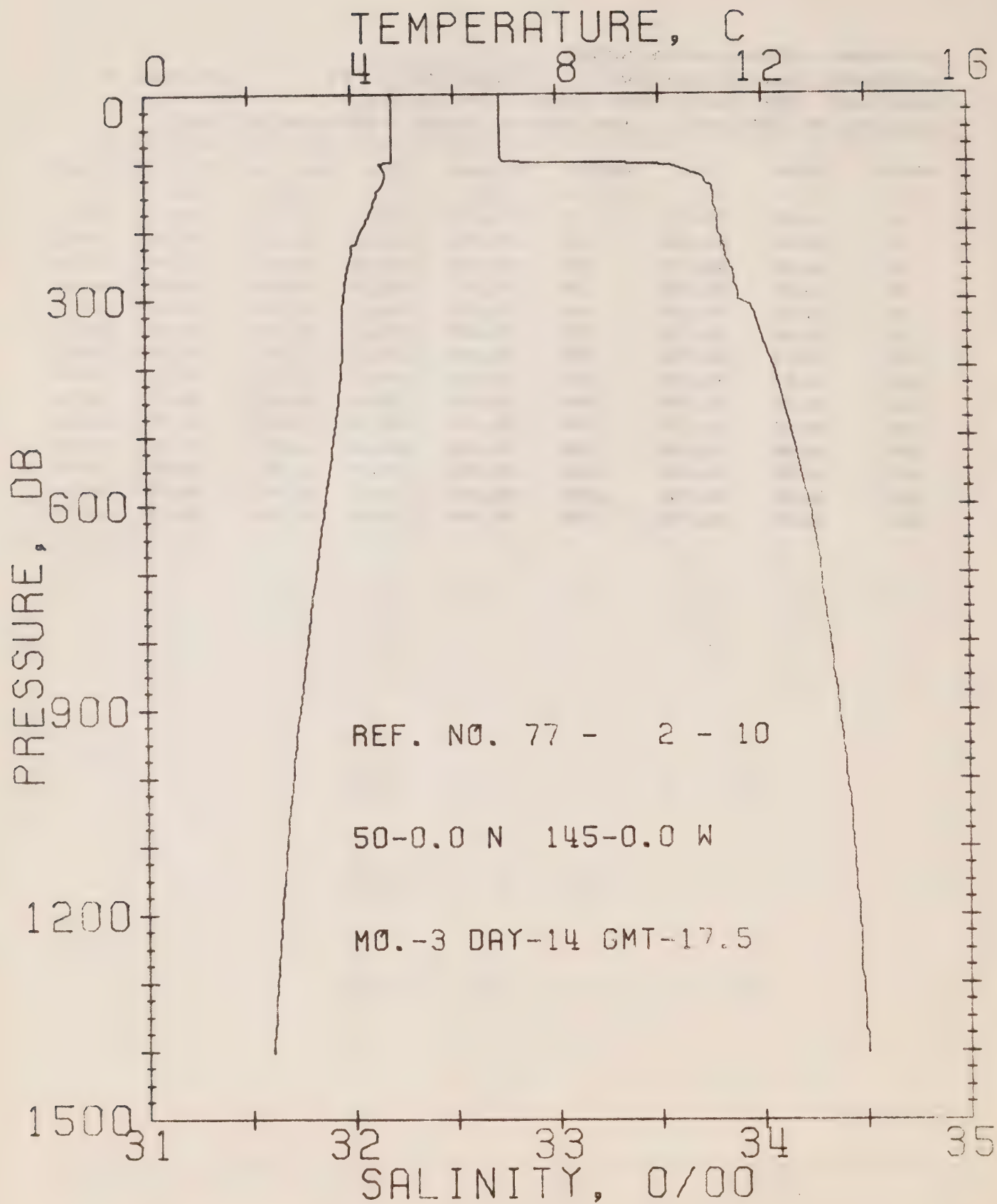
DATE 13/ 3/77

STATION P

POSITION 50- 0.0N, 145- 0.0W GMT 17.4

RESULTS OF STP CAST 118 POINTS TAKEN FROM ANALOG TRACE

PRESS	TEMP	SAL	DEPTH	SIGMA T	SVA	DELTA D	POT. EN	SOUND
0	5.22	32.70	0	25.85	215.4	0.0	0.0	1469.
10	5.22	32.69	10	25.85	216.5	0.22	0.01	1469.
20	5.23	32.70	20	25.85	216.3	0.43	0.04	1469.
30	5.23	32.69	30	25.85	216.7	0.65	0.10	1469.
50	5.22	32.70	50	25.85	216.1	1.08	0.28	1470.
75	5.18	32.71	75	25.87	215.2	1.62	0.62	1470.
100	5.13	32.72	99	25.88	214.0	2.16	1.10	1470.
125	4.72	33.58	124	26.61	145.5	2.57	1.57	1470.
150	4.57	33.74	149	26.75	132.3	2.92	2.05	1470.
175	4.23	33.77	174	26.81	126.3	3.24	2.59	1469.
200	4.06	33.80	199	26.85	122.5	3.55	3.18	1469.
225	3.92	33.83	223	26.89	119.4	3.85	3.84	1469.
250	3.88	33.86	248	26.92	116.8	4.15	4.55	1469.
300	3.87	33.91	298	26.96	113.3	4.72	6.16	1470.



OFFSHORE OCEANOGRAPHY GROUP

REFERENCE NO. 77- 2- 10

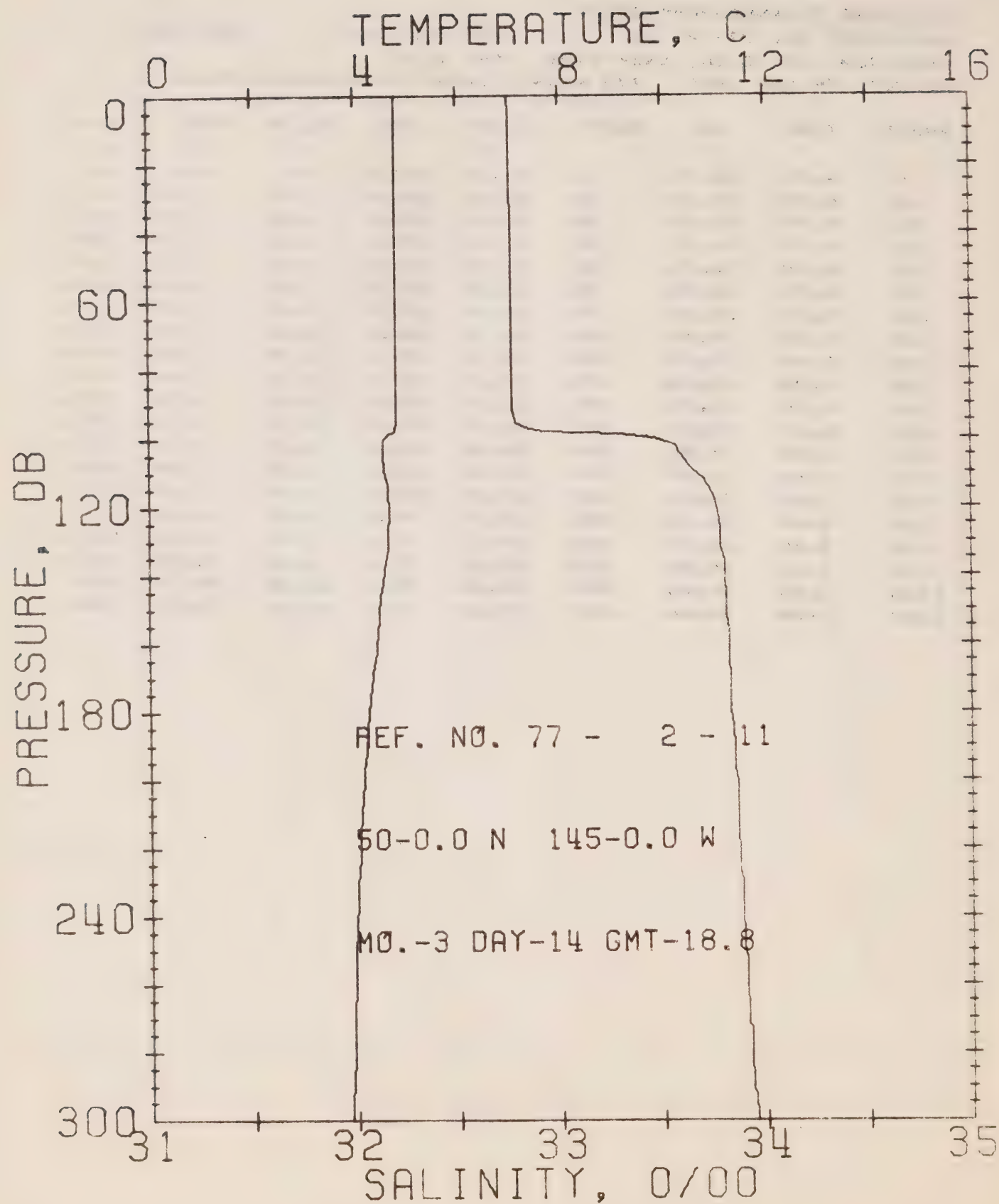
DATE 14/ 3/77

STATION P

POSITION 50- 0.0N, 145- 0.0W GMT 17.5

RESULTS OF STP CAST 173 POINTS TAKEN FROM ANALOG TRACE

PRESS	TEMP	SAL	DEPTH	SIGMA T	SVA	DELTA D	POT. EN	SOUND
0	4.78	32.73	0	25.93	208.6	0.0	0.0	1467.
10	4.79	32.73	10	25.93	208.9	0.21	0.01	1467.
20	4.79	32.73	20	25.93	209.0	0.42	0.04	1467.
30	4.79	32.73	30	25.93	209.1	0.63	0.10	1468.
50	4.79	32.73	50	25.93	209.3	1.05	0.27	1468.
75	4.79	32.73	75	25.93	209.5	1.57	0.60	1468.
100	4.77	32.87	99	26.04	199.0	2.09	1.07	1469.
125	4.65	33.72	124	26.73	134.0	2.45	1.47	1470.
150	4.48	33.77	149	26.78	129.0	2.78	1.93	1470.
175	4.35	33.78	174	26.80	127.0	3.10	2.46	1470.
200	4.19	33.79	199	26.83	124.8	3.41	3.06	1469.
225	4.01	33.82	223	26.87	120.9	3.72	3.73	1469.
250	3.94	33.84	248	26.90	118.6	4.02	4.46	1469.
300	3.84	33.89	298	26.94	114.6	4.60	6.08	1470.
400	3.80	34.06	397	27.08	102.5	5.67	9.89	1471.
500	3.65	34.15	496	27.17	94.9	6.65	14.41	1472.
600	3.45	34.23	595	27.25	87.5	7.57	19.51	1473.
800	3.11	34.33	793	27.36	77.8	9.22	31.24	1475.
1000	2.80	34.40	990	27.45	70.1	10.69	44.77	1477.
1200	2.58	34.46	1188	27.52	64.8	12.04	59.81	1480.



OFFSHORE OCEANOGRAPHY GROUP

REFERENCE NO. 77- 2- 11

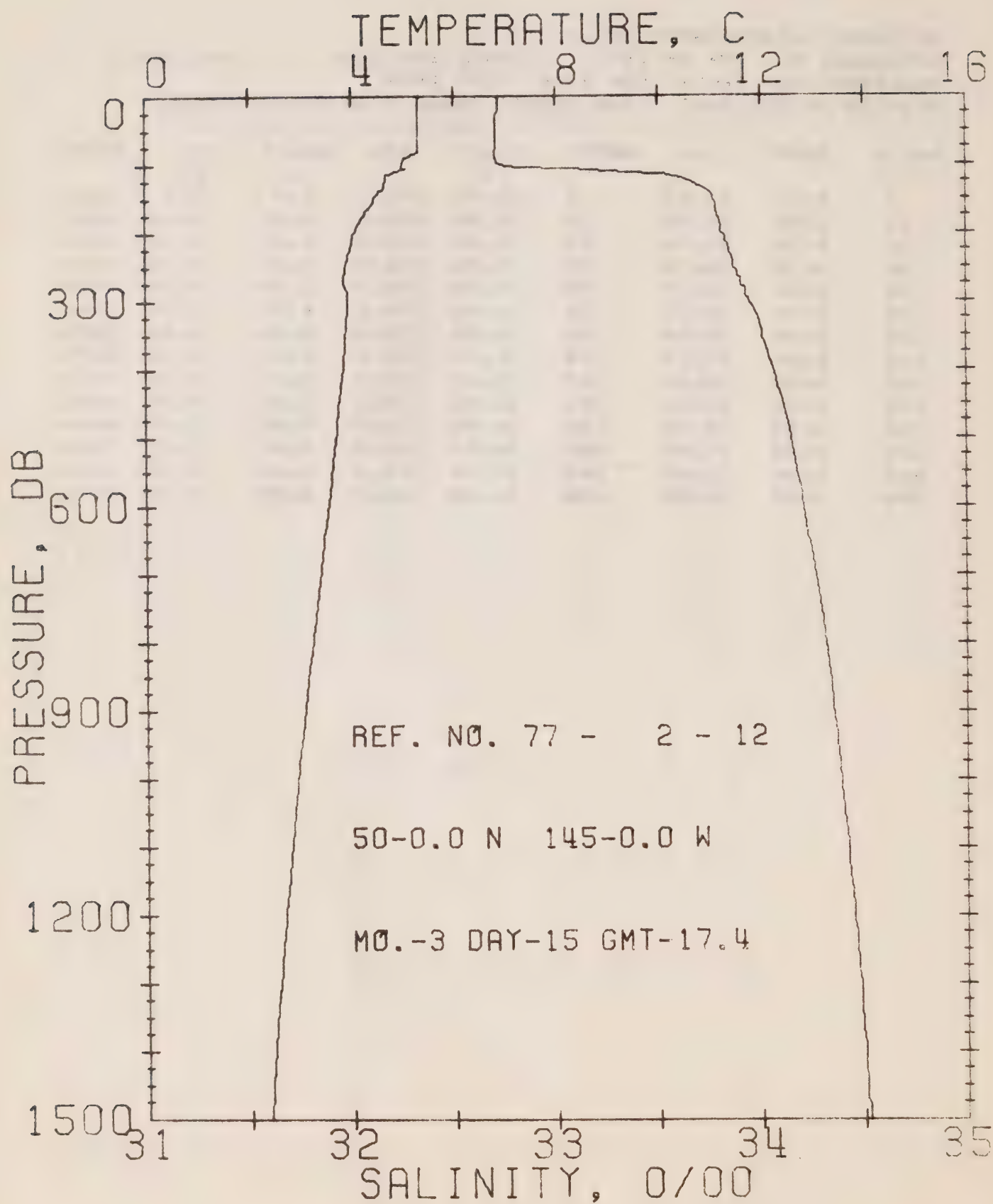
DATE 14/ 3/77

STATION P

POSITION 50- 0.0N, 145- 0.0W GMT 18.8

RESULTS OF STP CAST 108 POINTS TAKEN FROM ANALOG TRACE

PRESS	TEMP	SAL	DEPTH	SIGMA T	SVA	DELTA D	POT. EN	SOUND
0	4.81	32.75	0	25.94	207.4	0.0	0.0	1467.
10	4.80	32.76	10	25.95	206.8	0.21	0.01	1467.
20	4.79	32.76	20	25.95	206.9	0.41	0.04	1468.
30	4.79	32.76	30	25.95	206.8	0.62	0.09	1468.
50	4.80	32.77	50	25.96	206.4	1.03	0.26	1468.
75	4.80	32.77	75	25.96	206.6	1.55	0.59	1468.
100	4.56	33.46	99	26.53	152.5	2.06	1.04	1469.
125	4.65	33.78	124	26.77	130.0	2.40	1.44	1470.
150	4.46	33.81	149	26.82	125.7	2.72	1.88	1470.
175	4.28	33.83	174	26.85	122.5	3.03	2.40	1469.
200	4.13	33.86	199	26.89	119.2	3.33	2.97	1469.
225	4.03	33.87	223	26.91	117.3	3.63	3.61	1469.
250	3.96	33.89	248	26.94	115.2	3.92	4.32	1469.
300	3.87	33.95	298	26.99	110.4	4.48	5.90	1470.



OFFSHORE OCEANOGRAPHY GROUP

REFERENCE NO. 77- 2- 12

DATE 15/ 3/77

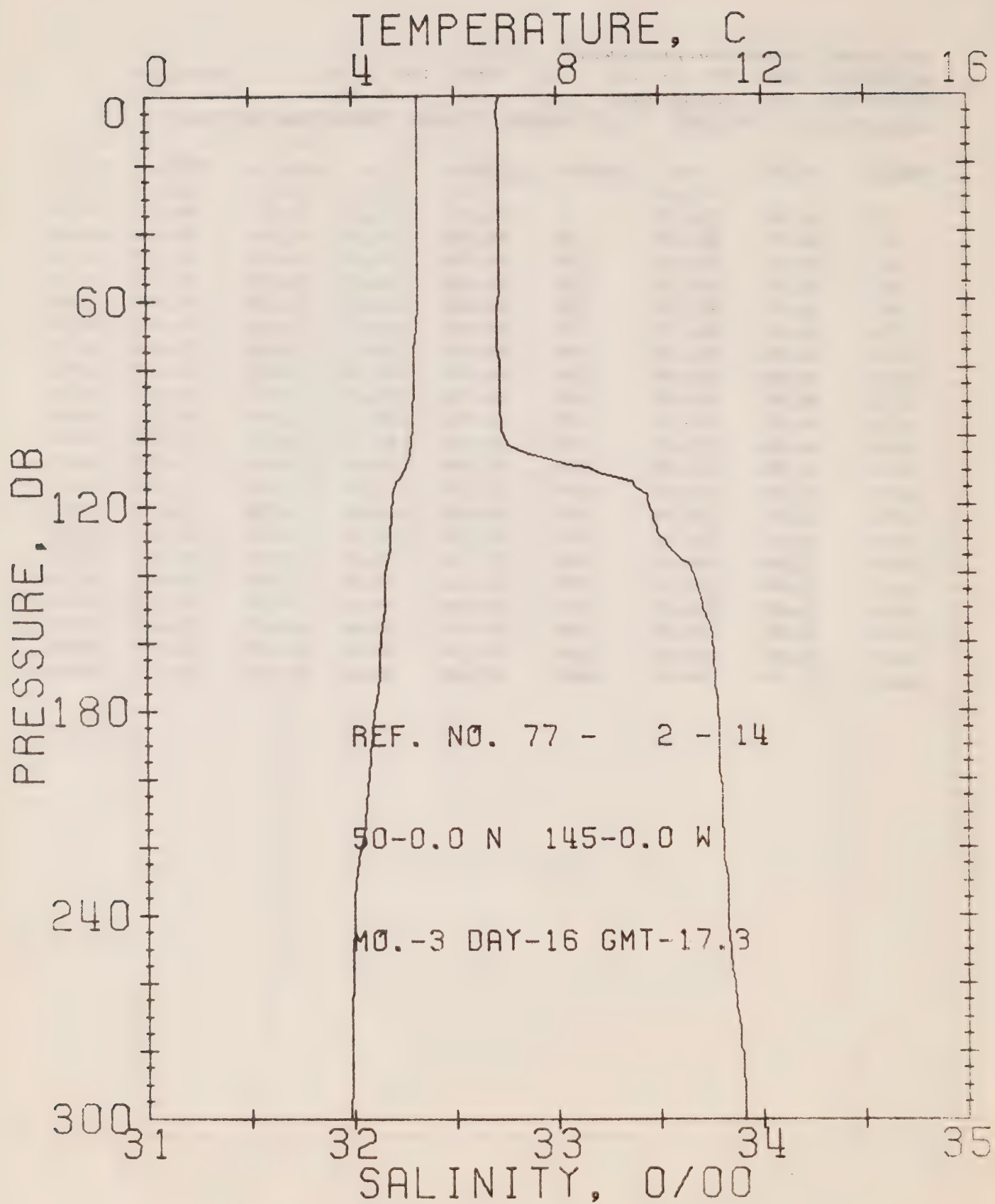
STATION P

POSITION 50- 0.0N. 145- 0.0W

GMT 17.4

RESULTS OF STP CAST 181 POINTS TAKEN FROM ANALCG TRACE

PRESS	TEMP	SAL	DEPTH	SIGMA T	SVA	DELTA D	POT. EN	SOUND
0	5.31	32.72	0	25.86	214.9	0.0	0.0	1469.
10	5.31	32.72	10	25.86	215.2	0.22	0.01	1469.
20	5.31	32.72	20	25.86	215.3	0.43	0.04	1470.
30	5.31	32.71	30	25.85	216.2	0.65	0.10	1470.
50	5.31	32.71	50	25.85	216.4	1.08	0.28	1470.
75	5.31	32.71	75	25.85	216.7	1.62	0.62	1470.
100	4.98	32.72	99	25.90	212.1	2.16	1.10	1470.
125	4.65	33.66	124	26.68	138.7	2.58	1.58	1470.
150	4.45	33.77	149	26.79	128.7	2.91	2.04	1470.
175	4.22	33.79	174	26.83	124.9	3.23	2.57	1469.
200	4.03	33.81	199	26.86	121.7	3.54	3.16	1469.
225	3.95	33.85	223	26.90	118.4	3.84	3.81	1469.
250	3.87	33.87	248	26.93	115.9	4.13	4.51	1469.
300	3.91	33.94	298	26.98	111.5	4.70	6.10	1470.
400	3.83	34.06	397	27.08	102.6	5.76	9.90	1471.
500	3.69	34.15	496	27.16	95.4	6.75	14.41	1473.
600	3.54	34.20	595	27.22	90.2	7.67	19.60	1474.
800	3.21	34.31	793	27.34	80.1	9.37	31.66	1476.
1000	2.91	34.39	990	27.43	72.6	10.89	45.60	1478.
1200	2.67	34.45	1188	27.50	66.6	12.28	61.19	1480.
1500	2.37	34.52	1483	27.58	59.6	14.17	87.07	1484.



OFFSHORE OCEANOGRAPHY GROUP

REFERENCE NO. 77- 2- 14

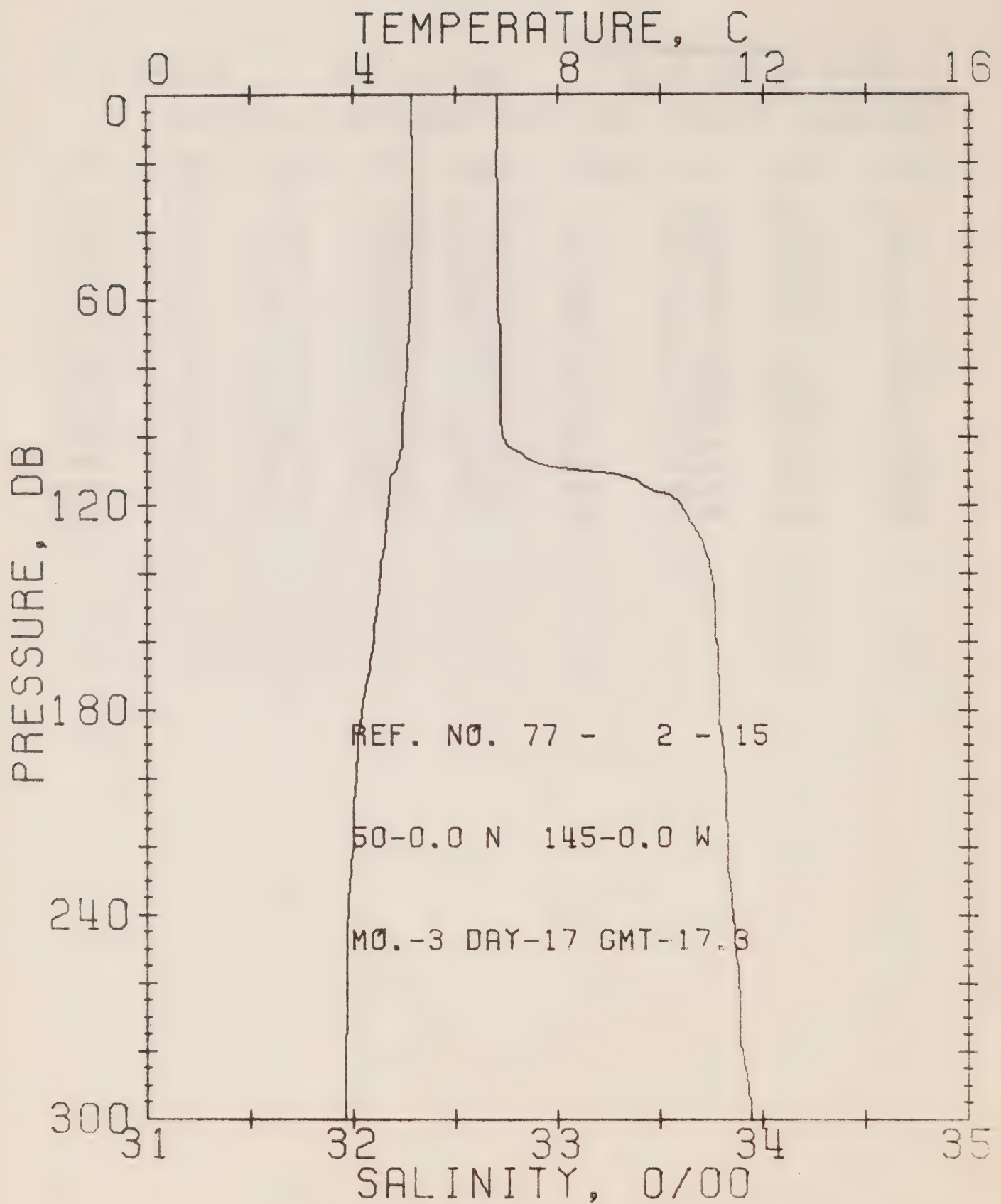
DATE 16/ 3/77

STATION P

POSITION 50- 0.0N, 145- 0.0W GMT 17.3

RESULTS OF STP CAST 108 POINTS TAKEN FROM ANALCG TRACE

PRESS	TEMP	SAL	DEPTH	SIGMA T	SVA	DELTA D	POT. EN	SOUND
0	5.28	32.72	0	25.86	214.6	0.0	0.0	1469.
10	5.27	32.72	10	25.86	214.9	0.22	0.01	1469.
20	5.27	32.72	20	25.86	214.9	0.43	0.04	1469.
30	5.27	32.72	30	25.86	215.0	0.65	0.10	1470.
50	5.27	32.72	50	25.86	215.2	1.08	0.27	1470.
75	5.20	32.71	75	25.87	215.2	1.61	0.62	1470.
100	5.16	32.74	99	25.89	213.0	2.15	1.10	1470.
125	4.74	33.48	124	26.52	153.4	2.59	1.60	1470.
150	4.62	33.71	149	26.72	134.9	2.95	2.09	1470.
175	4.47	33.77	174	26.79	128.6	3.27	2.64	1470.
200	4.29	33.79	199	26.82	125.5	3.59	3.24	1470.
225	4.06	33.81	223	26.86	121.9	3.90	3.91	1469.
250	3.98	33.84	248	26.89	119.3	4.20	4.64	1469.
300	3.93	33.91	298	26.95	114.0	4.78	6.27	1470.



OFFSHORE OCEANOGRAPHY GROUP

REFERENCE NO. 77- 2- 15

DATE 17/ 3/77

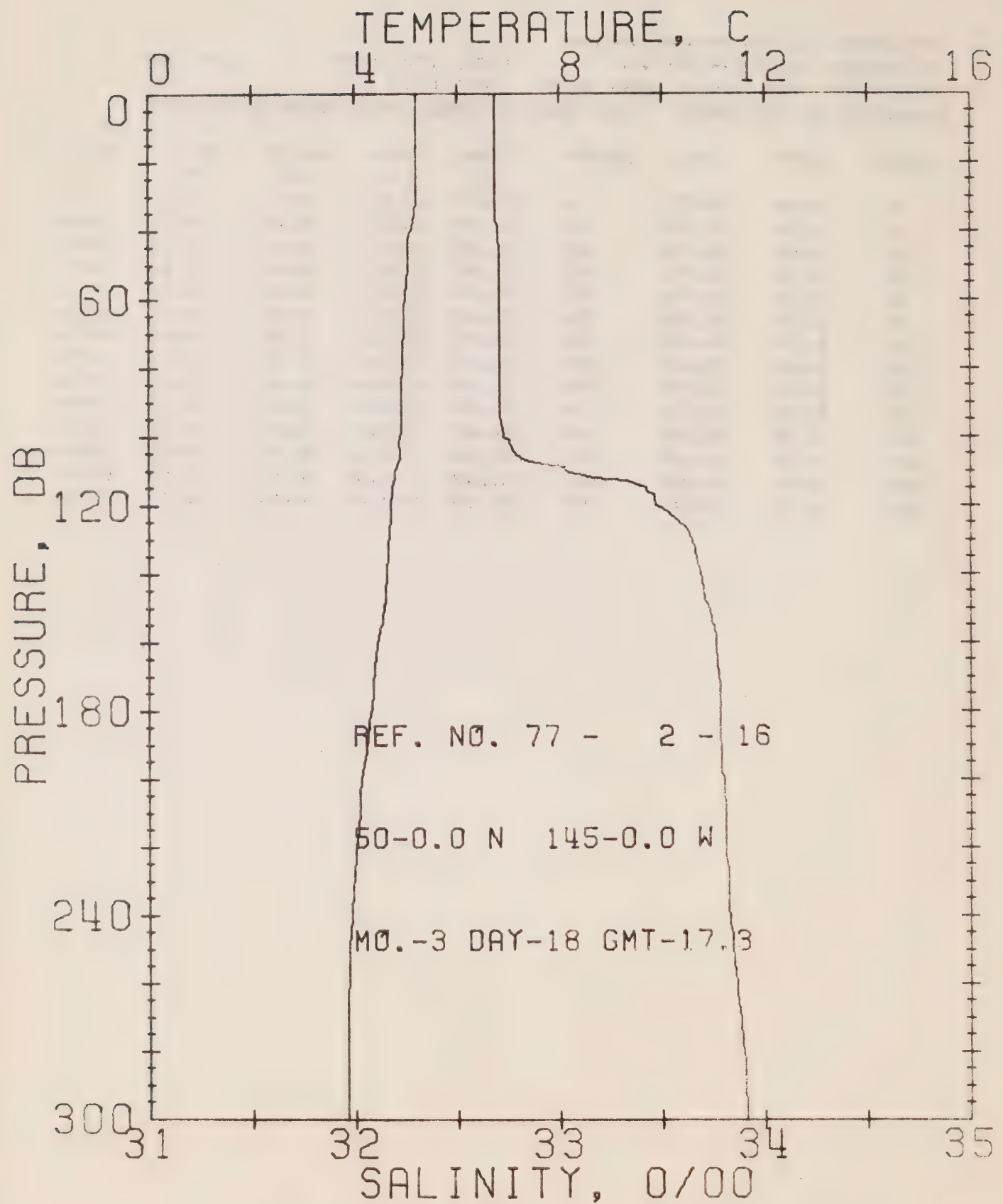
STATION P

POSITION 50- 0.0N, 145- 0.0W

GMT 17.3

RESULTS OF STP CAST 106 POINTS TAKEN FROM ANALOG TRACE

PRESS	TEMP	SAL	DEPTH	SIGMA T	SVA	DELTA D	POT. EN	SOUND
0	5.16	32.71	0	25.87	214.1	0.0	0.0	1469.
10	5.16	32.71	10	25.87	214.4	0.21	0.01	1469.
20	5.17	32.70	20	25.86	215.3	0.43	0.04	1469.
30	5.17	32.71	30	25.87	214.7	0.64	0.10	1469.
50	5.15	32.71	50	25.87	214.7	1.07	0.27	1469.
75	5.08	32.72	75	25.89	213.4	1.61	0.61	1470.
100	4.97	32.73	99	25.91	211.7	2.14	1.09	1469.
125	4.65	33.65	124	26.67	139.4	2.57	1.58	1470.
150	4.47	33.77	149	26.78	128.9	2.90	2.04	1470.
175	4.23	33.79	174	26.83	125.0	3.22	2.57	1469.
200	4.04	33.82	199	26.87	121.0	3.53	3.16	1469.
225	3.95	33.83	223	26.89	119.6	3.83	3.81	1469.
250	3.87	33.87	248	26.92	116.3	4.12	4.52	1469.
300	3.84	33.94	298	26.98	110.8	4.69	6.11	1470.



OFFSHORE OCEANOGRAPHY GROUP

REFERENCE NO. 77- 2- 16

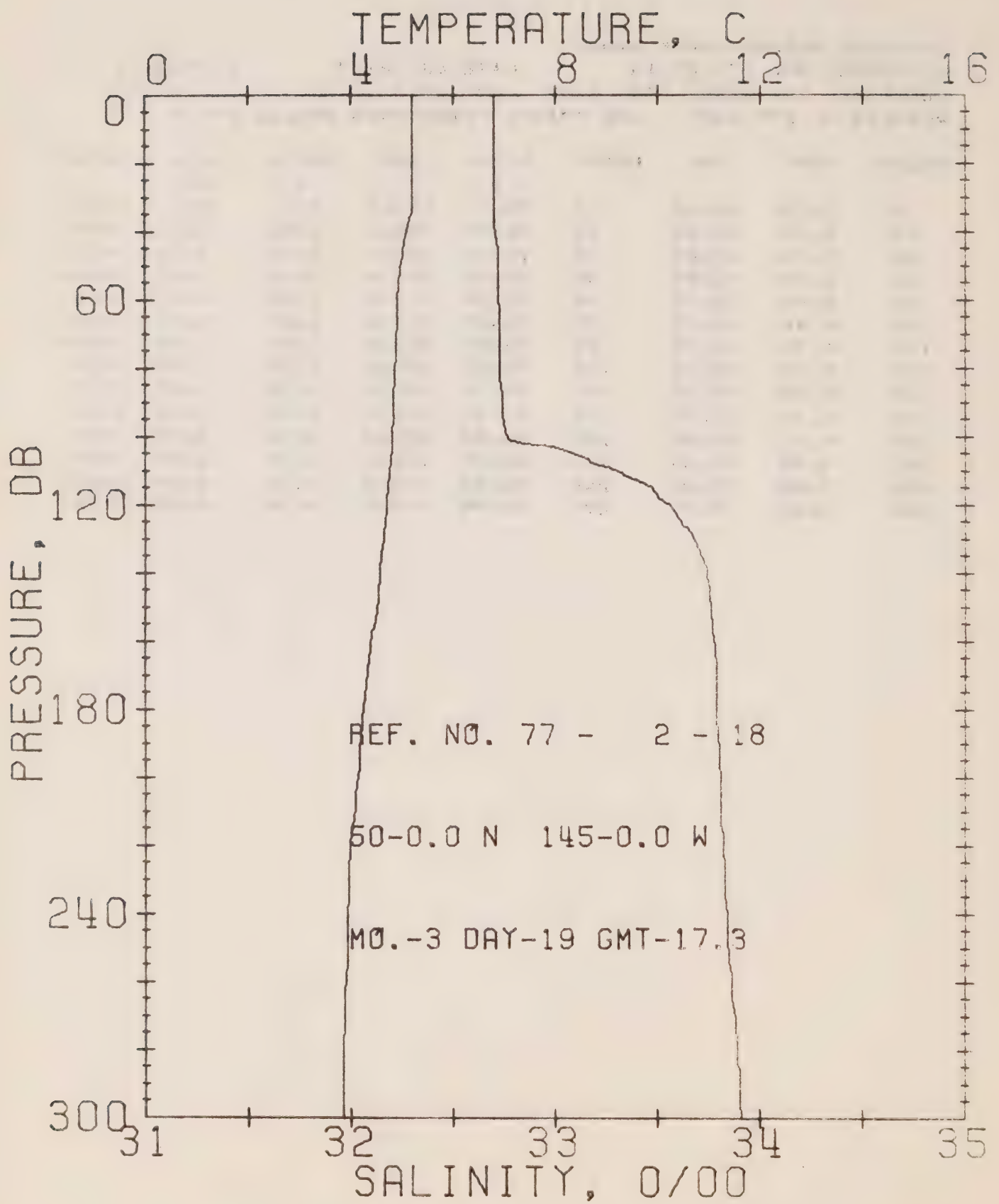
DATE 18/ 3/77

STATION P

POSITION 50- 0.0N, 145- 0.0W GMT 17.3

RESULTS OF STP CAST 108 POINTS TAKEN FROM ANALOG TRACE

PRESS	TEMP	SAL	DEPTH	SIGMA T	SVA	DELTA D	POT. EN	SOUND
0	5.19	32.69	0	25.85	215.9	0.0	0.0	1469.
10	5.19	32.69	10	25.85	216.2	0.22	0.01	1469.
20	5.19	32.69	20	25.85	216.3	0.43	0.04	1469.
30	5.19	32.69	30	25.85	216.4	0.65	0.10	1469.
50	5.04	32.71	50	25.88	213.5	1.08	0.27	1469.
75	4.94	32.71	75	25.89	212.6	1.61	0.61	1469.
100	4.89	32.73	99	25.91	210.8	2.14	1.09	1469.
125	4.68	33.59	124	26.62	144.5	2.58	1.59	1470.
150	4.56	33.72	149	26.74	133.1	2.93	2.07	1470.
175	4.34	33.78	174	26.81	126.9	3.25	2.60	1469.
200	4.11	33.80	199	26.85	123.2	3.56	3.20	1469.
225	3.99	33.81	223	26.87	121.1	3.87	3.87	1469.
250	3.88	33.84	248	26.90	118.0	4.17	4.59	1469.
300	3.83	33.91	298	26.96	113.0	4.74	6.20	1470.



OFFSHORE OCEANOGRAPHY GROUP

REFERENCE NO. 77- 2- 18

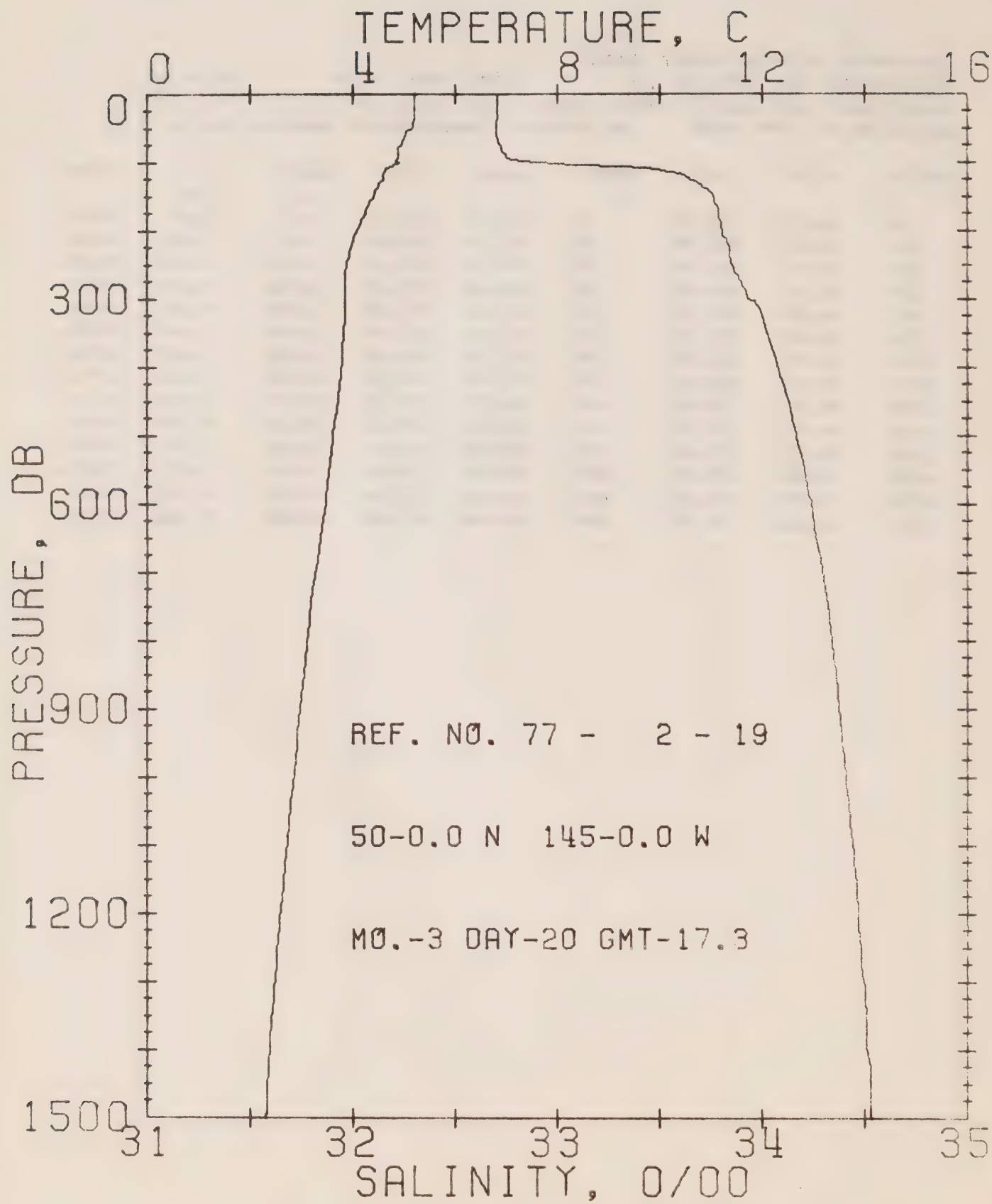
DATE 19/ 3/77

STATION P

POSITION 50- 0.0N, 145- 0.0W GMT 17.3

RESULTS OF STP CAST 96 POINTS TAKEN FROM ANALOG TRACE

PRESS	TEMP	SAL	DEPTH	SIGMA T	SVA	DELTA D	POT. EN	SOUND
0	5.21	32.70	0	25.86	215.3	0.0	0.0	1469.
10	5.21	32.70	10	25.86	215.7	0.22	0.01	1469.
20	5.21	32.70	20	25.86	215.8	0.43	0.04	1469.
30	5.20	32.70	30	25.86	215.8	0.65	0.10	1469.
50	4.97	32.72	50	25.90	211.9	1.08	0.27	1469.
75	4.87	32.73	75	25.92	210.4	1.60	0.61	1469.
100	4.81	32.76	99	25.95	207.7	2.13	1.08	1469.
125	4.66	33.62	124	26.64	142.0	2.54	1.55	1470.
150	4.51	33.76	149	26.77	130.1	2.87	2.02	1470.
175	4.28	33.79	174	26.82	125.5	3.19	2.54	1469.
200	4.12	33.81	199	26.85	122.6	3.50	3.14	1469.
225	3.95	33.83	223	26.88	119.8	3.81	3.79	1469.
250	3.92	33.84	248	26.90	118.4	4.11	4.51	1469.
300	3.84	33.91	298	26.96	113.1	4.68	6.13	1470.



OFFSHORE OCEANOGRAPHY GROUP

REFERENCE NO. 77- 2- 19

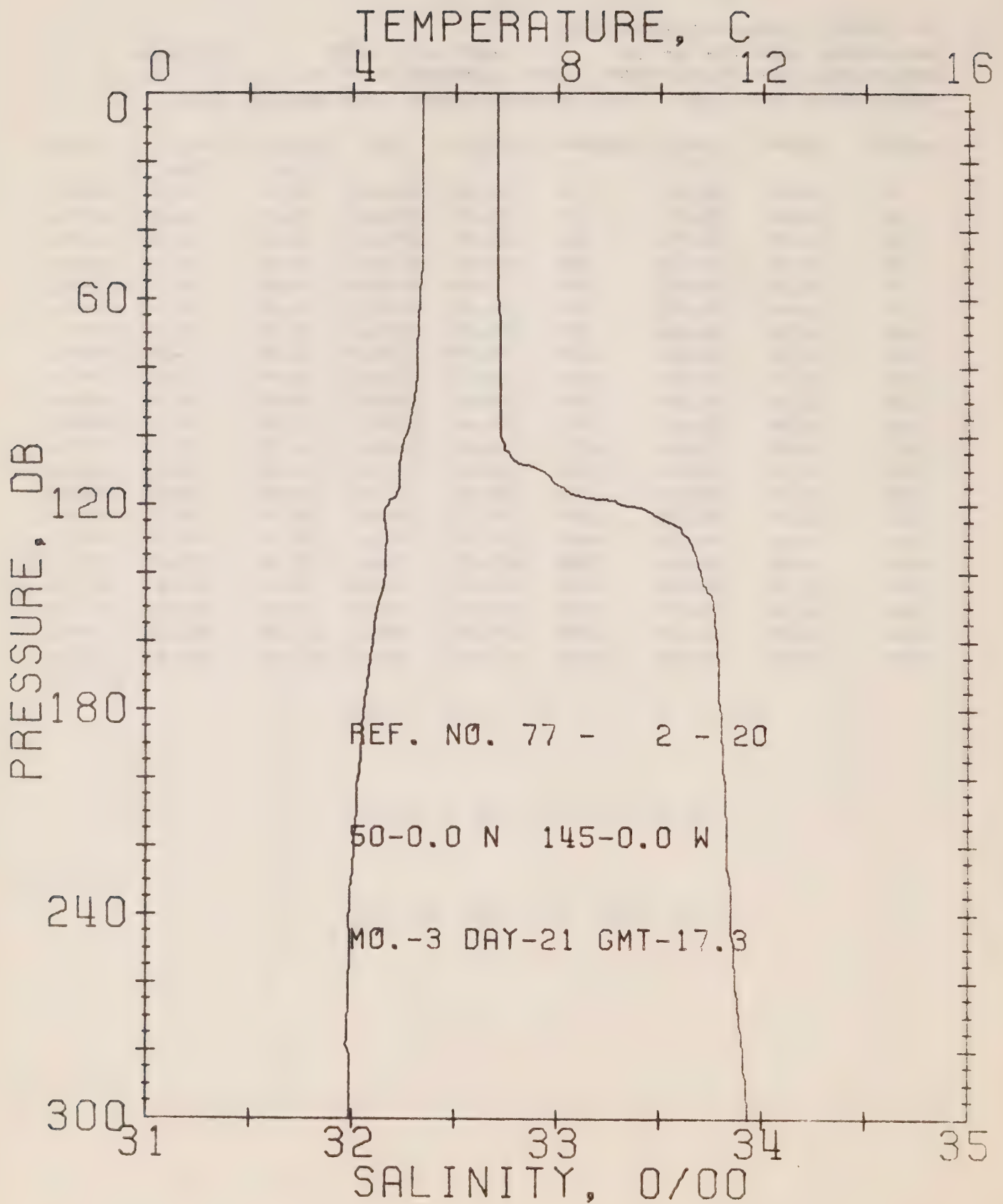
DATE 20/ 3/77

STATION P

POSITION 50- 0.0N, 145- 0.0W GMT 17.3

RESULTS OF STR CAST 173 POINTS TAKEN FROM ANALOG TRACE

PRESS	TEMP	SAL	DEPTH	SIGMA T	SVA	DELTA D	POT. EN	SOUND
0	5.20	32.71	0	25.86	214.5	0.0	0.0	1469.
10	5.21	32.71	10	25.86	214.9	0.21	0.01	1469.
20	5.21	32.71	20	25.86	214.9	0.43	0.04	1469.
30	5.19	32.71	30	25.87	214.9	0.64	0.10	1469.
50	5.15	32.70	50	25.86	215.4	1.08	0.27	1469.
75	4.94	32.72	75	25.90	212.0	1.61	0.61	1469.
100	4.92	32.91	99	26.05	197.6	2.13	1.08	1470.
125	4.59	33.65	124	26.68	138.9	2.52	1.53	1470.
150	4.39	33.76	149	26.78	128.8	2.86	1.99	1469.
175	4.23	33.79	174	26.83	125.0	3.17	2.51	1469.
200	4.06	33.81	199	26.86	122.3	3.48	3.11	1469.
225	3.94	33.84	223	26.90	118.7	3.78	3.76	1469.
250	3.87	33.85	248	26.91	117.3	4.08	4.47	1469.
300	3.83	33.93	298	26.98	111.4	4.65	6.07	1470.
400	3.77	34.08	397	27.10	100.5	5.70	9.80	1471.
500	3.61	34.17	496	27.19	92.8	6.66	14.22	1472.
600	3.45	34.24	595	27.26	86.6	7.56	19.24	1473.
800	3.10	34.34	793	27.37	77.0	9.19	30.83	1475.
1000	2.83	34.41	990	27.45	70.3	10.66	44.27	1477.
1200	2.57	34.47	1188	27.52	64.1	11.99	59.26	1480.
1500	2.30	34.53	1483	27.60	58.0	13.81	84.22	1484.



OFFSHORE OCEANOGRAPHY GROUP

REFERENCE NO. 77- 2- 20

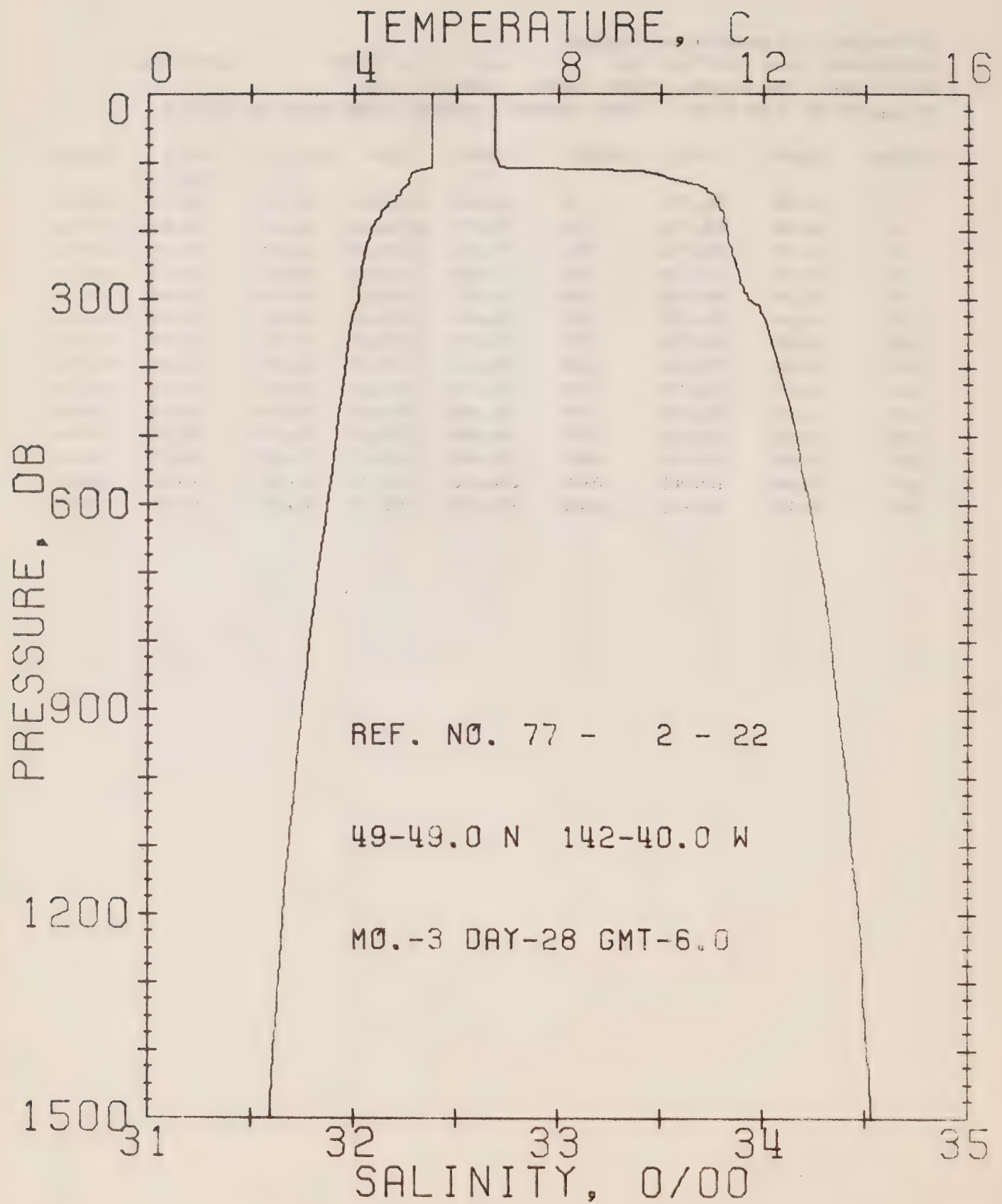
DATE 21/ 3/77

STATION P

POSITION 50- 0.0N, 145- 0.0W GMT 17.3

RESULTS OF STP CAST 112 POINTS TAKEN FROM ANALOG TRACE

PRESS	TEMP	SAL	DEPTH	SIGMA T	SVA	DELTA D	POT. EN	SOUND
0	5.35	32.71	0	25.85	216.2	0.0	0.0	1469.
10	5.36	32.71	10	25.85	216.6	0.22	0.01	1470.
20	5.37	32.71	20	25.85	216.8	0.43	0.04	1470.
30	5.37	32.71	30	25.85	216.9	0.65	0.10	1470.
50	5.35	32.71	50	25.85	216.9	1.08	0.28	1470.
75	5.26	32.72	75	25.87	215.3	1.62	0.62	1470.
100	5.00	32.72	99	25.89	212.8	2.16	1.10	1470.
125	4.62	33.54	124	26.59	147.4	2.63	1.64	1470.
150	4.49	33.76	149	26.77	129.8	2.97	2.11	1470.
175	4.27	33.79	174	26.82	125.4	3.29	2.64	1469.
200	4.10	33.81	199	26.86	122.0	3.60	3.23	1469.
225	4.00	33.83	223	26.88	120.1	3.90	3.89	1469.
250	3.94	33.86	248	26.91	117.4	4.20	4.60	1469.
300	3.95	33.93	298	26.97	112.7	4.77	6.21	1470.



OFFSHORE OCEANOGRAPHY GROUP

REFERENCE NO. 77- 2- 22

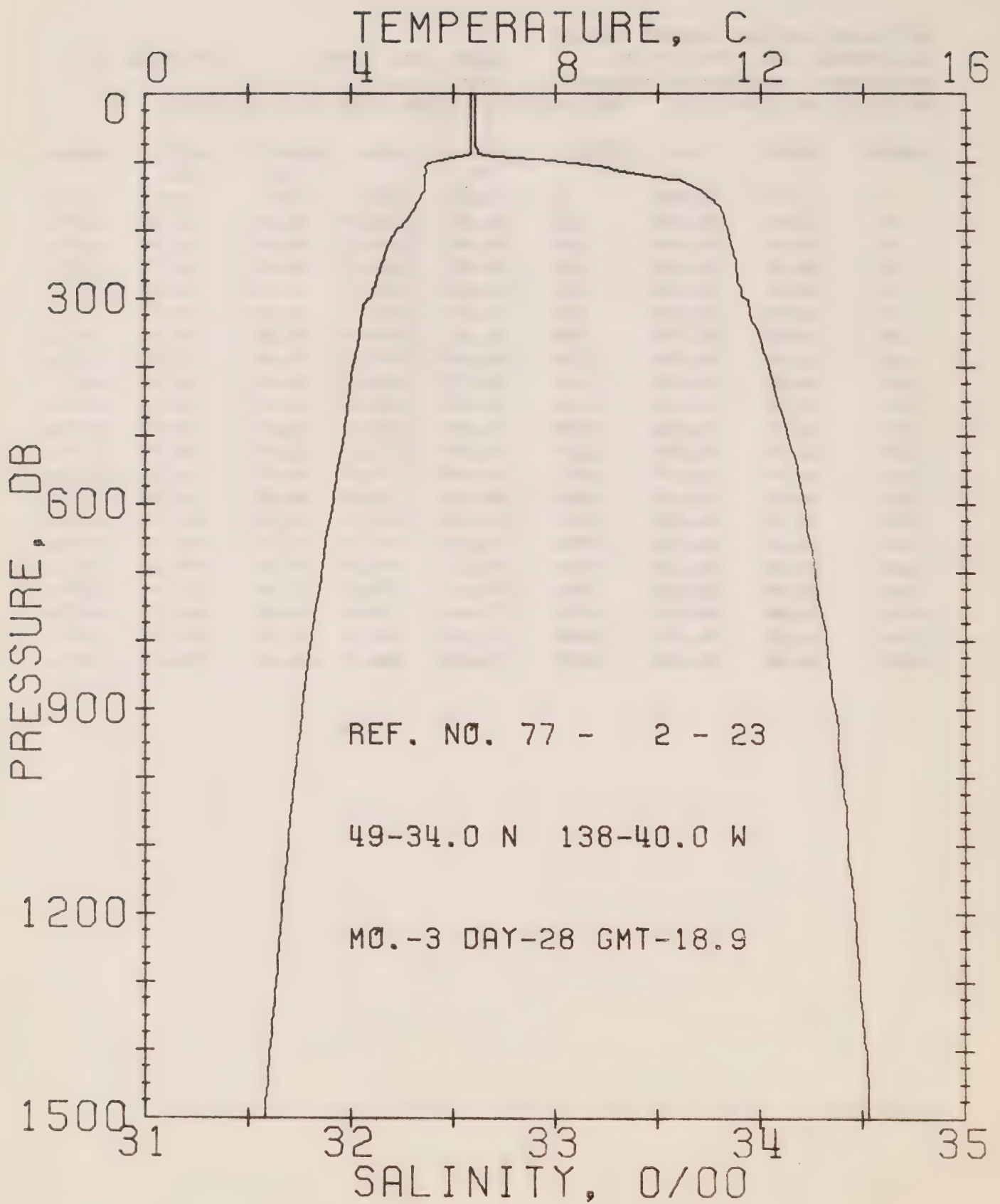
DATE 28/ 3/77

STATION 12

POSITION 49-49.0N, 142-40.0W GMT 6.0

RESULTS OF STP CAST 141 POINTS TAKEN FROM ANALOG TRACE

PRESS	TEMP	SAL	DEPTH	SIGMA T	SVA	DELTA D	POT. EN	SOUND
0	5.51	32.69	0	25.81	219.4	0.0	0.0	1470.
10	5.51	32.69	10	25.81	219.7	0.22	0.01	1470.
20	5.51	32.69	20	25.81	219.8	0.44	0.04	1470.
30	5.51	32.69	30	25.81	219.9	0.66	0.10	1471.
50	5.51	32.69	50	25.81	220.1	1.10	0.28	1471.
75	5.51	32.69	75	25.81	220.4	1.65	0.63	1471.
100	5.52	32.70	99	25.82	220.0	2.20	1.12	1472.
125	5.05	33.56	124	26.56	150.2	2.66	1.64	1471.
150	4.83	33.75	149	26.73	133.8	3.01	2.13	1471.
175	4.52	33.81	174	26.81	126.8	3.33	2.67	1470.
200	4.31	33.82	199	26.84	123.7	3.64	3.27	1470.
225	4.22	33.85	223	26.87	121.1	3.95	3.93	1470.
250	4.14	33.87	248	26.90	119.0	4.25	4.66	1470.
300	4.07	33.93	298	26.95	113.9	4.84	6.29	1471.
400	3.82	34.07	397	27.09	101.3	5.89	10.05	1471.
500	3.65	34.16	496	27.18	93.8	6.87	14.51	1472.
600	3.47	34.23	595	27.25	87.7	7.77	19.60	1473.
800	3.14	34.33	793	27.37	77.8	9.42	31.34	1475.
1000	2.86	34.41	990	27.45	70.5	10.91	44.93	1478.
1200	2.62	34.47	1188	27.52	64.7	12.26	60.07	1480.
1500	2.36	34.53	1483	27.59	58.8	14.11	85.45	1484.



OFFSHORE OCEANOGRAPHY GROUP

REFERENCE NO. 77- 2- 2J

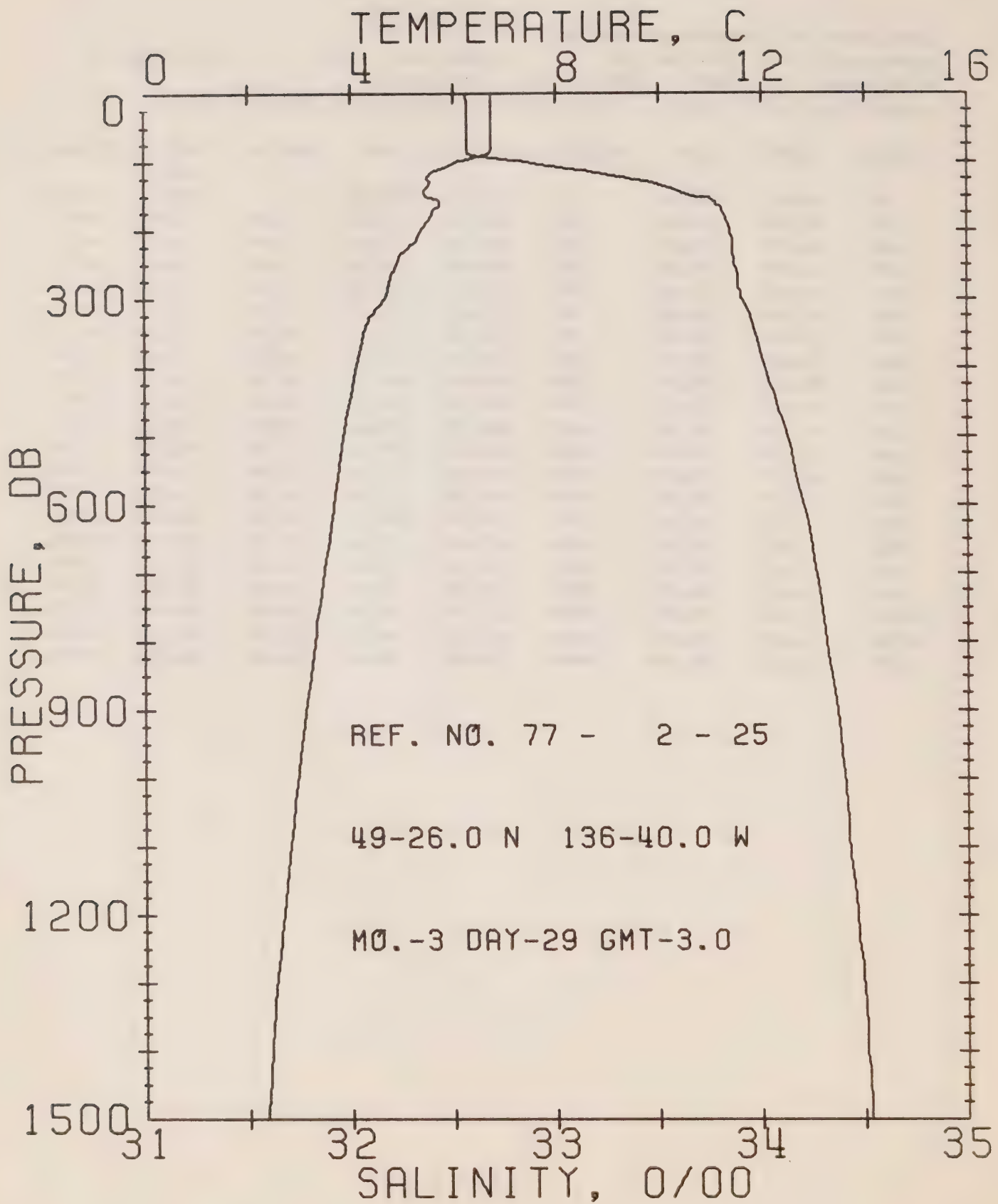
DATE 28/ 3/77

STATION 10

POSITION 49-34.0N, 138-40.0W GMT 18.9

RESULTS OF STP CAST 159 POINTS TAKEN FROM ANALOG TRACE

PRESS	TEMP	SAL	DEPTH	SIGMA T	SVA	DELTA D	POT. EN	SOUND
0	6.34	32.61	0	25.65	235.0	0.0	0.0	1473.
10	6.34	32.61	10	25.65	235.4	0.24	0.01	1473.
20	6.34	32.61	20	25.65	235.5	0.47	0.05	1474.
30	6.34	32.61	30	25.65	235.6	0.71	0.11	1474.
50	6.34	32.61	50	25.65	235.8	1.18	0.30	1474.
75	6.34	32.61	75	25.65	236.1	1.77	0.68	1475.
100	5.64	33.02	99	26.06	197.4	2.34	1.18	1473.
125	5.45	33.56	124	26.51	155.1	2.77	1.68	1473.
150	5.37	33.74	149	26.66	141.0	3.14	2.19	1473.
175	5.18	33.81	174	26.74	133.5	3.48	2.76	1473.
200	4.89	33.84	199	26.79	128.6	3.81	3.38	1472.
225	4.71	33.86	223	26.83	125.4	4.13	4.07	1472.
250	4.59	33.88	248	26.86	122.8	4.44	4.82	1472.
300	4.37	33.92	298	26.91	117.9	5.04	6.51	1472.
400	4.03	34.04	397	27.04	106.1	6.15	10.47	1472.
500	3.86	34.13	496	27.14	98.1	7.17	15.15	1473.
600	3.63	34.21	595	27.22	90.6	8.11	20.42	1474.
800	3.21	34.32	793	27.35	79.4	9.82	32.54	1476.
1000	2.90	34.40	990	27.44	71.5	11.32	46.33	1478.
1200	2.64	34.46	1188	27.51	65.3	12.69	61.64	1480.
1500	2.32	34.53	1484	27.59	58.3	14.54	86.96	1484.



OFFSHORE OCEANOGRAPHY GROUP

REFERENCE NO. 77- 2- 25

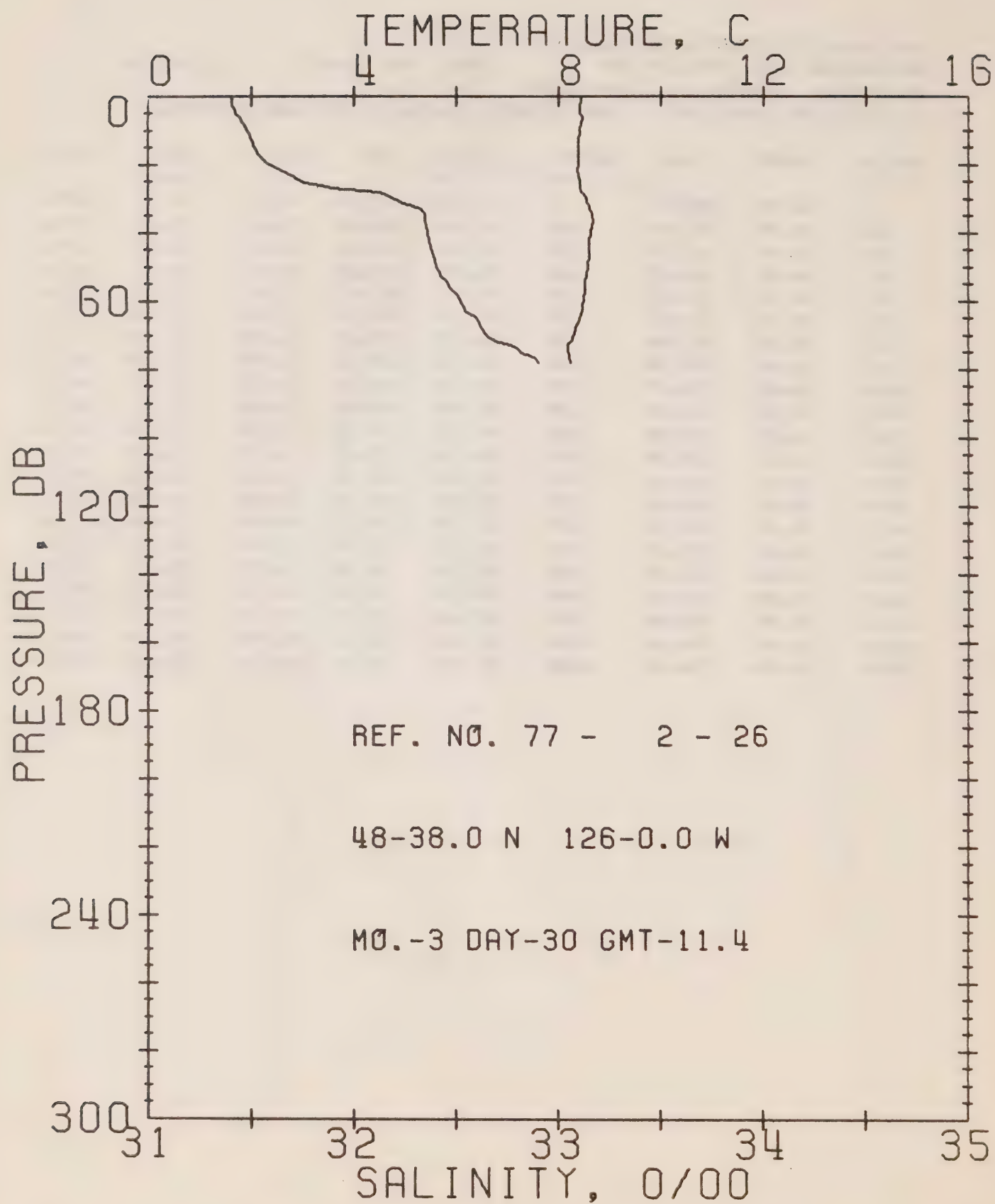
DATE 29/ 3/77

STATION 9

POSITION 49-26.0N, 136-40.0W GMT 3.0

RESULTS OF STP CAST 152 POINTS TAKEN FROM ANALOG TRACE

PRESS	TEMP	SAL	DEPTH	SIGMA T	SVA	DELTA D	POT. EN	SOUND
0	6.76	32.57	0	25.56	243.1	0.0	0.0	1475.
10	6.75	32.56	10	25.56	243.8	0.24	0.01	1475.
20	6.75	32.57	20	25.56	243.5	0.49	0.05	1475.
30	6.75	32.57	30	25.56	243.6	0.73	0.11	1475.
50	6.74	32.57	50	25.57	243.7	1.22	0.31	1476.
75	6.74	32.57	75	25.57	244.1	1.83	0.70	1476.
100	6.08	32.84	99	25.87	215.7	2.42	1.23	1474.
125	5.51	33.38	124	26.36	169.2	2.90	1.78	1473.
150	5.47	33.66	149	26.58	148.1	3.30	2.33	1474.
175	5.59	33.81	174	26.69	138.4	3.65	2.91	1475.
200	5.36	33.85	199	26.75	133.2	3.99	3.56	1474.
225	5.12	33.86	223	26.78	129.9	4.32	4.28	1474.
250	4.86	33.87	248	26.82	126.6	4.64	5.05	1473.
300	4.65	33.90	298	26.87	122.5	5.26	6.79	1473.
400	4.09	34.01	397	27.02	108.7	6.40	10.84	1472.
500	3.85	34.13	496	27.13	98.7	7.44	15.59	1473.
600	3.66	34.21	595	27.21	91.5	8.39	20.91	1474.
800	3.28	34.32	793	27.34	80.6	10.10	33.10	1476.
1000	2.94	34.41	990	27.44	71.6	11.62	46.99	1478.
1200	2.67	34.46	1188	27.51	65.7	12.99	62.40	1480.
1500	2.33	34.53	1484	27.59	58.4	14.84	87.70	1484.



OFFSHORE OCEANOGRAPHY GROUP

REFERENCE NO. 77- 2- 26

DATE 30/ 3/77

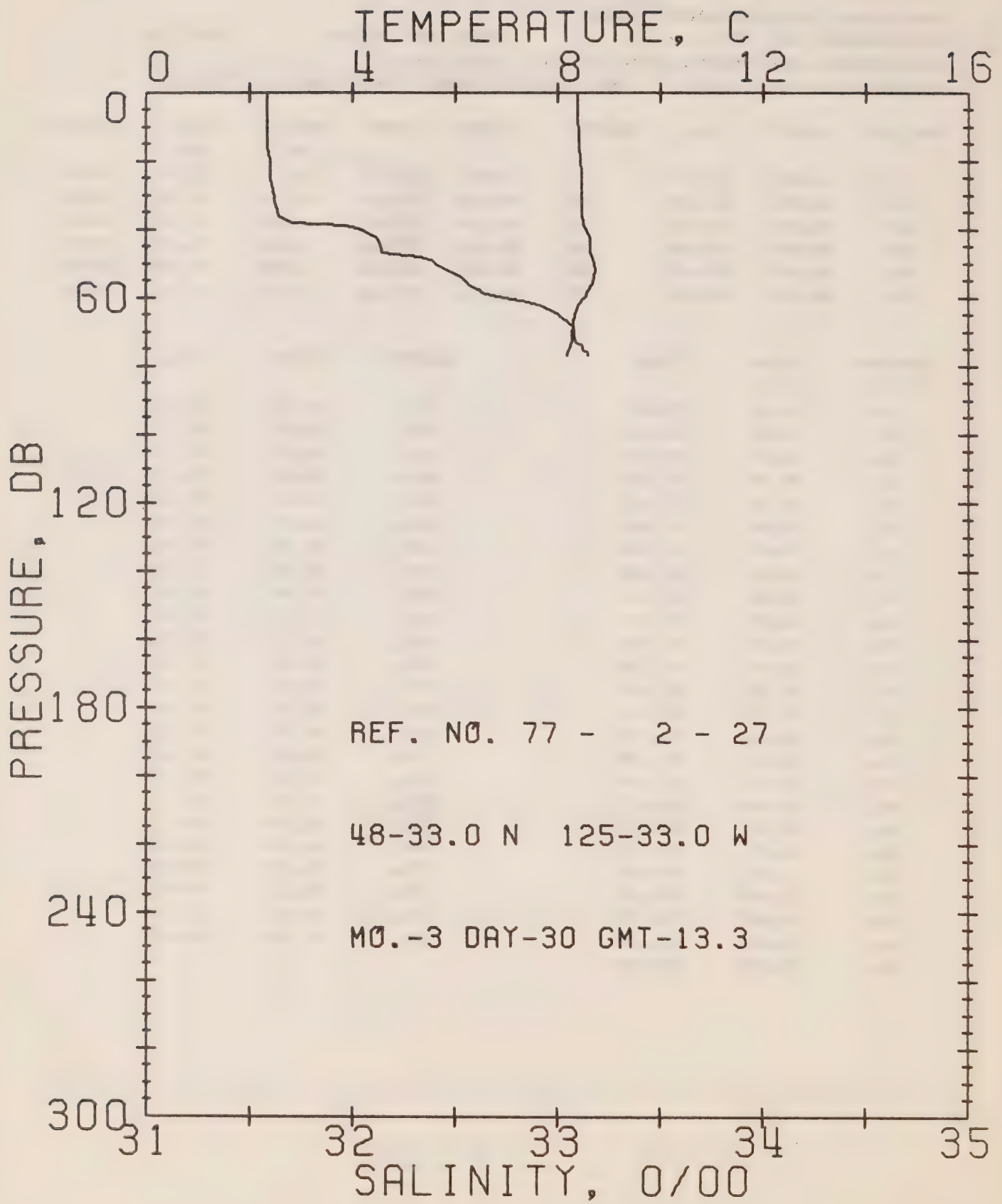
STATION 2

POSITION 48-38.0N, 126- 0.0W GMT 11.4

RESULTS OF STP CAST 49 POINTS TAKEN FROM ANALOG TRACE

PRESS	TEMP	SAL	DEPTH	SIGMA T	SVA	DELTA D	POT. EN	SOUND
0	8.46	31.41	0	24.42	352.2	0.0	0.0	1480.
10	8.44	31.48	10	24.48	347.1	0.35	0.02	1480.
20	8.39	31.59	20	24.57	338.3	0.69	0.07	1480.
30	8.55	32.20	30	25.02	295.4	1.02	0.15	1482.
50	8.58	32.40	50	25.17	281.2	1.59	0.38	1483.
75	8.19	32.82	75	25.56	244.8	2.25	0.81	1482.

DEPTH	TEMP	SAL	DEPTH	TEMP	SAL
0.	8.46	31.41	37.	8.68	32.35
1.	8.45	31.41	40.	8.65	32.36
2.	8.45	31.41	43.	8.62	32.37
3.	8.44	31.41	46.	8.61	32.38
4.	8.44	31.42	47.	8.61	32.39
5.	8.44	31.43	50.	8.58	32.40
6.	8.47	31.44	53.	8.55	32.43
7.	8.49	31.45	54.	8.54	32.45
10.	8.44	31.48	56.	8.54	32.47
14.	8.41	31.51	58.	8.53	32.50
17.	8.40	31.53	59.	8.52	32.51
19.	8.39	31.56	63.	8.49	32.54
20.	8.39	31.59	64.	8.45	32.58
22.	8.38	31.66	65.	8.43	32.60
25.	8.42	31.75	68.	8.34	32.62
26.	8.43	31.84	70.	8.31	32.65
27.	8.44	31.89	71.	8.29	32.66
28.	8.46	32.12	72.	8.23	32.71
29.	8.52	32.16	73.	8.19	32.77
30.	8.55	32.20	74.	8.18	32.80
31.	8.56	32.22	75.	8.19	32.82
32.	8.58	32.29	76.	8.21	32.87
33.	8.62	32.33	77.	8.22	32.89
34.	8.63	32.34	78.	8.23	32.90
35.	8.66	32.35			



OFFSHORE OCEANOGRAPHY GROUP

REFERENCE NO. 77- 2- 27

DATE 30/ 3/77

STATION 1

POSITION 48-33.0N, 125-33.0W GMT 13.3

RESULTS OF STP CAST 43 POINTS TAKEN FROM ANALOG TRACE

PRESS	TEMP	SAL	DEPTH	SIGMA T	SVA	DELTA D	POT. EN	SOUND
0	8.39	31.59	0	24.57	337.8	0.0	0.0	1480.
10	8.40	31.59	10	24.57	338.4	0.34	0.02	1480.
20	8.45	31.60	20	24.57	338.4	0.68	0.07	1481.
30	8.48	31.62	30	24.58	337.8	1.02	0.16	1481.
50	8.73	32.40	50	25.15	283.4	1.65	0.41	1483.
75	8.24	33.13	75	25.80	222.5	2.27	0.80	1483.

DEPTH	TEMP	SAL	DEPTH	TEMP	SAL
0.	8.39	31.59	50.	8.73	32.40
4.	8.40	31.59	52.	8.75	32.47
6.	8.39	31.59	54.	8.72	32.53
8.	8.39	31.59	56.	8.70	32.56
12.	8.42	31.59	57.	8.65	32.59
15.	8.43	31.59	58.	8.62	32.62
16.	8.43	31.59	59.	8.59	32.65
20.	8.45	31.60	60.	8.54	32.74
24.	8.47	31.60	61.	8.49	32.82
25.	8.47	31.60	62.	8.43	32.91
31.	8.48	31.62	63.	8.40	32.94
32.	8.48	31.62	64.	8.38	32.98
36.	8.47	31.64	67.	8.33	33.05
38.	8.50	31.71	69.	8.31	33.08
39.	8.52	31.97	70.	8.30	33.08
40.	8.55	32.04	72.	8.30	33.08
42.	8.60	32.11	73.	8.30	33.09
43.	8.63	32.12	74.	8.26	33.12
46.	8.65	32.14	75.	8.24	33.13
47.	8.65	32.14	76.	8.21	33.15
48.	8.66	32.33	77.	8.20	33.15
49.	8.70	32.38			

Surface Salinity and Temperature Observations
(P-77-2)

SURFACE SALINITY AND TEMPERATURE OBSERVATIONS
CRUISE REFERENCE NUMBER 77- 2

DATE/TIME				SALINITY	TEMP	LONGITUDE
YR	MO	DAY	GMT			
				0/00	C	WEST
77	2	11	2320	32.301	9.5	125-33
77	2	12	100	32.348	9.6	126- 0
77	2	12	250	32.348	9.6	126-40
77	2	12	550	32.508	9.8	127-40
77	2	12	905	32.335	9.0	128-40
77	2	12	1300	32.497	9.4	129-40
77	2	12	1600	32.454	9.3	130-40
77	2	12	2010	32.431	9.2	131-40
77	2	12	2355	32.314	8.9	132-40
77	2	13	350	32.382	8.2	133-40
77	2	13	800	32.424	8.2	134-40
77	2	13	1200	32.458	8.1	135-40
77	2	13	1545	32.454	7.9	136-40
77	2	13	2220	32.535	7.2	137-40
77	2	14	200	32.561	7.2	138-40
77	2	14	515	32.594	6.9	139-40
77	2	14	820	32.637	7.0	140-40
77	2	14	1205	32.609	6.2	141-40
77	2	14	1810	32.621	5.9	143-40
77	2	15	0	32.625	5.6	ON STATION
77	2	16	0	32.641b	5.6	ON STATION
77	2	17	0	32.650	5.7	ON STATION
77	2	19	0	32.644	5.5	ON STATION
77	2	20	0	32.657	5.5	ON STATION
77	2	21	0	32.640	5.5	ON STATION
77	2	22	0	32.676	5.1	ON STATION
77	2	23	0	32.668	5.2	ON STATION
77	2	24	0	32.661	5.5	ON STATION
77	2	25	0	32.679	5.2	ON STATION
77	2	26	0	32.681	5.4	ON STATION
77	2	27	0	32.661	5.8	ON STATION
77	2	27	300	32.620	5.5	142-40
77	2	27	600	32.625	6.5	141-40
77	2	27	900	32.606	6.7	140-48
77	2	27	1200	32.593	6.5	139-58
77	2	27	1500	32.574	6.6	138-59
77	2	27	1800	32.546	7.1	138- 0
77	2	27	2100	32.534	7.1	137- 0
77	2	28	0	32.477	7.6	136- 8
77	2	28	300	32.480	7.5	135- 6
77	2	28	600	32.466	7.9	134- 6
77	2	28	900	32.379	8.0	133-10
77	2	28	1200	32.350	8.5	132- 7
77	2	28	1500	32.380	8.6	131-17

SURFACE SALINITY AND TEMPERATURE OBSERVATIONS
CRUISE REFERENCE NUMBER 77-12

DATE/TIME				SALINITY	TEMP	LONGITUDE
YR	MO	DAY	GMT			
				0/00	C	WEST
77	2	28	1800	32.468	8.8	130-17
77	2	28	2100	32.503	9.1	129-17
77	3	1	300	32.437	9.1	127-23
77	3	1	600	32.154	9.2	126-22
77	3	4	305	31.004	8.4	125- 0
77	3	4	500	31.385	9.1	125-33
77	3	4	650	31.514	8.8	126- 0
77	3	4	900	32.375		126-40
77	3	4	1240	32.437		127-40
77	3	4	1615	32.351	8.5	128-40
77	3	5	35	32.318	8.6	130-40
77	3	5	710	32.344	8.5	132-40
77	3	5	1330	32.478	7.5	134-40
77	3	5	2010	32.522	7.4	136-40
77	3	6	300	32.558	6.8	138-40
77	3	6	1800	32.611	6.5	139-52
77	3	6	2100	32.632	6.3	140- 5
77	3	7	0	32.627	6.4	140-24
77	3	7	300	32.615	6.5	140-43
77	3	7	600	32.597	6.6	141-20
77	3	7	900	32.638	5.9	142- 8
77	3	8	0	32.679	5.5	ON STATION
77	3	9	0	32.701	4.8	ON STATION
77	3	10	0	32.714	5.0	ON STATION
77	3	11	0	32.721	4.9	ON STATION
77	3	12	0	32.765	4.3	ON STATION
77	3	13	0	32.768	4.5	ON STATION
77	3	14	0	32.717	5.2	ON STATION
77	3	16	0	32.722	5.1	ON STATION
77	3	17	0	32.720	5.4	ON STATION
77	3	18	0	32.714	5.4	ON STATION
77	3	19	0	32.706	5.4	ON STATION
77	3	20	0	32.708	5.4	ON STATION
77	3	21	0	32.717	5.4	ON STATION
77	3	22	0	32.693	5.2	ON STATION
77	3	23	0	32.710	5.1	ON STATION
77	3	24	0	32.711	5.1	ON STATION
77	3	25	0	32.703	5.3	ON STATION
77	3	26	0	32.708	5.2	ON STATION
77	3	27	0	32.742	4.5	ON STATION
77	3	28	140	32.710		143-40
77	3	28	600	32.697	5.4	142-40
77	3	28	1000	32.657		141-40
77	3	28	1345	32.651	6.0	140-40

SURFACE SALINITY AND TEMPERATURE OBSERVATIONS
 CRUISE REFERENCE NUMBER 77- 2

DATE/TIME				SALINITY	TEMP	LONGITUDE
YR	MO	DAY	GMT	0/00	C	WEST
77	3	28	1855	32.621	6.3	138-40
77	3	29	0	32.606		137-40
77	3	29	300	32.569	6.7	136-40
77	3	29	640	32.541		135-40
77	3	29	940	32.496	7.2	134-40
77	3	29	1240	32.433		133-40
77	3	29	1545	32.422	7.9	132-40
77	3	29	1845	32.497	8.1	131-40
77	3	29	2135	32.426	8.0	130-40
77	3	30	25	32.474	8.3	129-40
77	3	30	330	32.444	8.3	128-40
77	3	30	630	32.450	8.4	127-40
77	3	30	920	31.840	8.3	126-40
77	3	30	1125	31.254	8.5	126- 0
77	3	30	1300	31.543	8.4	125-33

B DENOTES SALINITY SAMPLE TAKEN FROM A
 BUCKET. ALL OTHER SAMPLES TAKEN FROM
 THE SEAWATER LOOP

LIST OF OMISSIONS FROM DATA

Hydrographic data:

Consec. #	Depth (m)	Temp.	Sal.	O ₂	Notes			Comments
					1.	2.	3.	
13	4216			*		*		no sample
	4216		*		*			
24	119		*					
	777		*			*		

Notes (MacNeill, 1977):

1. The data is suspect because of a reversal of gradient by $>.01^{\circ}/\text{oo}$ (salinity) or $>.08 \text{ ml/l}$ (oxygen).
2. The data is deleted because of very irregular data values (usually a mis-tripping or leaking bottle if both oxygen and salinity are irregular).
3. The data is deleted because duplicate samples at a depth were not within $.01^{\circ}/\text{oo}$ (salinity) or $.08 \text{ ml/l}$ (oxygen).

STD data:

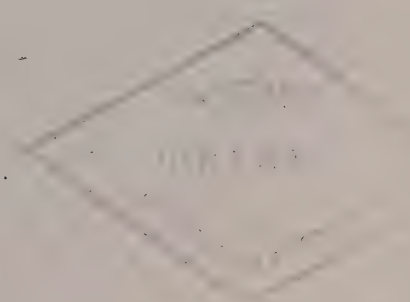
Consecutive #	Comments
2	not included; trace too erratic

CAI
EP 321
- 77R15

AIRBORNE MEASUREMENTS OF HORIZONTAL WIND

BY

B.M. Oliver and J.F.R. Gower



Institute of Ocean Sciences, Patricia Bay
Sidney , B.C.

For addition copies or further information please write to:

Department of Fisheries and the Environment

Institute of Ocean Sciences, Patricia Bay

P.O. Box 5000

Sidney, B.C.

V8L 4B2

AIRBORNE MEASUREMENTS OF HORIZONTAL WIND

by

B.M. Oliver and J.F.R. Gower

Institute of Ocean Sciences, Patricia Bay
Sidney, B.C.
October 1977

This is a manuscript which has received only limited circulation. On citing this report in a bibliography, the title should be followed by the words "UNPUBLISHED MANUSCRIPT" which is in accordance with accepted bibliographic custom.

Contents

<u>Section</u>	<u>Page</u>
1. Introduction	1
2. Inertial and Data Acquisition Systems	1
3. Inertial System Drift	2
4. Wind Measuring Sensors	4
5. Pitot and Yaw In Flight Calibration	7
6. Wind measurements in Juan de Fuca Strait	9
7. Summary and Conclusions	10
8. References	12

1. Introduction

Airborne-measurements of air motion have been a subject of considerable interest for the past twenty years. Because of a lack of an accurate ground reference, early investigations were limited mainly to measurements of vertical air motion obtained by monitoring the vertical motion of the aircraft, or long term average measurements of horizontal wind components using standard navigational procedures.

With the introduction of precise aircraft inertial navigation equipment which enabled accurate readings of aircraft attitude and motion to be made, the task of routinely measuring winds from an airborne platform was greatly simplified (Axford, 1968, Telford *et al*, 1974 and 1977). Certain problems still exist, however, including that of measuring the aircraft's attack angles relative to the airstream, and of compensating for the inherent drift which is characteristic of all inertial systems.

In this report, we discuss the results of several wind measuring test flights made in the Beechcraft 18 aircraft at present on lease to the Remote Sensing Section of the Institute of Ocean Sciences, Patricia Bay. The aircraft is equipped with an inertial navigation and data acquisition system enabling highly accurate aircraft attitude and navigational data to be recorded.

The system uses a visual sight to make periodic fixes of landmarks of known position on the earth's surface in order to determine the drift of the inertial unit (Oliver and Gower, 1977, Grasty *et al*, 1977). Additional sensors have been incorporated into the system to allow for measurement of air temperature, aircraft sideslip, pitot and static pressures which are required for the determination of wind velocity.

2. Inertial and Data Acquisition Systems

Details of the inertial/sighting system have been described previously (Grasty *et al*, 1977), and only a brief description is presented here. The inertial navigation unit (INU) used is a Litton LTN-51 with standard software designed for airline navigation. The unit operates by sensing aircraft accelerations along three mutually perpendicular axes on a gyrostabilized level platform. The platform is maintained level by applying torquing signals to the gyro axes derived from the movement of the aircraft over the earth's surface. The computations necessary to provide the correct torquing signals are performed by the unit's own internal digital computer. These calculations assume a spheroidal earth with a flattening ratio of 1:297 and a constant aircraft altitude of about 10,000 m. This computer also calculates standard output data from the INU including aircraft position and velocity data as well as navigation information useful in commercial airline operations. In addition, high accuracy aircraft attitude (pitch, roll and azimuth) is available directly from angle resolvers attached to the level platform.

The standard output data is of limited value because of two factors: 1) the computer cycle time gives relatively infrequent updating of this data, and 2) intentional internal rounding reduces its accuracy. In order to circumvent these problems, a specialized data acquisition system, MIDAS (Marine Inertial Data Acquisition System), was developed. This system was designed and

constructed by MacDonald Dettwiler and Associates Ltd. of Vancouver and is an outgrowth of the system they designed and constructed for the Canada Centre for Remote Sensing in Ottawa (Baker and MacDonald, 1974). MIDAS allows direct readout of the INU's internal computer memory, to give rapid access to the high precision navigation data. This data is output at a rate of 20 samples/sec and is used to calculate high precision aircraft position, velocity and direction. MIDAS allows, in addition, data to be input from eight analog channels (100 samples/sec) with a voltage range of 0-10 V and a resolution of 10 m V. The system records this data together with the observation time on either video or computer compatible magnetic tape. In the latter case, the user has the option of choosing between several recording modes depending on the frequency at which data recording is desired. Normally, INS data is output at the maximum rate of 20 samples/sec (100 samples/sec for the analog channels). For most of the flights, however, where no additional sensors are present, INS and sight data need only to be recorded at discrete time (i.e., when a target is being sighted) and in short bursts lasting about one second. In order to reduce the amount of output data in these flights, MIDAS was modified to allow for a much slower background recording rate of only one sample/sec between these bursts. This background recording rate was found to be more than adequate for post flight data analysis.

3. Inertial System Drift

In order to maintain the gyro stabilized platform level as the aircraft moves over the earth's surface, the INU's internal computer provides gyro torquing voltages calculated from the measured horizontal movement of the aircraft. The LTN-51 inertial unit used in this study is "Schuler tuned", that is, the torquing voltages are made proportional to the aircraft's angular velocity relative to the center of the earth. The inertial platform, therefore, behaves as a Schuler pendulum (Beck, 1971) and as such, if perturbed undergoes stable oscillation about the level position with a period T given by

$$T = 2\pi\left(\frac{R}{g}\right)^{\frac{1}{2}} \quad (1)$$

where R is the earth's radius and g is the acceleration of gravity. This oscillation, which has a period T = 84.4 minutes, results in an approximately sinusoidal drift in the calculated positions (latitude and longitude) returned by the INU. The fact that the INU drift is not perfectly sinusoidal arises from additional error mechanisms within the inertial system. The amplitude of the mean drift, in normal circumstances, is of the order of 2 km per hour.

The magnitude of this position drift is obtained during flight by sighting known landmarks on the earth's surface using a target sight located in the transparent nose of the Beechcraft 18 aircraft used. The angular direction data from the sight in conjunction with the aircraft's attitude and barometric altitude is used to establish the aircraft's "true" position using the known position of the sighted landmark. It should be mentioned here, that the relatively large position drift of the INU results from only relatively small ($\sim 1'$ arc) angular errors in the gyro stabilized level platform. Thus errors present in the attitude data are very small and will be negligible in comparison to the estimated errors in the sighting angles. The difference

between this "true" position and that returned by the INU determines the error due to inertial system drift (north and east) at the time the target was sighted. During flight, target sightings were generally restricted to observing angles less than 30° off nadir in order to reduce the effects of errors in sighting angles and in the aircraft's indicated altitude. A complete description of the target sight and its use has been given previously (Oliver and Gower, 1977).

The position fixes obtained using the target sight enable the inertial system drift to be determined at discrete times during the flight. An estimate of the drift for intermediate times is then obtained by fitting a modified cubic spline to the discrete drift data. An estimate of the possible error involved in the predicted inertial system position drift (from the cubic spline fit) was obtained by fitting the cubic spline, using various initial conditions, to a hypothetical set of discrete drift data generated assuming a perfectly sinusoidal drift with time (Oliver and Gower, 1977). The results of these tests showed that under normal operating conditions, the RMS interpolation error will be approximately equal to the assumed RMS error in the individual position fixes provided these fixes (discrete drift data) are determined at least every 10 minutes in time during the flight. For the present sighting system, this represents an error of about 5 m at an aircraft altitude of 300 m.

Of more importance, if one is interested in measuring wind velocity, is the velocity drift of the inertial system obtained from the first derivative of the cubic spline fit to the discrete position drift data. An estimate of the velocity error resulting from this procedure was obtained in the same manner as for the position drift error. Again, for time intervals between 100-600 secs the RMS velocity error was seen to be approximately constant at a value of order $\sigma/\Delta t$, where σ , again, is about 5 m.

It should be mentioned, however, that both error estimates (and in particular the velocity error) hold only if the drift of the inertial system behaves smoothly between position fixes. This has been found to be largely the case for test flights of the present system. Manoeuvre dependent error mechanisms in the INU such as that caused by gyro azimuth drift will introduce small errors in the indicated positions which will be largely a function of distance travelled from the nearest position fix and as such will not follow the time dependent Schuler drift. Azimuth errors of up to $7'$ arc have been identified in the present system in several test flights resulting in cross-track drift of up to 2.5 m per km. Assuming an aircraft speed of about 75 m/s, this would result in a short term velocity perturbation between fixes of up to 0.2 m/s.

An example of this may be seen by analyzing the data from the test flight of Dec. 5, 1975. This flight was one of several tests of the inertial-sighting system used to determine the accuracy of post-flight path recovery for geophysical survey applications (Grasty *et al*, 1977). During the flight, multiple passes were made over two local coastal navigation markers, Panther Point and Enterprise Reef, in Trincomali Channel between the islands of Galiano and Salt Spring off the eastern coast of Vancouver Island. These two markers lay roughly on a line NNE separated by a distance of about 17 km.

By fitting the cubic spline to the discrete position drift data obtained from the sightings of both landmarks and then comparing this with a second spline fit to the data from one landmark only (Enterprise Reef) one can see the effect on the inertial system drift due to gyro azimuth errors. The resulting position drift curves (for both latitude and longitude) are shown in Fig. 1. The relative crosstrack drift of the inertial system between the two landmarks is easily evident as an offset (ΔS) in the position of one landmark relative to the other. For this particular test, the offset amounted to -15 ± 7 m in latitude and -32 ± 13 m in longitude. The effect of this azimuth error is even more pronounced in the resulting velocity (first derivative) drift curves shown in Fig. 2. Here, the maximum velocity perturbation (ΔV) is about 0.08 m/s in latitude and 0.15 m/s in longitude. As was previously mentioned, these errors will be roughly proportional to the distance of the aircraft from the nearest sighted landmark, in this case the distance between Panther Pt. and Enterprise Rf. (17 km). For most flights within coastal waters landmarks can usually be found with relative distance spacings in this range. Thus, the above position and velocity errors should reasonably represent upper limits on these two quantities.

4. Wind Measuring Sensors

After compensation for inertial system drift, the aircraft's position and velocity in addition to aircraft altitude are accurately known throughout the flight. In order to determine the direction and magnitude of the local horizontal air movement the additional parameters of airspeed and direction are required. To a good approximation, the airspeed may be obtained from the expression:

$$V_a = \left| \frac{2RT\Delta P}{MP_s} (1-K) \right|^{\frac{1}{2}} \quad (2)$$

where V_a is the airspeed, R is the gas constant (8.31 J/mole K°), T is the air temperature, ΔP is the pitot-static pressure, M is the molecular weight, P_s is the static pressure and K is a first order correction term for the air's compressibility. Here, K may be expressed as (Gorlin and Slezinger, 1964) $K = \frac{m^2}{4}$, where m is the mach number (aircraft velocity divided by velocity of sound in air). For an aircraft velocity of about 75 m/s, $k \approx 0.013$. The pitot-static and static pressure were measured by a low range differential pressure transducer and by a higher range, single ended pressure transducer respectively. The air temperature was measured by a thermistor mounted under the nose of the aircraft.

Because of various aerodynamical considerations, the direction of the airstream is not in general directly given by the actual heading of the aircraft. This is caused by the fact that an aircraft can yaw, or sideslip, while turning or even while undergoing level flight. Because of the nature of the vector calculations involved in obtaining wind measurements from the motion of the aircraft this yaw angle (θ_y), which under normal circumstances will be $\leq 5^\circ$, will, if not taken into account, dramatically affect the wind.

This may be seen by considering Fig. 3. Here, the relevant vector quantities required for the calculations are shown in the x,y coordinate system of the inertial platform. In this representation, all angles are measured positive clockwise with respect to the positive x axis. \vec{V}_a , \vec{V}_g and \vec{V}_w are the air, ground and wind velocity vectors respectively, θ_z is the local azimuth angle measure between the aircraft's longitudinal (heading) axis and the positive x axis and α is the inertial platform wander angle measured between the positive x axis and true north. From Fig. 2, the measured wind vector \vec{V}_w is given by the vector difference of \vec{V}_g and \vec{V}_a ($\vec{V}_w = \vec{V}_g - \vec{V}_a$), two vectors whose magnitude and direction are of similar value. If the aircraft yaws, the aircraft's heading will not correspond to the true direction of the airstream. This error in θ_z , which is the apparent direction of \vec{V}_a , will result in a relatively large error in the calculated \vec{V}_w . Although the direction of \vec{V}_a will be in error, the magnitude of \vec{V}_a will remain essentially constant for normal yaw angles however, due to the relative insensitivity of pitot tubes to angles of attack up to 10-15° (Gorlin and Slezinger, 1966; Lenschaw, 1971). Accounting for the aircraft yaw, the x and y components of the wind, from Fig. 3, can be expressed as

$$V_{wx} = V_x - V_a \cos(\theta_z - \theta_y) \quad (3)$$

$$V_{wy} = V_y + V_a \sin(\theta_z - \theta_y) \quad (4)$$

Here, V_x and V_y are the corrected (for drift) ground velocity components in the inertial platform frame. Positive yaw refers to clockwise rotation of the aircraft about the vertical axis. Relative to a north-east coordinate system, the wind speed and direction are given by:

$$|V_w| = \sqrt{V_{wx}^2 + V_{wy}^2} \quad (5)$$

$$\text{Heading} = \alpha - \tan^{-1}(V_{wy}/V_{wx}) \quad (6)$$

In order to obtain a measure of the aircraft yawing motion, a rotatable vane was mounted on the underside of the nose assembly adjacent to the air temperature sensing thermistor. The axis shaft for the vane was connected to a precision potentiometer similar to the ones used on the alt/azimuth target sight, thus enabling the yaw angle to be monitored. Because of the location of the vane in the airstream and because the vane was not statically balanced, the output from the vane was found to be non-

linear for induced angles of yaw $> 5^\circ$ or for roll angles $> 10^\circ$. One or both of these conditions will normally exist during aircraft turns resulting in a larger degree of error in the calculated wind. With proper flight planning, however, plane manoeuvres can be restricted so as to occur over areas of less importance and in any event, will likely represent only a small fraction of the total flight time.

Each of the sensors' input to MIDAS are voltage conditioned to yield a maximum of 10 V output within the normal range of operation. This is particularly important in that the analog channels in MIDAS have no voltage overload or reverse polarity protection. If one (or more) channels overload or experience a negative voltage, all eight channels become inoperative for the duration of the fault. Calibration of each of the various sensors was performed either in the laboratory or in the aircraft and the estimated RMS errors for each are listed in Table I.

Table I
Wind Measuring Sensors and Calibration Accuracy

<u>Sensor</u>	<u>Description</u>	<u>Estimated RMS Accuracy</u>
Static Pressure	Hamilton Standard Model PT-020S-5D (0-20 PSIA)	$\pm 0.001\%$ FS RMS (± 0.014 mb)
Pitot-Static Pressure	Edcliff Model 4-10S-2.50 (± 2.5 PSID)	± 0.02 mb RMS linearity ± 0.03 mb resolution
Temperature Sensor	Thermistor feedback op-amp	$\pm 0.04^\circ\text{K}$ RMS $\pm 0.03^\circ\text{K}$ resolution
Yaw Indicator	Precision single turn potentiometer	$\pm 0.2^\circ$ RMS linearity $\pm 0.12^\circ$ resolution

The differential pressure transducer and associated 6X amplifier were calibrated using the static pressure transducer as a standard. The stated accuracy of the static pressure transducer is as given by the manufacturer. Calibration of the temperature-sensor was conducted in a stirred glycerin bath using an accurate digital quartz thermometer with the entire bath assembly contained within a controlled environment chamber. Using the data in Table I, in conjunction with Eq. (1), the estimated RMS error in V_a , as measured from the pitot tube, should be < 0.1 m/s. Combining this estimate with a ground speed error of 0.2 m/s and a yaw error of 0.3° results in an estimated total wind velocity error vector of magnitude 0.5 - 0.6 m/s.

5. Pitot and Yaw in-Flight Calibration

The laboratory calibration of the pitot and yaw assemblies discussed above determined the relative accuracy of the two sensors. Absolute calibration, i.e., relating actual airspeed to measured airspeed, and actual yaw angle to measured yaw angle, of these two sensors was determined during each flight by analysing the calculated wind derived at various aircraft headings. Specifically, we consider that $V_a = C_1 V_a'$ and $\theta_y = \theta_y' + C_2$. That is, the true airspeed V_a is given by the measured airspeed V_a' from Eq.(2) multiplied by a correction coefficient C_1 . The magnitude of C_1 will be of order unity; its actual value being determined by the design of the pitot tube (Gorlin and Slezinger, 1966) and any additional systematic measurement errors in air temperature and density (e.g., due to changes in humidity). Similarly, the true aircraft yaw angle θ_y is given by the measured yaw θ_y' plus an offset constant C_2 . This constant will account for any error in the zero setting of the yaw sensor in addition to any misalignment of either the inertial unit or the pitot tube with respect to the longitudinal axis of the aircraft. Applying these corrections to V_a and θ_y in Fig. 3, we can see that C_1 will result in an error vector in V_w which is essentially along track whereas C_2 will result in an essentially crosstrack error. The resulting situation is shown in Fig. 4. As is evident, the result will be an error in both the magnitude and direction of V_w which will be dependent on the heading of the aircraft. Thus, if the aircraft travels along two different headings in a region of assumed constant wind, an error in either (or both) of C_1 and C_2 will result in a different apparent wind vector along each heading. By adjusting the values of C_1 and C_2 so as to minimize the variation in the calculated winds around a turn, a reasonably efficient method of calibration is realized. Because wind fields in any given area are never absolutely constant, calibration checks were taken at several locations during each flight in order to produce average values for C_1 and C_2 . These locations were chosen to be regions of relatively steady wind in which the aircraft turned through an angle of $> 90^\circ$. Approximately equal numbers of samples were used in the calibration along each turning leg so as not to weight one leg of the turn more heavily than another. During some flights a square pattern was flown and the resulting calibration performed for the entire square. Comparison could then be made of the values of C_1 and C_2 obtained in this manner as compared to analyzing individually each of the four separate 90° turns. As was mentioned earlier, the yaw sensor used in the current tests could be expected to provide reasonably accurate measurements provided the roll angle of the plane did not exceed about 10° . For this reason, wind data obtained while the roll exceeded 10° was not used for any of the wind calculations. An improvement in both the yaw sensor design and its location would be required for accurate wind measurements under high aircraft roll or yaw.

Table II shows the results of the inflight pitot and yaw calibrations for various test flights.

TABLE II

Pitot and Yaw Inflight Calibrations

Flight Date	\bar{C}_1	$\bar{C}_2(^{\circ})$	\bar{V}_w (m/s)	\bar{RMS} (m/s)	Number
Jan. 27, 1977	1.005 \pm 0.004	-0.6 \pm 0.2	7.1	0.7	5
March 30, 1977	1.018 \pm 0.004	-0.6 \pm 0.2	2.6	0.5	6
March 31, 1977	1.032 \pm 0.007	-0.4 \pm 0.5	10.7	1.1	8
May 19, 1977	1.017 \pm 0.003	-0.5 \pm 0.4	7.7	0.8	6
June 14, 1977	1.025 \pm 0.001	-0.6 \pm 0.1	6.0	0.7	5
June 17, 1977	1.022 \pm 0.001	-0.6 \pm 0.2	5.8	0.7	5

Here, the average values of C_1 , C_2 and V_w are given together with the RMS deviation for each average and the number of calibration locations for each. As is evident, the variability in C_1 , C_2 and V_w increase for larger amplitude winds, a result which is most likely due to increased air turbulence under higher wind conditions. Because of the large inertia of the aircraft as compared to the small yaw sensor, short period air turbulence (or wind gusts) will show in the data as a change in the aircraft yaw angle. The computed wind vector in such cases will remain accurate provided that the turbulent components of the wind normal to the mean wind direction are sufficiently small such that the effective angle of attack of the pitot tube remains within the previously specified limits of 5-10°. For larger effective attack angles, a trigonometric correction to the measured airspeed would need to be applied. It should also be mentioned that under conditions of heavy turbulence, the assumption of a constant wind field during calibration is also likely suspect. Calibrations computed in any given flight without using the yaw sensor data resulted in an increased RMS deviation in the average values for both C_1 and C_2 computed for the complete flight. This indicates that within the limitations of the yaw angle sensor used here, the yaw angle data does lead to improved internal consistency and overall accuracy of the resulting wind calculations.

Variations in the average values of both calibration constants from flight to flight are partly attributable to long term mechanical and electrical drifts associated with the various sensors involved. In particular, in the period between the January 27th and the March 30th flights, the pitot and static pressure transducers were removed from the aircraft, possibly accounting for the jump in value of C_1 over this period. Averaging, the last five flights results in overall average values for C_1 and C_2 of 1.023 \pm 0.006 and -0.5 \pm 0.1° respectively. For an average airspeed of 75 m/s, the combined RMS deviations in the above values will result in an RMS wind

error vector of magnitude about 0.6 m/s, a value which is in very good agreement with the predicted estimated error given previously. The altitudes at which most of the calibrations occurred ranged from 30-300 m. For the June 14th test however, in flight calibrations were conducted at altitudes of 30 m and 3000 m. These calibrations resulted in essentially identical values for C_1 and C_2 at both altitudes indicating that the pitot and static pressure sensitivities are relatively independent of altitude up to this height.

6. Wind Measurements in Juan de Fuca Straits

During the first half of 1977 six flight tests of the system were conducted in Juan de Fuca Strait off Victoria, B.C. The majority of these flights were undertaken in cooperation with the Tides and Currents section of the Institute of Ocean Sciences, Patricia Bay, for the purpose of studying the feasibility of measuring near surface wind fields for use in various oil spill prediction models of the strait. The results of these test flights are discussed below.

The computed wind vectors, for each flight, calculated using the various values of C_1 and C_2 in Table II are shown in Figs. 5 through 10. In each case, the wind vectors represent an average over a time span of 30 seconds, representing a spatial averaging distance of about 2 km. The original plots were computer generated on a natural scale of 1:250,000 and then subsequently overlaid on a topographic map of the region for hand drafting of the coastline along the strait and the southern tip of Vancouver Island. In each test, the flight path was chosen to encompass a sufficient number of surface landmarks for post-flight inertial system drift analysis (as discussed previously).

As is evident in all six flights, the winds in Juan de Fuca Strait are predominantly directed along the strait. This result is typical due to the funnelling effect of the Olympic mountain range along the southern border of the strait and the coastal mountains along the northern border of the strait on Vancouver Island. For four of the flights, on March 30 and 31, May 19 and June 14, the winds in the strait were towards the east ranging from 6 to 17 m/s. In each case, the winds down the strait tend to split as they approach the mouth of Haro Strait and Puget Sound, with the winds in the northern strait tending northward up Haro Strait and the winds in the southern part of Juan de Fuca Strait tending southward down Puget Sound. Also evident is a distinctive shading of the wind, by the land mass near Victoria, causing a drop in wind speed up the western side of Haro Strait.

Conversely, for the flights on January 27 and June 17, where the winds in the strait were to the west, a reciprocal process (at least as concerns Haro Strait) is seen with the wind flowing southward down Haro Strait and then being funnelled along Juan de Fuca Strait to the west. As evidenced in the June 17 flight, the winds in the center of the strait seem to suggest an origin in Puget Sound. Unfortunately, no wind measurements were taken along the southern reaches of the strait or near the mouth of Puget Sound. Measurements of this kind would have been valuable in determining if a completely reciprocal process had been occurring here, that is, if the air mass along the southern section of Juan de Fuca Strait had its origin in Puget Sound to the south.

Some conclusions might also be drawn from the May 19 flight concerning the character of the winds in the strait proper. Here, several cross-strait sections were flown in addition to sections along the northern and southern boundaries. Similar sections were also flown during the March 30th flight but for this flight the winds were too variable to be of any significant value. As is evidenced in the measured winds on May 19, the winds in the north and center sections of the strait are seen to be relatively uniform. Along the southern boundary of the strait, however, the wind tends to be less uniform. Part of this is most likely due to the much more irregular nature of the shoreline along the Olympic Peninsula. Certainly near Cape Flattery, at the southern mouth of the strait, the decreased effect of the Olympic mountain range can be seen by the fact that the wind is more to the south rather than being directed along the strait to the south-east.

As mentioned above, the purpose of these flights was to measure near surface wind fields in Juan de Fuca. To this end, the aircraft was flown as low as possible (20-30 m) while over areas of interest. While away from the strait, and while flying over surface landmarks, the altitude of the aircraft was considerably higher, ranging up to 500 m. Thus, much of the variability in the wind plots is due to aircraft altitude changes. These changes in altitude are indicated in Figs. 5-10 by bars superimposed on the wind vectors. Here, no bars signify altitudes to 60 m, one bar altitudes to 200 m and two bars, altitudes above 200 m. Viewing the wind measurements in Figs. 5-10 as a whole, the fact the averaged winds in any given location measured at the same altitude at varying aircraft headings show very good internal consistency is verification of the inherent accuracy of the system as discussed above. Additional evidence for this can be obtained from the wind data during the last flight on June 17. For this test, anemometer wind measurements were also taken aboard a vessel on lease to the Tides and Currents Section, stationed near the center of the strait. This wind data consisted of one minute time averaged wind speed and direction obtained approximately 5 m above sea level. In order to use this data for comparison with the airborne system, several square patterns were flown at low altitude (< 20 m) around the vessel during a portion of the flight. Averaging the calculated winds over these squares (a total time of about 7 minutes) resulted in a mean speed and direction of 5.0 ± 1.6 m/s and $-40 \pm 13^\circ$ respectively. Over this same time period, the corresponding average of the anemometer data was 4.6 ± 0.4 m/s and $-50 \pm 5^\circ$. Considering the altitude difference of the two measurements and that the airborne data represents a spatial, in addition to time average, the agreement between these two sets of data is very good.

7. Summary and Conclusions

Airborne measurements of wind have been made from an aircraft using data from the aircraft's pitot/static system in conjunction with data from an onboard inertial navigation unit. The inertial navigation unit is a Litton LTN-51 interfaced to a specialized data acquisition system. Additional sensors have been incorporated into the system to measure the additional parameters of air temperature and aircraft sideslip which are required for the calculation of wind velocity. Inertial system drift is compensated for by fixing the aircraft's position using target sighting apparatus located in the transparent nose of the aircraft.

Accounting for additional residual errors in the inertial system as well as errors in the various wind measuring sensors, we estimate that the resulting wind velocity measurements will be accurate (for aircraft roll $\leq 10^\circ$) to about ± 0.5 m/s. Viewing the results of the various test flights of the system to date, in particular the internal consistency shown in the calculated winds in the same area and at the same altitude, it is difficult in fact to imagine any instrument effect which could cause the observed winds to be in error beyond the calculated accuracy limit stated above.

Given this accuracy, it is felt that the present system can provide useful wind data for a variety of applications, such as atmospheric models and/or oil spill prediction. This data would be of significantly greater use than present data available from moored buoys or onshore weather stations.

8. References

- Axford, D.N., 1968. On the Accuracy of Wind Measurements Using an Inertial Platform in an Aircraft, and an Example of a Measurement of the Vertical Mesostructure of the Atmosphere, *J. of Appl. Meteorology* 7(8), 645-666.
- Baker, R.C. and J.S. MacDonald, 1974. An Integrated Airborne Data Acquisition System for Remote Sensing, 2nd Can. Rem. Sens. Symp., Guelph, Ontario, Canada. pp. 671-674.
- Gorlin, S.M. and I.I. Slezinger, Ed., 1966. Wind Tunnels and Their Instrumentation, Israel Program for Scientific Translations, Jerusalem.
- Grasty, R.L., J.F.R. Gower and B.M. Oliver, 1977. Inertial Navigation for Flight Path Recovery, Geological Survey of Canada paper 76/30.
- Lenschow, D.H., 1971. Vanes for Sensing Incidence Angles of the Air from an Aircraft, *J. Appl. Meteorology* 10(12), 1339-1343.
- Oliver, B.M. and J.F.R. Gower, 1977. Use of An Inertial Navigation System for Accurate Track Recovery and Coastal Oceanographic Measurements, Proc. Eleventh Int. Symp. Rem. Sens. Envir., Ann Arbor, Mich. In press.
- Telford, J.W., 1974. The Measurement of Horizontal Air Motion near Clouds from Aircraft, *J. of Atmos. Sci.* 31(11), 2066-2080.
- Telford, J.W., P.B. Wagner and A. Vaziri, 1977. The Measurement of Air Motion from Aircraft, *J. Appl. Meteorology* 16(2), 156-166.

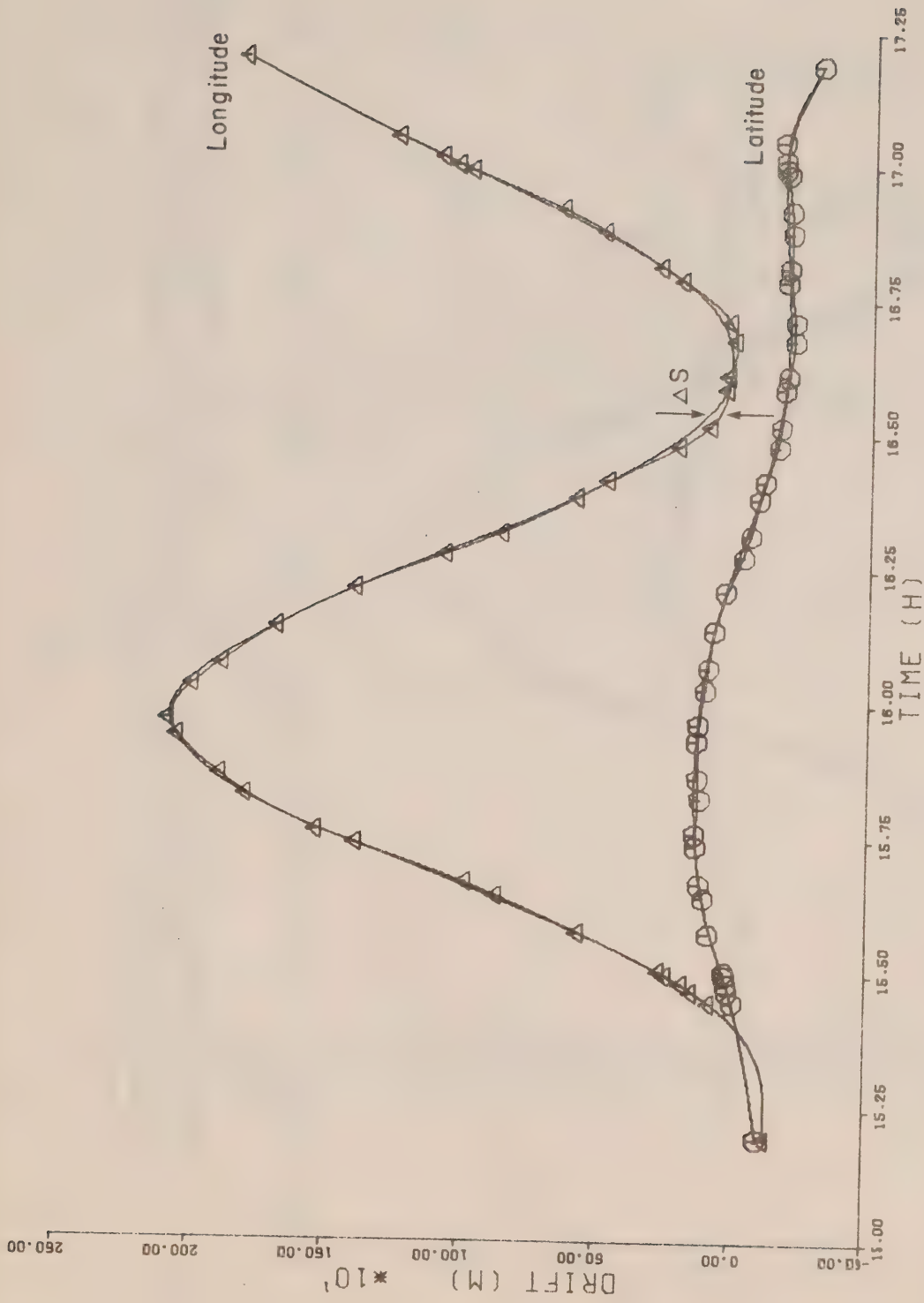


Figure 1. Discrete latitude and longitude inertial system position drift for the Dec. 5, 1975 test flight. The solid lines show two separate spline fits to the data, one being fitted to all the data and the other fitted to approximately half the data.

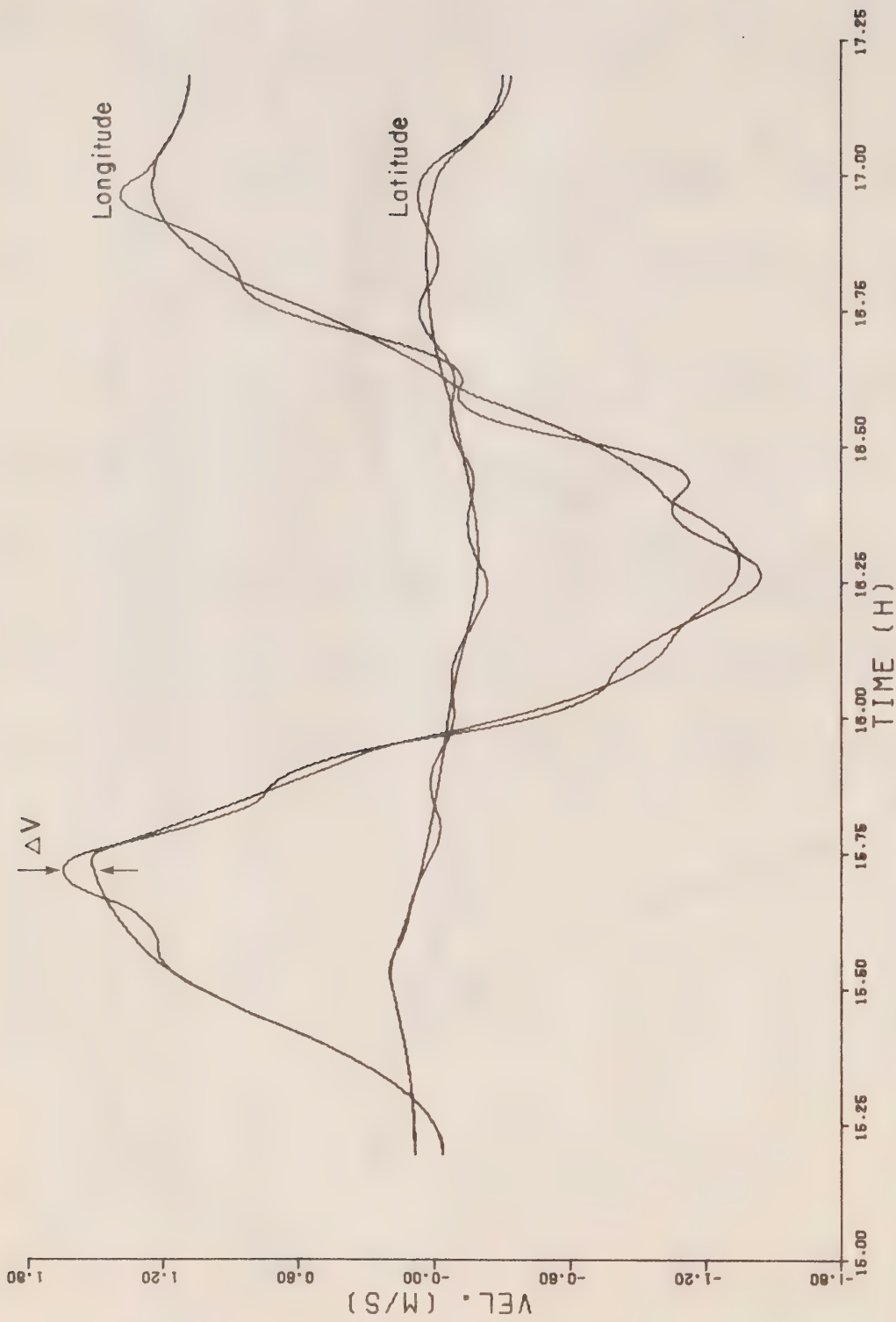


Figure 2. Inertial system velocity drift for the Dec. 5, 1975 flight obtained from the derivative of the cubic splines shown in Fig. 1. The deviations between the two sets of curves, ΔV , due to azimuth gyro drift, is seen as a high frequency wobble on the lower frequency Schuler drift.

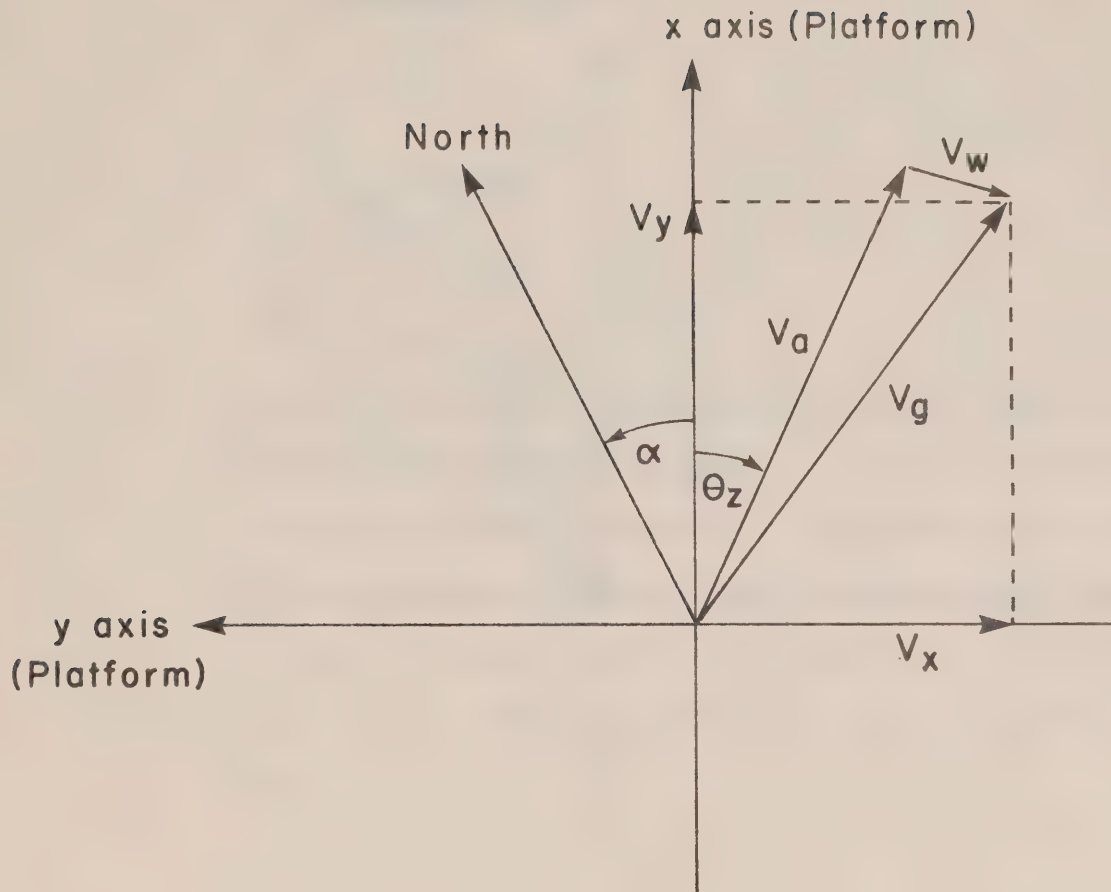


Figure 3. Vector quantities involved in the calculation of wind velocity. The x , y coordinate system represents the axes of the inertial platform.

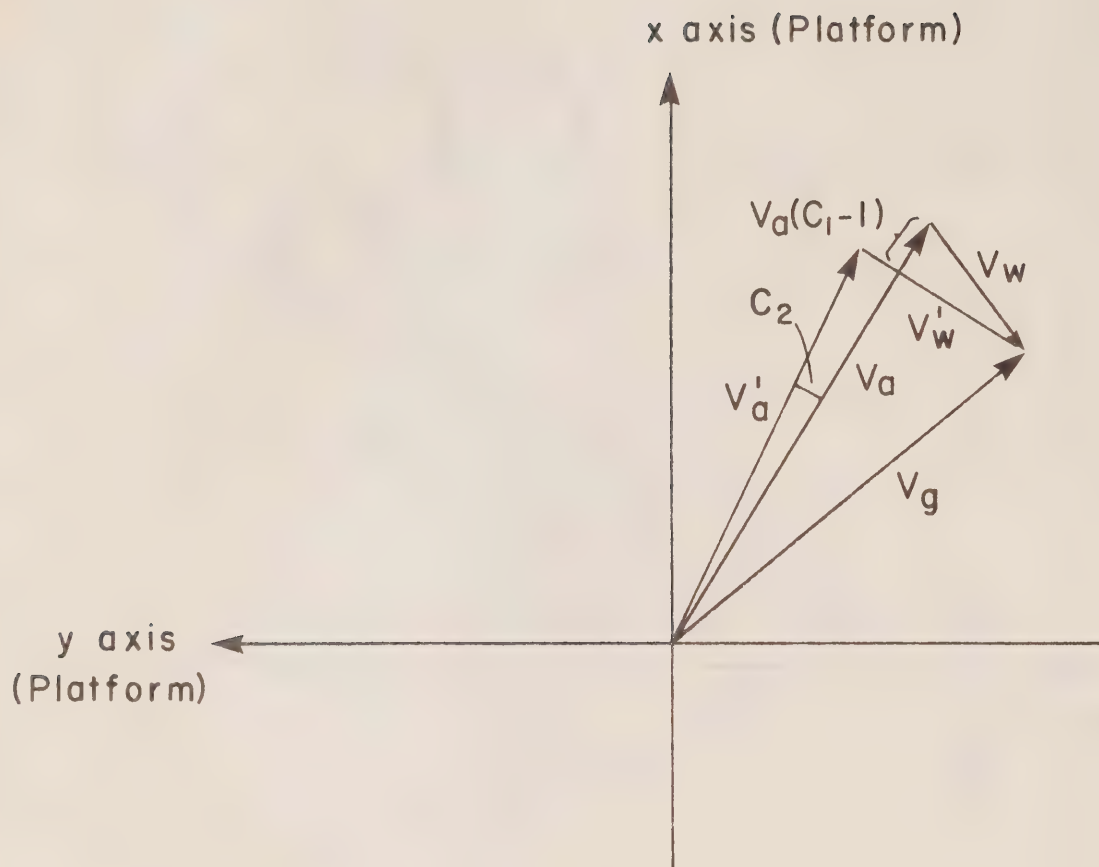


Figure 4. Perturbation to the calculated wind velocity vector caused by applying angle and amplitude corrections C_1 and C_2 to the measured airspeed direction and amplitude respectively.

Figures

5-10.

Calculated airborne wind vectors for six test flights of the system in the first half of 1977. In each case, the vectors represent 30 second time averages. The approximate altitude of the aircraft is indicated by bars superimposed on the body of each wind vector. Here, no bars indicates altitudes to 60 m; 1 bar, altitudes to 200 m and 2 bars, altitudes above 200 m.

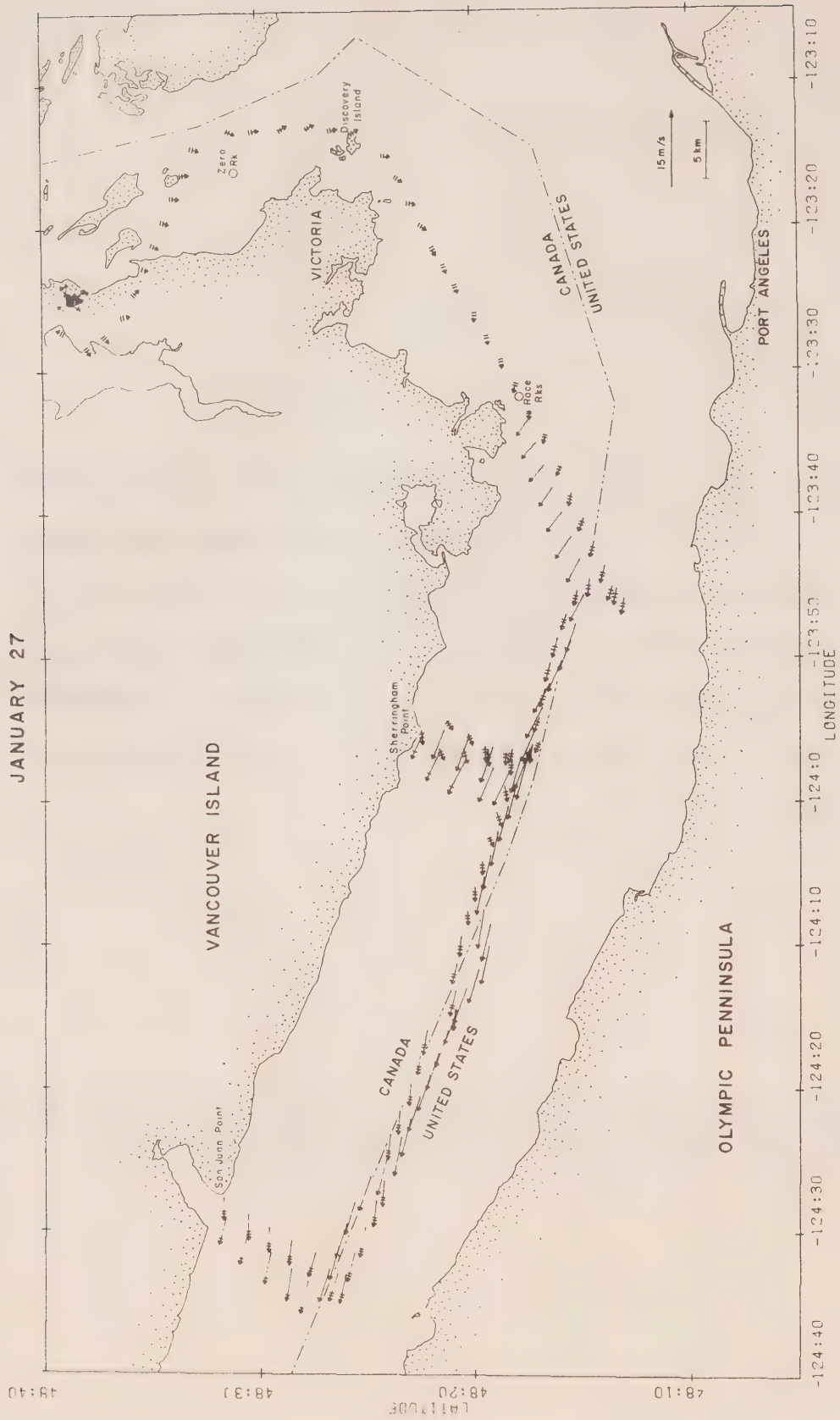


Figure 5.

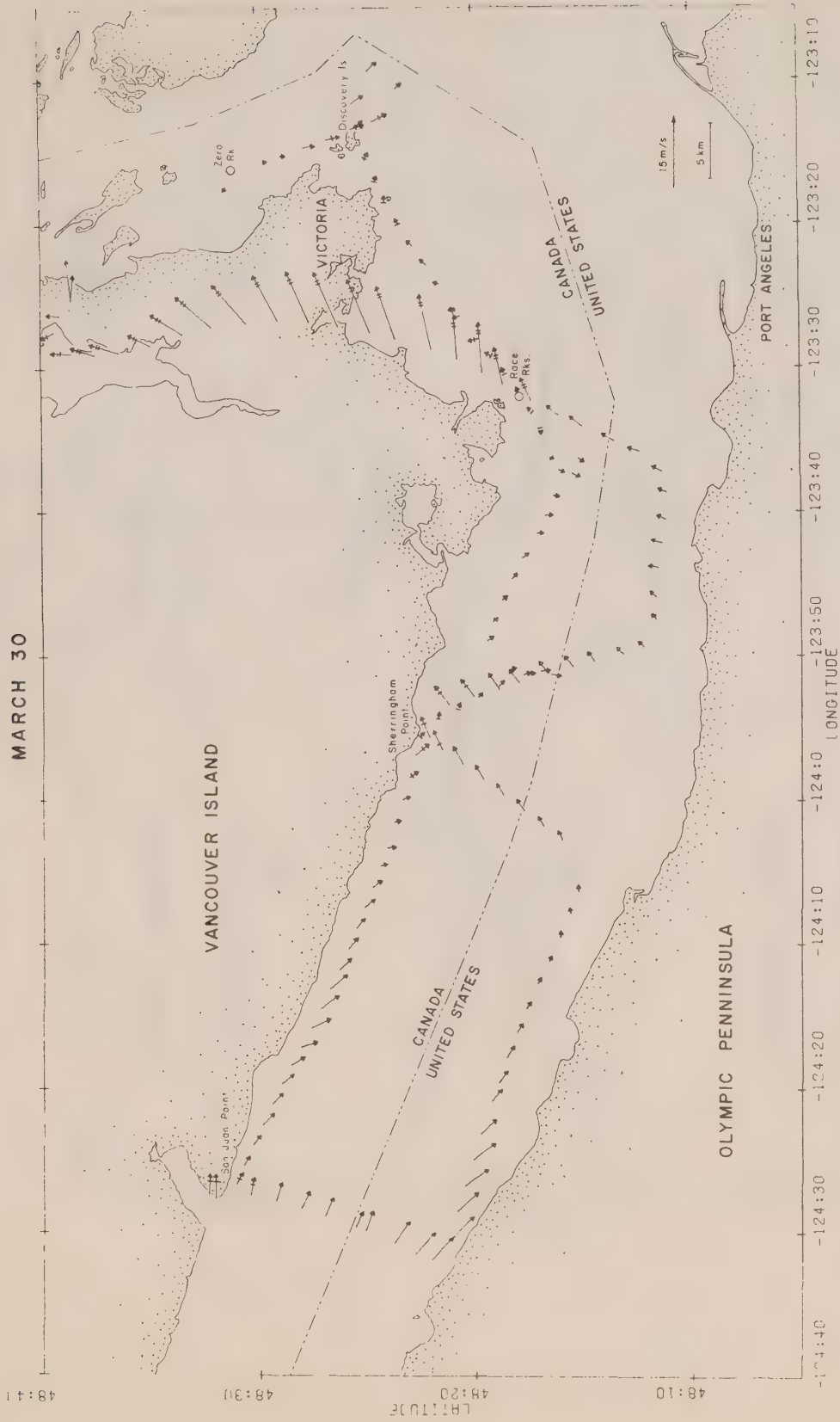


Figure 6.



Figure 7.

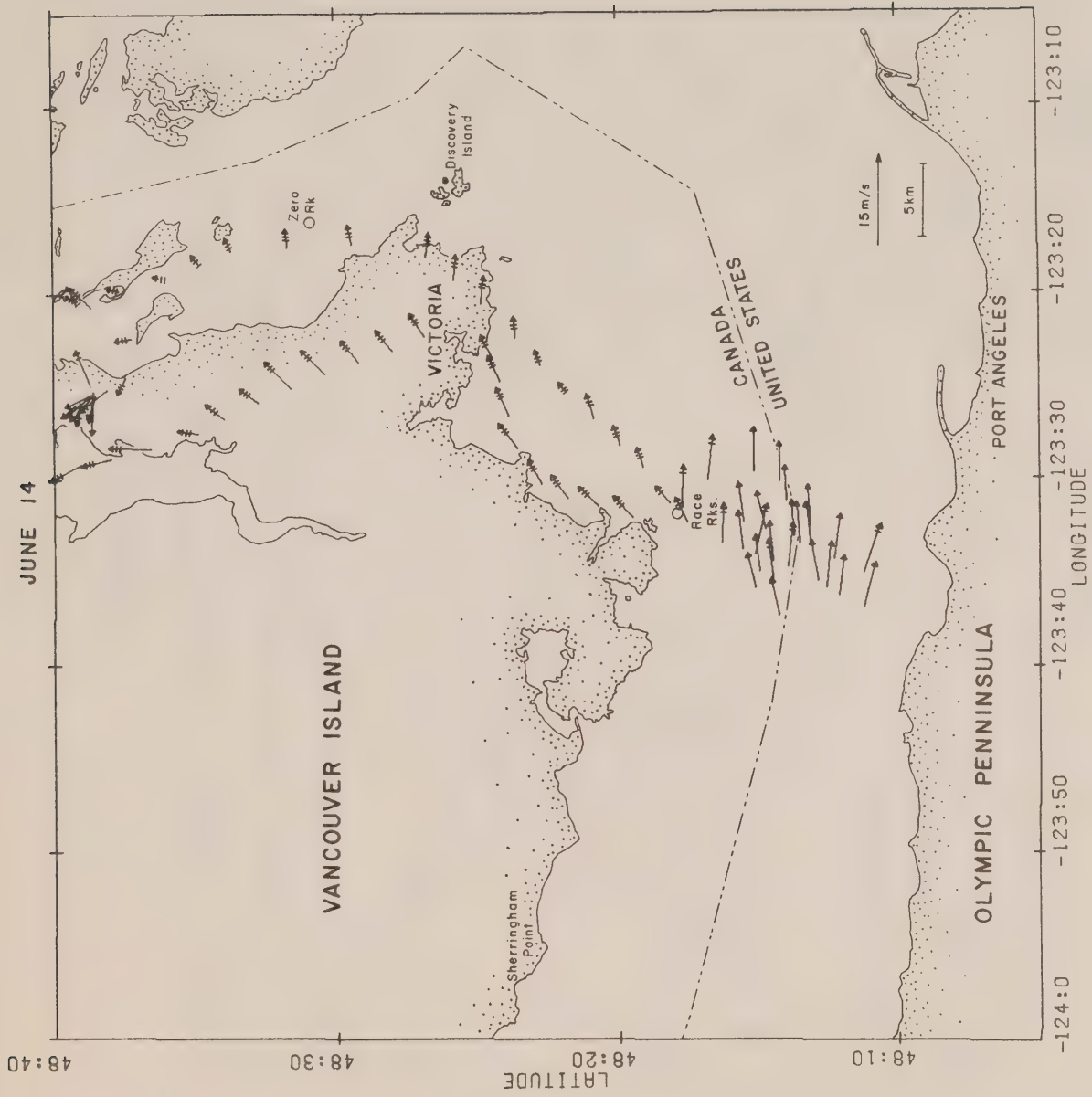


Figure 8.

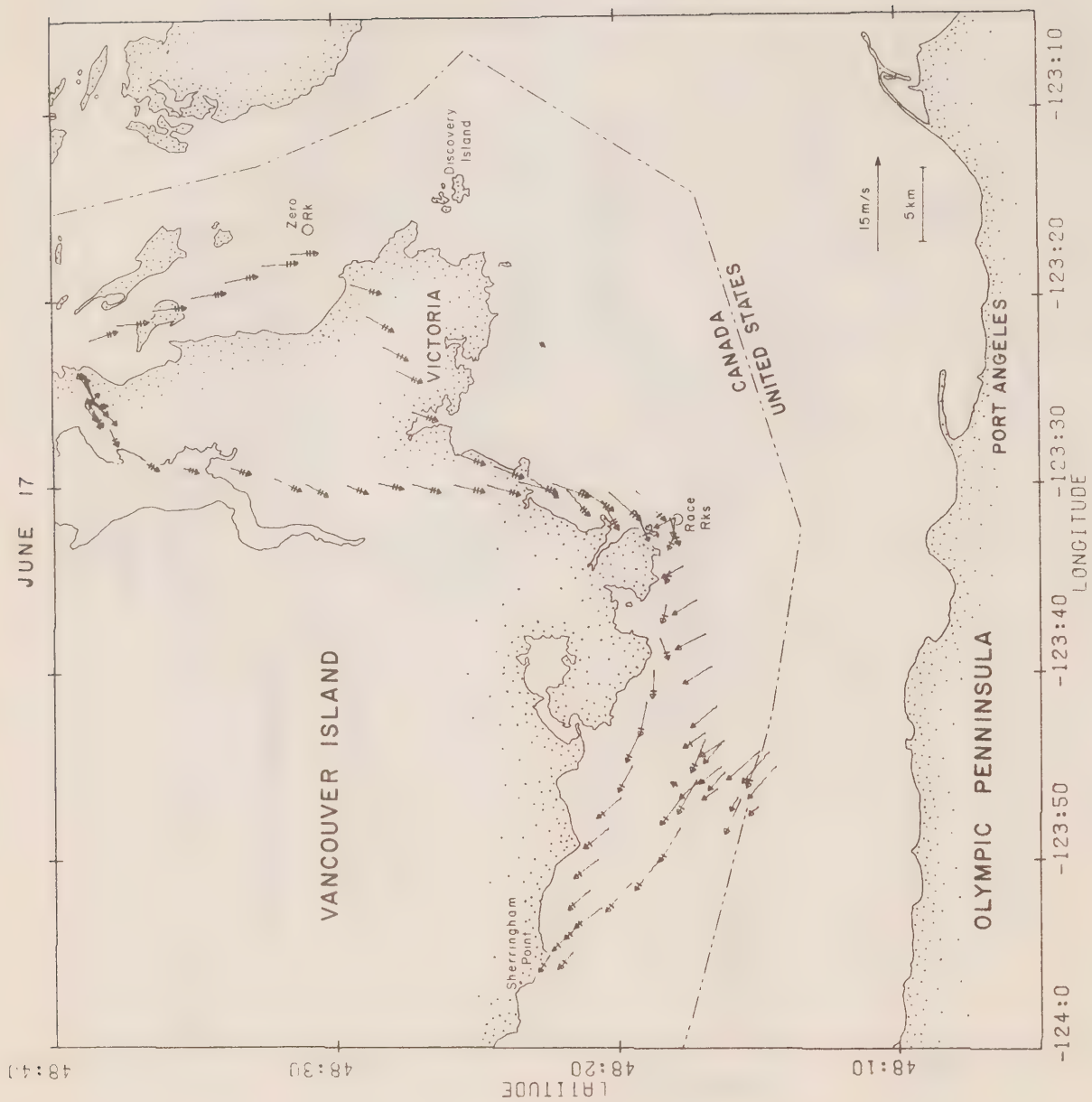
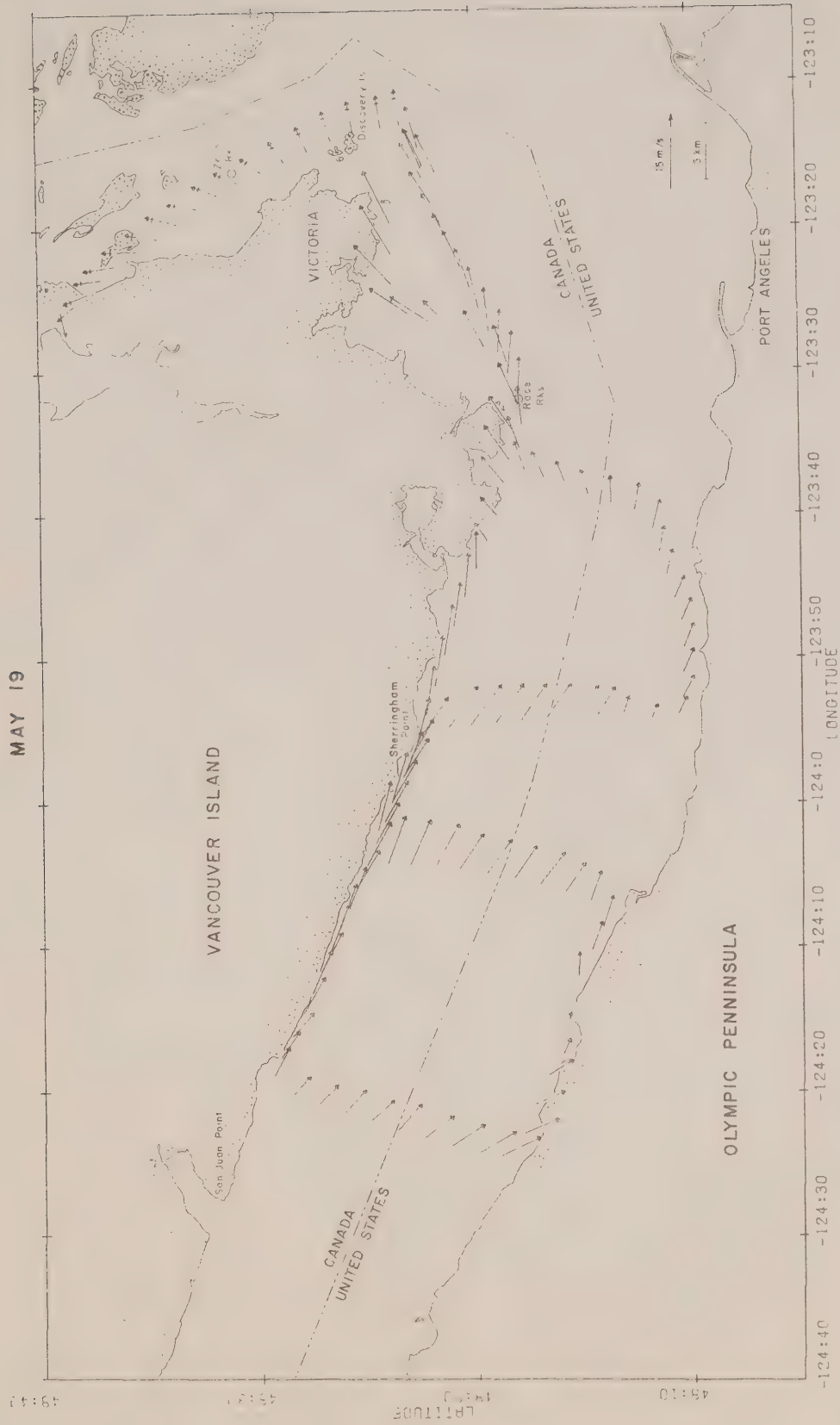


Figure 9.



CAI
EP 321
-77R16

AN *IN SITU* DRAG COEFFICIENT DETERMINATION FOR AN AANDERAA THERMISTOR CHAIN

by
W.H. Bell



Institute of Ocean Sciences, Patricia Bay
Sidney, B.C.

For addition copies or further information please write to:

Department of Fisheries and the Environment

Institute of Ocean Sciences, Patricia Bay

P.O. Box 5000

Sidney, B.C.

V8L 4B2

AN *IN SITU* DRAG COEFFICIENT DETERMINATION
FOR AN AANDERAA THERMISTOR CHAIN

by

W.H. Bell

Institute of Ocean Sciences, Patricia Bay
Sidney, B.C.
October 1977

This is a manuscript which has received only limited circulation. On citing this report in a bibliography, the title should be followed by the words "UNPUBLISHED MANUSCRIPT" which is in accordance with accepted bibliographic custom.

ABSTRACT

Lack of knowledge regarding the drag forces on a thermistor chain moored in tidal currents led to uncertainties in the design of such moorings using a surface buoy. In an attempt to resolve the problem, a field experiment was conducted using a thermistor chain, current meters and pressure sensors suspended from a subsurface buoy. An empirical value for the thermistor chain drag coefficient is obtained using the field data and a mathematical simulation of the mooring. Then, using the model to simulate a surface mooring, the effect of thermistor chain drag on cable tension and required anchor weight is investigated.

Acknowledgements

Grateful acknowledgement is made to A. Stickland, R. Bigham and L. Spearing for their efforts in arranging, installing and retrieving the test mooring and to the captain and crew of the Dobrocky Seatech vessel "Sea Lion" for their assistance with the field work.

TABLE OF CONTENTS

	<u>Page</u>
Abstract	i
Acknowledgements	ii
Table of Contents	iii
List of Figures	iv
List of Tables	iv
Introduction	1
Sensor Data	1
The Mooring Model	4
Thermistor Chain Drag Coefficient	6
Thermistor Chains With a Surface Mooring	6
Conclusion	11
References	14
Appendix I - Model Input Parameters	15

LIST OF FIGURES

	<u>Page</u>
Fig. 1. Mooring Arrangement	2
Fig. 2. Current Speed <i>vs</i> Cable Tension for a Surfaced-Moored Thermistor Chain	10
Fig. 3. Graph of $1/\mu = (W_A - T_Z)/T_X$ <i>vs</i> Velocity	12

LIST OF TABLES

Table I. Data Obtained From Current Meter Sensors	3
Table II. Sensor Data Converted to Ft-Lb-Sec System	4
Table III. Mooring Component Rest Position Distances	5
Table IV. Checks on Drag Coefficient Estimate	7

Introduction

Aanderaa thermistor chains are often moored beneath a surface buoy for the purpose of determining the thermal structure of the water. Each chain is made up of 11 thermistors enclosed in a plastic hose with a diameter of 16 mm and a length of about 50 m. Because the drag coefficient of the hose (when attached to a wire rope forming part of a taut-line mooring cable) was not known, there was some uncertainty as to how many such thermistor chains could be safely used on one mooring in strong currents. It was decided to attempt an *in situ* determination of the drag coefficient by using data obtained from a thermistor chain and Aanderaa current meters, attached to a sub-surface mooring, in conjunction with a numerical mooring model (Bell, 1977a, b). With a velocity profile obtained from the current meters, and a measure of the vertical excursion of the mooring obtained from pressure sensors incorporated in the current meters, it would be possible to obtain an estimate of the thermistor chain drag coefficient from the mooring model.

A mooring was deployed on May 30, 1977 in Haro Strait at the position 48° 35.6'N, 123° 15.5'W. Previous experience at this location has shown that the velocity profile is usually quite uniform in both amplitude and direction during periods of large tidal range. When this condition prevails, the subsequent analysis is facilitated. The water depth at the site is approximately 207 m. The mooring arrangement is shown in Fig. 1, together with an indication of the component distances along the cable, referred to the anchor location. The distances include an allowance for the strain induced by cable tension. The mooring was retrieved on June 6, 1977.

Sensor Data

The sampling interval used for data acquisition was 2 minutes. In the sampling scheme used by the Aanderaa current meters the direction and pressure data are obtained as instantaneous values, whereas the speed is integrated over the sample period. A sample set was chosen from a portion of the record where there was some reasonable correspondence between speeds and directions at the three current meter positions. This set is presented in Table I. Subsequently, in the model, the mean of the samples is used. This is an aid in smoothing out irregularities in the data arising from the difference in sampling technique between speed and pressure, or from non-uniformities in the velocity profile between current meter locations. Although oceanographic data are normally reported in metric units, as in Table I, they are here converted to the ft-lb-sec system for use in the model because of the present utility of the force unit (lb). Table II presents some pertinent data thus converted. An obvious inconsistency is apparent, inasmuch as the change in depth is shown to be slightly greater for the middle sensor than for the top one in the array. This is readily accounted for by the considerable difference in actual accuracies of the pressure sensors. The top sensor has a range of 0-200 psi and the other two both have a range of 0-1000 psi, while the accuracy is 1% of full scale in all cases. The height of the column of water equivalent to the accuracy is about 4.5 ft for the top sensor and 22.5 ft for the others. Because the drag coefficient is determined by comparing actual and predicted vertical excursions, which are the difference between two pressure readings for the actual case, only the values obtained from the more accurate sensor will be used in the determination. The mean depth used in the calculation is adjusted relative to the rest position

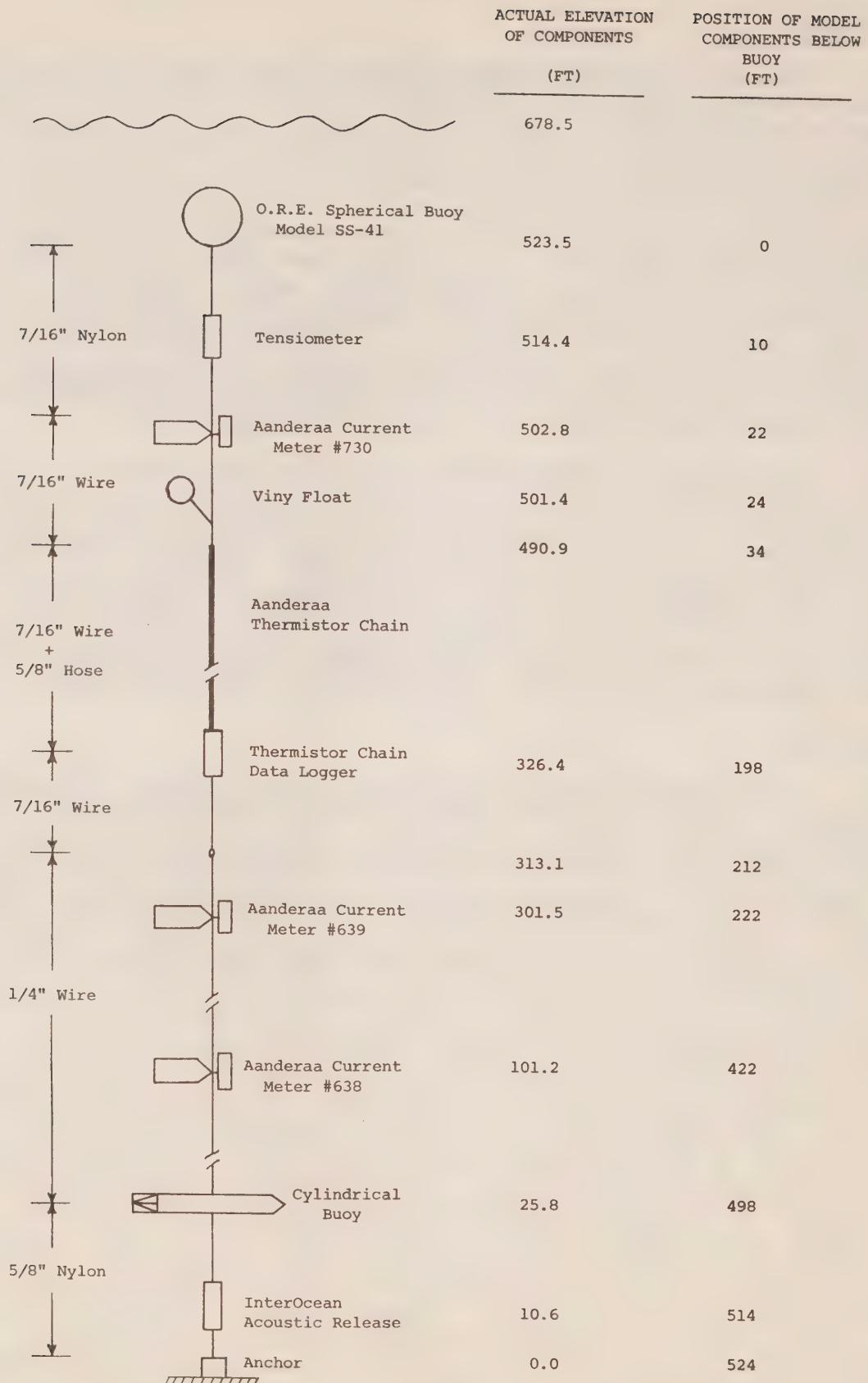


FIGURE 1 - Mooring arrangement.

TABLE I. Data Obtained From Current Meter Sensors

Record No.	Instrument No.					
	730			639		
	Pressure (m)*	Direction ($^{\circ}$ T)	Speed (cm/sec)	Pressure (m)*	Direction ($^{\circ}$ T)	Speed (cm/sec)
616	60.8	348	81.4	121.5	336	73.2
617	61.6	349	91.7	122.2	337	81.4
618	61.1	348	89.6	121.5	340	81.4
619	60.7	344	85.5	120.7	341	83.5
620	60.7	338	75.3	120.7	340	87.6
621	60.7	336	75.3	121.5	341	89.6
622	61.0	336	81.4	122.2	340	91.7
623	62.0	337	85.5	123.0	340	87.6
624	63.2	336	87.6	124.5	338	87.6
625	63.4	338	95.8	125.2	335	97.8
Mean Value	61.5	341	84.9	122.3	339	86.1
Rest Position	54.8			115.5		
				177.0	343	86.4
				175.5		
				177.0	338	99.9
				177.0	337	95.8
				178.5	337	89.6
				177.0	339	79.4
				177.0	339	87.6
				176.2	341	85.5
				177.0	344	79.4
				176.2	348	81.4
				177.0	353	85.5
				177.0	353	79.4

Mean value of all speed samples = 85.8 cm/sec

Mean value of all direction samples = 341° T

* Pressure unit is meters of fresh water

depth, as shown in Table II, to account for the differing tide heights occurring at the times of the measurements for the instrument rest position and the position assumed by the instrument under the action of the current. The tide of the test mooring site is assumed to be that predicted for Hanbury Point on San Juan Island, immediately adjacent to the test site.

TABLE II. Sensor Data Converted to Ft-Lb-Sec System

	Instrument No.		
	730	639	638
Mean Depth (ft)*	197.1	391.8	567.0
Mean Depth Adjusted for Tide Height (ft)	193.8	388.5	563.7
Rest Position (ft)*	175.7	370.0	562.2
Change in depth (ft)	18.1	18.5	1.8

Mean speed = 2.8 ft/sec

* Depth is obtained from the pressure reading and includes the effect due to the water column being saline (specific gravity = 1.024).

The Mooring Model

Mathematical simulation of the mooring system is accomplished by writing the appropriate static force balance equations for the buoy, the cable and the instruments, and solving them simultaneously using a numerical integration procedure. Boundary conditions are established by the buoy at the upper end of the cable and the integration proceeds from there, in discrete steps, to the anchor end of the cable. Here, the anchor and the bottom must coincide (within a specified limit) or an iteration is necessary. Because of the step-wise integration, the cable consists of an integral number of segment lengths and instruments can only be inserted between segments. As a result, the model dimensions must be altered slightly from those of the real system it is intended to simulate. The effect of this is shown in Table III and Fig. 1 for the present case. Again, a discrepancy is noted in connection with the pressure sensor data since the measured distance between sensors does not agree with that derived from the pressure information. Part of the discrepancy may be due to a small error in the reported rest positions, arising from an incomplete knowledge of the velocity profile, but most is undoubtedly a result of sensor inaccuracy. This data supports the decision to derive the drag coefficient from the information supplied by the uppermost pressure sensor. The next requirement is one of setting out the remaining model input parameters with reasonable accuracy, as presented in

TABLE III. Mooring Component Rest Position Distances (ft above bottom)

Component	Distance			Model
	Planned	Measured	Pressure*	
Bottom sensor	100	101.2	116.3	102
Middle Sensor	300	301.5	308.5	302
Top Sensor	500	502.8	502.8	502
Buoy	520	523.5	523.5	524

Model cable segment length = 2 ft

No. of segments = 262

* Derived from pressure sensor data assuming a water depth of 678.5 ft so that the top sensor position coincides with the measured value.

Appendix I. The only item which requires some explanation (besides the Vinyl float which remained attached through an error) is the value of the diameter of the thermistor chain-wire rope combination. These two components are initially fastened together in a slack condition with their axes parallel to one another, using plastic ties spaced several inches apart. When the wire rope comes under tension, after installation of the mooring, it has a tendency to unwind because it is not torque-balanced. Wire rope is used in preference to a torque-balanced synthetic plastic cable to prevent undue stretching of the thermistor chain under tension. The net result of the unwinding tendency is that the thermistor chain assumes a helical shape about the wire rope, increasing the cross-sectional area presented to the flow. (However, this shape may inhibit vortex shedding and, hence, strumming with its resulting higher drag.) The effective, or average, diameter of the combination is therefore assumed to be the sum of the largest diameter (in this case, the hose) and one-half of the smallest diameter (the wire rope). The definition of diameter is not of great import so long as it is used consistently in any subsequent calculations involving the derived drag coefficient.

A value for the drag coefficient of the thermistor chain is assumed and the model predictions for the change in depth of the sensors under the influence of the given current are computed. When this is done for two or three different values of drag coefficient, an interpolation can be made for that coefficient which corresponds to the measured depth excursions. Mention should be made of the fact that only the normal drag force is considered here, consisting principally of form drag, but including a small additive skin friction term. Longitudinal drag is neglected as an unnecessary complication (although provision for calculating it is included in the model). Thus, if the cable is at an angle to the flow, the drag is taken basically as the product of the square of the sine of the angle and the drag which would occur

normal to the flow. So long as the angles involved are reasonably close to 90° , the error due to the omission of frictional drag in the axial direction is small. Also, buoy tilt may be quite pronounced at high current speeds and no attempt is made to include the effect of this in the model.

Thermistor Chain Drag Coefficient

Two model simulations were made, using drag coefficient values of 1.8 and 2.1. These resulted in predicted depth excursions which bracketed the actual excursion of the uppermost current meter. A linear interpolation was then made, indicating coincidence of the measured and predicted excursions at a drag coefficient value of $C_D = 1.97$. Some uncertainty in this value results from measurement errors, some from the tide height prediction and some from errors in estimating drag coefficients for the other mooring components. The greatest source of uncertainty, though, arises from the lack of complete knowledge of the velocity profile, because the square of the velocity is involved in the determination. It is not possible to assign limits to this uncertainty with any degree of confidence. However, as a check on the validity of the estimate, it can be used for predictions of instrument excursions corresponding to other points in the empirical data set. This is done below. Because of the uncertainty, the value of the coefficient is henceforth rounded off to:

$$C_D = 2.0$$

Table IV sets out the details for the comparison of some additional model predictions for the current meter elevations with the corresponding empirical data. The first check was made for the case of relatively strong currents, about twice the speed of the current used in arriving at the drag coefficient value. The effect of this higher speed should be to magnify any errors in predicted depths. Also, only one sample set was used in the comparison, although it should have reasonable validity because it was chosen from a section of the data record where the velocity and pressure appeared to be smoothly varying functions. The remaining three checks are all based on the average of five sample sets. The first three checks involve a uniform velocity profile, whereas the fourth has a linear variation in velocity with depth. The greatest error for the predicted depth of any of the current meters in any of the checks is about 4% of the indicated depth. Since the predicted depths err on both the high and low sides of the indicated depths, it is likely that the chief source of the error is the uncertainty in the velocity profile for each case.

Thermistor Chains With a Surface Mooring

Now that an estimate of the thermistor chain drag coefficient has been obtained, we can use it in a model simulation of a surface mooring to determine the constraints imposed on a system using one or more thermistor chains.

The model mooring uses a Geodyne toroid buoy for surface support. A typical water depth for such a mooring in coastal waters might be 900 ft, as

TABLE IV - Checks on Drag Coefficient Estimate

CHECK NO. 1

	Instrument No.		
	730	639	638
Indicated current speed (ft/sec)	5.76	5.63	5.76
Current direction (°T)	344	337	310
Model current speed (ft/sec)	5.7	5.7	5.7
Indicated depth (ft)	354.5	506.9	605.4
Indicated depth adjusted for tide height (ft)	347.3	499.7	598.2
Predicted depth (ft)	336.3	505.2	623.3
Percent depth difference	3.2	-1.1	-4.2
Rest depth (ft)	175.7	370.0	562.2
Indicated change in depth (ft)	171.6	129.7	36.0
Predicted change in depth (ft)	159.9	128.7	46.8

Remarks:

Reference data is Record No. 2169, chosen from smoothly varying section of data. Predicted line angle is very large so speed recorded by C.M. #638 may be about 15% low and direction may be inaccurate.

CHECK NO. 2

	Instrument No.		
	730	639	638
Indicated current speed (ft/sec)	3.28	3.17	3.16
Current direction (°T)	174	183	166
Model current speed (ft/sec)	3.2	3.2	3.2
Indicated depth (ft)	214.5	407.4	576.8
Indicated depth adjusted for tide height (ft)	210.4	403.3	572.7
Predicted depth (ft)	206.5	402.0	586.6
Percent depth difference	1.9	0.3	-2.4
Rest depth (ft)	175.7	370.0	562.2
Indicated change in depth (ft)	34.7	33.3	10.5
Predicted change in depth (ft)	30.0	25.5	10.1

Remarks:

Reference data is mean value of Record Nos. 4134-4138, incl.

TABLE IV (Cont'd)

CHECK NO. 3

	Instrument No.		
	730	639	638
Indicated current speed (ft/sec)	3.65	3.51	3.57
Current direction (°T)	350	348	345
Model current speed (ft/sec)	3.6	3.6	3.6
Indicated depth (ft)	221.1	411.8	577.5
Indicated depth adjusted for tide height (ft)	217.7	408.4	574.1
Predicted depth (ft)	221.5	414.6	591.4
Percent depth difference	-1.8	-1.5	-3.0
Rest depth (ft)	175.7	370.0	562.2
Indicated change in depth (ft)	42.0	38.4	11.9
Predicted change in depth (ft)	45.0	38.1	14.9

Remarks:

Reference data is mean value of Record
Nos. 1365-1369, inc.

CHECK NO. 4

	Instrument No.		
	730	639	638
Indicated current speed (ft/sec)	2.85	2.13	1.38
Current direction (°T)	169	171	176
Model current speed (ft/sec)	2.86	2.11	1.39
Indicated depth (ft)	197.4	391.6	575.1
Indicated depth adjusted for tide height (ft)	189.5	383.7	567.2
Predicted depth (ft)	188.9	386.6	580.2
Percent depth difference	0.3	-0.8	-2.3
Rest depth (ft)	175.1	370.0	562.2
Indicated change in depth (ft)	14.4	13.7	5.0
Predicted change in depth (ft)	12.4	10.1	3.7

Remarks:

Reference data is mean value of Record
Nos. 3861-3865, inc.
Linear velocity profile assumed for model.

assumed here. The total unstretched mooring line length is also made 900 ft so that the elasticity of the cable only causes a tension force in the line under the condition of non-zero tidal current speed. (Normally, the installation would be made with some pre-tension at zero speed, but this is just an additive constant.) The thermistor chain portion of the cable begins immediately below the buoy. Each thermistor chain is 165 ft in length and consists of 5/8-inch hose attached with cable ties to 7/16-inch wire rope. It is assumed to be inextensible so all the stretch occurs in the remaining portion of the cable. This latter is 5/8-inch prestretched Samson 2-in-1 nylon braided rope. A deadweight anchor is used to hold the mooring in position. For the sake of simplicity, no current meters or other instrument packages are included in the simulation. In any case, the drag on such instruments is small compared to the drag on the thermistor chain. A uniform velocity profile is assumed.

In the course of referring to the manufacturer's literature to determine the strain equation coefficients (Bell, 1977a) for the Samson nylon rope, it was discovered that a change has recently occurred in the method of rope construction. This change results in a much reduced elasticity for the new construction compared to the old method. The old construction is preferred for taut-line surface moorings because it results in reduced cable tension for a given water velocity and less side thrust tending to drag the anchor. Further inquiry elicited the information that it is a simple operation to convert the manufacturing machinery back to the old method, a change in gear ratios being all that is required, and that this could be done for any rope order when specified. A discrepancy was also discovered in referring to the manufacturer's literature in connection with the toroidal buoy. In this case, the stated buoyancy was 5% greater than that obtained by calculation using the given buoy dimensions. The model uses the given dimensions to calculate the buoyancy for any depth of immersion so, for complete immersion, the buoyancy is somewhat less than that claimed by the manufacturer. Also, the value of drag coefficient for a toroidal buoy is uncertain and is here assumed to be unity regardless of the immersion depth.

The results of several simulations are presented in Fig. 2 for cable having the old construction. The curve for a mooring using the old-style cable and two thermistor chains corresponds very closely to the results obtained using cable of new construction and a single thermistor chain. Only normal cable drag is considered for the curves shown in the figure; one simulation was done which included some longitudinal drag, but the results were little different from the equivalent system with longitudinal drag ignored. An examination of the curves makes it apparent that, for a region such as Haro Strait in the Pacific Northwest, where current speeds occasionally reach 7 or 8 ft/sec, the buoy may become completely immersed at times, even when only a single thermistor chain is used. Note that, once the buoy is completely submerged, the tension increases only slightly with increasing current speed. There is no particular cause for concern on this account, so long as the tension remains within the normal working range of the cable. However, the resulting side thrust on the anchor may present a problem as next discussed.

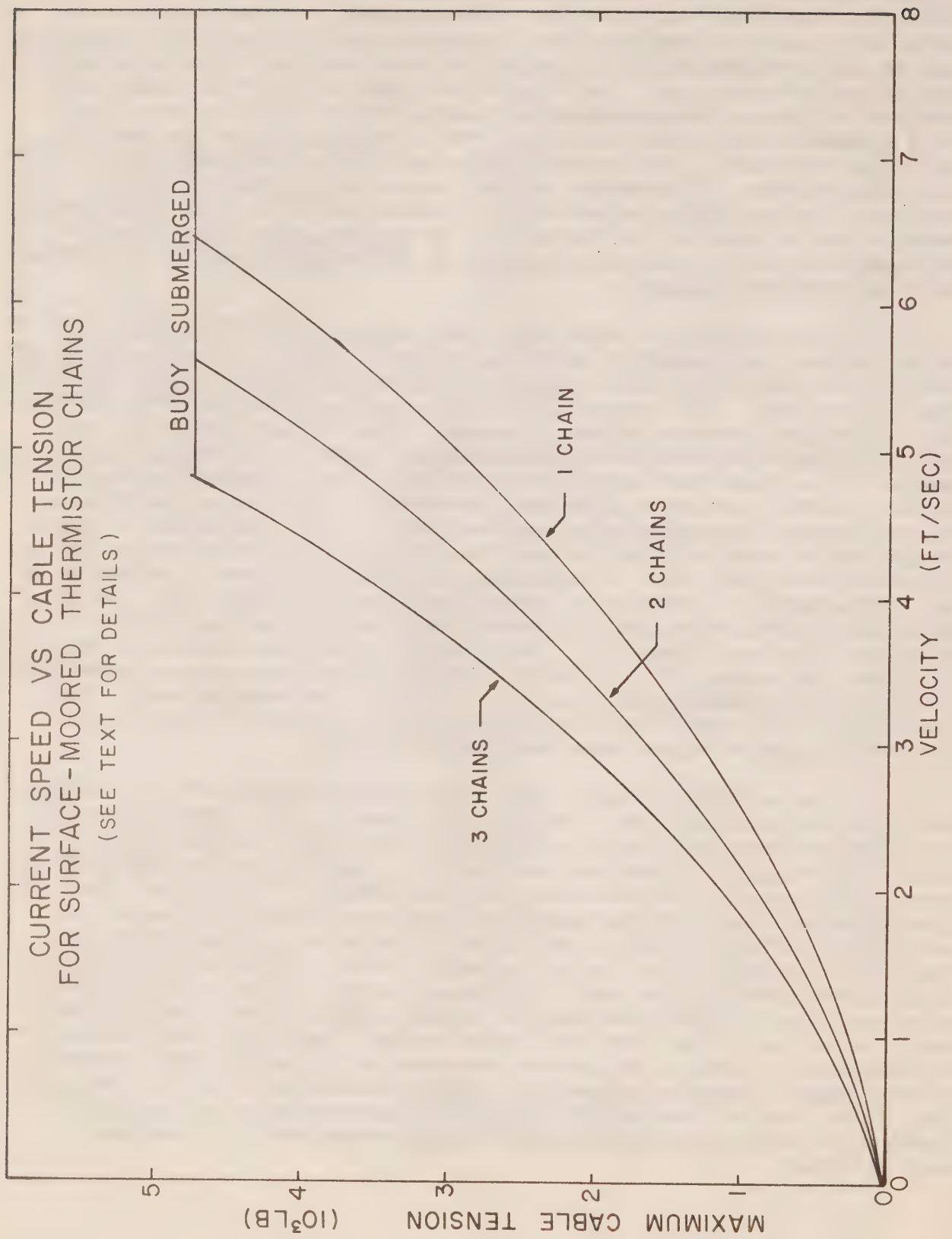


FIGURE 2

The situation regarding anchor movement is a difficult one to resolve, depending as it does on the nature of both the anchor and the sea bottom, in addition to the cable tension. If it is assumed that the bottom surface of a deadweight anchor is in contact with a flat, level sea bottom, then the frictional force F (the resisting force which prevents the anchor from dragging) is given by:

$$F = \mu(W_A - T_Z)$$

where μ is the coefficient of friction, W_A is the weight of the anchor in water and T_Z is the vertical component of cable tension. If F is less than the horizontal component of cable tension, T_X , then the anchor will drag. Therefore, the criterion which must be met to prevent the anchor from dragging in the specified case is:

$$\frac{T_X}{W_A - T_Z} < \mu$$

Using the previously described model mooring, with a single thermistor chain and a series of anchor weights, a family of curves can be plotted for current speed v vs the reciprocal friction coefficient, as in Figure 3. Then any combination of speed and $1/\mu$ lying to the right of a particular anchor weight curve will result in that anchor being dragged, and any combination to the left of the curve will be safe. The situation for an anchor weight of 2000 lb is indicated in the figure. If an estimate for the coefficient of friction is available (admittedly very difficult to obtain) then the curves permit an estimate of the anchor weight required to hold a mooring in position under the influence of a given current. For example, suppose $W_A = 4000$ lb and $\mu = 1$. Then the anchor will start to drag when the velocity exceeds about 5 ft/sec, for the system as postulated. The above exposition represents a simplistic approach to the problem of anchor movement (especially since it ignores any imbedment) but it can provide some useful information concerning the constraints on a particular mooring system.

Conclusion

The Aanderaa thermistor chains present a relatively high resistance to flow, having a drag coefficient of about 2.0 for the presently-used configuration of 5/8-inch diameter plastic hose strapped to 7/16-inch diameter wire rope. The drag could probably be reduced by attaching the hose to a torque-free rope to reduce the effective frontal area of the combination.

For the typical mooring examined, as the current speed increases, the surface buoy is pulled below the water surface before the tension in the cable reaches a critical value. After immersion, the cable tension is essentially equivalent to the net buoyancy of the buoy, increasing only slightly with speed. However, the horizontal force at the anchor continues

GRAPH OF $1/\mu = (W_A - T_A) / T_x$ VS VELOCITY
 FOR SURFACE-MOORED THERMISTOR CHAIN
 (SEE TEXT FOR DETAILS)

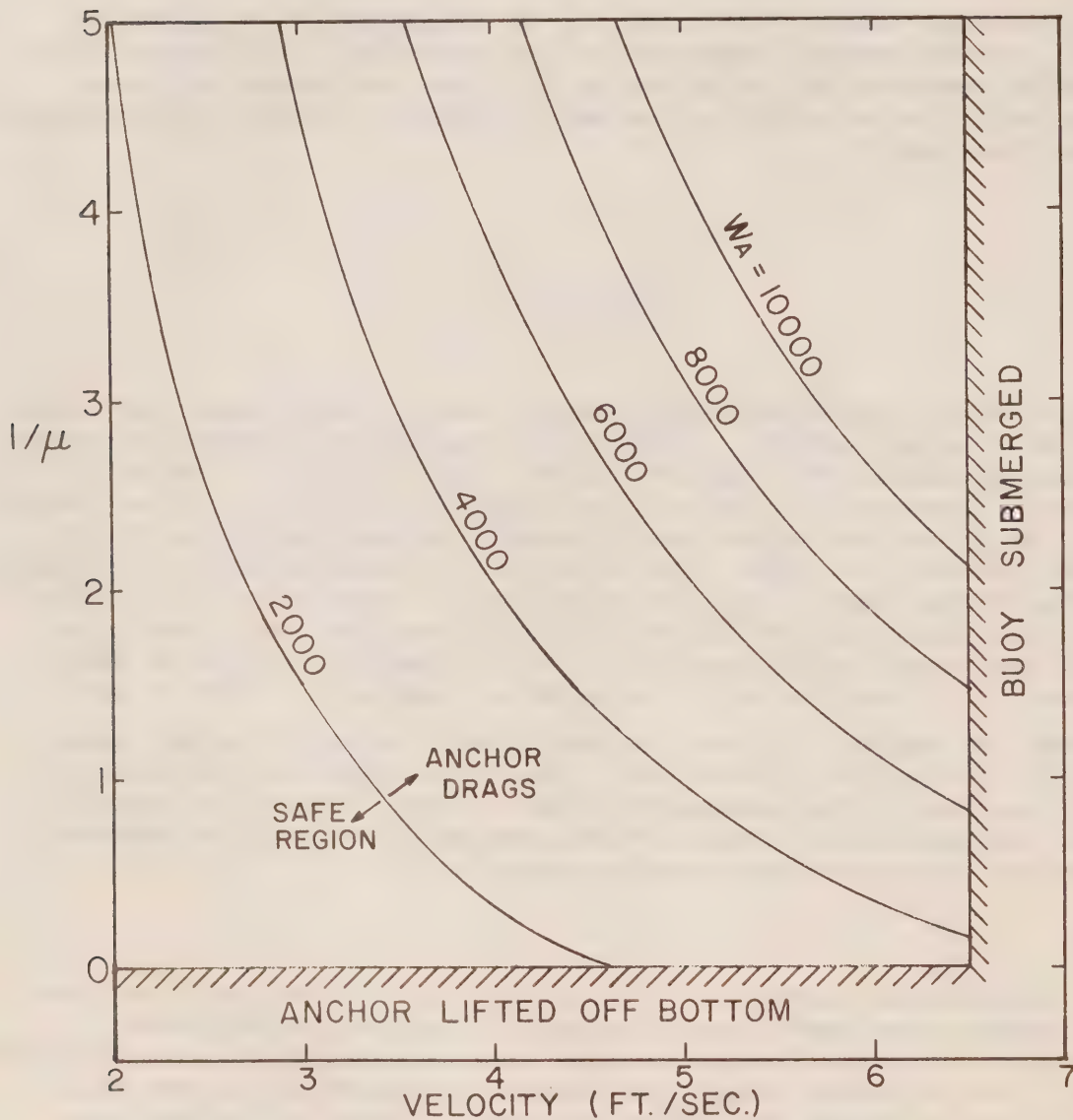


FIGURE 3.

to increase, and the vertical force to decrease, because the cable inclination is being reduced by the increased hydrodynamic drag on the system. The combination of these component forces influences the point at which the anchor starts to drag.

It is advisable to continue using the old construction of nylon cable for taut-line surface moorings because it has more stretch than the new construction. This extra stretch results in reduced tension in the cable, reduced pull on the anchor and a reduced immersion depth for the buoy at any given current speed.

References

- Bell, W.H. 1977a. Static Analysis of Single-Point Moorings. Pacific Marine Science Report 77-12. Institute of Ocean Sciences, Patricia Bay, Victoria, B.C.
- . 1977b. The Use of Extruded Plastic Fairing For a Subsurface Mooring. Pacific Marine Science Report 77-8. Institute of Ocean Sciences, Patricia Bay, Victoria, B.C.

APPENDIX I - Model Input Parameters

1. Velocity Profile:

Uniform, 2.8 ft/sec

2. Buoys:

(a) Spherical Buoy

Radius = 1.733 ft

Reynolds No. = 6.5×10^5 (super-critical) $C_D = 0.2$ Buoyancy = 1395 lb (for specific weight of water = 64 lb/ft³)

Weight = 418 lb (including shackle and pinger)

(b) Cylindrical Buoy

Buoyancy = 1278 lb

Weight = 947 lb (including shackles and pinger)

Frontal area = 2.41 ft² $C_D = 0.7$

(c) Viny Float

Buoyancy = 50 lb

Weight = 6 lb

Frontal area = 1.04 ft² $C_D = 0.2$

3. Cables:

(a) Nylon (7/16") - Samson 2-in-1

Diameter = 0.036 ft

 $C_D = 1.4$

Weight = 0.051 lb/ft

Buoyancy = 0.065 lb/ft

(b) Nylon (5/8") - Samson 2-in-1

Diameter = 0.052 ft

 $C_D = 1.4$

Weight = 0.120 lb/ft

Buoyancy = 0.136 lb/ft

(c) Wire Rope (1/4") - 6x19

Diameter = 0.021 ft

 $C_D = 1.4$

Weight = 0.100 lb/ft

Buoyancy = 0.022 lb/ft

(d) Wire Rope (7/16") - 6x19

Diameter = 0.036 ft

 $C_D = 1.4$

Weight = 0.310 lb/ft

Buoyancy = 0.065 lb/ft

(e) Thermistor Chain

Diameter = 0.052 ft

Weight = 24.0 lb/164 ft

Buoyancy = 22.3 lb/164 ft

(f) Thermistor chain in combination with 7/16" wire rope

Diameter = $0.052 + (0.036/2) = 0.070$ ftWeight = $0.310 + (24/164) = 0.456$ lb/ftBuoyancy = $0.065 + (22.3/164) = 0.201$ lb/ft $C_D =$ To be determined

4. Instruments:

(a) Aanderaa Current Meters

Weight = 54 lb (plus shackles and swivels where appropriate)

Buoyancy = 17 lb

Frontal area = 0.5 ft² $C_D = 1.1$

(b) Aanderaa Data Logger

Weight = 30 lb

Buoyancy = 10 lb

Frontal area = 0.46 ft² $C_D = 1.1$

(c) Tensiometer

Weight = 37 lb (including shackles)

Buoyancy = 12 lb

Frontal area = 0.64 ft² $C_D = 1.1$

(d) Acoustic Release

Weight = 48 lb

Buoyancy = 22 lb

Frontal area = 0.90 ft² $C_D = 1.2$

